KfK 3962
EUR 9610e
Oktober 1985

Analysis of Unsteady Two-Phase Flow Through Perforated Plates: Experimental Results

G. P. Tartaglia
Institut für Neutronenphysik und Reaktortechnik
Projekt Schneller Brüter

Kernforschungszentrum Karlsruhe

KERNFORSCHUNGSZENTRUM KARLSRUHE

Institut für Neutronenphysik und Reaktortechnik
Projekt Schneller Brüter

KfK 3962
EUR 9610e

Analysis of Unsteady Two-Phase Flow Through Perforated Plates : Experimental Results

G. P. Tartaglia

Kernforschungszentrum Karlsruhe Gmbh, Karlsruhe

Kernforschungszentrum Karlsruhe GmbH
ISSN 0303-4003

ANALYSIS OF UNSTEADY TWO-PHASE FLOW THROUGH PERFORATED PLATES : EXPERIMENTAL RESULTS

ABSTRACT

The coolant flow through the perforated dip-plate during a hypothetical core disruptive accident (HCDA) in a liquid metal fast breeder reactor was simulated in a one dimensional model. Several experiments (110) with a water-air mixture as fluid simulating the coolant were run. The pressure drop through the dip-plate, the forces acting on the dip-plate and on the upper plate, acceleration and displacement of the piston, the air volumetric fraction and the size of the air bubbles were measured in a wide range of Strouhal and acceleration numbers. The flow pattern downstream the dip-plate was filmed by using a high speed camera. The present report contains the most significative experimental results.

UNTERSUCHUNG DER INSTATIONÄREN ZWEIPHASENSTRÖMUNG DURCH PERFORIERTE PLATTEN : EXPERIMENTELLE ERGEBNISSE

ZUSAMMENFASSUNG

Die bei einem hypothetischen Störfall mit Kernzerstörung in einem natriumgekühlten " Schnellen Brüter " Reaktor (HCDA) auftretenden fluidmechanischen Phänomene und daraus resultierenden Krafteinwirkungen auf Reaktorstrukturen werden durch eine aus Ähnlicheitsbetrachtungen hergeleiteten Versuchsanordnung simuliert. Diese beschreibt eindimensional die Strömung der Kühlmittelmasse oberhalb der Kernstrukturen durch die Tauchplatte an den Reaktordeckel. Mehrere Versuche (110) mit einer Wasser-Luft Mischung als Modellfluid wurden durchgeführt. Gemessen wurden die Druckverluste an der Tauchplatte, die Kräfte auf dieselbe und auf die obere Platte, die Beschleunigung und die Bewegung des Kolbens sowie der Luftvolumenanteil für verschiedene Strouhal- und Beschleunigungszahlen. Die Strömung abwärts der perforierten Platte wurde von einer Hochgeschwindigkeitskamera gefilmt. Dieser Bericht enthält die wichtigsten experimentellen Ergebnisse.

TABLE OF CONTENTS

1 - INTRODUCTION

During a hypothetical core disruptive accident (HCDA) in a sodium-cooled fast breeder reactor (LMFBR), a large amount of energy is released within a very short period of time. The pressure in the core region is expected to raise strongly until a multiphase mixture of fuel, particles, cladding and sodium vapor is discharged into the liquid sodium pool. The coolant is pushed upwards, it compresses the inert cover gas and hits the top of the reactor. In order to reduce the possible structural damages, protective structures, i.e. shield tank or dip-plate (s. Fig. 1.1) are installed in the reactor tank.

In the present work the flow of the coolant through the dip-plate, a plate with circular holes placed at some distance under the sodium level above the core region, has been investigated.

While it was too complicated a simulation of the whole reactor, it was decided to simulate only an axial part of the upper region from the core to the top of the reactor (s. Fig. 1.2) with a one dimensional model.

A two-phase flow mixture (water-air) replaces the multiphase mixture (sodium, sodium vapor, fuel, particles and so on) of the reactor. The two-phase flow investigated is formed by small air bubbles in a liquid continuous phase.

For the analysis of this type of accident computer-codes have been developed (for istance SIMMER /1/). Up to now these codes do not allow a detailled description of the dip-plate. An experimental investigation of the unsteady two-phase flow of the coolant through the dip-plate with a reasonable modelization of the geometric and of the flow parameters is very important for observing the consequences of a Hypothetical Core Disruptive Accident (HCDA).

The work has also a general validity because the unsteady two-phase flow through perforated structures occurs in many other branches of the technology.

The theoretical aspects of the problem and their consequences have been already discussed in a previous report /2/.

In the present report are presented only the most important experimental results after a short description of the experimental device and of the instrumentation.

2 - EXPERIMENTAL SETUP

2.1 - TEST SECTION

A schematic view of the text section is given in the Fig 2.1. The test device consists of a 110. mm i.d. lower steel cylinder, a perforated plate simulating the dip-plate of the reactor, an upper transparent plexiglass cylinder, a second upper steel cylinder, and an upper plate simulating the reactor upper plug.

Within the bottom cylinder a piston is placed that accelerates the two-phase mixture of water and air simulating the mixture of liquid and vaporized sodium of the reactor. The air reaches the cylinder through nozzles placed just above the piston or through a porous bronze plate placed in the front head of the piston. The transient experiment starts only when equilibrium conditions between the water and the air bubbles percolating through the water have been reached.

At this point the piston is accelerated and pushes the water-air mixture through the dip-plate. Three different devices were realized to accelerate the piston : two full-stroke safety valves opening at extremely high speed and an explosion nut. The acceleration of the piston equals zero at the beginning of the tests with the valves, then it gradually increases up to a maximum value when air flows into the cylinder and decreases subsequently. In the tests performed with the explosion nut the maximum acceleration is attained shortly after the onset of the test, then the acceleration gradually decreases due to the movement of the piston and the consequent reduction of pressure below the piston.

More details about the test device are given in /2/.

2.2 - INSTRUMENTATION

A schematic wiew of the instrumentation layout is given in Fig. 2.2 Pressures (P1 to P7) and forces (Fu, Fd) were measured by means of piezoelectric and piezoresistive transducers. These signals are amplified through charge amplifiers (detail A in the Fig. 2.2) and then recorded on the tape unit.

The displacement of the piston is measured through a steel rod (detail L in the Fig. 2.2) with many bores connected with the piston. The rod moves together with the piston, a photodiode sends a light beam across it. At the other side of the rod a photosensible element receives the light and generates a signal directly recorded on the tape unit. The acceleration of the piston is measured by means of an accelerometer placed in the top of the piston (detail B in the

Fig. 2.2); this signal is first amplified and then recorded on the tape unit.

A digital clock generates a coded signal that is both recorded on the analogic tape unit and impressed on one edge of the film in the high speed camera. This allows the synchronization, during the analysis of the results, between the recorded signals and the data attained from the film frames. Moreover the camera is connected with a 1000 Hz oscillator which impresses its signal on the other edge of the film. This allows the computation of the velocity of the camera in frames per second.

The beginning of the experiment is regulated by a control unit. The magnetic tape has to be accelerated until it reaches the desired speed. At this moment, by pressing a button on the control unit, the experiment is started. Since the high speed camera needs a certain time to accelerate the film up to the wished speed, the control unit contains a time-delay device which provides the desired delay between the instant when the button is pressed and the actual beginning of the test (send of an electric signal opening the valve or firing the explosive nut). The electric signal which starts the experiments is recorded by the tape unit on a separated channel and also sent to a flash which marks the initial time on the film.

The signals collected on the tape unit are digitized through a Digital- PDP11 computer and then elaborated with the central computer (IBM System).

2.3 - MEASURED VARIABLES

The following variables were measured in all the tests :

1. The pressure at seven axial points (P1-P7 in Fig. 2.2)
2. The force acting on the dip-plate and on the upper plate
3. The piston displacement
4. The piston acceleration
5. The size of the air bubbles

Moreover the flow downstream the dip-plate was filmed by using a high speed camera in the transparent plexiglass channel (680 mm long) of the test device. From the analysis of the films the following data were obtained :

1. Displacement and velocity of the mixture level

2. Displacement and velocity of the jets coming out from the dip-plate

3. Size and velocity of the air bubbles in the plexiglass channel.

3 - PARAMETER OF THE EXPERIMENTAL ANALYSIS

The parameters, which have been varied during the present work, are :

1. The perforation ratio of the dip-plate (R_p = Ratio between the area of the bores of the dip-plate and the area of the plexiglass channel). Three different perforation ratios were investigated : $R_p = 0.12$, $R_p = 0.171$, $R_p = 0.25$.

2. The number of the bores of the dip-plate. Dip-plates with one bore and with seven bores have been used, the latter to investigate the interaction of several jets flowing side by side.

3. The height of the fluid over the dip-plate. The experiments were performed with different values of the height of the fluid over the dip-plate. These values were in the range between 0 and 300 mm.

4. Acceleration of the fluid. The development with time of velocity during a transient in a HCDA is undefined since it can differ from case to case /1,2/. For this reason it was specified to study three different types of velocity and acceleration curves.

5. Air volumetric fraction. The composition of the multiphase mixture during a HCDA is unknown. For this reason it was decided to perform experiments in a wide range of air volumetric fraction α : $0 \leqslant \alpha \leqslant 0.28$.

6. Size of the air bubbles. The initial size of the air bubbles in the water-air mixture (d_b=diameter of a bubble) was variied in the following range 2 mm $\leqslant d_b \leqslant$ 6 mm.

4 - PERFORMED EXPERIMENTS

Several experiments (110) were performed in order to analyse the effect of the parameters described in the Chapter 3. A list of the performed experiments is given in the Table 4.1.

In the first 12 experiments only the water was used to simulate the coolant (one-phase flow experiments). The experiment Nr. 23 was performed with the same characteristics of the experiment Nr. 11, but with degassed water.

The experiments 13-22 were performed by using the valve 1 as accelerating device and the air was blown through the nozzles. The dip-plate had a perforation ratio $R_p = 0.17$. The pressure in the chamber K1 (s. Fig. 2.1) was variied between 60 and 80 bar.

The air was blown through the plates of porous bronze in the experiments 24 to 35. All the parameters were variied for these experiments.

The experiments 36-78 were performed by using the valve 2 as accelerating device. The initial pressure was variied in the range 62 up to 100 bar. These experiments were performed with the different dip-plates, different plates of porous bronze and different height of the mixture over the dip-plate.

The experiments 79-108 were performed by using the explosive nut as accelerating device. As for the previous experiments all the parameters were variied for this type of experiment.

TABLE : 4.1

List of the experiments : explanation of the numbers between brackets at the end of the table.

Exp. Nr. (1)	DATUM	Accel. dev. (2)	Press. (bar)(3)	Plate (4)	Mixt. level mm(5)	Water level mm(6)	L.S. (7)	FILM (8)	IP (9)	ROC (10)	TEMP. W C (11)	TEMP. L C (12)	Air % (13)	Bubble dev. (14)	Poros. mm-mu (15)	Press. (bar) (16)
1	25. 4.83	1	40.- 80.	3	227.0	227.0	1	1	1	1	21.70	20.00	0.0	0	0.0	0.0
2	28. 4.83	1	40.-120.	3	227.0	227.0	1	1	1	1	19.00	20.00	0.0	0	0.0	0.0
3	4. 5.83	1	40.- 60.	3	227.0	227.0	1	1	1	1	22.00	22.00	0.0	0	0.0	0.0
4	9. 5.83	1	40.- 60.	3	227.0	227.0	1	1	1	1	20.00	20.00	0.0	0	0.0	0.0
5	13. 5.83	1	40.- 80.	3	220.0	220.0	1	1	1	1	17.30	17.00	0.0	0	0.0	0.0
6	16. 5.83	3	40.- 80.	3	227.0	227.0	1	1	1	1	20.20	20.00	0.0	0	0.0	0.0
7	17. 5.83	3	40.- 92.	3	195.0	195.0	1	1	1	1	22.80	22.50	0.0	0	0.0	0.0
8	17. 5.83	3	40.- 90.	3	220.0	220.0	1	1	1	1	22.00	22.00	0.0	0	0.0	0.0
9	18. 5.83	3	40.- 60.	3	210.0	210.0	1	1	1	1	21.20	21.00	0.0	0	0.0	0.0
10	19. 5.83	3	40.-105.	3	227.0	227.0	1	1	1	1	19.90	19.00	0.0	0	0.0	0.0
11	27. 5.83	2	100.- 0.	3	233.0	233.0	1	1	1	1	17.20	17.00	0.0	0	0.0	0.0
12	8. 6.83	2	130.- 0.	3	233.0	233.0	1	1	1	1	23.80	23.00	0.0	0	0.0	0.0
13	15. 6.83	2	110.- 0.	3	260.0	227.0	1	1	1	1	21.50	21.00	3.8	1	0.2	5.0
14	20. 6.83	1	40.- 80.	1	164.0	139.0	1	1	1	1	20.00	20.00	2.8	1	0.2	3.5
15	21. 6.83	1	40.- 80.	1	160.0	139.0	1	1	1	1	25.20	24.00	2.3	1	0.2	3.5
16	24. 6.83	1	40.- 85.	1	164.0	139.0	1	1	1	1	24.20	23.00	2.8	1	0.2	3.5
17	26. 6.83	1	40.-105.	1	227.0	162.0	1	1	1	1	23.03	23.00	3.3	1	0.2	3.5
18	30. 8.83	1	40.-105.	1	172.0	142.0	1	1	1	1	23.80	23.00	3.3	1	0.2	3.5
19	30. 8.83	1	40.-118.	1	170.0	140.0	1	1	1	1	26.00	24.50	3.3	1	0.2	3.5
20	7. 9.83	1	40.- 85.	1	286.0	144.0	1	1	1	1	25.00	24.50	14.4	2	20.0	0.7
21	6.10.83	1	40.- 62.	1	315.0	142.0	1	1	1	1	20.00	19.50	17.1	2	20.0	0.7
22	7.10.83	1	40.- 50.	1	370.0	139.0	1	1	1	1	20.00	19.50	21.0	2	20.0	0.7
23	18.10.83	2	100.- 0.	3	233.0	233.0	1	1	1	1	20.80	19.50	0.0	0	0.0	0.0
24	6.12.83	1	40.- 60.	1	218.0	147.0	1	1	1	1	17.00	17.00	7.0	2	8.0	0.3
25	7.12.83	1	40.- 60.	1	228.0	38.0	1	1	1	1	20.00	20.00	18.7	2	8.0	1.6
26	8.12.83	1	40.- 59.	1	240.0	98.0	1	1	1	1	18.00	18.00	13.8	2	8.0	0.7
27	11.12.83	1	40.- 80.	1	231.0	98.0	1	1	1	1	17.50	17.20	13.0	2	8.0	0.4
28	12.12.83	1	40.-100.	1	227.0	98.0	1	1	1	1	18.00	18.00	12.7	2	8.0	0.4
29	12.12.83	1	40.- 84.	1	227.0	98.0	1	1	1	1	19.00	19.00	12.7	2	8.0	0.4
30	13.12.83	1	40.-116.	1	227.0	98.0	1	1	1	1	19.00	18.80	12.7	2	8.0	0.4
31	15.12.83	1	40.- 60.	1	246.0	-4.0	1	1	1	1	18.00	18.00	24.2	2	8.0	2.5
32	18.12.83	1	40.- 60.	1	106.0	33.0	1	1	1	1	18.00	18.00	8.1	2	8.0	0.3
33	20.12.83	1	40.- 60.	1	162.0	93.0	1	1	1	1	18.00	18.00	7.2	2	8.0	0.3
34	23.12.83	1	40.- 80.	1	149.0	98.0	1	1	1	1	19.00	19.00	5.3	2	8.0	0.3
35	23.12.83	1	40.- 80.	1	300.0	98.0	1	1	1	1	18.50	18.50	18.6	2	8.0	1.4
36	30.12.83	3	46.- 80.	1	200.0	106.0	1	1	1	1	18.50	18.50	9.4	2	8.0	0.4
37	2. 1.84	3	44.- 76.	1	200.0	98.0	1	1	1	1	18.50	18.00	10.3	2	8.0	0.8
38	2. 1.84	3	46.-100.	1	232.0	162.0	1	1	1	1	18.50	18.00	6.8	2	8.0	0.4
39	4. 1.84	3	46.-104.	1	235.0	162.0	1	1	1	1	18.50	18.00	7.0	2	8.0	0.7
40	4. 1.84	3	46.- 76.	1	235.0	162.0	1	1	1	1	18.50	18.00	7.0	2	8.0	0.4
41	4. 1.84	3	46.- 60.	1	227.0	162.0	1	1	1	1	18.50	18.00	7.0	2	8.0	0.4
42	7. 1.84	3	46.- 80.	1	197.0	106.0	1	1	1	1	18.50	18.00	9.2	2	30.0	0.3
43	8. 1.84	3	46.- 70.	1	203.0	106.0	1	1	1	1	18.50	18.00	9.7	2	30.0	0.3
44	10. 1.84	3	46.-100.	1	208.0	106.0	1	1	1	1	18.50	18.00	10.2	2	30.0	0.3
45	10. 1.84	3	46.- 80.	1	0.0	-200.0	1	1	1	1	18.50	18.00	2.3	2	30.0	0.2

TABLE : 4.1 (Follow)

List of the experiments : explanation of the numbers between brackets at the end of the table.

Exp. Nr. (1)	DATUM	Accel. dev. (2)	Press. (bar)(3)	Plate (4)	Mixt. level mm(5)	Water level mm(6)	L.S. (7)	FILM (8)	IP (9)	ROC (10)	TEMP. W C (11)	TEMP. L C (12)	Air % (13)	Bubble dev. (14)	Poros. mm-mu (15)	Press. (bar) (16)
46	11. 1.84	3	46.- 80.	1	227.0	98.0	1	1	1	1	18.50	18.00	12.7	2	30.0	0.4
47	11. 1.84	3	46.- 70.	1	227.0	162.0	1	1	1	1	18.50	18.00	6.3	2	30.0	0.4
48	11. 1.84	3	46.- 90.	1	233.0	162.0	1	1	1	1	18.50	18.00	6.9	2	30.0	0.3
49	12. 1.84	3	46.- 62.	1	197.0	106.0	1	1	1	1	18.50	18.00	9.2	2	60.0	0.4
50	13. 1.84	3	46.-100.	1	197.0	106.0	1	1	1	1	18.50	18.00	9.2	2	60.0	0.5
51	13. 1.84	3	46.- 80.	1	227.0	98.0	1	1	1	1	18.22	18.00	12.7	2	60.0	0.9
52	13. 1.84	3	46.- 80.	1	234.0	162.0	1	1	1	1	18.20	18.00	7.0	2	60.0	0.3
53	17. 1.84	3	46.- 80.	4	227.0	98.0	1	1	1	1	18.20	18.00	12.7	2	8.0	0.5
54	17. 1.84	3	46.-100.	4	227.0	162.0	1	1	1	1	18.20	18.00	7.1	2	8.0	0.3
55	17. 1.84	3	46.- 80.	4	0.0	-200.0	1	1	1	1	18.20	18.00	2.0	2	8.0	0.2
56	18. 1.84	3	46.- 80.	4	228.0	162.0	1	1	1	1	18.20	18.00	6.3	2	8.0	0.3
57	19. 1.84	3	46.-120.	4	228.0	162.0	1	1	1	1	18.20	18.00	6.3	2	8.0	0.4
58	19. 1.84	3	46.-120.	2	227.0	162.0	1	1	1	1	18.20	18.00	6.3	2	8.0	0.4
59	20. 1.84	3	46.-100.	2	227.0	162.0	1	1	1	1	18.20	18.00	6.3	2	8.0	0.4
60	21. 1.84	3	46.- 80.	2	227.0	162.0	1	1	1	1	18.10	18.00	6.3	2	8.0	0.3
61	21. 1.84	3	46.- 80.	2	227.0	98.0	1	1	1	1	18.20	17.90	12.6	2	8.0	0.8
62	22. 1.84	3	46.-100.	2	233.0	98.0	1	1	1	1	18.20	18.00	13.1	2	8.0	0.9
63	22. 1.84	3	46.- 80.	2	155.0	98.0	1	1	1	1	18.20	18.00	5.9	2	8.0	0.3
64	22. 1.84	3	46.- 80.	2	0.0	-252.0	1	1	1	1	18.30	18.00	2.6	2	8.0	0.3
65	22. 1.84	3	46.- 80.	2	227.0	185.0	1	1	1	1	18.20	18.00	4.0	2	8.0	0.3
66	24. 1.84	3	46.-120.	3	227.0	162.0	1	1	1	1	18.10	18.00	6.3	2	8.0	0.3
67	25. 1.84	3	46.-100.	3	227.0	162.0	1	1	1	1	18.20	18.20	6.3	2	8.0	0.3
68	25. 1.84	3	46.- 80.	3	230.0	162.0	1	1	1	1	18.50	18.20	6.6	2	8.0	0.3
69	26. 1.84	3	46.- 80.	3	222.0	98.0	1	1	1	1	18.40	18.20	12.3	2	8.0	0.9
70	26. 1.84	3	46.- 80.	3	156.0	98.0	1	1	1	1	18.20	20.00	6.1	2	8.0	0.3
71	27. 1.84	3	46.- 80.	3	233.0	185.0	1	1	1	1	18.20	18.00	4.6	2	8.0	0.3
72	28. 1.84	3	46.-100.	4	233.0	162.0	1	1	1	1	18.20	18.00	6.7	2	8.0	0.4
73	28. 1.84	3	46.- 80.	4	227.0	162.0	1	1	1	1	18.20	18.00	6.2	2	8.0	0.4
74	2. 2.84	3	46.- 80.	4	227.0	98.0	1	1	1	1	20.40	19.40	12.7	2	8.0	0.4
75	3. 2.84	3	46.- 80.	5	227.0	162.0	1	1	1	1	20.30	19.50	7.1	2	8.0	0.3
76	3. 2.84	3	46.- 80.	5	268.0	162.0	1	1	1	1	20.40	20.00	9.8	2	8.0	0.3
77	3. 2.84	3	46.- 80.	5	227.0	98.0	1	1	1	1	21.00	20.50	12.4	2	8.0	0.7
78	3. 2.83	3	46.- 80.	5	83.0	40.0	1	1	1	1	21.00	20.40	4.7	2	8.0	0.3
79	30. 5.84	3	80.	1	227.0	162.0	1	1	1	0	21.00	20.50	7.1	1	8.0	0.3
80	1. 6.84	2	80.	1	227.0	162.0	1	1	1	1	21.50	20.30	7.9	2	8.0	0.4
81	1. 6.84	2	80.	1	227.0	200.0	1	1	1	1	21.50	21.00	3.2	2	8.0	0.3
82	5. 6.84	2	80.	1	245.0	110.0	1	1	1	1	21.50	21.00	16.2	2	8.0	0.6
83	5. 6.84	2	40.	1	227.0	162.0	1	1	1	1	21.50	21.00	7.9	2	8.0	0.4
84	5. 6.84	2	60.	1	233.0	162.0	1	1	1	1	22.50	22.00	8.5	2	8.0	0.4
85	6. 6.84	2	40.	1	227.0	162.0	1	1	1	1	22.50	22.00	7.9	2	60.0	0.3
86	6. 6.84	2	80.	1	232.0	162.0	1	1	1	1	23.00	22.00	8.4	2	60.0	0.3
87	7. 6.84	2	60.	1	235.0	162.0	1	1	1	1	23.00	22.00	8.8	2	60.0	0.3
88	7. 6.84	2	60.	1	166.0	100.4	1	1	1	1	22.00	21.50	8.6	2	8.0	0.3
89	8. 6.84	2	60.	1	100.0	45.3	1	1	1	1	22.00	21.50	7.8	2	8.0	0.3
90	8. 6.84	2	60.	1	40.0	-9.9	1	1	1	1	22.00	21.50	7.8	2	8.0	0.3

TABLE : 4.1 (Follow)

List of the experiments : explanation of the numbers between brackets at the end of the table.

Exp. Nr. (1)	DATUM	Accel. dev. (2)	Press. (bar)(3)	Plate (4)	Mixt. level mm(5)	Water level mm(6)	L.S. (7)	FILM (8)	IP (9)	ROC (10)	TEMP. W C (11)	TEMP. L C (12)	Air % (13)	Bubble dev. (14)	Poros. mm-mu (15)	Press. (bar) (16)
91	9. 6.84	2	20.	1	227.0	162.0	1	1	1	1	22.70	21.00	7.9	2	8.0	0.3
92	9. 6.84	2	80.	1	297.0	227.0	1	1	1	1	22.00	21.00	7.8	2	8.0	0.5
93	9. 6.84	2	80.	1	230.0	98.0	1	1	1	1	22.50	22.00	16.1	2	8.0	0.3
94	11. 6.84	2	60.	1	0.0	-200.0	1	1	1	1	22.00	21.00	3.1	2	8.0	0.3
95	11. 6.84	2	40.	2	227.0	162.0	1	1	1	1	22.30	21.80	7.9	2	8.0	0.3
96	11. 6.84	2	60.	2	227.0	162.0	1	1	1	1	22.20	21.40	7.9	2	8.0	0.3
97	12. 6.84	2	80.	2	227.0	162.0	1	1	1	1	22.80	22.30	7.9	2	8.0	0.3
98	12. 6.84	2	80.	2	227.0	200.0	1	1	1	1	22.00	21.50	3.1	2	8.0	0.2
99	12. 6.84	2	80.	2	227.0	110.0	1	1	1	1	22.20	21.80	14.2	2	8.0	0.5
100	13. 6.84	2	60.	3	227.0	162.0	1	1	1	1	22.90	22.00	7.9	2	8.0	0.3
101	13. 6.84	2	80.	3	227.0	162.0	1	1	1	1	22.20	21.80	7.9	2	8.0	0.3
102	14. 6.84	2	80.	3	227.0	162.0	1	1	1	1	22.80	22.00	7.9	2	8.0	0.3
103	14. 6.84	2	80.	3	227.0	200.0	1	1	1	1	22.50	22.00	3.2	2	8.0	0.3
104	14. 6.84	2	80.	3	227.0	110.0	1	1	1	1	20.00	21.50	14.3	2	8.0	0.6
105	15. 6.84	2	60.	5	224.0	162.0	1	1	1	1	25.20	24.80	7.3	2	8.0	0.3
106	15. 6.84	2	80.	5	226.0	162.0	1	1	1	1	24.20	23.50	7.6	2	8.0	0.3
107	11.12.84	2	50.	2	180.0	164.0	1	1	1	1	18.20	18.00	2.8	1	0.2	2.4
108	12.12.84	2	60.	2	227.0	162.0	1	1	1	1	18.20	18.00	7.9	2	8.0	0.3

Explanations :

(1) Number of the experiment

(2) Accelerating device

1. Valve 1

2. Explosive nut

3. Valve 2

(3) Pressures - For the experiments with the valves these are the pressures in the chambers K1 and K2.

- For the experiments with explosive nut this is the pressure in the chamber K below the piston.

(4) Dip-plates

1. 1 = 0.17 Perforation Ratio - 1 Bore

2. 2 = 0.25 Perforation Ratio - 1 Bore

3. 3 = 0.12 Perforation Ratio - 1 Bore

4. 4 = 0.12 Perforation Ratio - 7 Bores

5. 5 = 0.17 Perforation Ratio - 7 Bores

(5) Mixture level - height of the fluid (water-air) over the dip-plate

(6) Water level - collapsed height of the water over the dip-plate

(7) Perforated rod signal (1=yes; 0=no)

(8) High speed film (1=yes; 0=no)

(9) Starting signal on tape (1=yes; 0=no)

(10) Digital clock signal on film (1=yes; 0=no)

(11) Temperature of the water

(12) Temperature near the test device

(13) Air volumetric fraction

(14) Device used to blow air into the water.

1. 0 = One phase-flow experiments. No blowing device.

2. 1 = Nozzles

3. 2 = Porous bronze plates

(15) Diameter of the hole of the nozzles (mm) or porosity of the porous bronze plates (µm).

(16) Pressure - Entry pressure of the air into the water through the nozzles or through the porous bronze plates.

5 - RESULTS FROM THE FILM ANALYSIS

The films, totaling 100 experiments (32 performed with valve 1, 41 with valve 2, and 27 with explosive nut), were evaluated.

The following variables were measured as a function of time in the transparent section of the test device:

1. The displacement of the mixture surface DS
2. The displacement of the jets DJ
3. The size of the air bubbles
4. The velocity of the air bubbles

All the peculiarities about the film analysis have been discussed in a previous report /2/. Here the most important experimental data are illustrated.

The figures 5.1 to 5.13 show the displacement of the surface of the mixture (DS) as a function of the displacement of the piston (DP). The plots are collected for different accelerating device, different air volumetric fraction and different perforation ratios. The abscissa represents the dimensionless piston displacement DP/DI (DI=110 mm is the diameter of the test channel), the ordinate represents the dimensionless displacement of the mixture surface DS/DI, with DS measured from the initial point of the mixture surface. The zero points of the x-axis coincides with the instant when the first movement of the mixture surface is observed.

It can be seen that the data lie on different lines, one for each perforation ratio or for each air volumetric fraction. The main parameter is the perforation ratio, but also the air volumetric fraction plays an important role because when it increases the piston can achieve higher acceleration and consequently also the velocity of the mixture surface over the dip-plate increases.

The behaviour of the displacement of the jets (DJ) plotted as a function of the piston displacement (DP) is similar. The figures 5.14 to 5.24 show the different cases.

The behaviour of the ratios RS (displacement of the mixture surface divided by the piston displacement) and of the ratios RJ (displacement of the jet divided by the piston displacement) are also plotted as a function of the dimensionless piston displacement (DP/DI) and the behaviour is, obviously, similar to that of figures 5.14 to 5.24. The figures 5.25 to 5.46 illustrate the different cases.

Analytical empirical plots of the form:

$$y = ax^b \tag{5.1}$$

have been fitted to the measured data. The coefficients a and b are listed in the Table 5.1 for the various cases together with the ranges of validity.

To be able to apply the results derived for the perforation ratios investigated (i.e., 0.12, 0.17 and 0.25) to other values of the perforation ratio, the coefficients a and b of Eq. (5.1) were fitted as a function of the perforation ratio R_p, through curves of the type :

$$a = f_1 + f_2R_p + f_3R_p^2 \tag{5.2}$$

$$b = g_1 + g_2R_p + g_3R_p^2 \tag{5.3}$$

or :

$$a = f_1 + f_2R_p + f_3R_p^2 \tag{5.4}$$

$$b = g_1 + R_p^{g_2} \tag{5.5}$$

The coefficients f_1, f_2, f_3, g_1, g_2, g_3 are listed in the Table 5.2 . The different interpolating curves are shown in the figures 5.47 to 5.54.

As for the perforation ratios, to be able to apply the results derived for the air volumetric fraction investigated to other values of the air volumetric fraction (α), the coefficients a and b of the Eq. (5.1) were fitted as a function of α through curves of the type :

$$a = c_1 + c_2\alpha + c_3\alpha^2 \tag{5.6}$$

$$b = d_1 + d_2\alpha + d_3\alpha^2 \tag{5.7}$$

The coefficients c_1, c_2, c_3, d_1, d_2, d_3 are listed in the Table 5.3 . The different interpolating curves are shown in the figures 5.55 to 5.64.

Valve Nr. 1

R_p	Mixture level(mm)	α	Reynolds-number-max ($*10^5$)	Strouhal number	y	a	b	y_1	a_1	b_1
0.171	160.-300.	0.03	3.3 - 3.4	0.127-0.505	D_s/D	2.37	1.42	R_s	2.34	0.51
					D_j/D	3.83	1.42	R_j	4.68	0.56
		0.05	3.4 - 3.5	0.059-0.484	D_s/D	2.53	1.42	R_s	2.64	0.42
					D_j/D	4.40	1.38	R_j	4.70	0.25
		0.13	4.2 - 5.0	0.424-0.850	D_s/D	2.60	1.43	R_s	3.18	0.53
					D_j/D	4.57	1.41	R_j	4.77	0.26
		0.15	4.1 - 4.2	0.096-0.660	D_s/D	2.73	1.43	R_s	3.20	0.38
					D_j/D	5.03	1.53	R_j	5.03	0.27
		0.17	4.5 - 4.6	0.070-0.620	D_s/D	2.78	1.44	R_s	3.23	0.35
					D_j/D	5.09	1.54	R_j	5.10	0.26
		0.21	3.3 - 3.4	0.052-0.464	D_s/D	2.90	1.46	R_s	3.24	0.33
					D_j/D	5.11	1.56	R_j	5.12	0.26
	0.0 -140.	0.07	3.2 - 3.3	0.275-0.578	D_s/D	4.89	1.47	R_s	4.98	0.29
					D_j/D	4.72	1.28	R_j	7.09	0.21
		0.09	3.3 - 3.4	0.283-0.582	D_s/D	4.91	1.47	R_s	4.98	0.29
					D_j/D	4.68	1.26	R_j	7.10	0.21

Tab. 5.1 - Coefficients for the Equations 5.1

Valve Nr. 2

R_p	Mixture level(mm)	α	Reynolds-number-max ($*10^5$)	Strouhal number	y	a	b	y_1	a_1	b_1
0.12	150.-233.	0.04	4.2 - 4.3	0.140-0.868	D_s/D	5.41	1.23	R_s	7.27	0.19
					D_j/D	10.22	1.55	R_j	13.50	0.41
		0.06	3.3 - 3.9	0.389-0.689	D_s/D	5.97	1.37	R_s	6.76	0.19
					D_j/D	6.50	1.07	R_j	15.00	0.42
		0.12	6.2 - 6.3	0.402-1.309	D_s/D	7.00	1.38	R_s	8.72	0.12
					D_j/D	15.23	1.74	R_j	21.50	0.45
0.171	197.-235.	0.06	1.4 - 6.9	0.598-1.121	D_s/D	3.25	1.64	R_s	3.24	0.62
					D_j/D	5.93	1.59	R_j	4.77	0.32
		0.09	3.7 - 4.8	0.189-0.991	D_s/D	3.92	1.70	R_s	3.85	0.60
					D_j/D	6.06	1.58	R_j	5.28	0.38
		0.11	4.4 - 5.9	0.361-1.241	D_s/D	3.88	1.61	R_s	3.97	0.48
					D_j/D	6.50	1.36	R_j	4.70	0.34
		0.13	6.6 - 6.8	0.353-1.123	D_s/D	4.70	1.75	R_s	4.08	0.54
					D_j/D	7.05	1.64	R_j	8.85	0.30
	0.0 -140.	0.02	2.4 - 2.5	0.101-0.370	D_s/D	-	-	R_s	-	-
					D_j/D	9.05	1.65	R_j	-	-

Tab. 5.1 - Coefficients for the Equations 5.1 (follow)

Valve Nr. 2

R_p	Mixture level(mm)	α	Reynolds-number-max ($*10^5$)	Strouhal number	y	a	b	y_1	a_1	b_1
0.171 (7Bohr.)	227.-268.	0.07	4.6 - 4.7	0.262-1.056	D_s/D	1.99	1.37	R_s	-	-
					D_j/D	4.08	1.22	R_j	-	-
		0.09	3.3 - 3.5	0.194-0.665	D_s/D	2.04	1.39	R_s	-	-
					D_j/D	4.10	1.24	R_j	-	-
		0.12	6.2 - 6.3	0.330-1.302	D_s/D	2.06	1.40	R_s	-	-
					D_j/D	4.15	1.23	R_j	-	-
	0.0 -83.	0.05	4.6 - 4.7	0.271-0.931	D_s/D	2.10	1.41	R_s	-	-
					D_j/D	4.31	1.30	R_j	-	-
0.250	155.-233.	0.04	5.3 - 5.4	0.020-0.702	D_s/D	2.36	1.52	R_s	2.94	0.64
					D_j/D	2.70	0.88	R_j	3.36	0.50
		0.05	5.1 - 5.2	0.137-0.601	D_s/D	2.74	1.29	R_s	3.50	0.58
					D_j/D	2.95	1.09	R_j	4.07	0.18
		0.06	5.2 - 5.9	0.545-0.825	D_s/D	2.80	1.30	R_s	3.51	0.54
					D_j/D	4.02	1.49	R_j	4.10	0.21
		0.13	6.7 - 7.7	0.566-1.736	D_s/D	3.82	1.64	R_s	3.67	0.50
					D_j/D	4.62	1.36	R_j	5.00	0.02
	0.0	0.02	5.4 - 5.5	0.160-0.601	D_s/D	3.82	1.64	R_s	3.67	0.50
					D_j/D	4.62	1.36	R_j	5.00	0.02

Tab. 5.1 - Coefficients for the Equations 5.1 (follow)

Valve Nr. 2

R_p	Mixture level(mm)	α	Reynolds-number-max ($*10^5$)	Strouhal number	y	a	b	y_1	a_1	b_1
0.120 (7Bohr.)	227.-233.	0.06	6.7 - 6.8	0.106-1.541	D_s/D	1.40	1.16	R_s	-	-
					D_j/D	2.70	0.88	R_j	-	-
		0.07	3.0 - 4.3	0.136-0.626	D_s/D	1.80	1.30	R_s	-	-
					D_j/D	2.95	1.09	R_j	-	-
		0.12	3.5 - 3.6	0.464-1.054	D_s/D	2.55	1.25	R_s	-	-
					D_j/D	4.02	1.49	R_j	-	-

Tab. 5.1 - Coefficients for the Equations 5.1 (follow)

Explosive Nut

R_p	Mixture level(mm)	α	Reynolds-number-max ($*10^5$)	Strouhal number	y	a	b	y_1	a_1	b_1
0.171	227.-297.	0.03	10.0 - 11.1	0.085-0.470	D_s/D	2.92	1.43	R_s	5.64	0.47
					D_j/D	3.80	1.29	R_j	3.60	0.19
		0.08	12.0 - 19.0	0.212-1.272	D_s/D	3.78	1.56	R_s	4.93	0.49
					D_j/D	4.71	1.56	R_j	3.49	0.36
		0.16	23.0 - 24.1	0.552-1.861	D_s/D	4.05	1.70	R_s	4.33	0.48
					D_j/D	4.85	1.57	R_j	2.95	0.29
	100.	0.02	14.2 - 14.6	0.189-0.709	D_s/D	5.98	1.72	R_s	4.36	0.42
					D_j/D	6.02	1.61	R_j	3.00	0.28
	0.0	0.02	11.6	0.156-0.396	D_s/D	-	-	R_s	-	-
					D_j/D	6.21	1.62	R_j	3.12	0.29
0.171 (7Bohr.)	227.-233.	0.07	13.9 - 17.4	0.119-1.349	D_s/D	2.64	1.46	R_s	2.40	0.34
					D_j/D	4.34	1.33	R_j	4.45	0.24

Tab. 5.1 - Coefficients for the Equations 5.1 (follow)

Explosive Nut

R_p	Mixture level(mm)	α	Reynolds-number-max ($*10^5$)	Strouhal number	y	a	b	y_1	a_1	b_1
0.25	227.	0.03	13.5 - 13.6	0.130-0.637	D_s/D	2.63	1.27	R_s	3.02	0.30
					D_j/D	3.10	1.17	R_j	3.57	0.21
		0.08	13.3 - 17.4	0.263-1.001	D_s/D	2.78	1.27	R_s	2.74	0.37
					D_j/D	3.46	1.50	R_j	3.34	0.06
		0.14	21.6 - 21.7	0.247-0.969	D_s/D	3.08	1.63	R_s	2.56	0.47
					D_j/D	3.52	1.41	R_j	2.82	0.27
0.12	227.	0.03	11.3 - 11.4	0.216-0.422	D_s/D	4.93	1.78	R_s	6.52	0.29
					D_j/D	4.78	1.18	R_j	4.64	0.42
		0.08	15.0 - 18.1	0.408-1.228	D_s/D	5.75	1.87	R_s	5.79	0.37
					D_j/D	5.98	1.88	R_j	5.78	0.43
		0.14	22.1 - 22.2	0.216-1.456	D_s/D	6.44	1.43	R_s	4.37	0.31
					D_j/D	6.22	1.90	R_j	7.40	0.33

Tab. 5.1 - Coefficients for the Equations 5.1 (follow)

Valve Nr. 2

α	y	f_1	f_2	g_1	g_2	g_3
0.04	D_s/D	0.47	-1.12	1.40	-2.7	10.22
	D_j/D	0.21	-1.80	0.308	-0.775	
0.07	D_s/D	0.63	-1.01	-0.81	27.13	-74.70
	D_j/D	0.61	-1.34	0.74	-0.409	
0.13	D_s/D	1.18	-0.82	-0.88	26.99	-67.50
	D_j/D	0.46	-1.61	0.86	-0.338	21.50

Explosive Nut

α	y	f_1	f_2	g_1	g_2	g_3
0.03	D_s/D	0.75	-0.84	1.36	-0.59	10.22
	D_j/D	0.66	-0.45	1.18	-0.016	
0.08	D_s/D	0.69	-0.98	1.24	-0.746	-74.70
	D_j/D	0.61	-0.53	1.05	-0.242	
0.16	D_s/D	0.74	-0.99	1.21	-0.78	-67.50
	D_j/D	1.15	-0.23	0.47	-0.66	21.50

Tab. 5.2 - Coefficients for the Equations 5.2 ÷ 5.5

Valve Nr. 1

R_p	y	c_1	c_2	c_3	d_1	d_2	d_3
0.171	D_s/D	1.75	0.167	-0.0068	1.43	-0.021	0.0013
	D_j/D	3.74	0.12	-0.003	1.42	-0.025	0.0019

Valve Nr. 2

R_p	y	c_1	c_2	c_3	d_1	d_2	d_3
0.12	D_s/D	3.40	0.51	-0.018	0.58	0.1825	-0.0093
	D_j/D	6.76	0.60	0.0036	1.94	-0.08	0.0052
0.171	D_s/D	1.96	0.245	-0.004	2.12	-0.1134	0.0065
	D_j/D	3.50	0.32	-0.0027	1.55	-0.0012	0.0003
0.25	D_s/D	1.57	0.21	-0.0028	2.32	-0.268	0.0166
	D_j/D	-0.1178	0.85	-0.0378	-0.055	0.29	-0.014

Tab. 5.3 - Coefficients for the Equations 5.6, 5.7

Explosive Nut

R_p	y	c_1	c_2	c_3	d_1	d_2	d_3
0.12	D_s/D	4.55	0.166	-0.003	2.65	-0.20	0.0103
	D_j/D	3.67	4.20	-0.016	0.68	0.21	-0.0086
0.171	D_s/D	2.33	0.24	-0.0085	2.07	-0.148	0.0079
	D_j/D	3.10	0.29	-0.0114	1.51	0.024	-0.0024
0.25	D_s/D	1.54	0.27	-0.011	1.89	-0.17	0.009
	D_j/D	2.76	0.126	-0.005	0.844	0.13	-0.006

Tab. 5.3 - Coefficients for the Equations 5.6, 5.7 (follow)

6 - RESULTS FROM THE DIGITIZED DATA

6.1 - PISTON DATA

The displacement and the acceleration of the piston are directly measured, as already discussed in the Chapter 2 , respectively through a perforated rod and through an accelerometer. The execution of the derivative of the signal of the perforated rod allows to compute the velocity and the acceleration of the piston; by integrating the signal of the accelerometer it is possible to compute the velocity and the displacement of the piston. The data attained with the two different methods are in a very good agreement as shown in /1/.

The figures 6.1 to 6.103 show the displacement D, the velocity V and the acceleration A of the piston for the performed experiments. The results shown in these figures are those obtained through the elaboration of the signal from the accelerometer.

6.2 - MEASURED RESISTANCE COEFFICIENTS

As discussed in /2/ the resistance coefficient for unsteady two-phase flow through the perforated plate can be attained through the relation:

$$Cu = \Delta P/(\rho v^2/2) \tag{6.1}$$

where ΔP is the pressure drop through the dip-plate (P6-P7), v is the velocity of the flow below the dip-plate, ρ is the density of the mixture,

or through the relation :

$$Cu = (F_d/S_e)/(\rho v^2/2) \tag{6.2}$$

where F_d is the force acting on the dip-plate and S_e is the effective area of the dip-plate, i.e. the total surface area of the dip-plate minus the area of the bore.

The pressure drop through the dip-plate (P6-P7) versus time is plotted in the figures 6.104 to 6.198 for the various experiments.

The figures 6.199 to 6.301 show the force acting on the dip-plate as a function of the square of the piston velocity. The points are represented by various symbols depending on the acceleration, with the range of acceleration for each symbol indicated in the table of each figure. The arrows show the time progress.

If we discuss, for istance, the Fig 6.282 (Exp.87), we can see that at the beginning of the two-phase flow experiments the points lay on the line F_d=0, because the movement of the piston is taken up by the compression of the air bubbles contained in the region below the perforated plate (between the points 0 and 1). When the piston has completely compressed the air below the dip-plate, the piston starts to push the mixture through the perforated dip-plate. Now it is possible to measure a force acting on the dip-plate that reaches a first maximum value (point 2). During the progress of the plotted curve to the point 3, the pressure P7 downstream the dip-plate increases and the force on the dip-plate decreases. Then the force increaes up to a maximum when also the pressure drop P6-P7 reaches a maximum value (point 4). When the transient is finished (point 5), the force decreases and at the end of the experiment steady state flow is attained.

From dimensional analysis, developed in /2/, it was found that it is possible to represent the resistance coefficient of unsteady two-phase flow through the dip-plate as a function of only two dimensionless numbers, that is :

$$Cu = Cu(\Gamma, Str) \qquad (6.3)$$

where :

$Str = v_{max}/D$ (Strouhal number)

$\Gamma = Da/(Csv^2)$ (acceleration number)

with :

a = acceleration of the flow below the dip-plate,

v_{max} = maximum velocity of the flow below the dip-plate,

D = equivalent diameter of the test channel,

Cs = resistance coefficient for the steady flow through the dip-plate.

The values of the resistance coefficients for fixed ranges of Strouhal and acceleration numbers have been given in a previous report /2/.

6.3 - FORCES ACTING ON THE UPPER PLATE

The maximum values of the forces acting on the upperplate and their time integral (impulses) are two important parameters in analyzing the loading of the upper structures of the reactor during a hy-

pothetical accident. The forces acting on the upper plate of the test section versus time are plotted in the figures 6.302 to 6.391.

The time integrals (impulses) of these forces are plotted also versus time in the figures 6.392 to 6.492.

It is interesting to compare the force acting on the upper plate with that acting on the dip-plate to analyze the distribution of load between the two structures. The figure 6.493 show for each test the ratio between the maximum force acting on the upper platte (F_{um}) and the maximum force acting on the dip-plate (F_{dm}). Since the cavitation has the strongest effect on the flow pattern over the dip-plate both for two-phase flow /2/ and for one-phase flow /3/ the ratios between the impulses have been plotted versus the cavitation number K_c.

The same ratio between these forces is plotted in the figure 6.494 as a function of the maximum pressure in the steel cylinder.

The ratio between the total impulses acting on the upper plate (I_{mu}) plate and on the dip-plate (I_{md}) is shown in the figures 6.495 to 6.497, respectively as a function of the cavitation number and of the maximal pressure of the steel cylinder.

From the analysis of the above listed figures it is possible to recognize that both the forces and the impulses are strongly depending on the perforation ratio R_p. The higher R_p is, the greater are the forces and the impulses acting on the upper plate as compared with those acting on the dip-plate. In the case of the plates with seven bores the ratios between the impulses are considerably lower than for the plates with one bore, due to mixing between the jets over the dip-plate and consequent dissipation of kinetic energy, which can take place if several holes have been provided. In all cases the ratio between the impulses decreases with K_c.

REFERENCES

/1/ L.L. Smith

SIMMER-II : A computer program for LMFBR disruptive core analysis. NUREG/CR-0.453, LA-7515-M, Rw. 1980.

/2/ G.P. Tartaglia

Experimentelle Unterusuchung der instationären Zweiphasenströmung durch perforierte Platten. KfK 3954, Kernforschungszentrum Karlsruhe, 1985

/3/ F. Casadei, M.Dalle Donne

Accelerated one-phase flow through perforated plates. Nuclear Technology, pag. 43, Vol. 64, Jan. 1984

NOMENCLATURE

1. Latin letters

a		coefficient
a	(m/s^2)	acceleration
a_1		coefficient
b		coefficient
b_1		coefficient
C	(-)	resistance coefficient
C_c	(-)	contraction coefficient
C_s	(-)	resistance coefficient by steady-state flow
C_u	(-)	resistance coefficient by unsteady-state flow
C_1		coefficient
C_2		coefficient
C_3		coefficient
DI	(m)	diameter of the plexiglass channel
d_b	(mm)	diameter of the air bubbles
DJ	(m)	displacement of the jet
DP	(m)	displacement of the piston
DS	(m)	displacement of the mixture level
d_1		coefficient
d_2		coefficient
d_3		coefficient
F	(N)	force
F_d	(N)	force on the dip-plate
F_{dm}	(N)	maximal force on the dip-plate
F_u	(N)	force on the upper plate
F_{um}	(N)	maximal force on the upper plate
f_1		coefficient
f_2		coefficient
f_3		coefficient
g_1		coefficient
g_2		coefficient
g_3		coefficient
h	(m)	mixture level over the dip-plate
I_{md}	(N*s)	Total impulse on the dip-plate
I_{mu}	(N*s)	Total impulse on the upper plate
K_c	(-)	cavitation number
P	(N/m^2)	pressure
P_v	(N/m^2)	water vapor saturation pressure
P1	(N/m^2)	pressure beneath the piston

P2	(N/m^2)	pressure above the piston
P3	(N/m^2)	pressure in the steel cylinder
P4	(N/m^2)	pressure in the steel cylinder
P5	(N/m^2)	pressure in the steel cylinder
P6	(N/m^2)	pressure upstream the dip-plate
P7	(N/m^2)	pressure downstream the dip-plate
R_p	(-)	Perforation ratio, ratio between the area of the holes and the total surface area of the dip-plate.
RJ	(-)	dimensionless displacement of the jet
RS	(-)	dimensionless displacement of the mixture level
S_e	(m^2)	effective surface area of the dip-plate, total surface area of the dip-plate minus area of the holes.
t	(s)	time
v	(m/s)	velocity
v_{max}	(m/s)	maximum value of the velocity
v_j	(m/s)	velocity of the jet
x		abscissa
y		ordinate

Greek Letters

ΔP	(N/m^2)	Pressure difference (P6-P7)
Γ		$(D*a)/(C_s*v^2)$ Acceleration number
α		air volumetric fraction
ρ	(Kg/m^3)	density

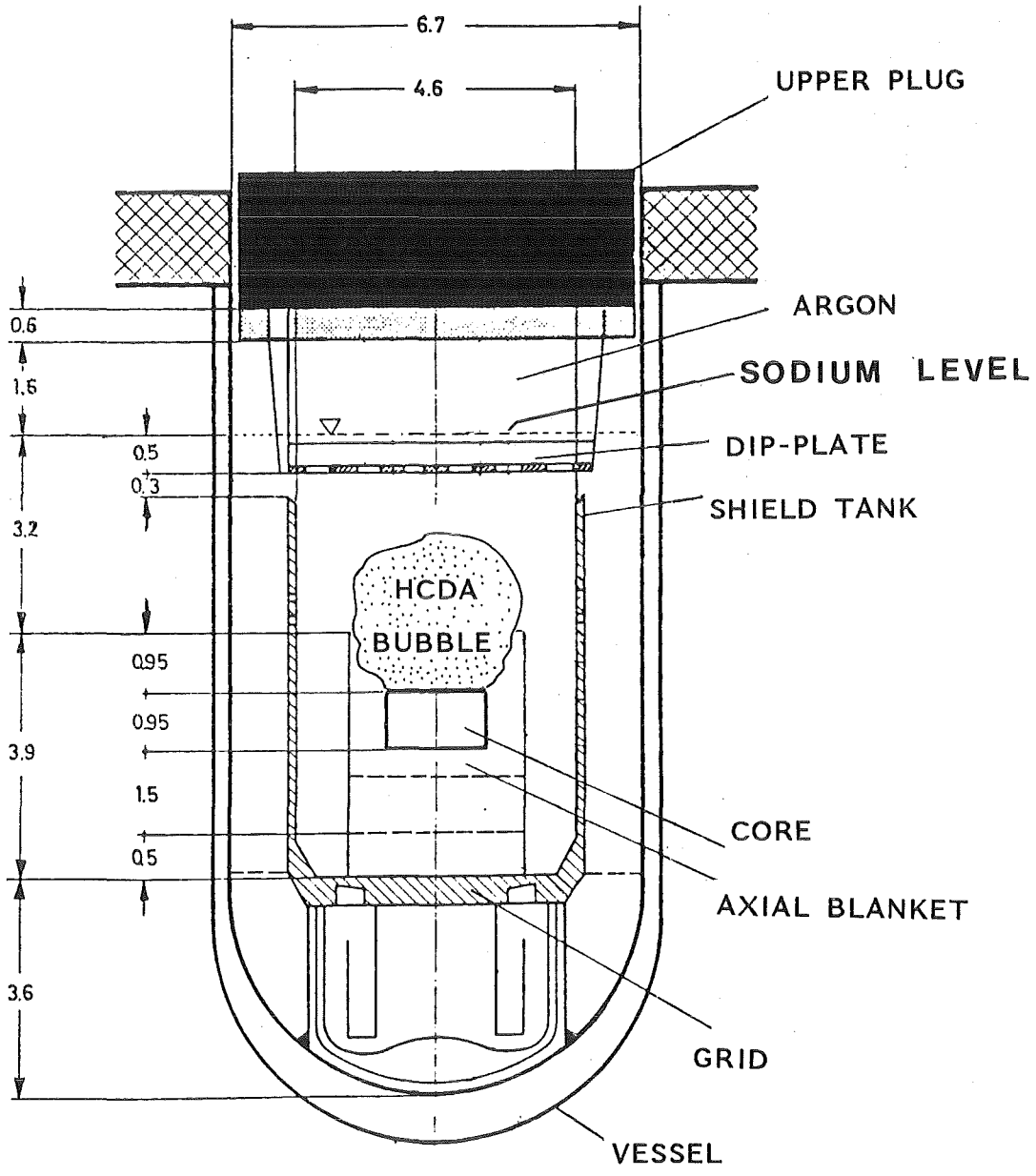

Fig. 1.1 - Schematic representation of the HCDA bubble discharge in the upper plenum of an LMFBR of the loop type. (The dimensions are in meters)

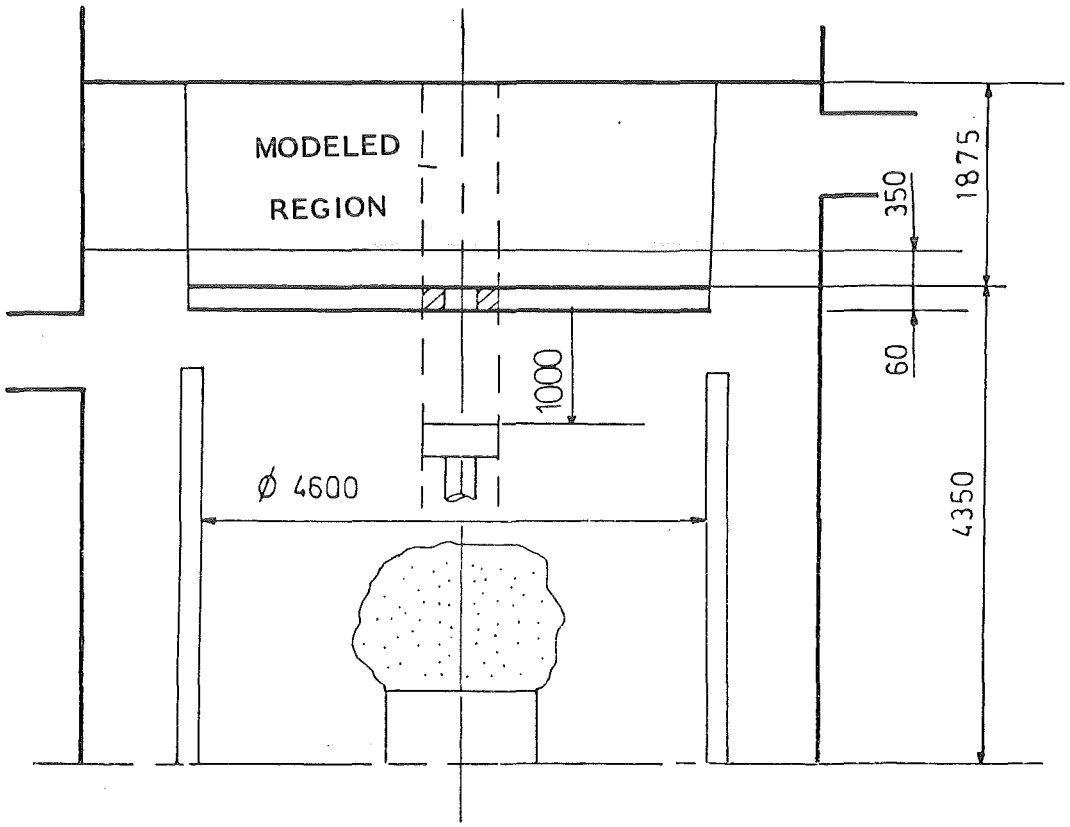

Fig. 1.2 - Upper part of an LMFBR and modeled region. The dimensions (in millimeters) are typical values for a 300 MW (electric) LMFBR.

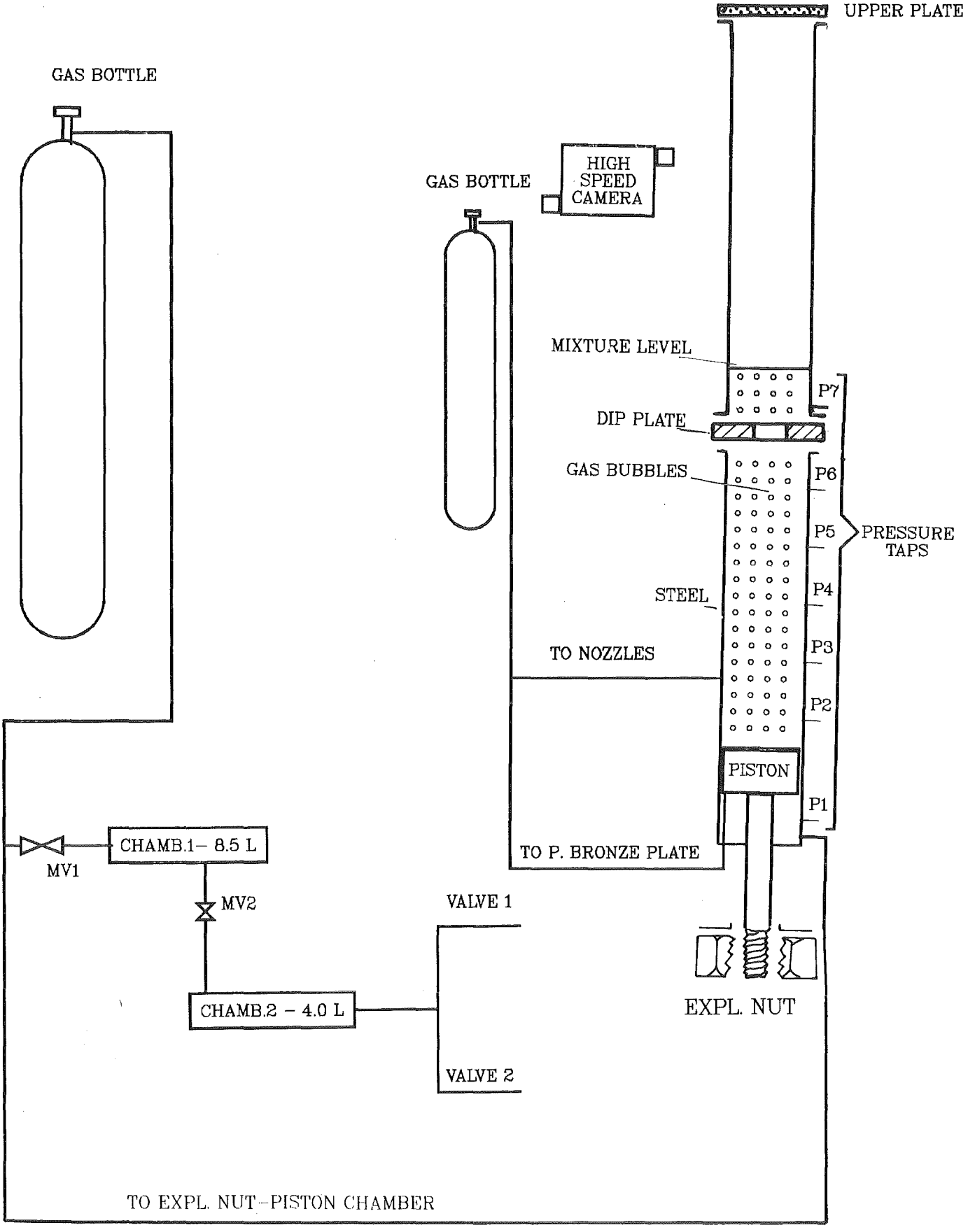

Fig. 2.1 - SCHEMATIC REPRESENTATION OF THE EXPERIMENTAL APPARATUS.

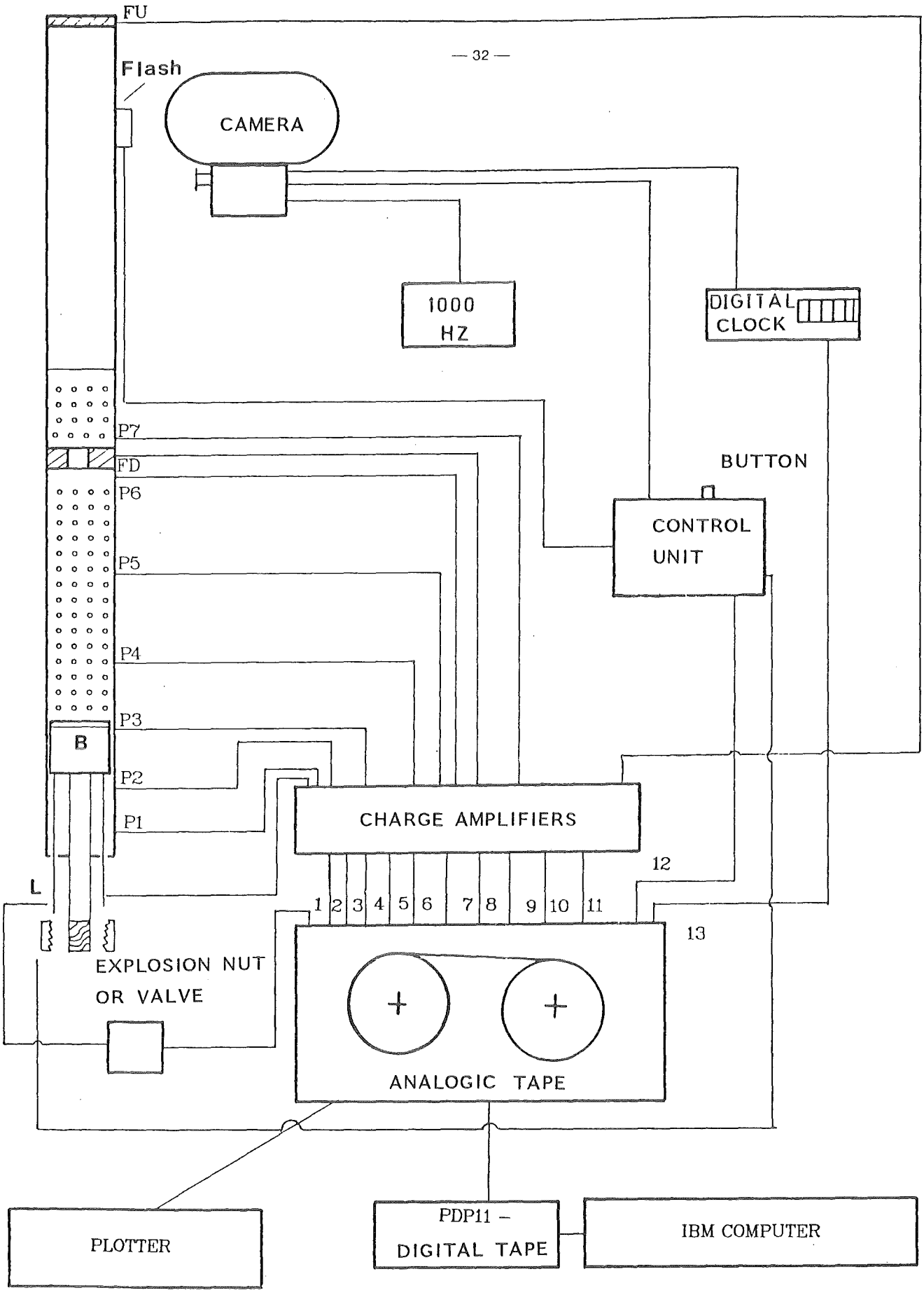

Fig. 2.2 - Schematic representation of the instrumentation.

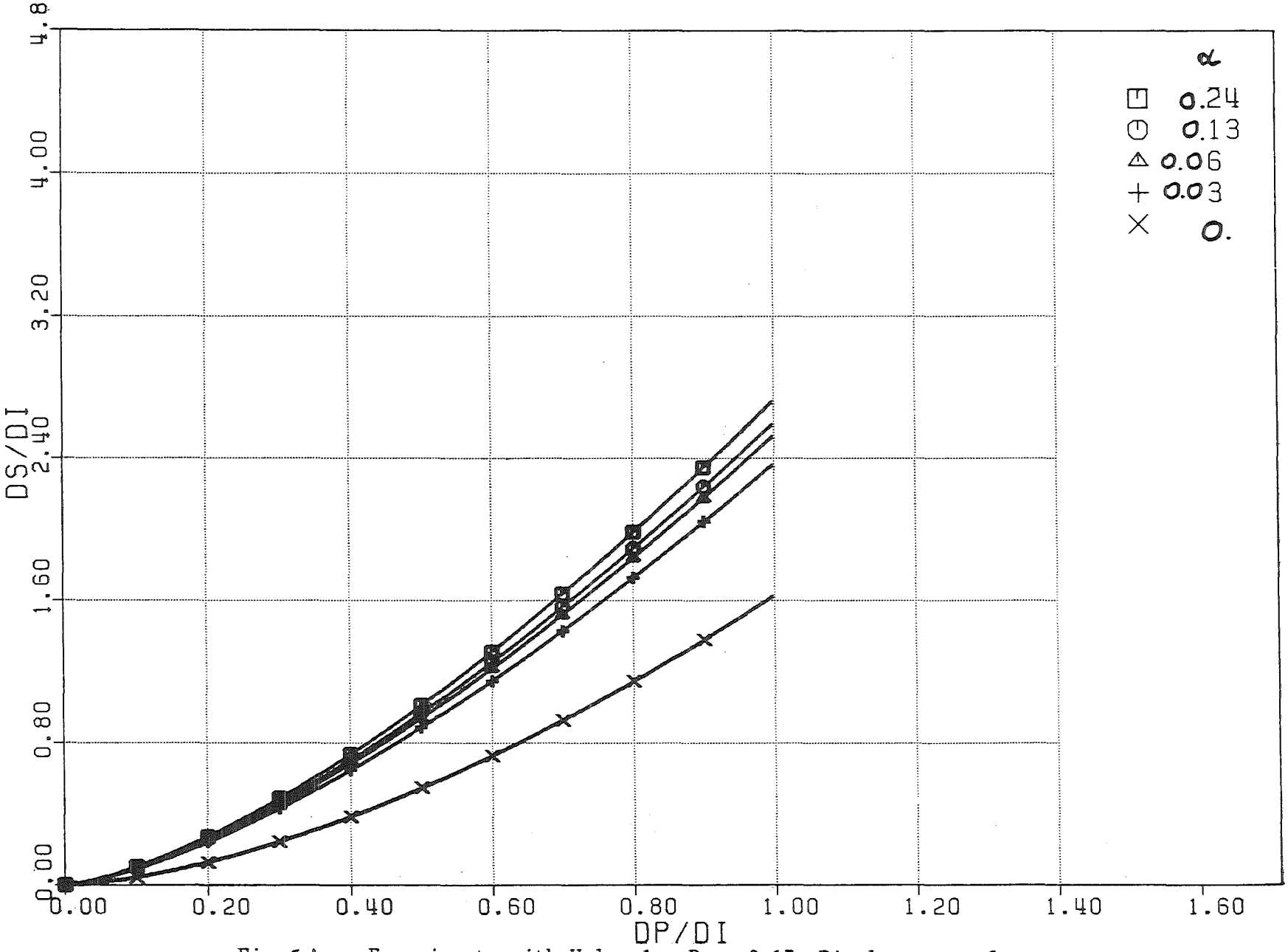

Fig. 5.1 - Experiments with Valve 1 . R_p = 0.17. Displacement of the surface for different values of the air volumetric fraction.

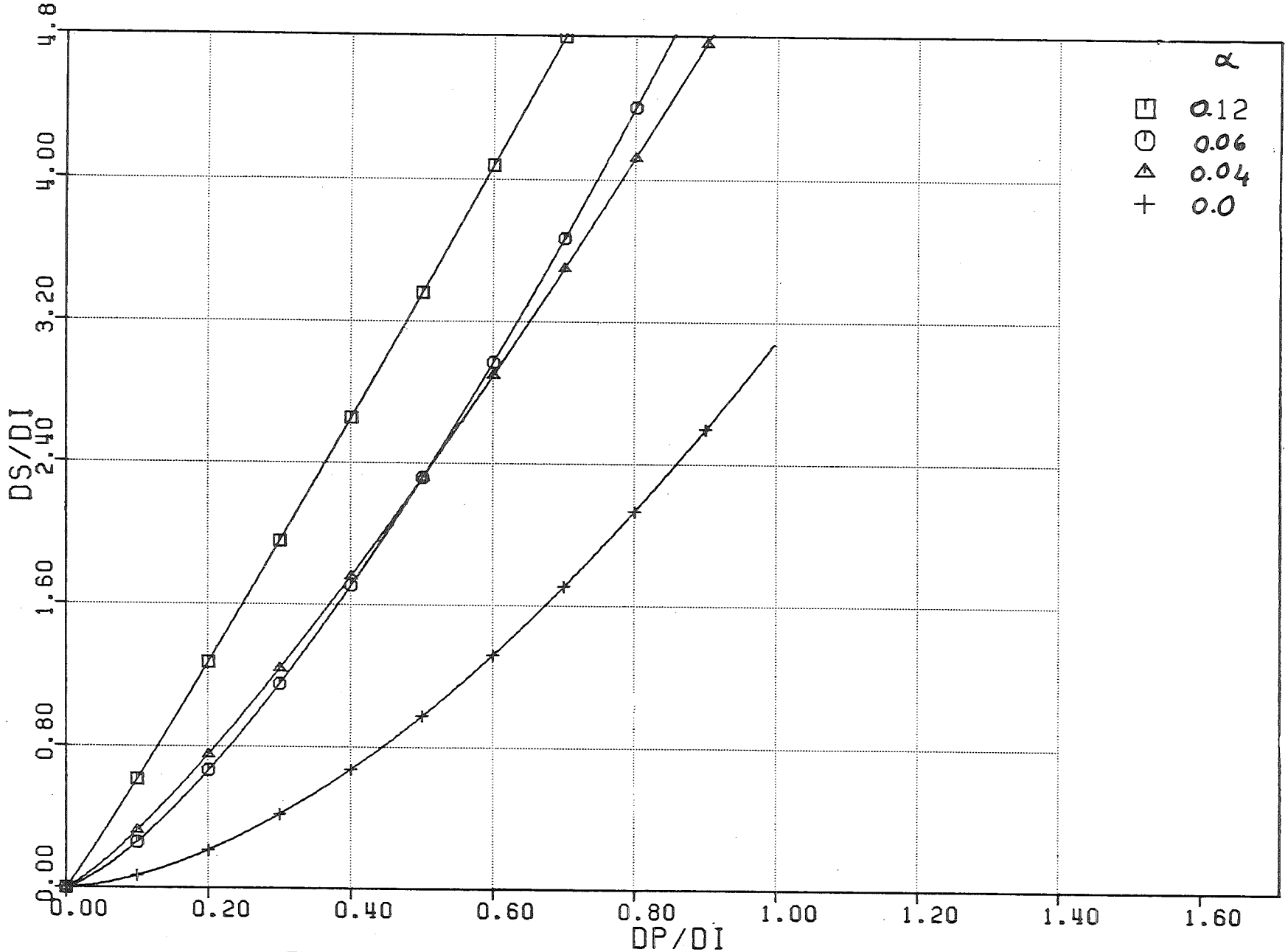

Fig. 5.2 - Experiments with Valve 2 . R_p = 0.12. Displacement of the surface for different values of the air volumetric fraction.

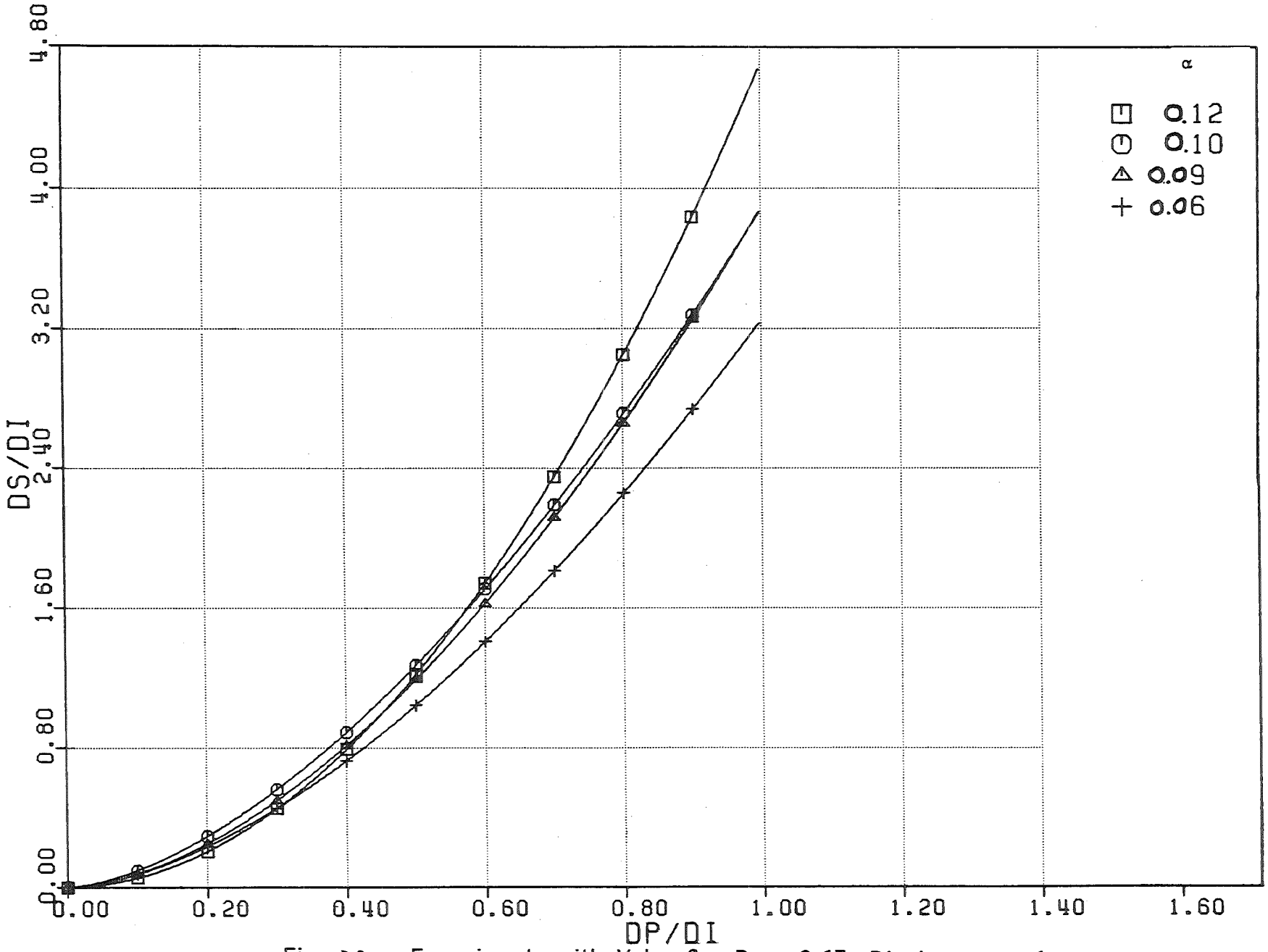

Fig. 5.3 - Experiments with Valve 2 . R_p = 0.17. Displacement of the surface for different values of the air volumetric fraction.

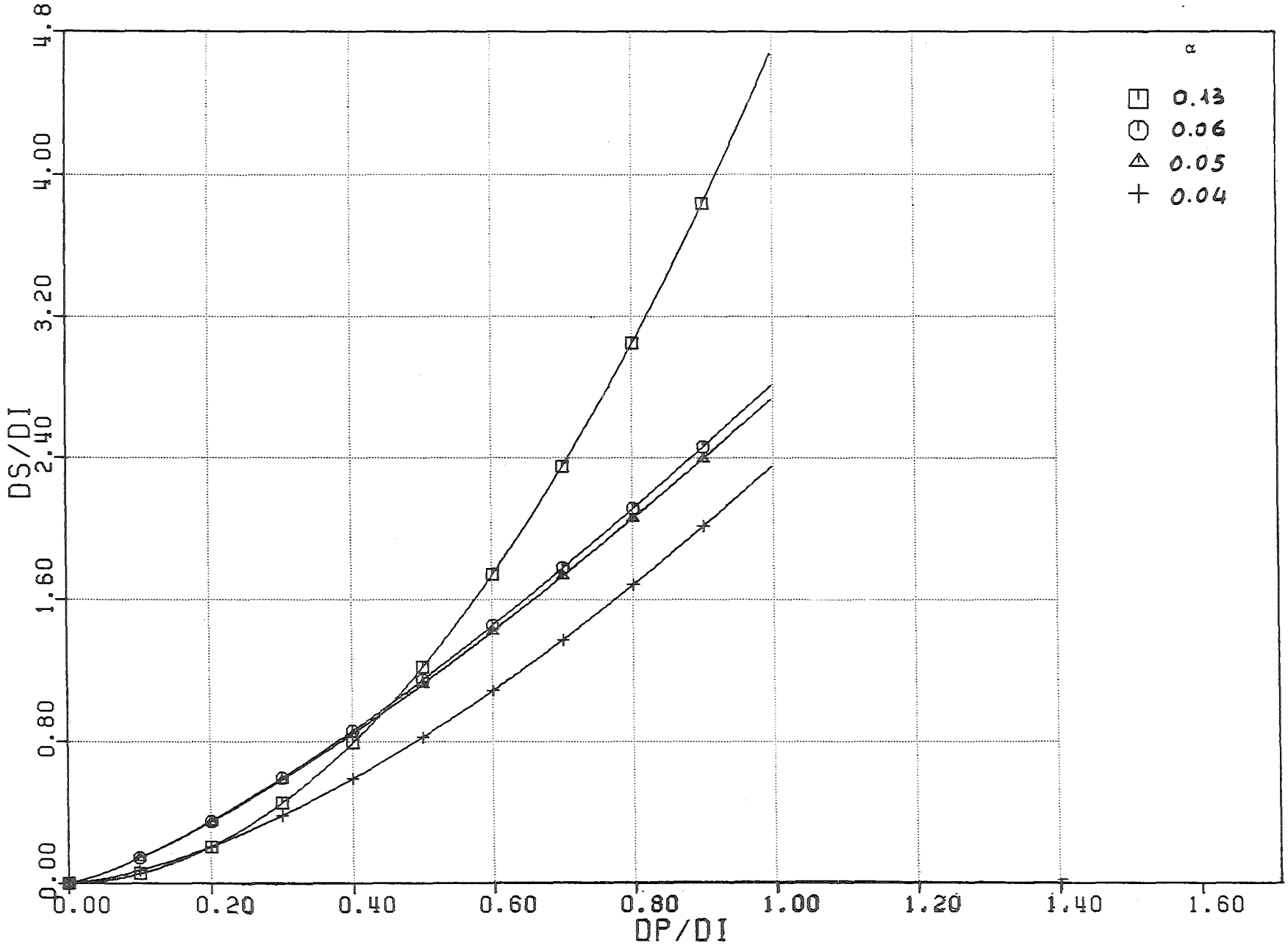

Fig. 5.4 - Experiments with Valve 2 . R_p = 0.25. Displacement of the surface for different values of the air volumetric fraction.

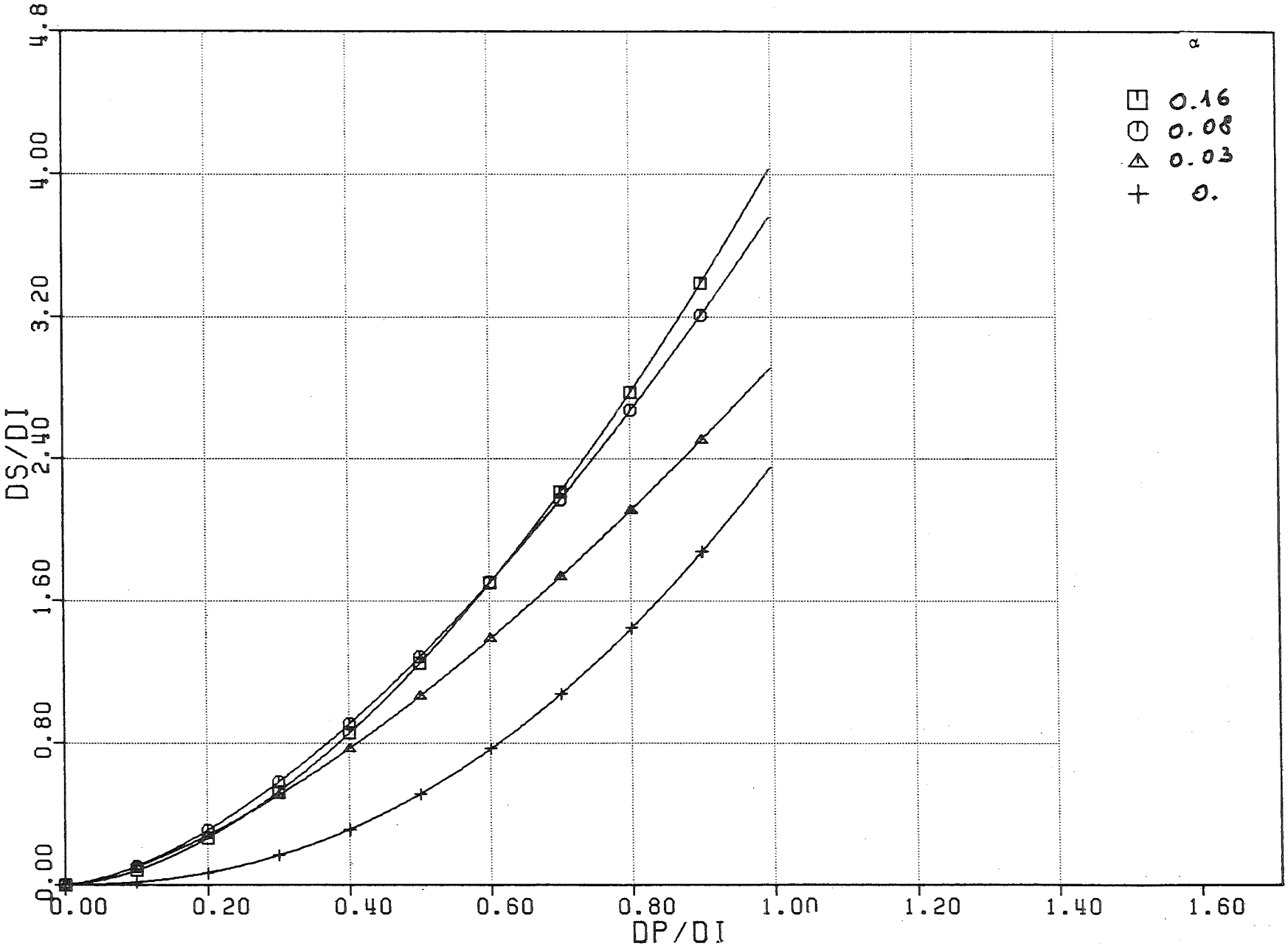

Fig. 5.5 - Experiments with Explosion Nut, R_p = 0.12. Displacement of the surface for different values of the air volumetric fraction.

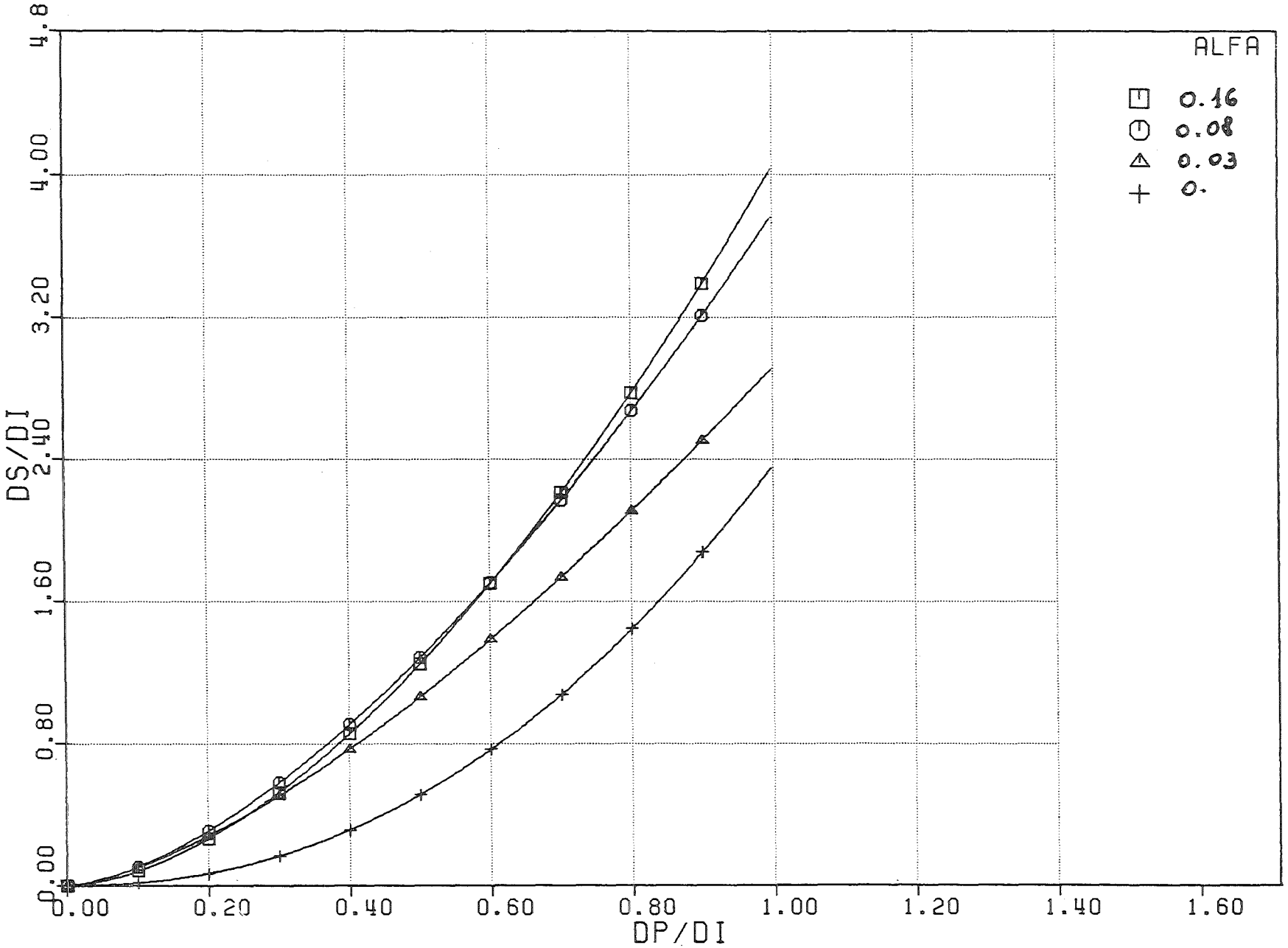

Fig. 5.6 - Experiments with Explosion Nut, R_p = 0.17. Displacement of the surface for different values of the air volumetric fraction.

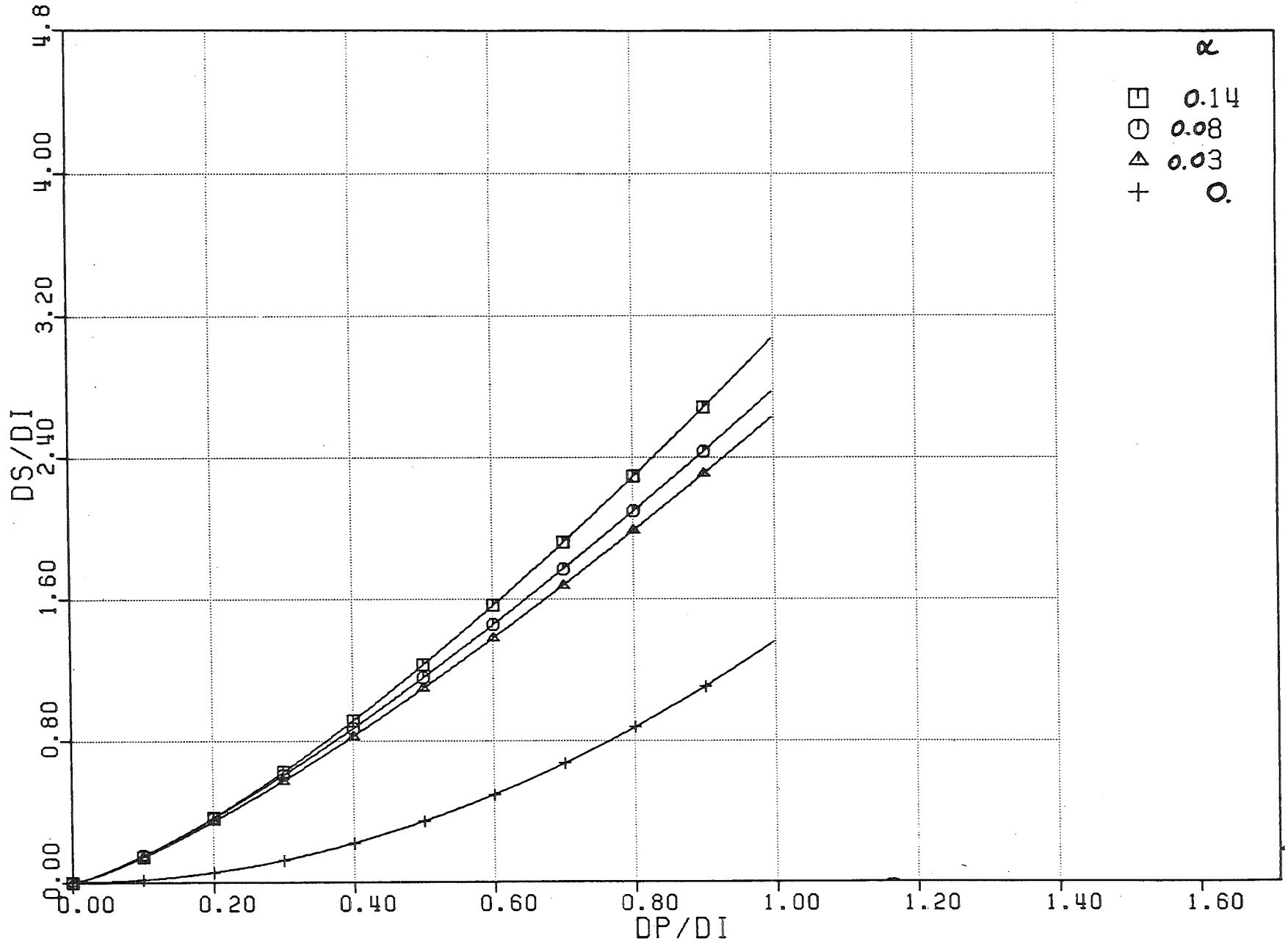

Fig. 5.7 - Experiments with Explosion Nut, R_p = 0.25. Displacement of the surface for different values of the air volumetric fraction.

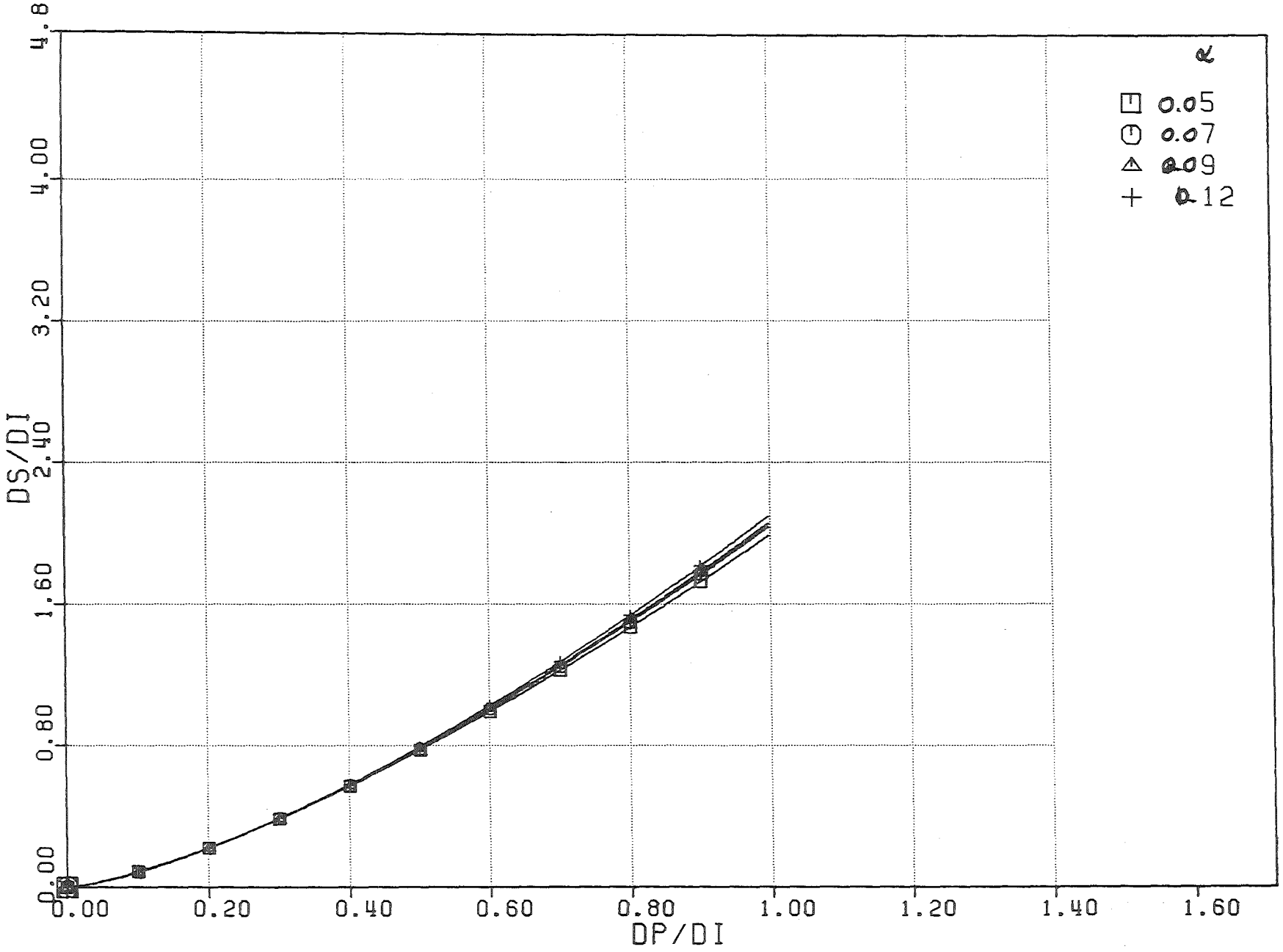

Fig. 5.8 - Experiments with Explosion Nut, R_p = 0.17, 7 Holes.
Displacement of the surface for different values of the air volumetric fraction.

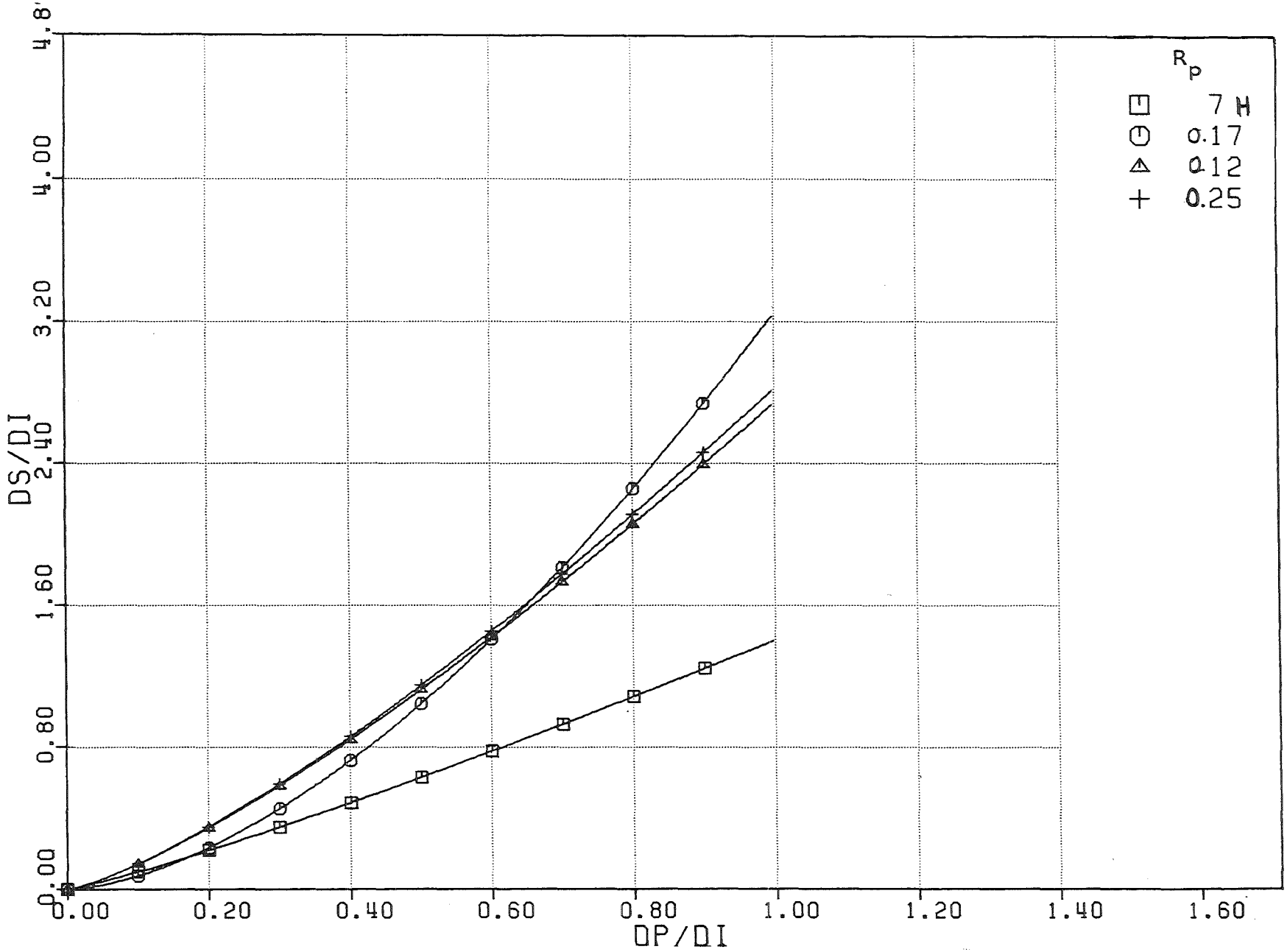

Fig. 5.9 - Experiments with Valve 2 . α = 0.06. Displacement of the surface for different values of the perforation ratio.

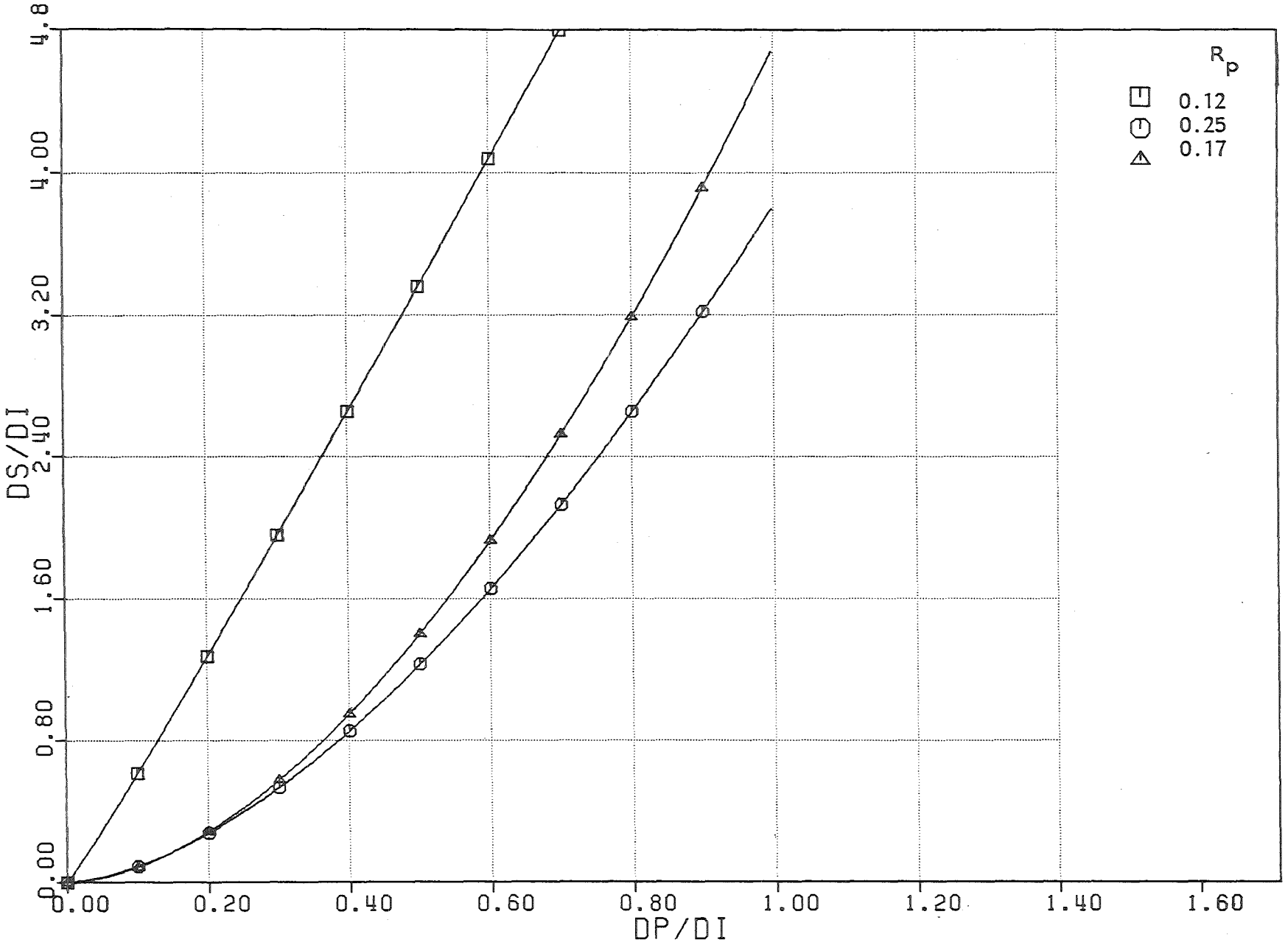

Fig. 5.10 - Experiments with Valve 2 . α = 0.12. Displacement of the surface for different values of the perforation ratio.

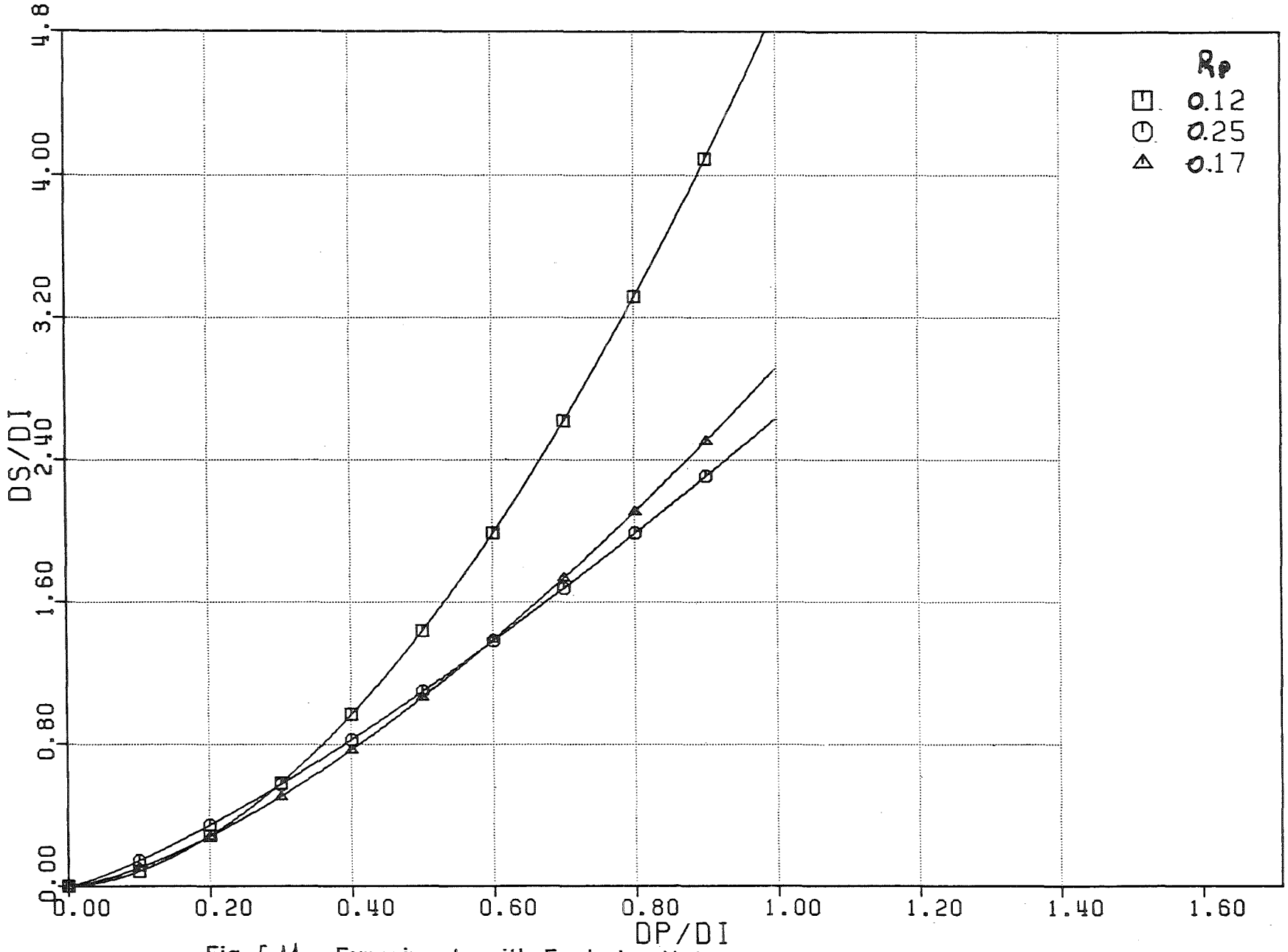

Fig. 5.11 - Experiments with Explosion Nut, α = 0.03. Displacement of the surface for different values of the perforation ratio.

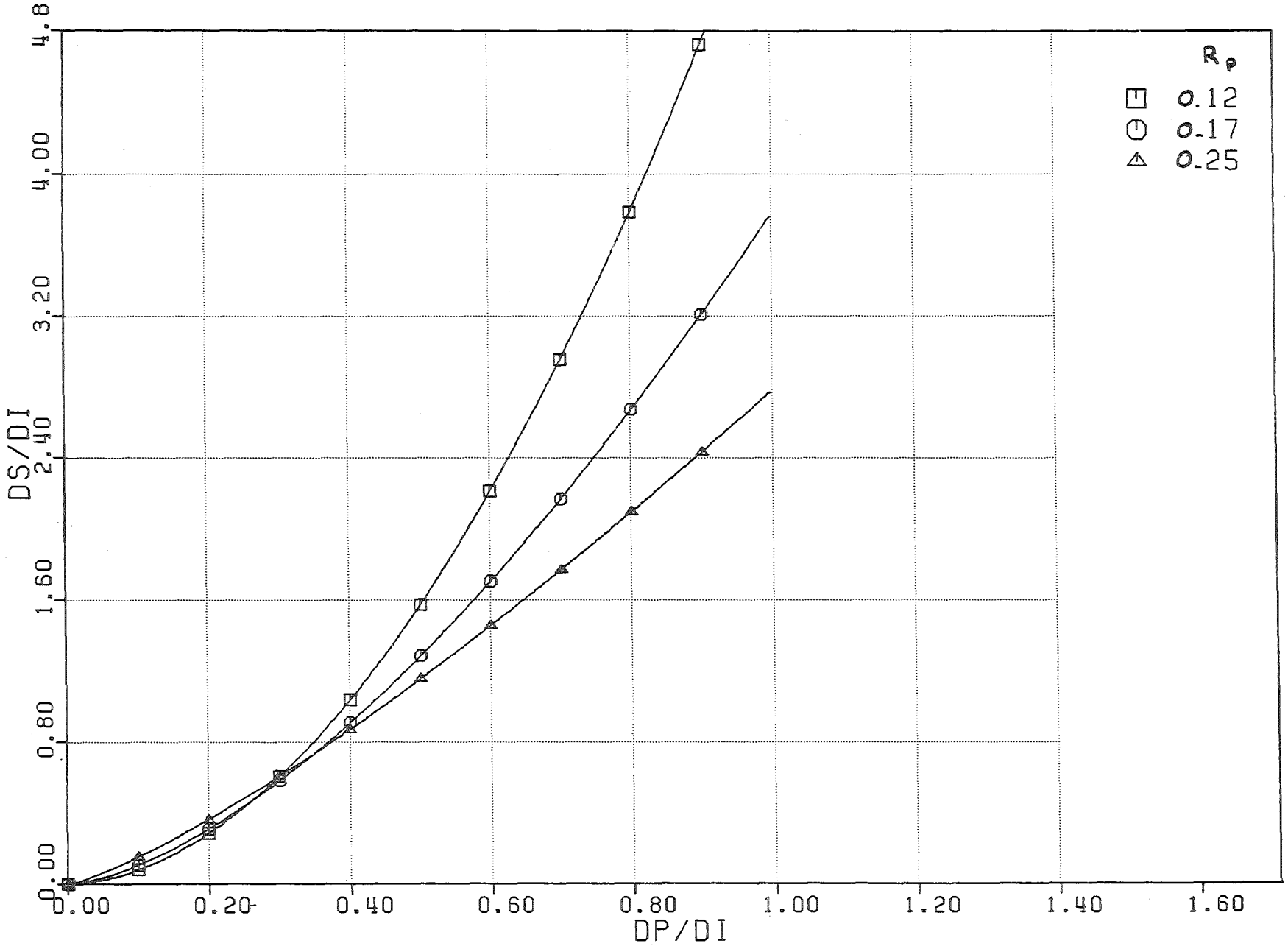

Fig. 5.12 - Experiments with Explosion Nut, α = 0.08. Displacement of the surface for different values of the perforation ratio.

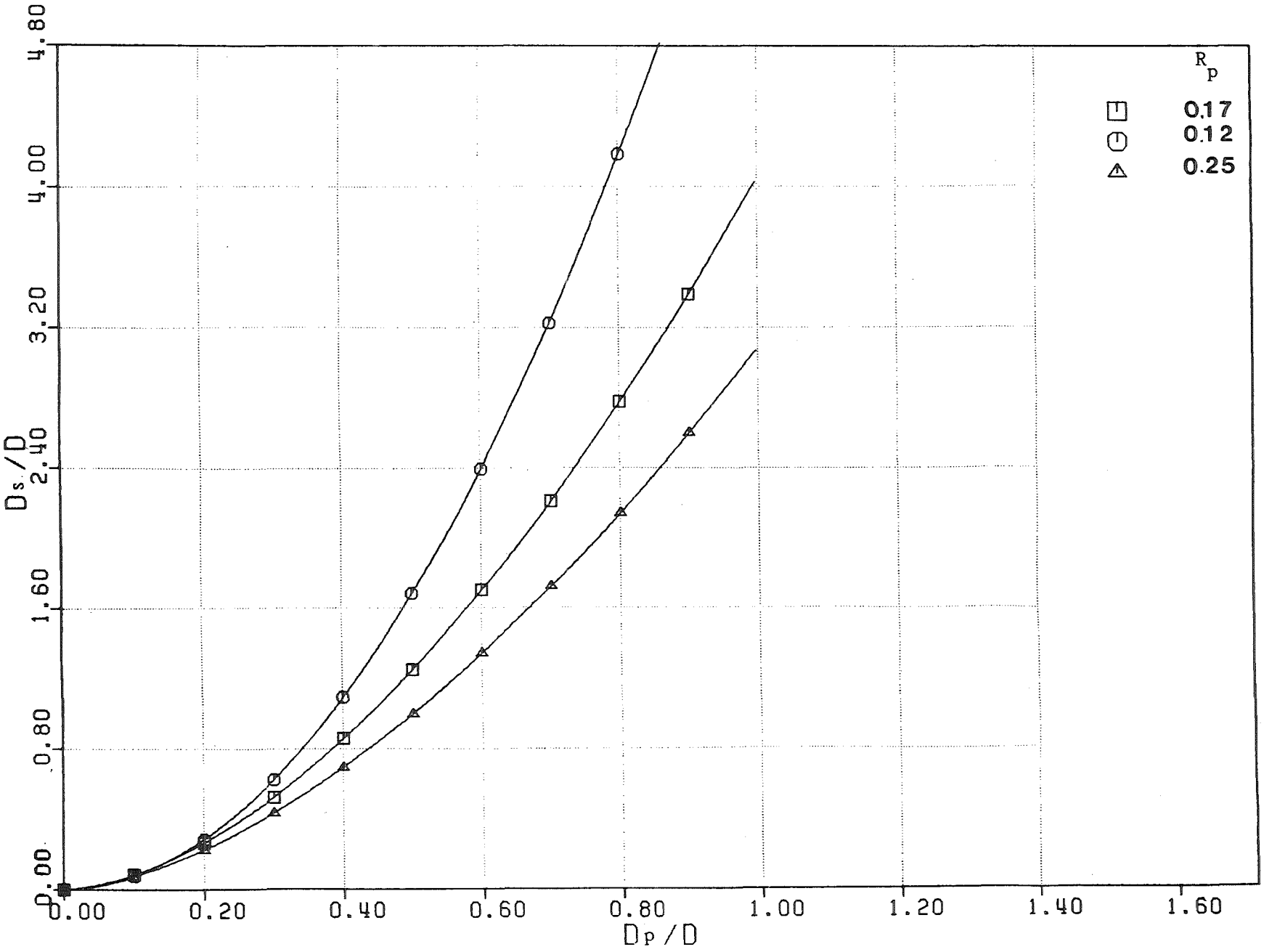

Fig. 5.13 - Experiments with Explosion Nut, α = 0.14. Displacement of the surface for different values of the perforation ratio.

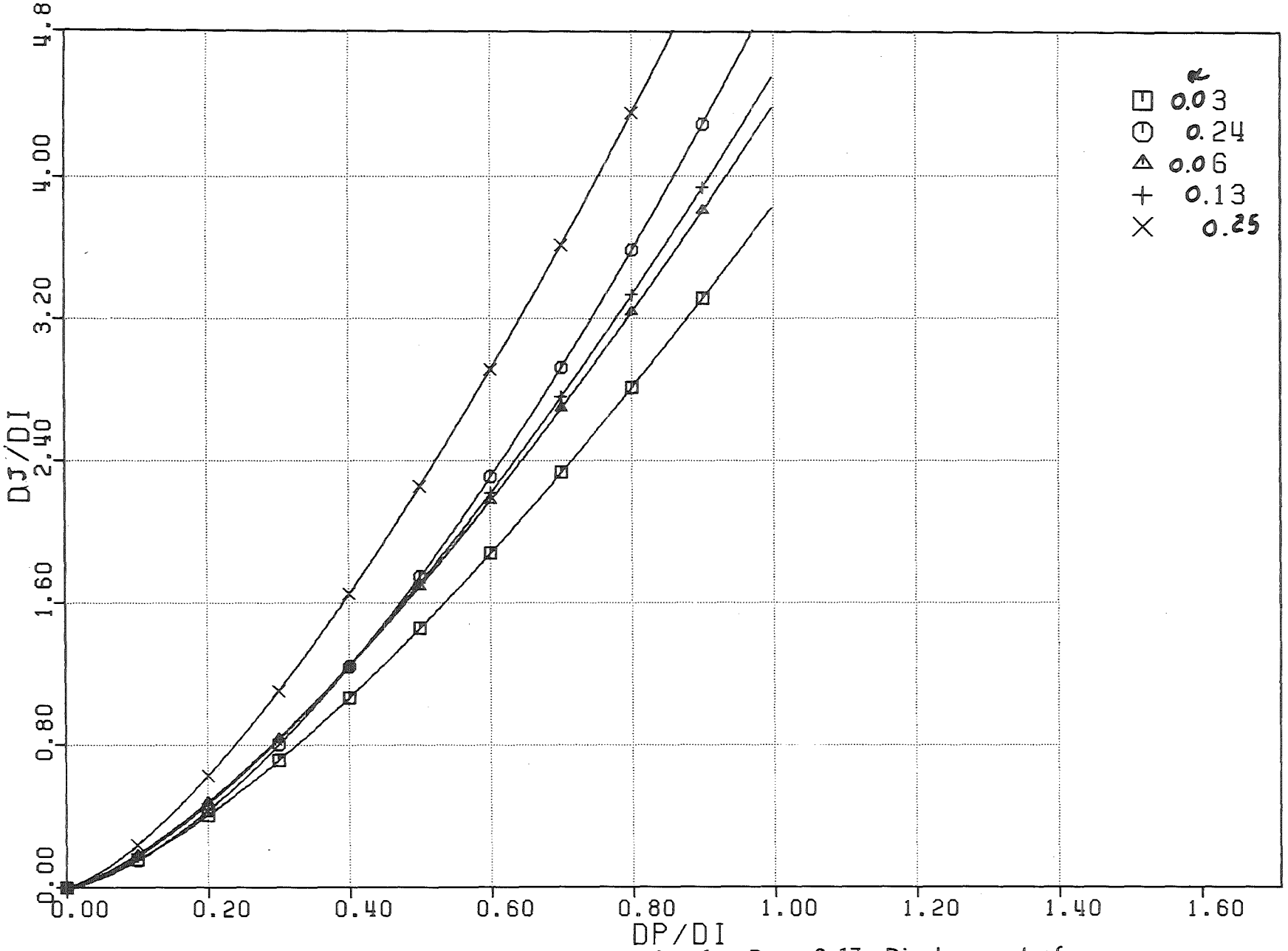

Fig. 5.14 - Experiments with Valve 1 . R_p = 0.17. Displacement of the jet for different values of the air volumetric fraction.

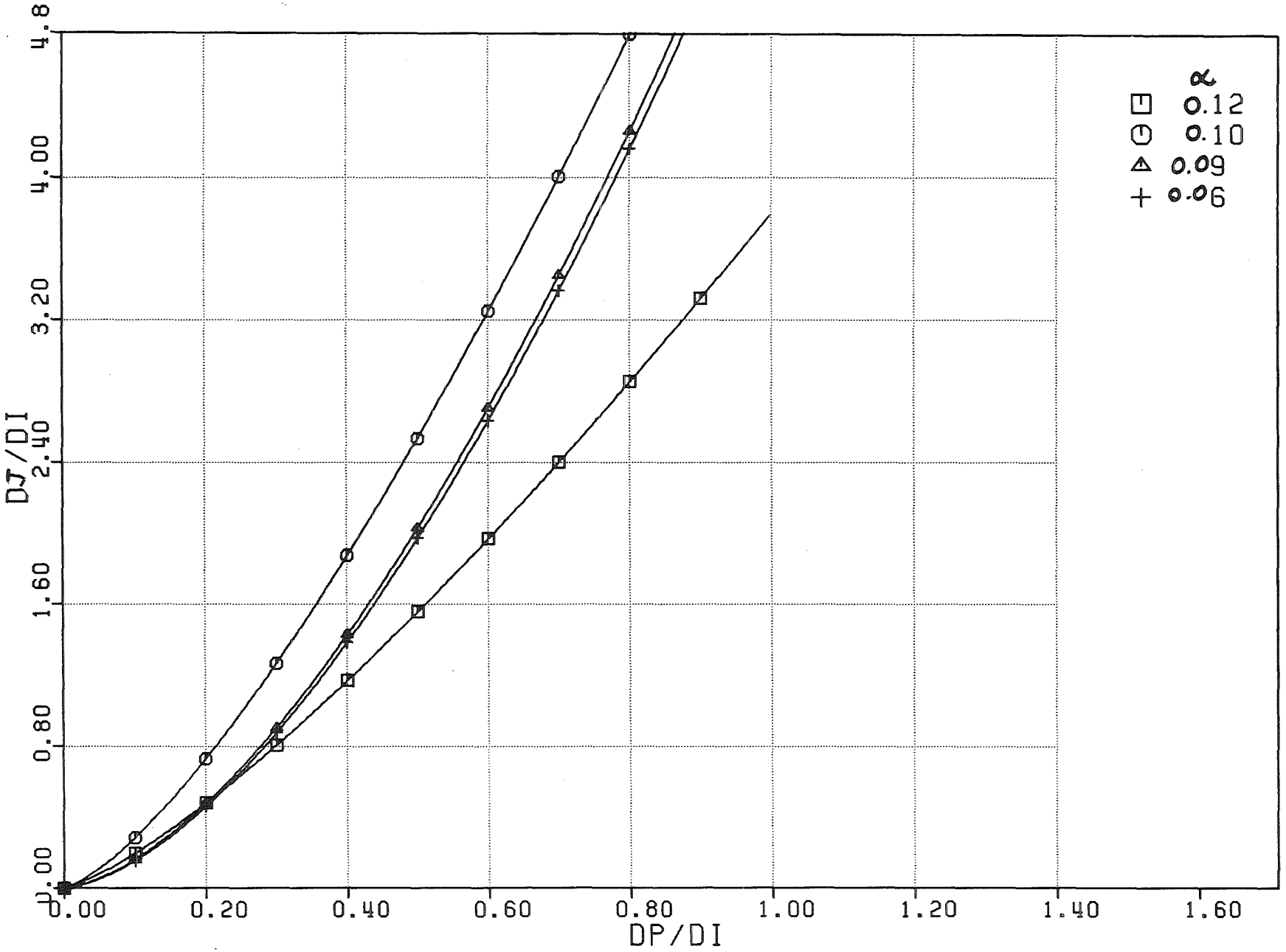

Fig. 5.15 - Experiments with Valve 2 . R_p = 0.17. Displacement of the jet for different values of the air volumetric fraction.

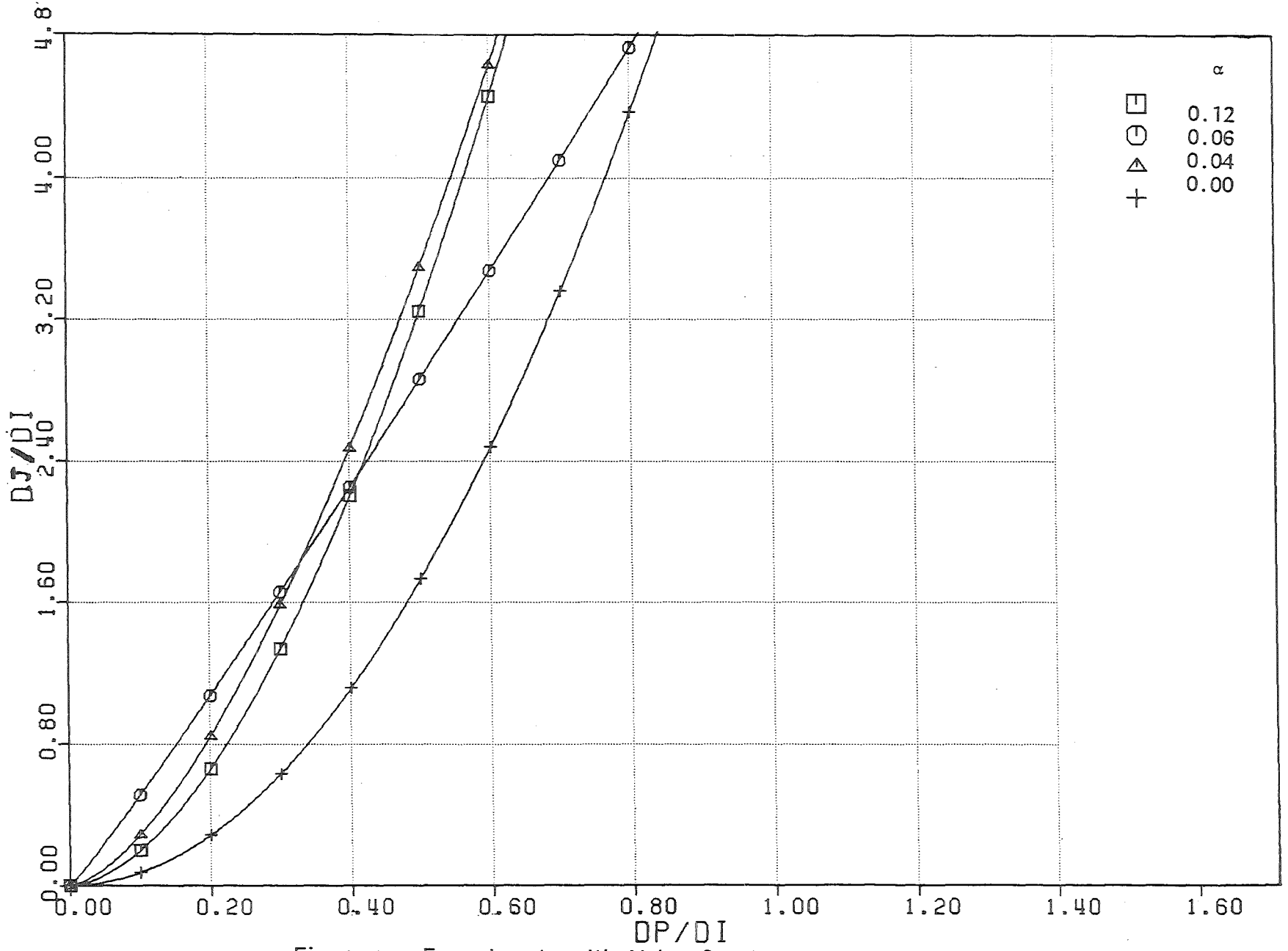

Fig. 5.16 - Experiments with Valve 2 . R_p = 0.12. Displacement of the jet for different values of the air volumetric fraction.

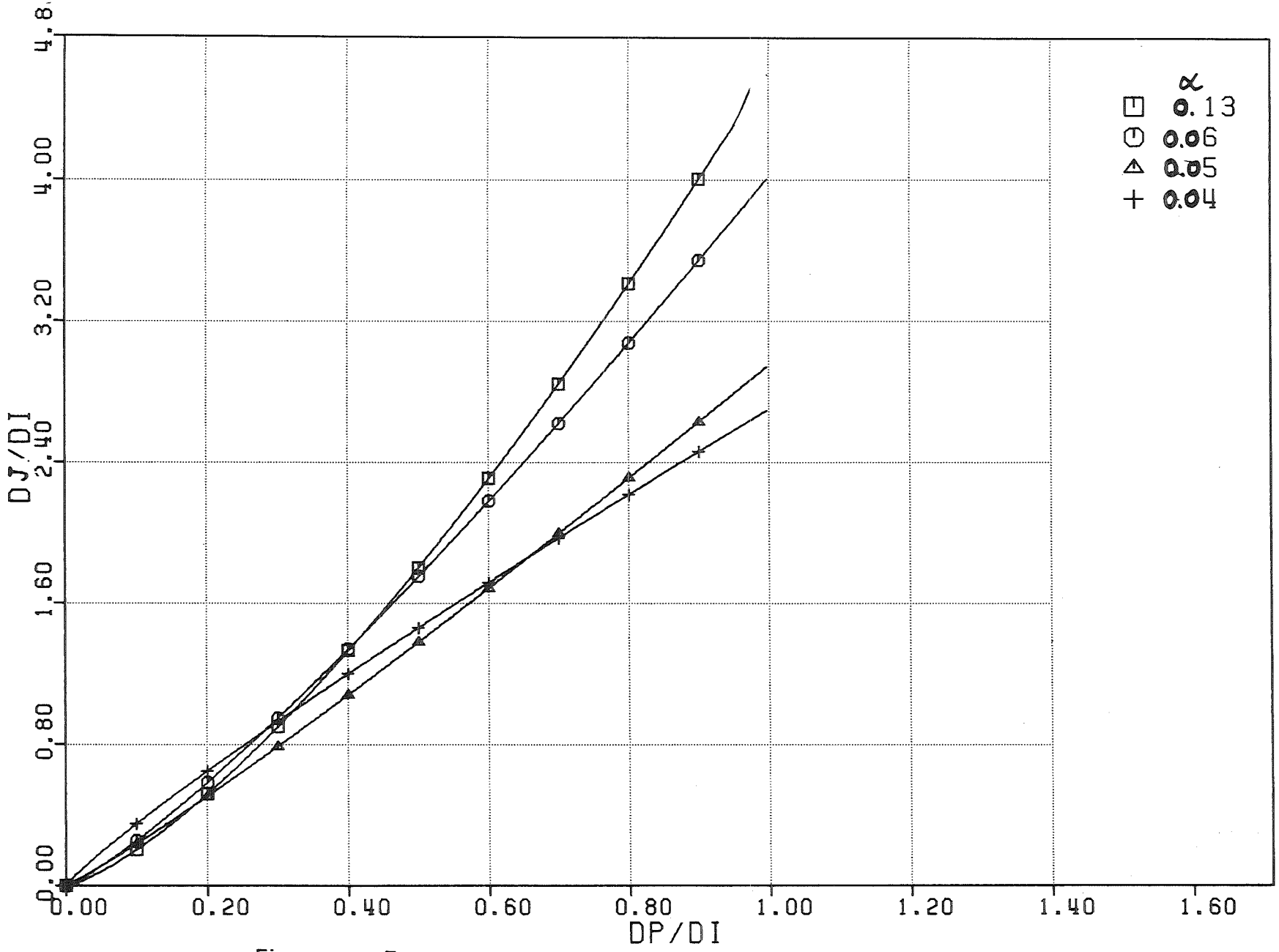

Fig. 5.17 - Experiments with Valve 2 . R_p = 0.25. Displacement of the jet for different values of the air volumetric fraction.

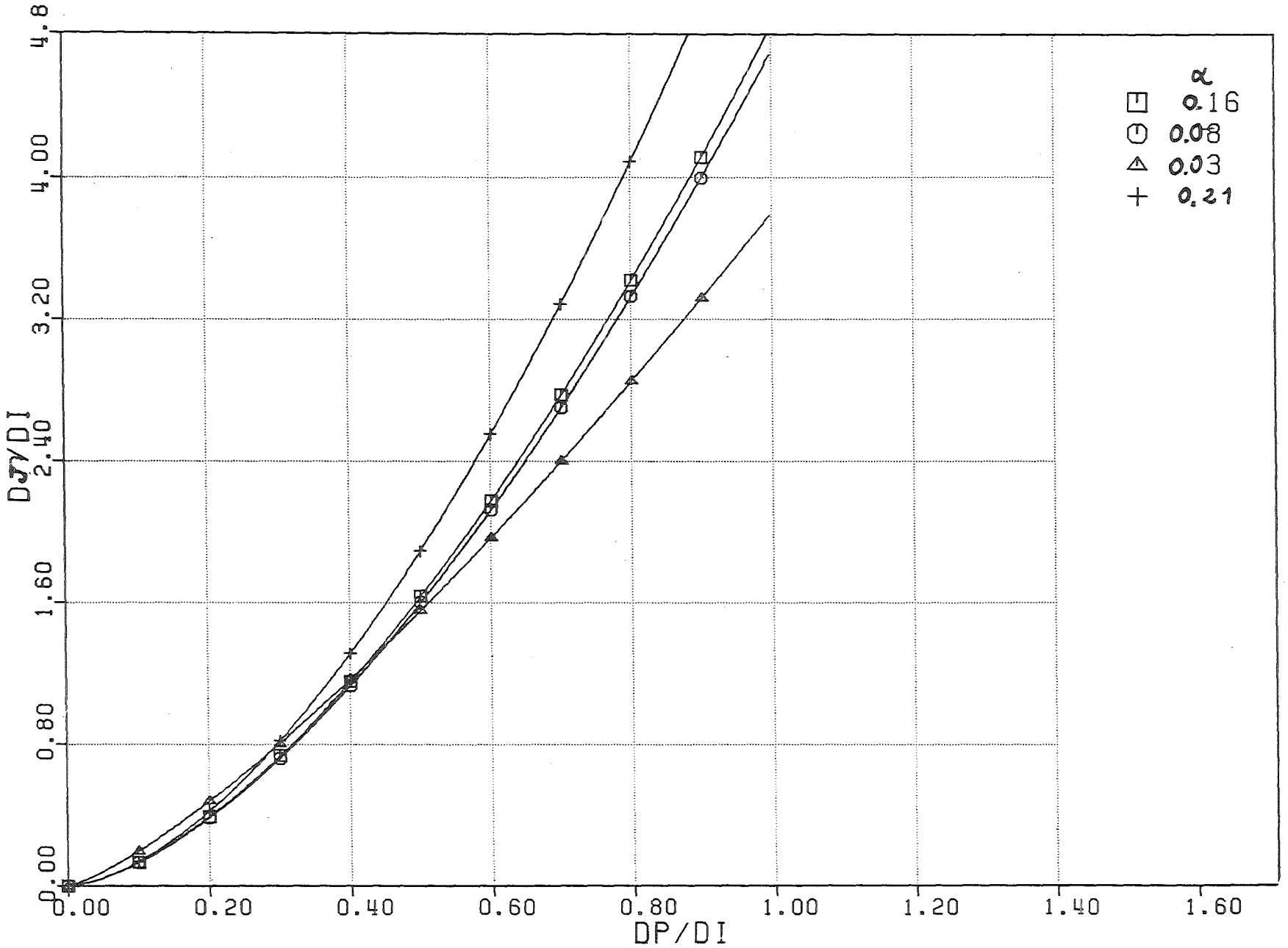

Fig. 5.18 - Experiments with Explosion Nut, R_p = 0.12. Displacement of the jet for different values of the air volumetric fraction.

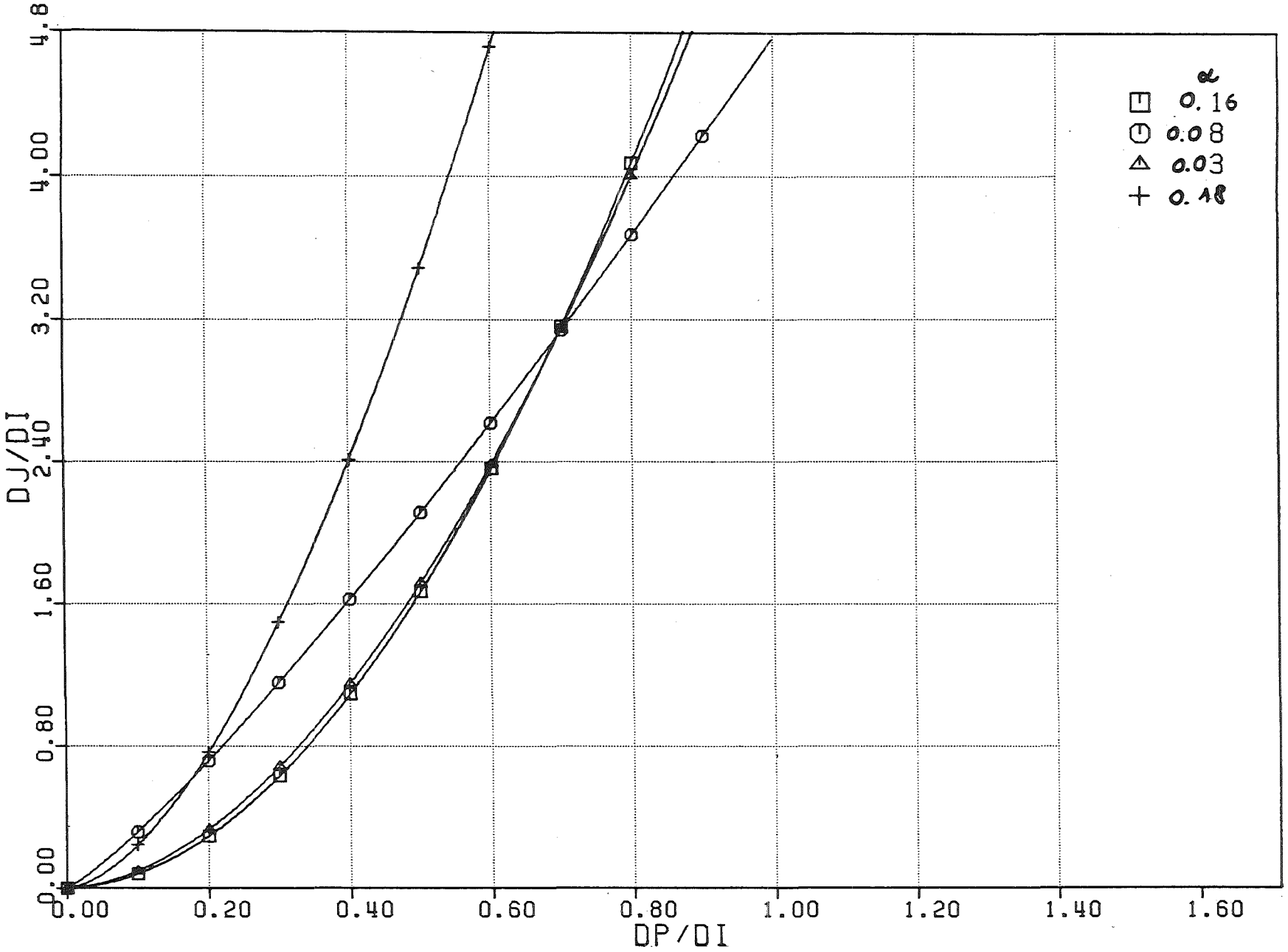

Fig.5.19 - Experiments with Explosion Nut, R_p = 0.17. Displacement of the jet for different values of the air volumetric fraction.

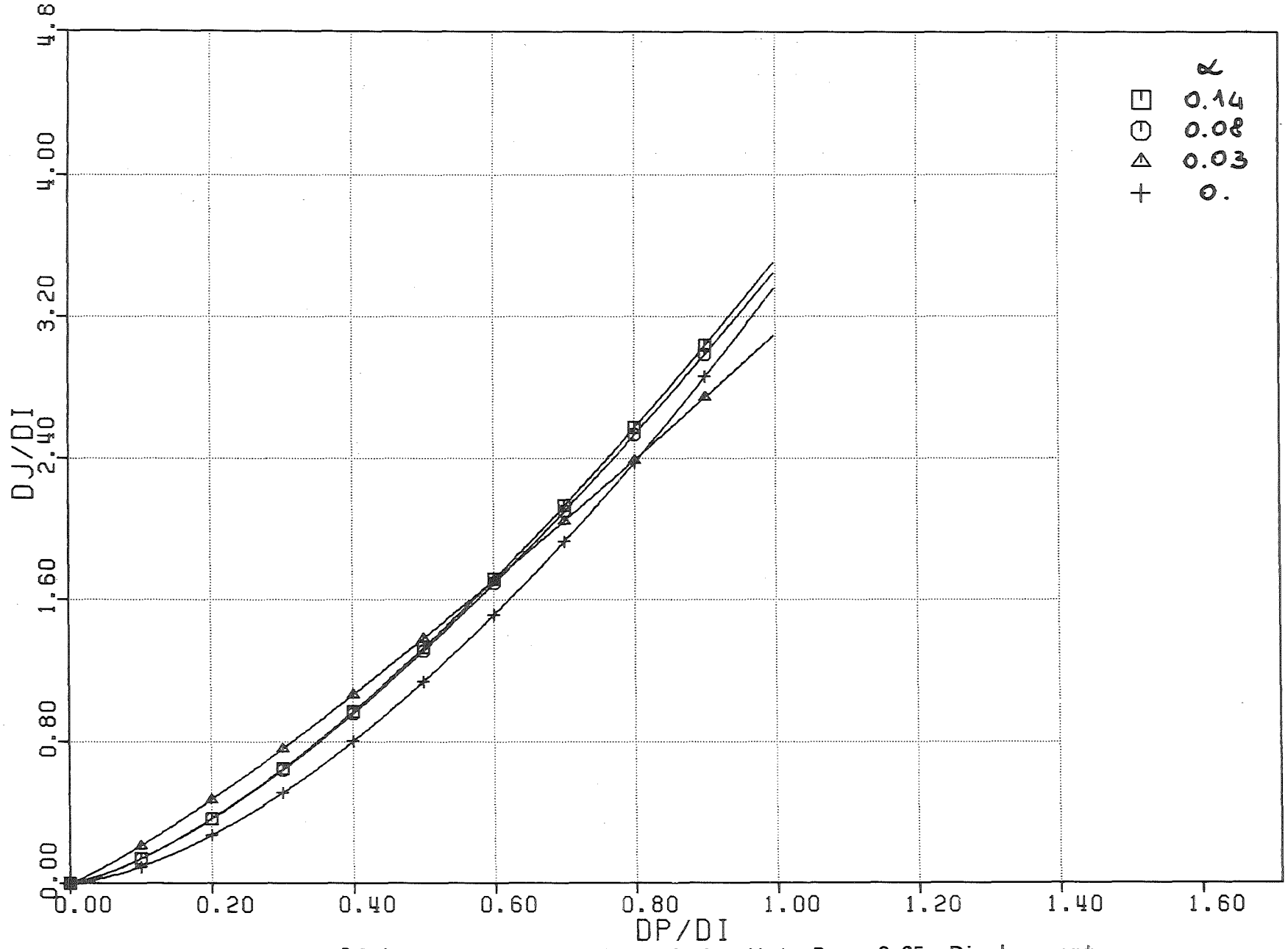

Fig.5.2.0 - Experiments with Explosion Nut, R_p = 0.25. Displacement of the surface for different values of the air volumetric fraction.

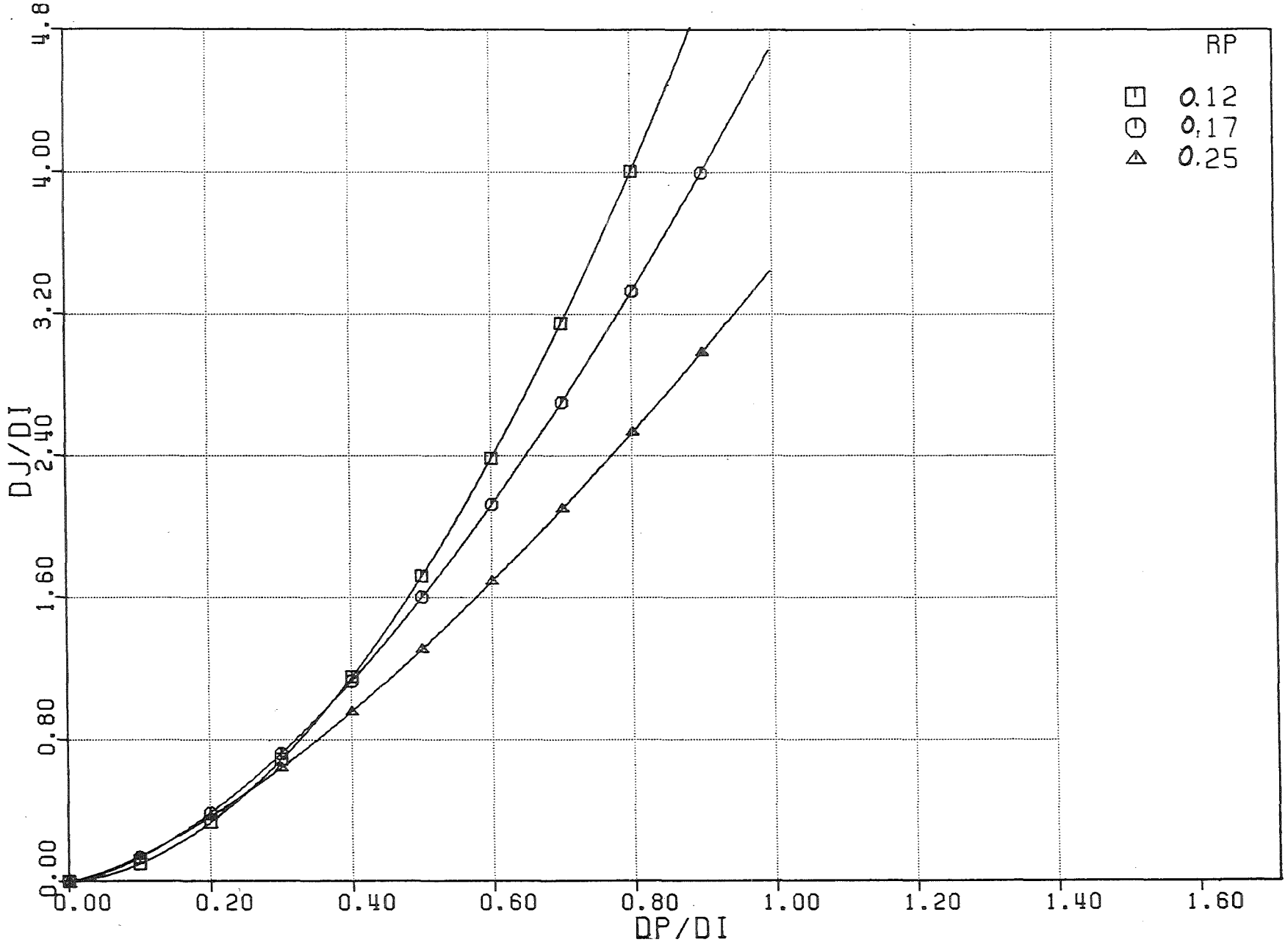

Fig. 5.21 - Experiments with Valve 2 . α = 0.06. Displacement of the jet for different values of the perforation ratio.

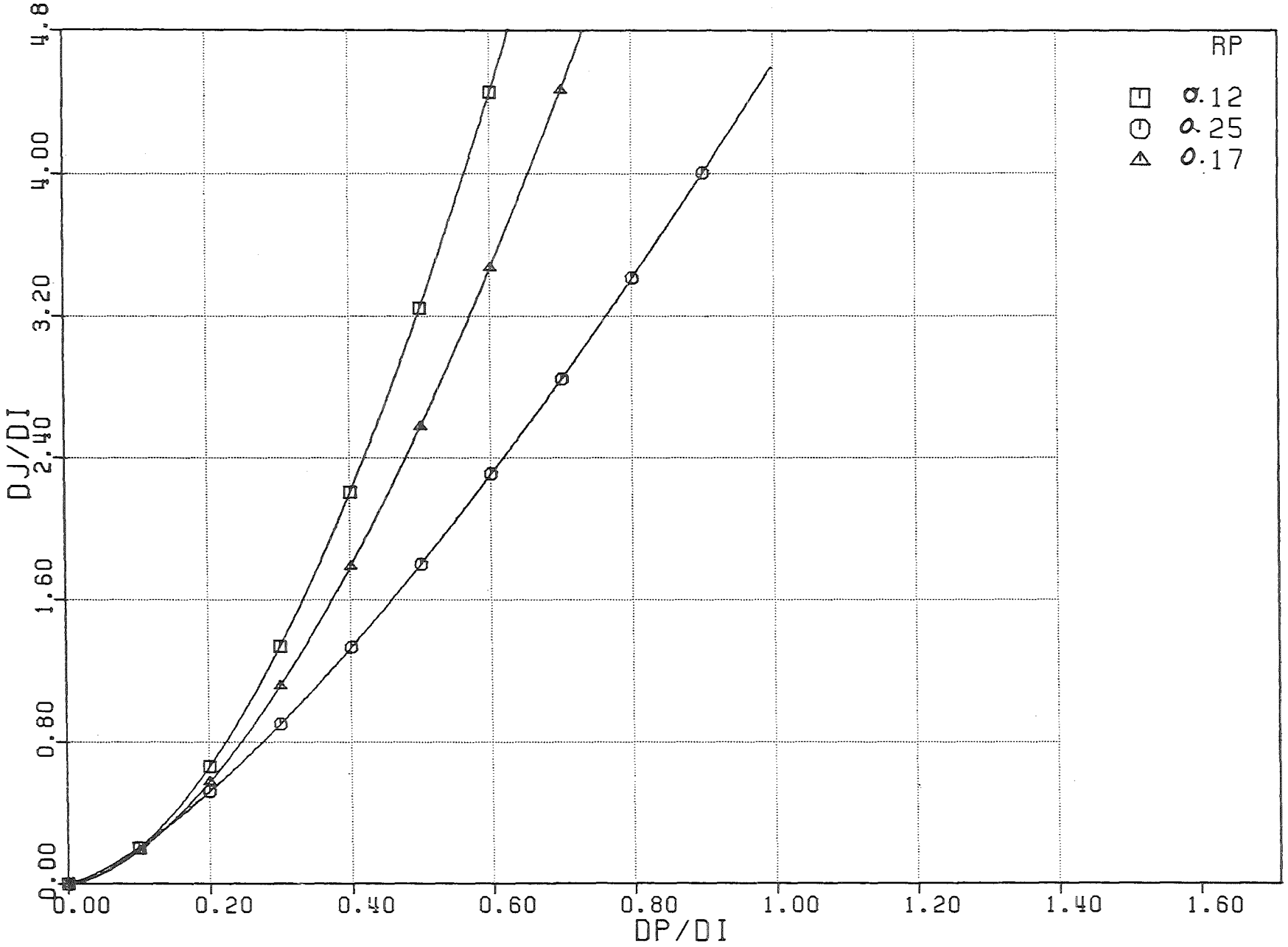

Fig. 5.22 - Experiments with Valve 2 . α = 0.12. Displacement of the jet for different values of the perforation ratio.

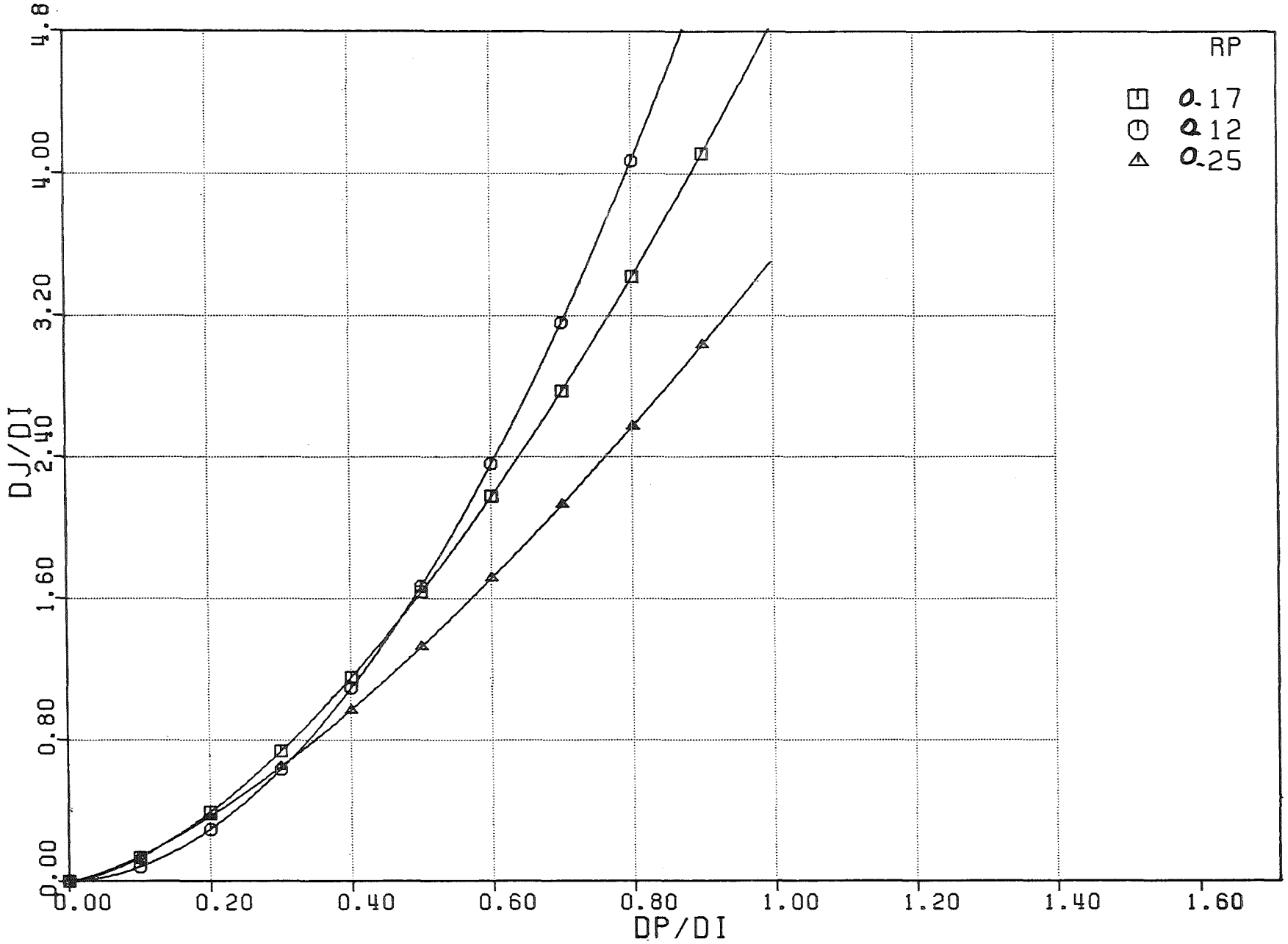

Fig. 5.23 - Experiments with Explosion Nut, α = 0.08. Displacement of the jet for different values of the perforation ratio.

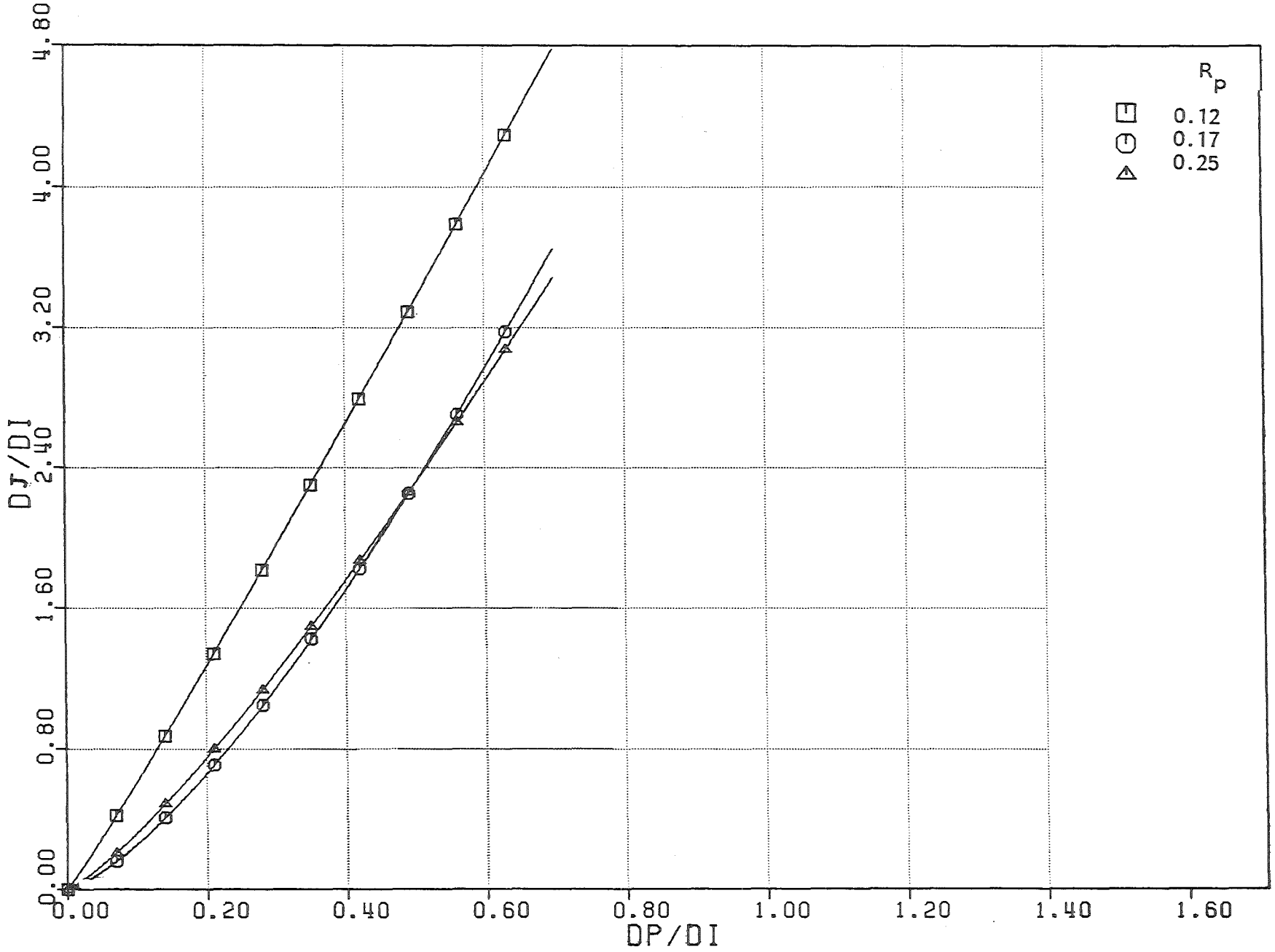

Fig.5.24 - Experiments with Explosion Nut, α = 0.14. Displacement of the jet for different values of the perforation ratio.

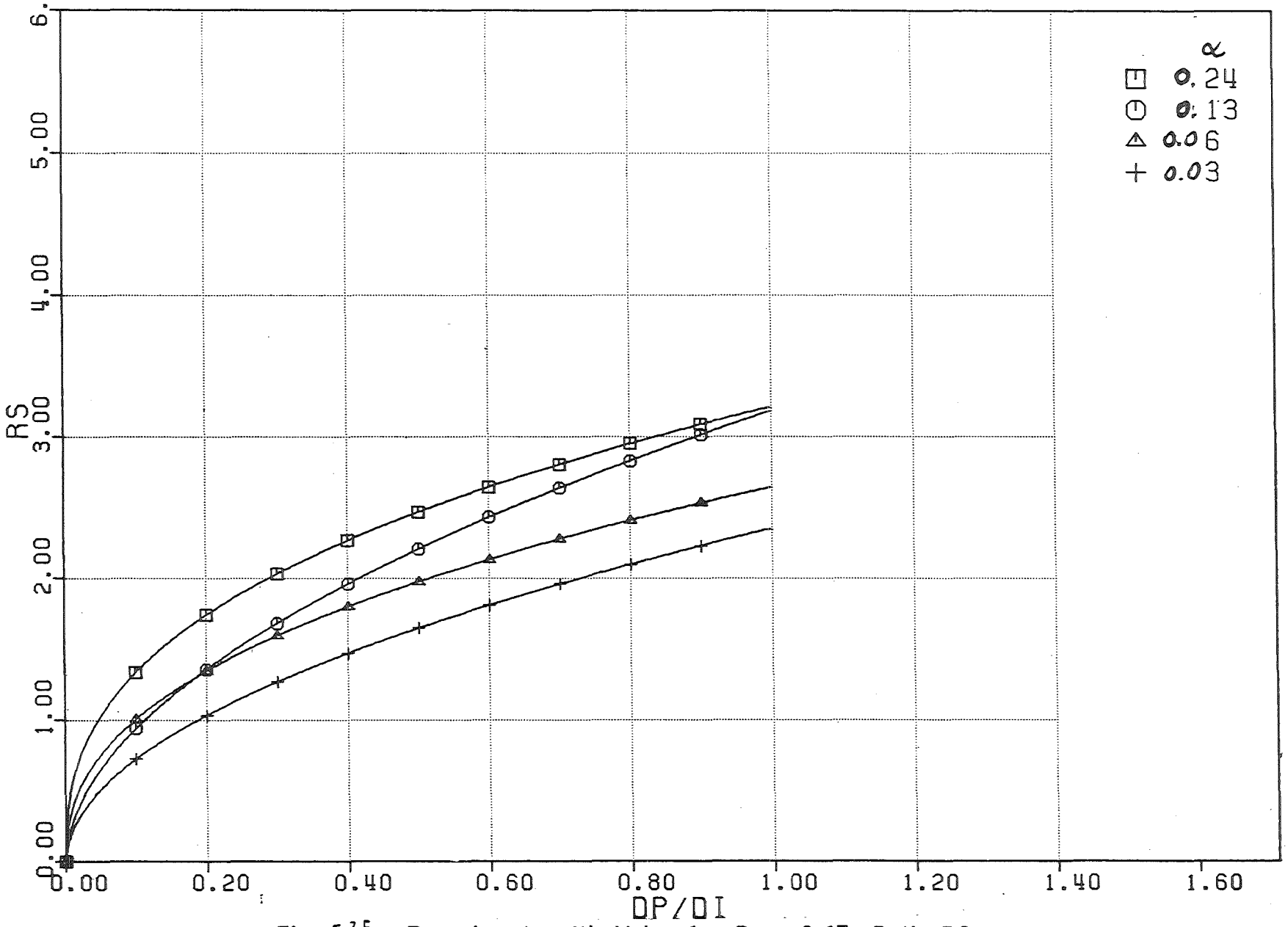

Fig. 5.25 - Experiments with Valve 1 . R_p = 0.17. Ratio RS plotted for different values of the air volumetric fraction

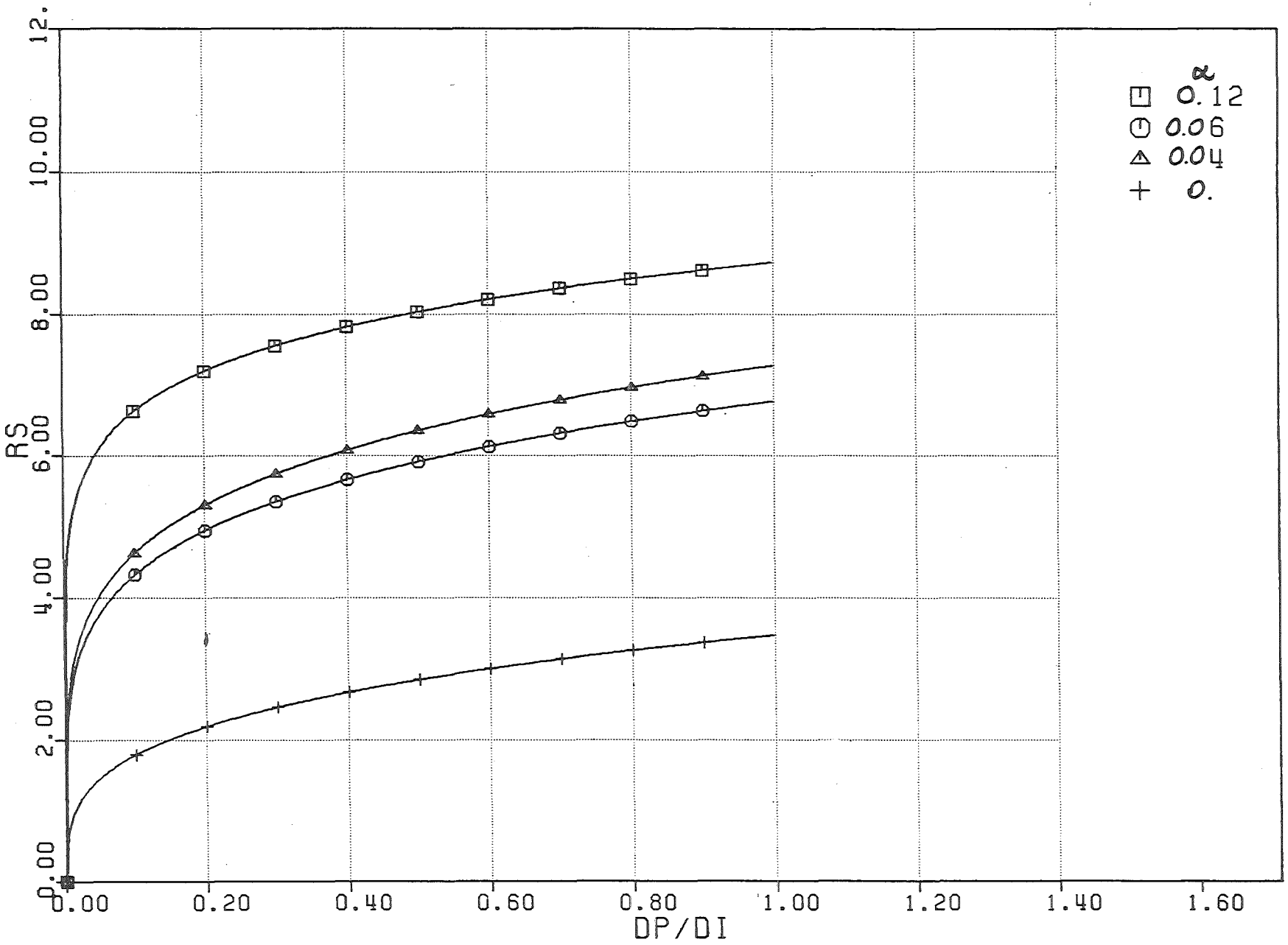

Fig. 5.26 - Experiments with Valve 2 . R_p = 0.12. Ratio RS plotted for different values of the air volumetric fraction

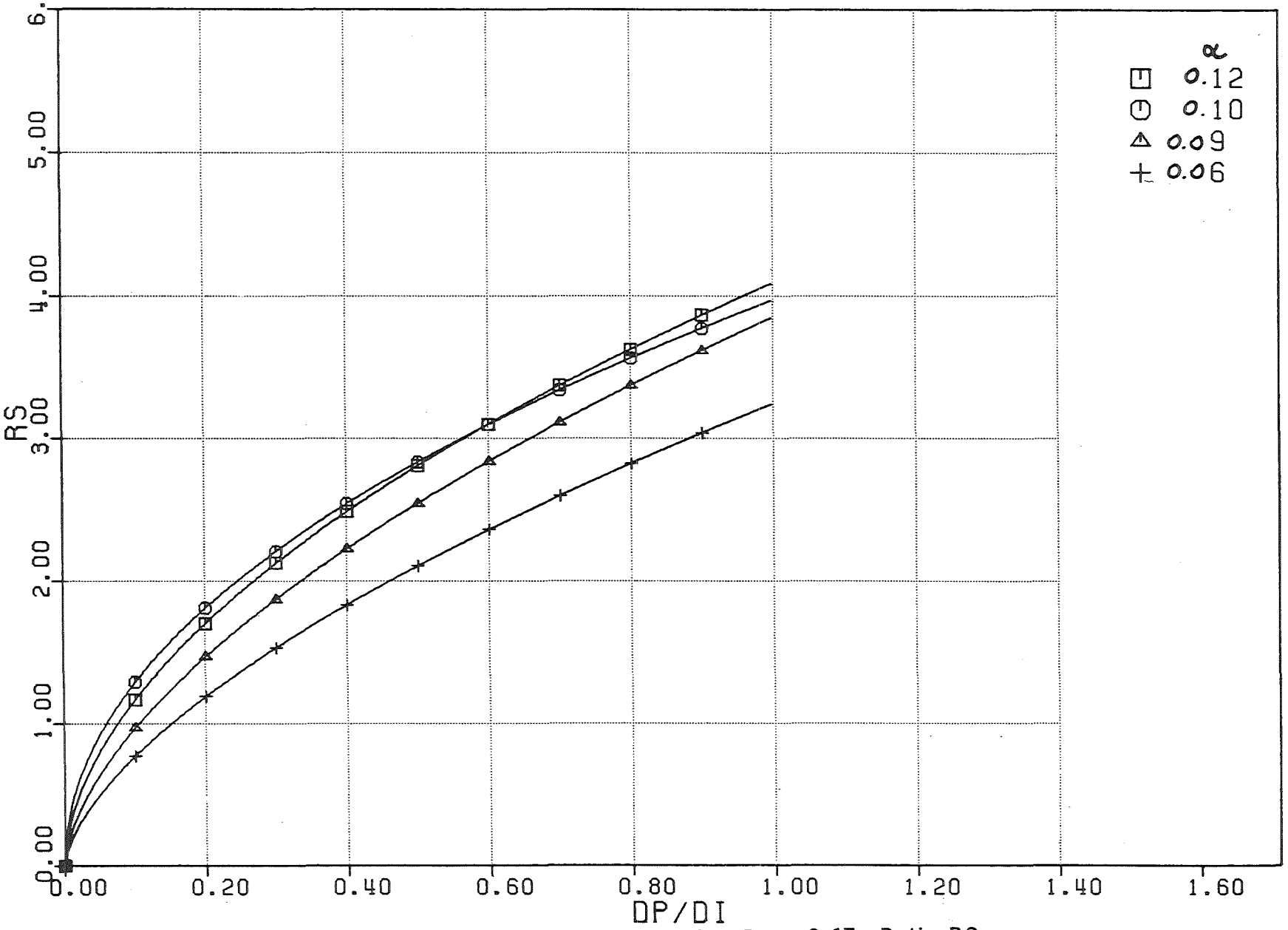

Fig. 5.27- Experiments with Valve 2 . R_p = 0.17. Ratio RS plotted for different values of the air volumetric fraction

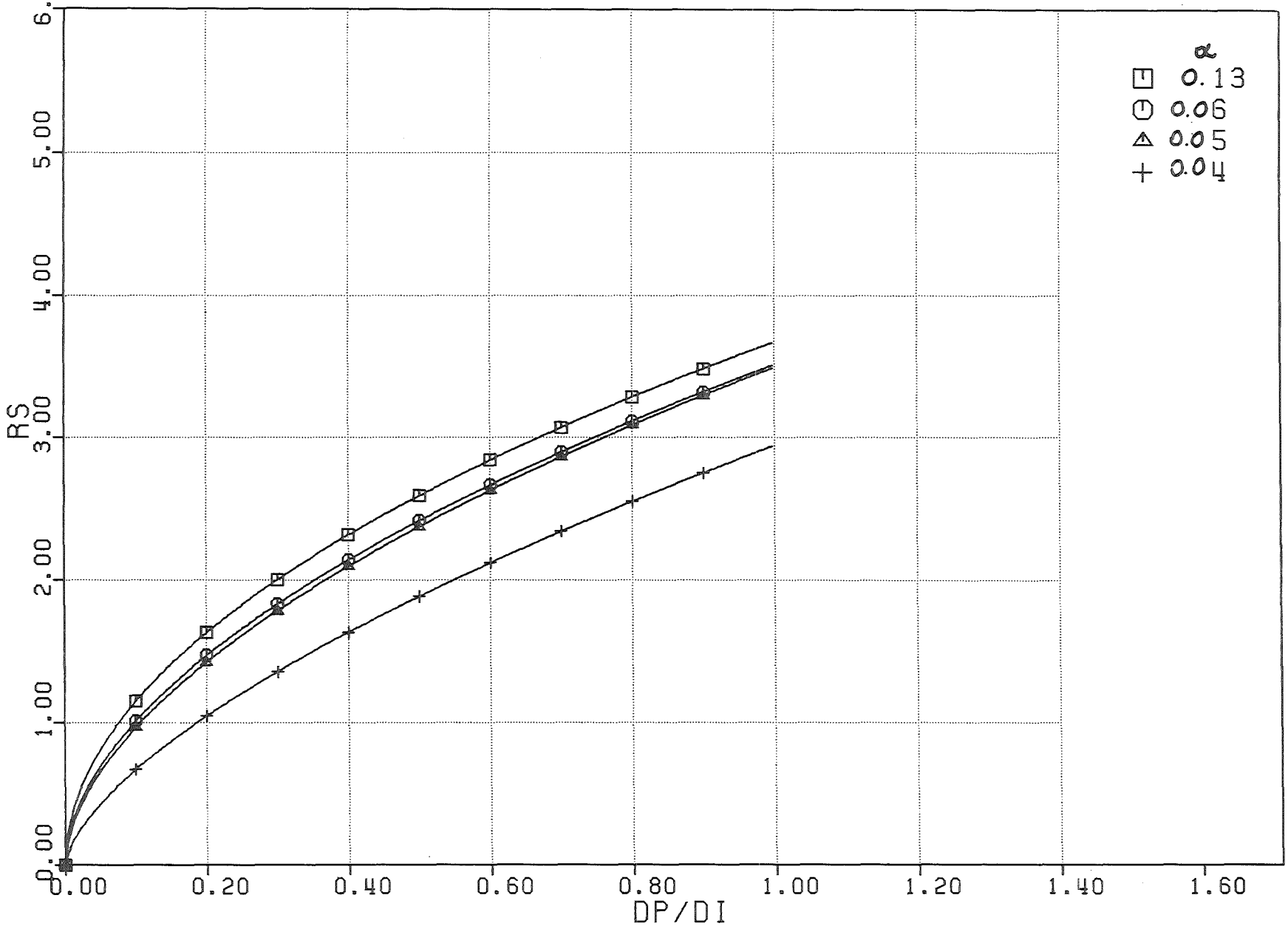

Fig. 5.2 8 - Experiments with Valve 2 . R_p = 0.25. Ratio RS plotted for different values of the air volumetric fraction

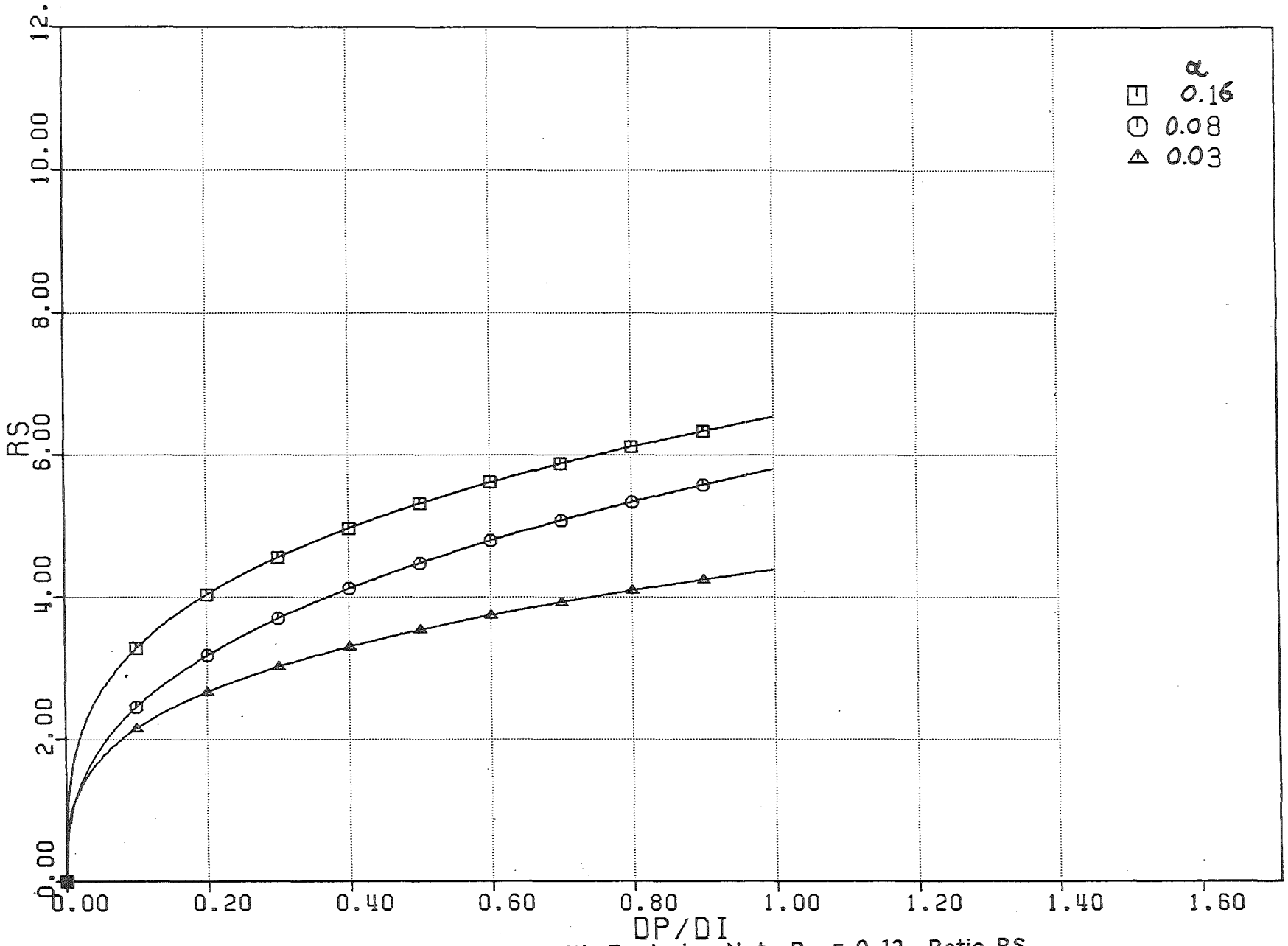

Fig.5.29 - Experiments with Explosion Nut, R_p = 0.12. Ratio RS plotted for different values of the air volumetric fraction

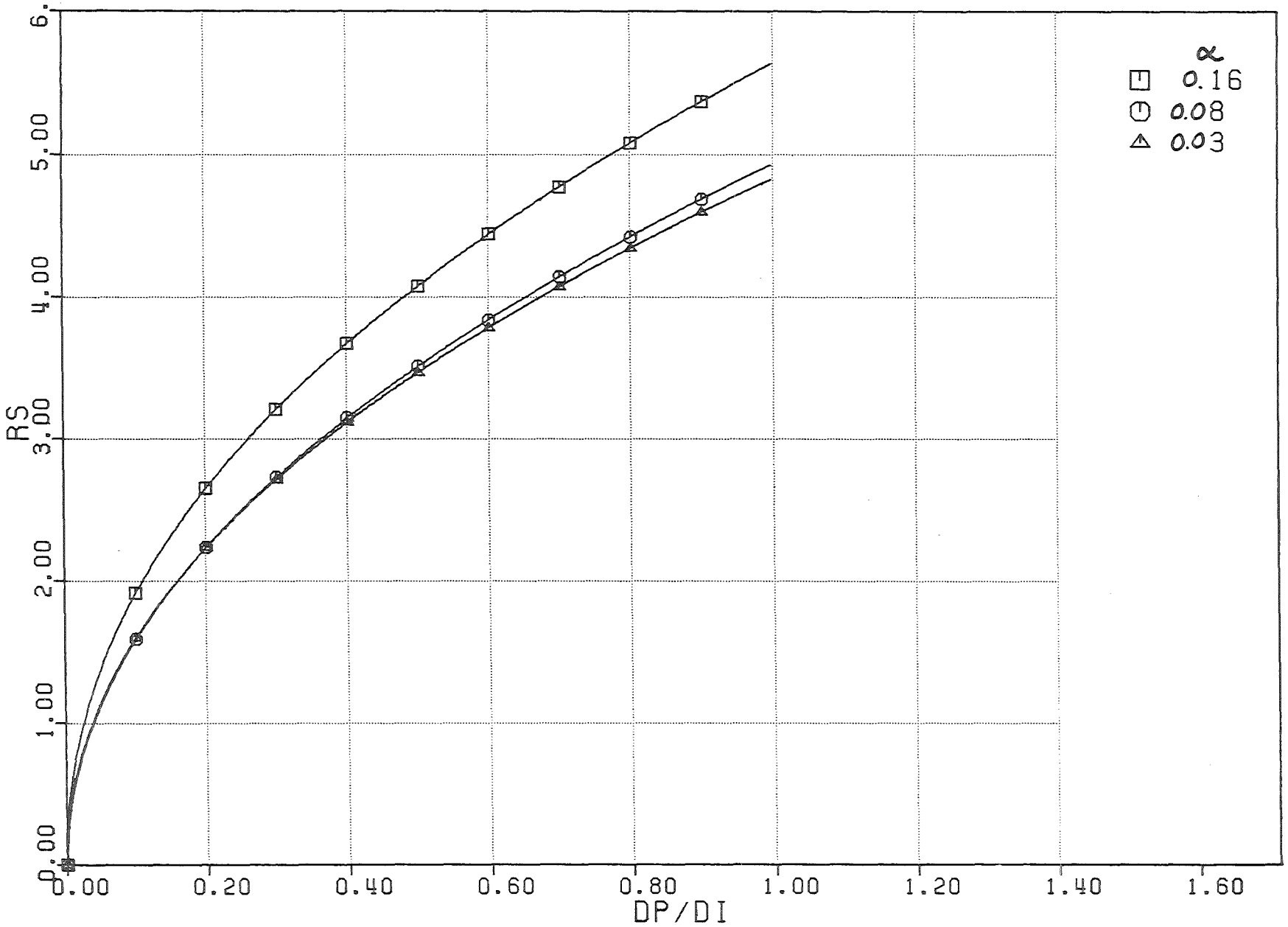

Fig. 5.30- Experiments with Explosion Nut, R_p = 0.17. Ratio RS plotted for different values of the air volumetric fraction

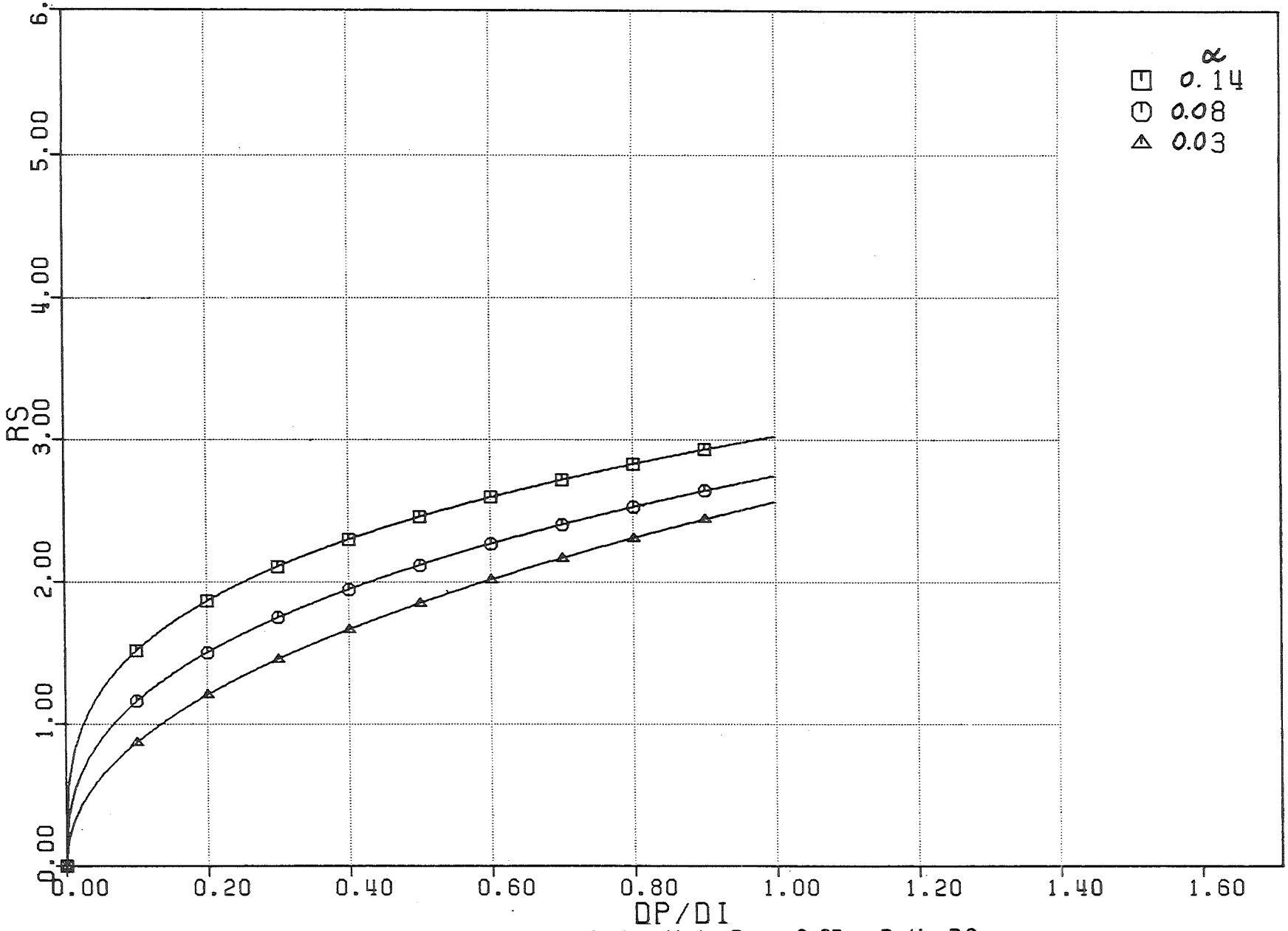

Fig. 5.31 - Experiments with Explosion Nut, R_p = 0.25. Ratio RS plotted for different values of the air volumetric fraction

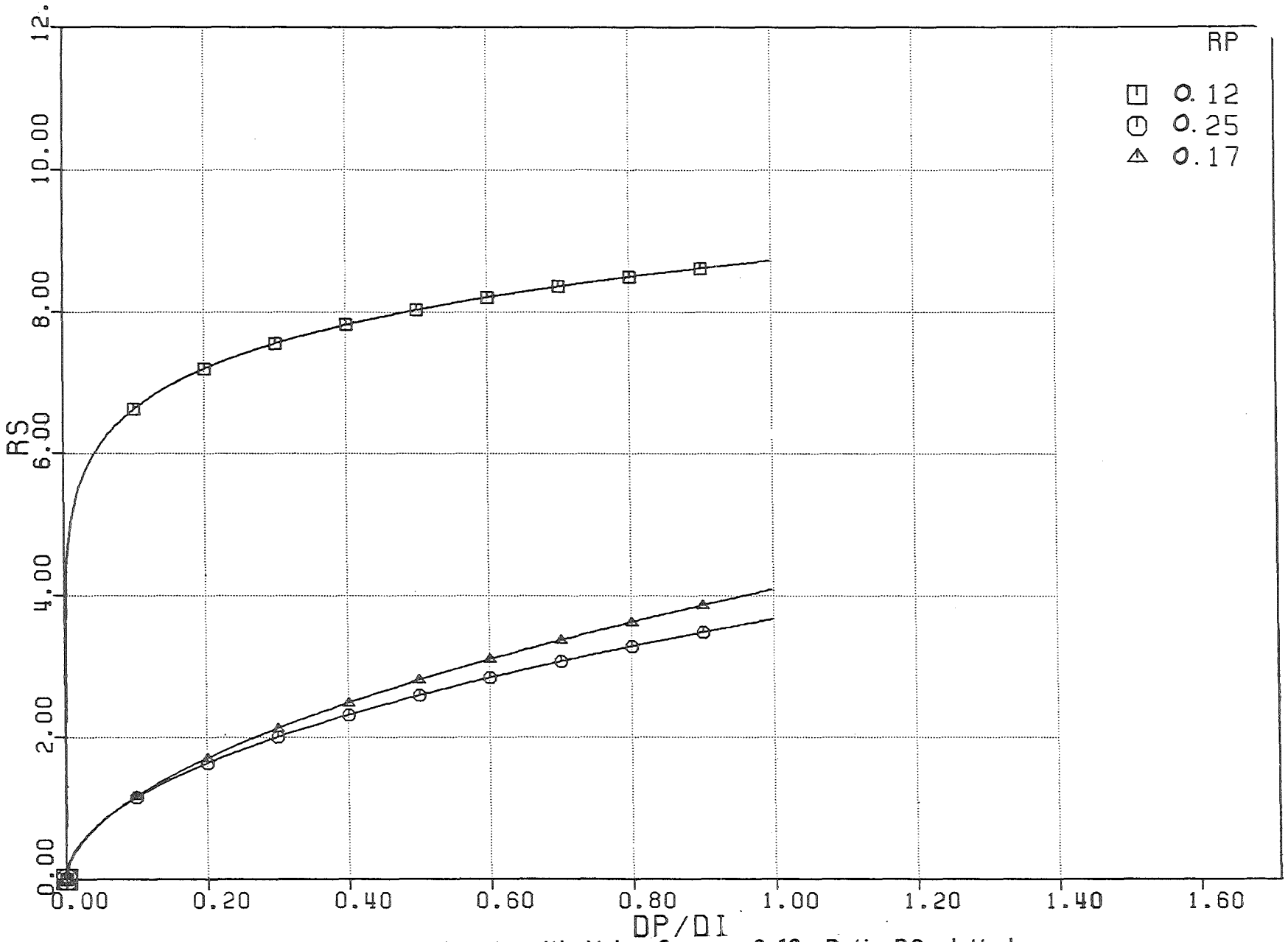

Fig. 5.32 - Experiments with Valve 2 . α = 0.12. Ratio RS plotted for different values of the perforation ratio.

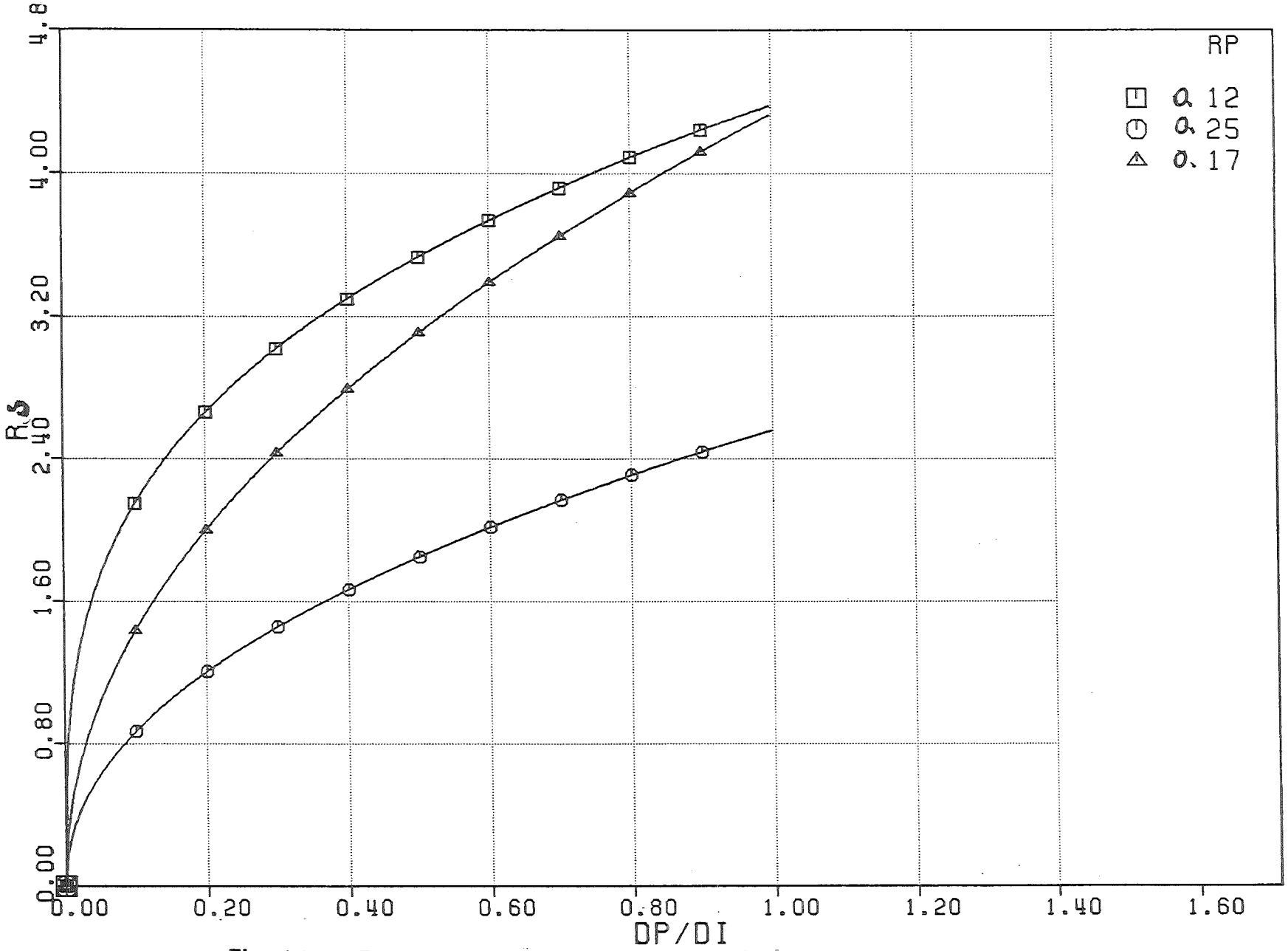

Fig. 5.33 - Experiments with Explosion Nut, $\alpha = 0.03$. Ratio RS plotted for different values of the perfoartion ratio.

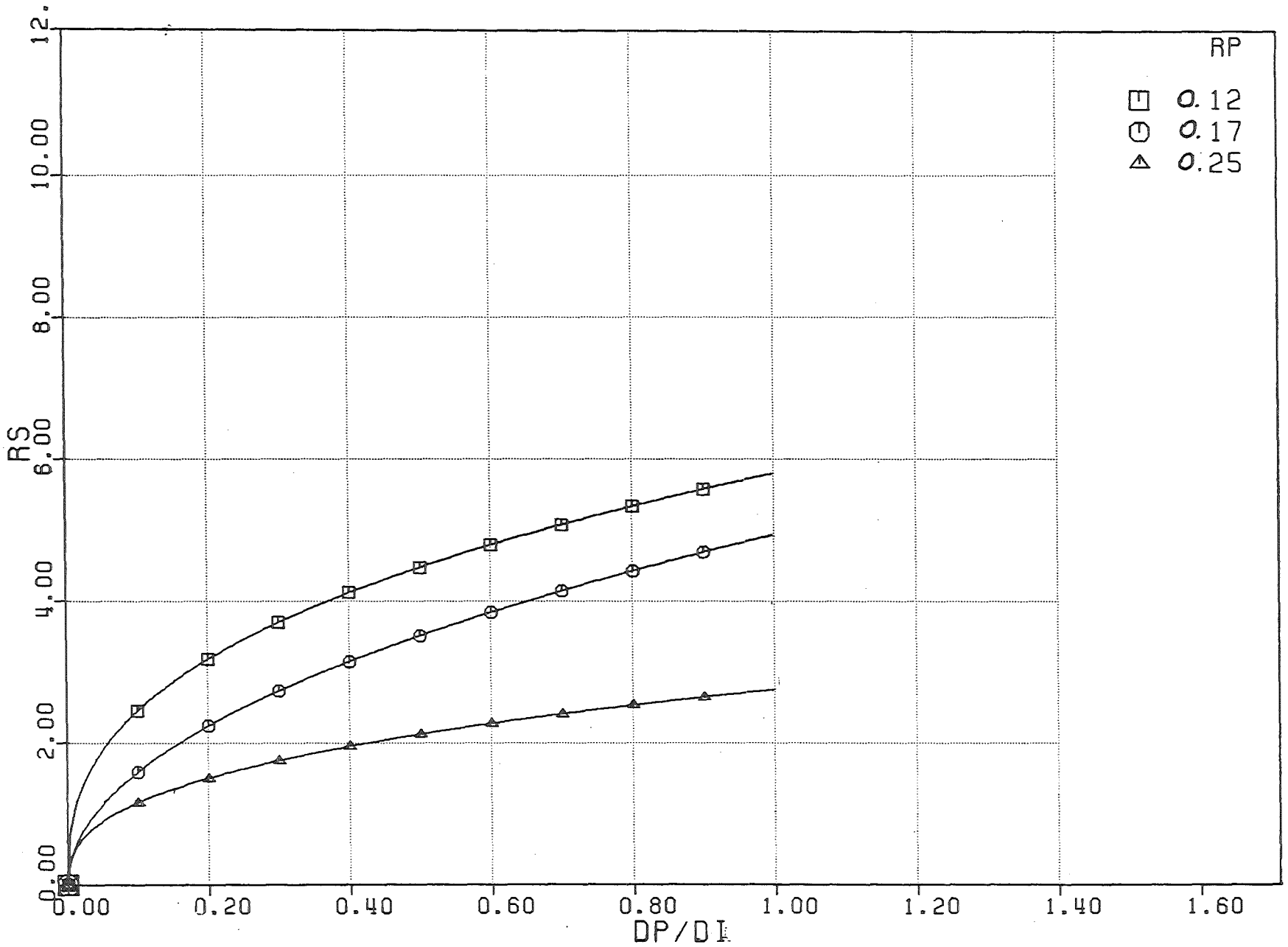

Fig. 5.34 - Experiments with Explosion Nut, α = 0.08. Ratio RS plotted for different values of the perforation ratio.

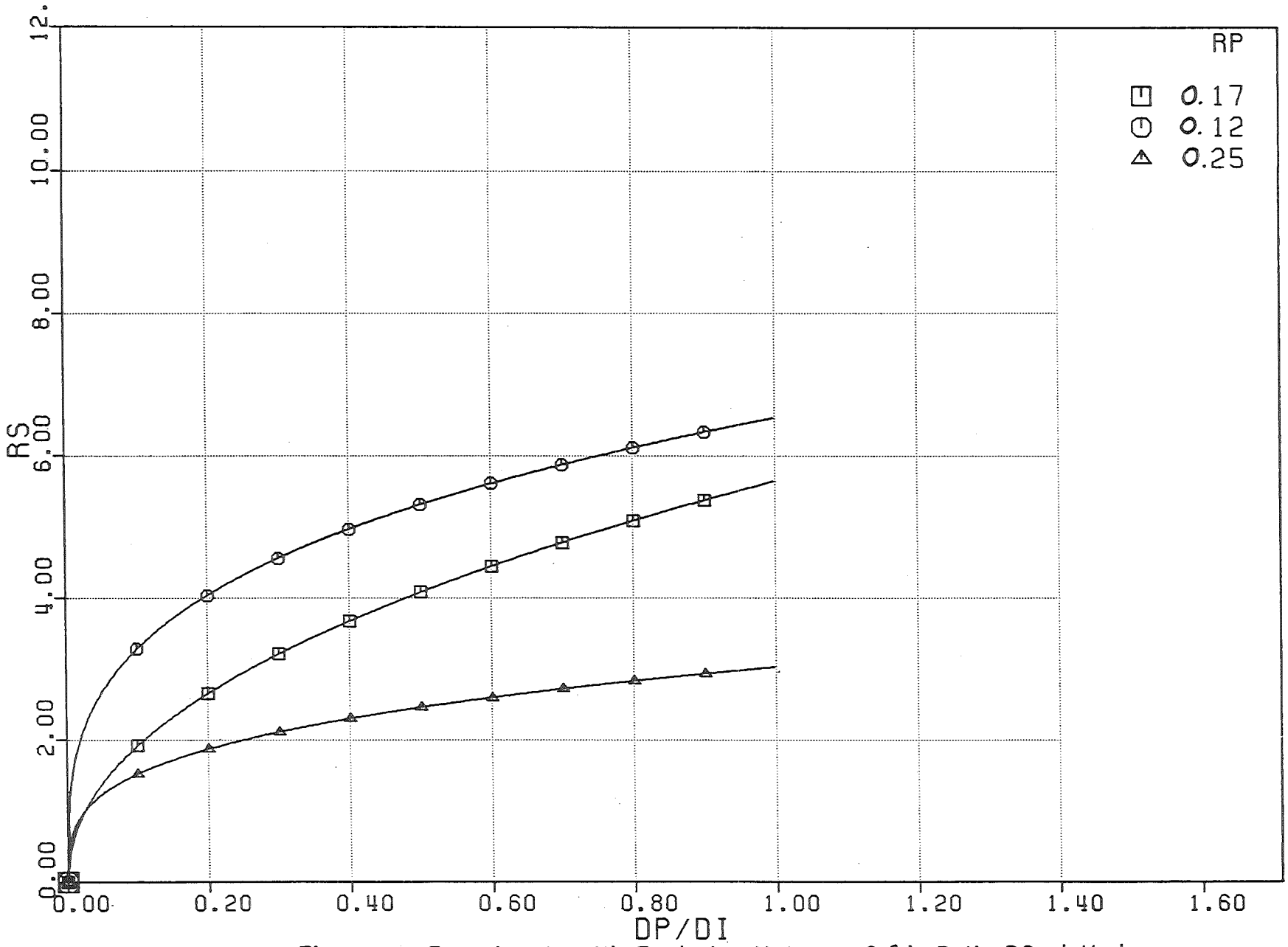

Fig. 5.35 - Experiments with Explosion Nut, $\alpha = 0.14$. Ratio RS plotted for different values of the perforation ratio.

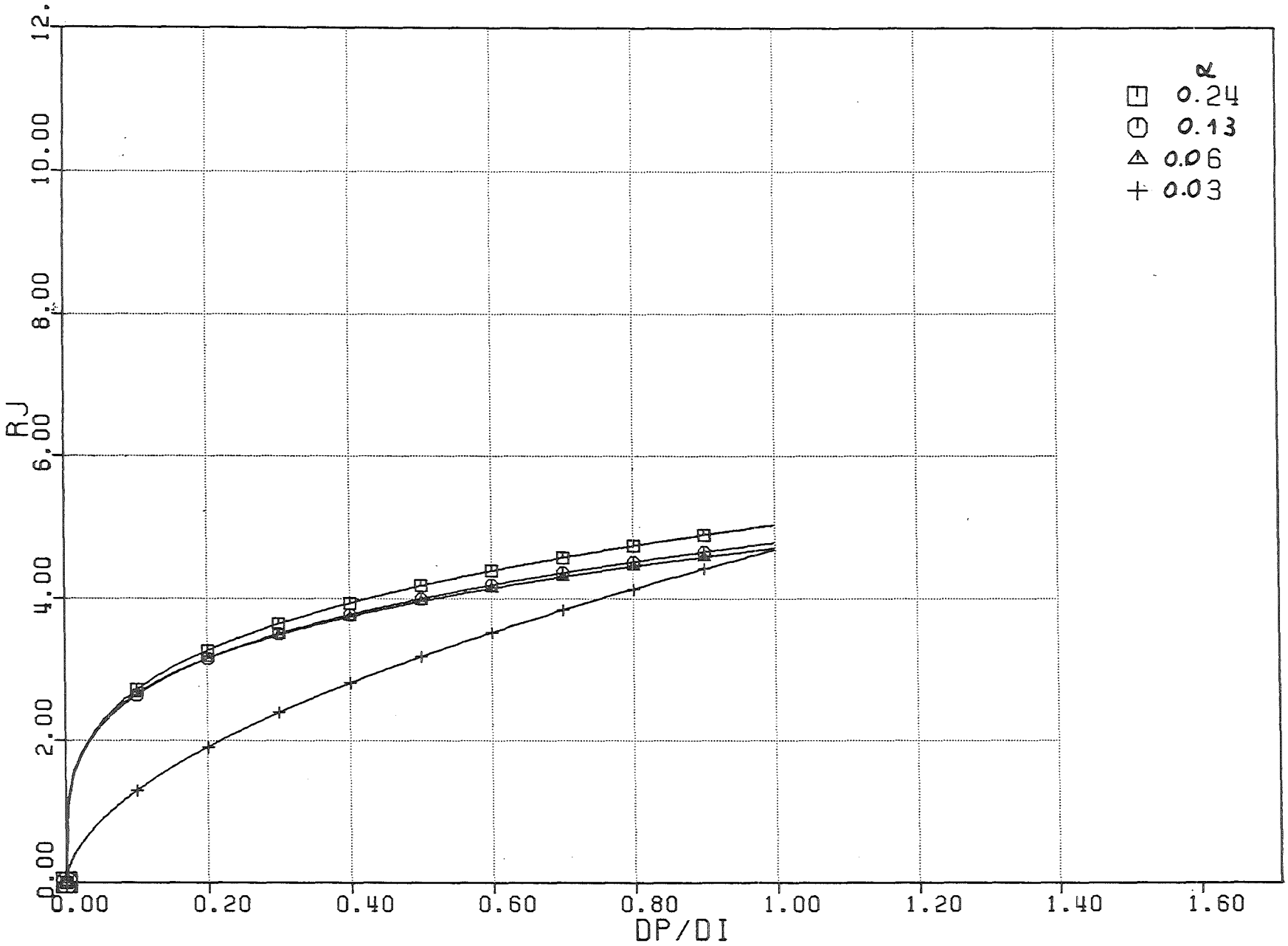

Fig. 5.36 - Experiments with Valve 1 . R_p = 0.17. Ratio RJ plotted for different values of the air volumetric fraction

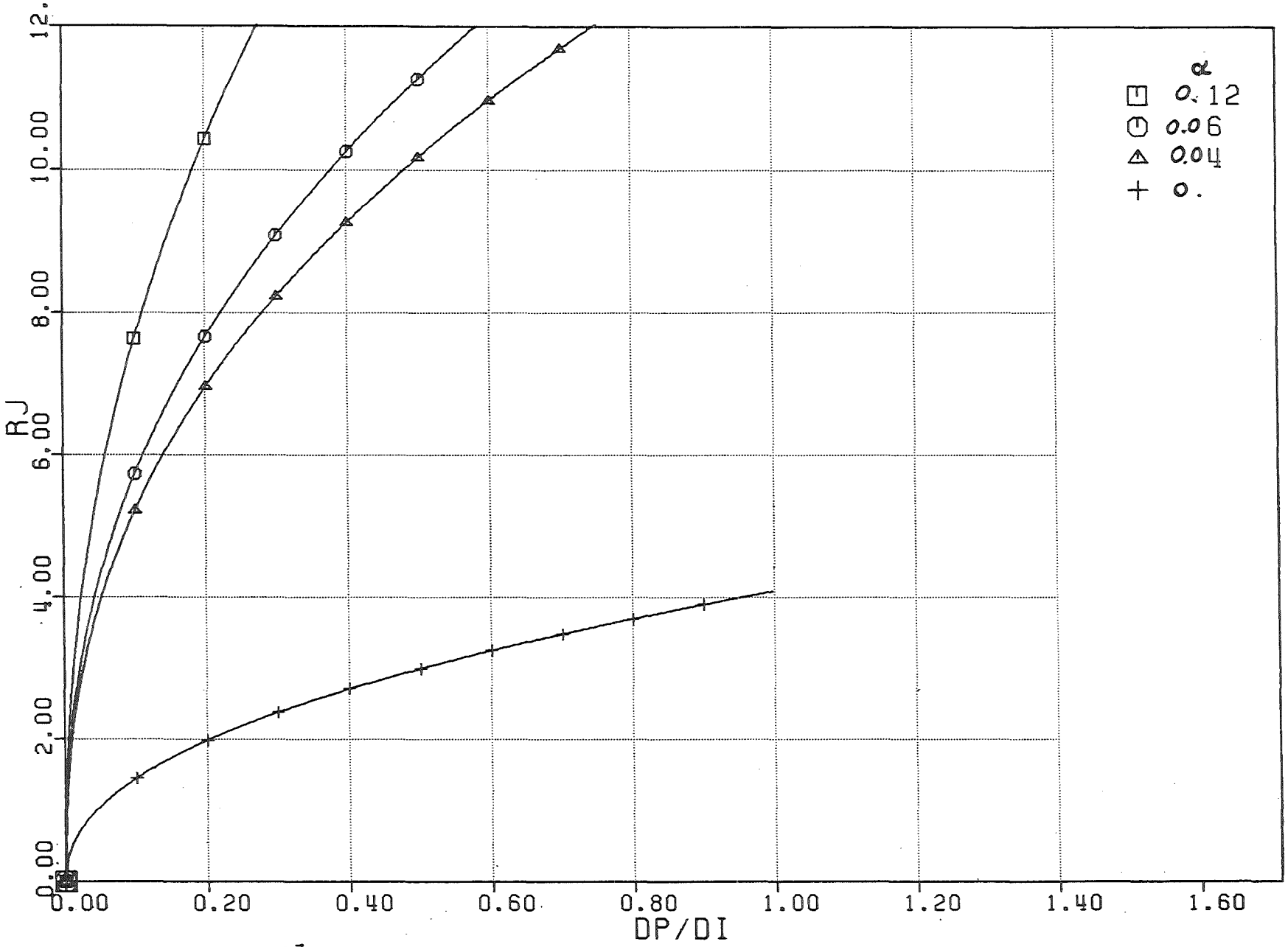

Fig. 5.37 - Experiments with Valve 2 . R_p = 0.12. Ratio RJ plotted for different values of the air volumetric fraction

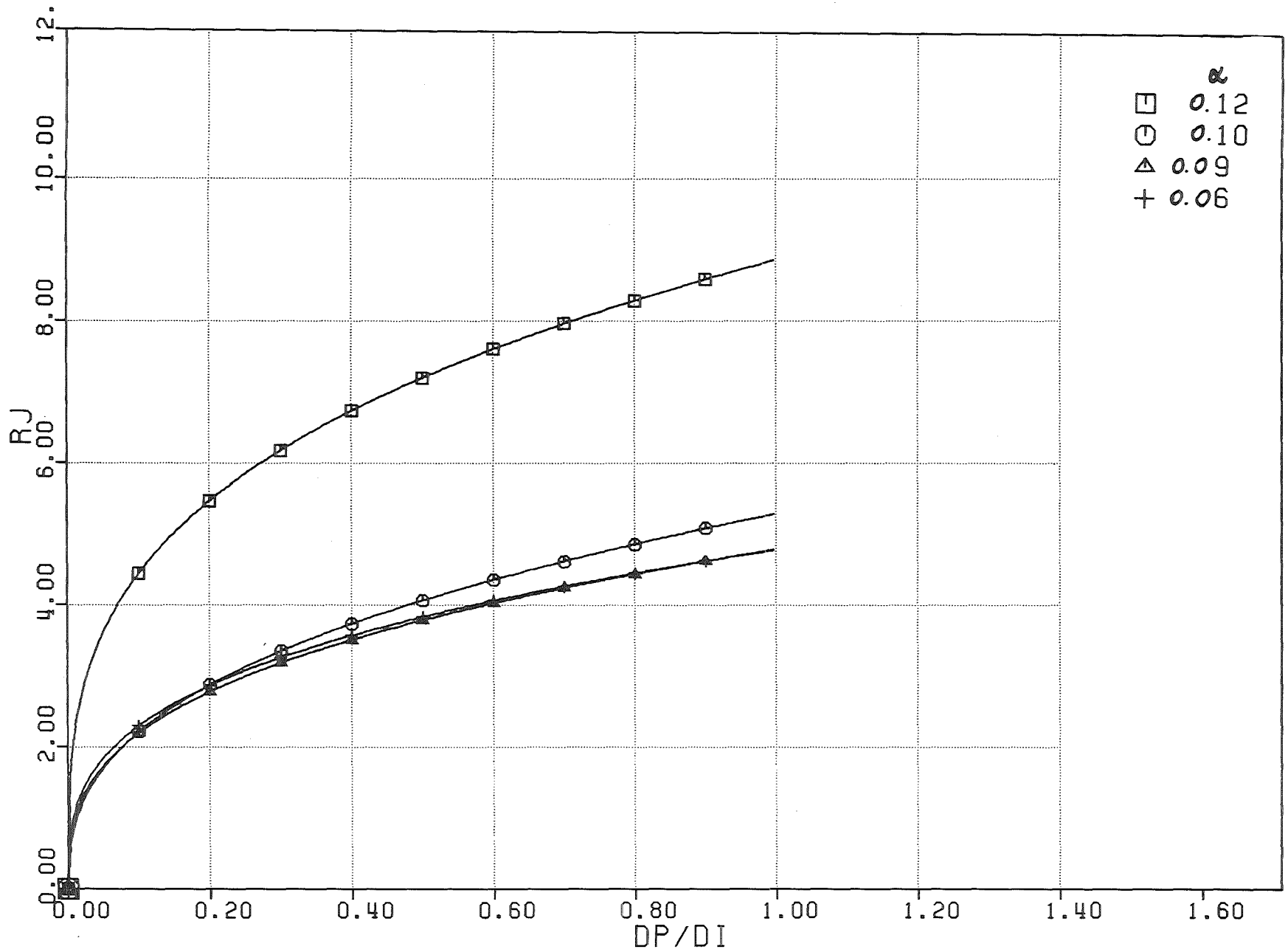

Fig. 5.3 - Experiments with Valve 2 . R_p = 0.17. Ratio RJ plotted for different values of the air volumetric fraction

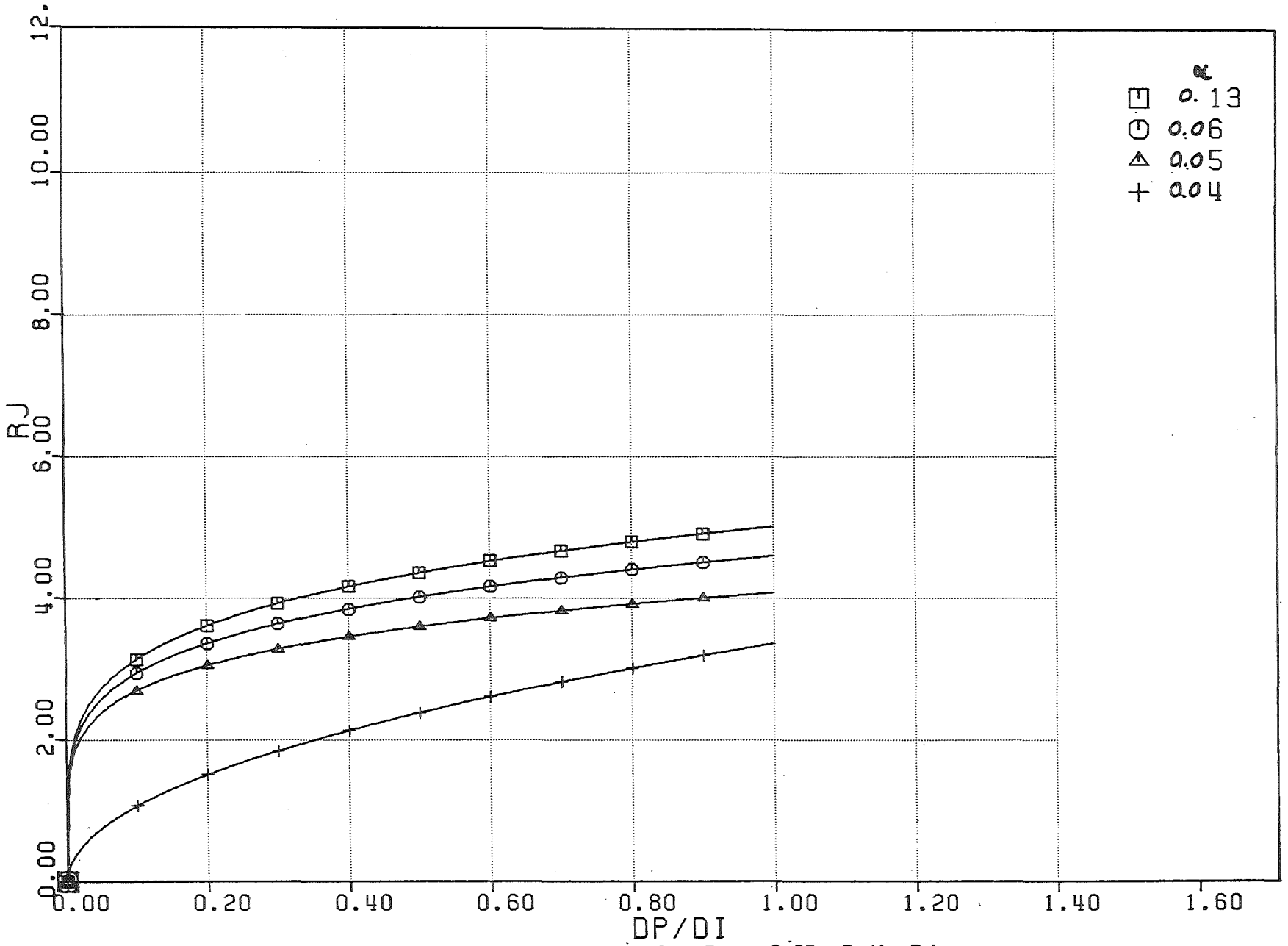

Fig. 5.39 - Experiments with Valve 2 . R_p = 0.25. Ratio RJ plotted for different values of the air volumetric fraction

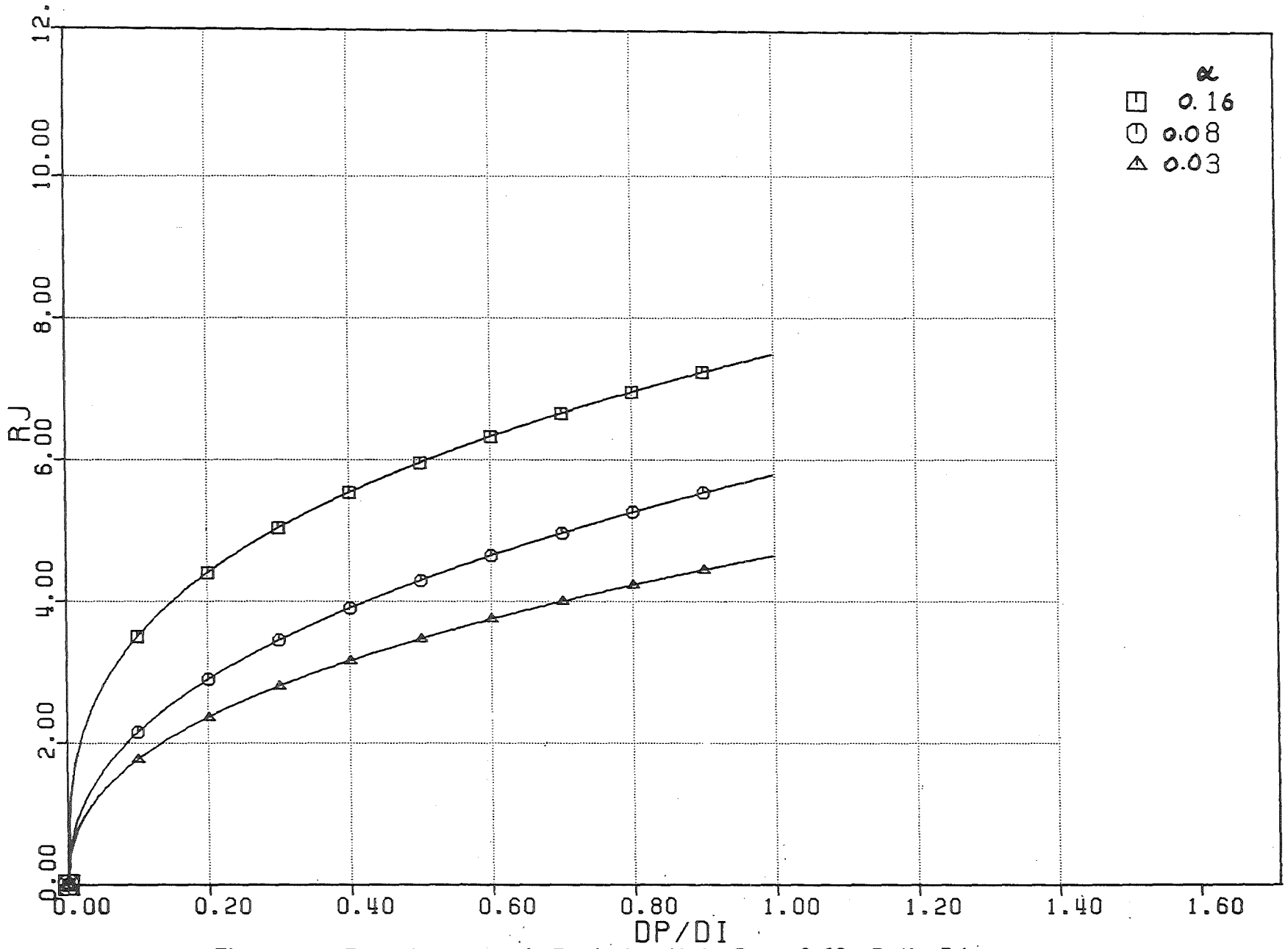

Fig. 5.40- Experiments with Explosion Nut, R_p = 0.12. Ratio RJ plotted for different values of the air volumetric fraction

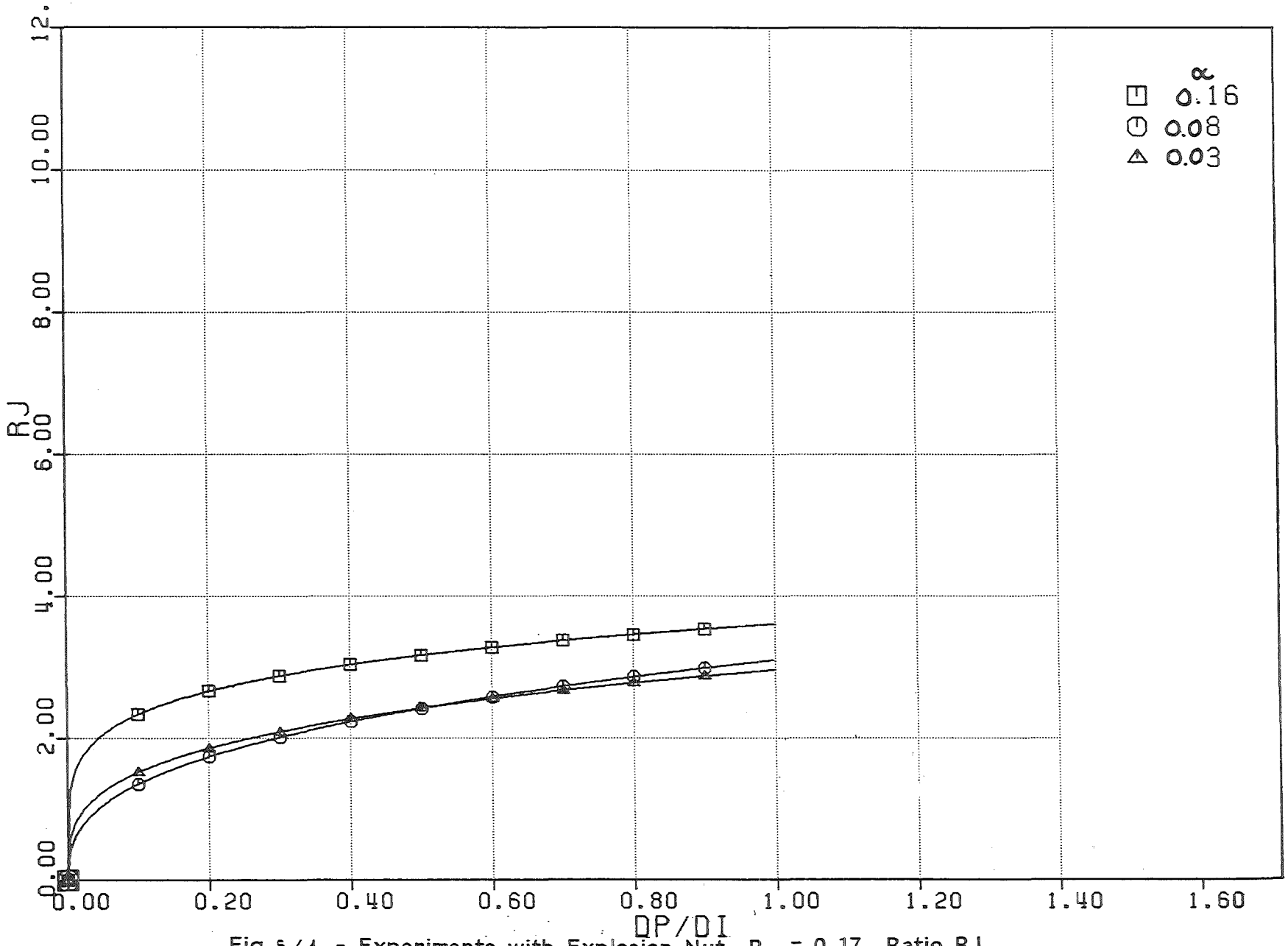

Fig.5.41 - Experiments with Explosion Nut, R_p = 0.17. Ratio RJ plotted for different values of the air volumetric fraction

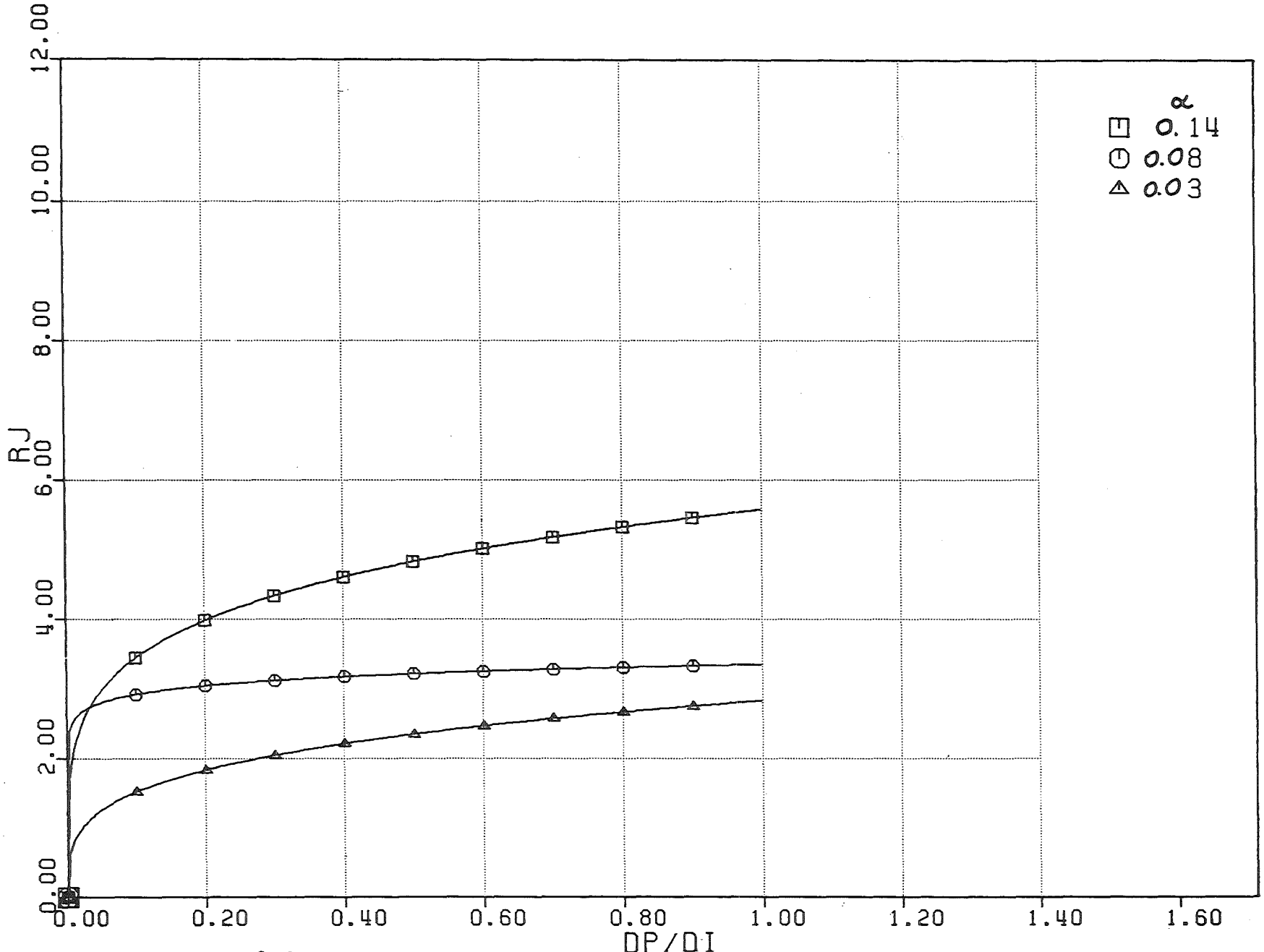

Fig. 5.42 - Experiments with Explosion Nut, R_p = 0.25. Ratio RJ plotted for different values of the air volumetric fraction

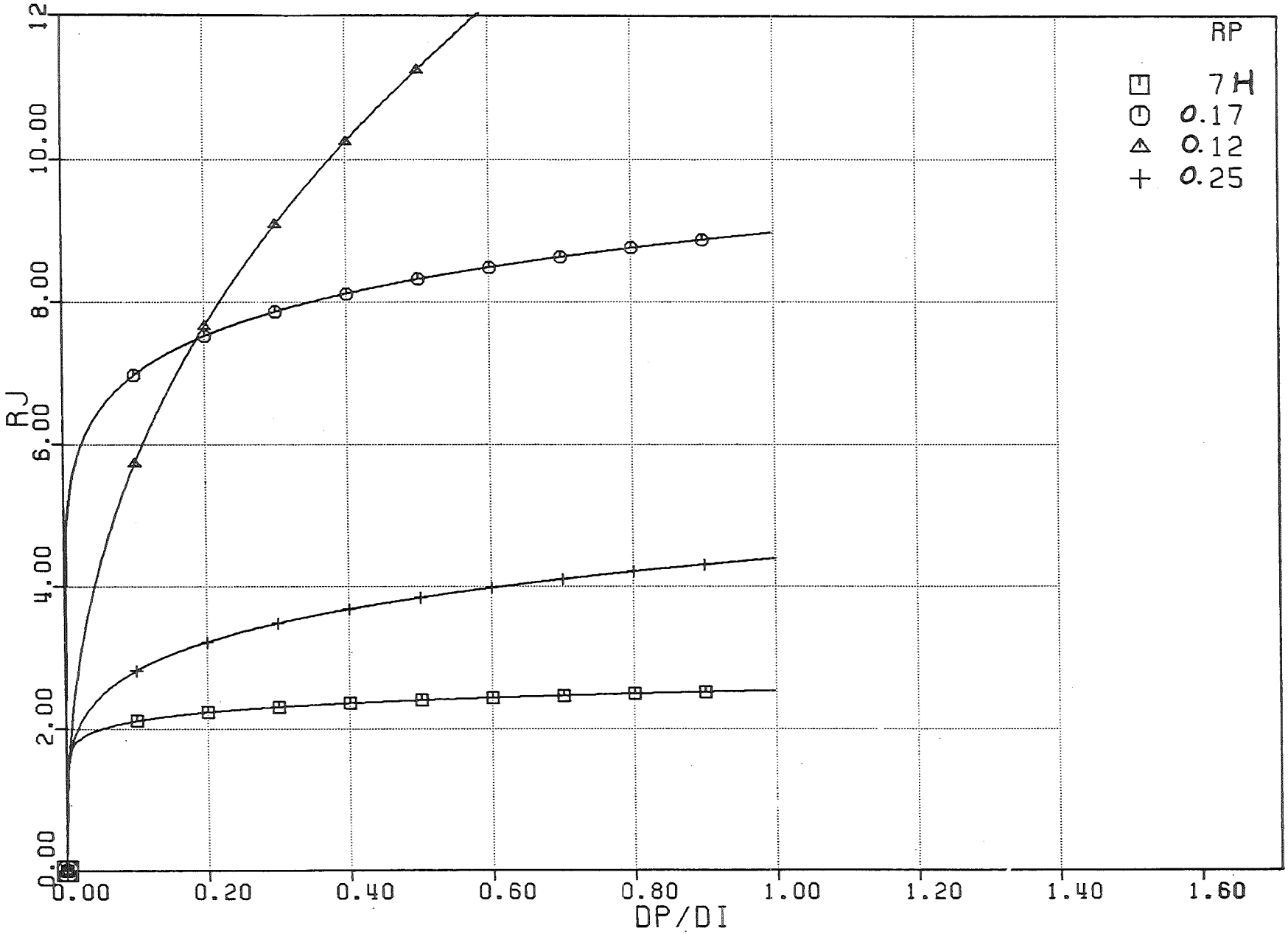

Fig.5.43 - Experiments with Valve 2 . α = 0.06. Ratio RJ plotted for different values of the perforation ratio.

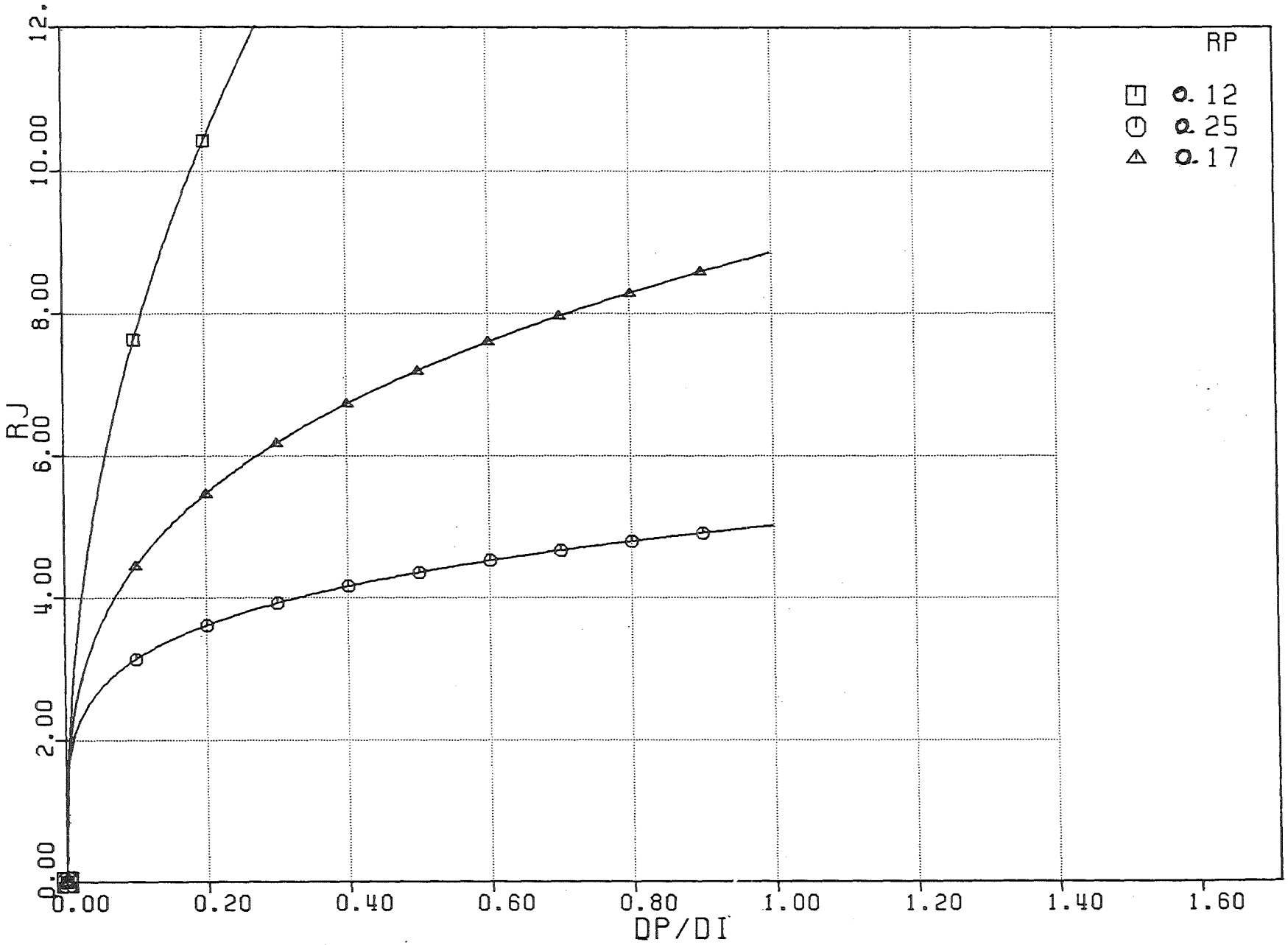

Fig. 44 - Experiments with Valve 2 . α = 0.12. Ratio RJ plotted for different values of the perforation ratio.

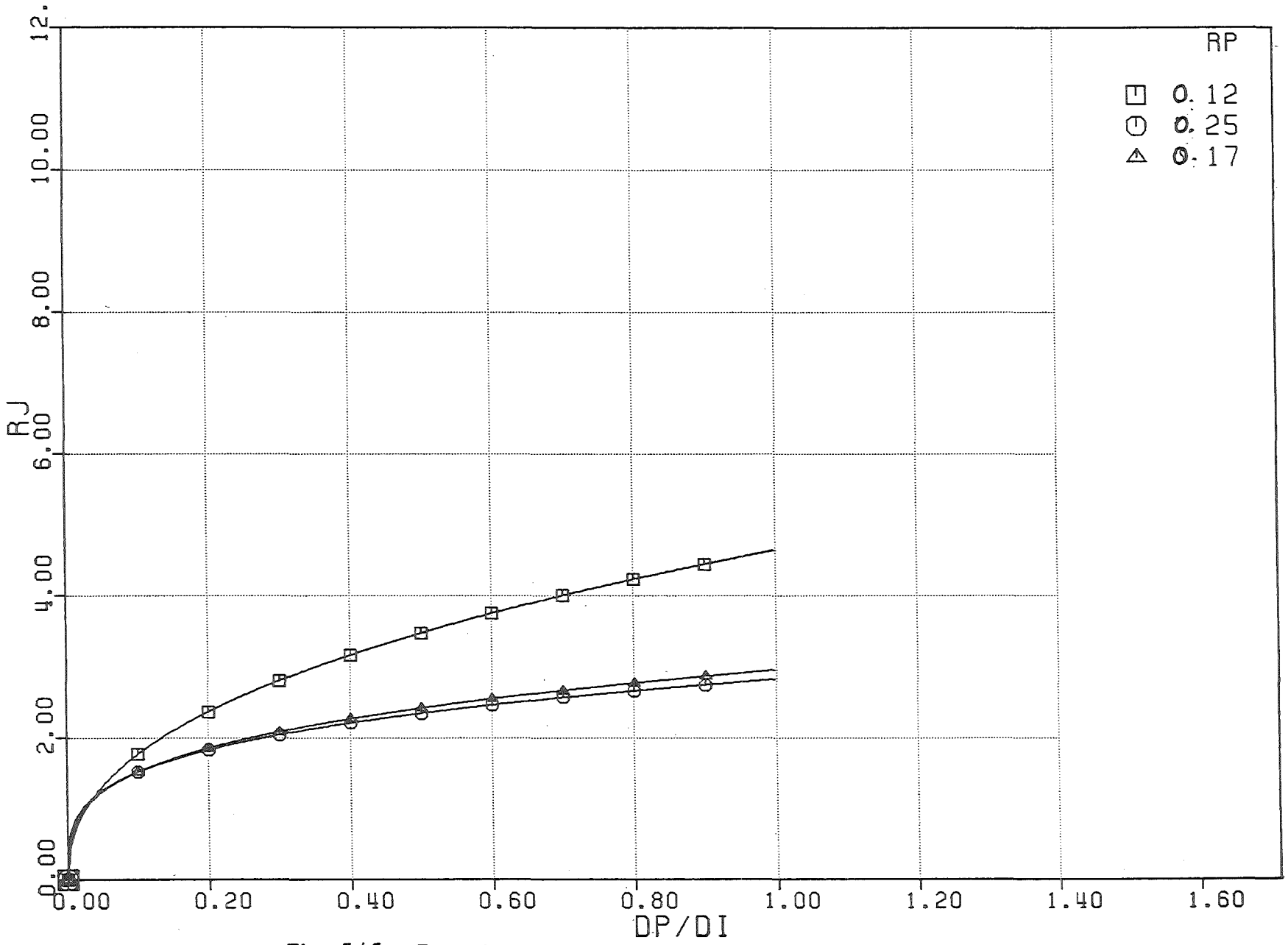

Fig. 5.45 - Experiments with Explosion Nut, α = 0.03. Ratio RJ plotted for different values of the perfoartion ratio.

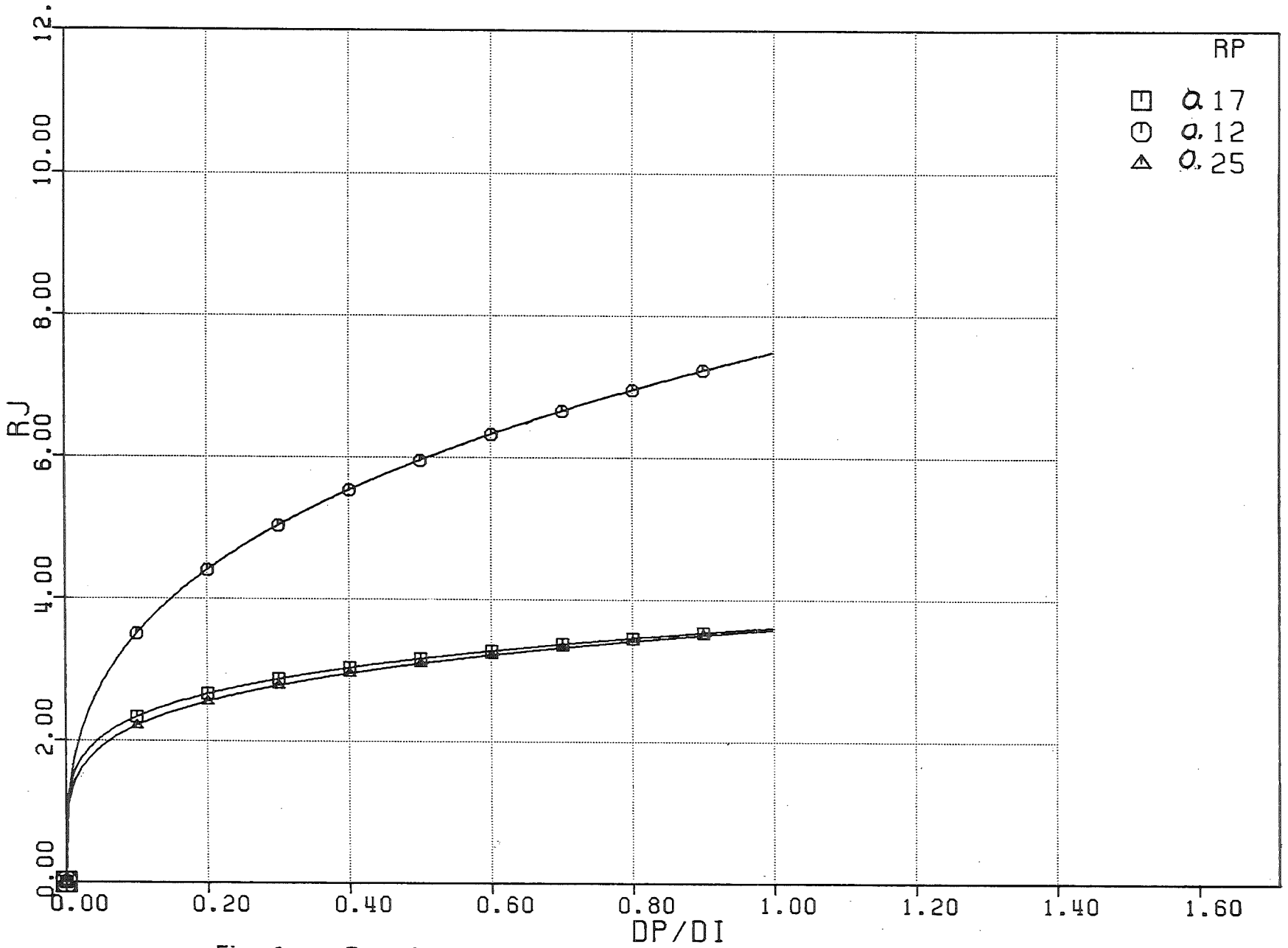

Fig. 5.46 - Experiments with Explosion Nut, $\alpha = 0.14$. Ratio RJ plotted for different values of the perforation ratio.

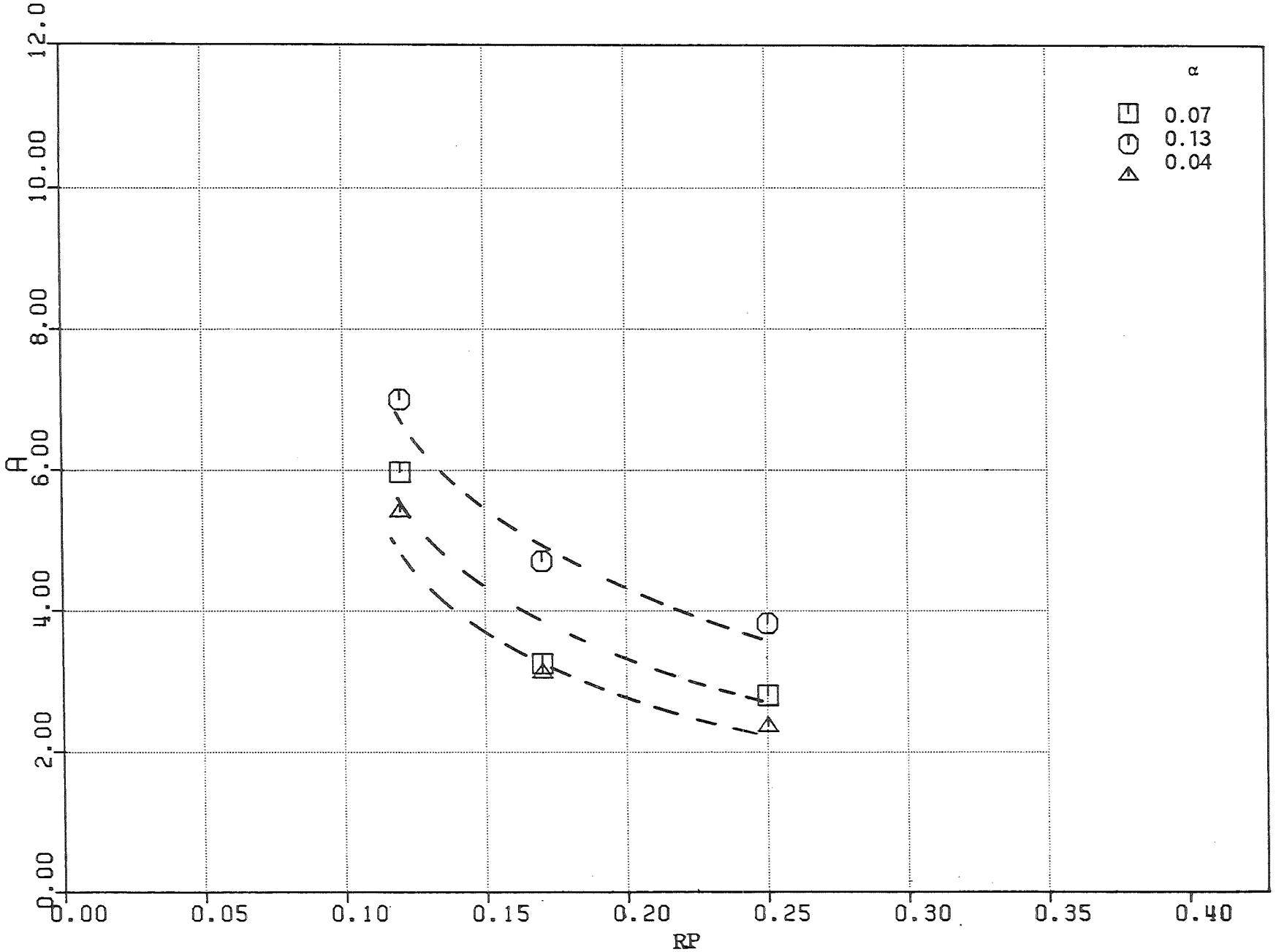

Fig. 5.47 - Experiments with Valve 2, α = 0.04, 0.07, 0.13.
Fit of the coefficients A (Eq. 5.1) for the displacement of the mixture surface.

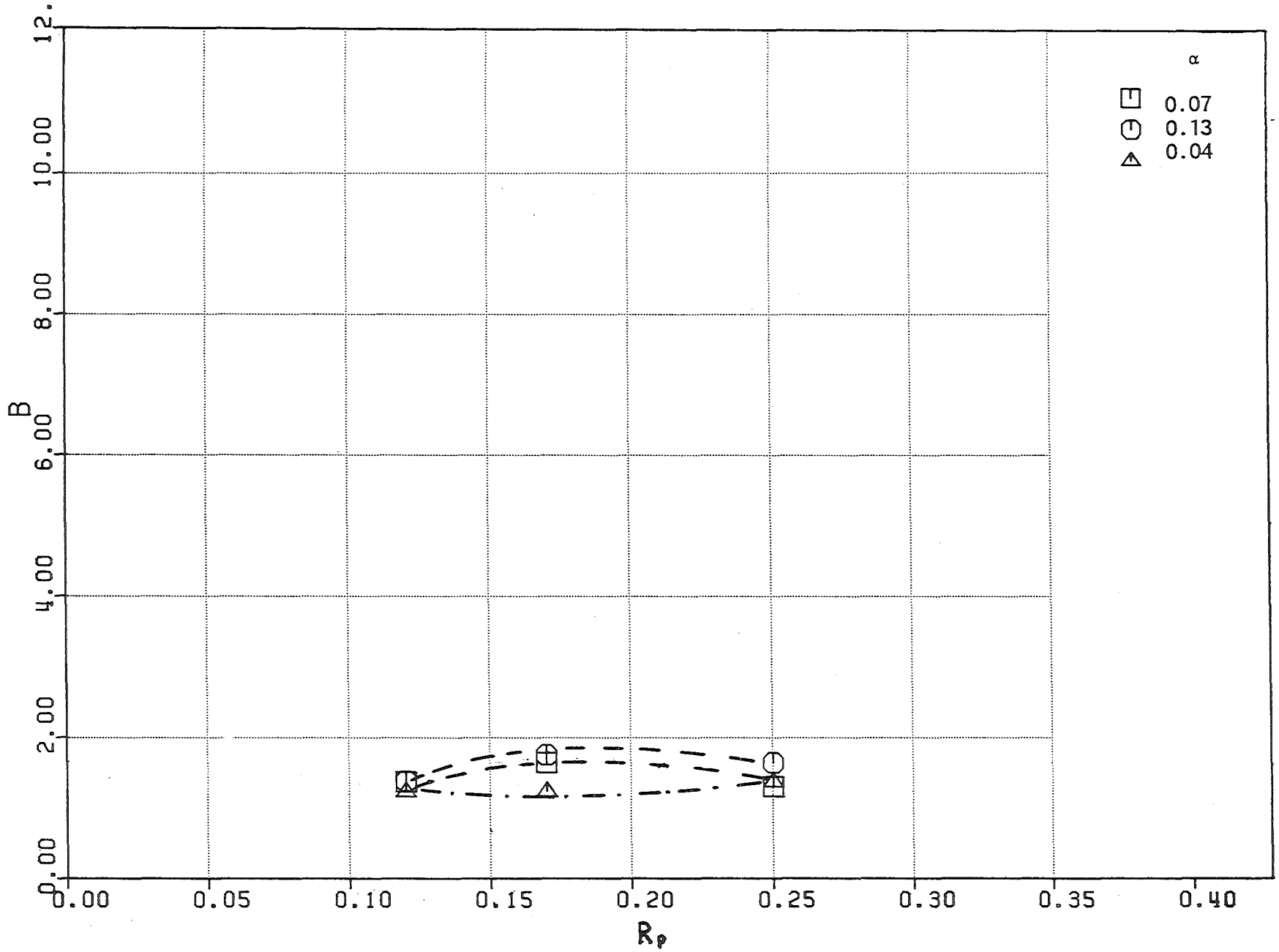

Fig. 5-48 - Experiments with Valve 2, α = 0.04, 0.07, 0.13.
Fit of the coefficients B (Eq. 5.1) for the displacement of the mixture surface.

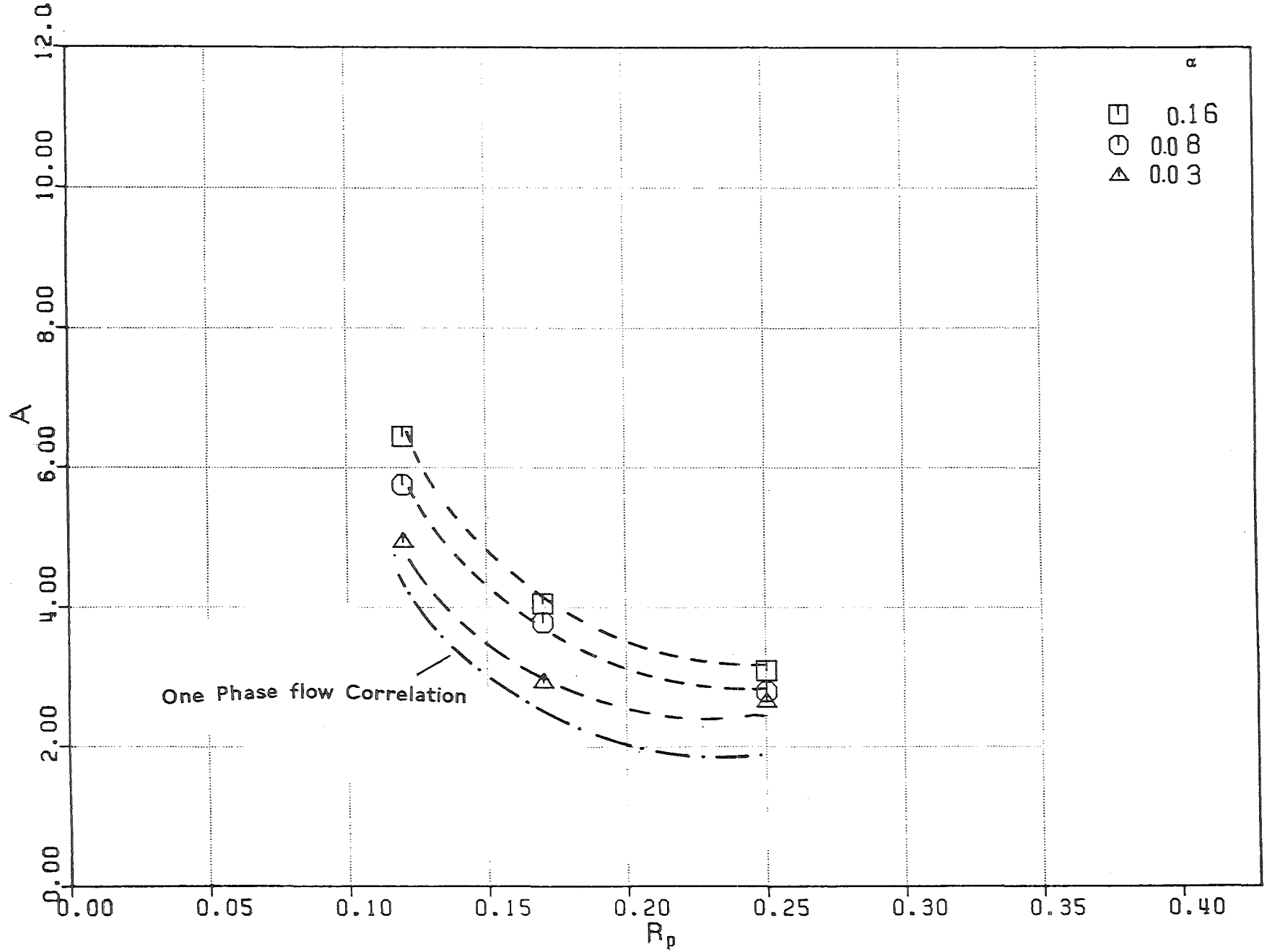

Fig. 5.49 - Experiments with Explosion Nut , α = 0.03, 0.08, 0.16. Fit of the coefficients A (Eq. 5.1) for the displacement of the mixture surface.

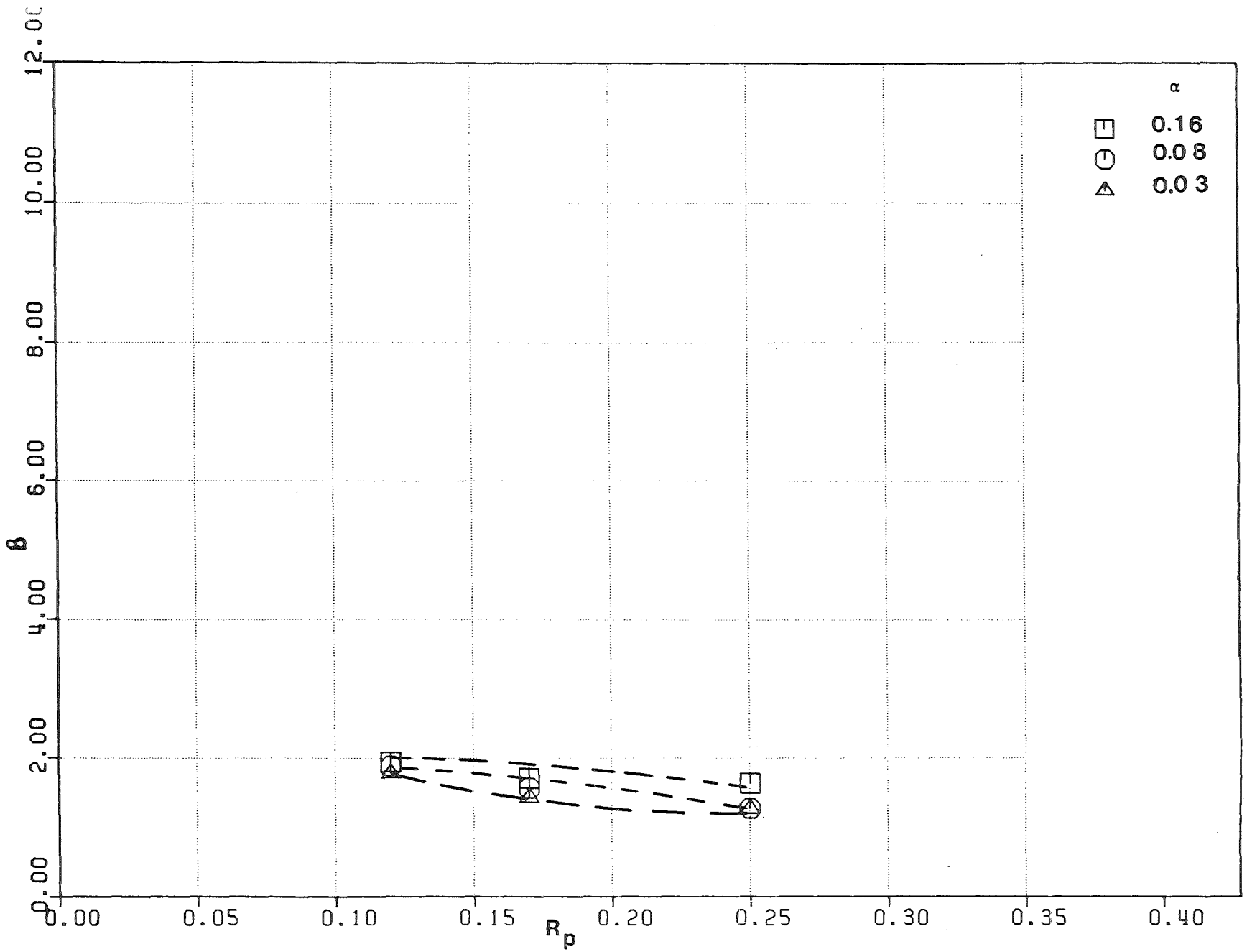

Fig.5.50 - Experiments with Explosion Nut , α = 0.03, 0.08, 0.16. Fit of the coefficients B (Eq. 5.1) for the displacement of the mixture surface.

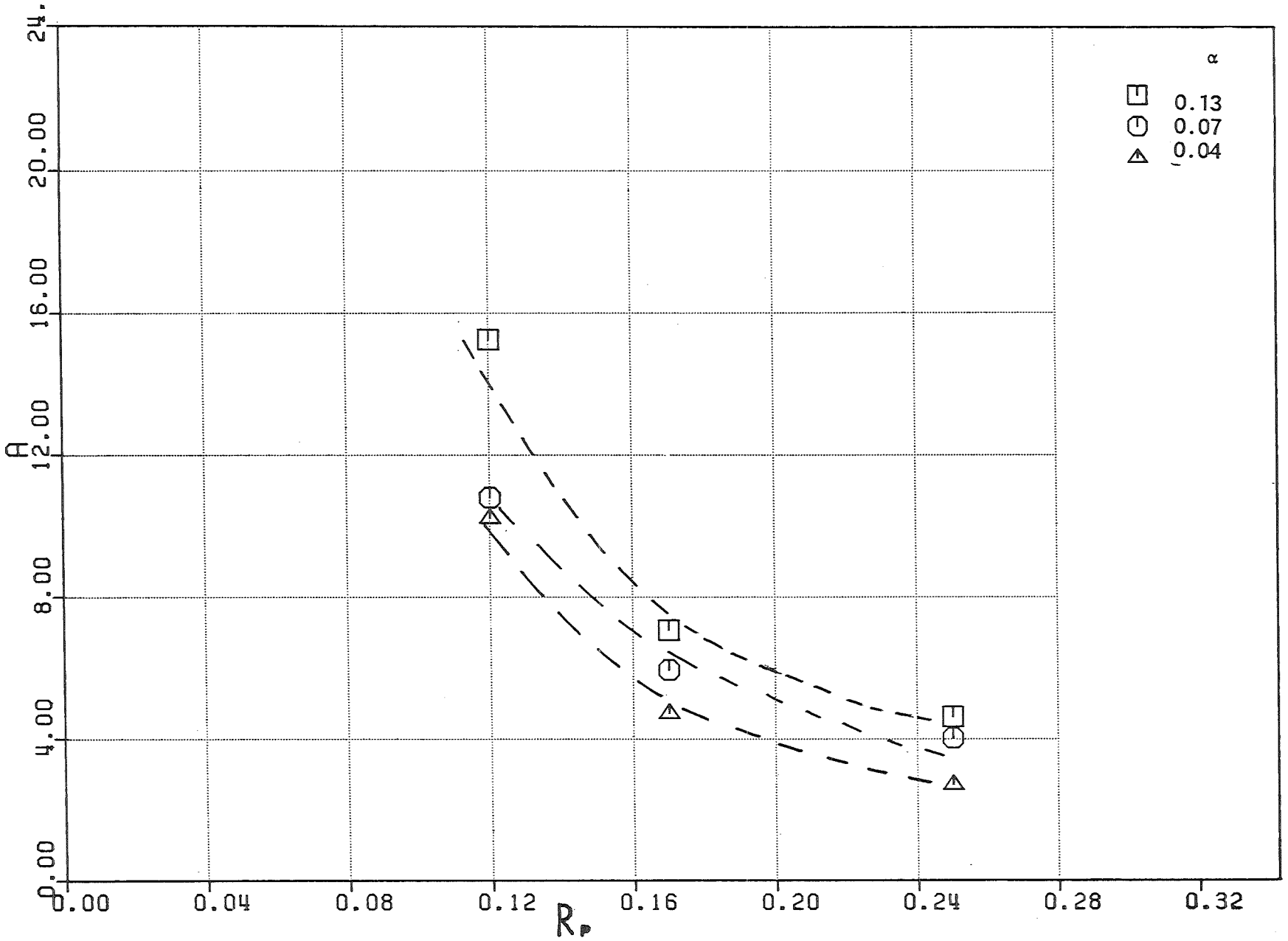

Fig. 5.51 - Experiments with Valve 2, α = 0.04, 0.07, 0.13.
Fit of the coefficients A (Eq. 5.1) for the displacement of the jet.

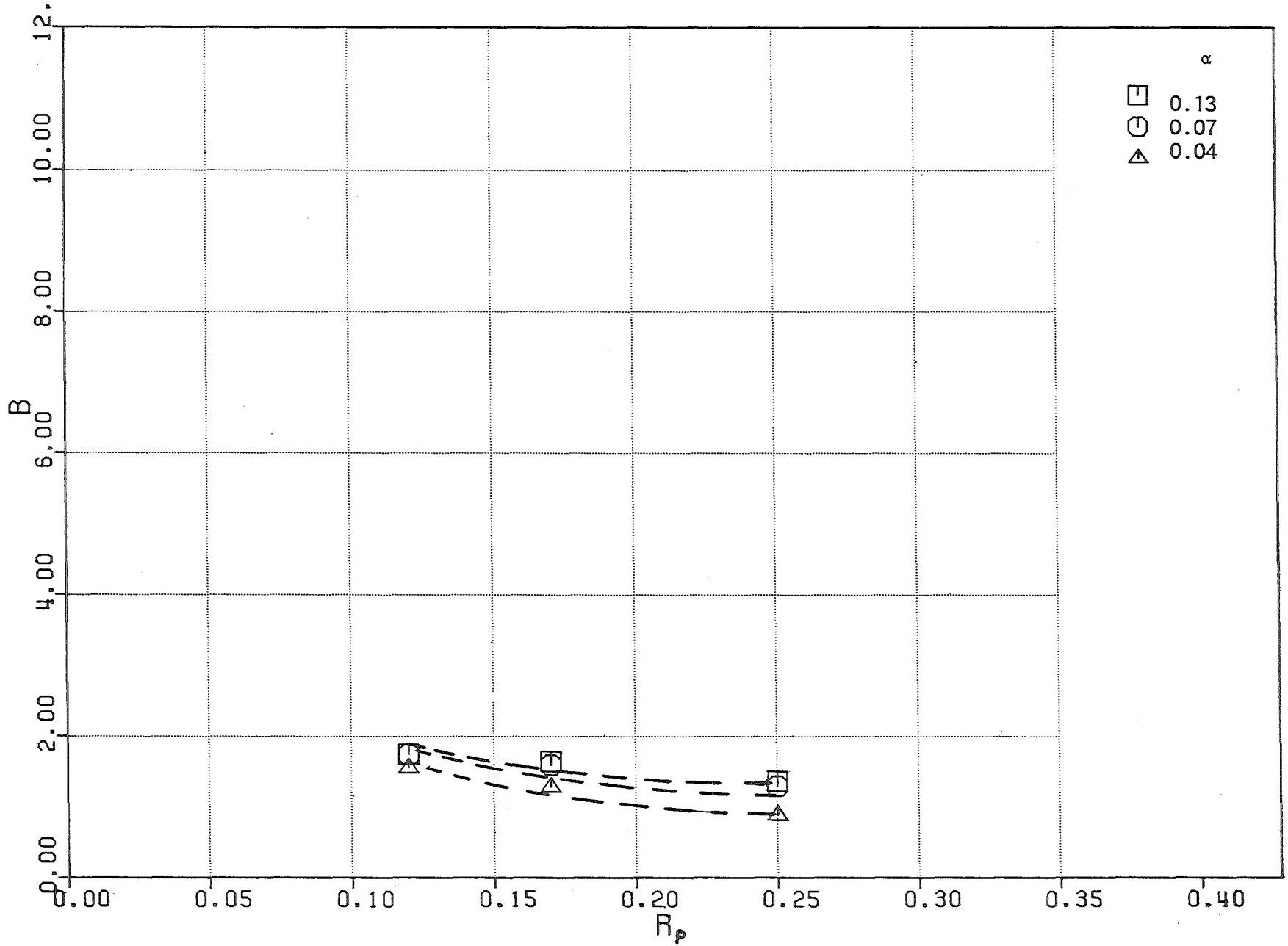

Fig.5.52 - Experiments with Valve 2, α = 0.04, 0.07, 0.13.
Fit of the coefficients B (Eq. 5.1) for the displacement of the jet.

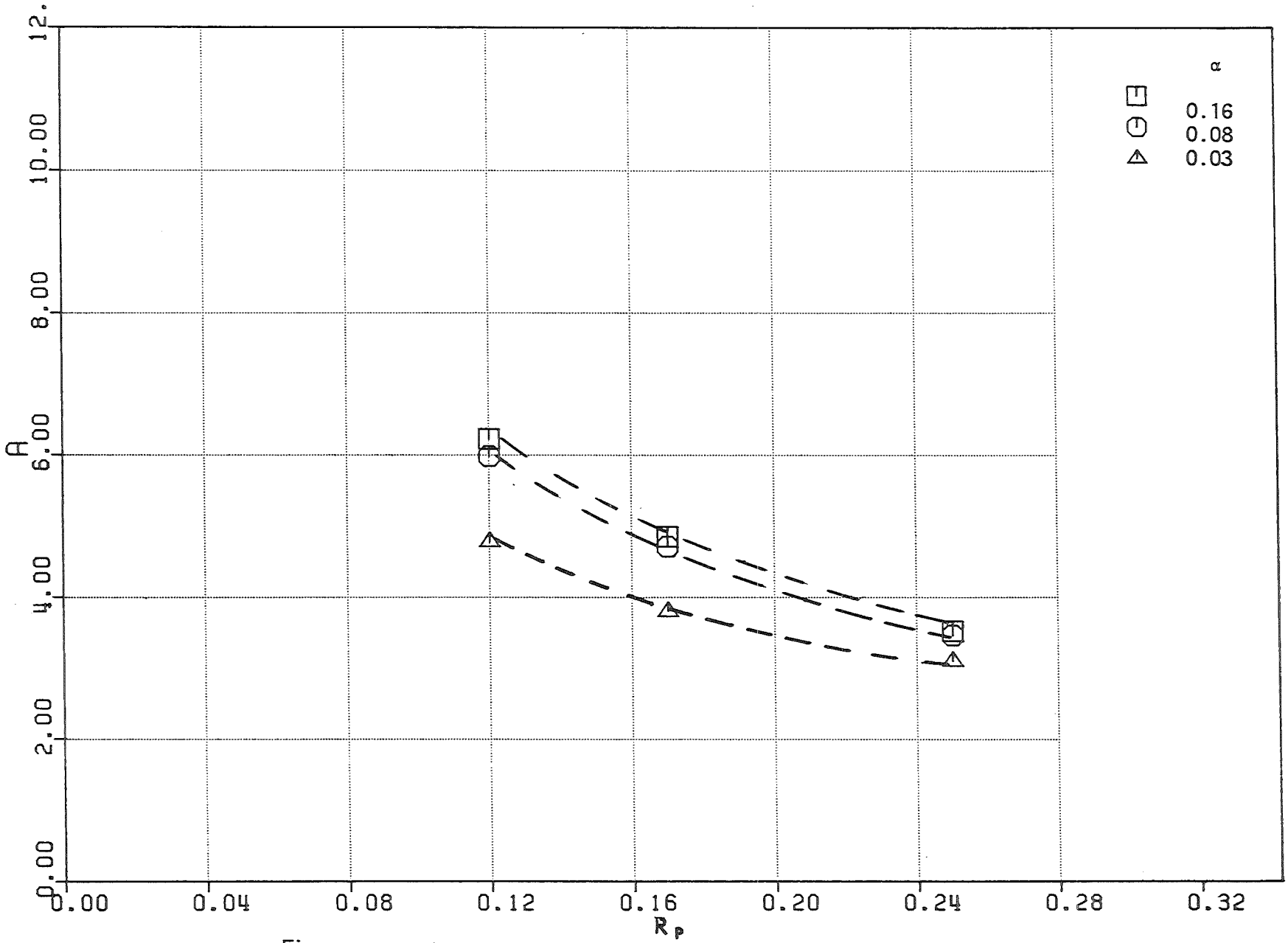

Fig. 5.53 - Experiments with Explosion Nut , α = 0.03, 0.08, 0.16. Fit of the coefficients A (Eq. 5.1) for the displacement of the jet.

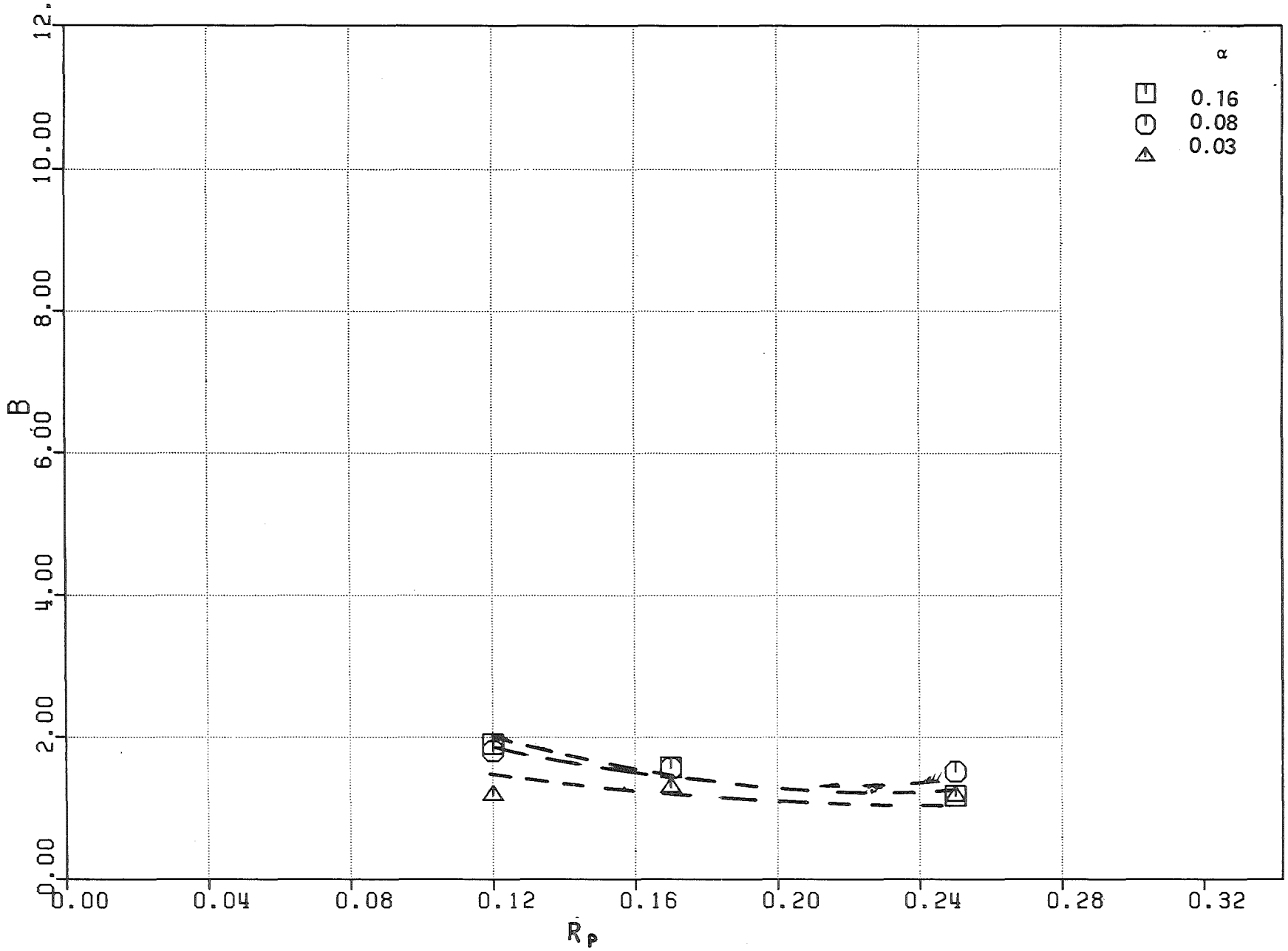

Fig. 5.54 - Experiments with Explosion Nut , α = 0.03, 0.08, 0.16. Fit of the coefficients B (Eq. 5.1) for the displacement of the jet.

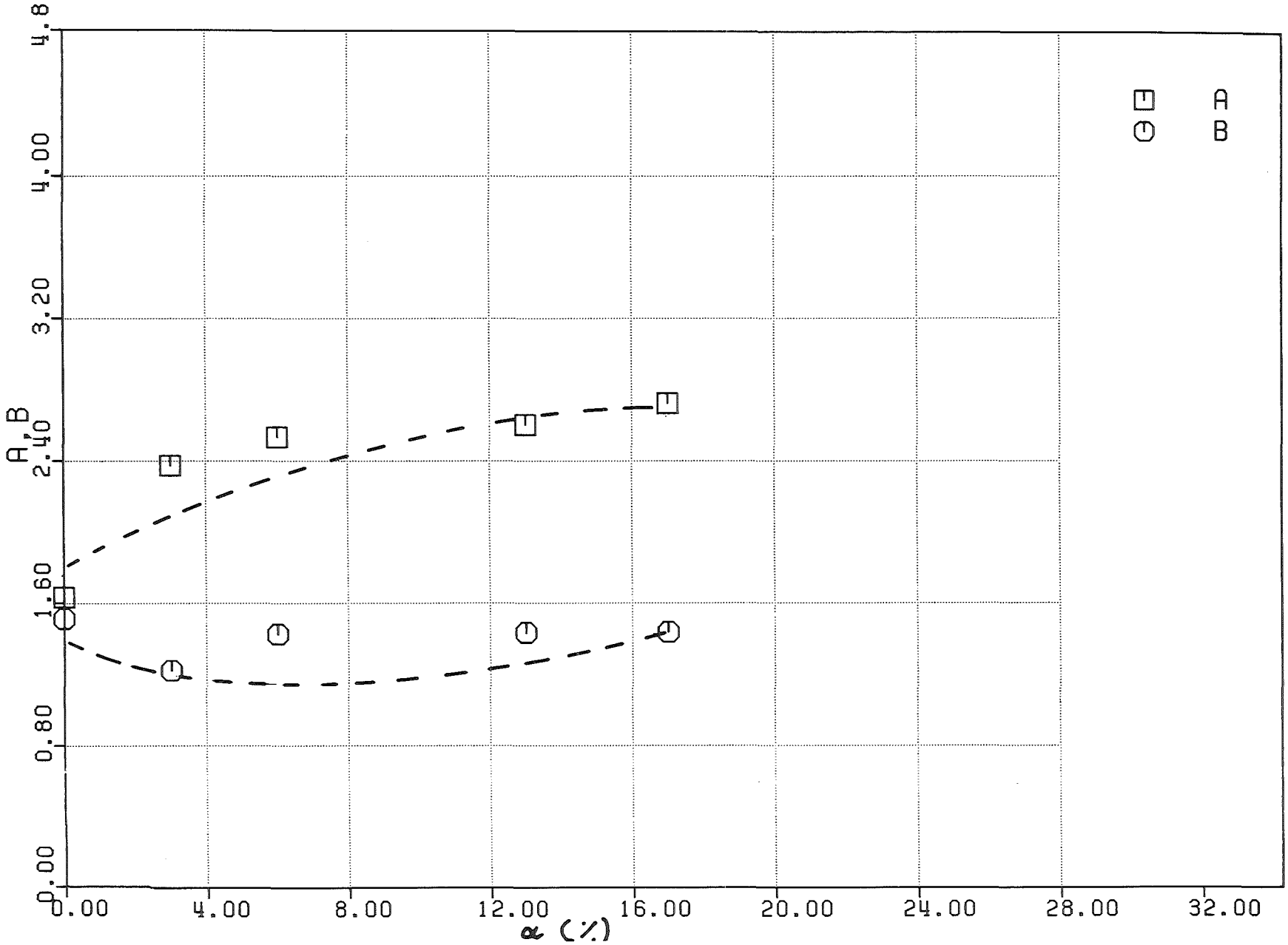

Fig. 5.55 - Experiments with Valve 1, R_p = 0.17. Fit of the coefficients A, B (Eq. 5.1) for the displacement of the mixture surface.

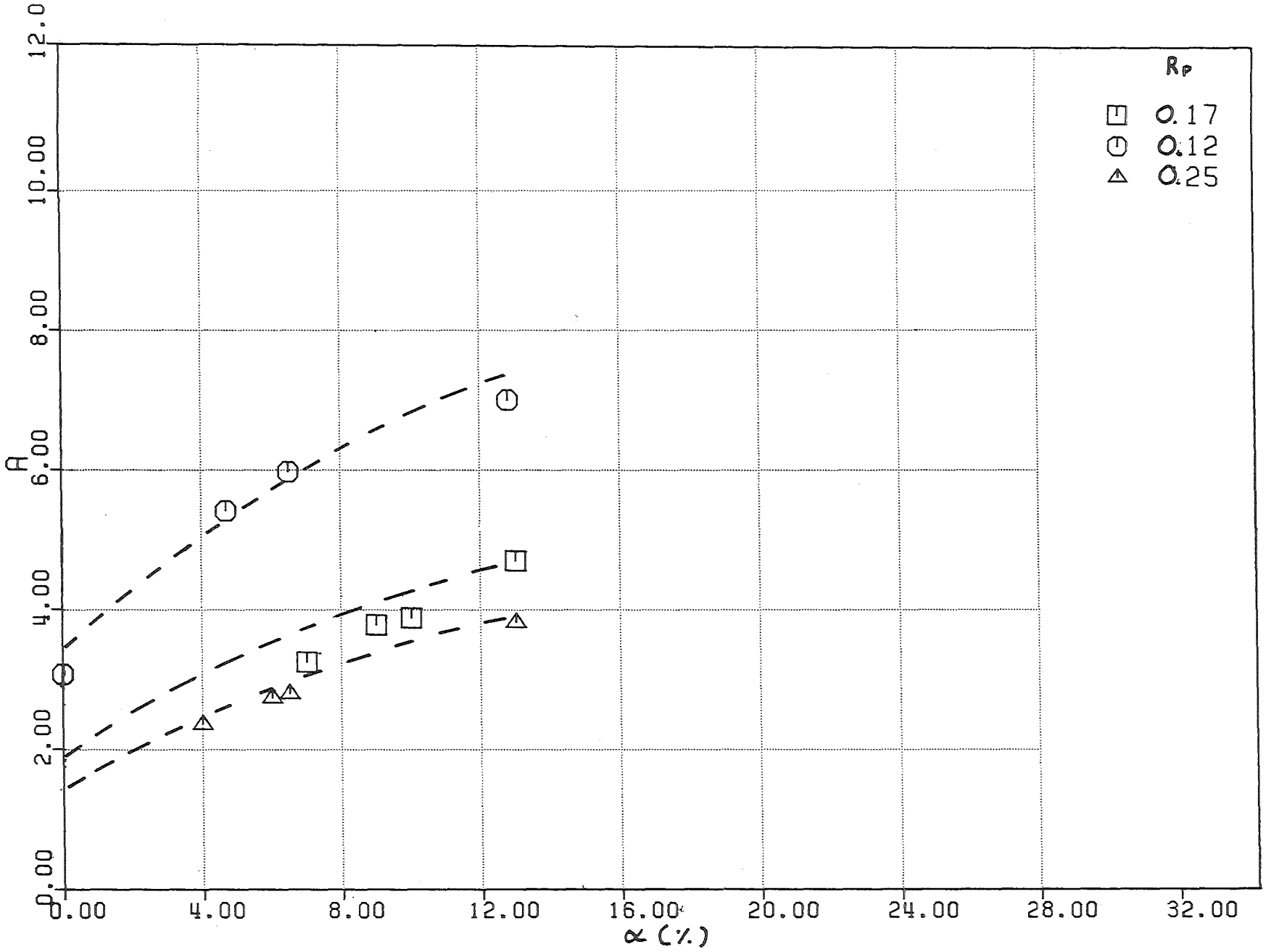

Fig. 5.56 - Experiments with Valve 2, R_p = 0.12, 0.17, 0.25.
Fit of the coefficients A (Eq. 5.1) for the displacement of the mixture surface.

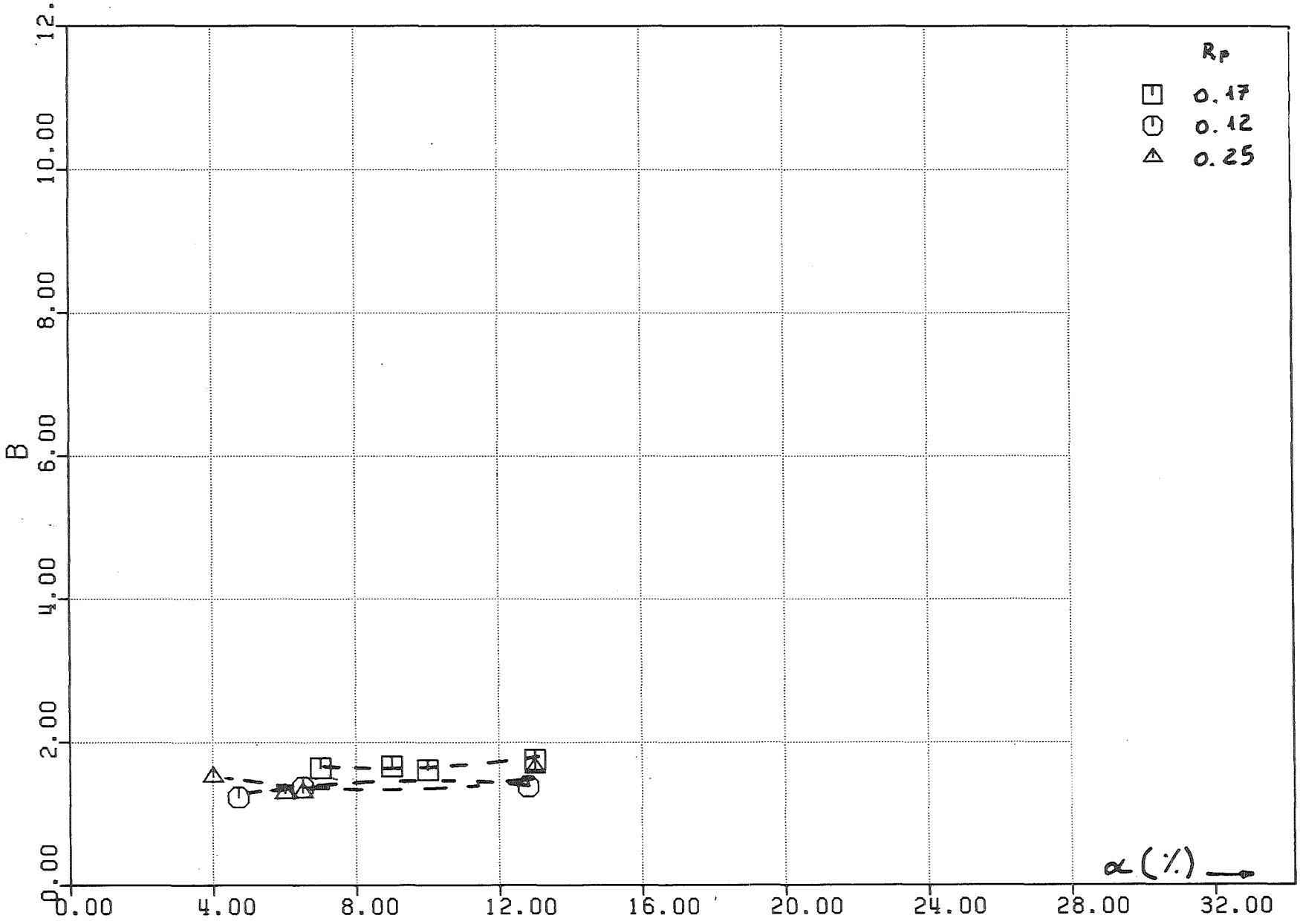

Fig. 5.57 - Experiments with Valve 2, R_p = 0.12, 0.17, 0.25.
Fit of the coefficients B (Eq. 5.1) for the displacement of the mixture surface.

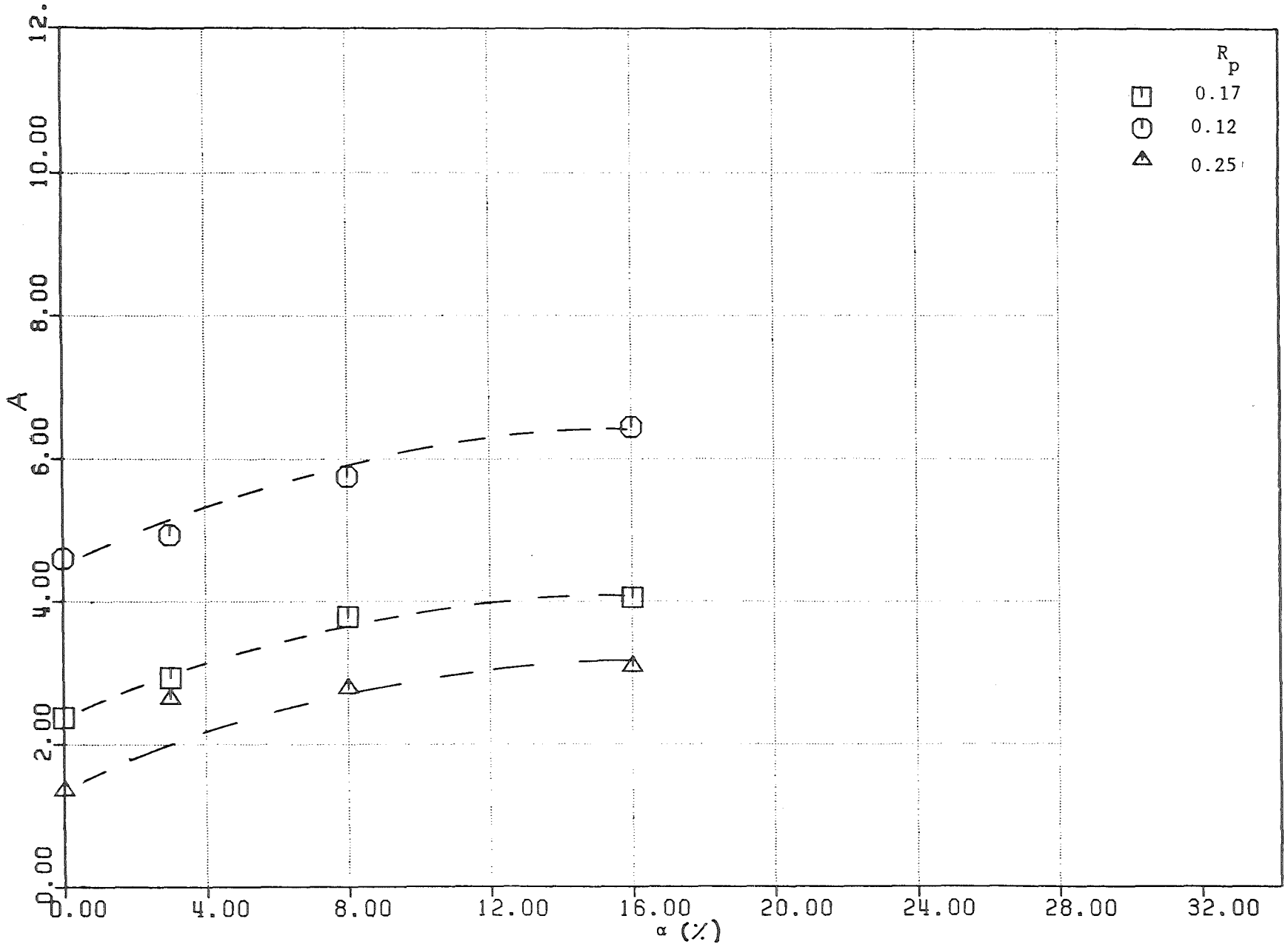

Fig. 5.58 - Experiments with Explosion Nut , R_p = 0.12, 0.17, 0.25
Fit of the coefficients A (Eq. 5.1) for the displacement of the mixture surface.

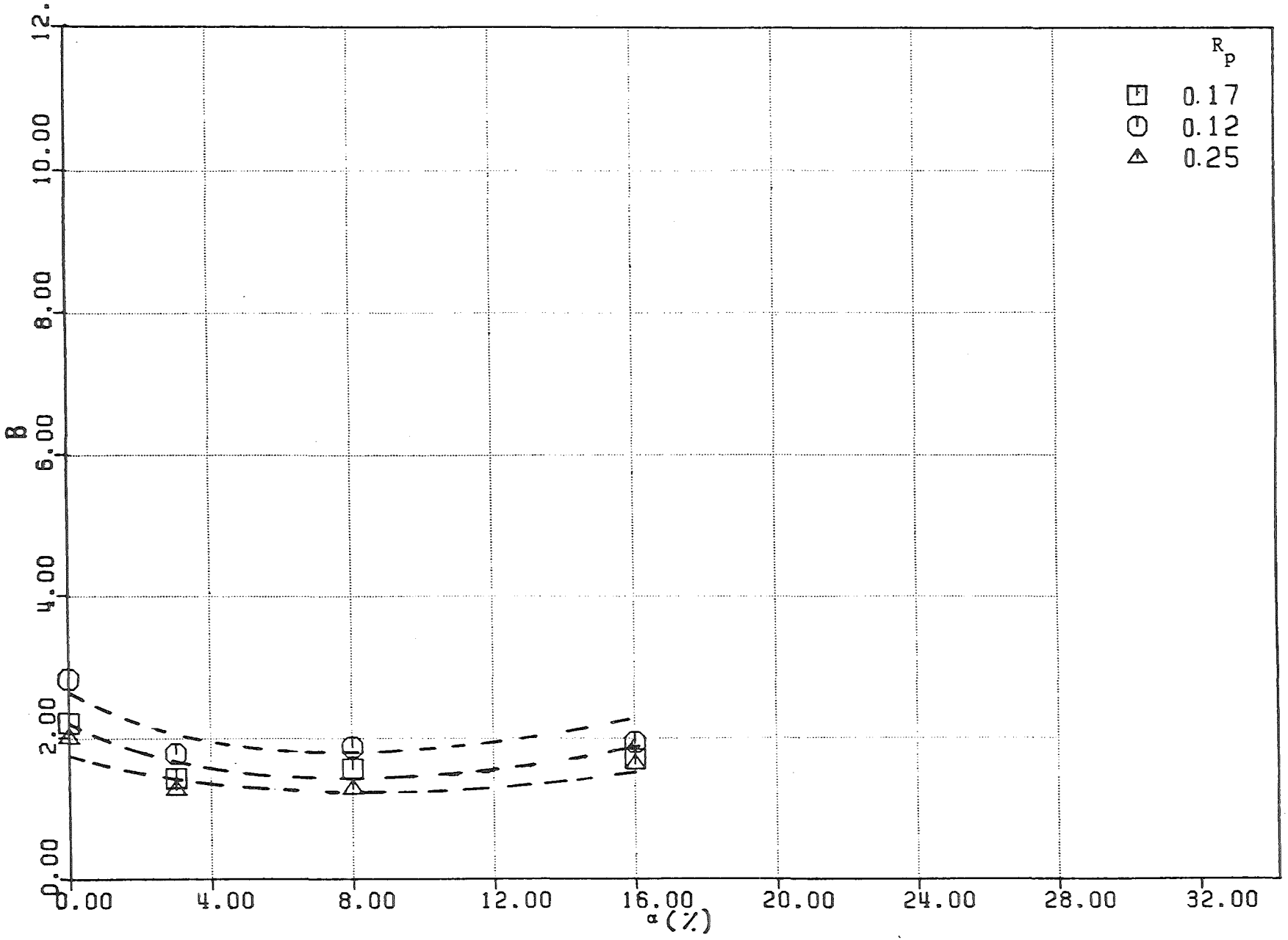

Fig. 5.59 - Experiments with Explosion Nut , R_p = 0.12, 0.17, 0.25
Fit of the coefficients B (Eq. 5.1) for the displacement of the mixture surface.

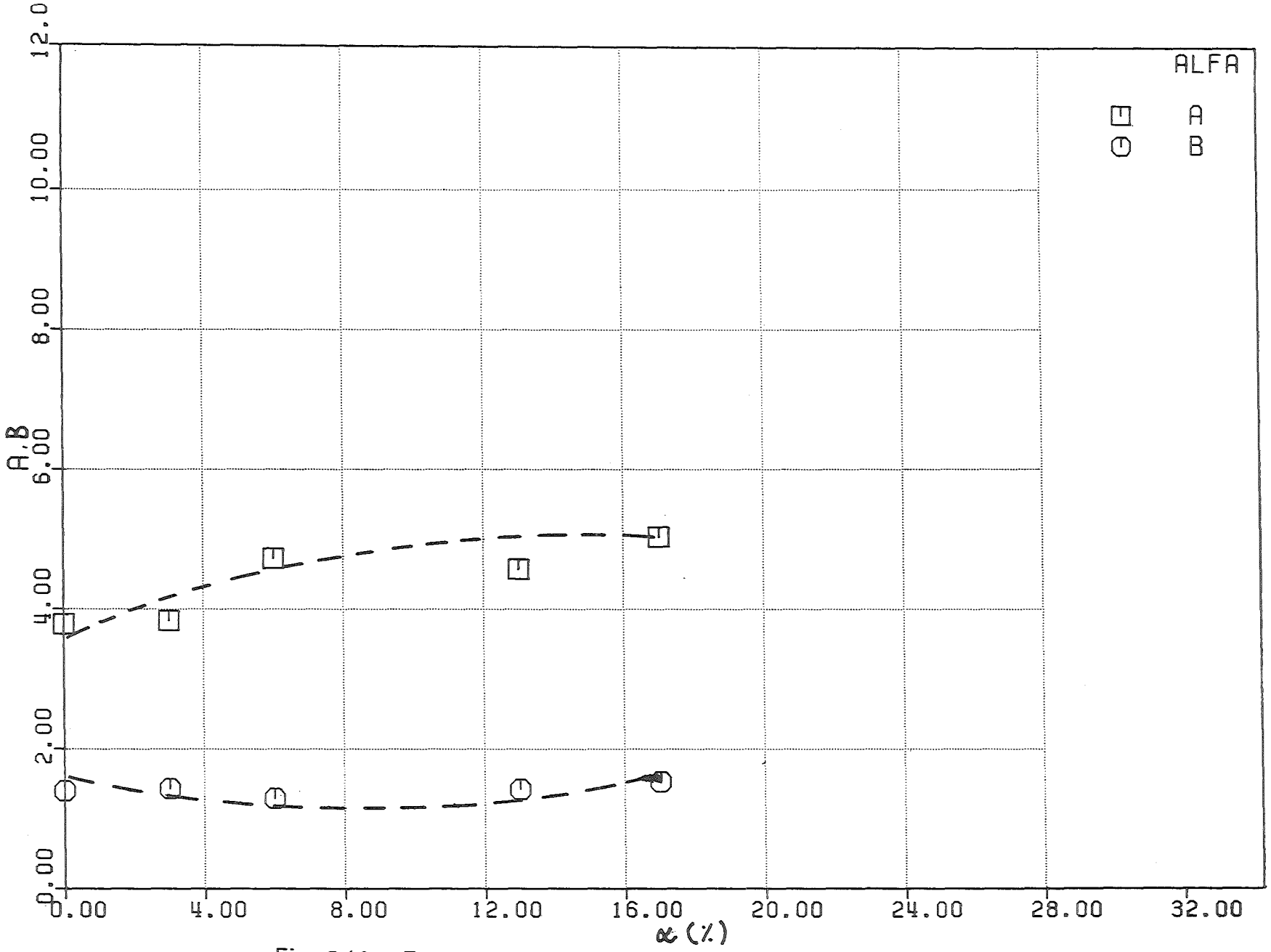

Fig. 5.60 - Experiments with Valve 1, R_p = 0.17. Fit of the coefficients A, B (Eq. 5.1) for the displacement of the jet.

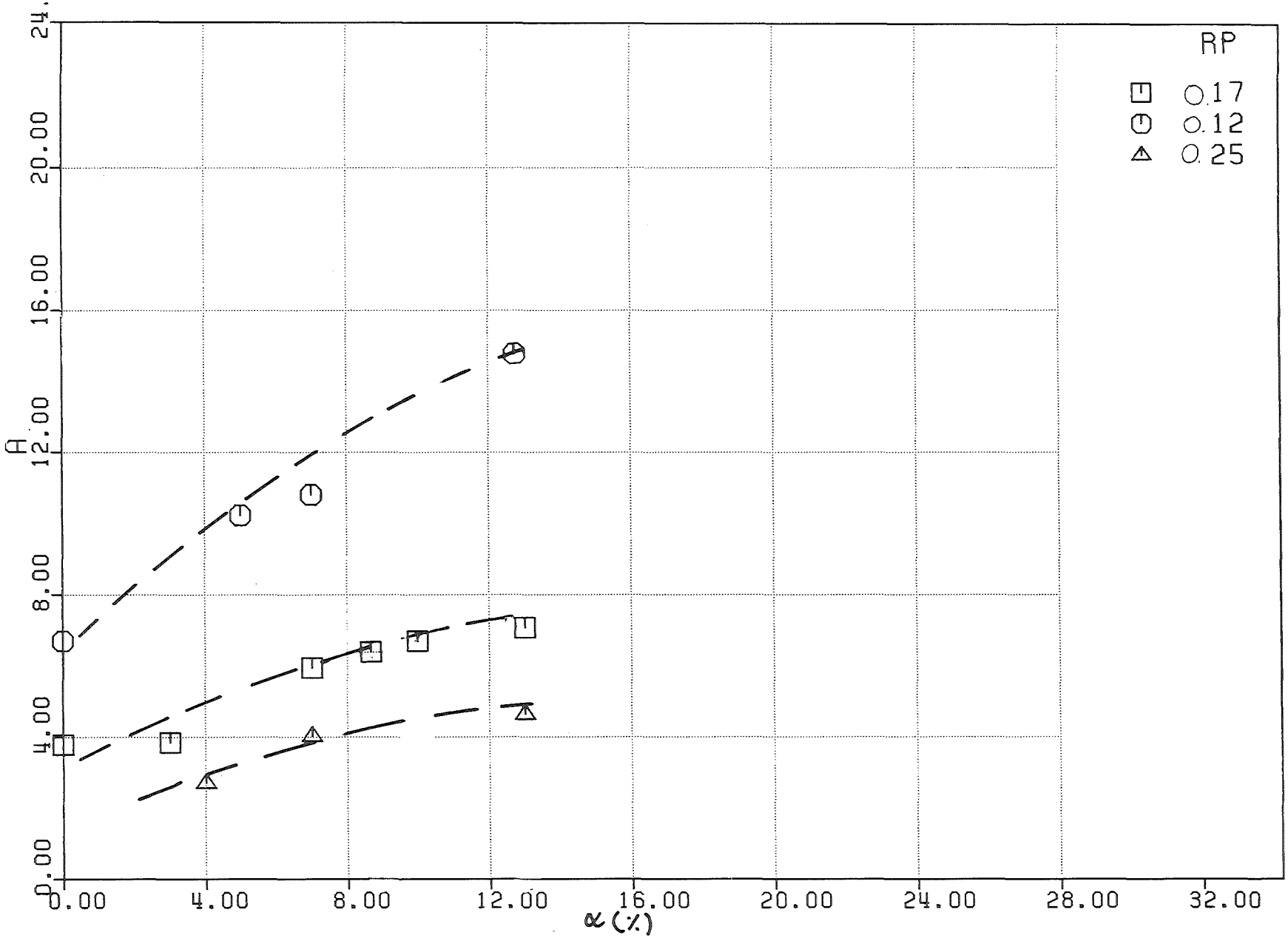

Fig.5-61 - Experiments with Valve 2, R_p = 0.12, 0.17, 0.25.
Fit of the coefficients A (Eq. 5.1) for the displacement of the jet.

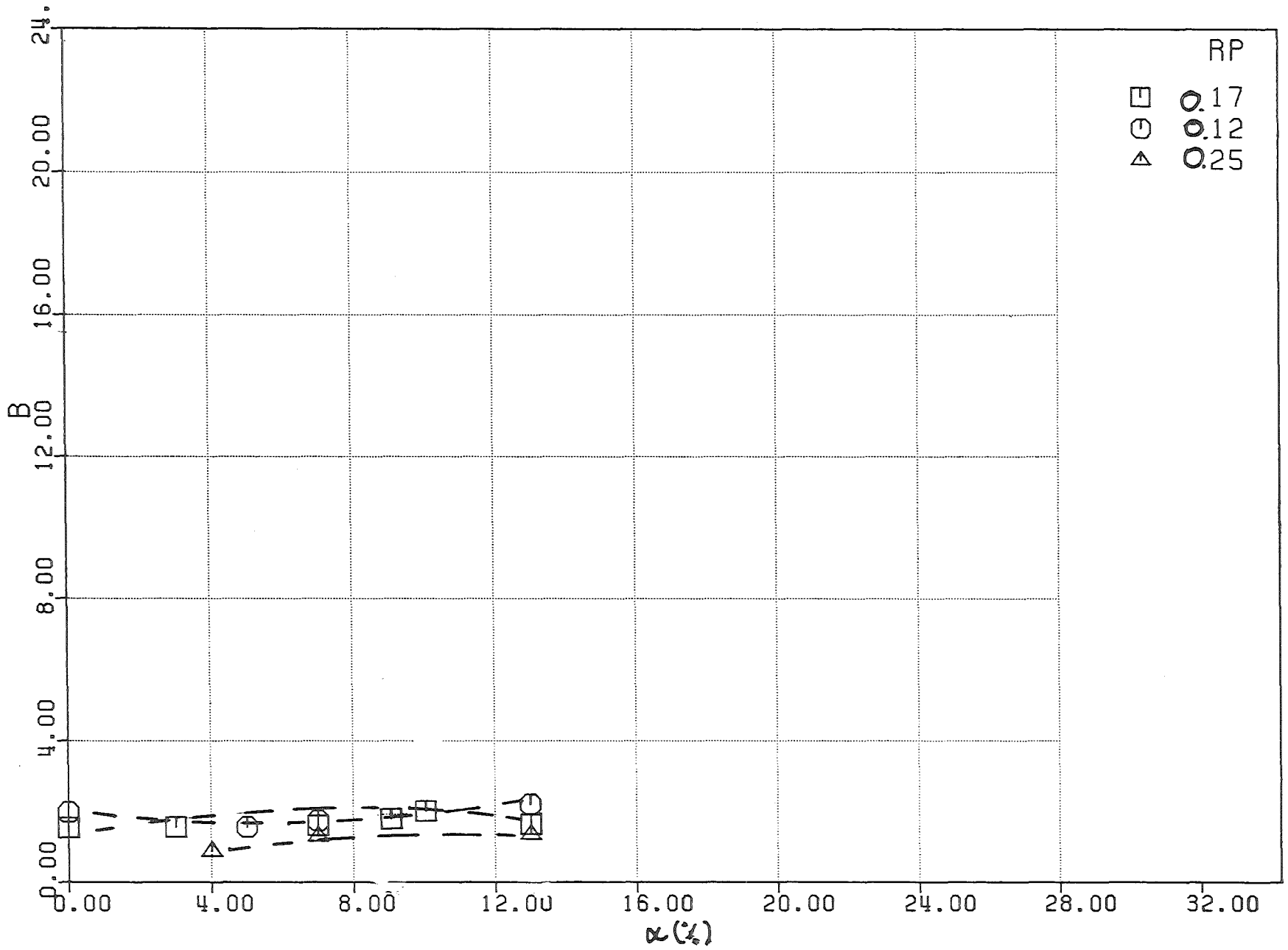

Fig. 5.62 - Experiments with Valve 2, R_p = 0.12, 0.17, 0.25.
Fit of the coefficients B (Eq. 5.1) for the displacement of the jet.

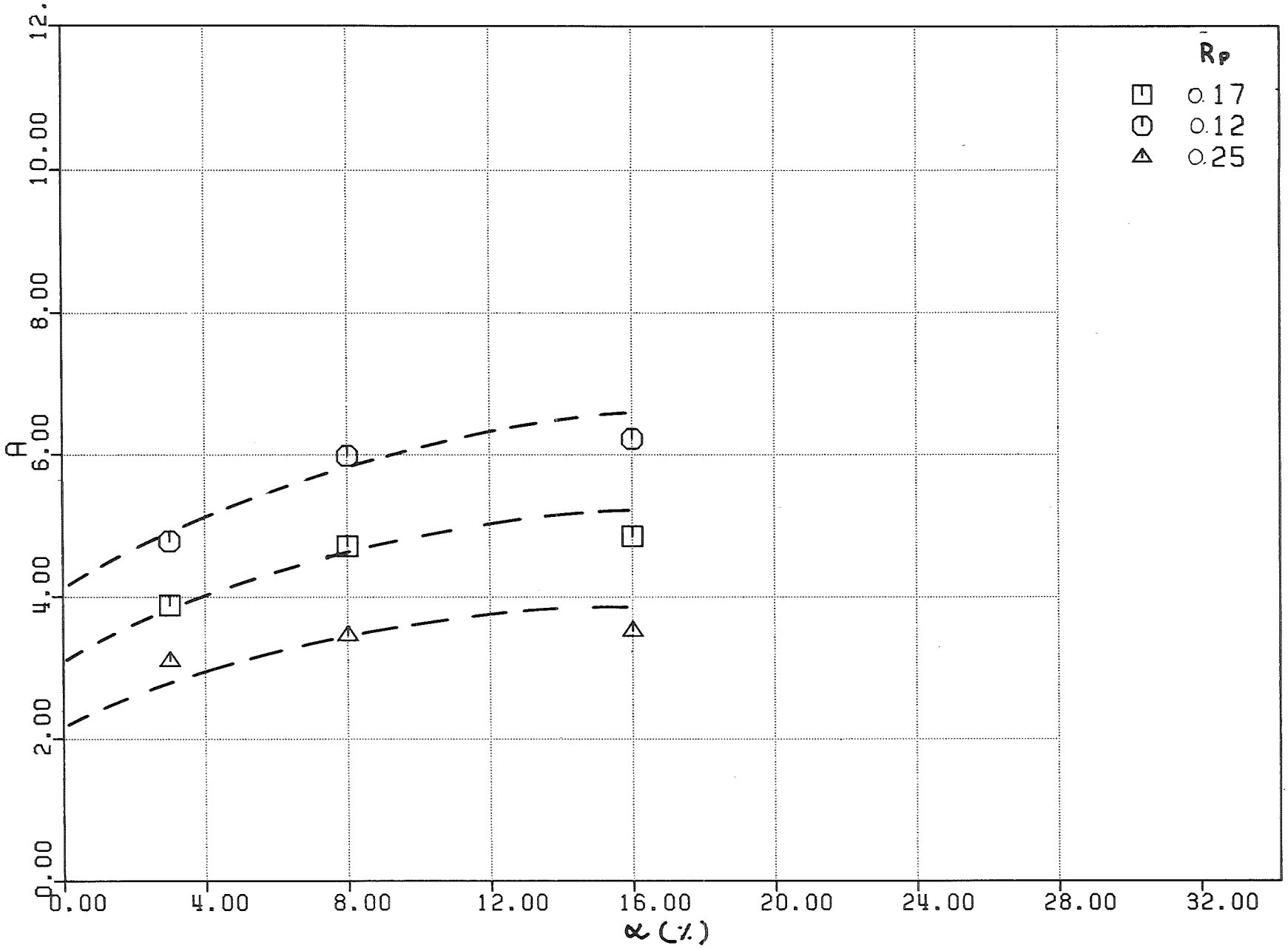

Fig. 5.63 - Experiments with Explosion Nut , R_p = 0.12, 0.17, 0.25

Fit of the coefficients A (Eq. 5.1) for the displacement of the jet.

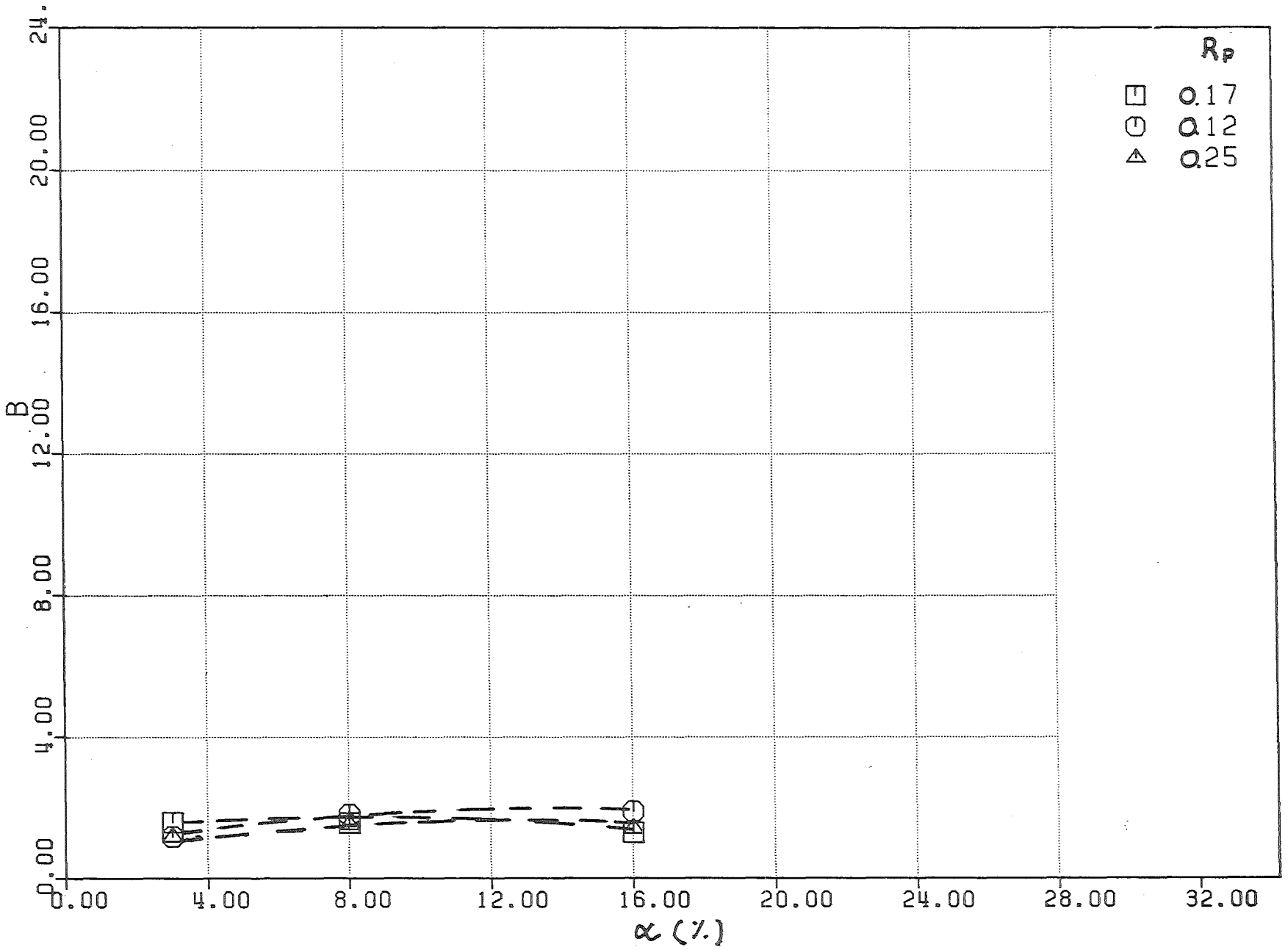

Fig. 5.64 - Experiments with Explosion Nut , R_p = 0.12, 0.17, 0.25
Fit of the coefficients B (Eq. 5.1) for the displacement of the jet.

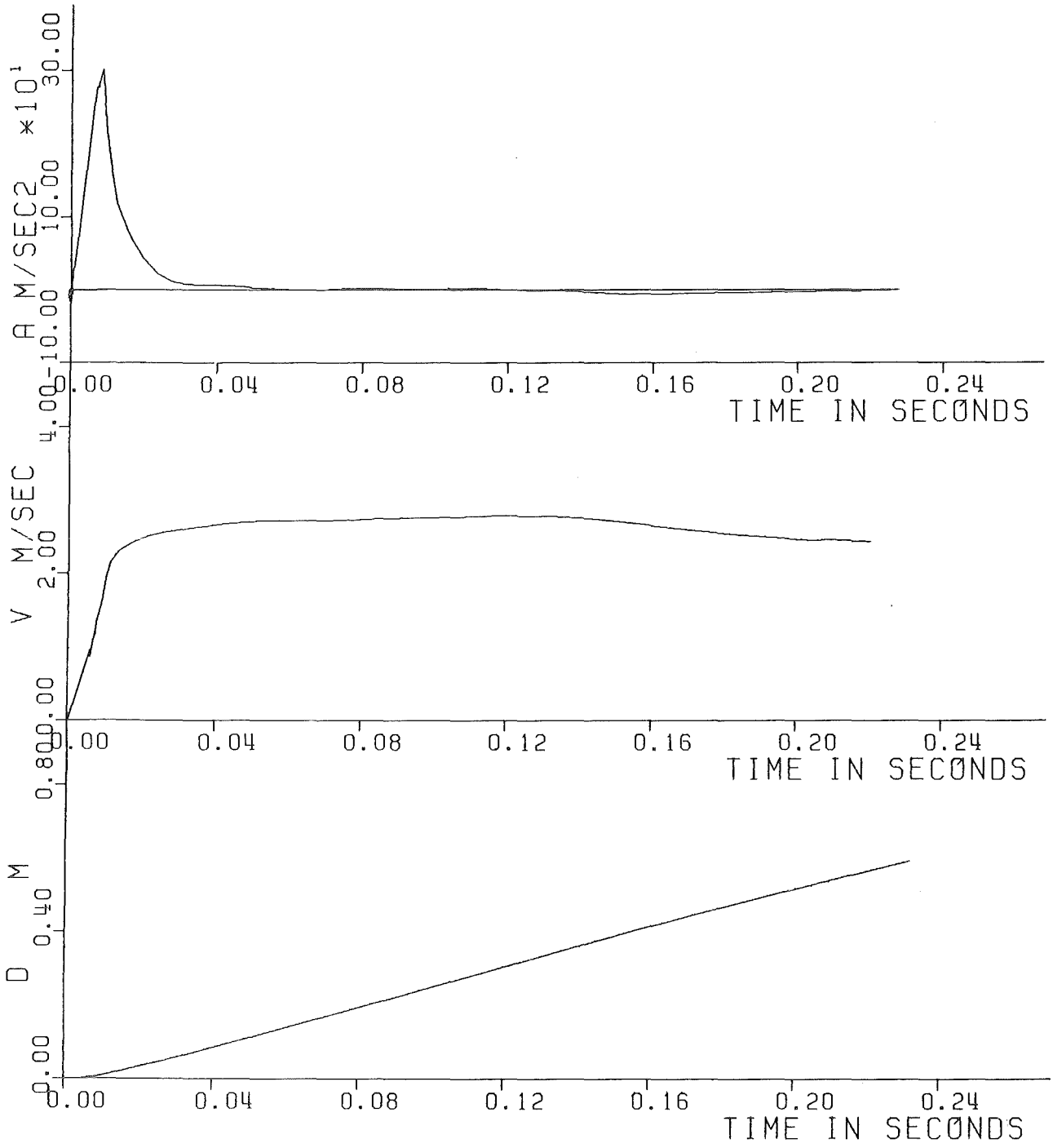

Fig. 61 - Experiment Nr. 1 - Displacement, Velocity and Acceleration of the piston.

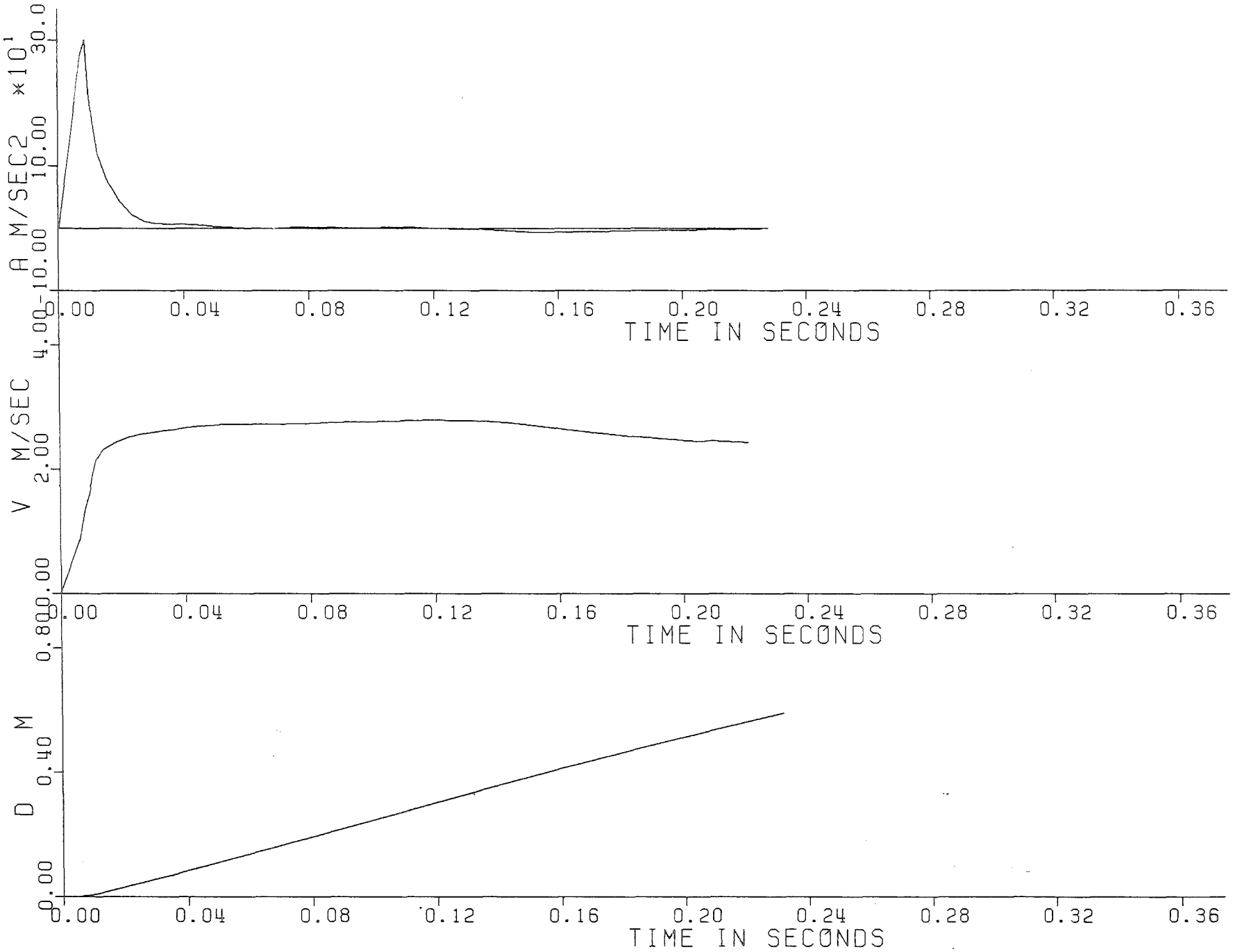

Fig. 6.2 - Experiment Nr. 2 - Displacement, Velocity and Acceleration of the piston.

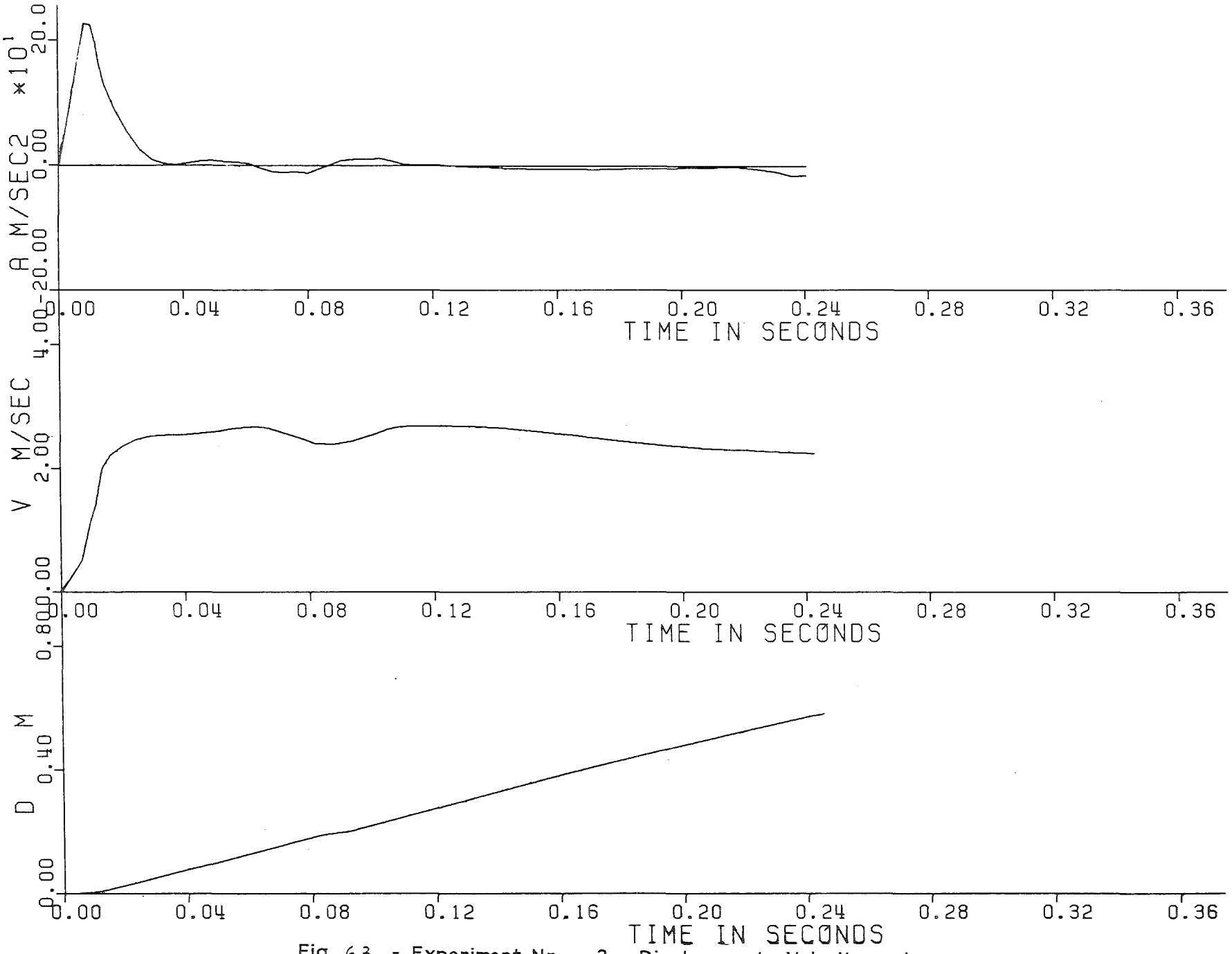

Fig. 6.3 - Experiment Nr. 3 - Displacement, Velocity and Acceleration of the piston.

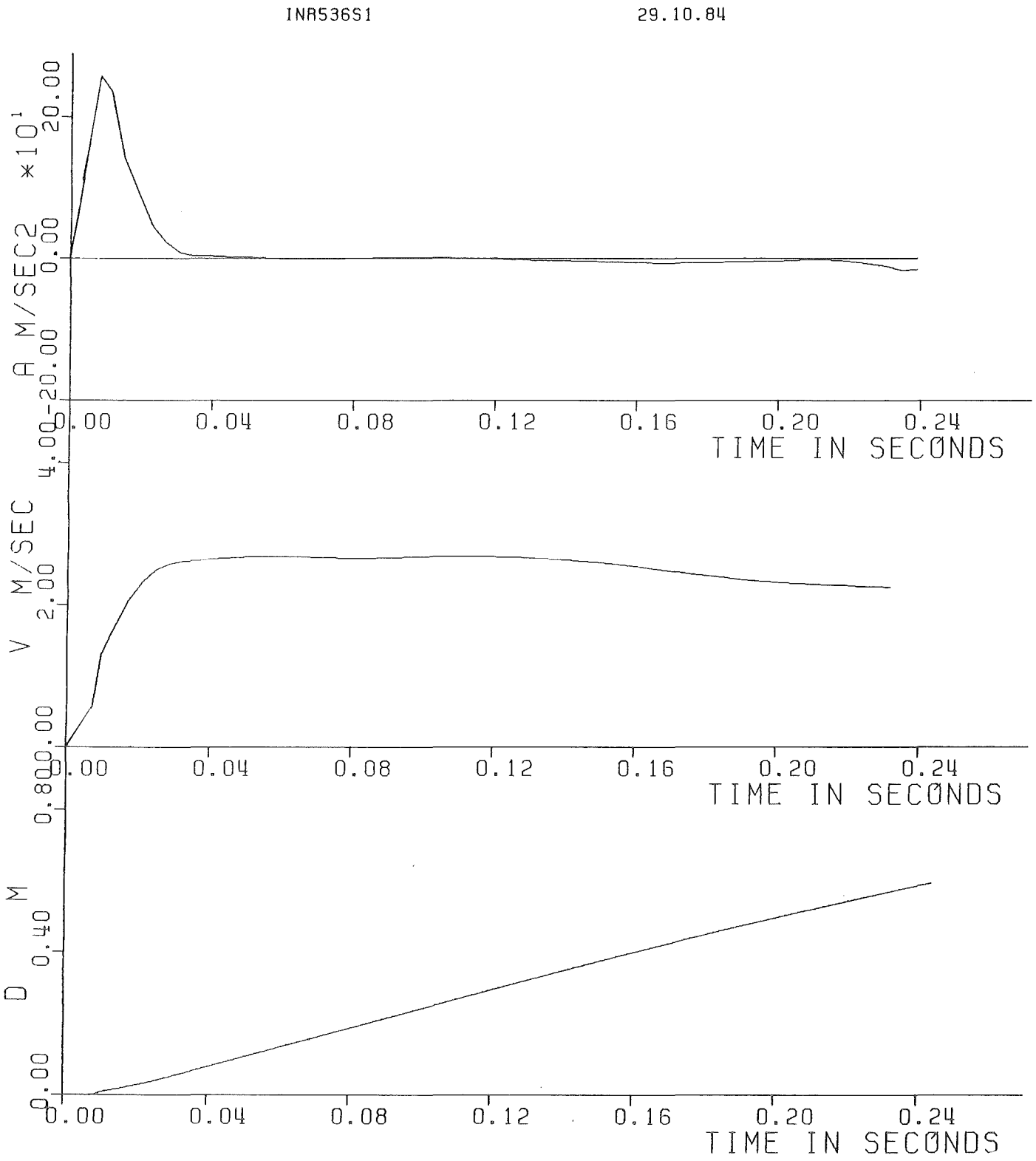

Fig. 6.4 - Experiment Nr. 4 - Displacement, Velocity and Acceleration of the piston.

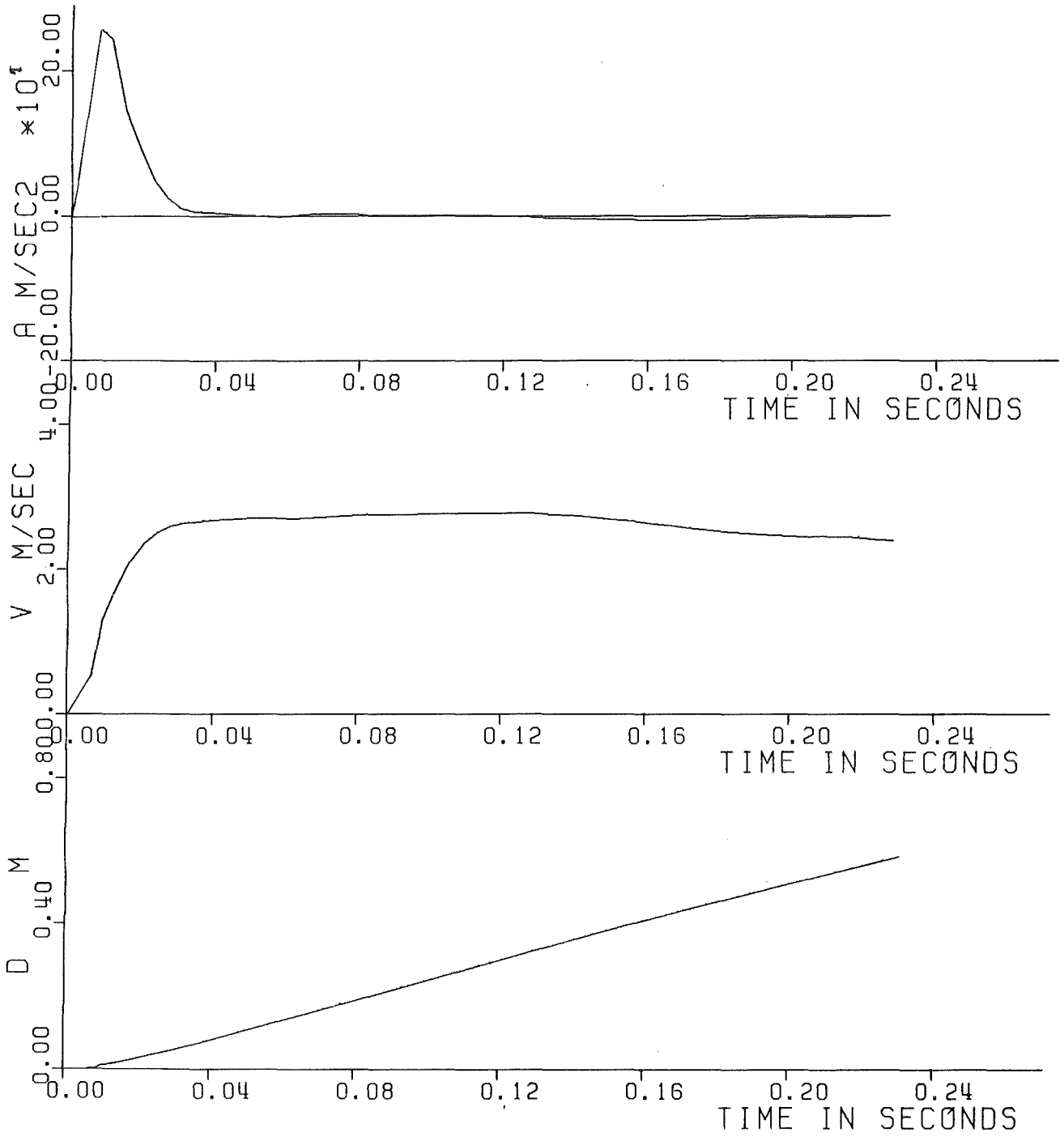

Fig. 6.5 - Experiment Nr. 5 - Displacement, Velocity and Acceleration of the piston.

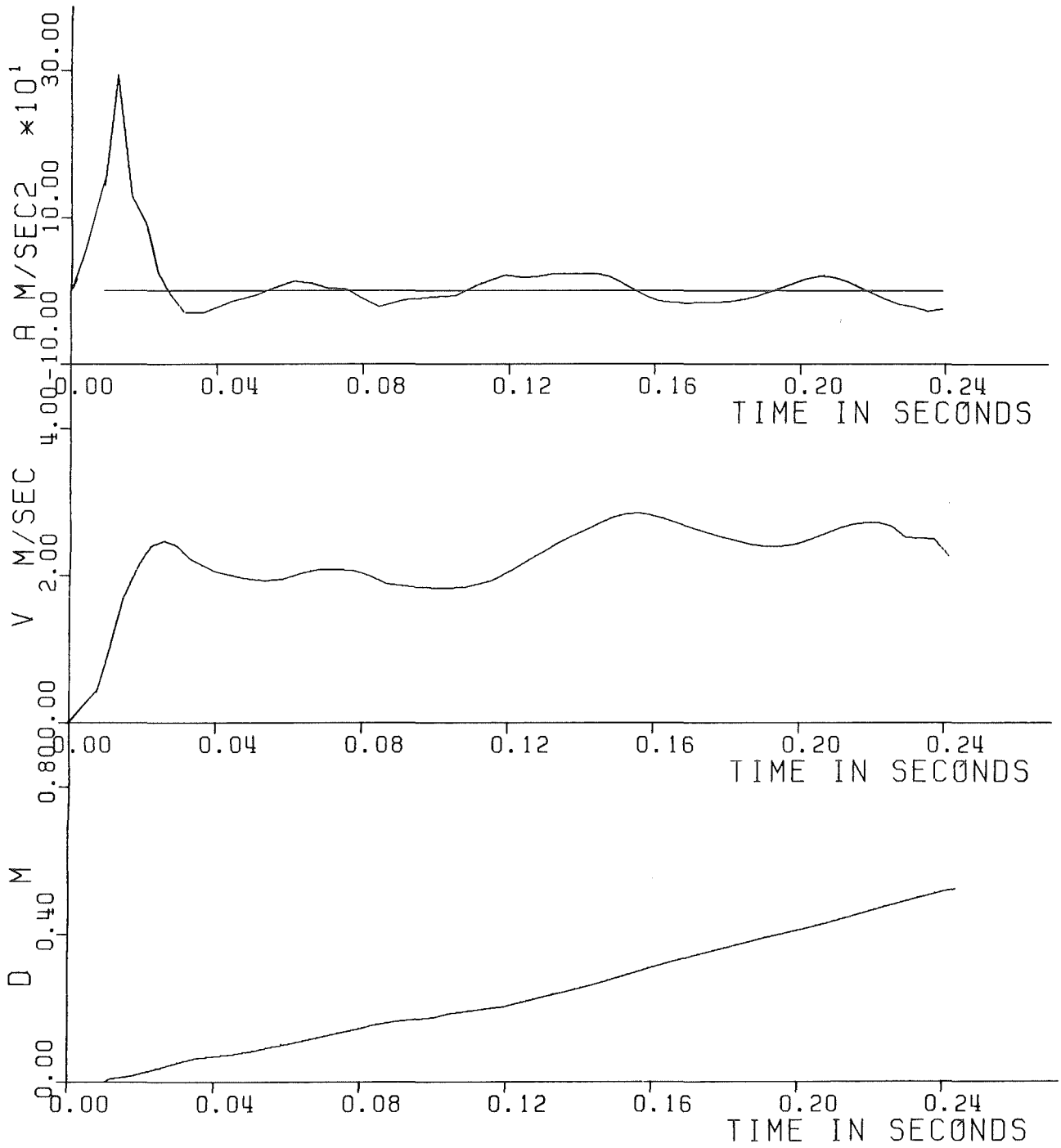

Fig. 6.6 - Experiment Nr. 6 - Displacement, Velocity and Acceleration of the piston.

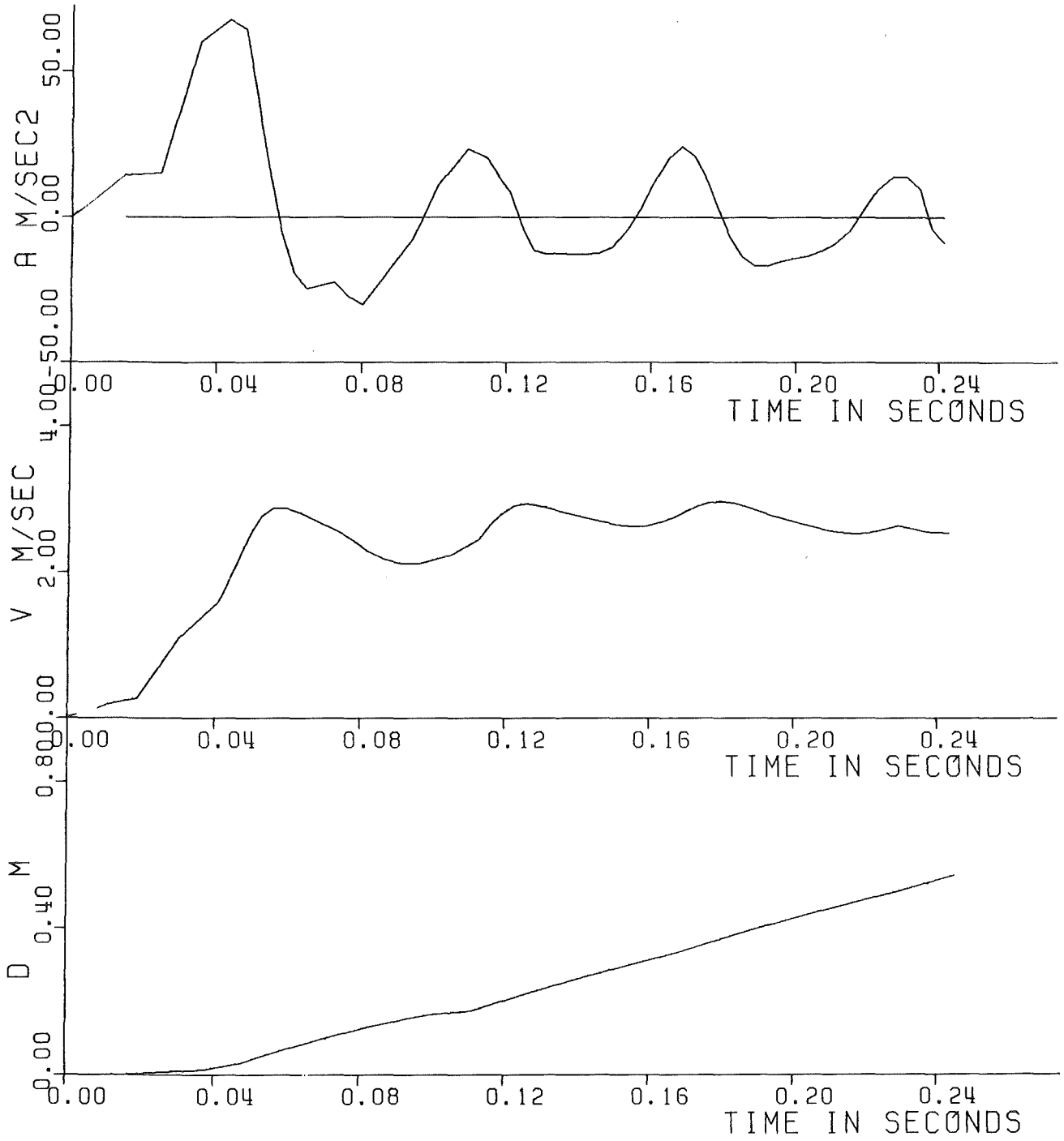

Fig. 6.7 - Experiment Nr. 7 - Displacement, Velocity and Acceleration of the piston.

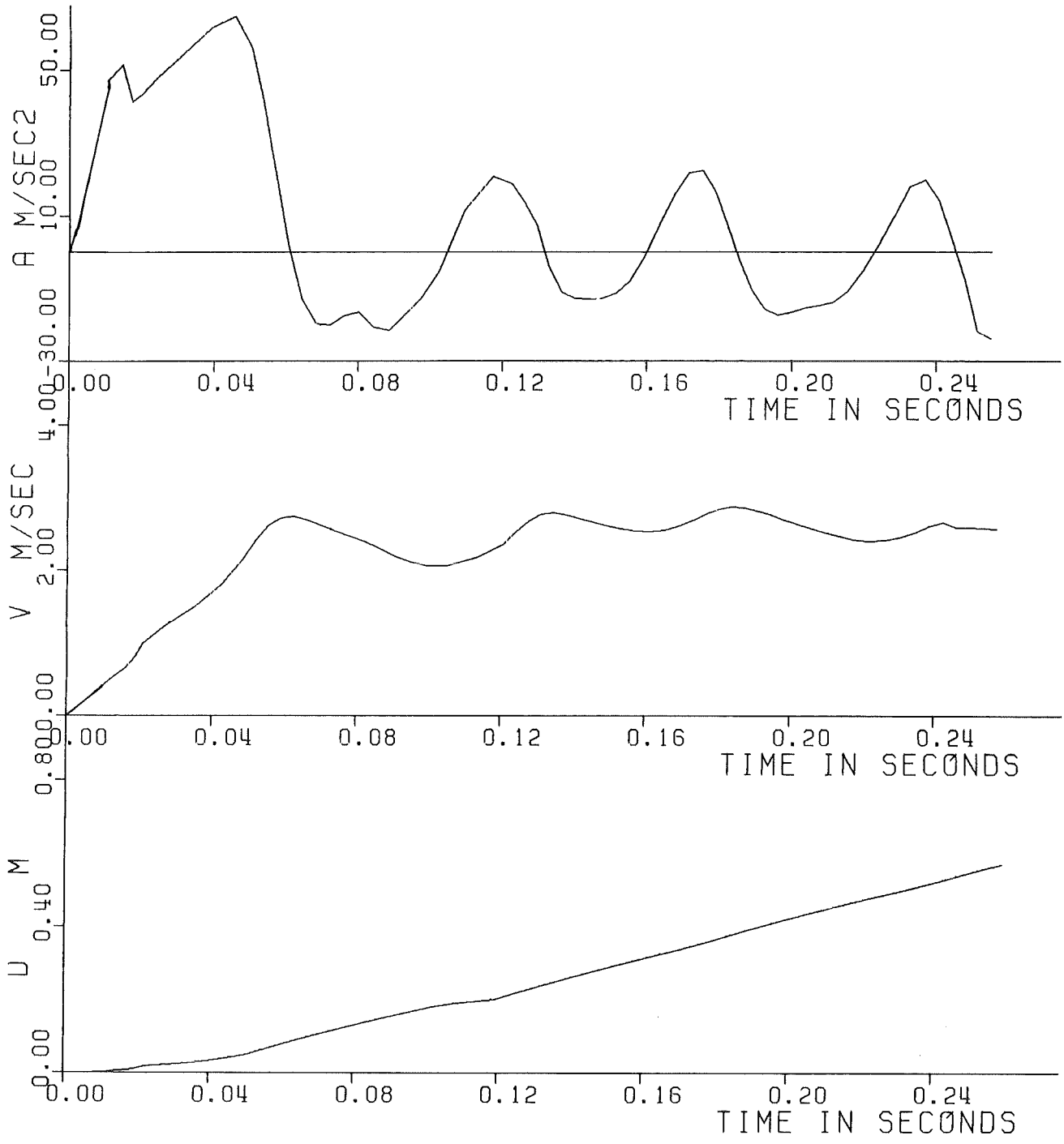

Fig. 6.8 - Experiment Nr. 8 - Displacement, Velocity and Acceleration of the piston.

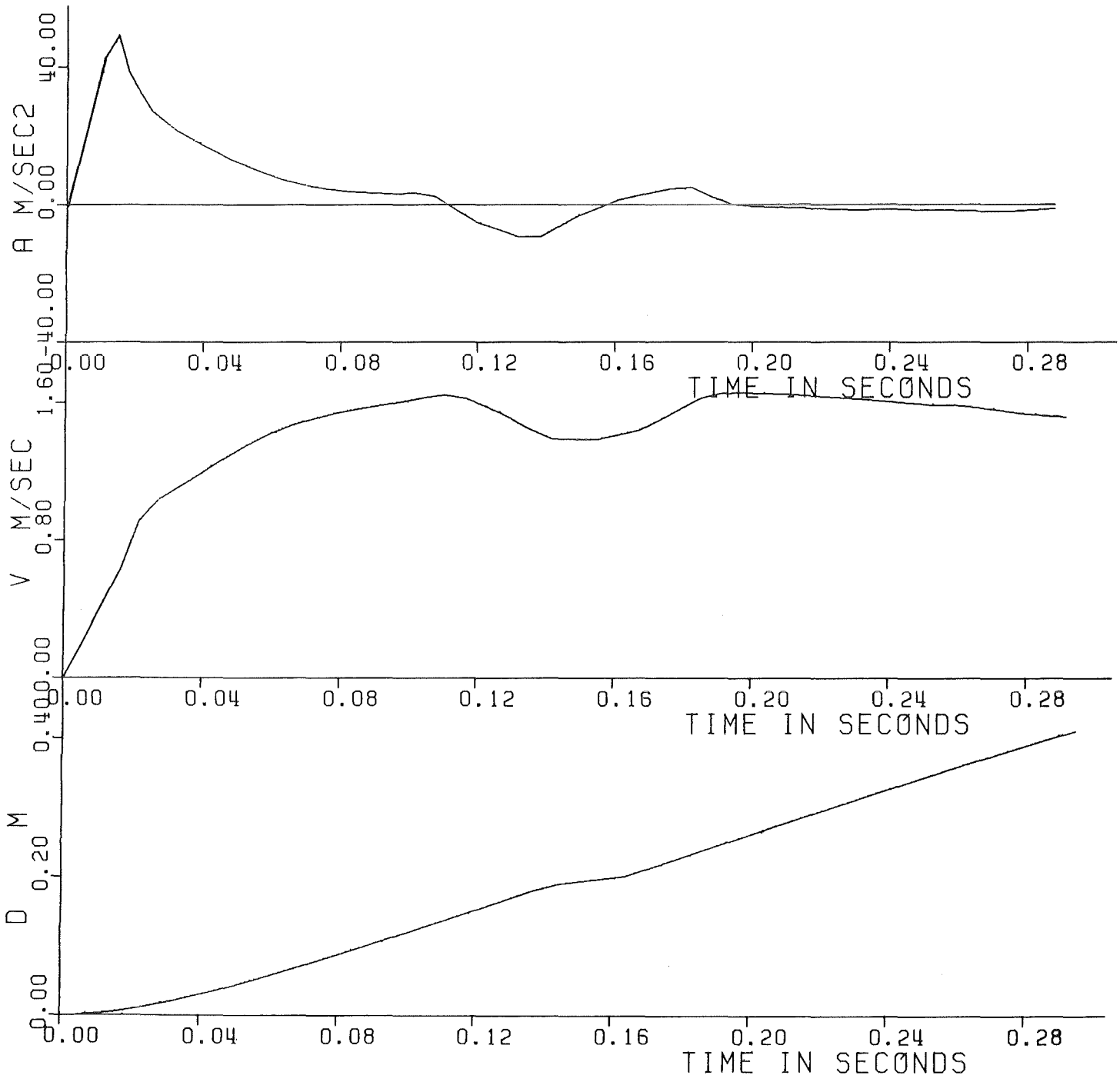

Fig. 6.9 - Experiment Nr. 9 - Displacement, Velocity and Acceleration of the piston.

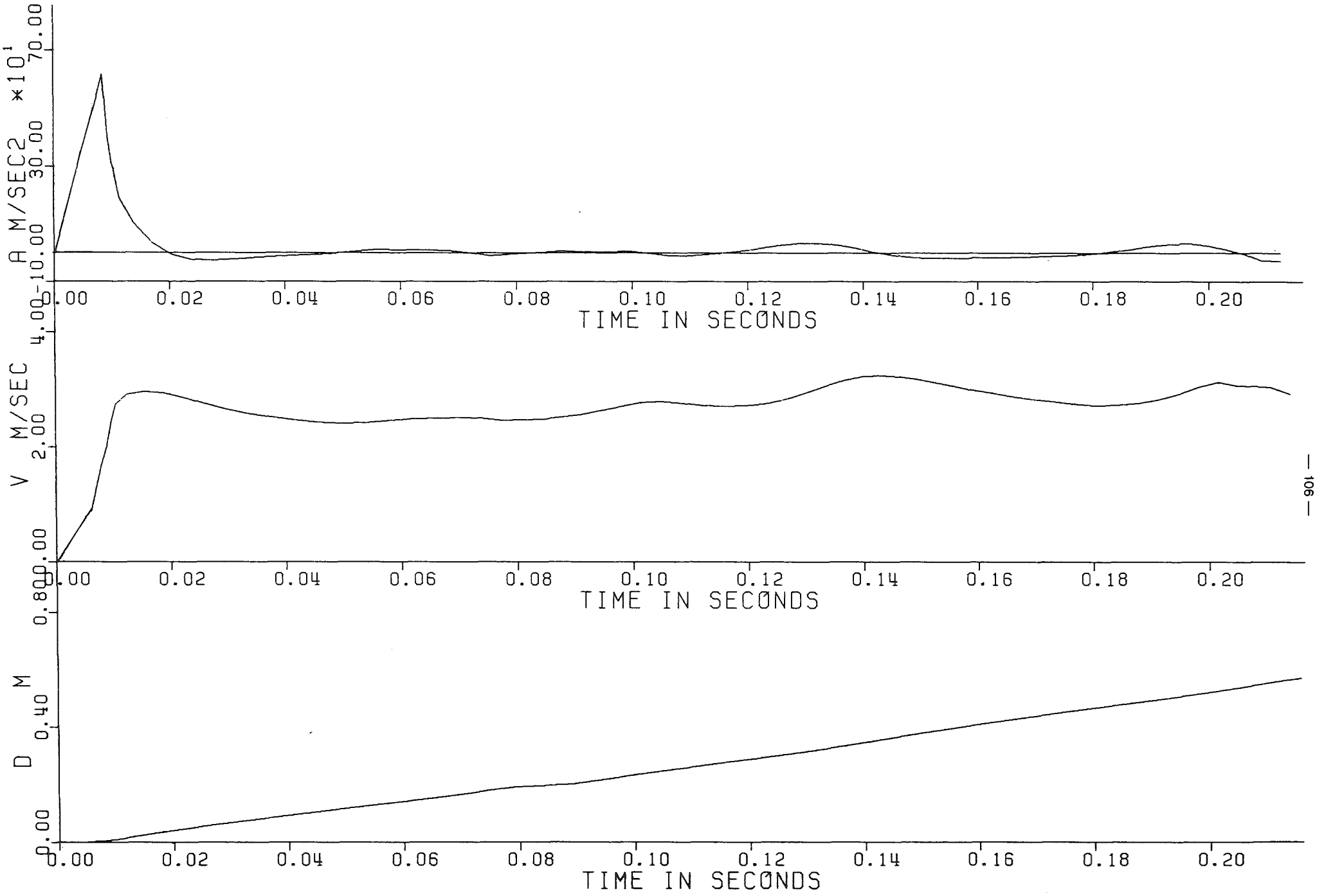

Fig. 6.10 - Experiment Nr. 10 - Displacement, Velocity and Acceleration of the piston.

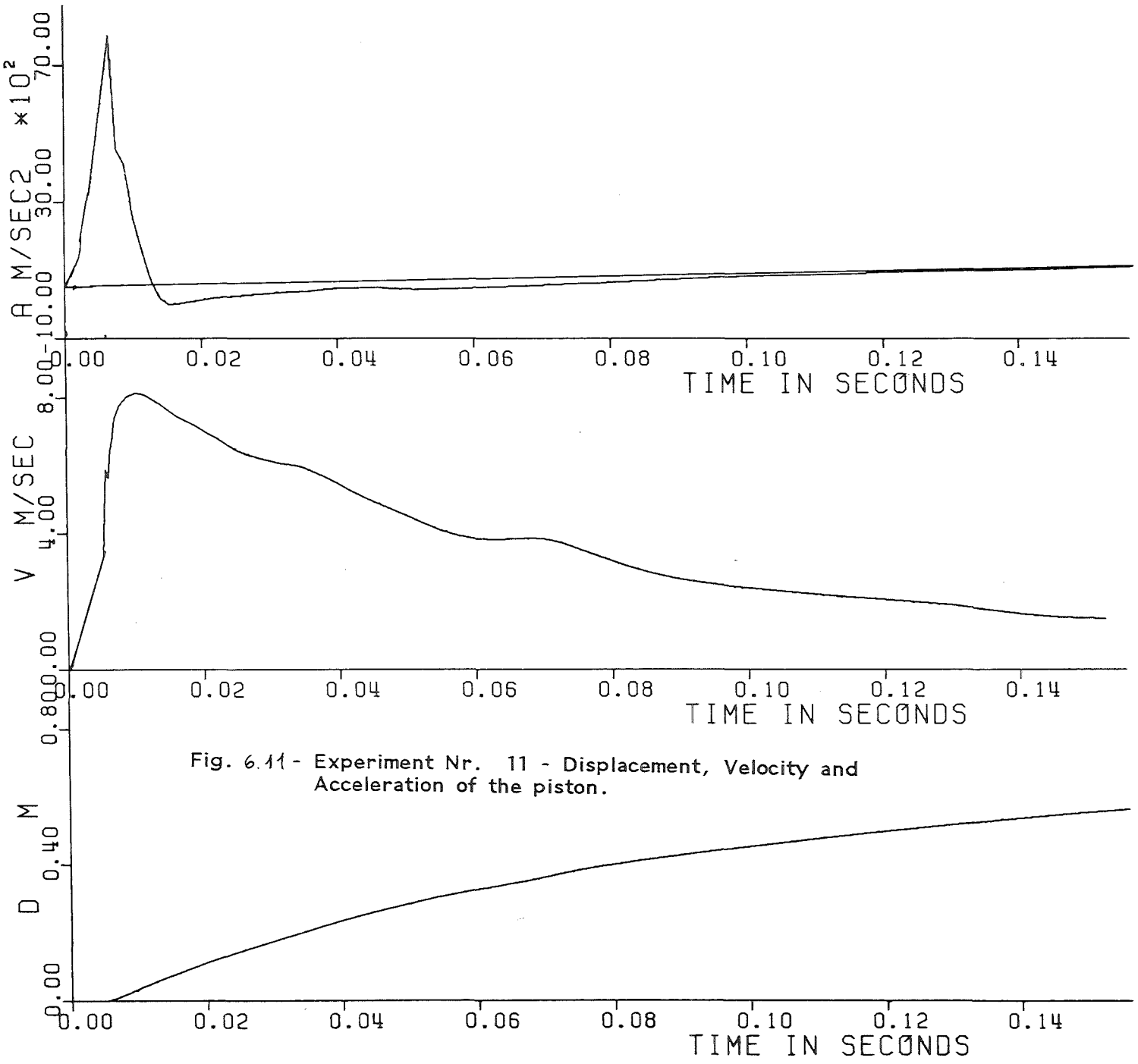

Fig. 6.11 - Experiment Nr. 11 - Displacement, Velocity and Acceleration of the piston.

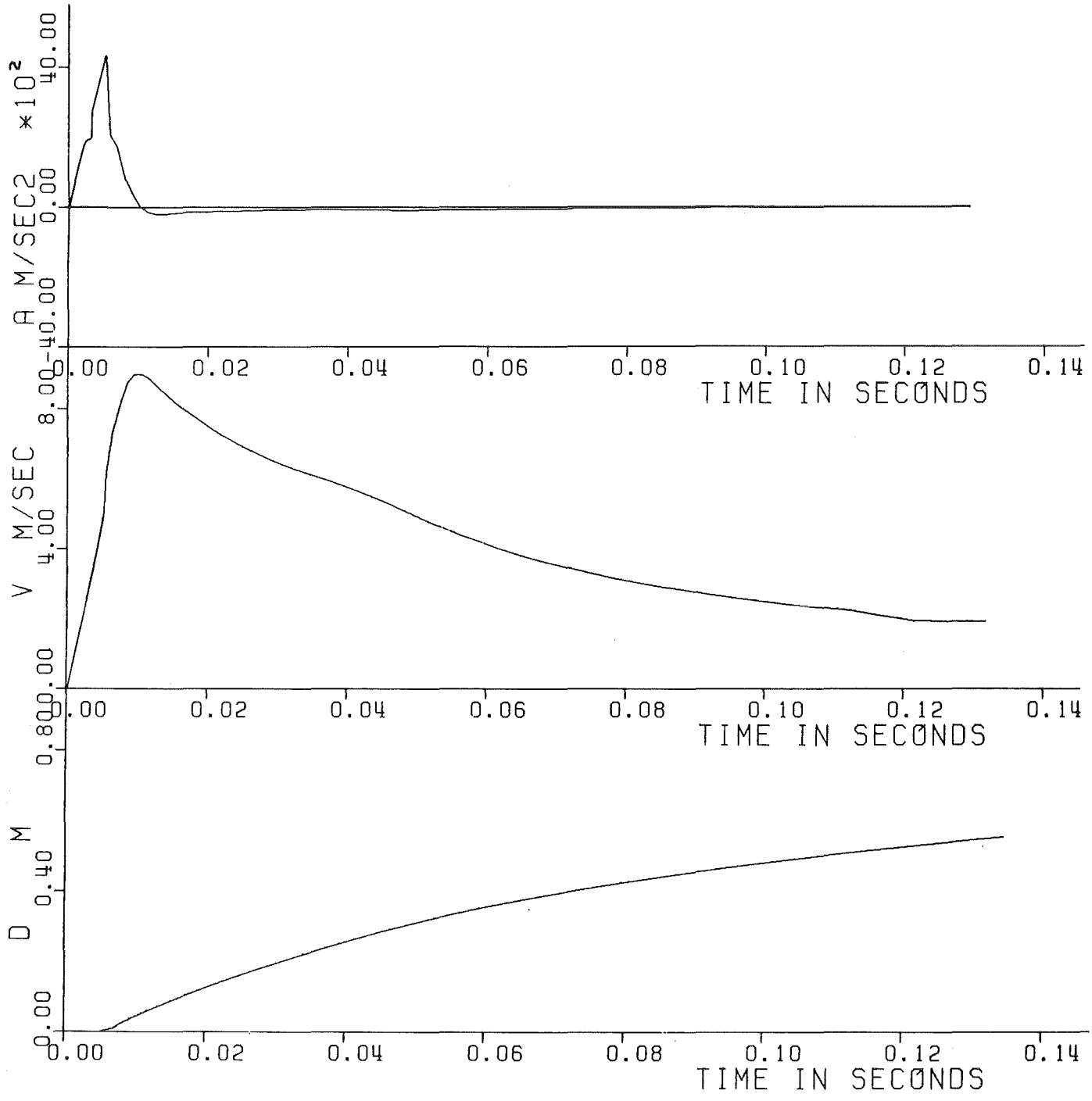

Fig. 6.12 - Experiment Nr. 12 - Displacement, Velocity and Acceleration of the piston.

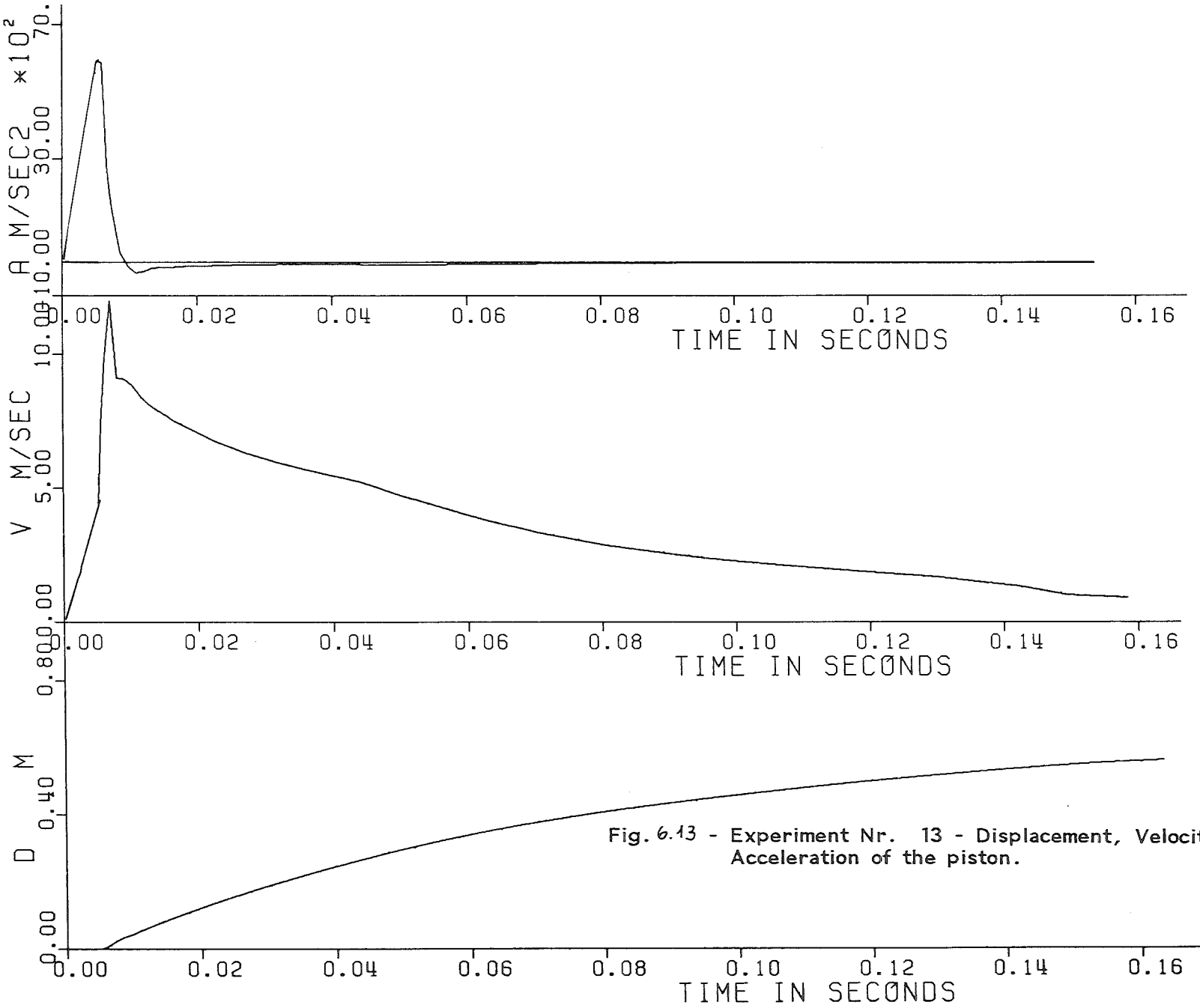

Fig. 6.13 - Experiment Nr. 13 - Displacement, Velocity and Acceleration of the piston.

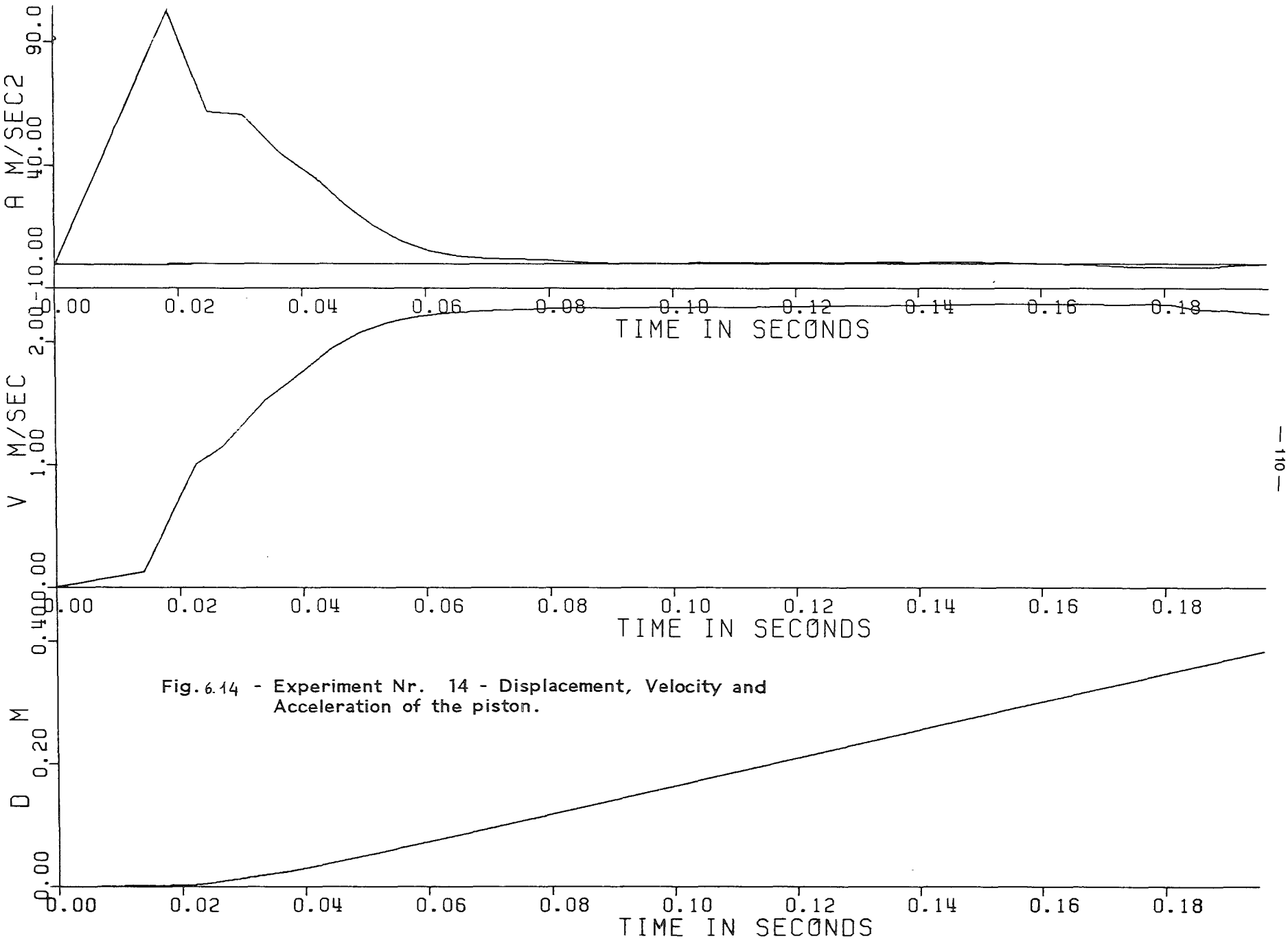

Fig. 6.14 - Experiment Nr. 14 - Displacement, Velocity and Acceleration of the piston.

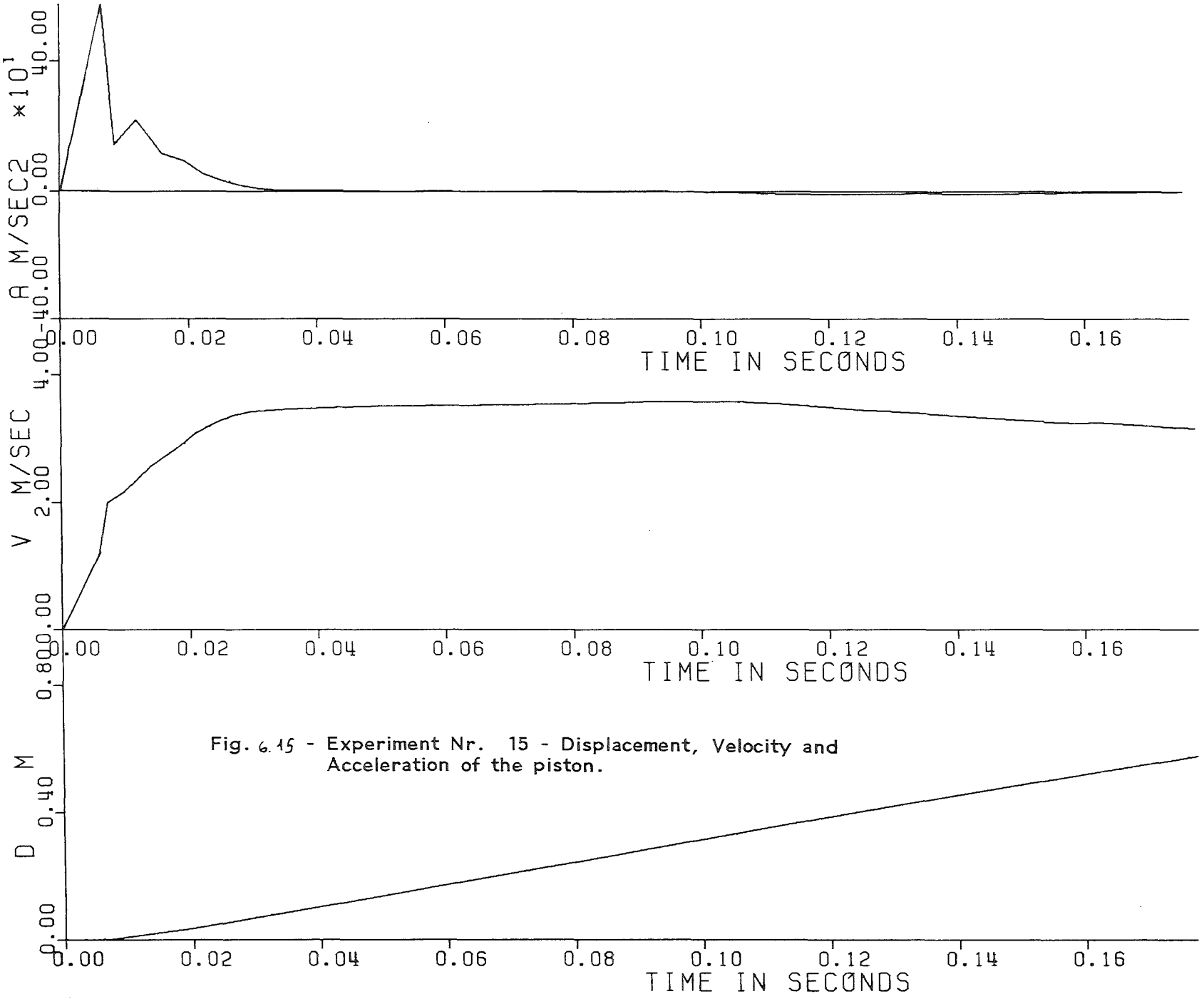

Fig. 6.15 - Experiment Nr. 15 - Displacement, Velocity and Acceleration of the piston.

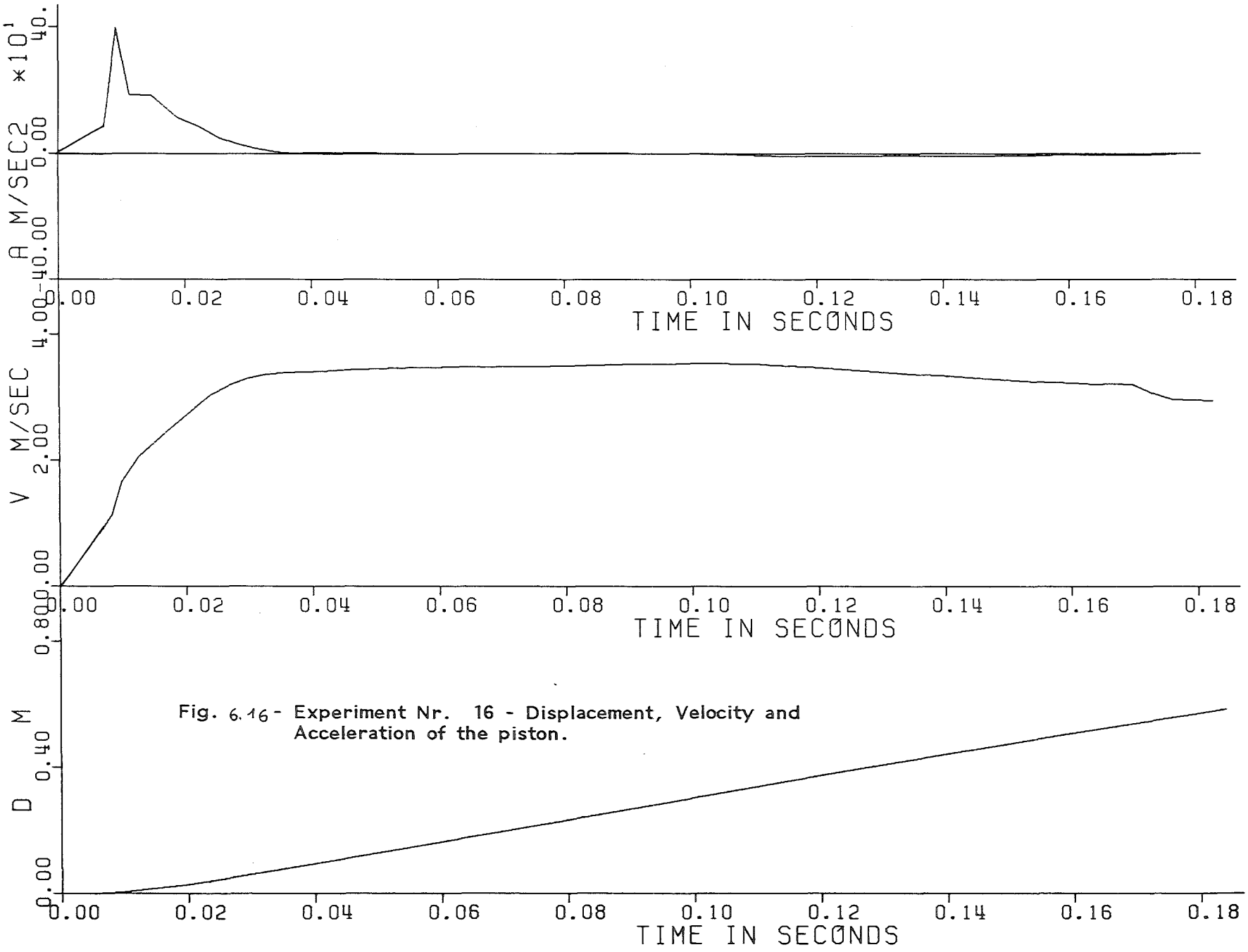

Fig. 6.16 - Experiment Nr. 16 - Displacement, Velocity and Acceleration of the piston.

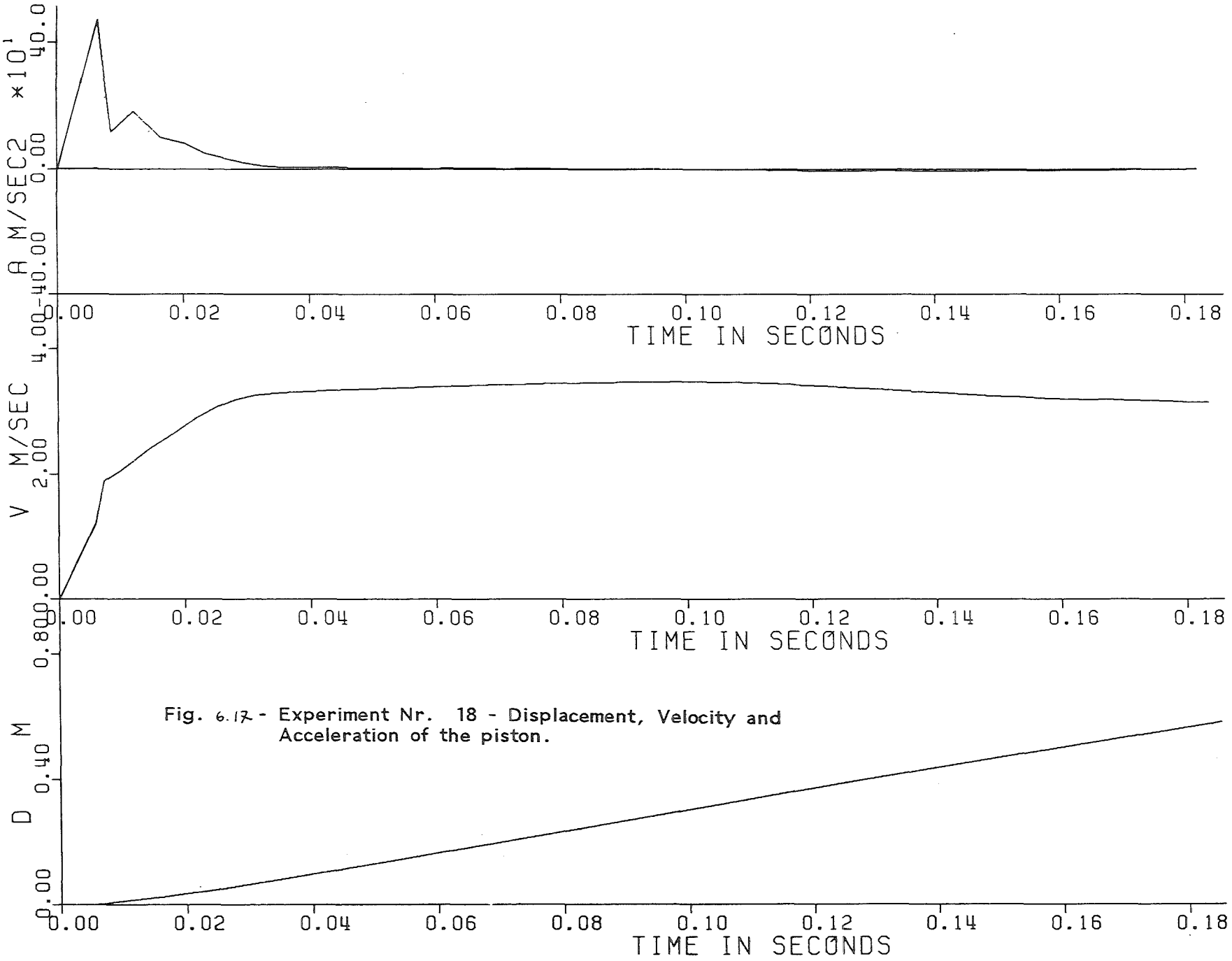

Fig. 6.17 - Experiment Nr. 18 - Displacement, Velocity and Acceleration of the piston.

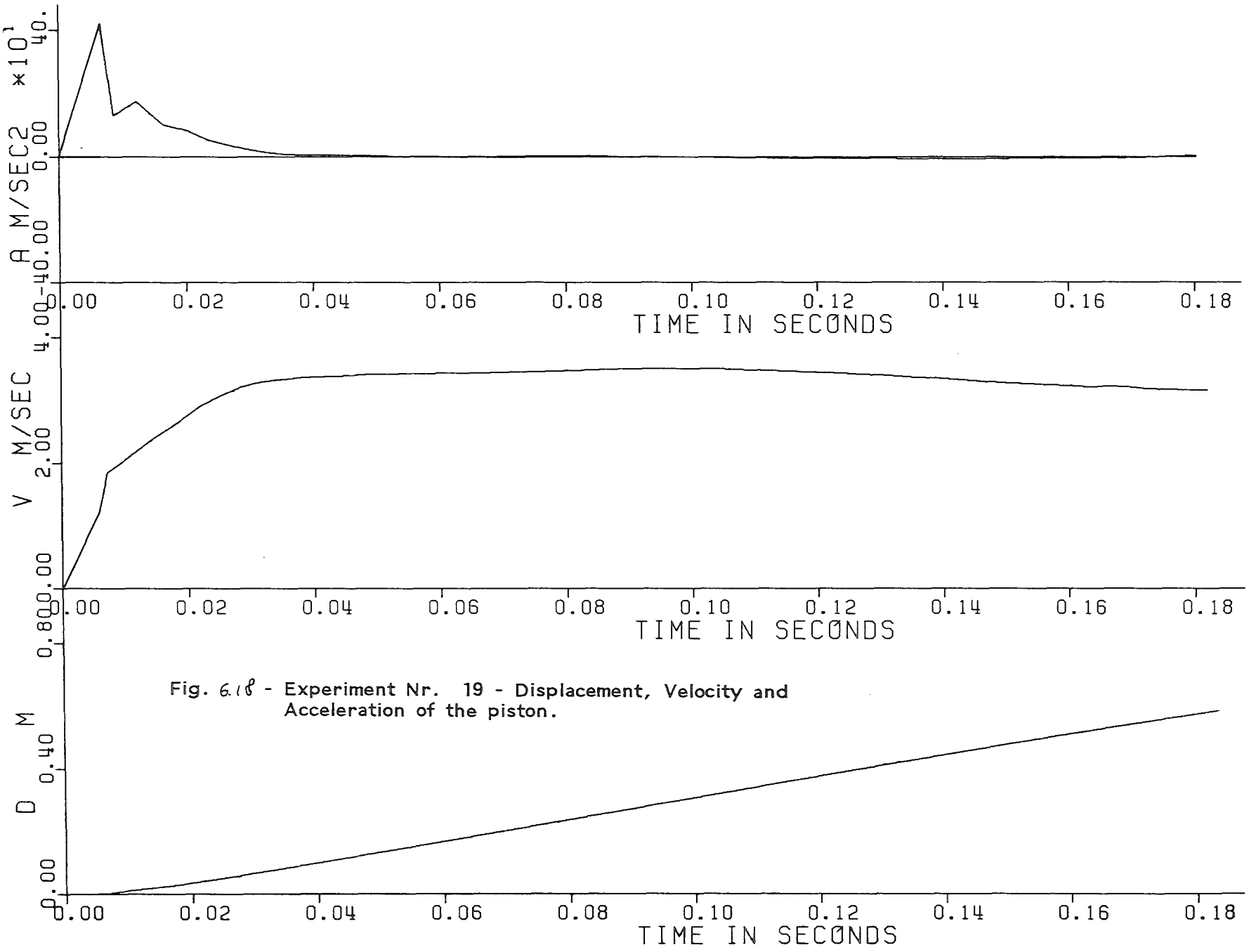

Fig. 6.18 - Experiment Nr. 19 - Displacement, Velocity and Acceleration of the piston.

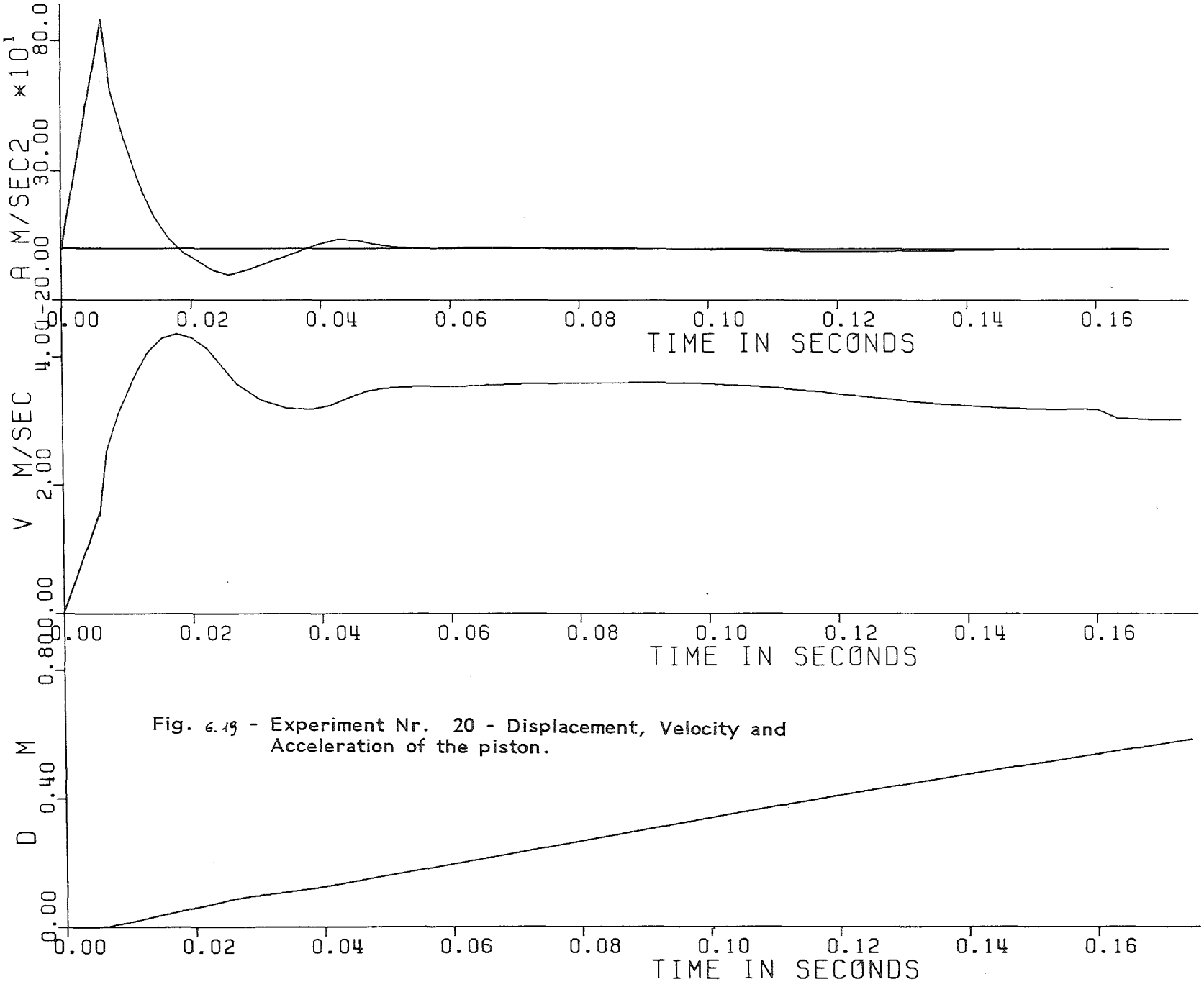

Fig. 6.19 - Experiment Nr. 20 - Displacement, Velocity and Acceleration of the piston.

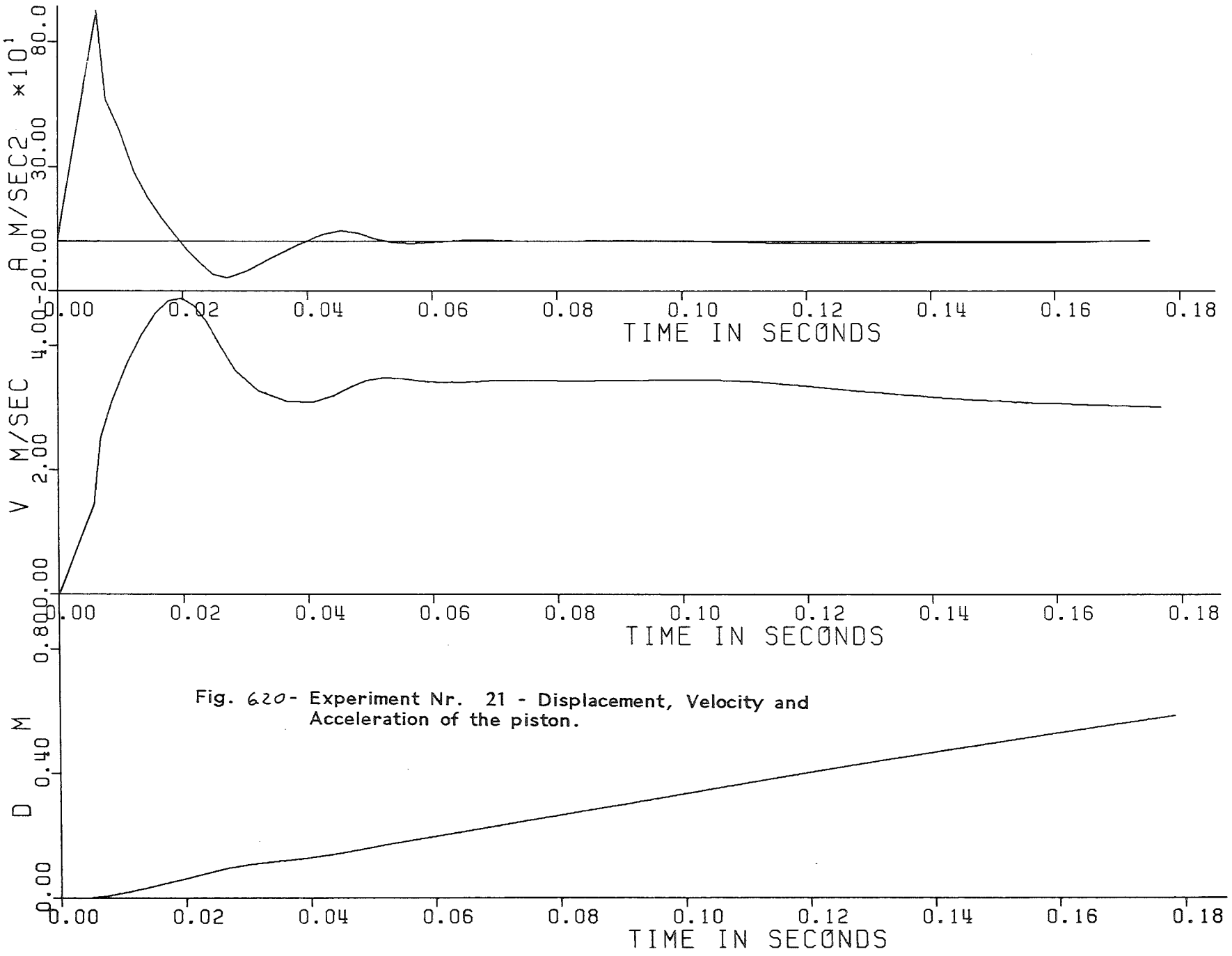

Fig. 620- Experiment Nr. 21 - Displacement, Velocity and Acceleration of the piston.

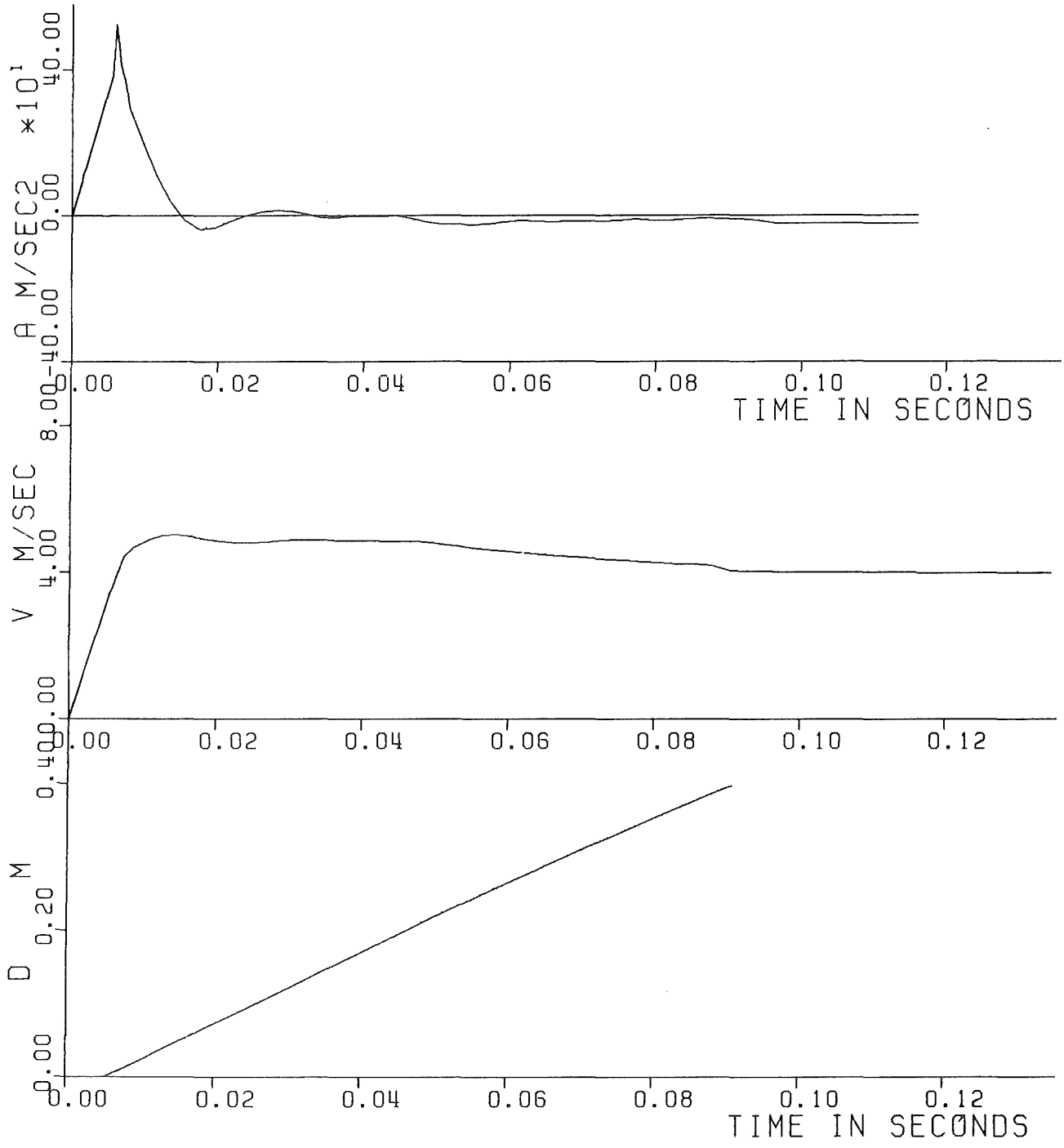

Fig. 6.21 - Experiment Nr. 22 - Displacement, Velocity and Acceleration of the piston.

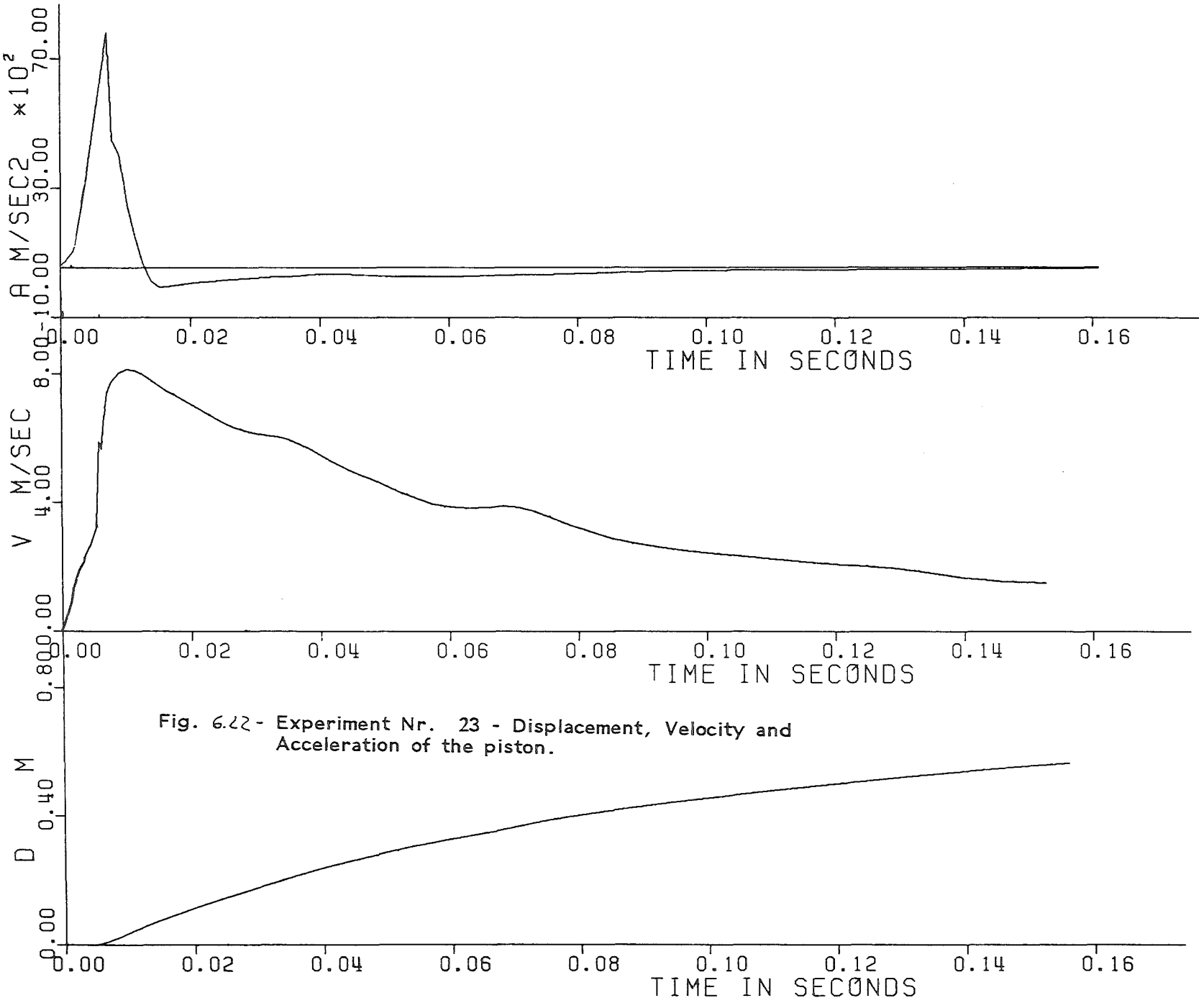

Fig. 6.22 - Experiment Nr. 23 - Displacement, Velocity and Acceleration of the piston.

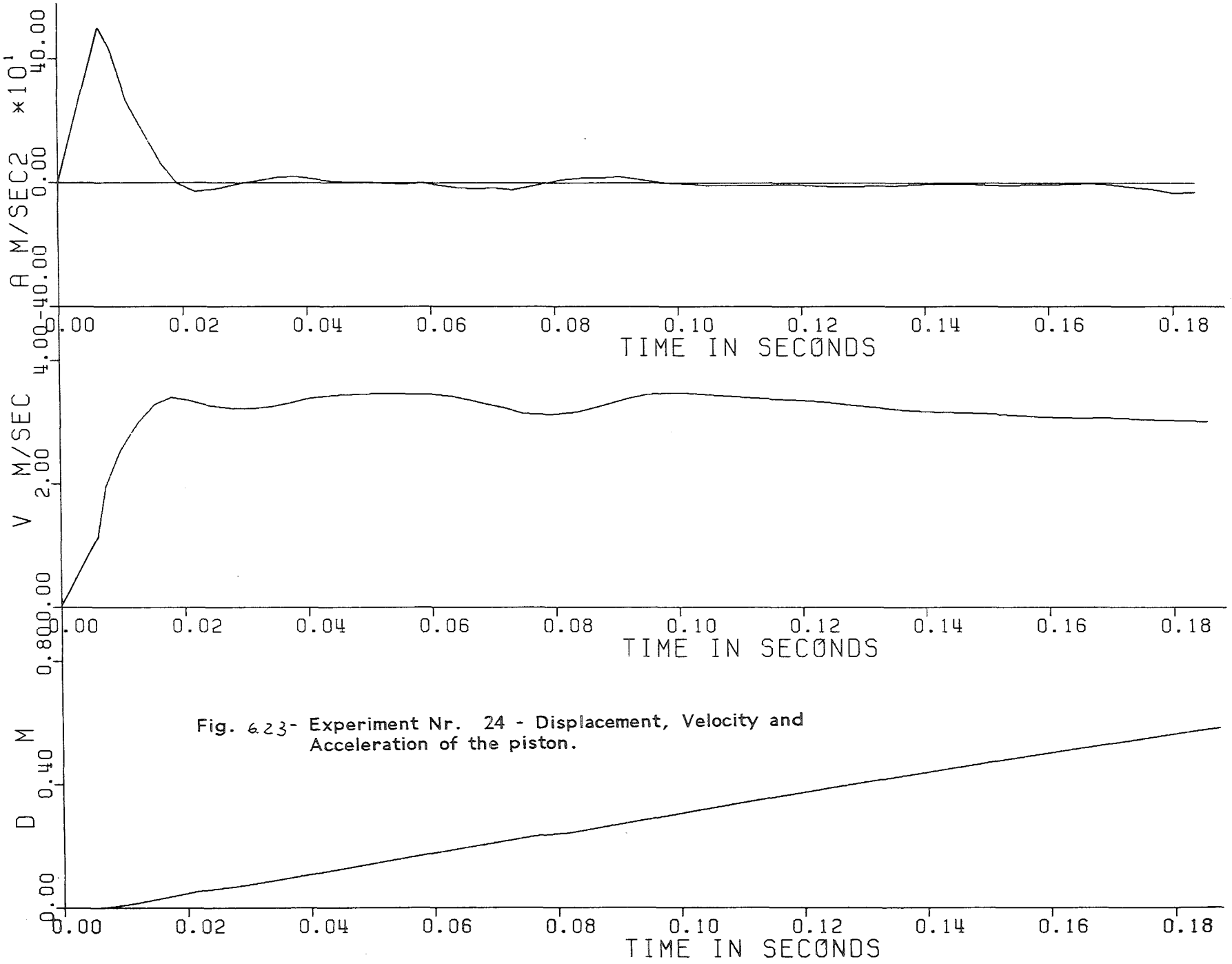

Fig. 623- Experiment Nr. 24 - Displacement, Velocity and Acceleration of the piston.

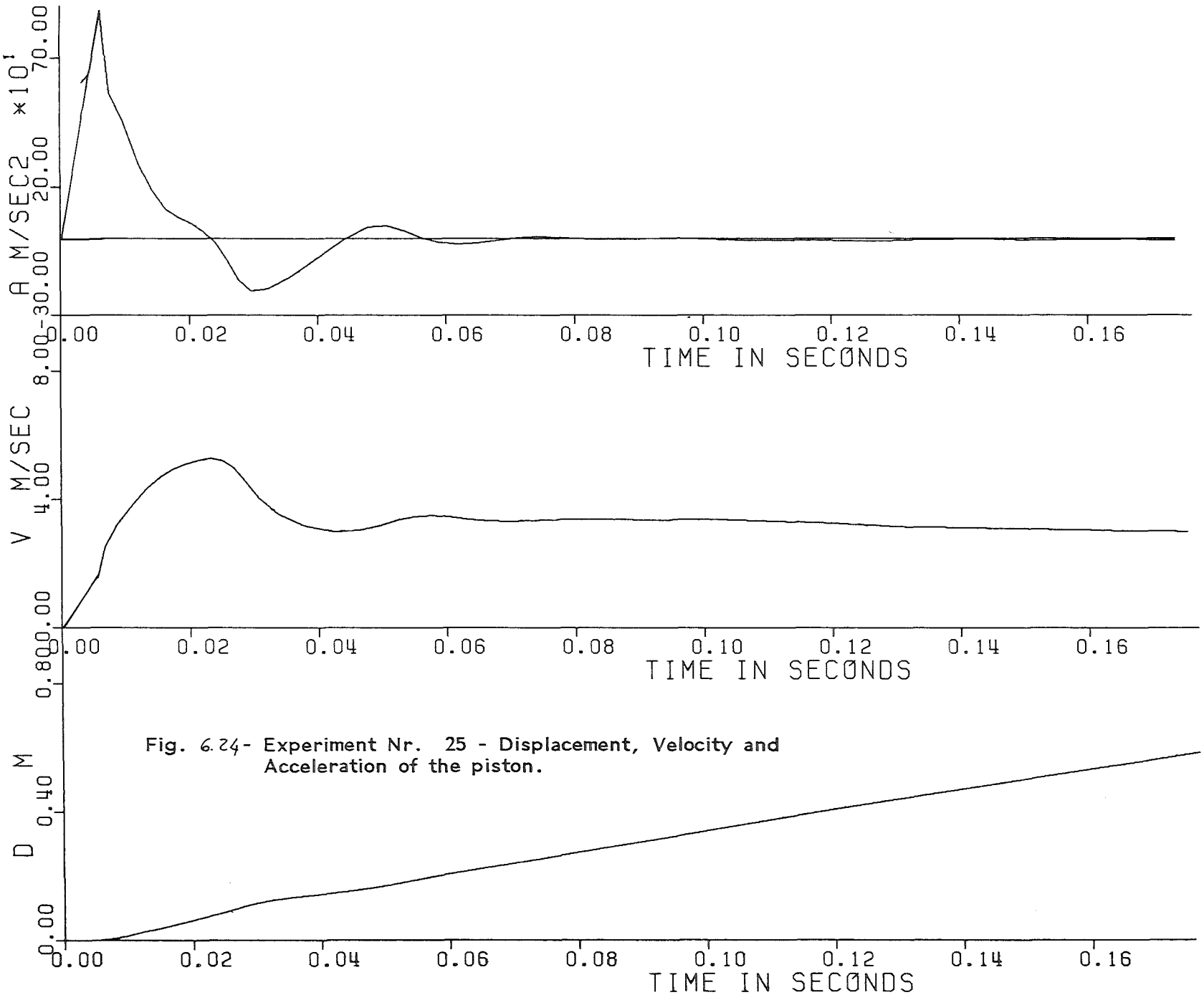

Fig. 6.24- Experiment Nr. 25 - Displacement, Velocity and Acceleration of the piston.

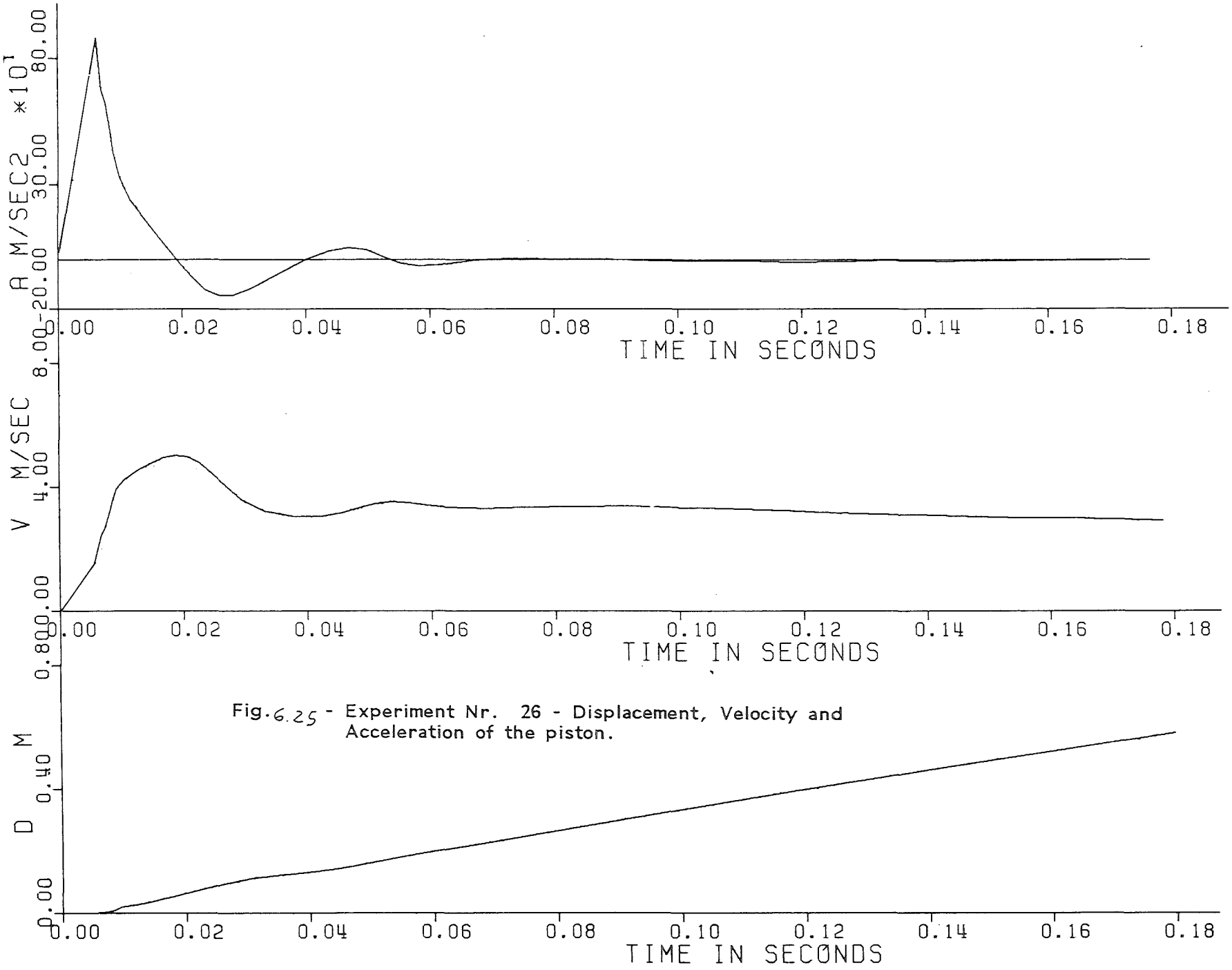

Fig. 6.25 - Experiment Nr. 26 - Displacement, Velocity and Acceleration of the piston.

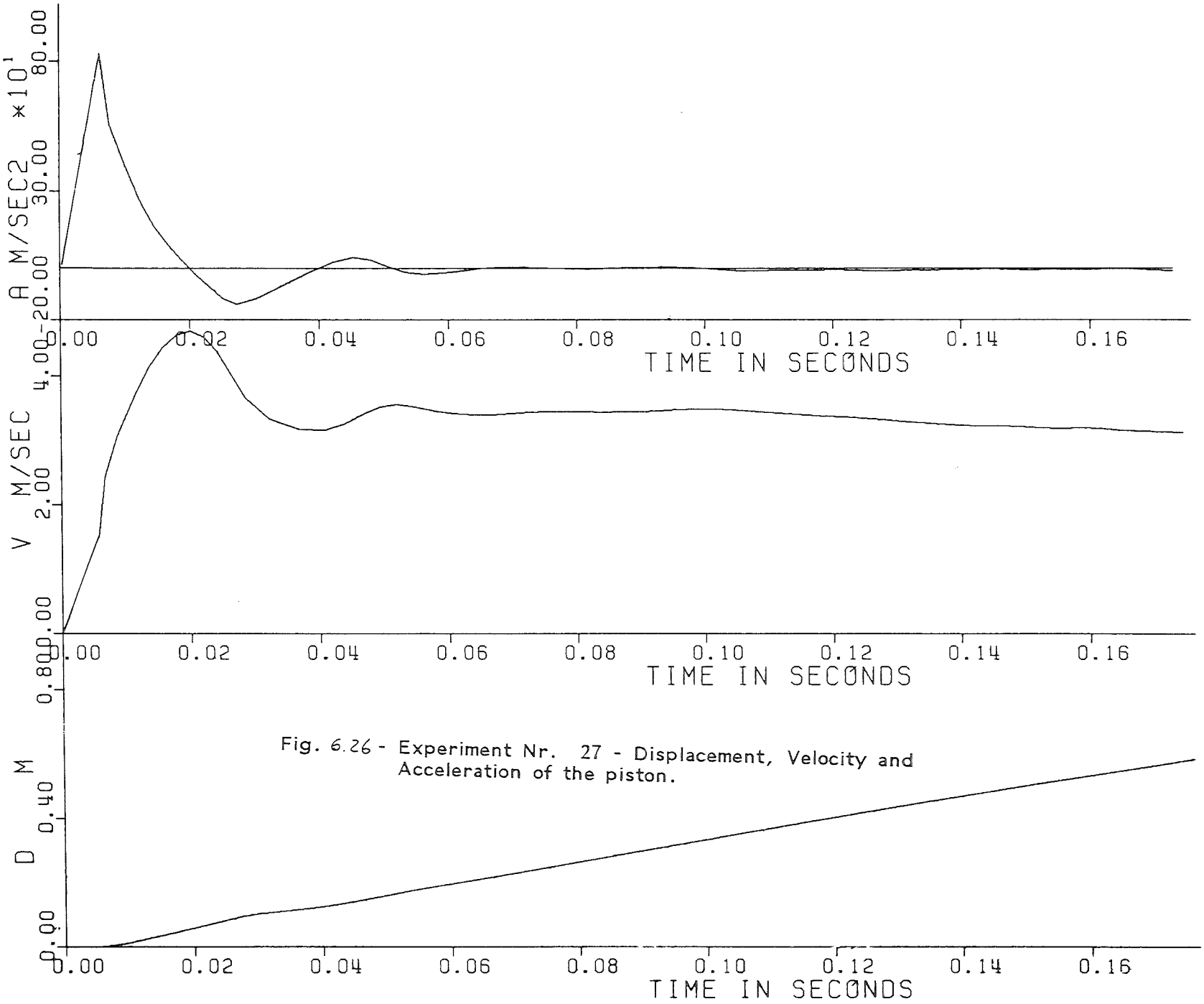

Fig. 6.26 - Experiment Nr. 27 - Displacement, Velocity and Acceleration of the piston.

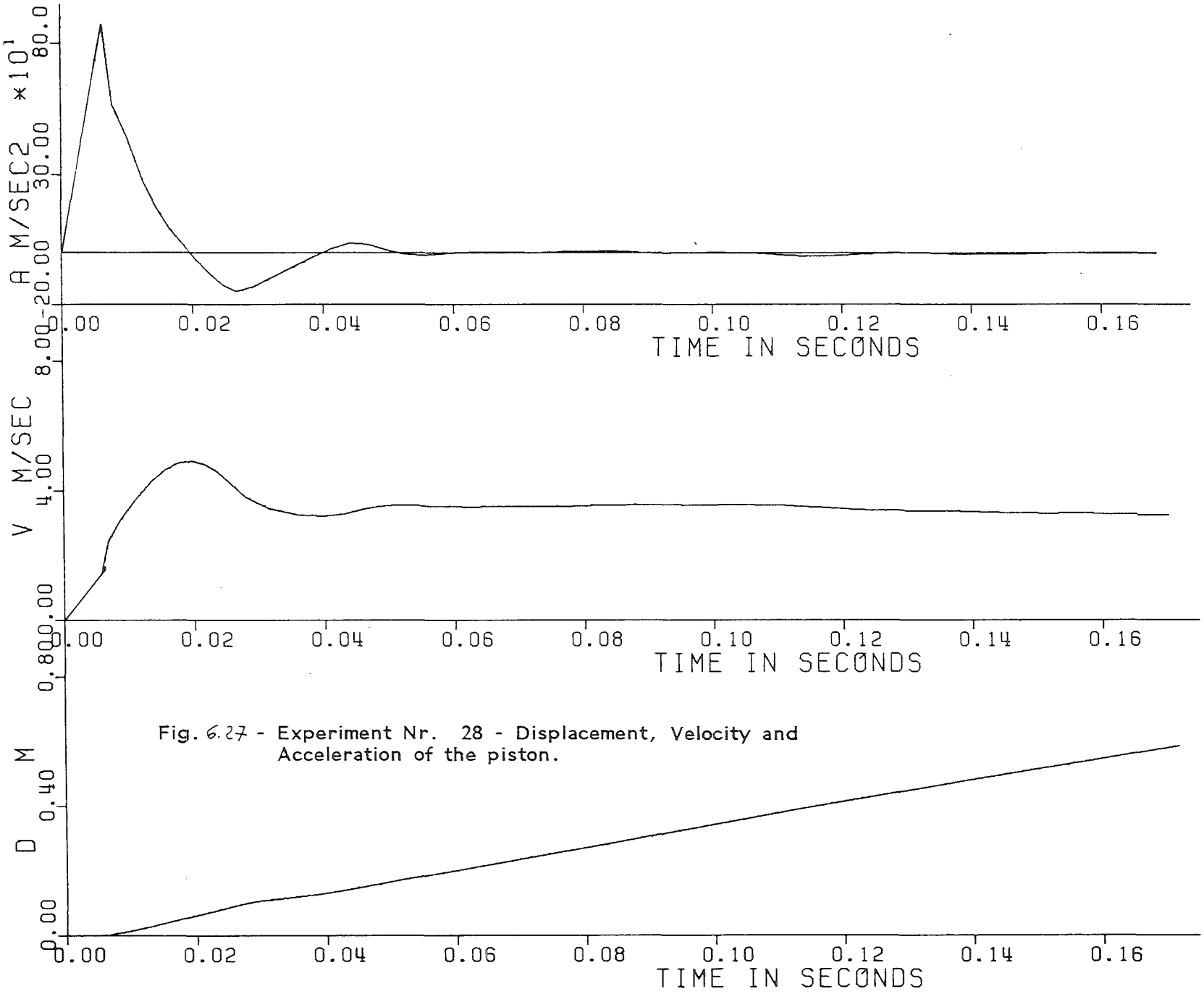

Fig. 6.27 - Experiment Nr. 28 - Displacement, Velocity and Acceleration of the piston.

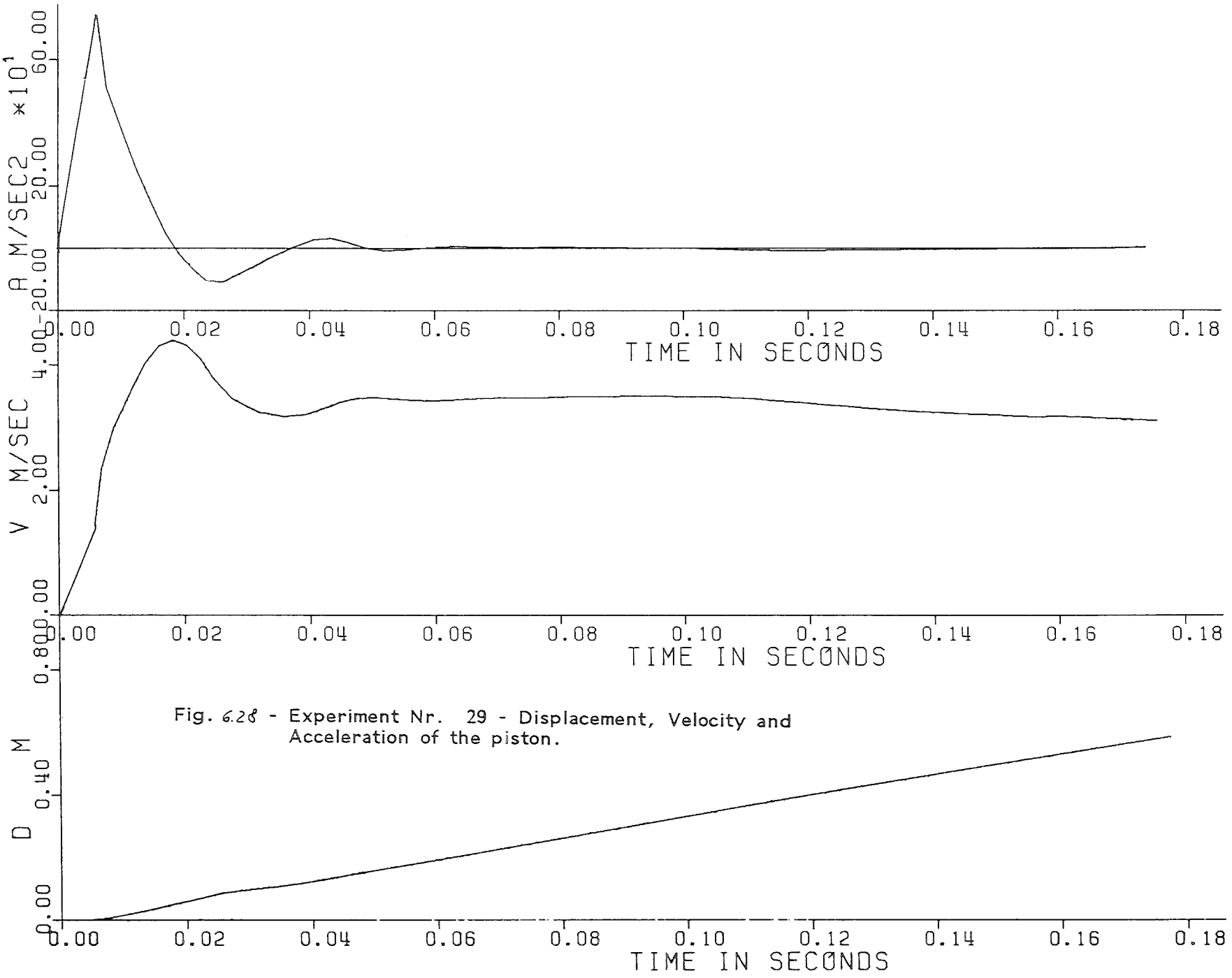

Fig. 6.28 - Experiment Nr. 29 - Displacement, Velocity and Acceleration of the piston.

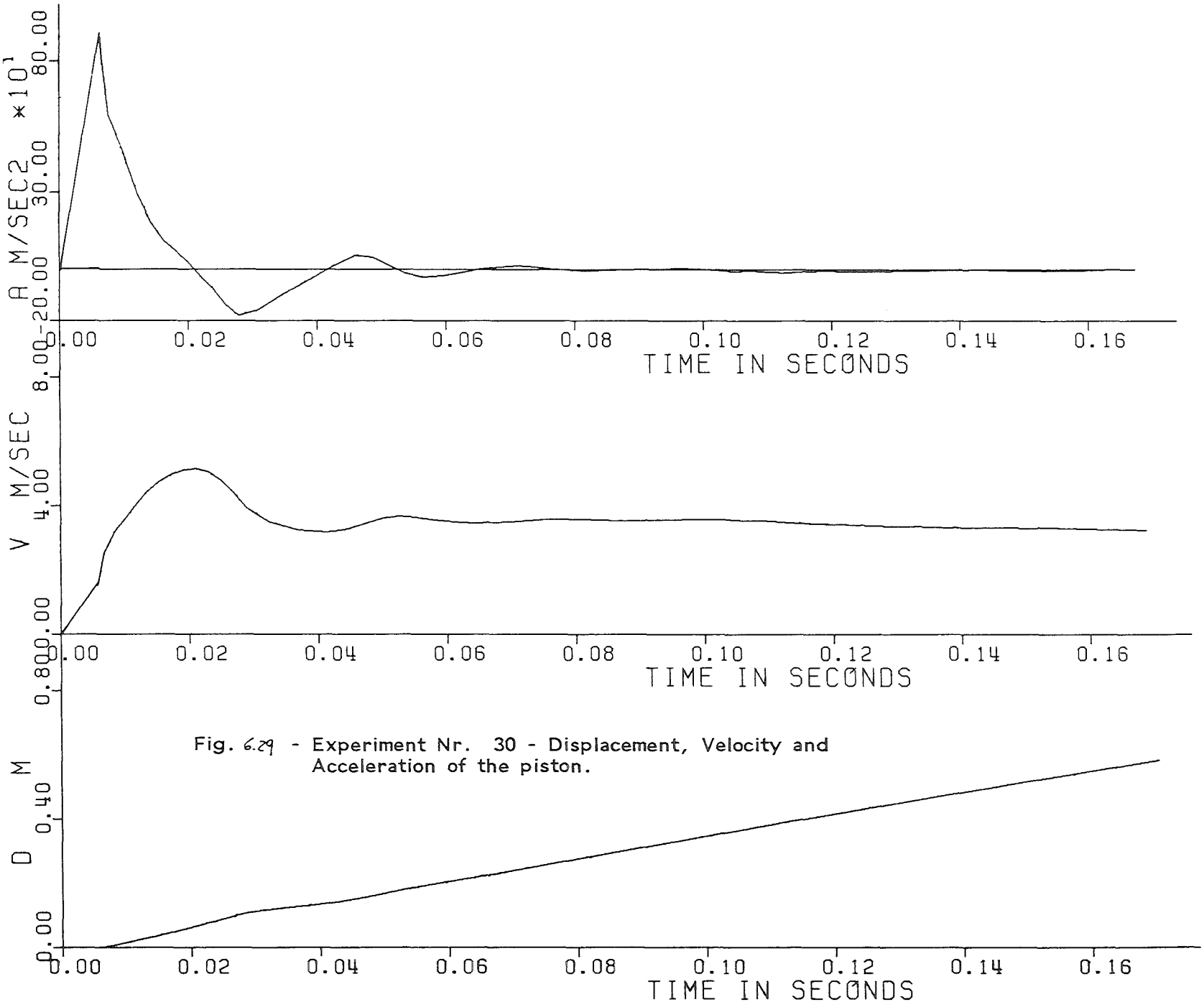

Fig. 6.29 - Experiment Nr. 30 - Displacement, Velocity and Acceleration of the piston.

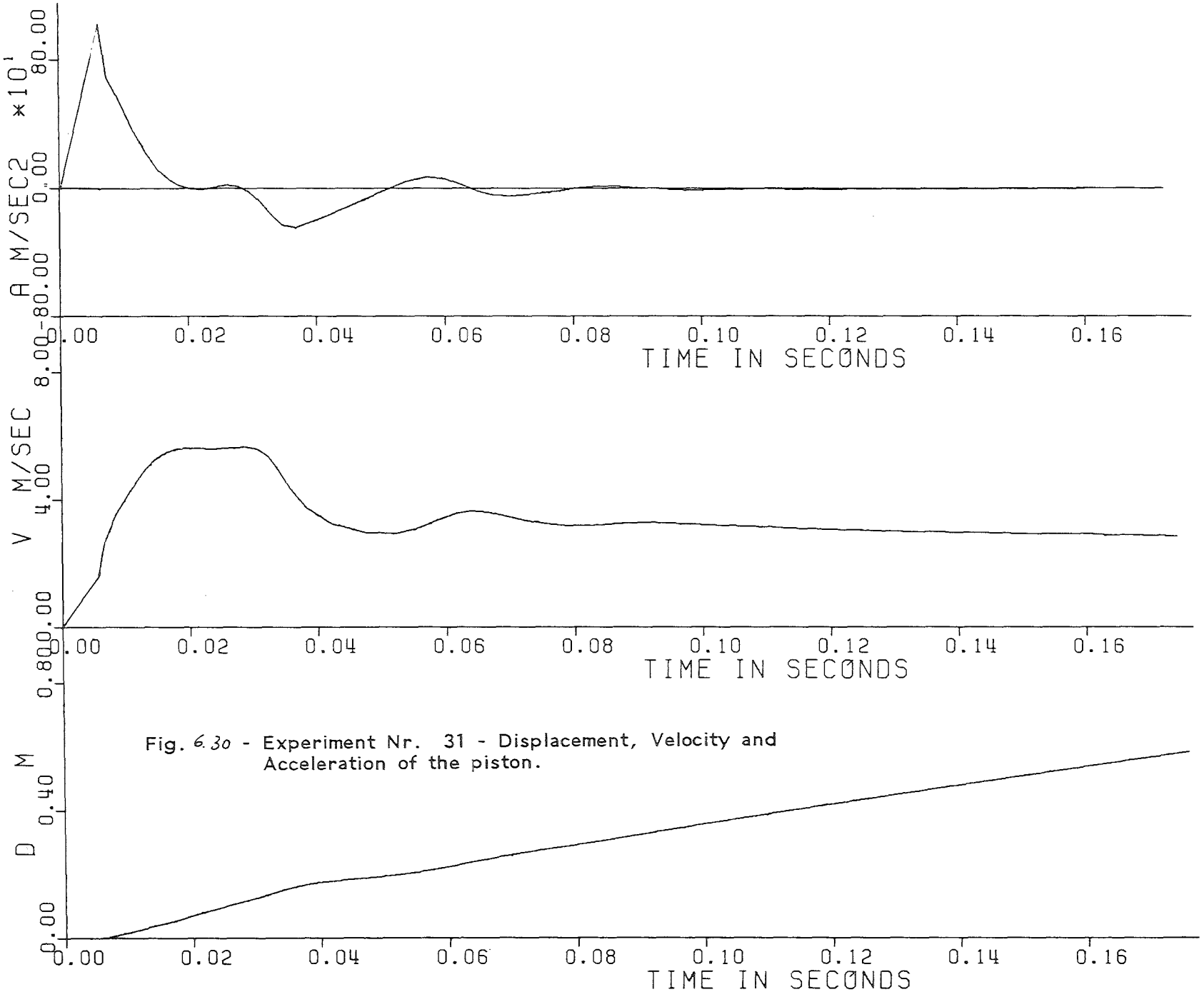

Fig. 6.30 - Experiment Nr. 31 - Displacement, Velocity and Acceleration of the piston.

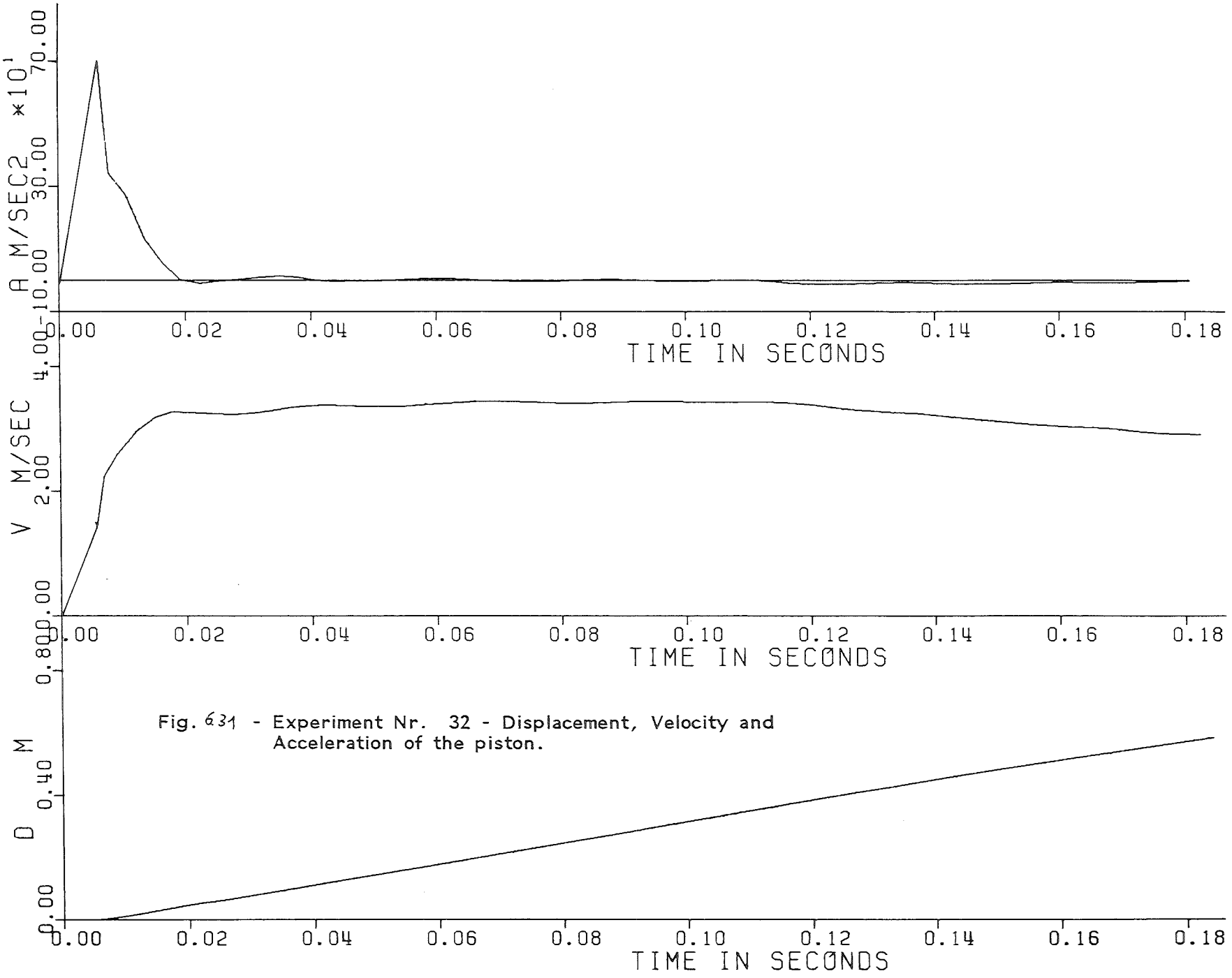

Fig. 631 - Experiment Nr. 32 - Displacement, Velocity and Acceleration of the piston.

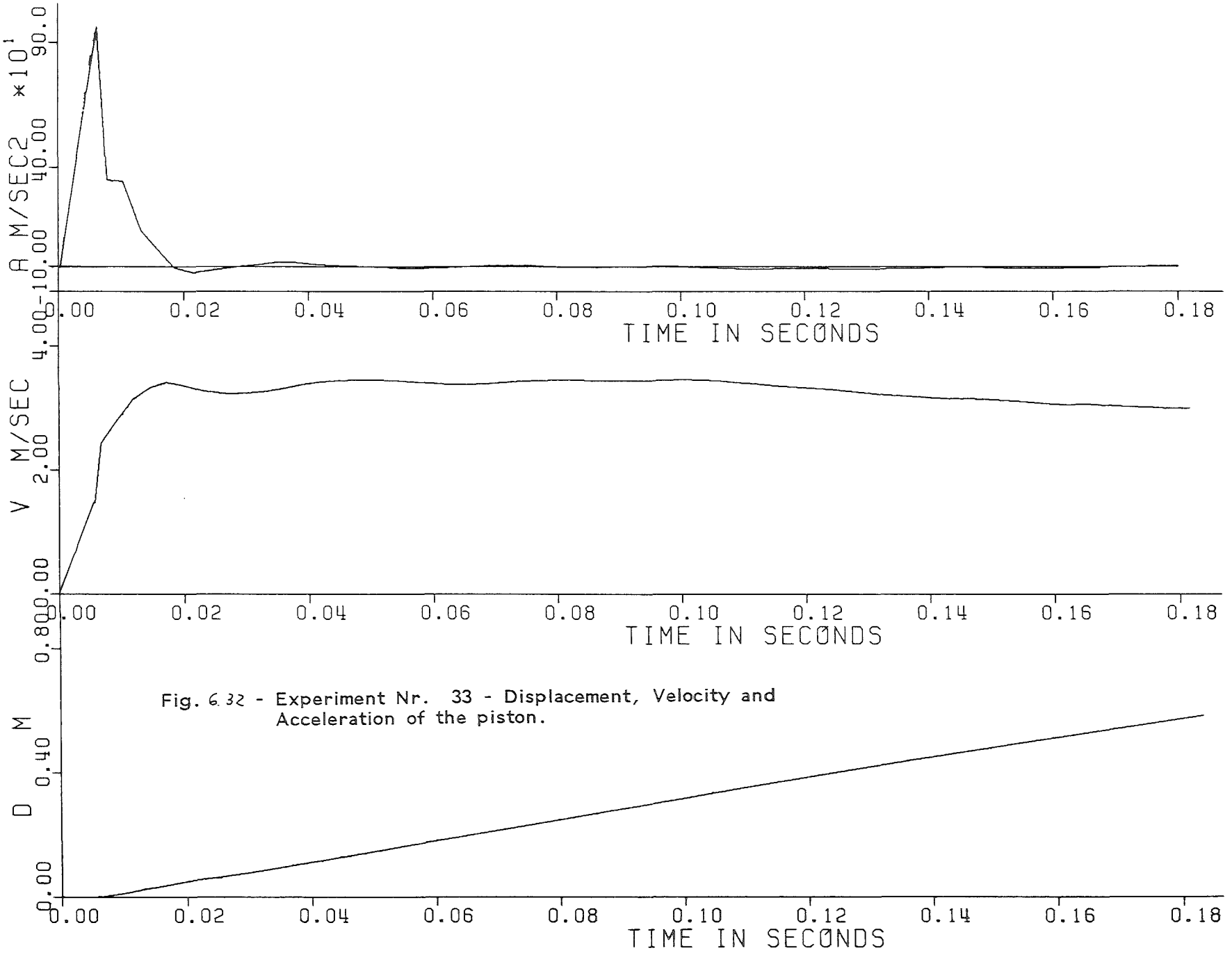

Fig. 6.32 - Experiment Nr. 33 - Displacement, Velocity and Acceleration of the piston.

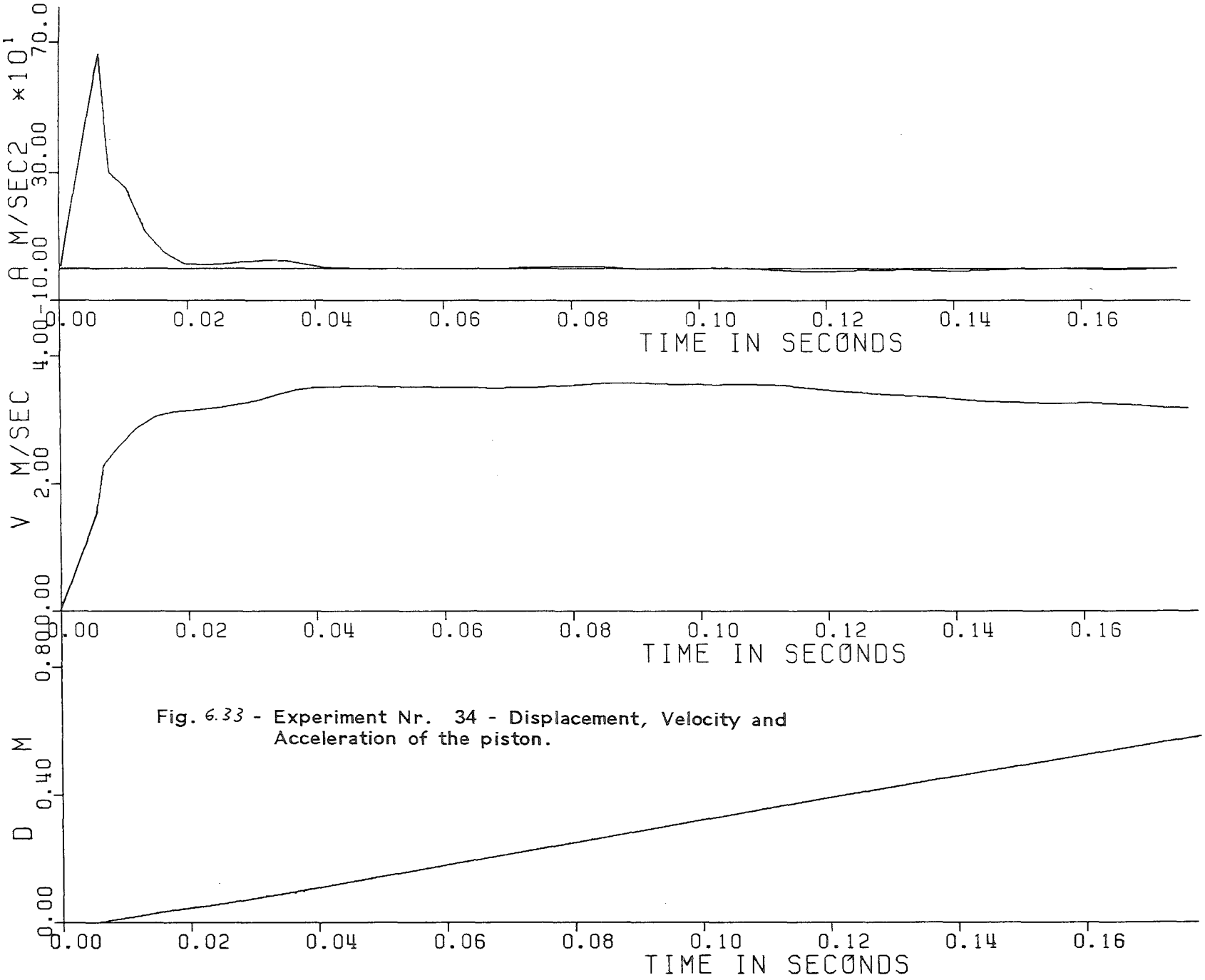

Fig. 6.33 - Experiment Nr. 34 - Displacement, Velocity and Acceleration of the piston.

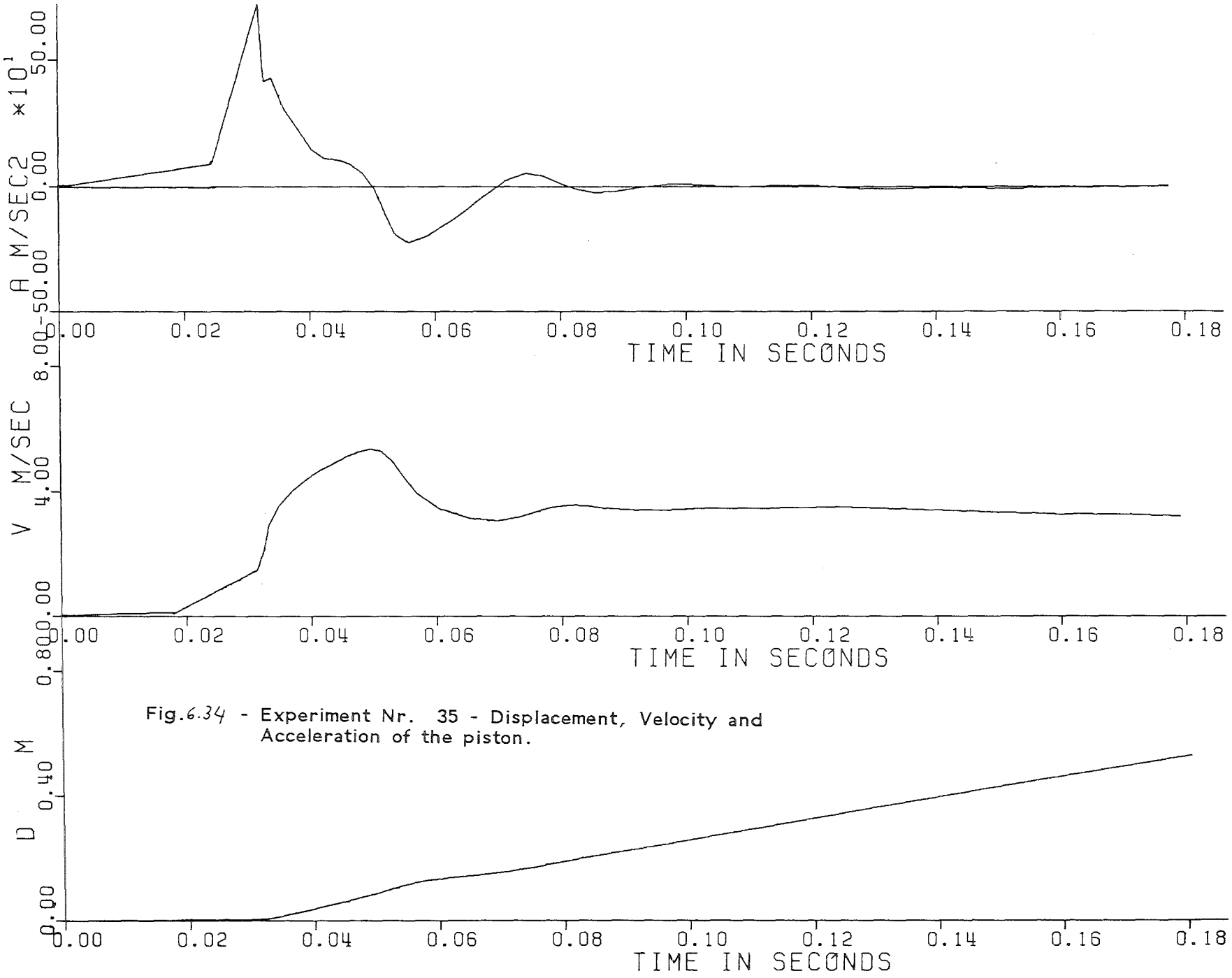

Fig.6.34 - Experiment Nr. 35 - Displacement, Velocity and Acceleration of the piston.

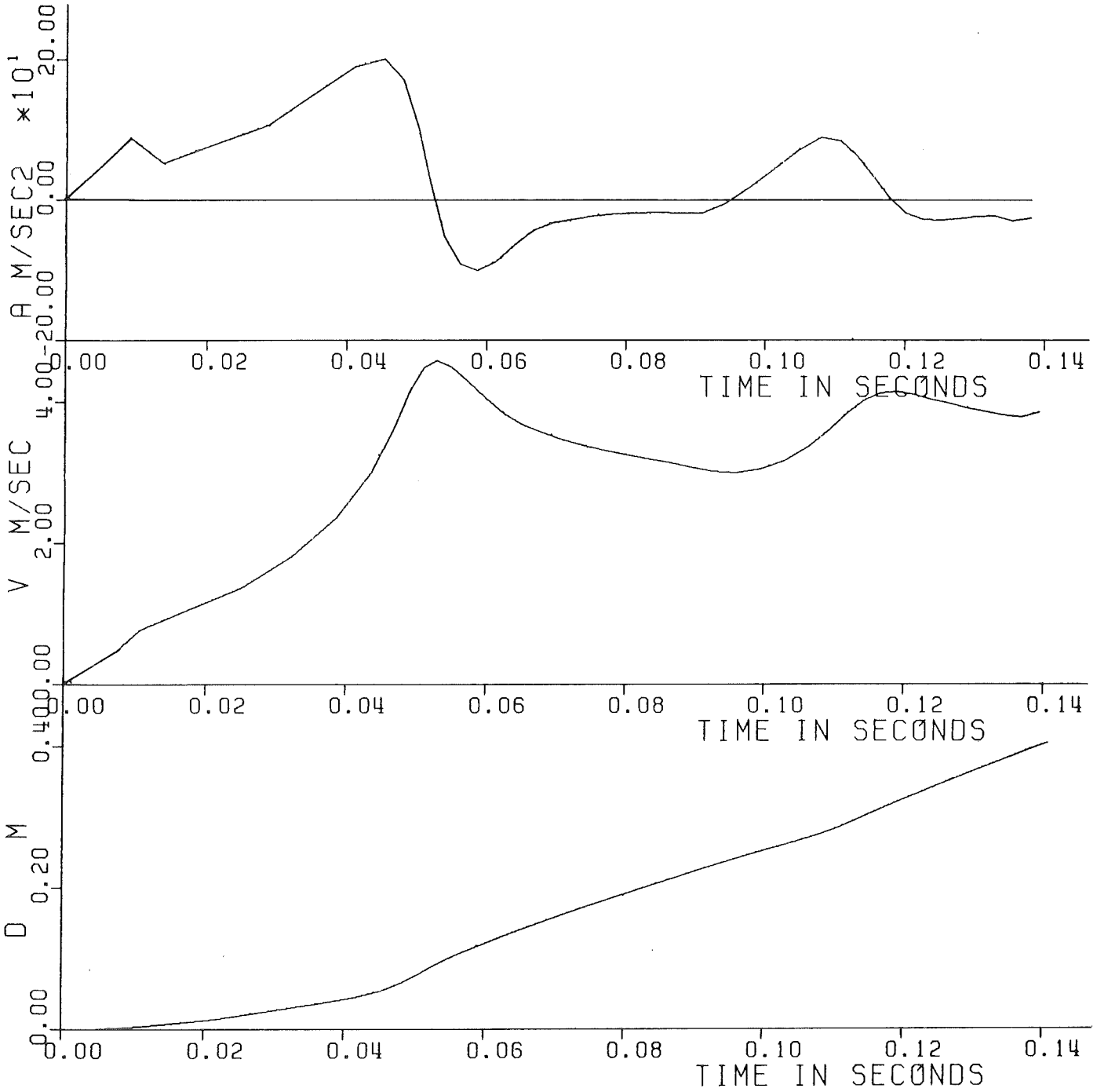

Fig. 6.35 - Experiment Nr. 36 - Displacement, Velocity and Acceleration of the piston.

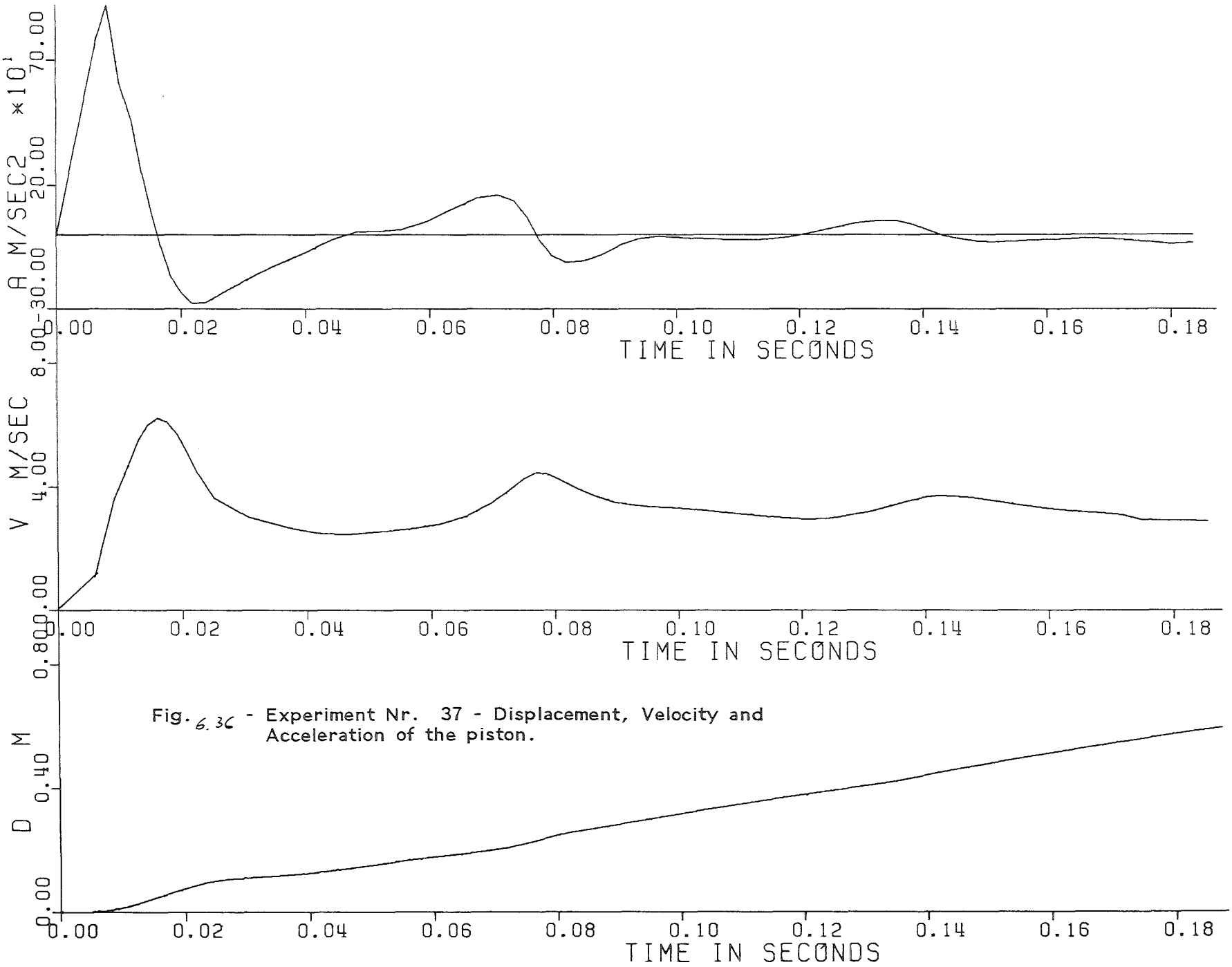

Fig. 6.36 - Experiment Nr. 37 - Displacement, Velocity and Acceleration of the piston.

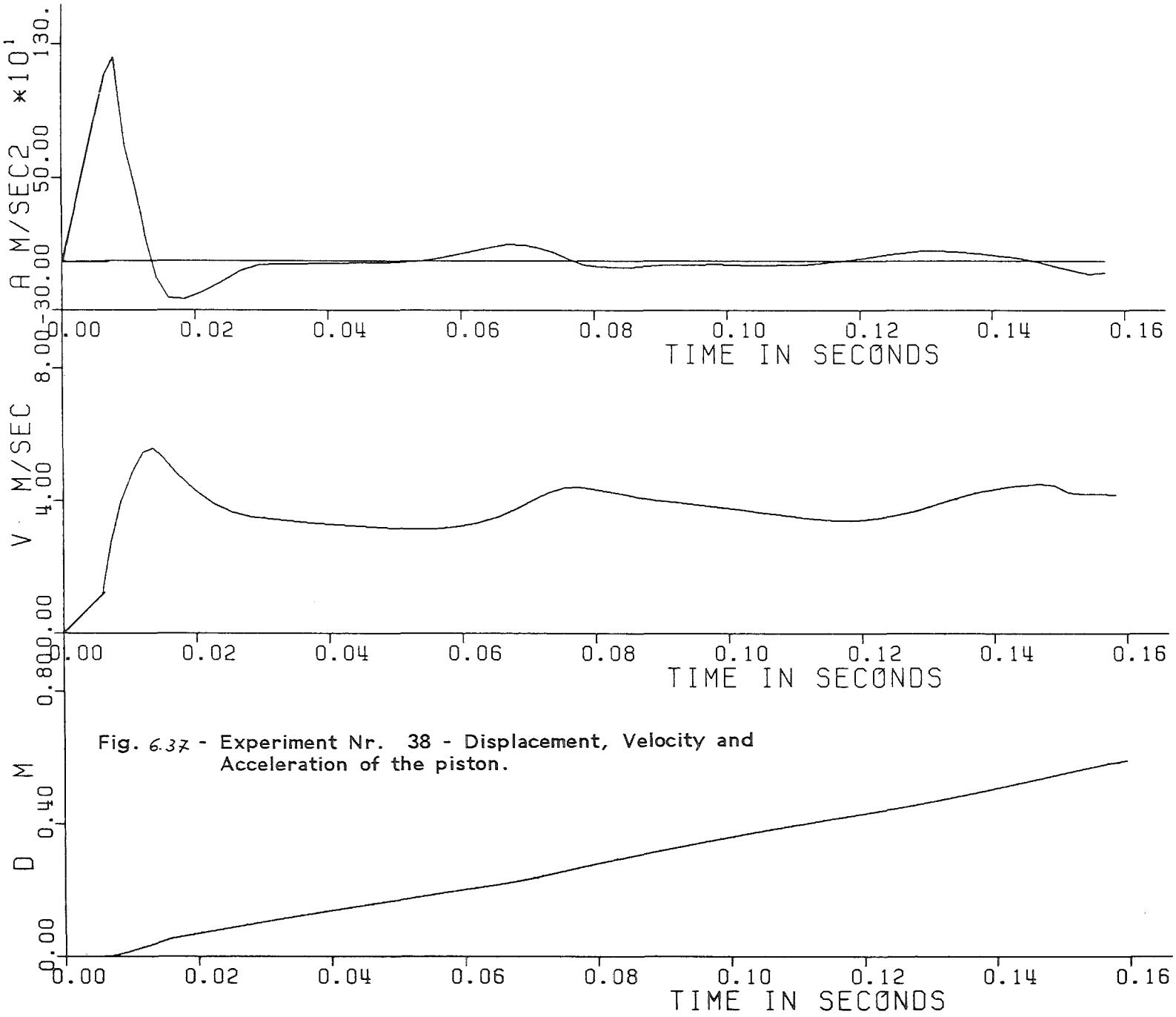

Fig. 6.37 - Experiment Nr. 38 - Displacement, Velocity and Acceleration of the piston.

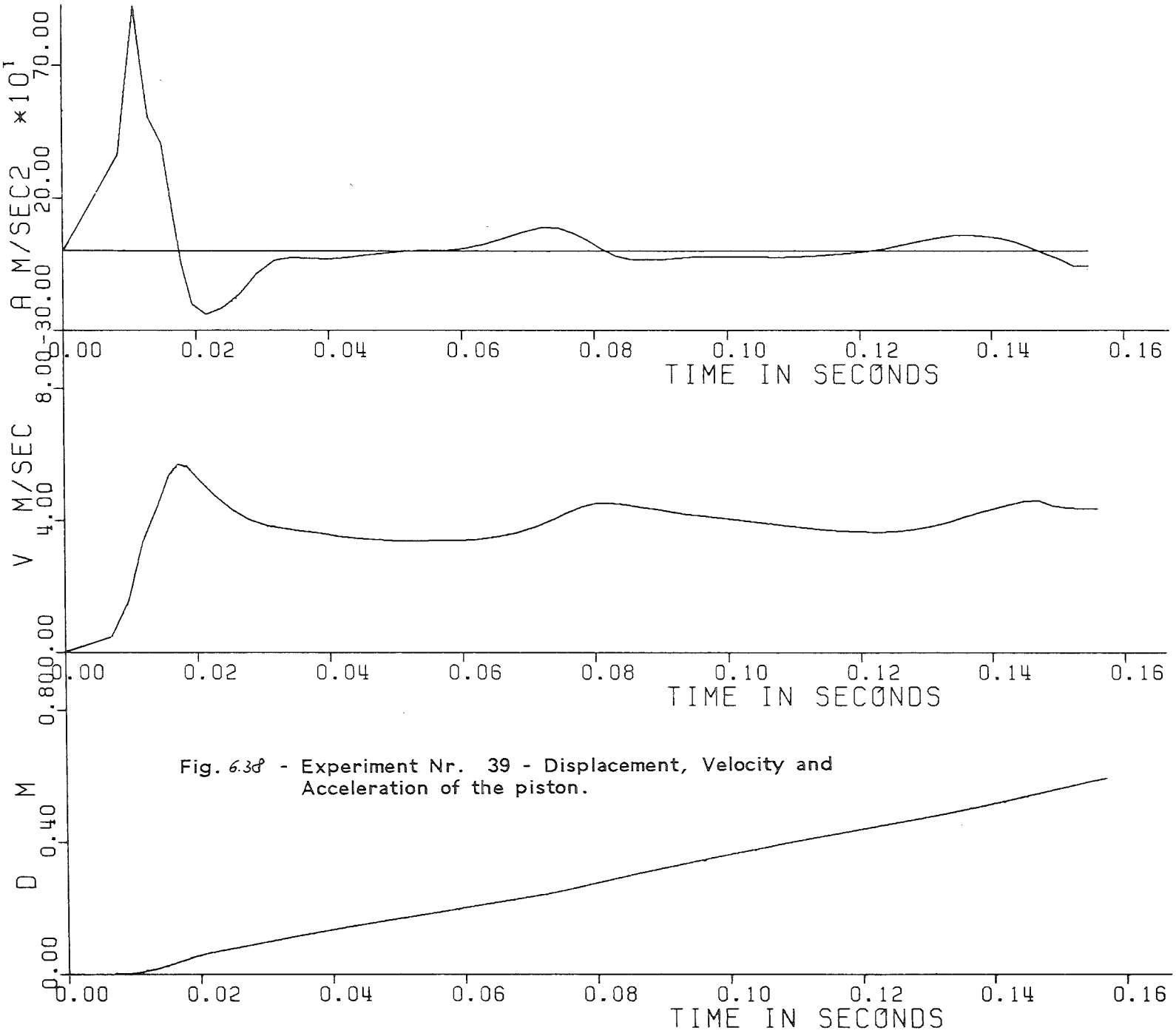

Fig. 6.38 - Experiment Nr. 39 - Displacement, Velocity and Acceleration of the piston.

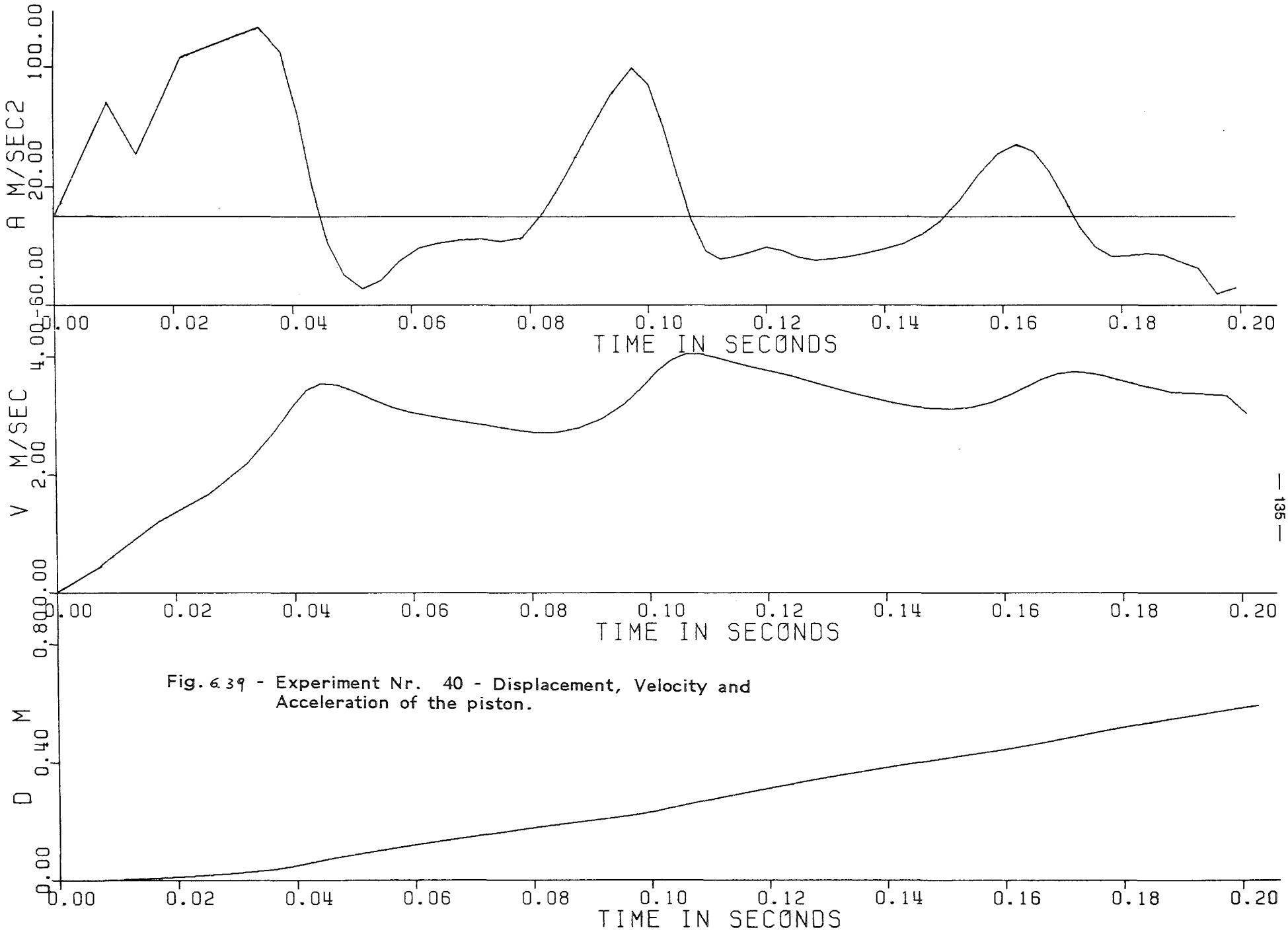

Fig. 6.39 - Experiment Nr. 40 - Displacement, Velocity and Acceleration of the piston.

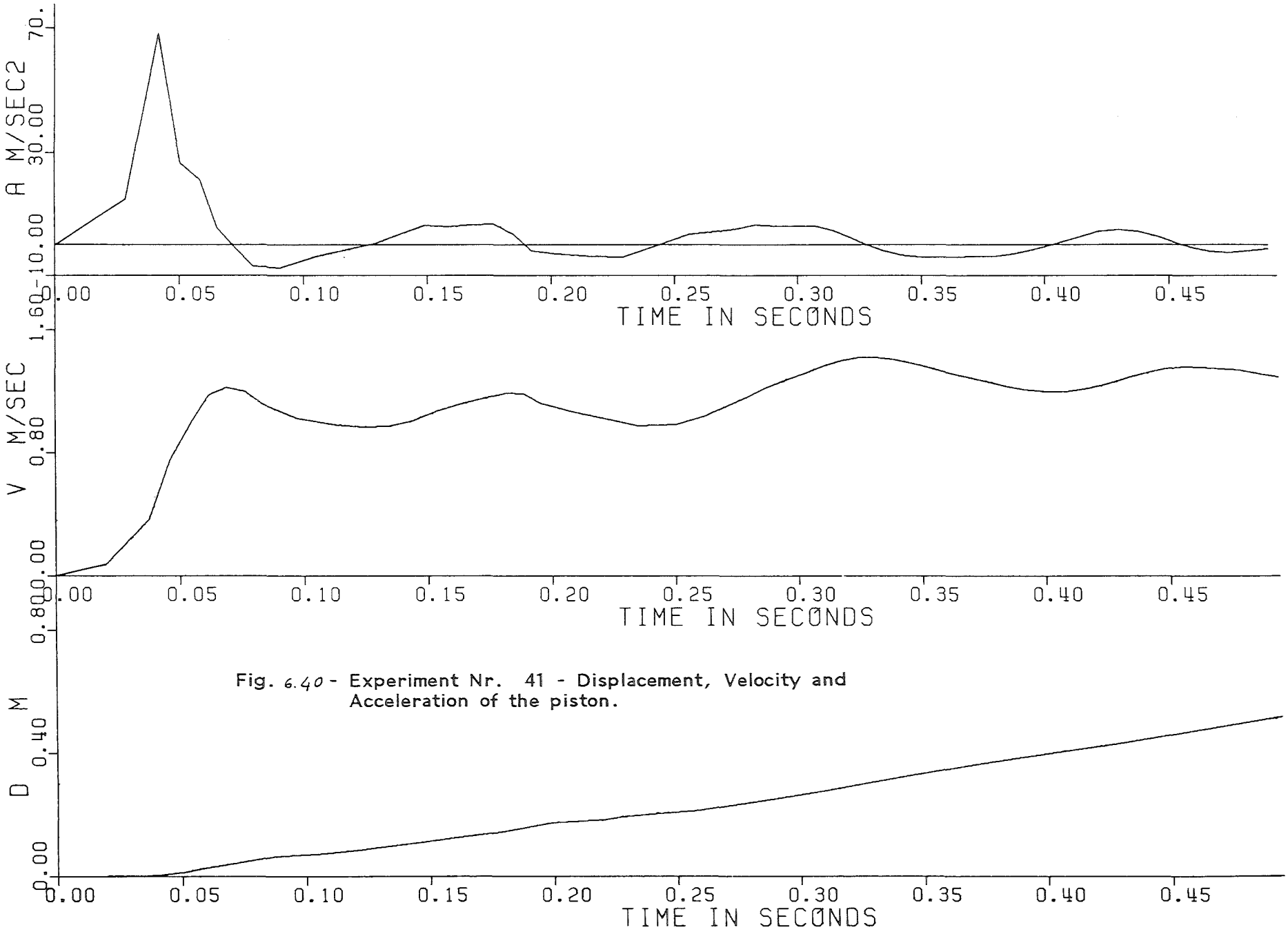

Fig. 6.40 - Experiment Nr. 41 - Displacement, Velocity and Acceleration of the piston.

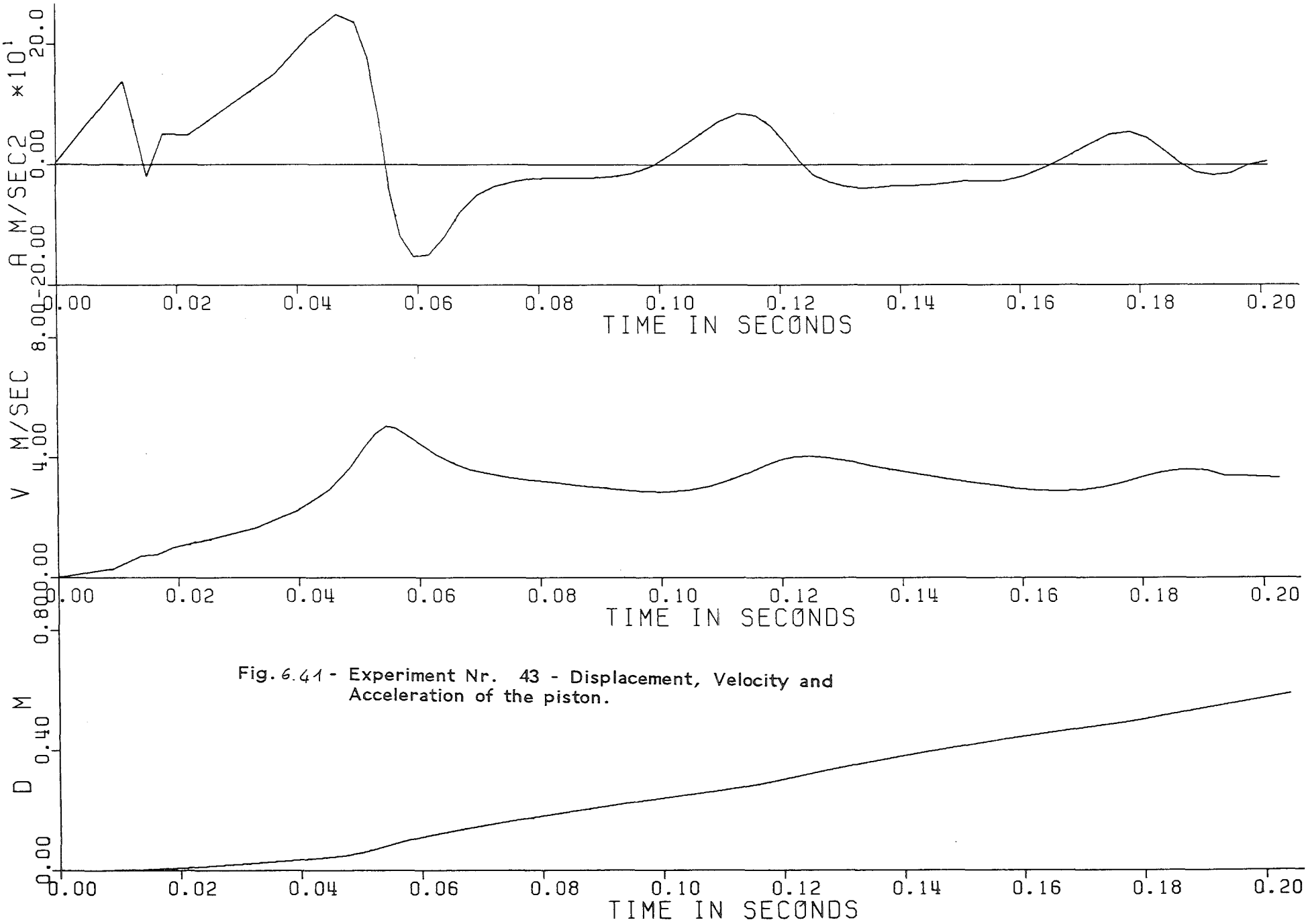

Fig. 6.41 - Experiment Nr. 43 - Displacement, Velocity and Acceleration of the piston.

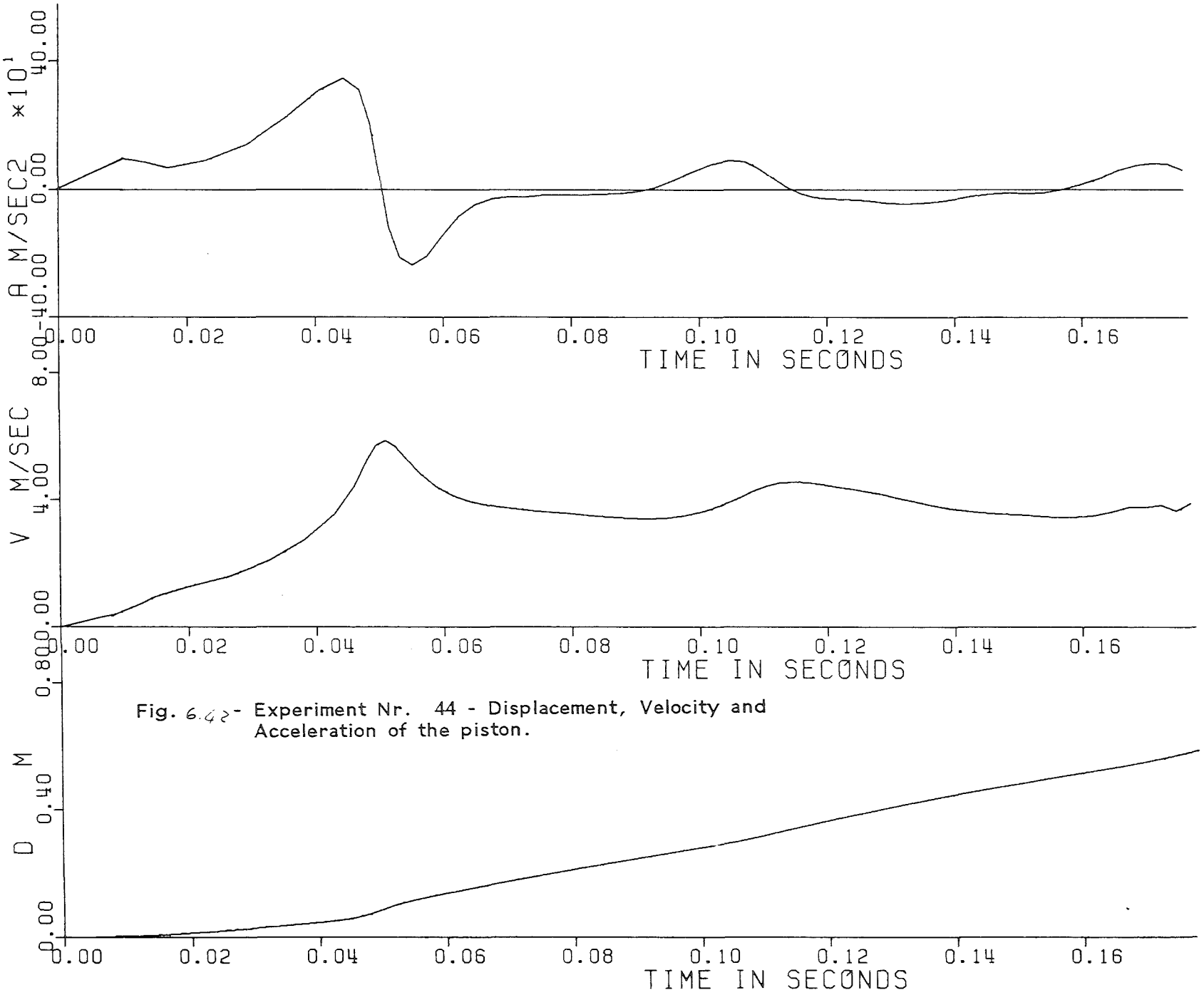

Fig. 6.42 - Experiment Nr. 44 - Displacement, Velocity and Acceleration of the piston.

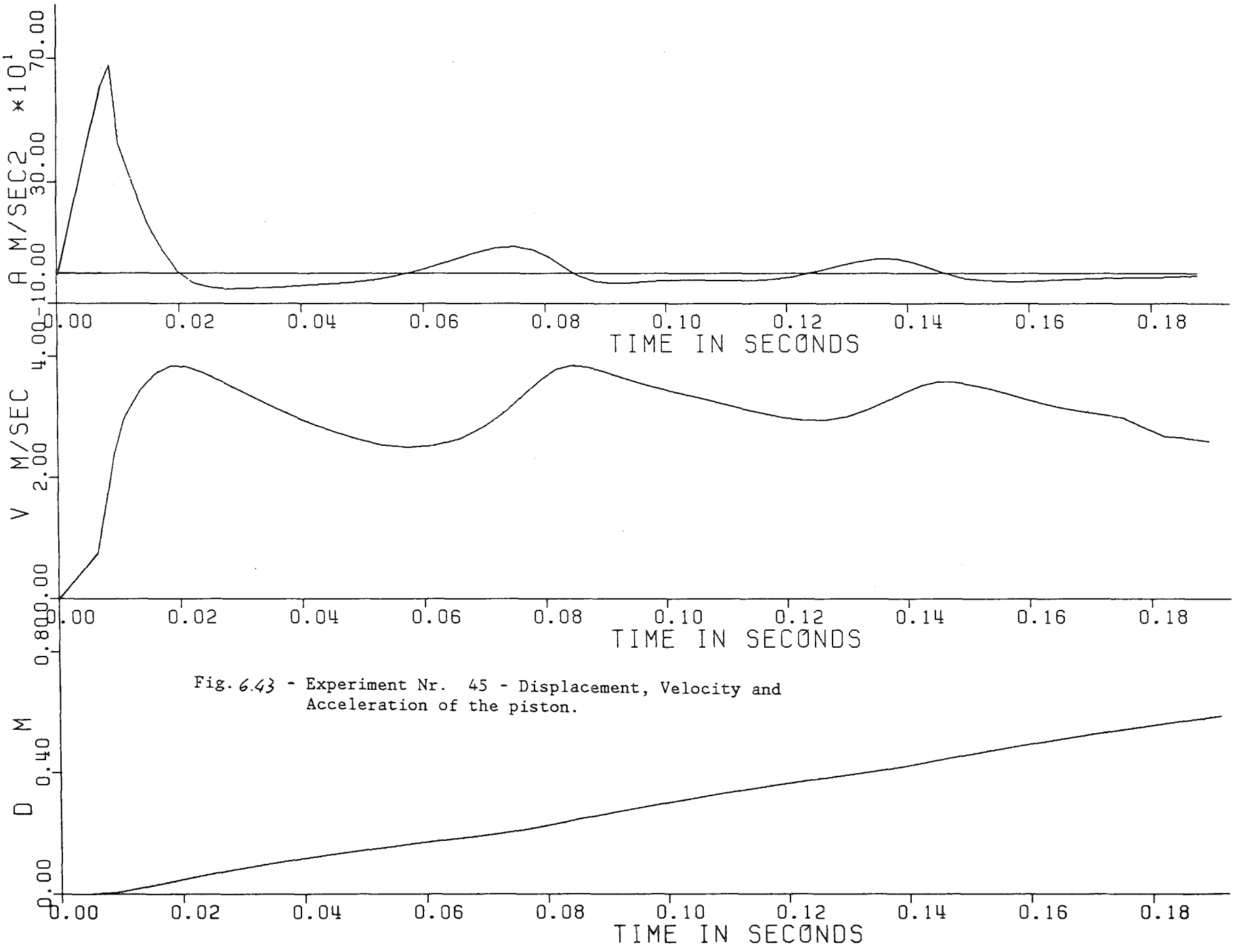

Fig. 6.43 - Experiment Nr. 45 - Displacement, Velocity and Acceleration of the piston.

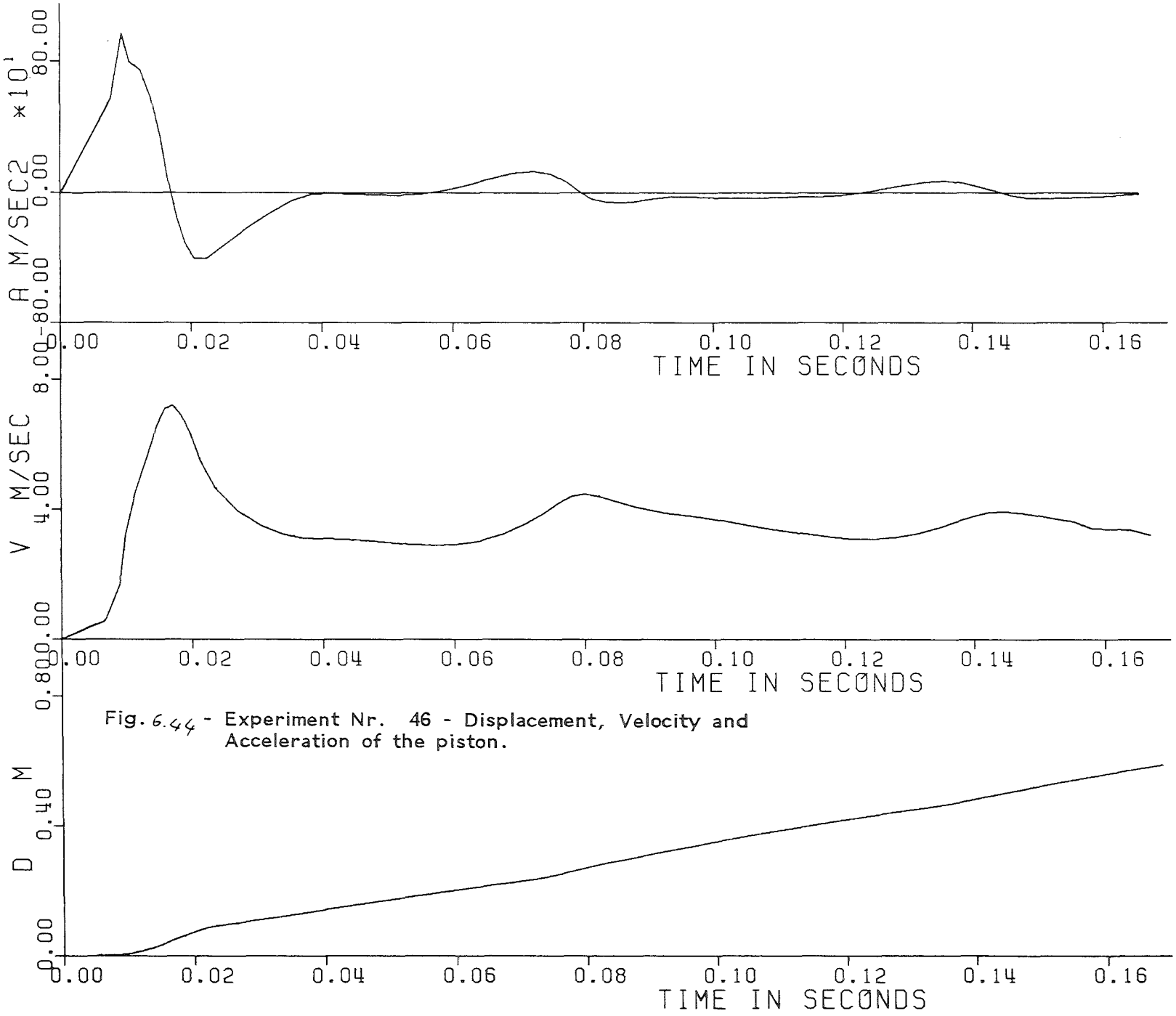

Fig. 6.44 - Experiment Nr. 46 - Displacement, Velocity and Acceleration of the piston.

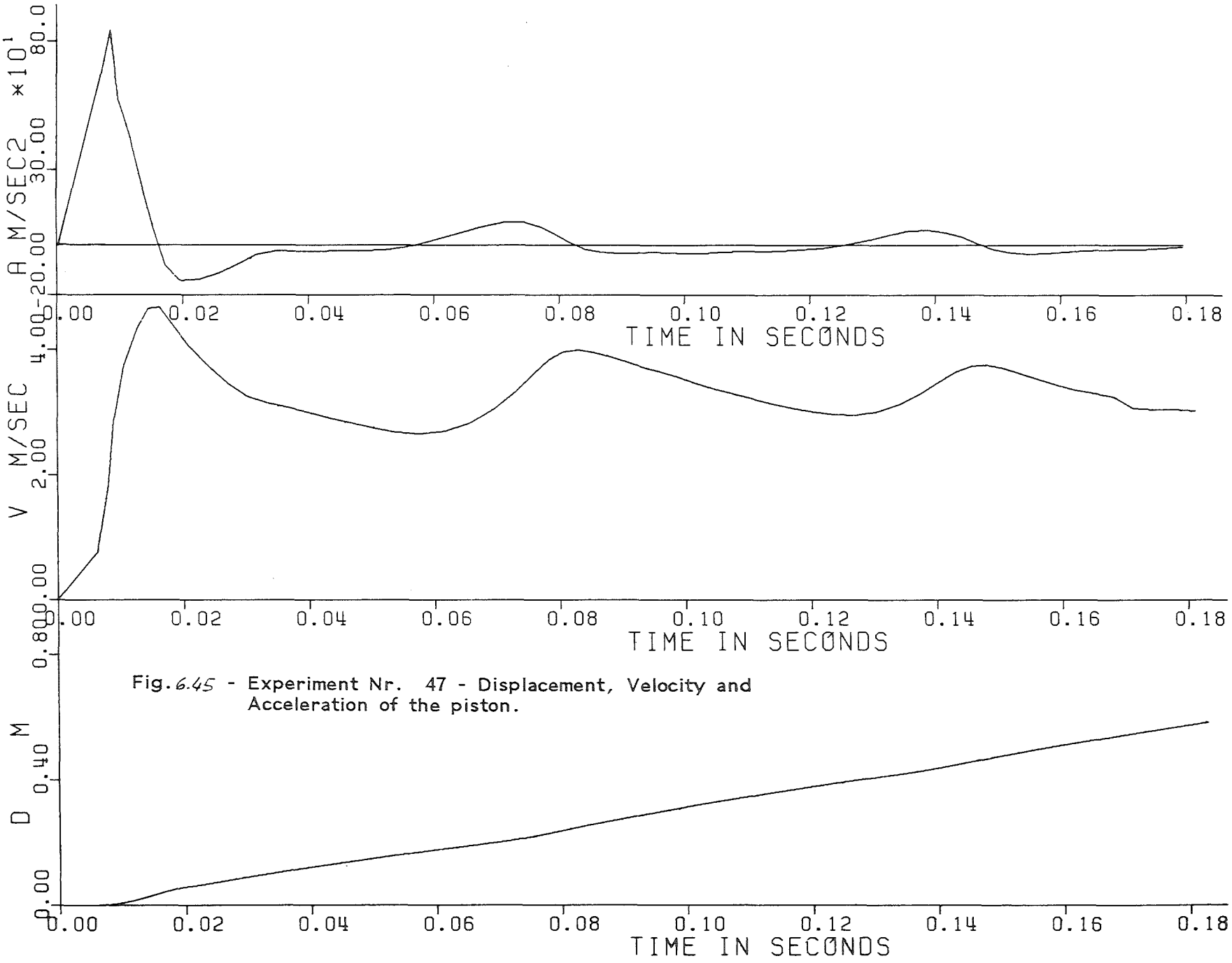

Fig. 6.45 - Experiment Nr. 47 - Displacement, Velocity and Acceleration of the piston.

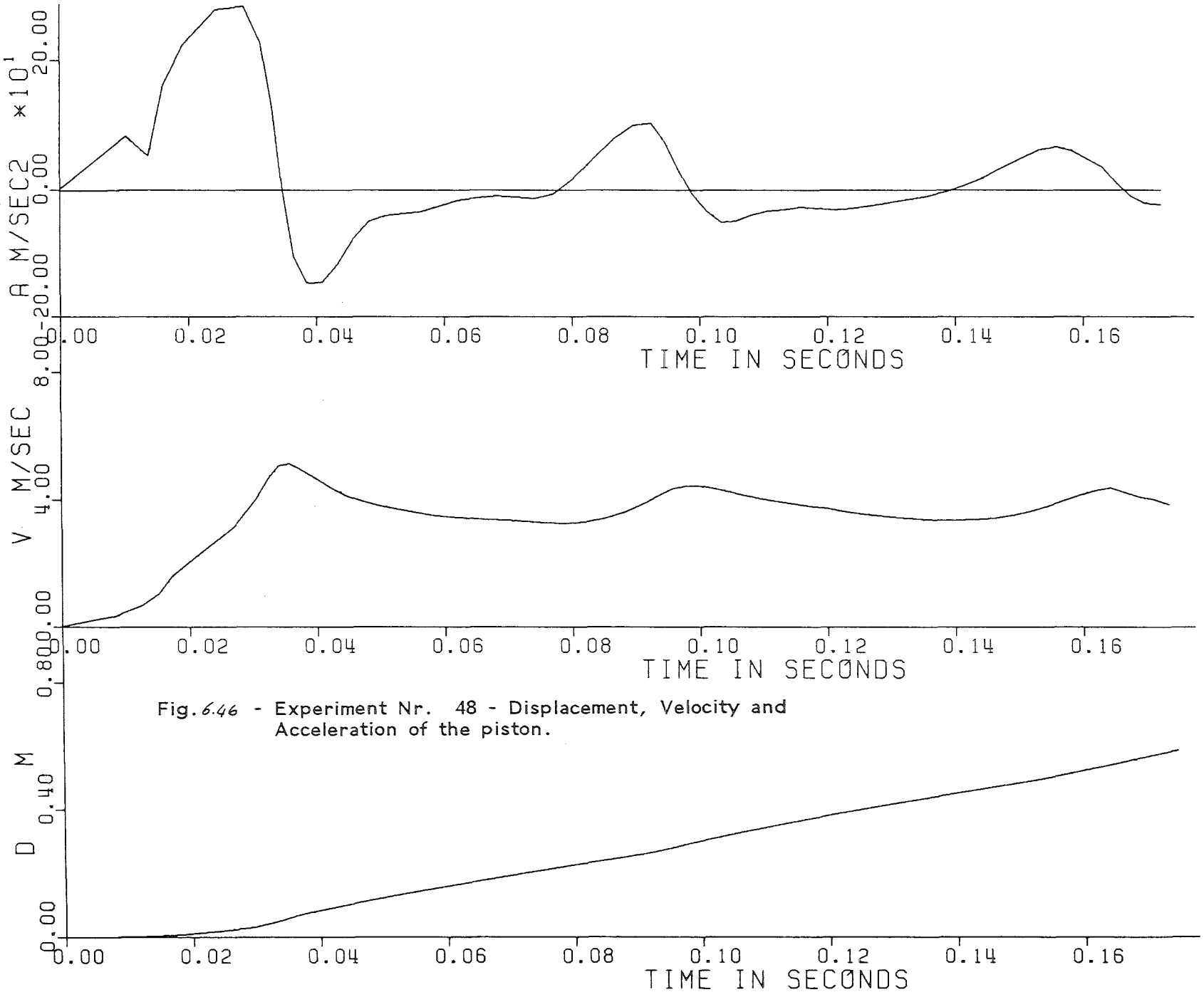

Fig. 6.46 - Experiment Nr. 48 - Displacement, Velocity and Acceleration of the piston.

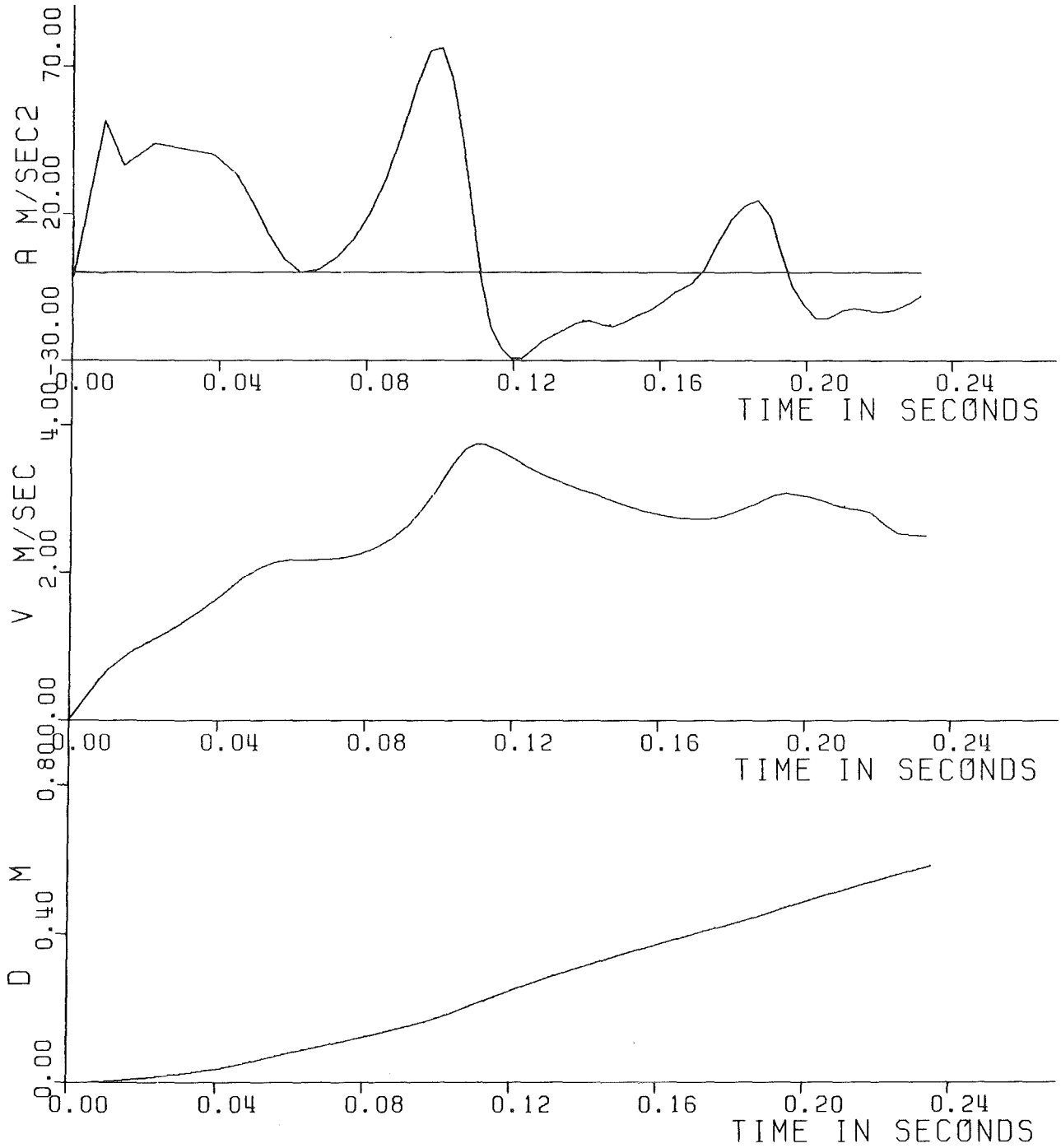

Fig.6.47 - Experiment Nr. 49 - Displacement, Velocity and Acceleration of the piston.

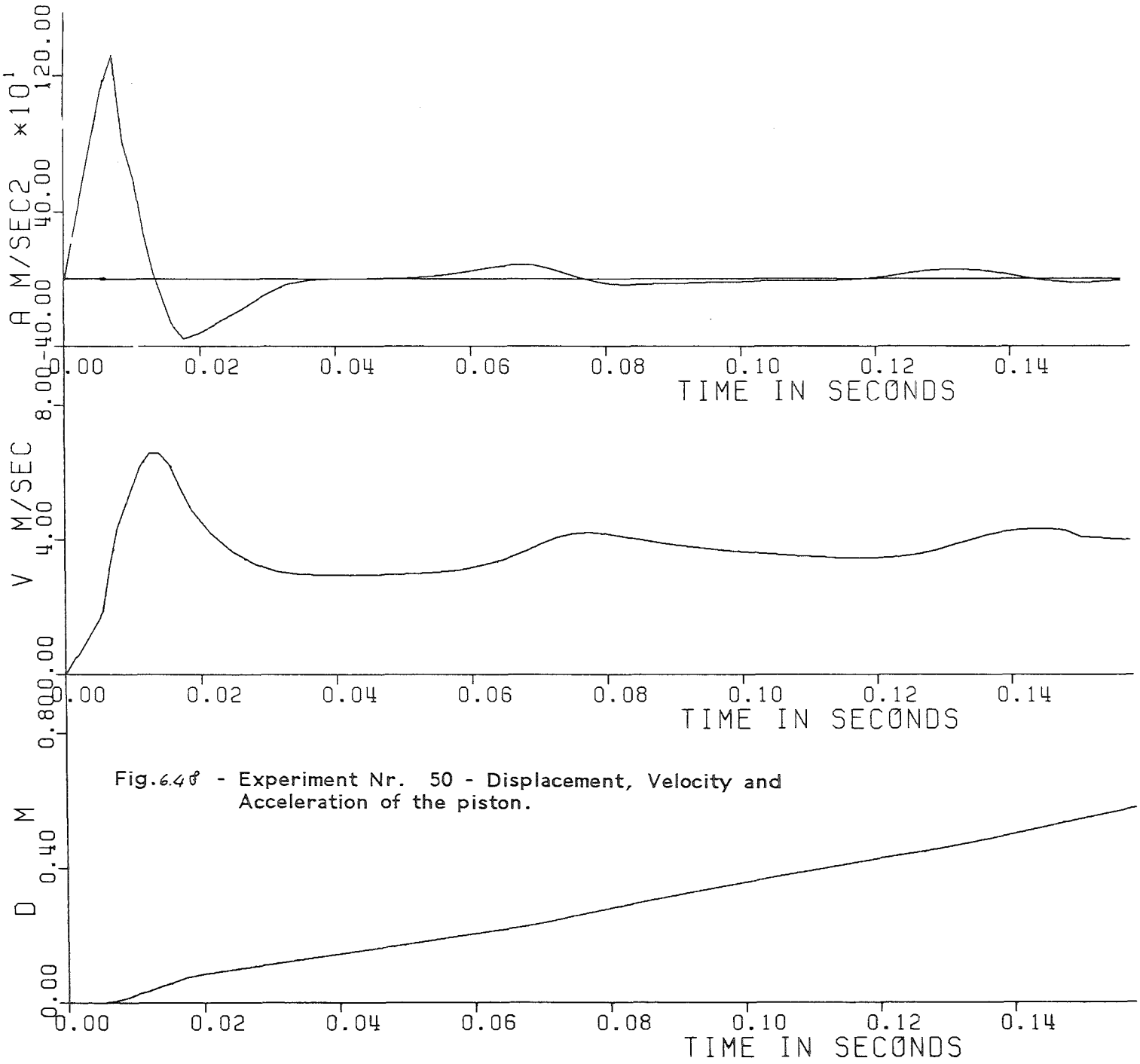

Fig.6.48 - Experiment Nr. 50 - Displacement, Velocity and Acceleration of the piston.

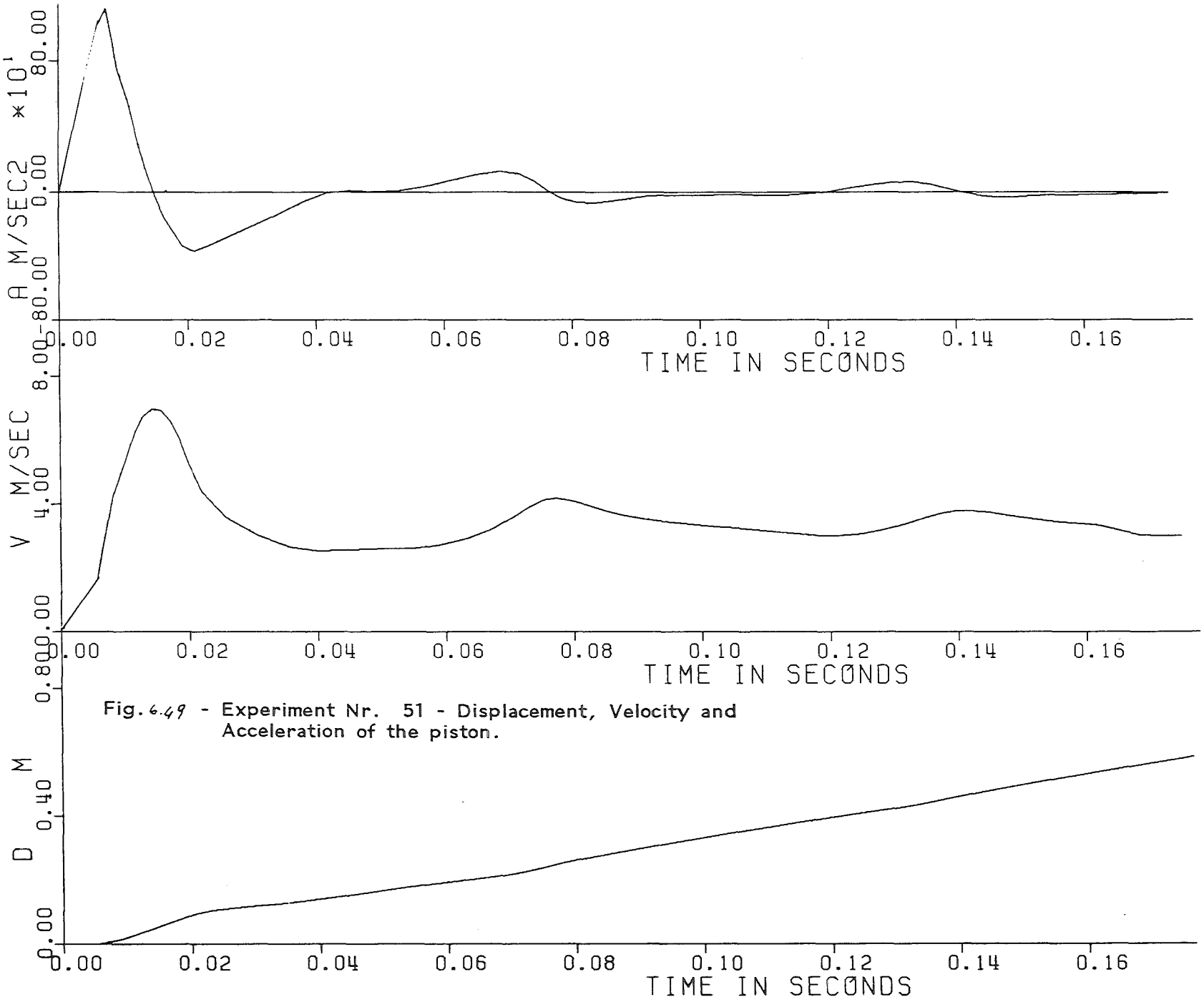

Fig. 6.49 - Experiment Nr. 51 - Displacement, Velocity and Acceleration of the piston.

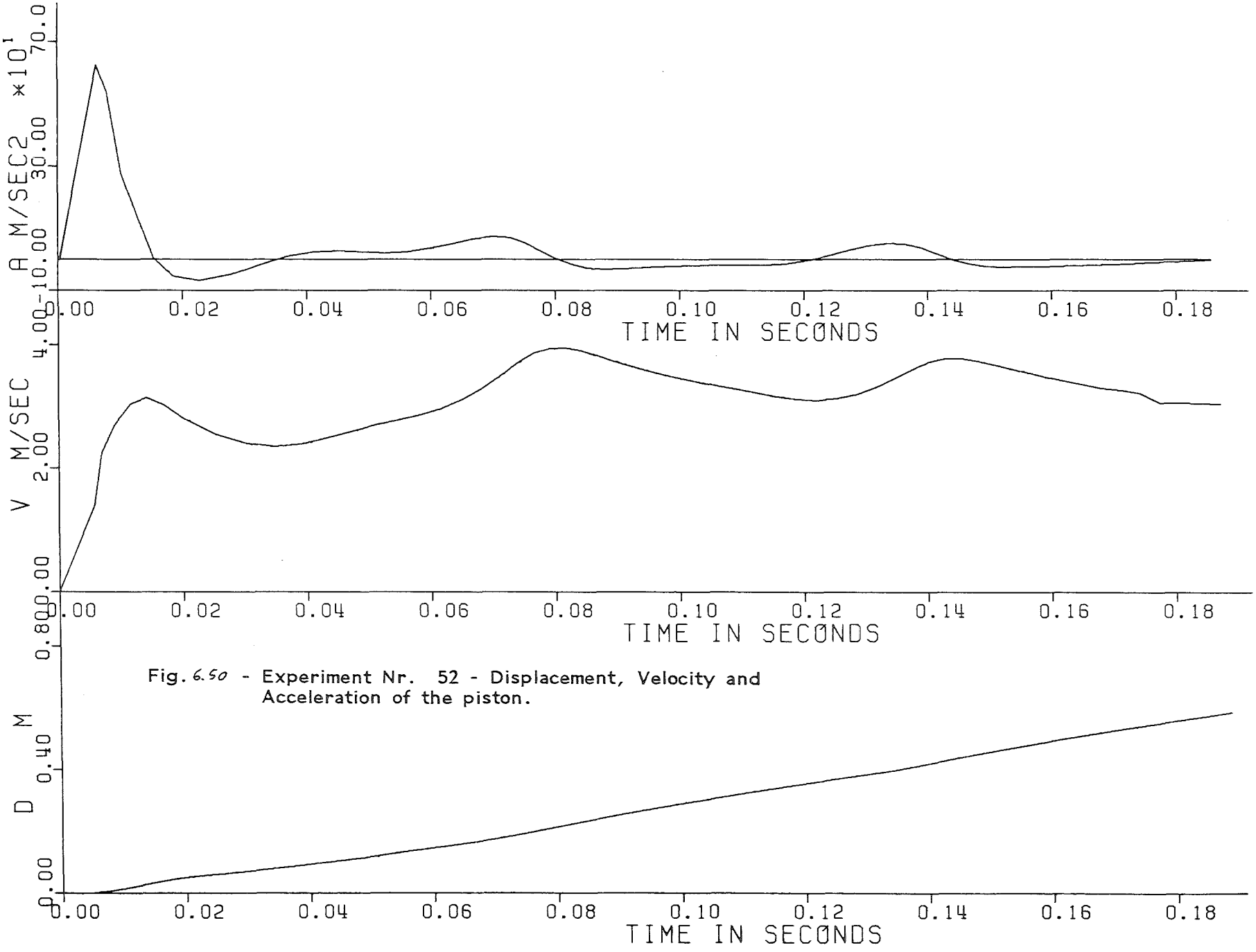

Fig. 6.50 - Experiment Nr. 52 - Displacement, Velocity and Acceleration of the piston.

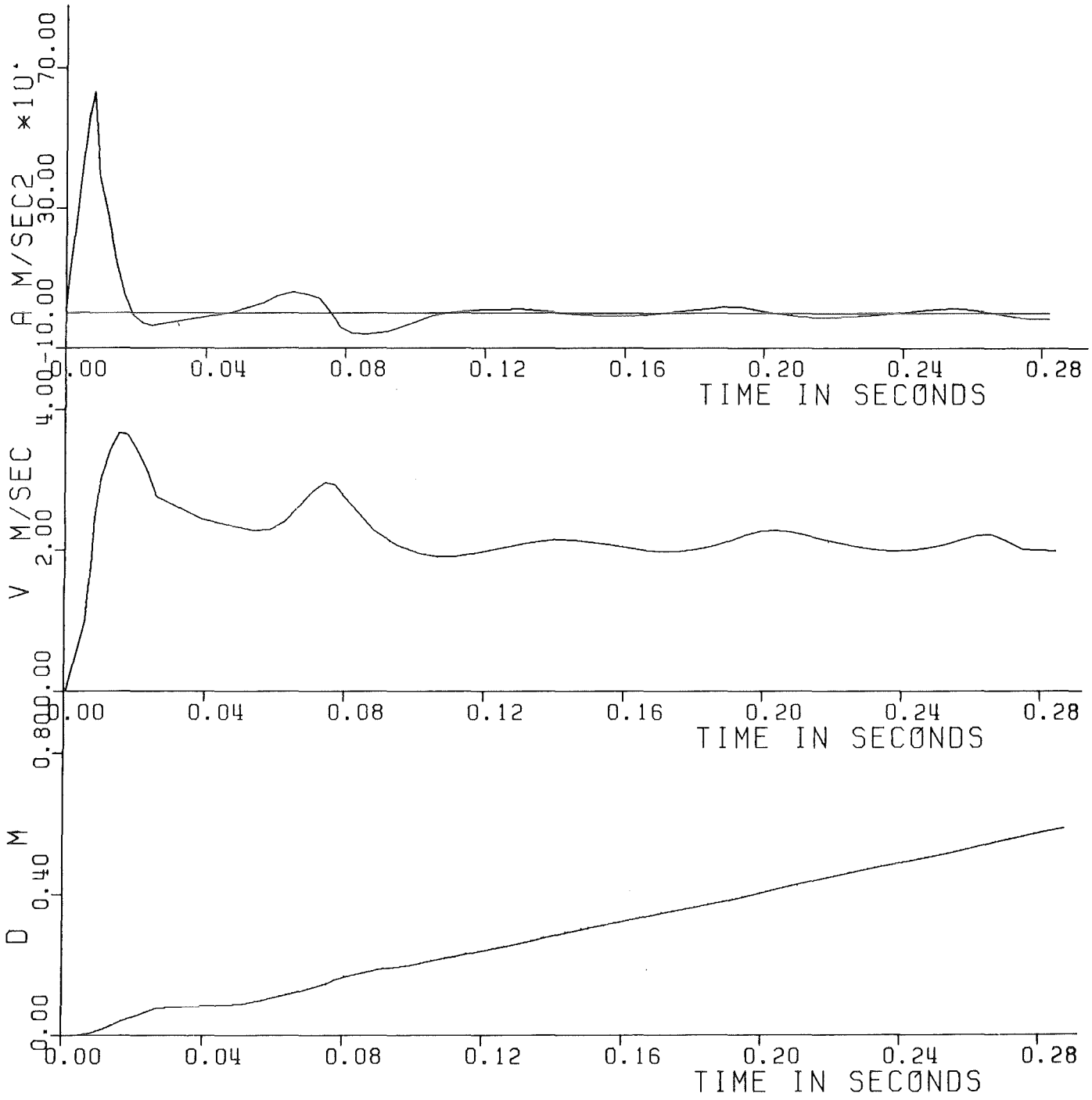

Fig. 6.51 - Experiment Nr. 53 - Displacement, Velocity and Acceleration of the piston.

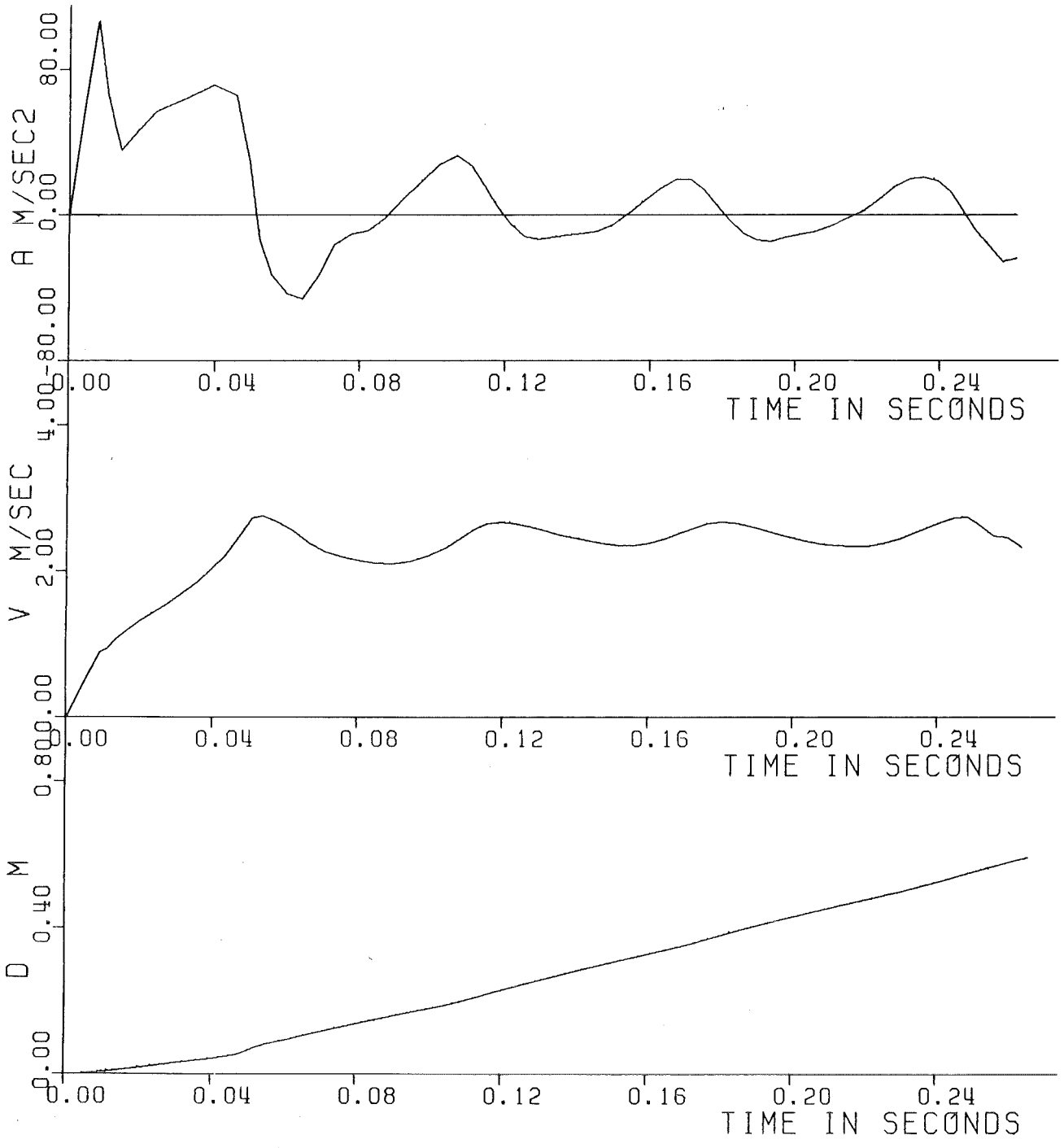

Fig.6.52 - Experiment Nr. 54 - Displacement, Velocity and Acceleration of the piston.

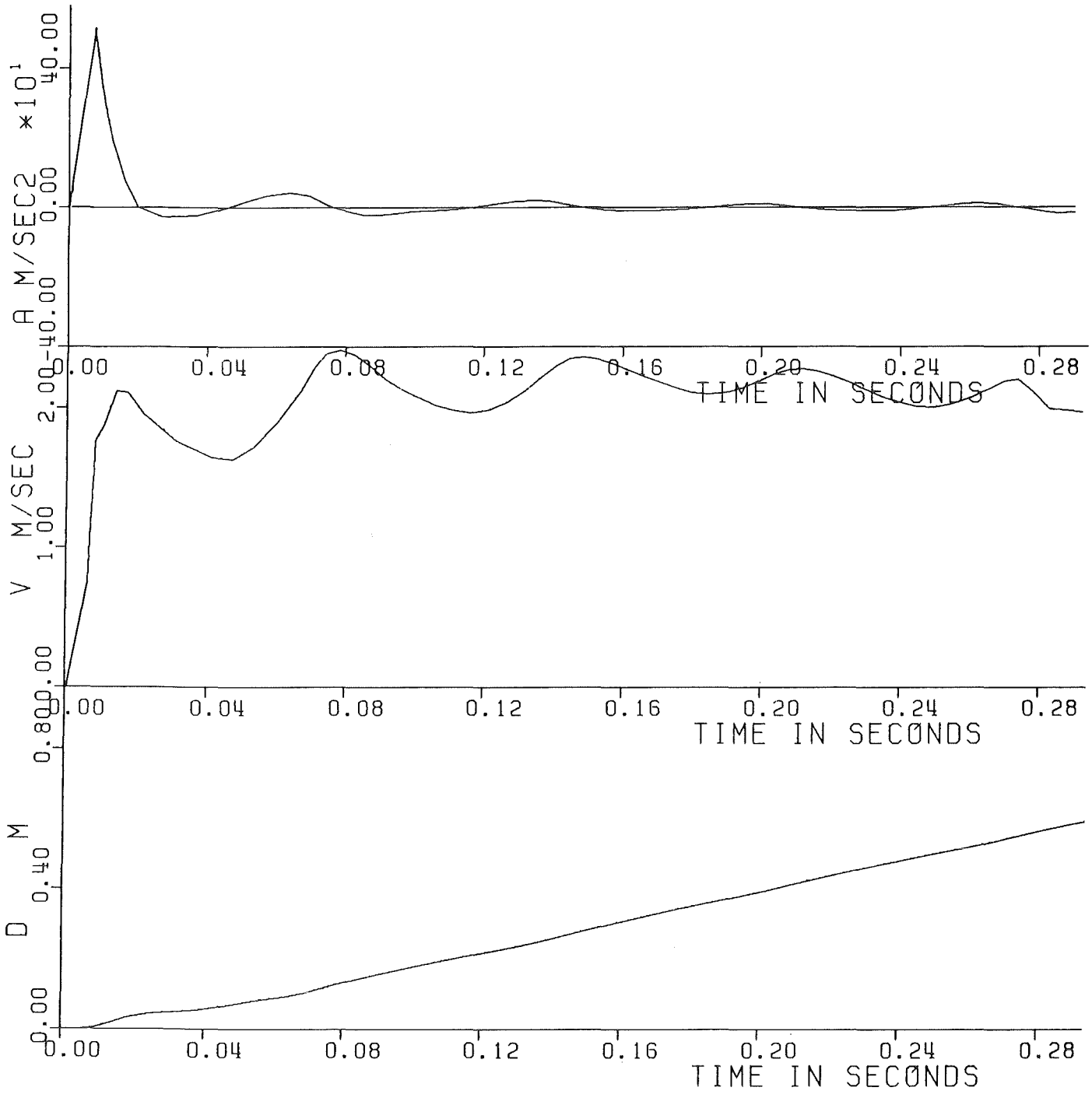

Fig.6.53 - Experiment Nr. 56 - Displacement, Velocity and Acceleration of the piston.

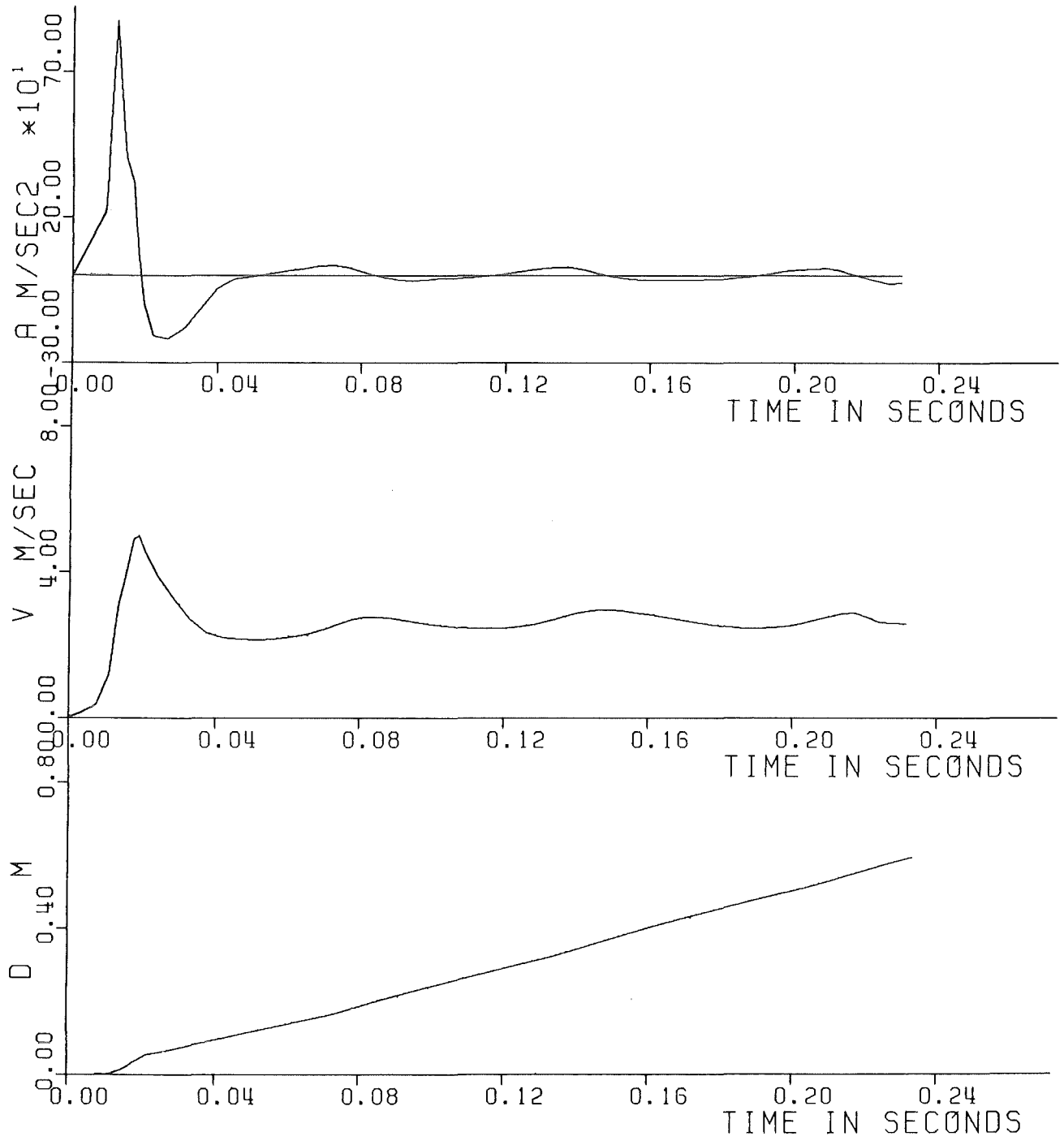

Fig. 6.54 - Experiment Nr. 57 - Displacement, Velocity and Acceleration of the piston.

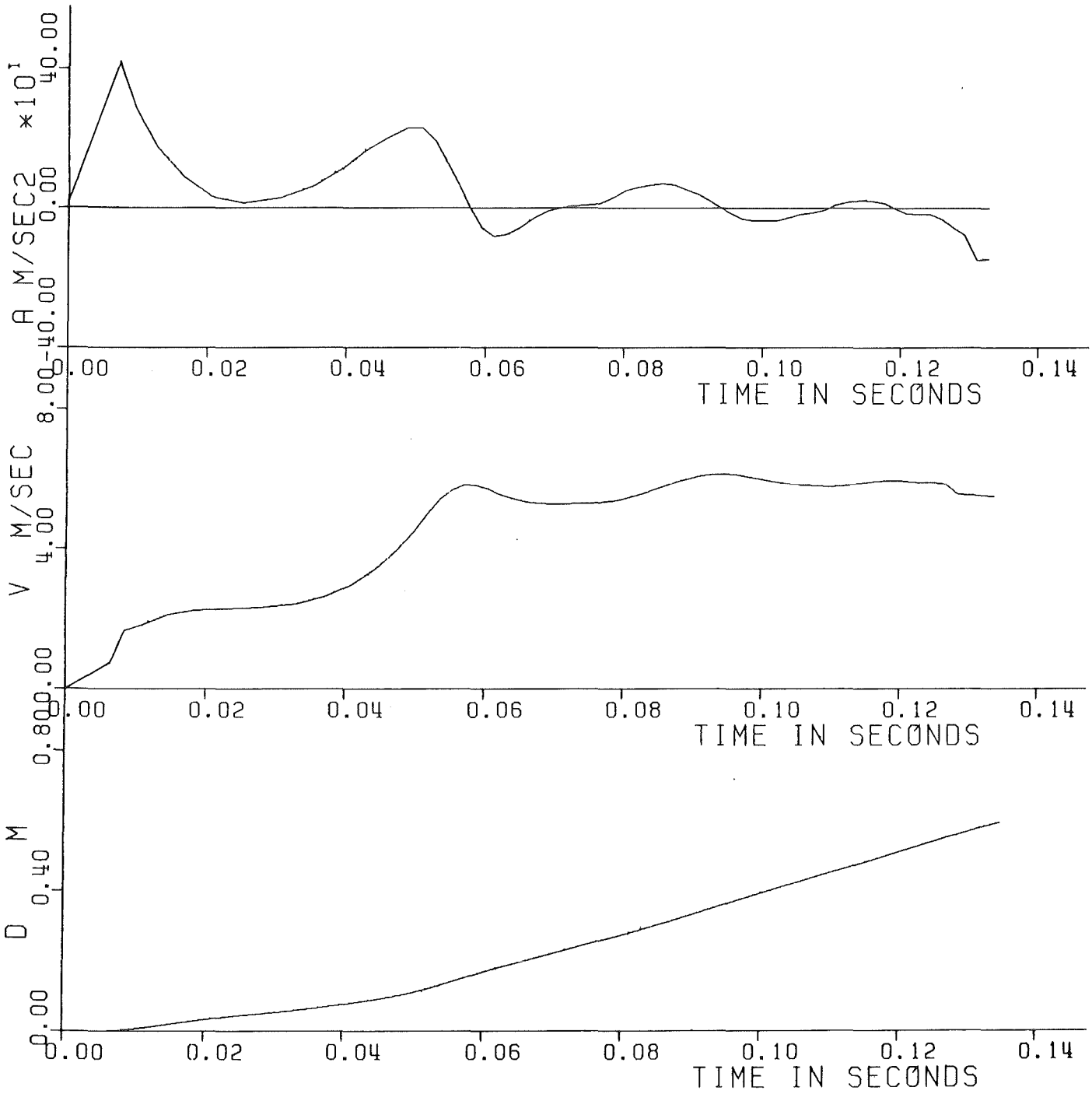

Fig. 6.55 - Experiment Nr. 58 - Displacement, Velocity and Acceleration of the piston.

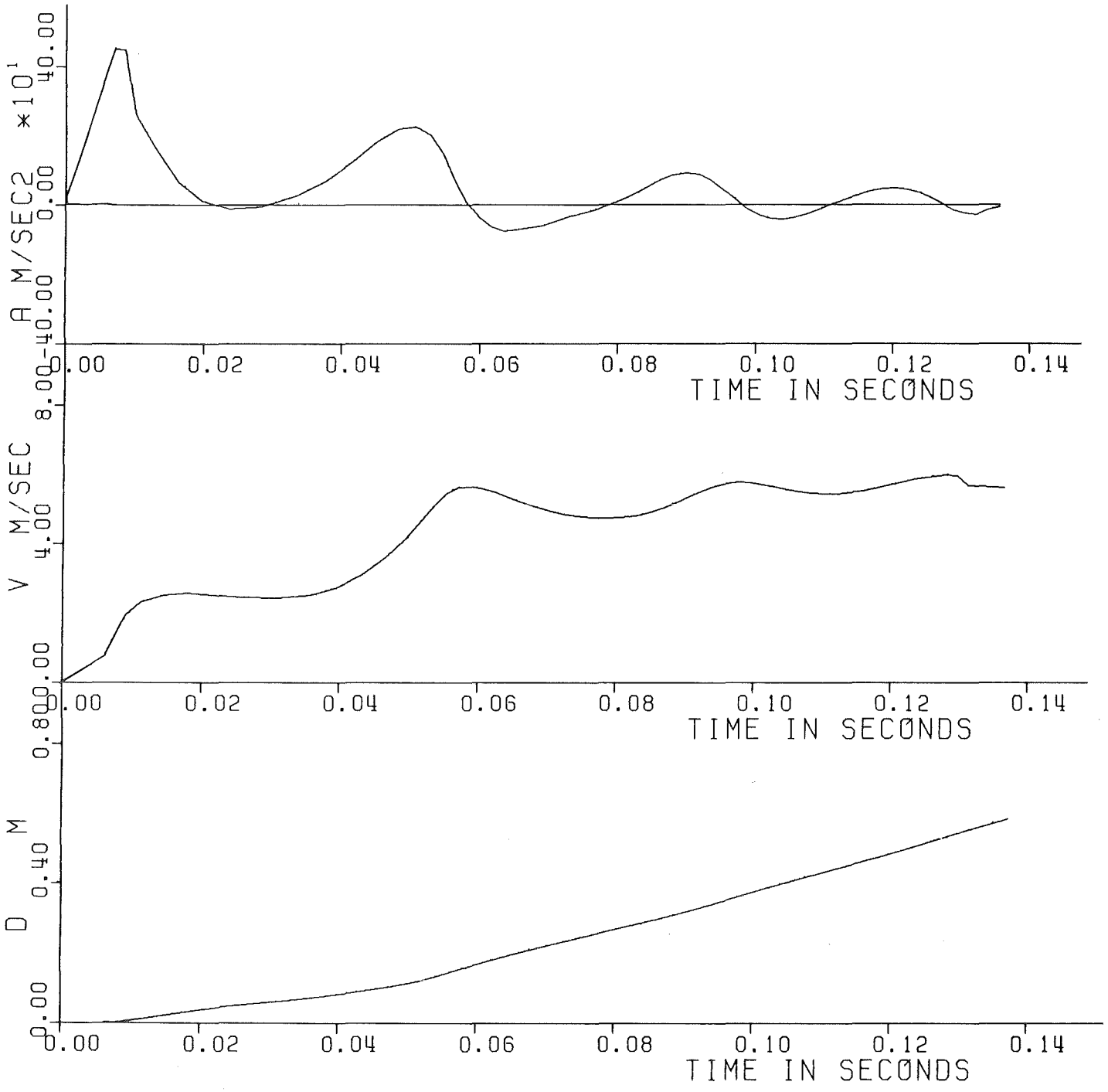

Fig. 6.56 - Experiment Nr. 59 - Displacement, Velocity and Acceleration of the piston.

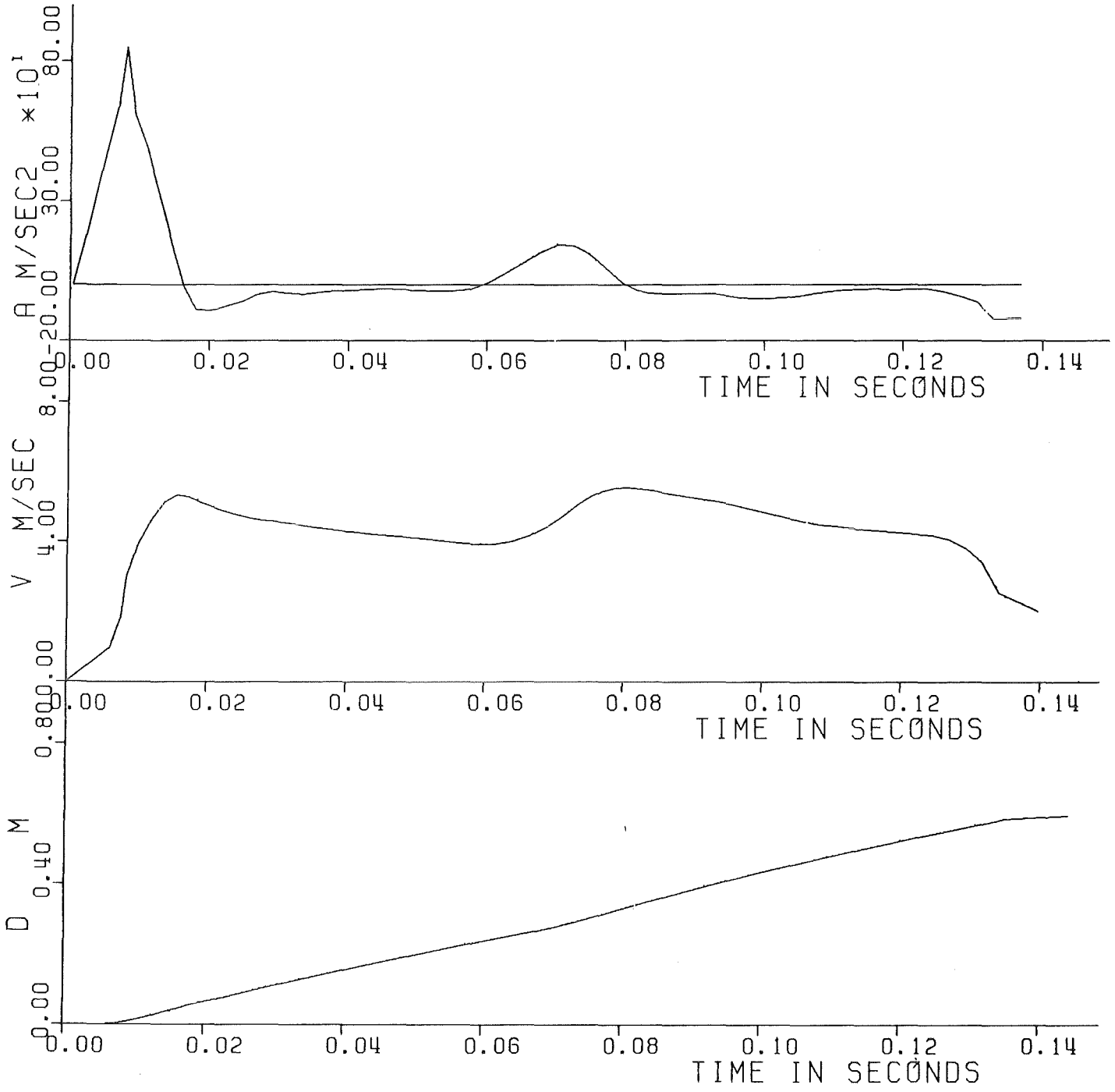

Fig. 6.57 - Experiment Nr. 60 - Displacement, Velocity and Acceleration of the piston.

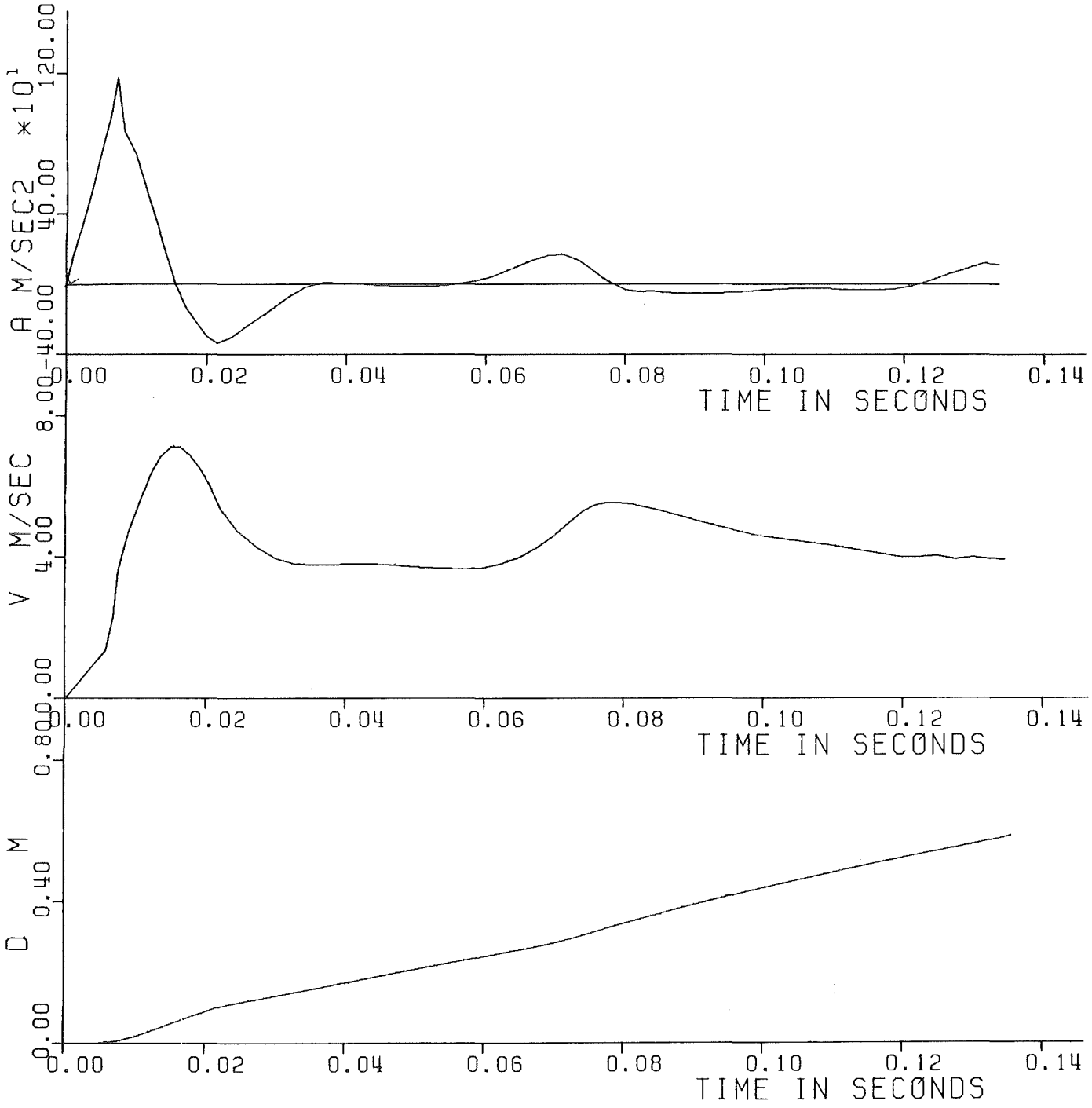

Fig. 6.58 - Experiment Nr. 61 - Displacement, Velocity and Acceleration of the piston.

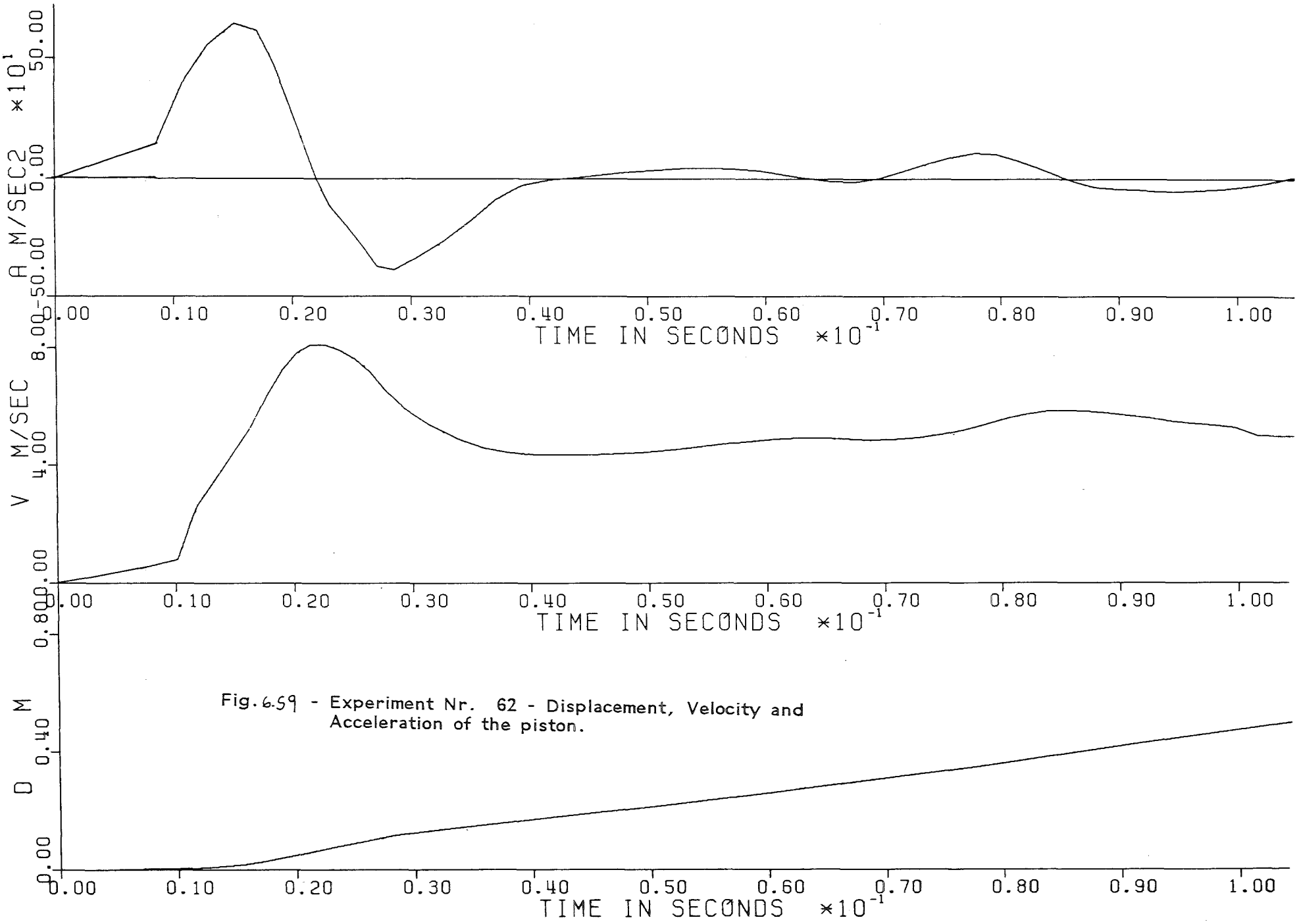

Fig. 6.59 - Experiment Nr. 62 - Displacement, Velocity and Acceleration of the piston.

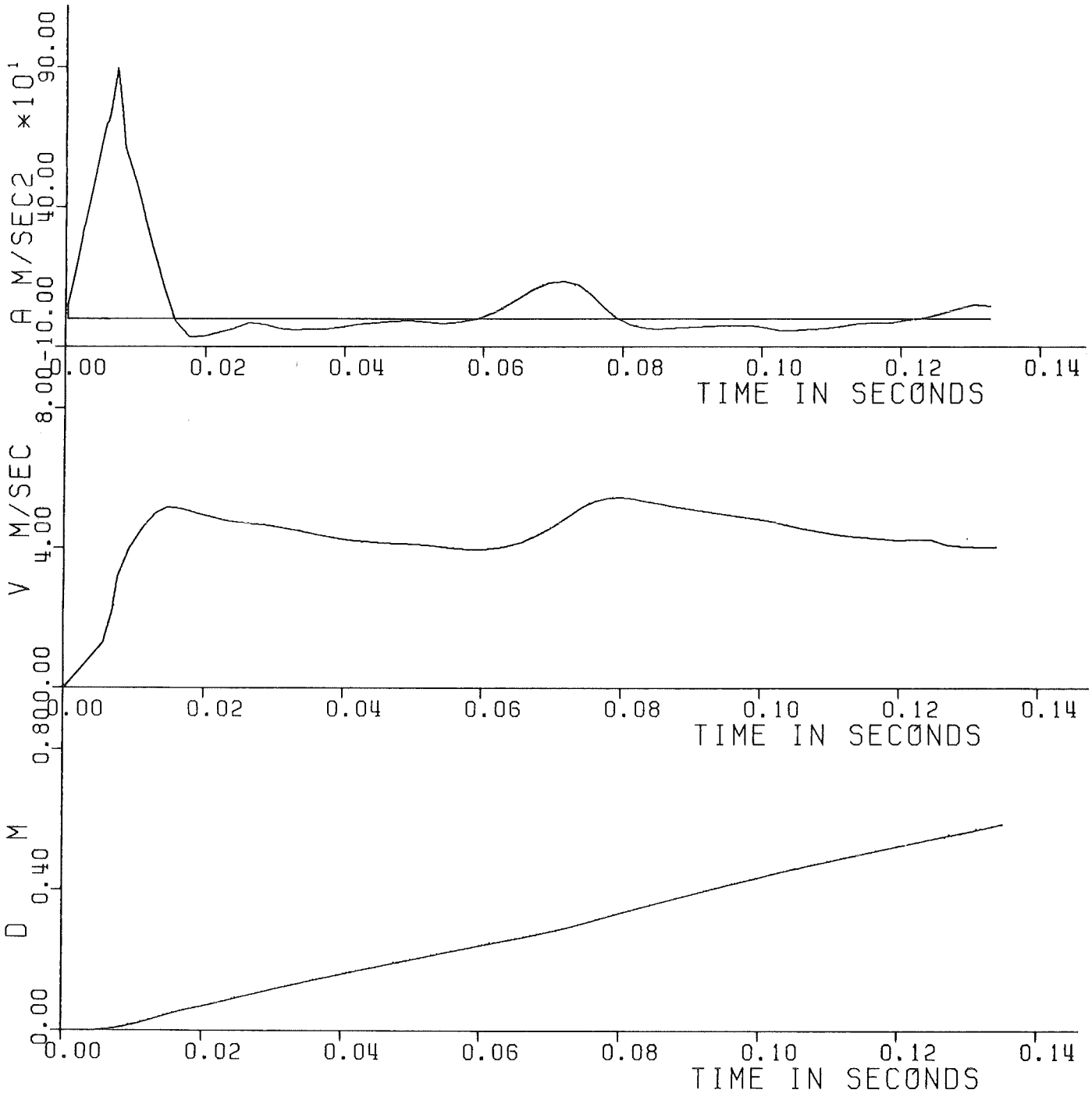

Fig. 6.60 - Experiment Nr. 63 - Displacement, Velocity and Acceleration of the piston.

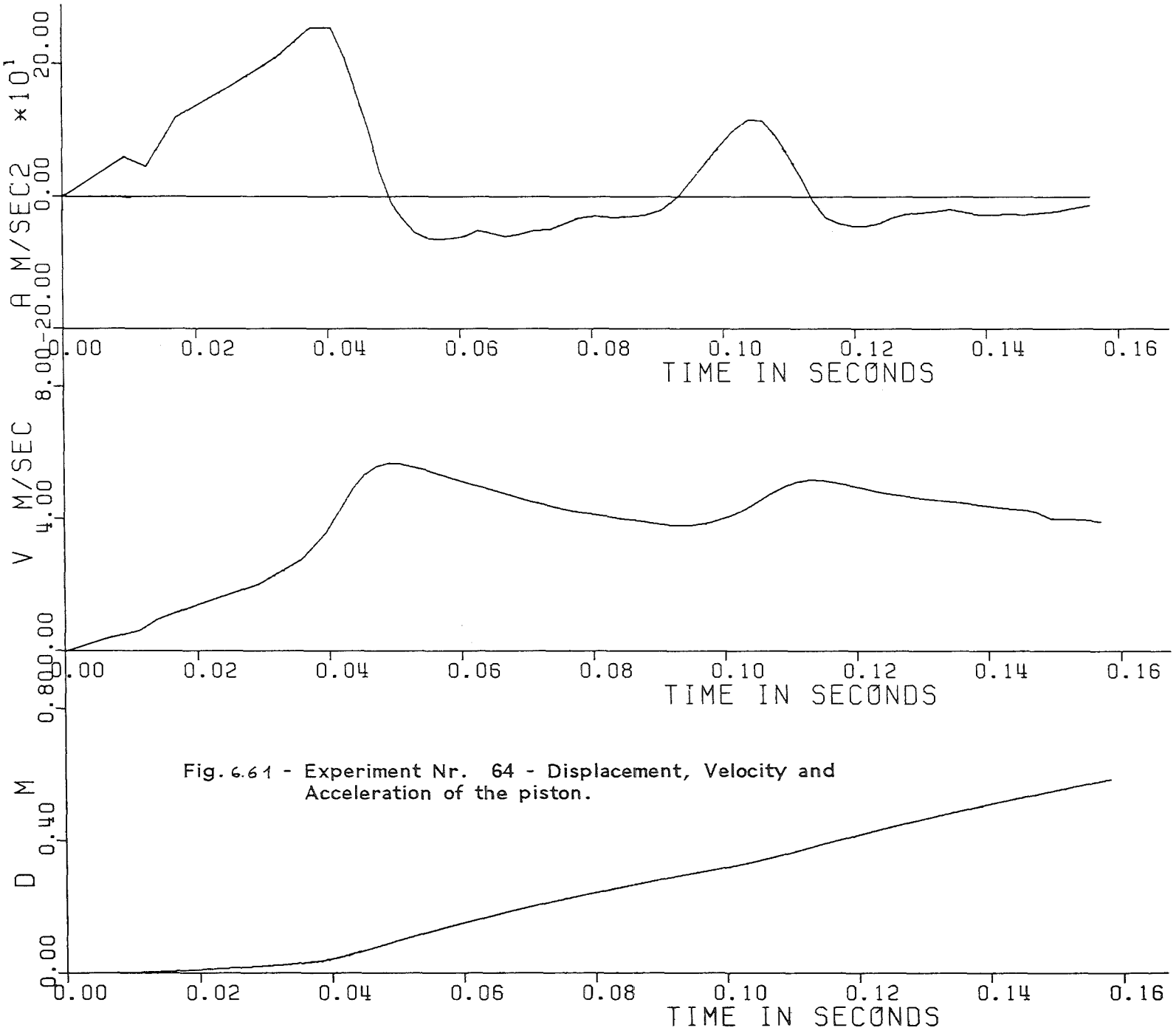

Fig. 6.61 - Experiment Nr. 64 - Displacement, Velocity and Acceleration of the piston.

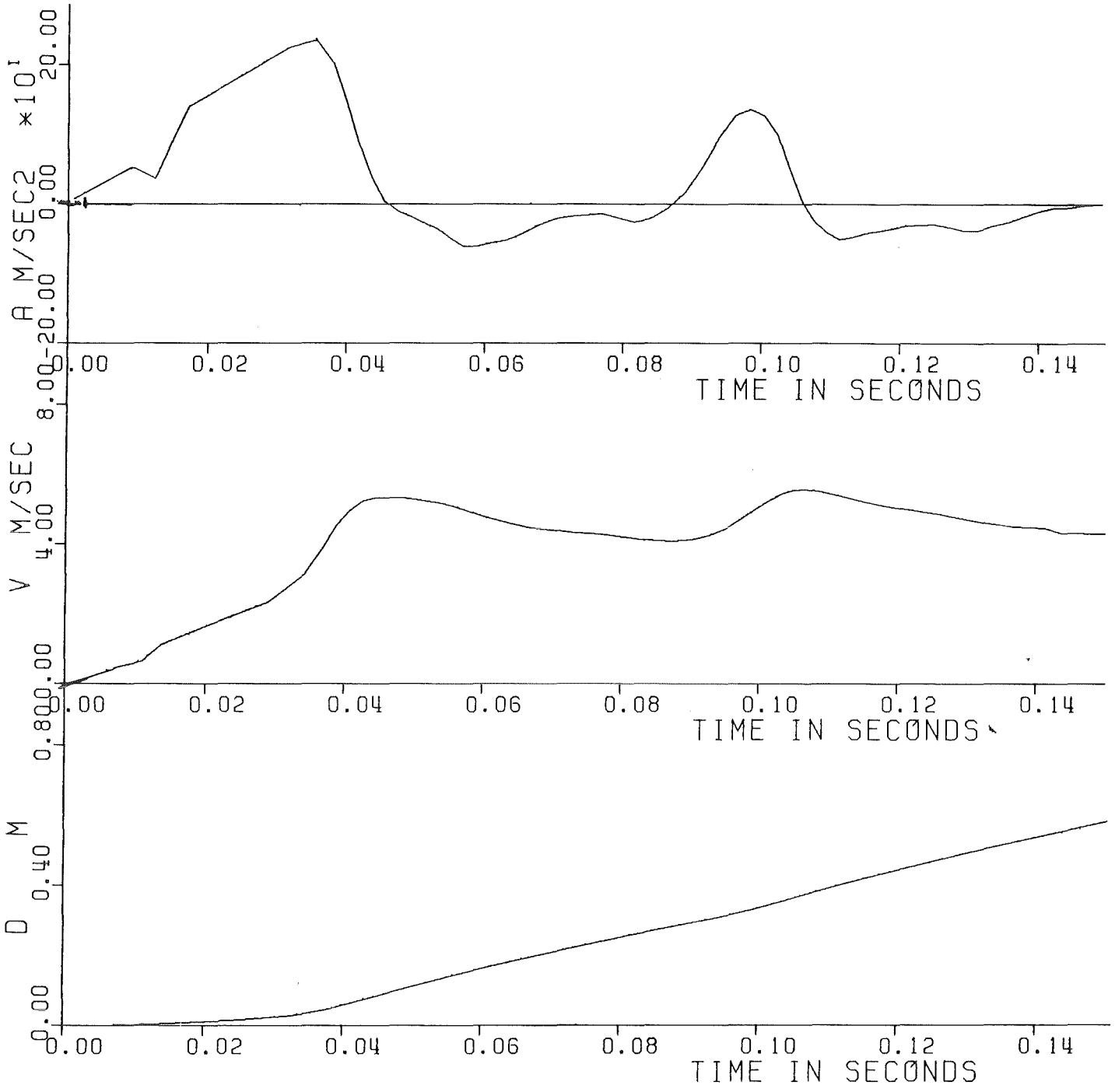

Fig. 6.62 - Experiment Nr. 65 - Displacement, Velocity and Acceleration of the piston.

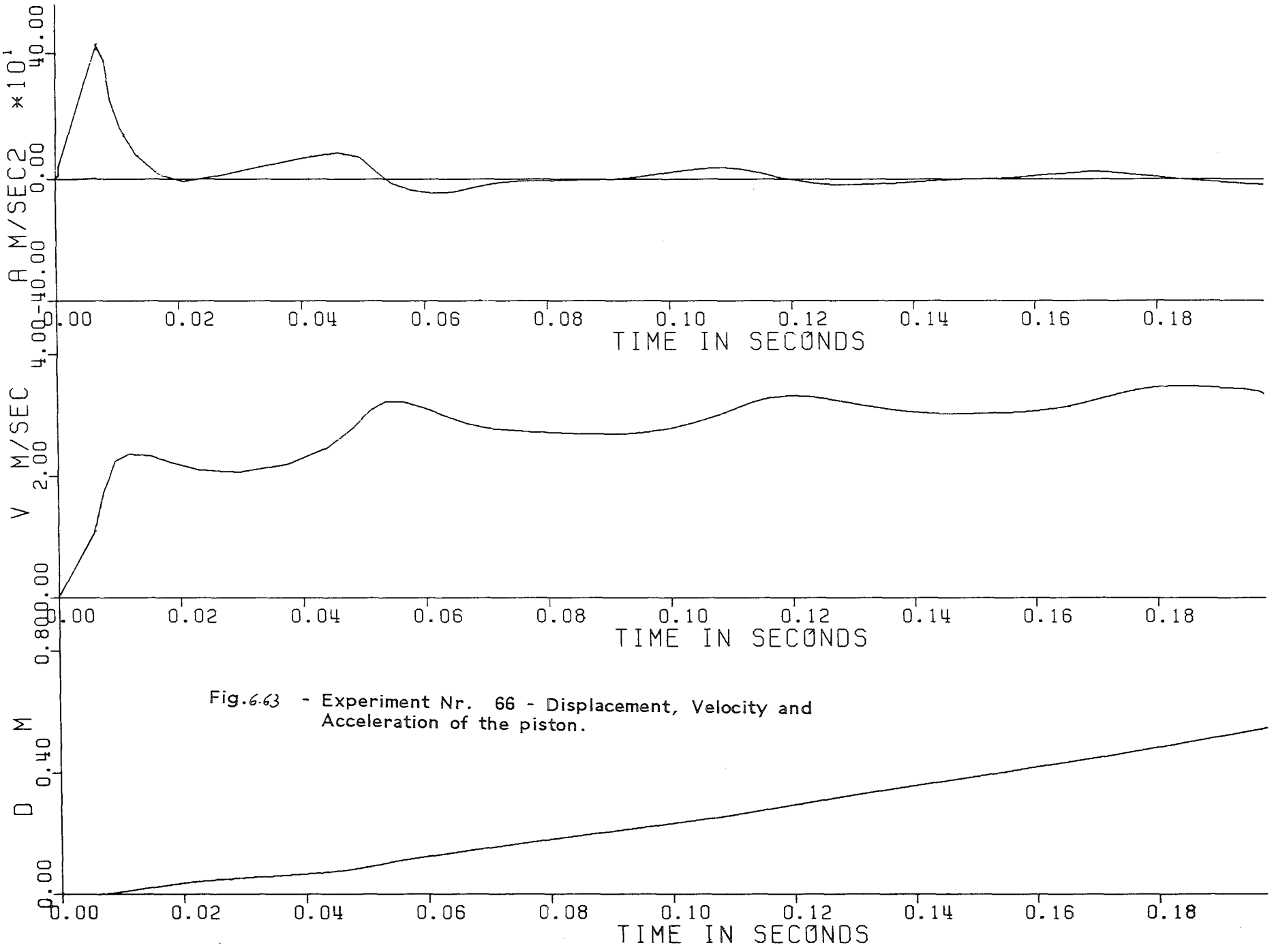

Fig.6.63 - Experiment Nr. 66 - Displacement, Velocity and Acceleration of the piston.

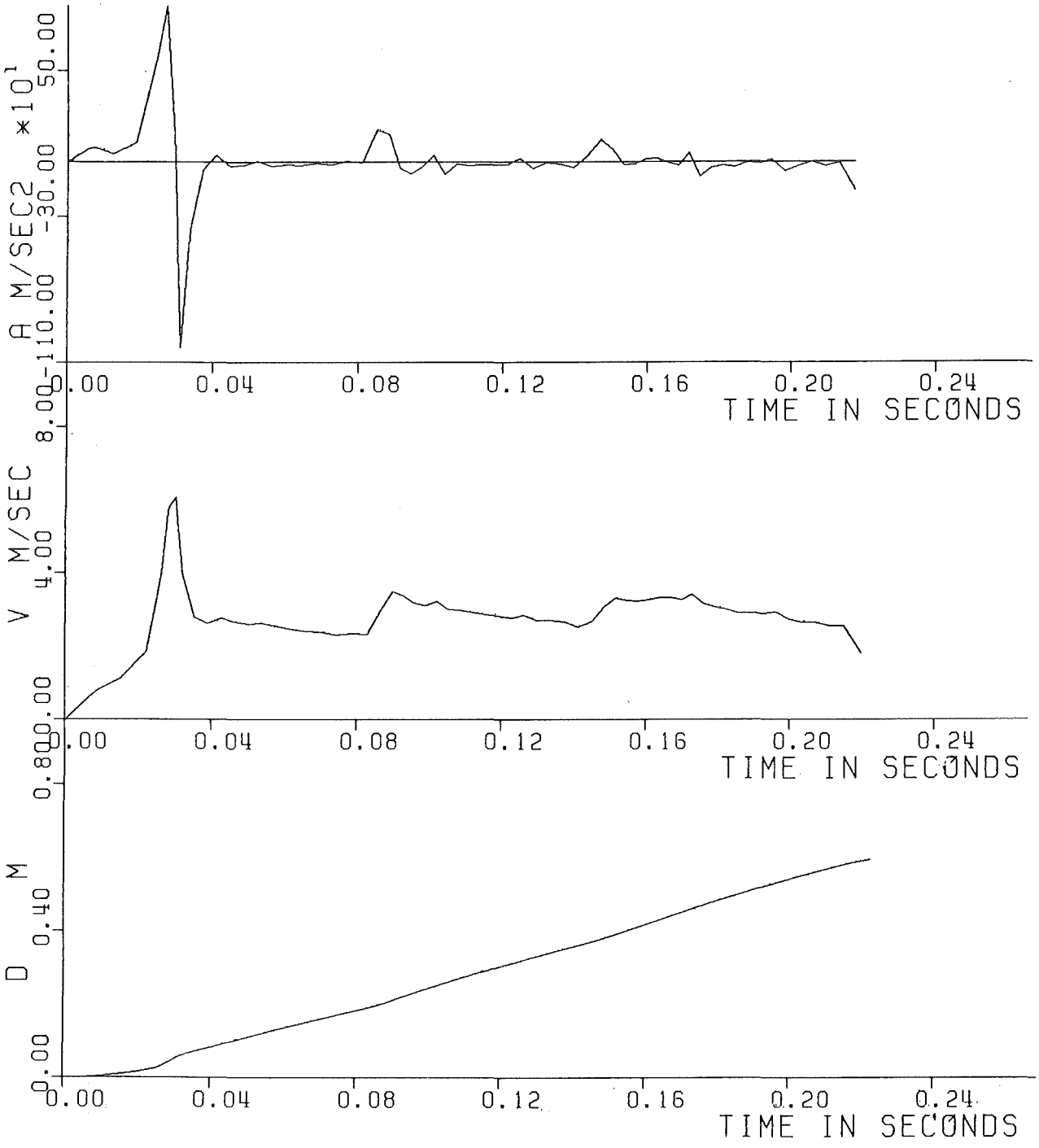

Fig. 6.64 - Experiment Nr. 67 - Displacement, Velocity and Acceleration of the piston.

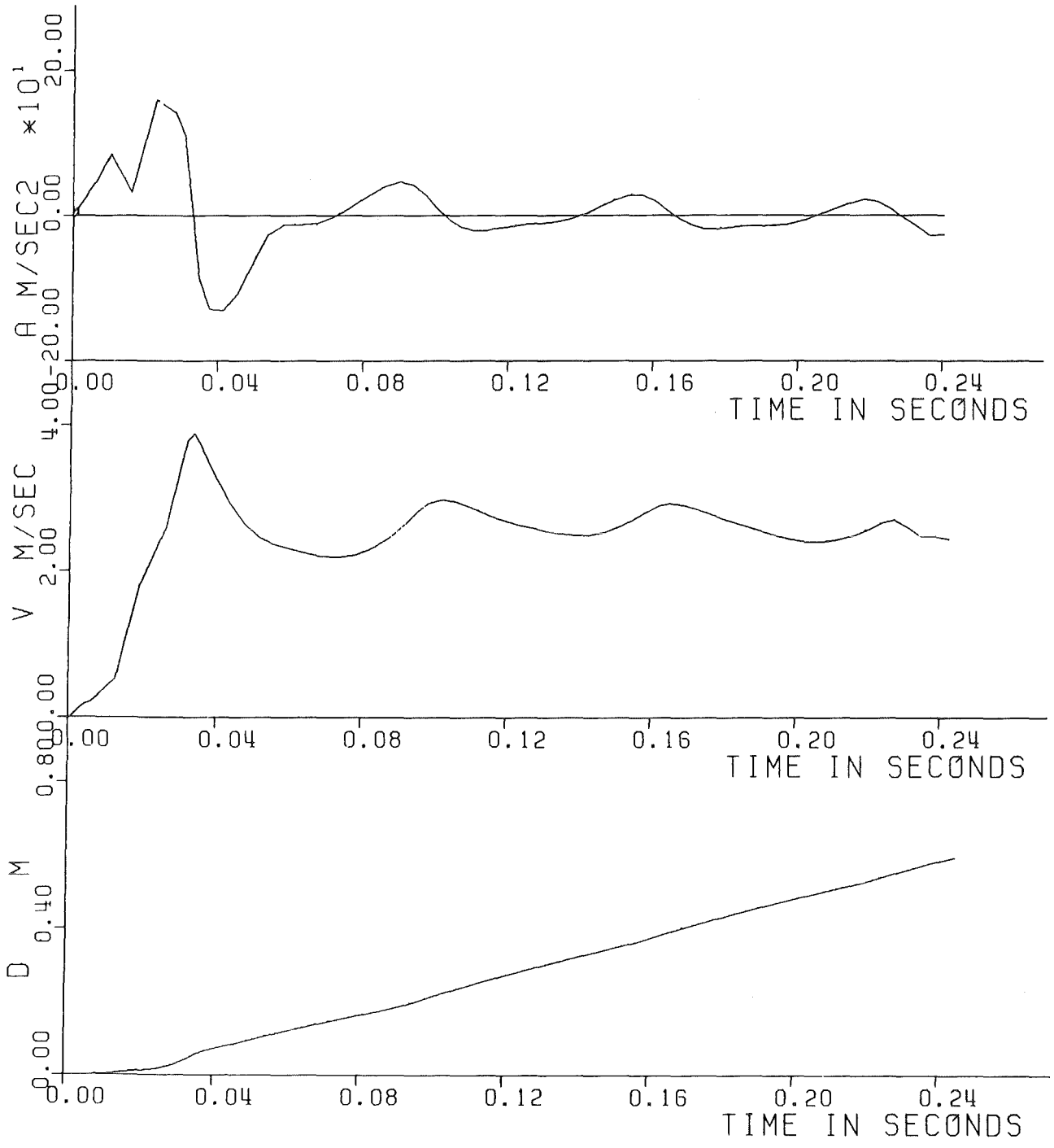

Fig. 6.65 - Experiment Nr. 68 - Displacement, Velocity and Acceleration of the piston.

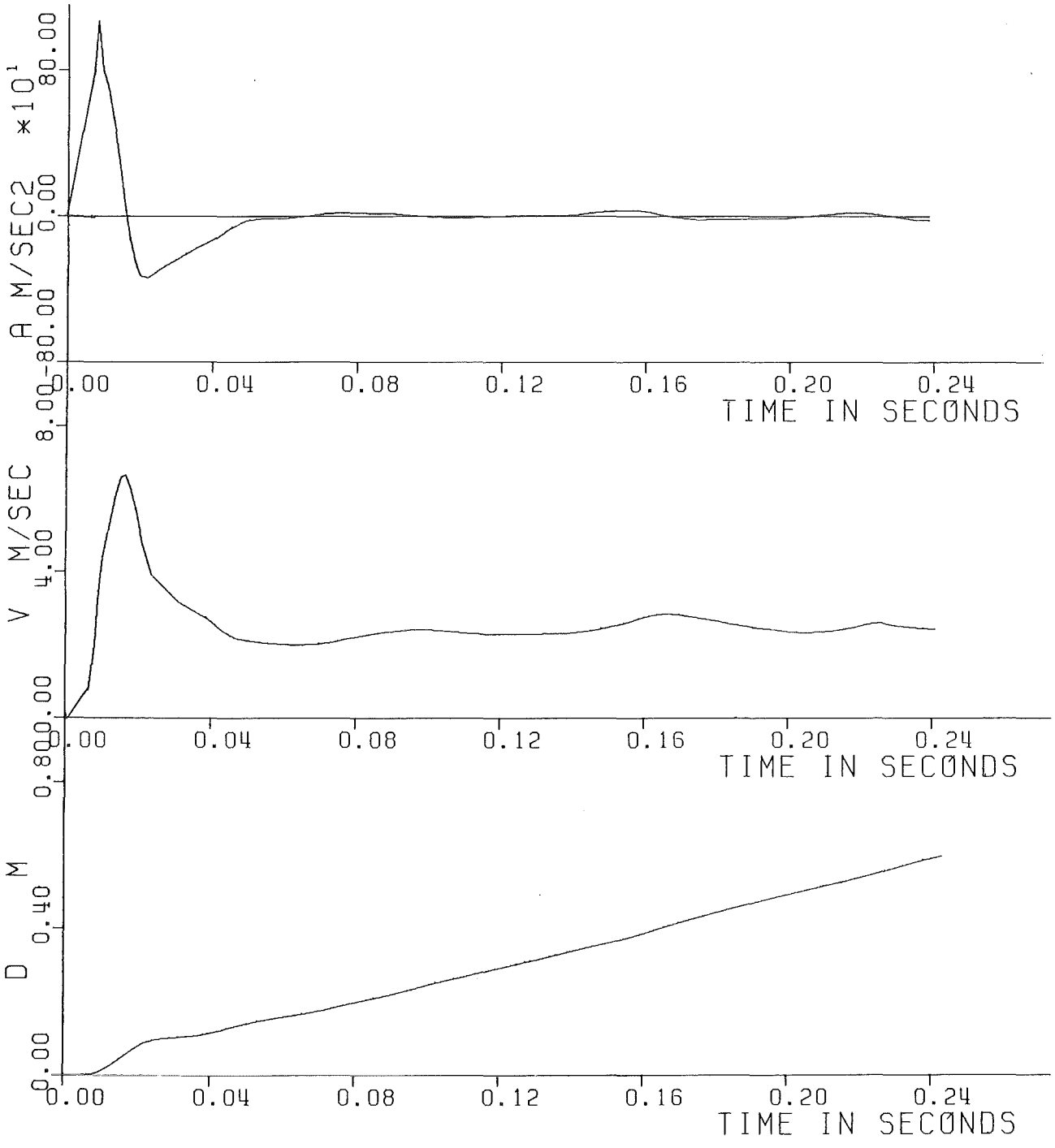

Fig. 6.66 - Experiment Nr. 69 - Displacement, Velocity and Acceleration of the piston.

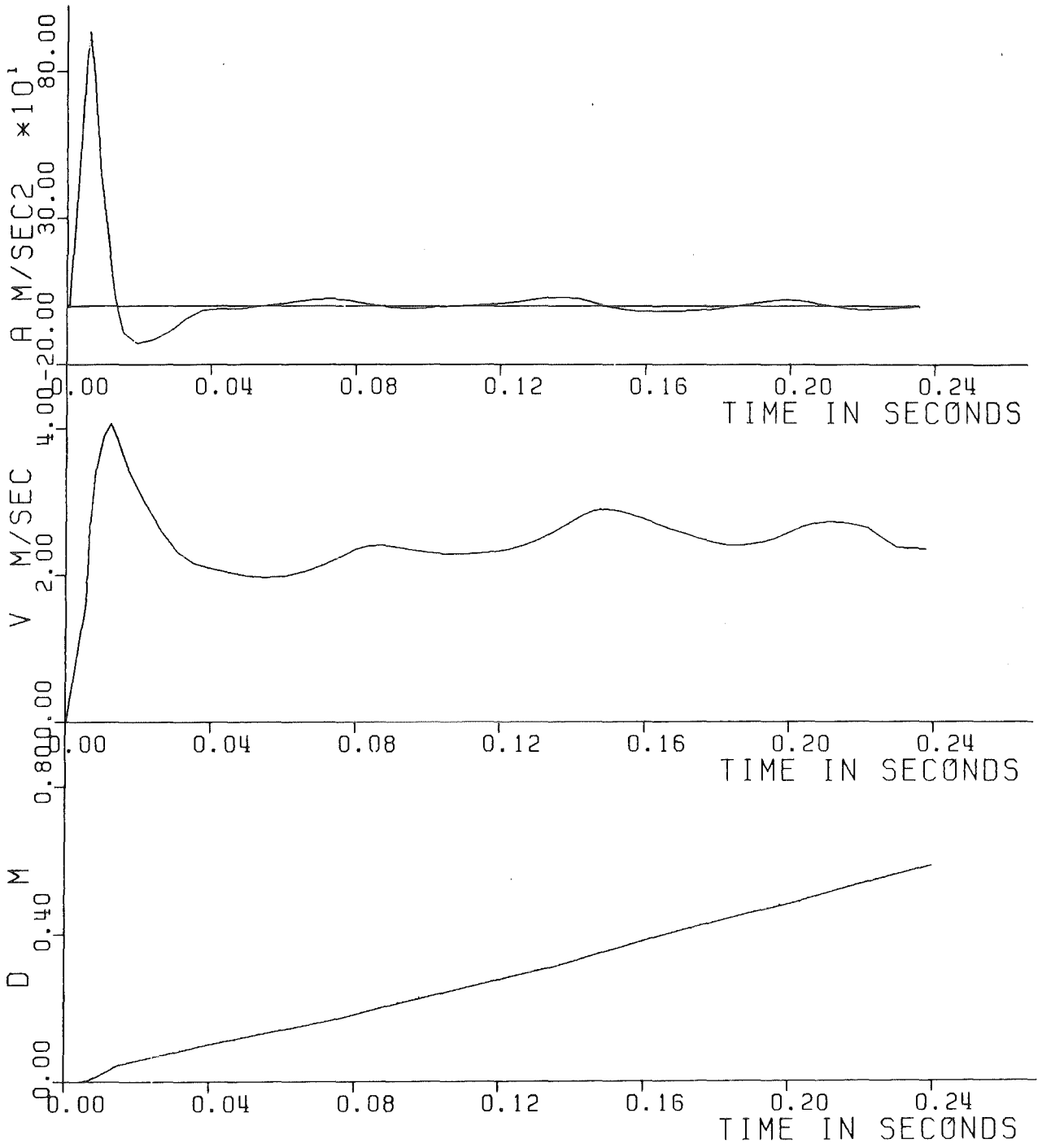

Fig. 6.67 - Experiment Nr. 70 - Displacement, Velocity and Acceleration of the piston.

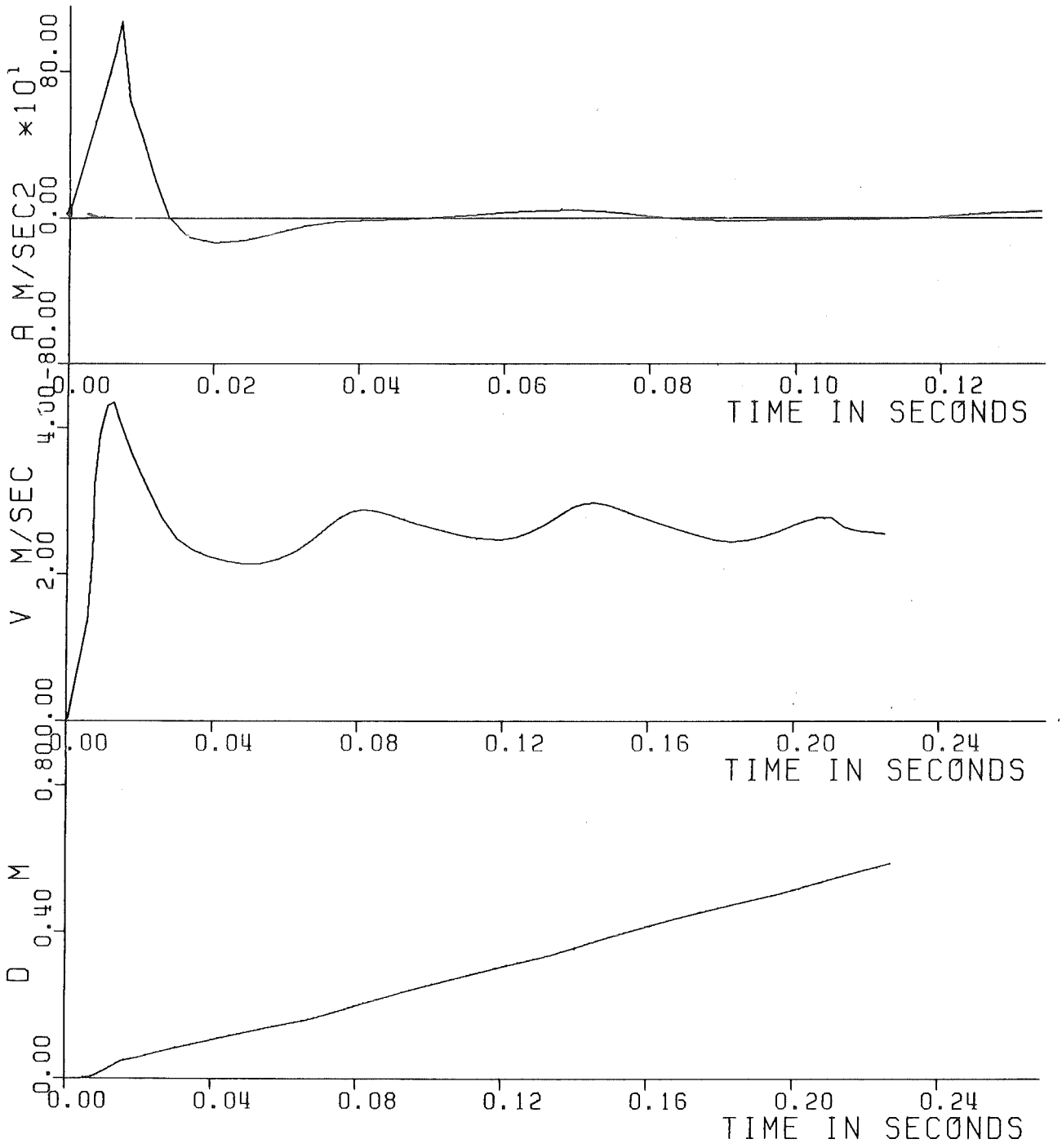

Fig. 6.68 - Experiment Nr. 71 - Displacement, Velocity and Acceleration of the piston.

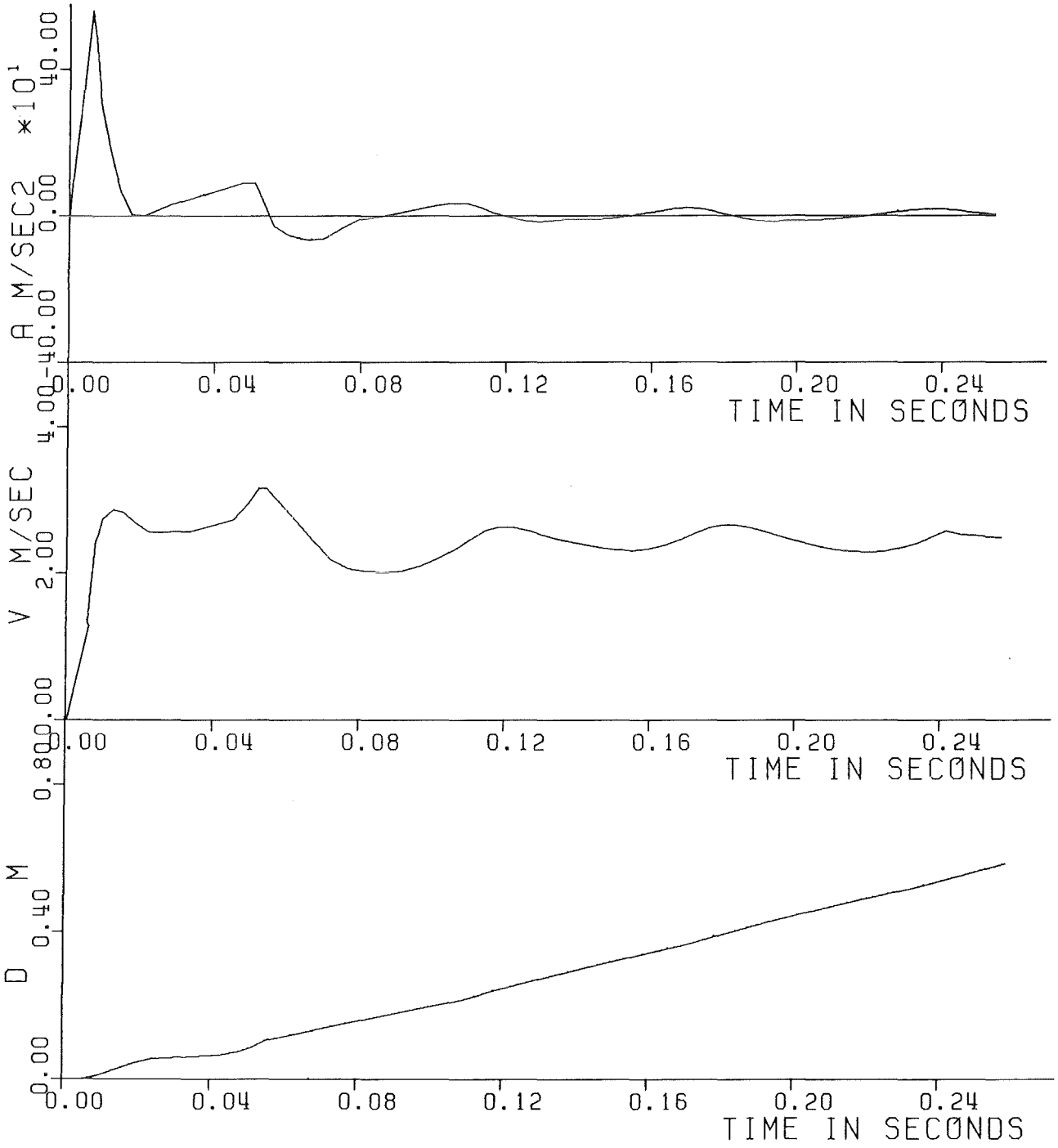

Fig.6.69 - Experiment Nr. 72 - Displacement, Velocity and Acceleration of the piston.

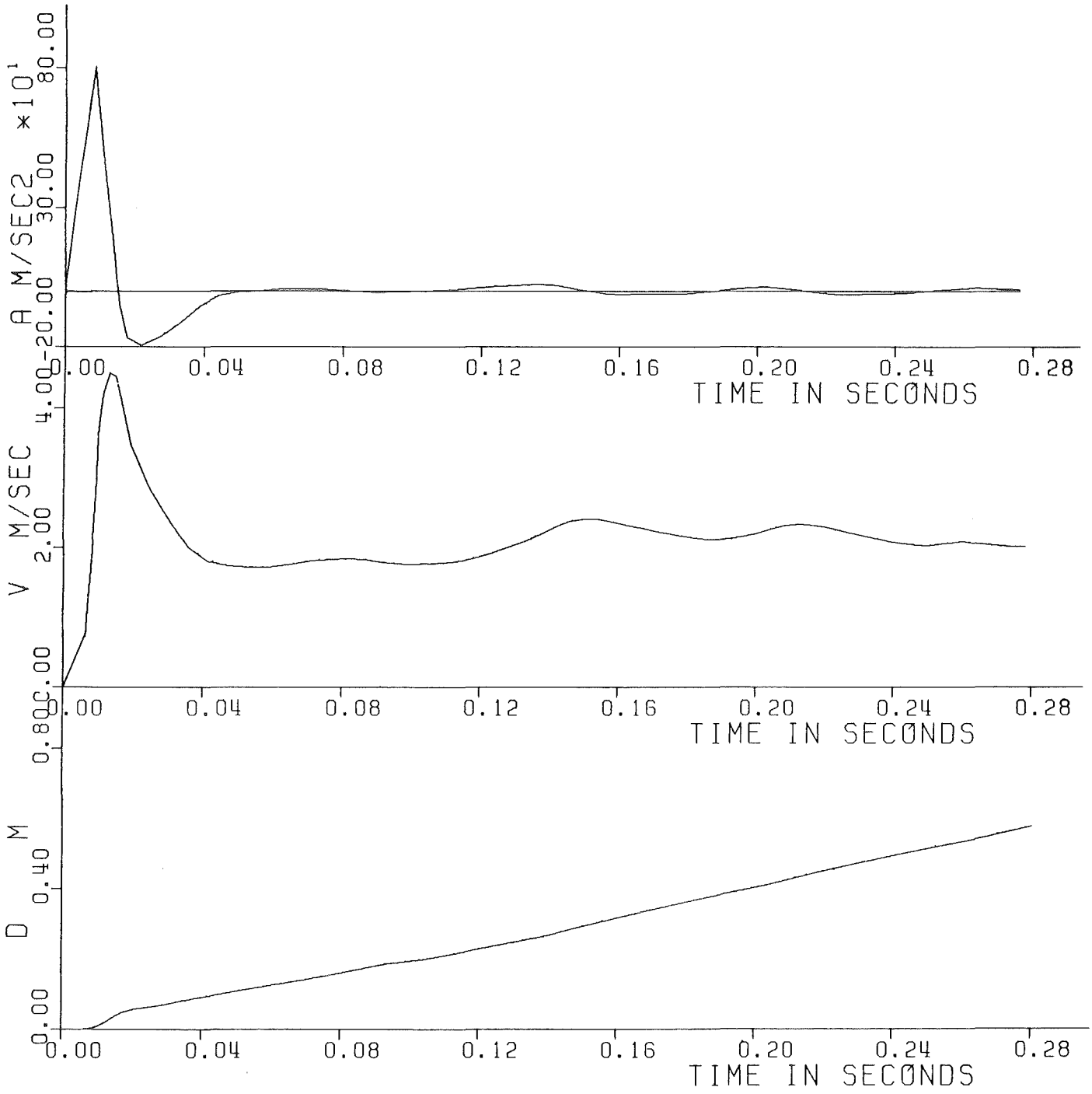

Fig. 6.70 - Experiment Nr. 73 - Displacement, Velocity and Acceleration of the piston.

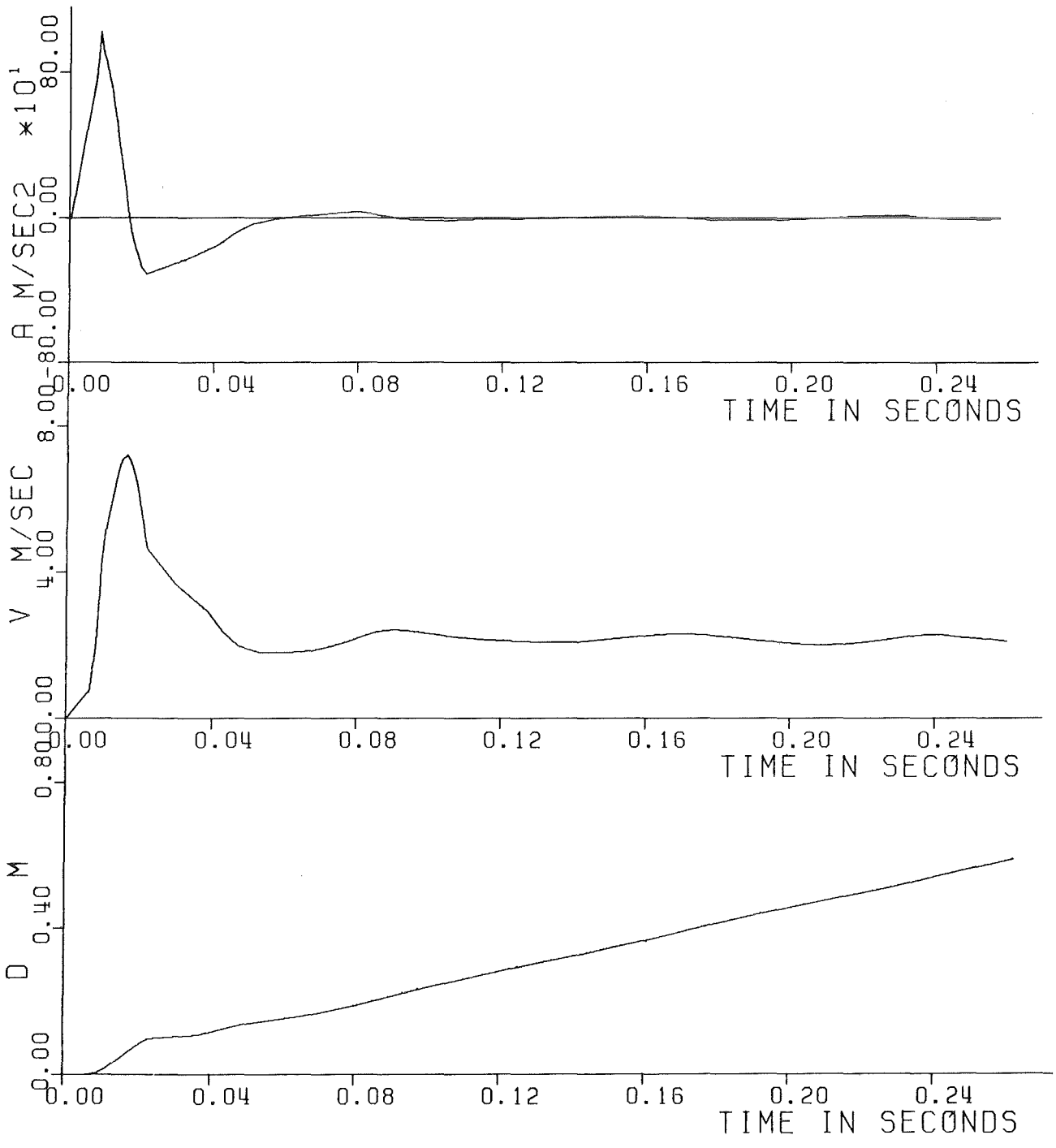

Fig. 6.71 - Experiment Nr. 74 - Displacement, Velocity and Acceleration of the piston.

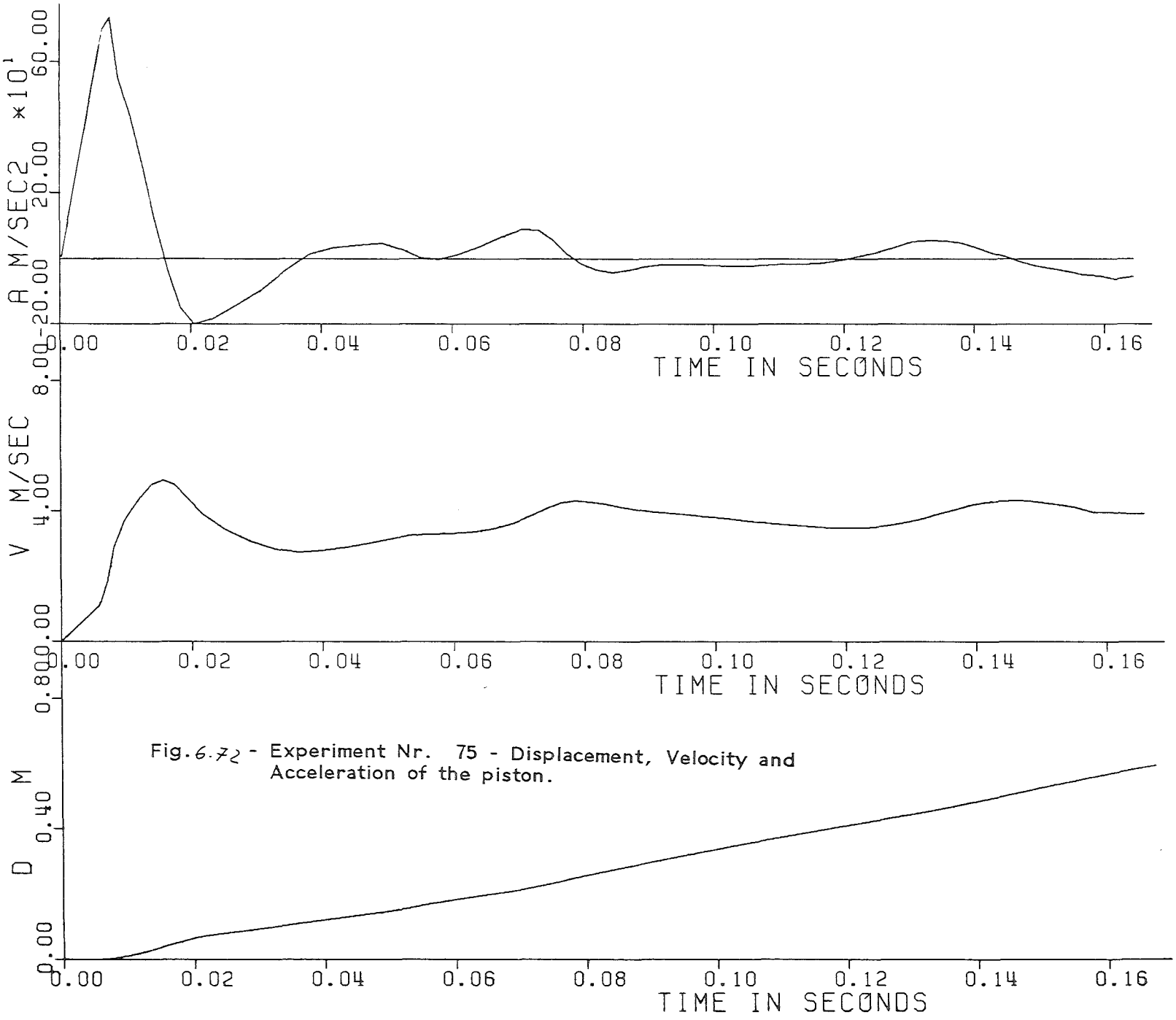

Fig. 6.72 - Experiment Nr. 75 - Displacement, Velocity and Acceleration of the piston.

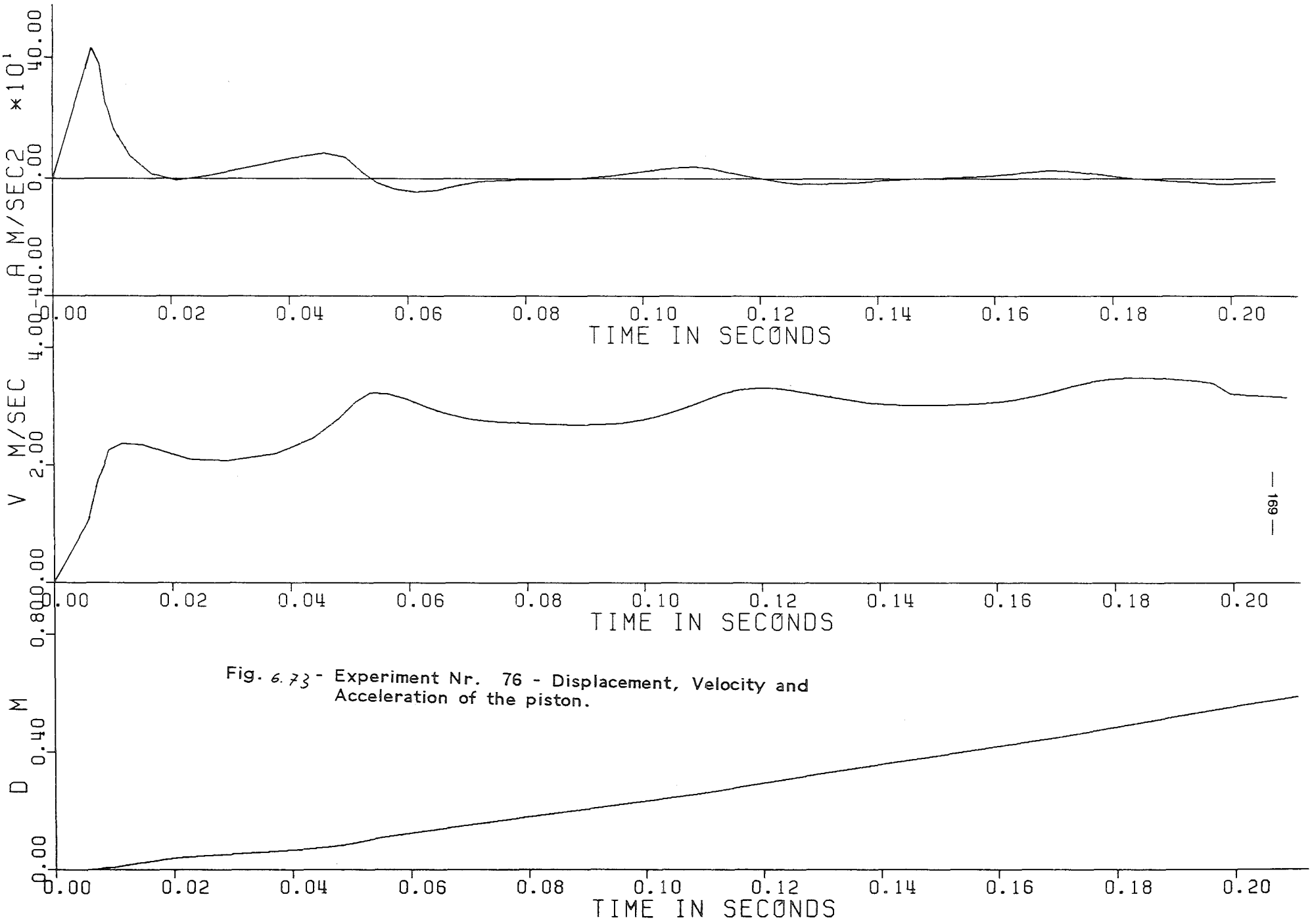

Fig. 6.73 - Experiment Nr. 76 - Displacement, Velocity and Acceleration of the piston.

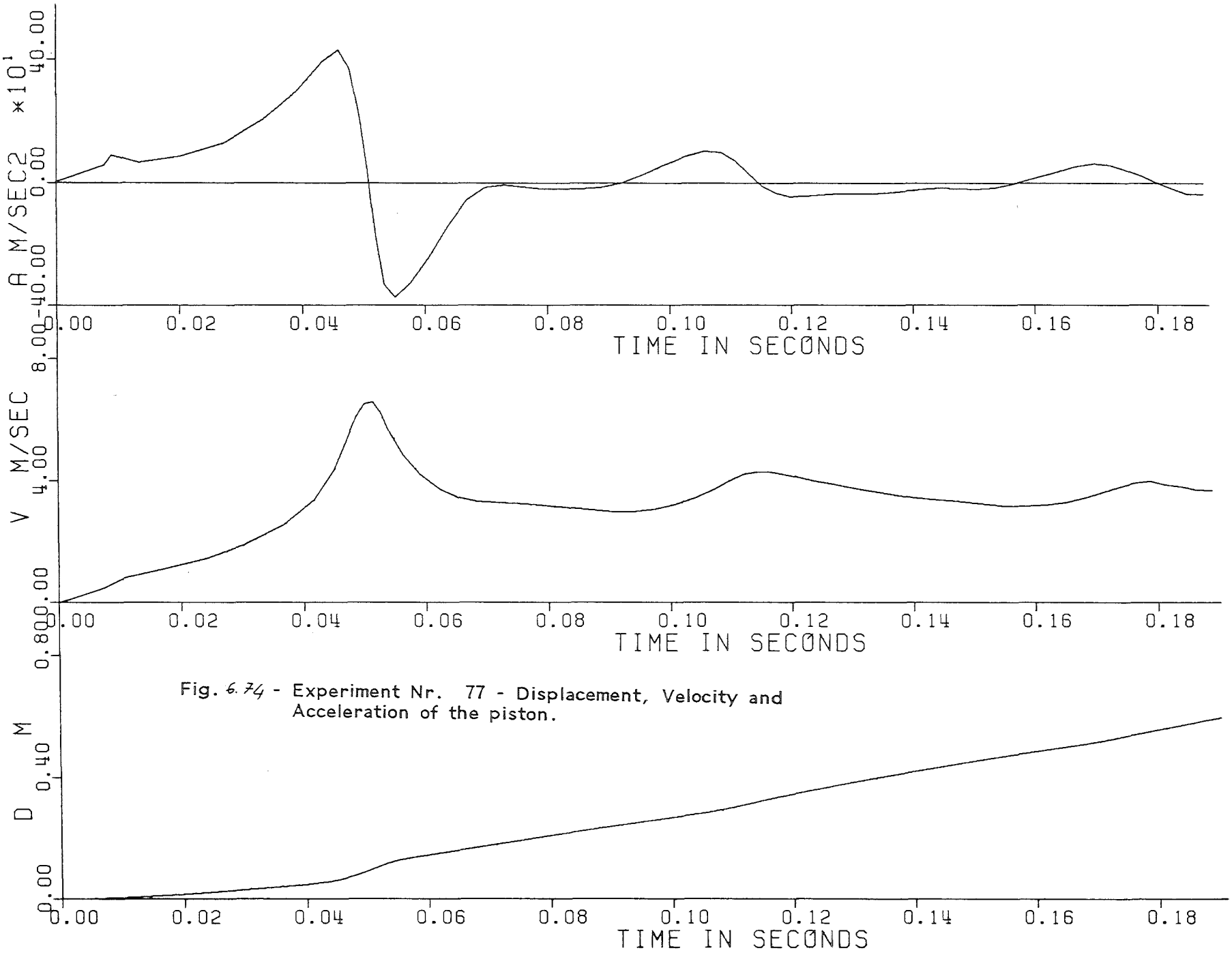

Fig. 6.74 - Experiment Nr. 77 - Displacement, Velocity and Acceleration of the piston.

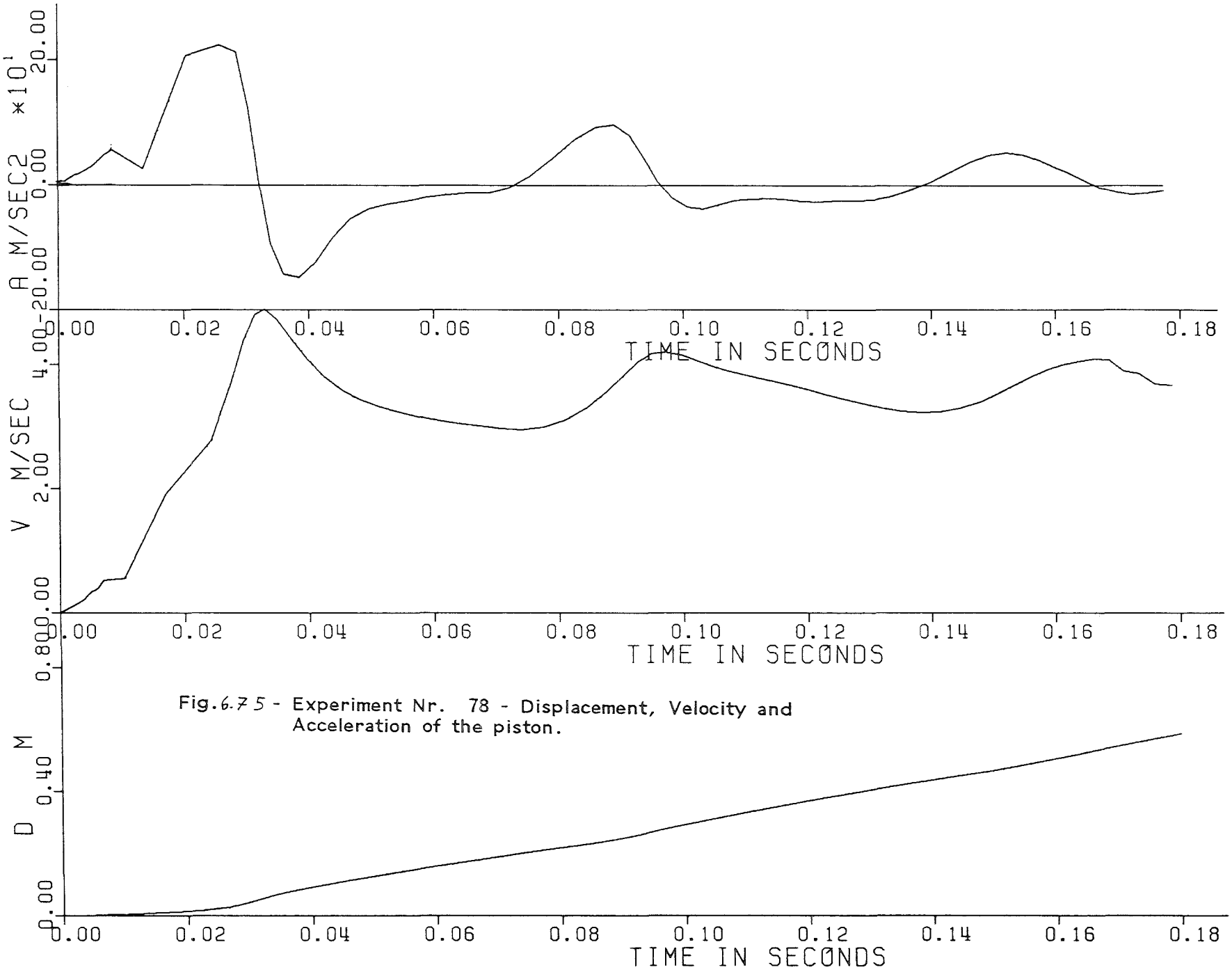

Fig.6.7.5 - Experiment Nr. 78 - Displacement, Velocity and Acceleration of the piston.

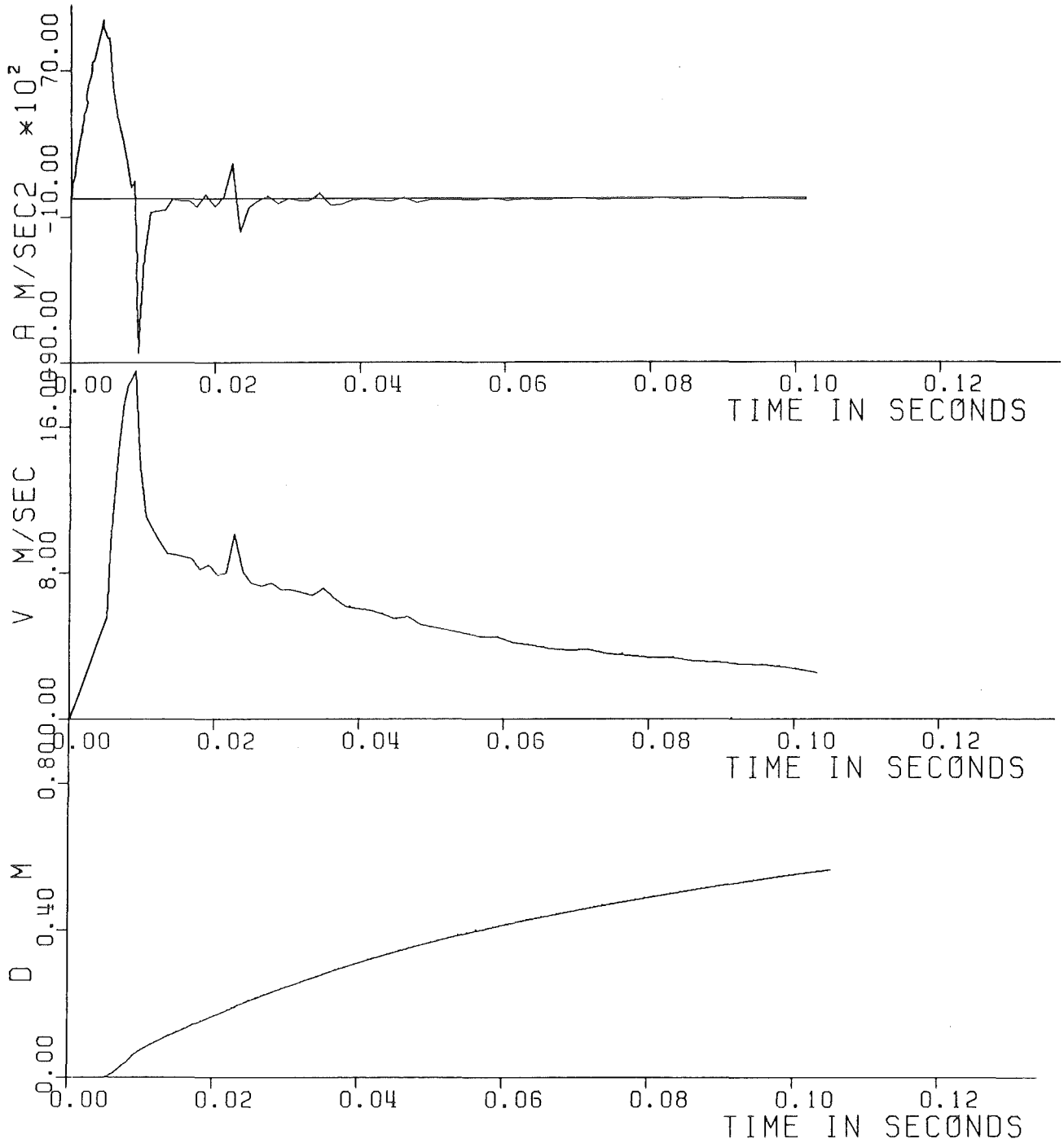

Fig. 6.76 - Experiment Nr. 79 - Displacement, Velocity and Acceleration of the piston.

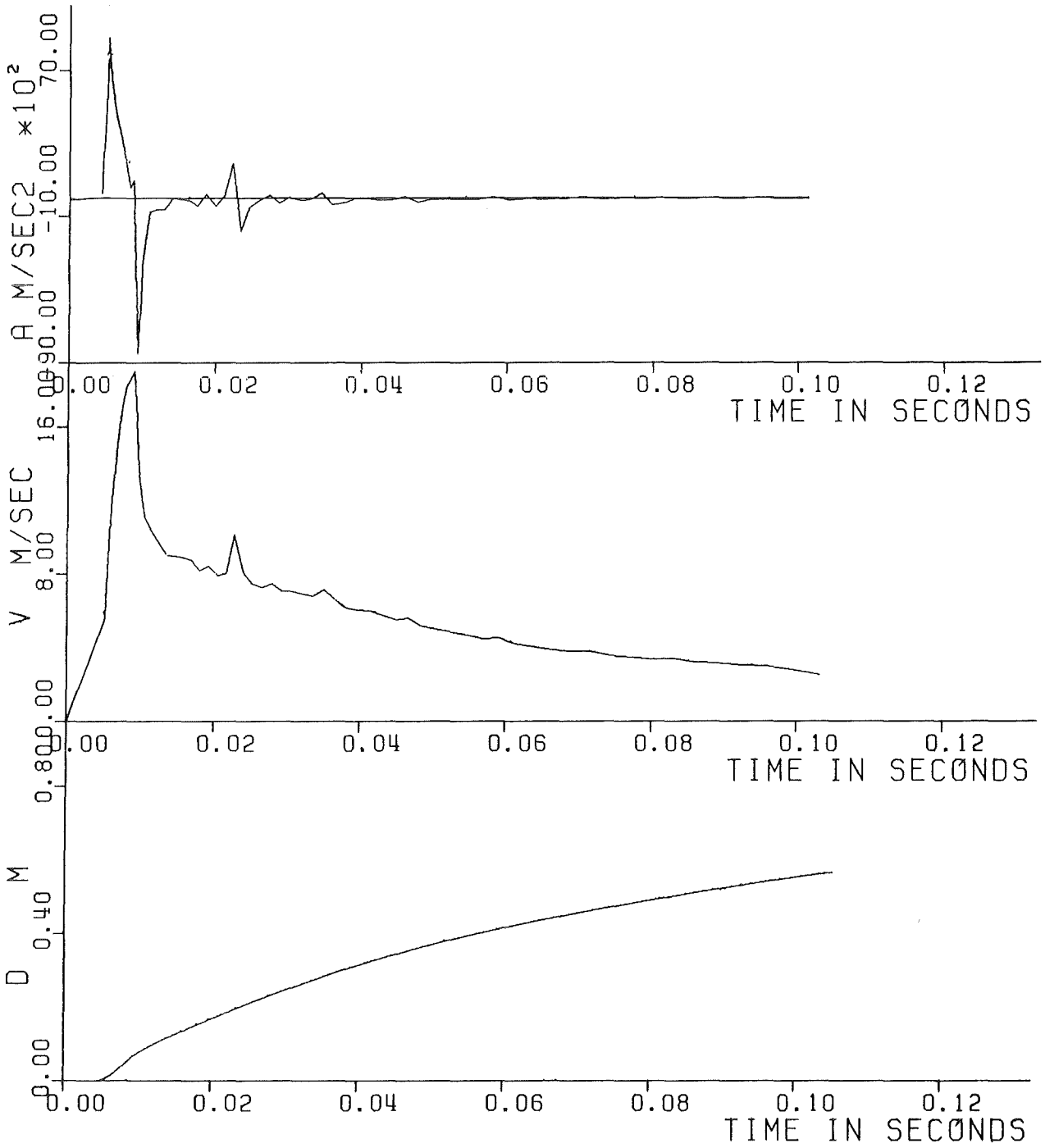

Fig. 6.77 - Experiment Nr. 80 - Displacement, Velocity and Acceleration of the piston.

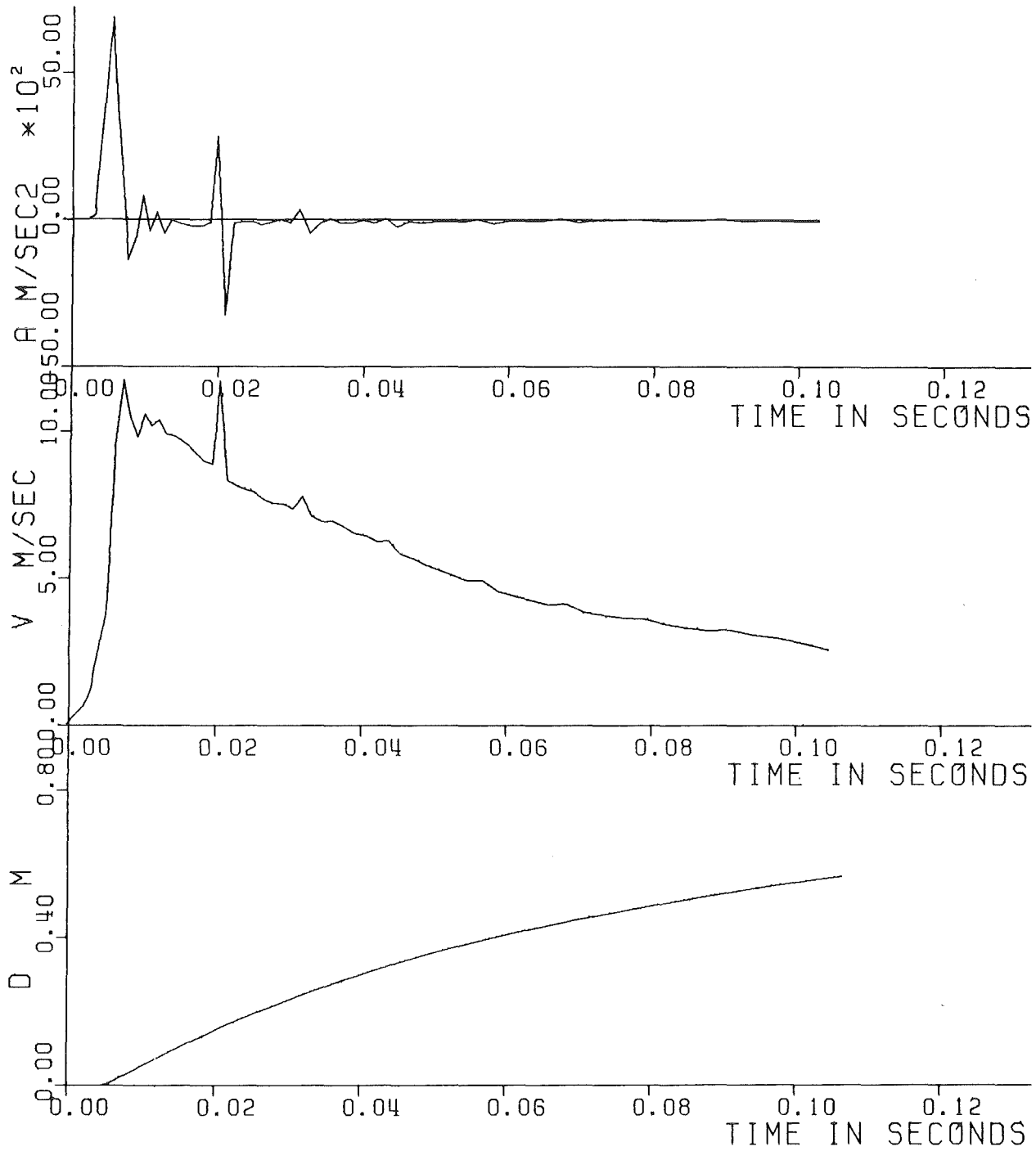

Fig. 6.78 - Experiment Nr. 81 - Displacement, Velocity and Acceleration of the piston.

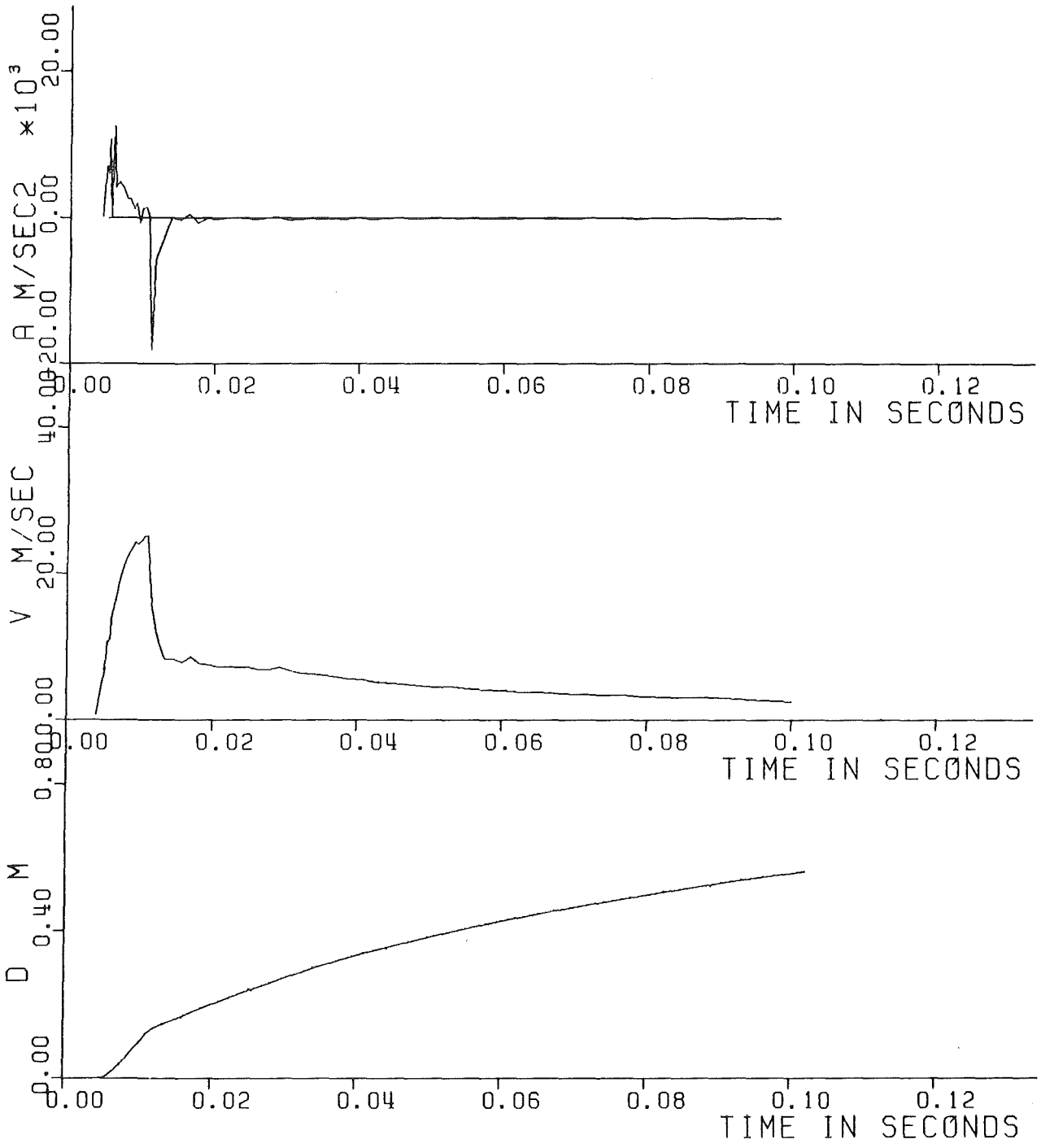

Fig. 6.79 - Experiment Nr. 82 - Displacement, Velocity and Acceleration of the piston.

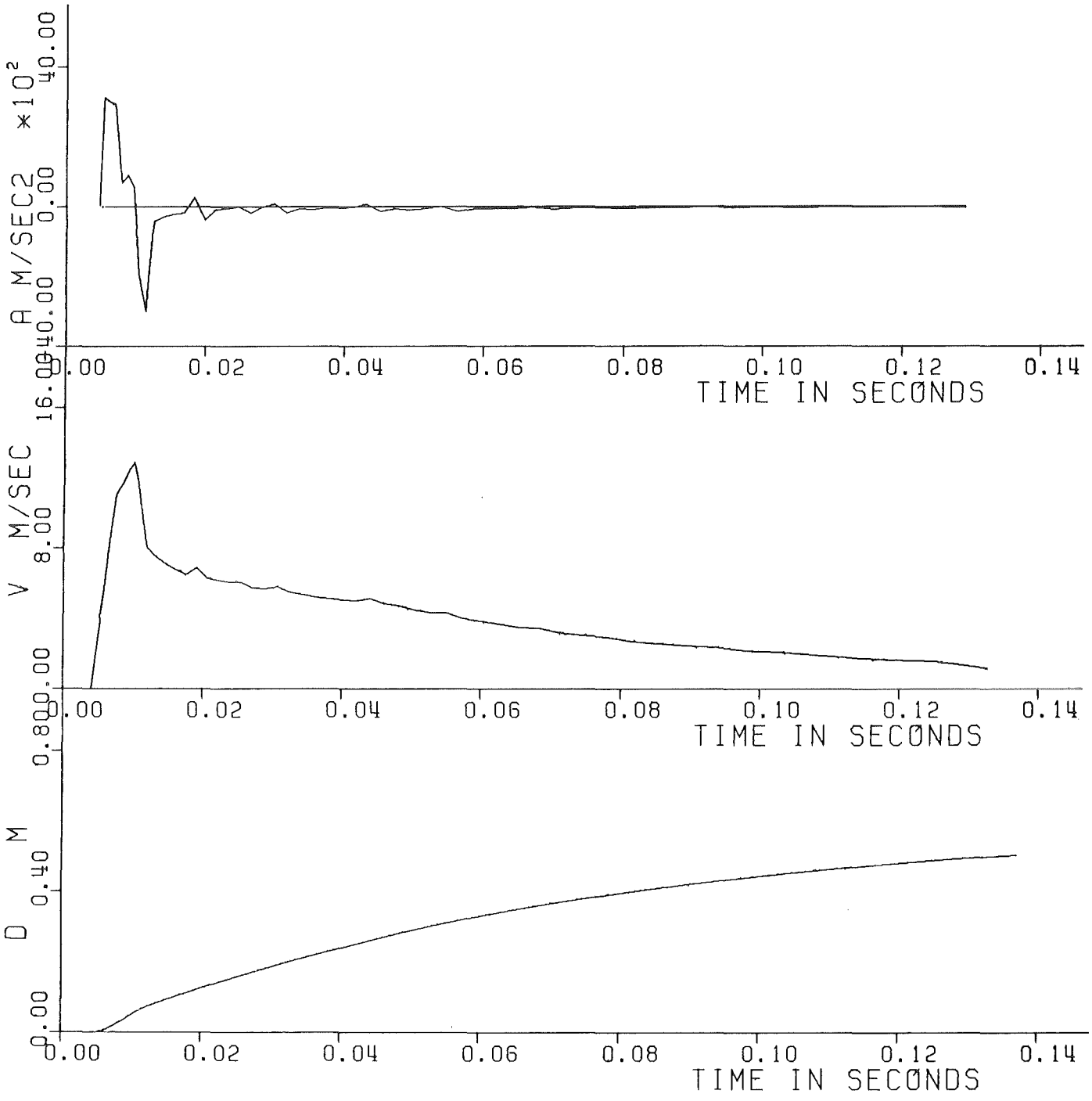

Fig.6.8o - Experiment Nr. 83 - Displacement, Velocity and Acceleration of the piston.

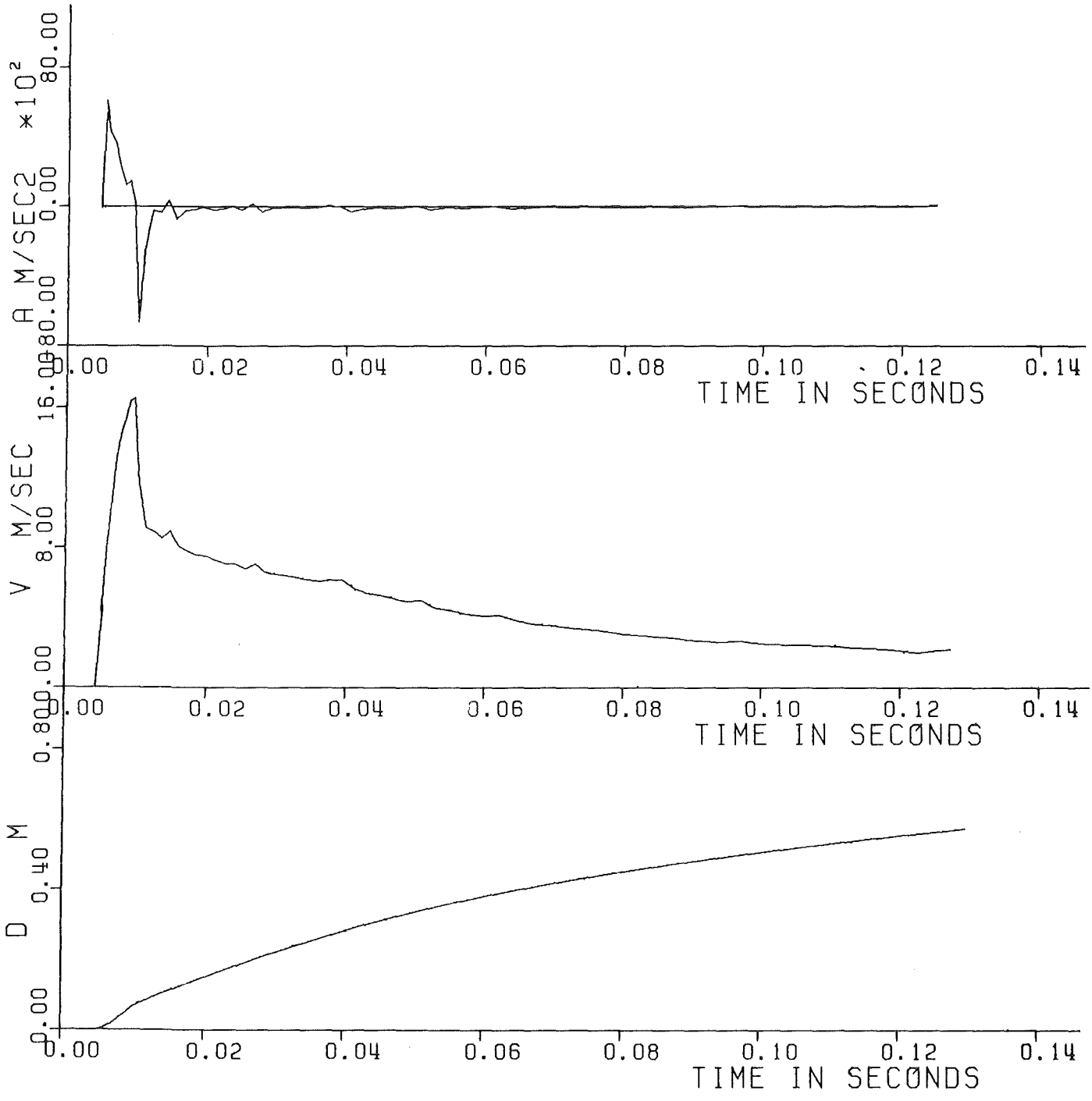

Fig. 6.81 - Experiment Nr. 84 - Displacement, Velocity and Acceleration of the piston.

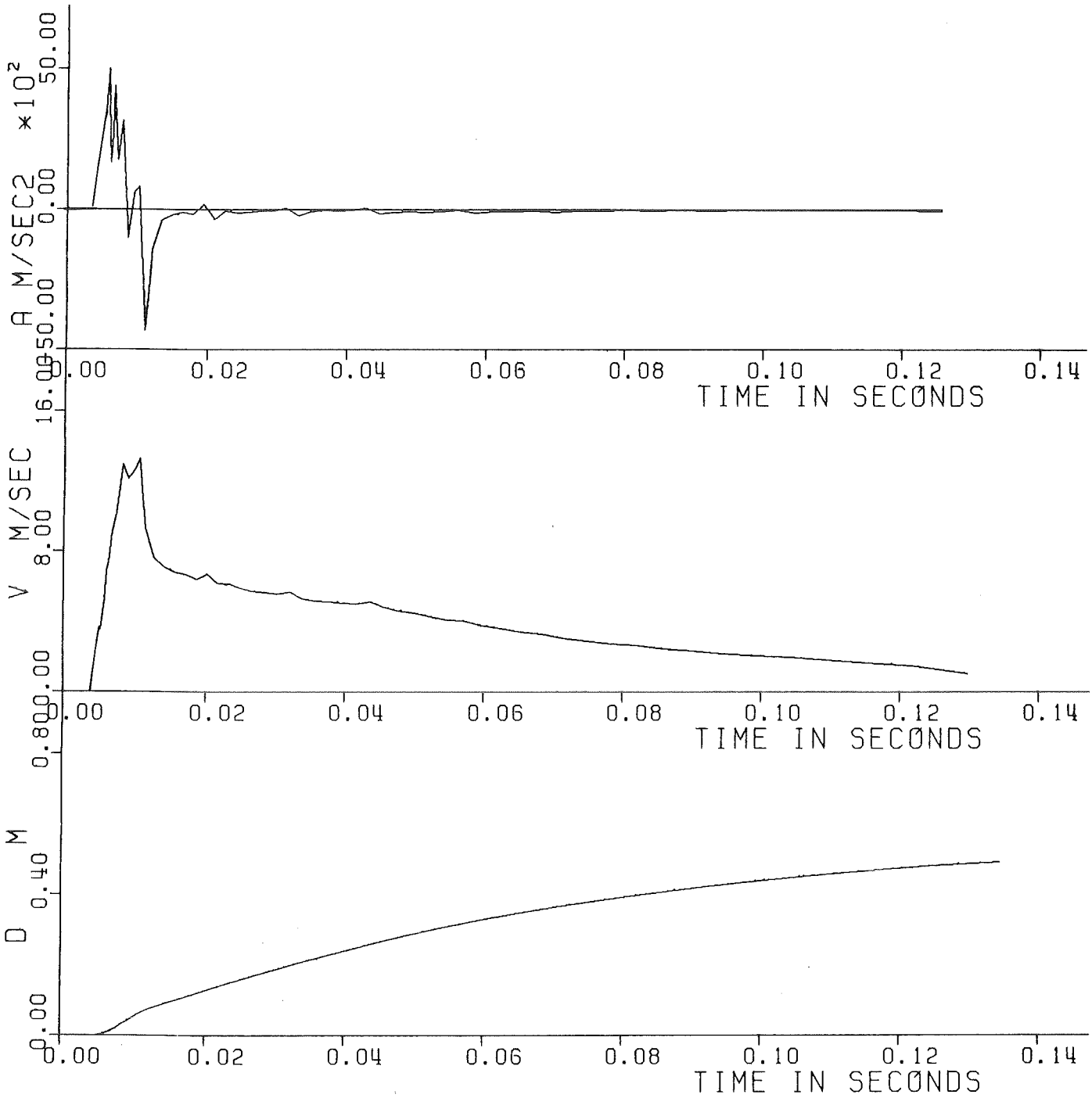

Fig. 6.82 - Experiment Nr. 85 - Displacement, Velocity and Acceleration of the piston.

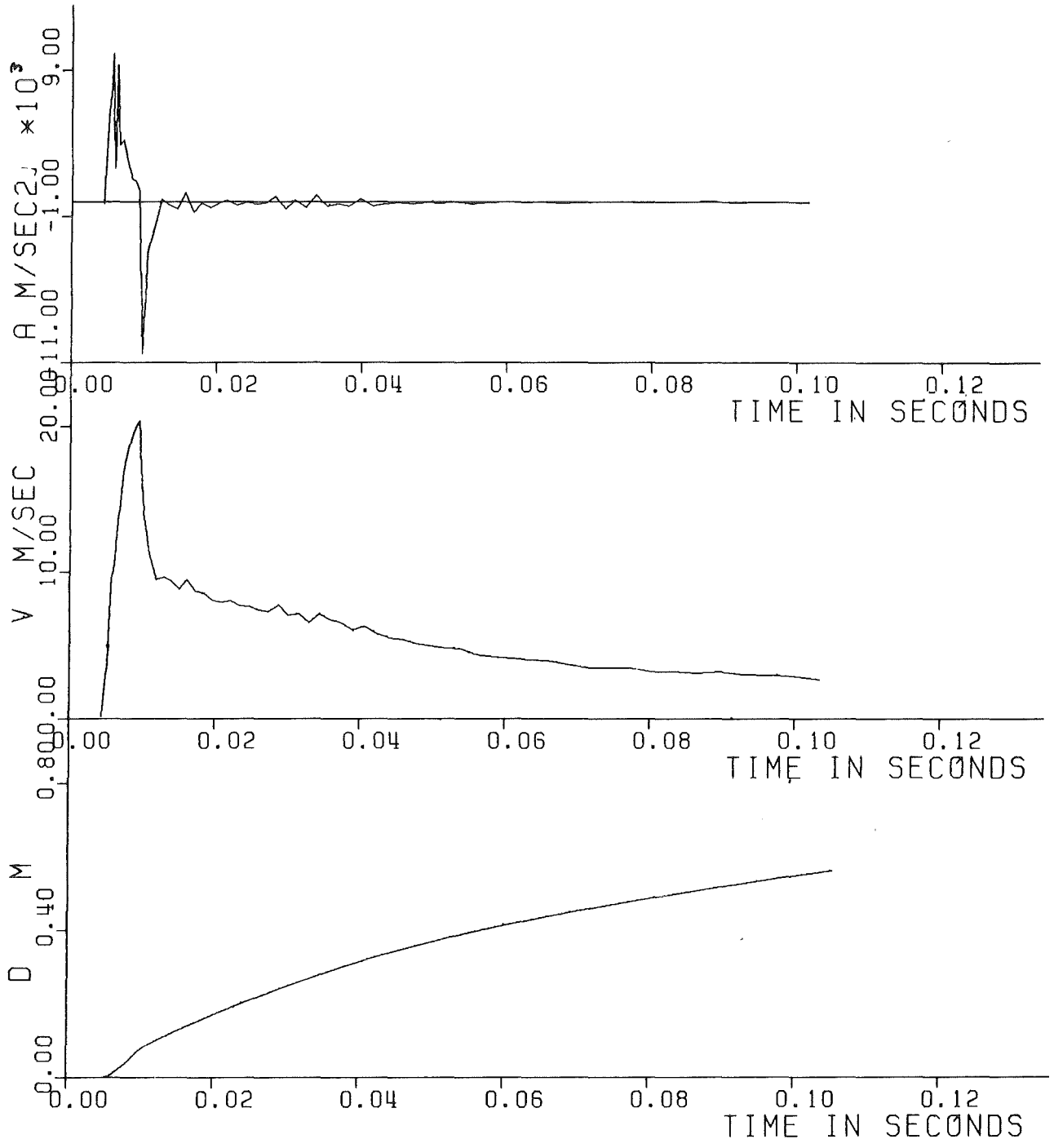

Fig. 6.83 - Experiment Nr. 86 - Displacement, Velocity and Acceleration of the piston.

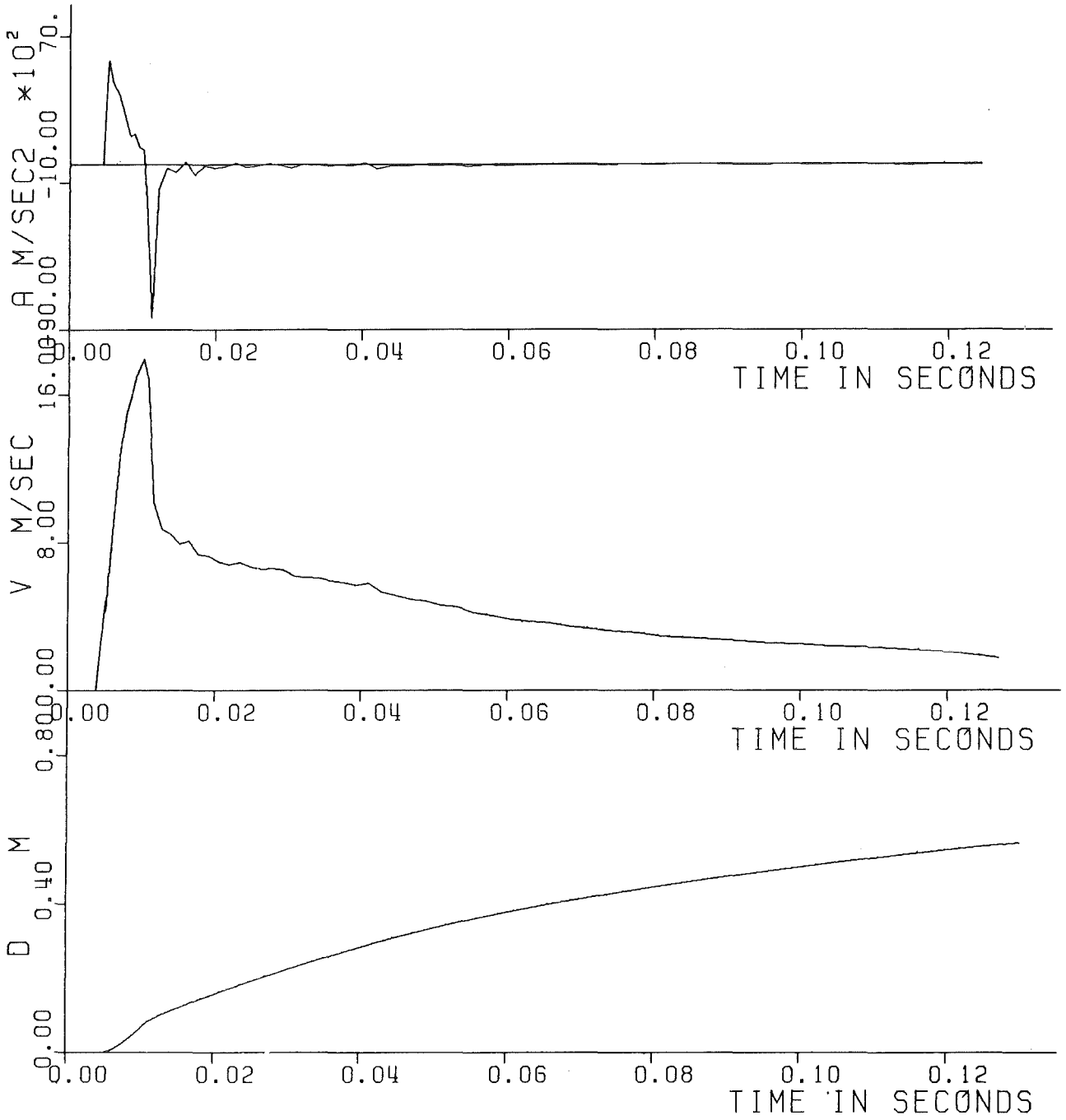

Fig. 6.84 - Experiment Nr. 87 - Displacement, Velocity and Acceleration of the piston.

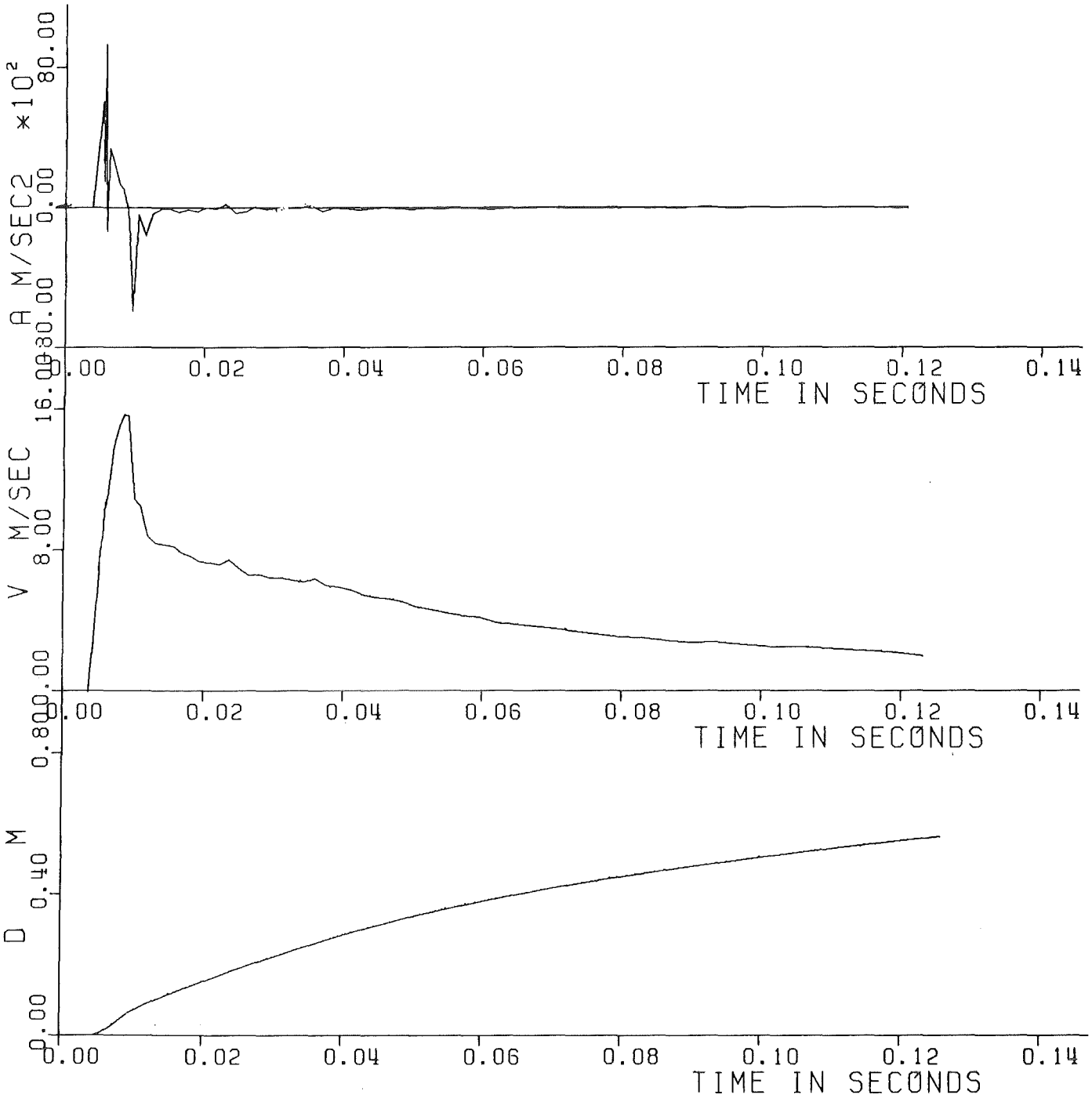

Fig. 6.85 - Experiment Nr. 88 - Displacement, Velocity and Acceleration of the piston.

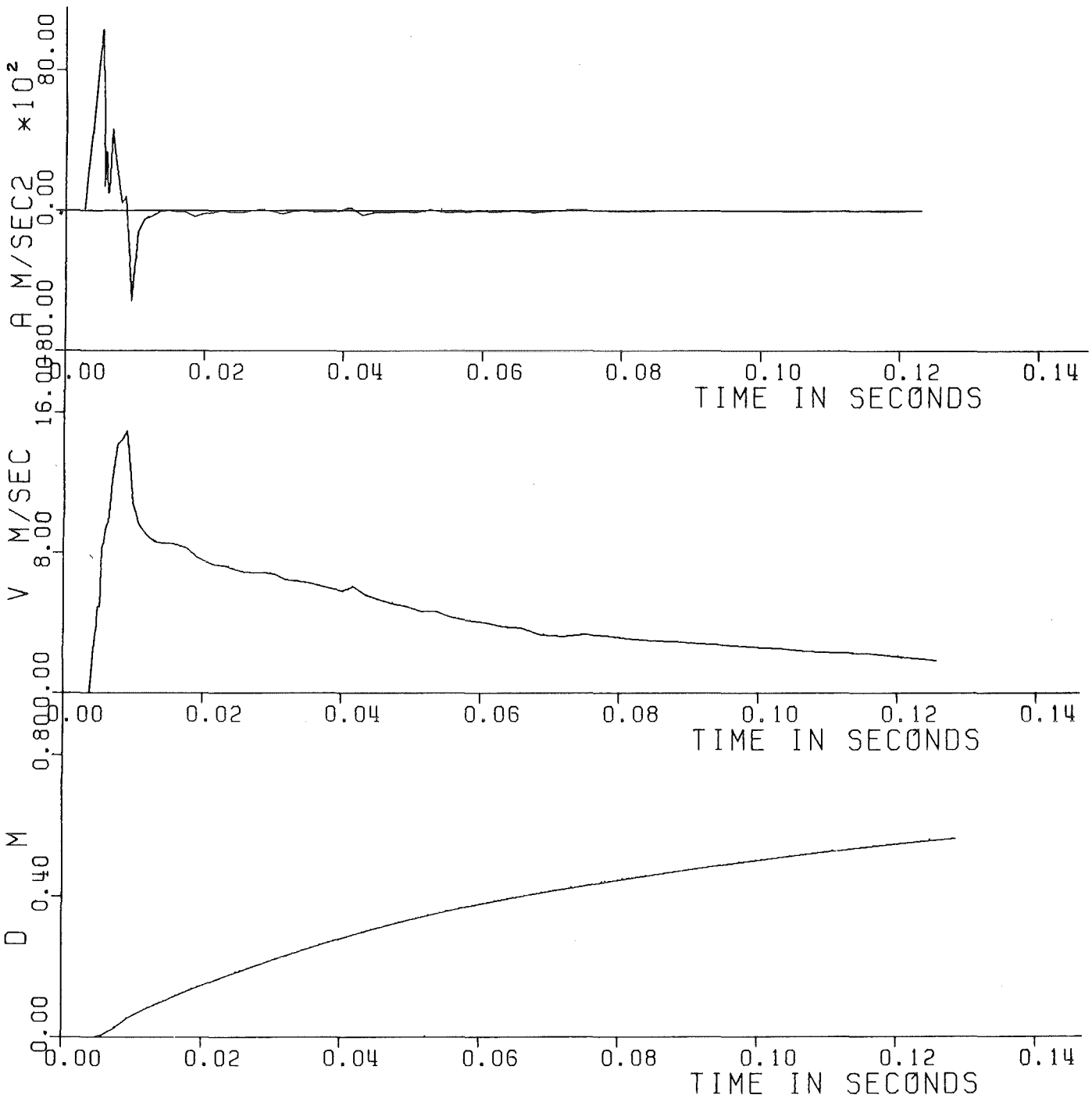

Fig. 6.86 - Experiment Nr. 89 - Displacement, Velocity and Acceleration of the piston.

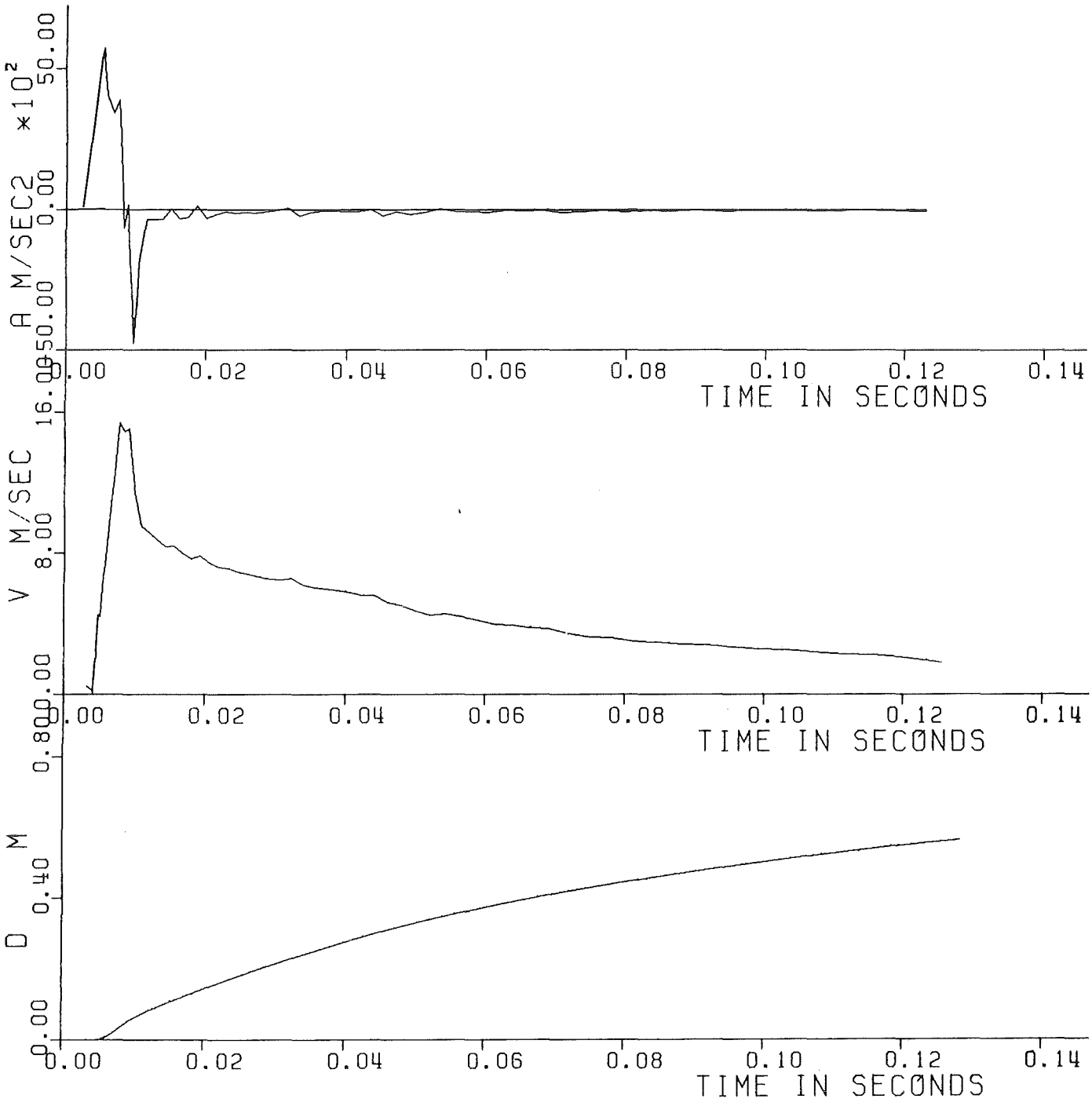

Fig.6.87 - Experiment Nr. 90 - Displacement, Velocity and Acceleration of the piston.

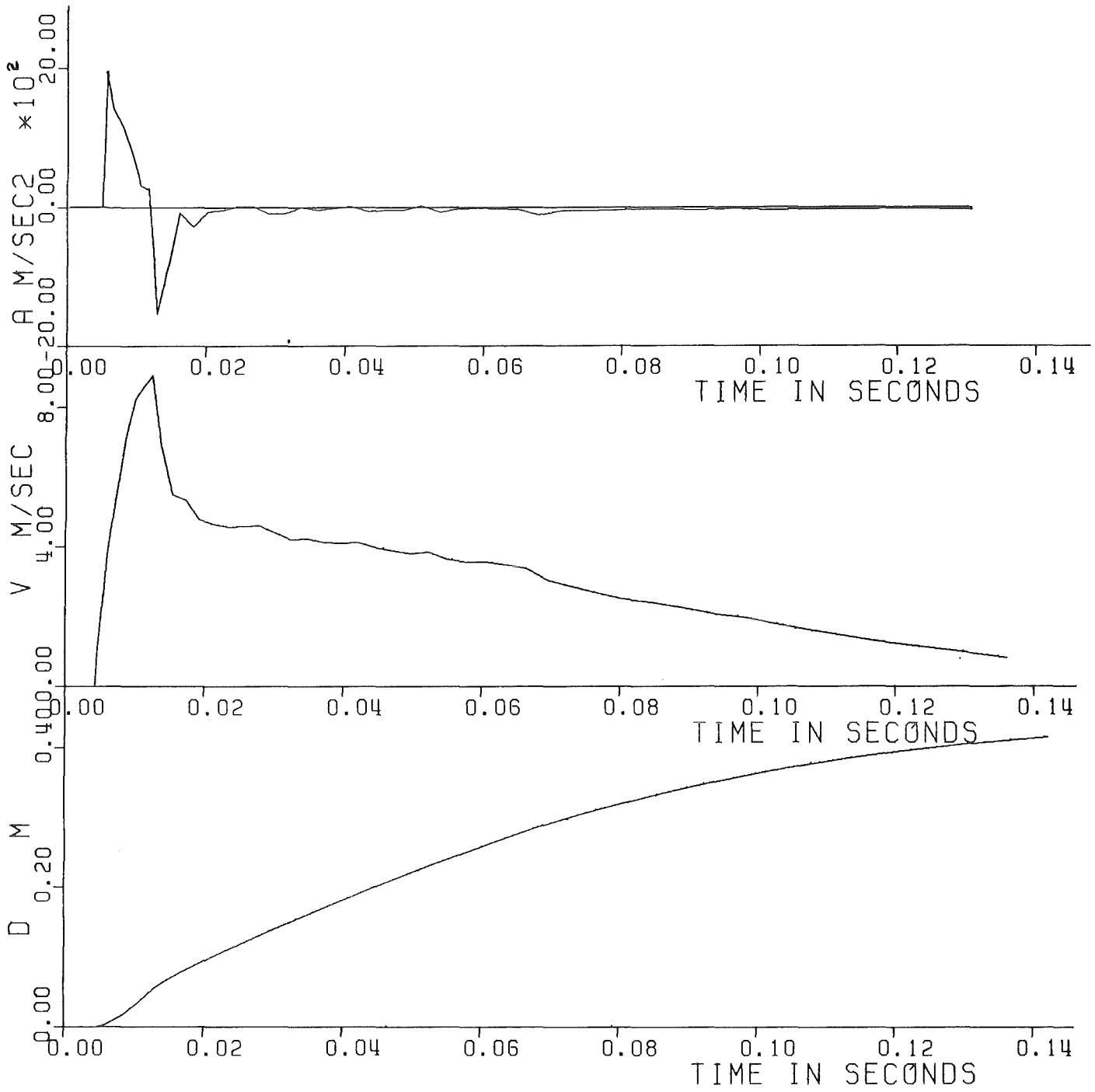

Fig. 6.88 - Experiment Nr. 91 - Displacement, Velocity and Acceleration of the piston.

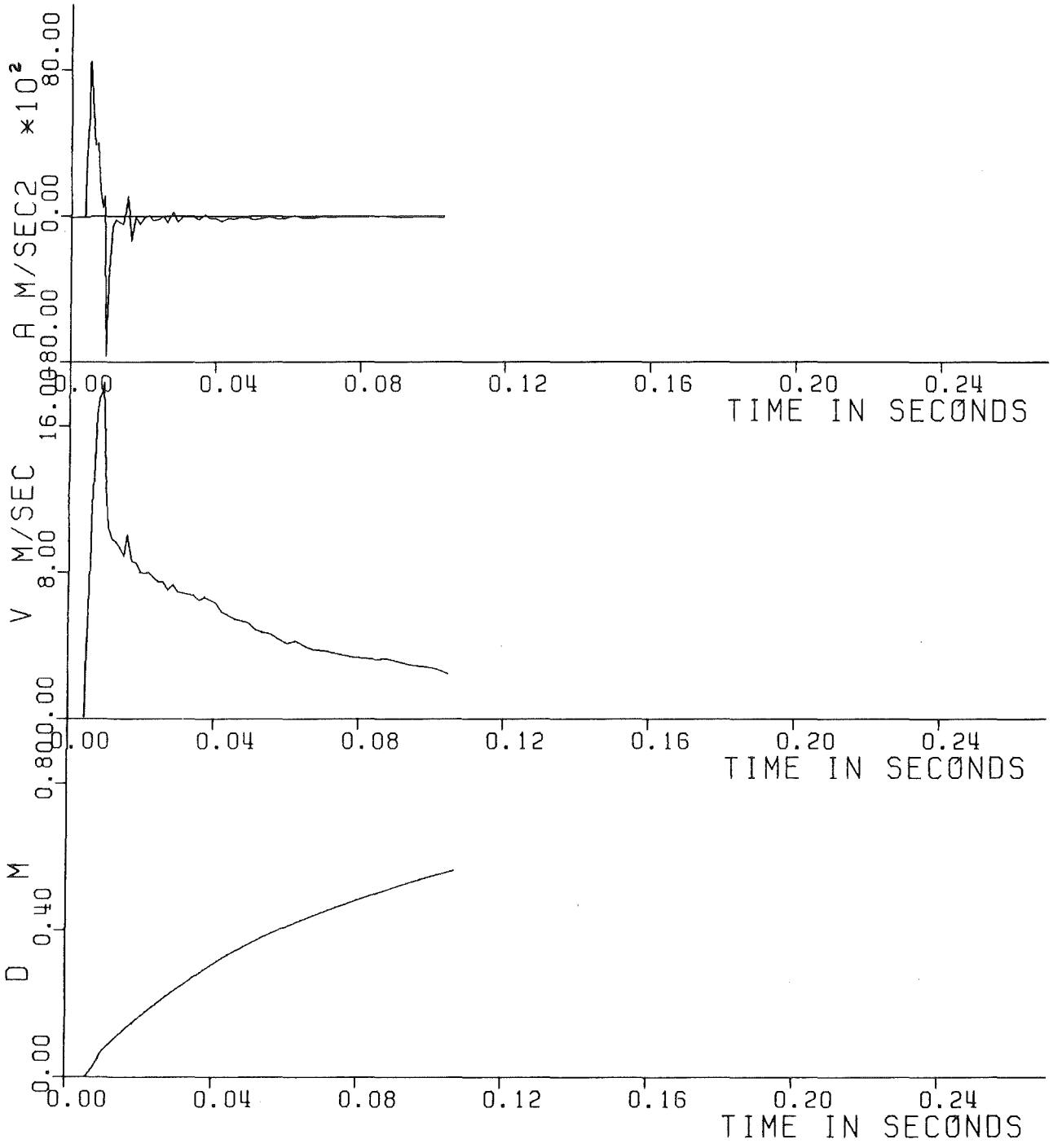

Fig. 6.89 - Experiment Nr. 92 - Displacement, Velocity and Acceleration of the piston.

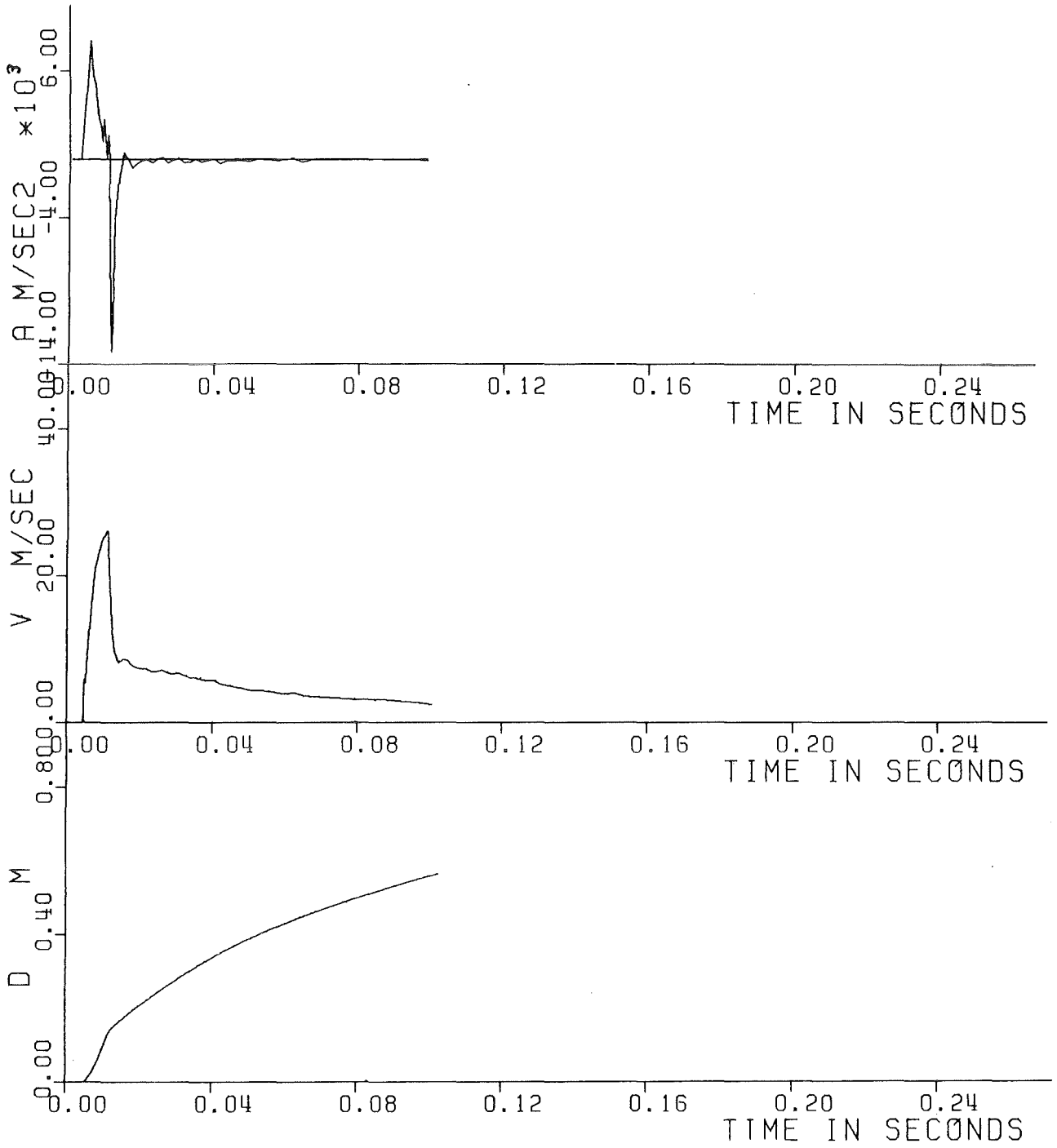

Fig. 6.90 - Experiment Nr. 93 - Displacement, Velocity and Acceleration of the piston.

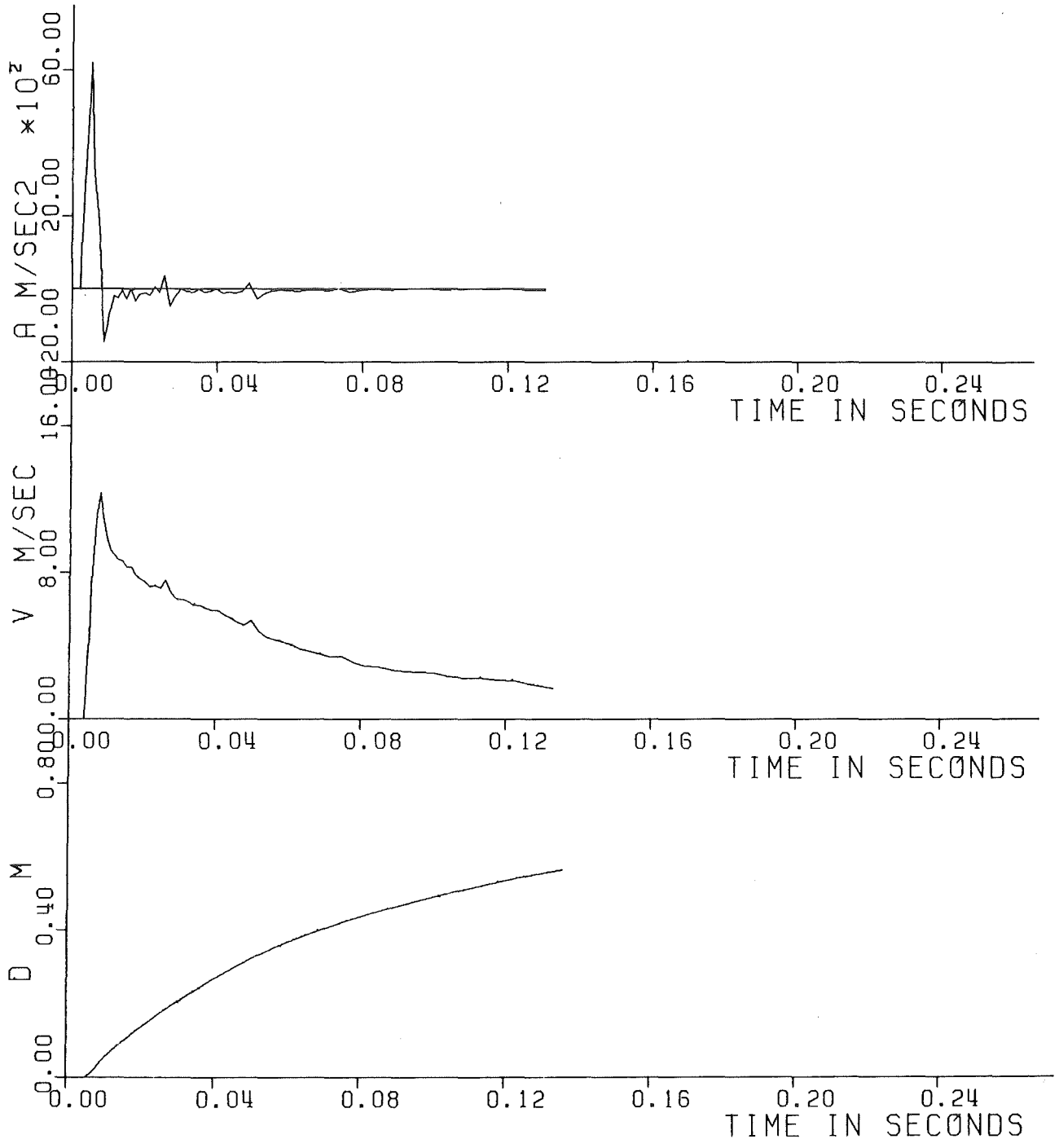

Fig. 6.9 1 - Experiment Nr. 94 - Displacement, Velocity and Acceleration of the piston.

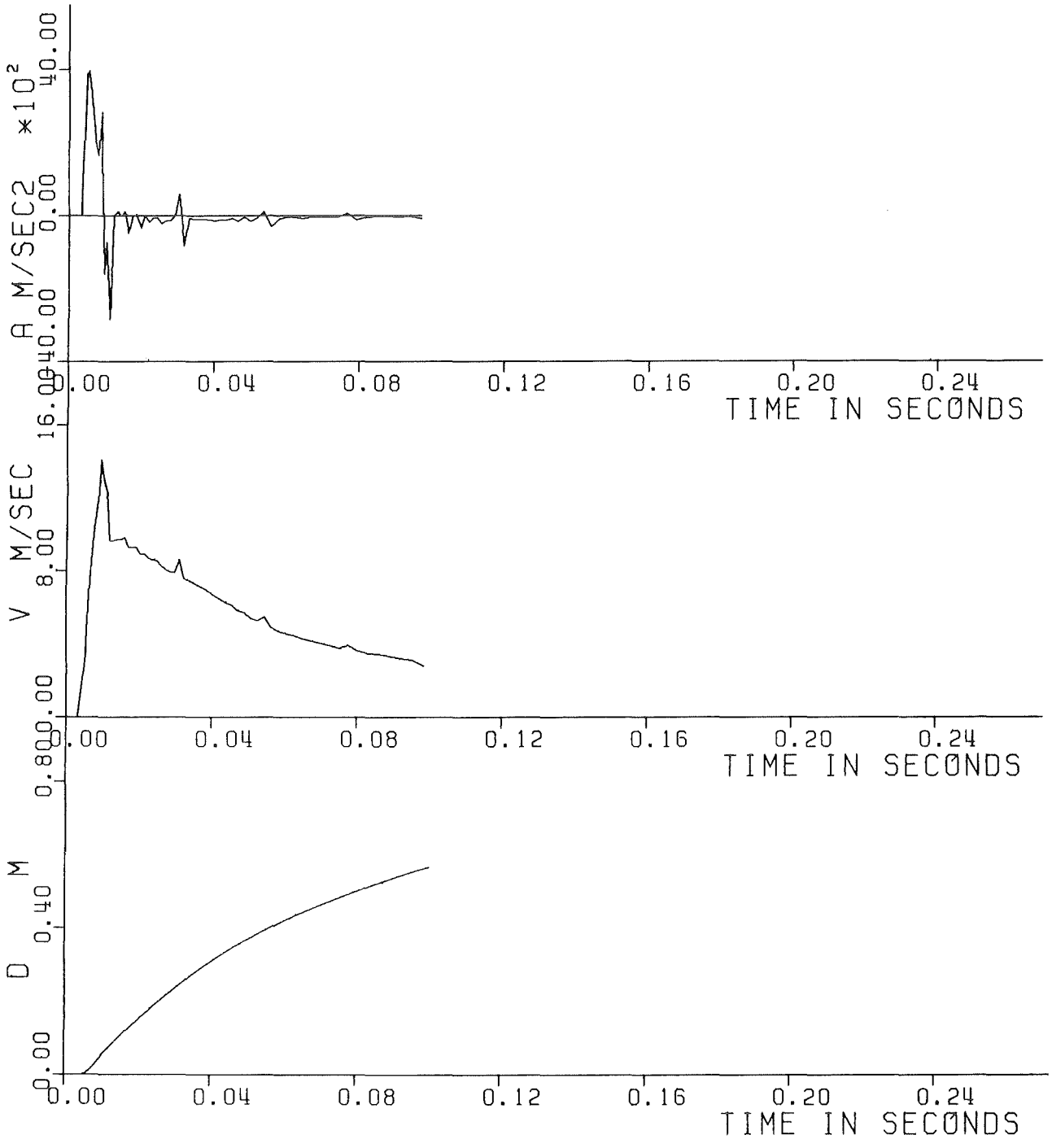

Fig. 6.92- Experiment Nr. 95 - Displacement, Velocity and Acceleration of the piston.

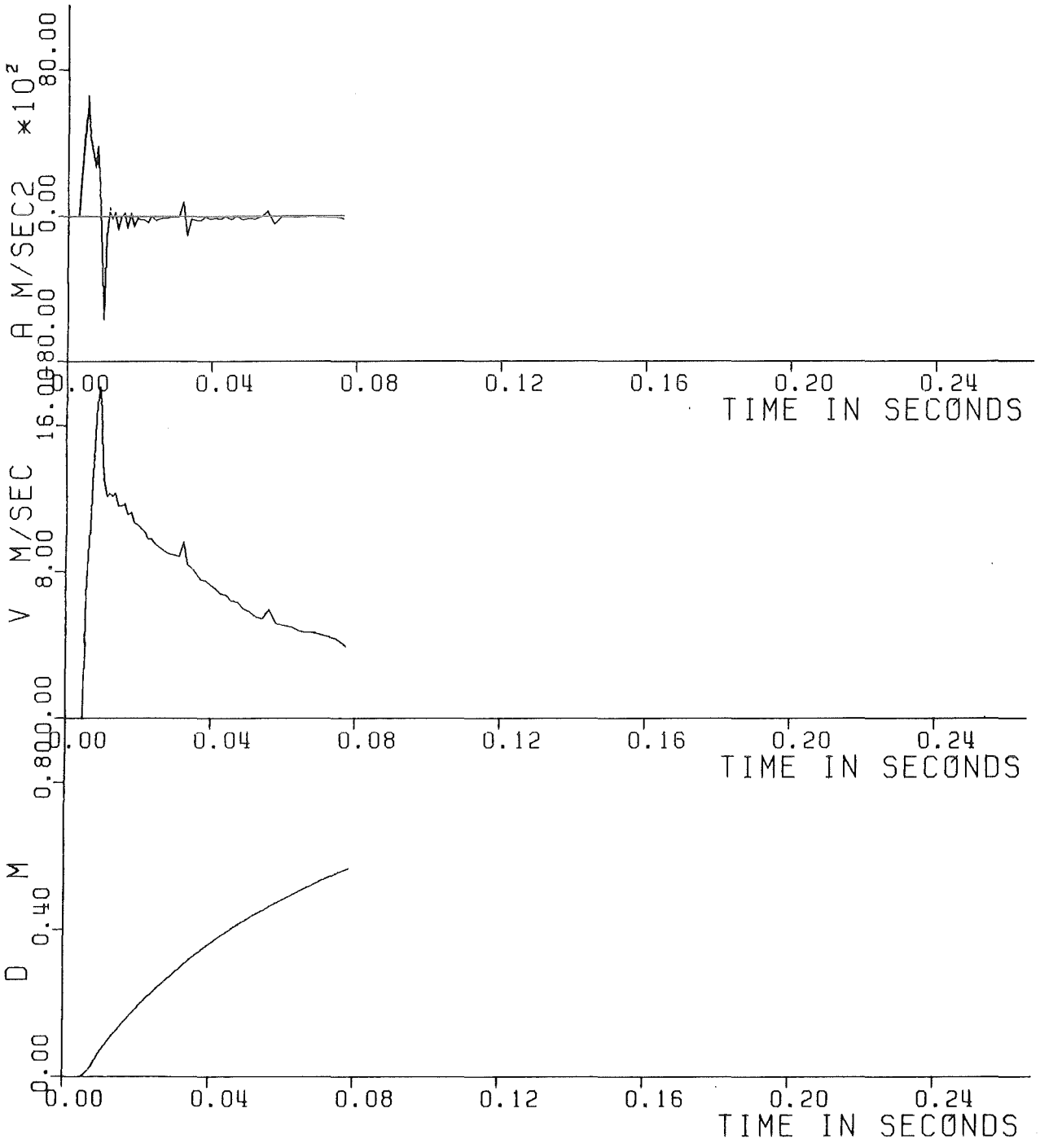

Fig. 6.93 - Experiment Nr. 96 - Displacement, Velocity and Acceleration of the piston.

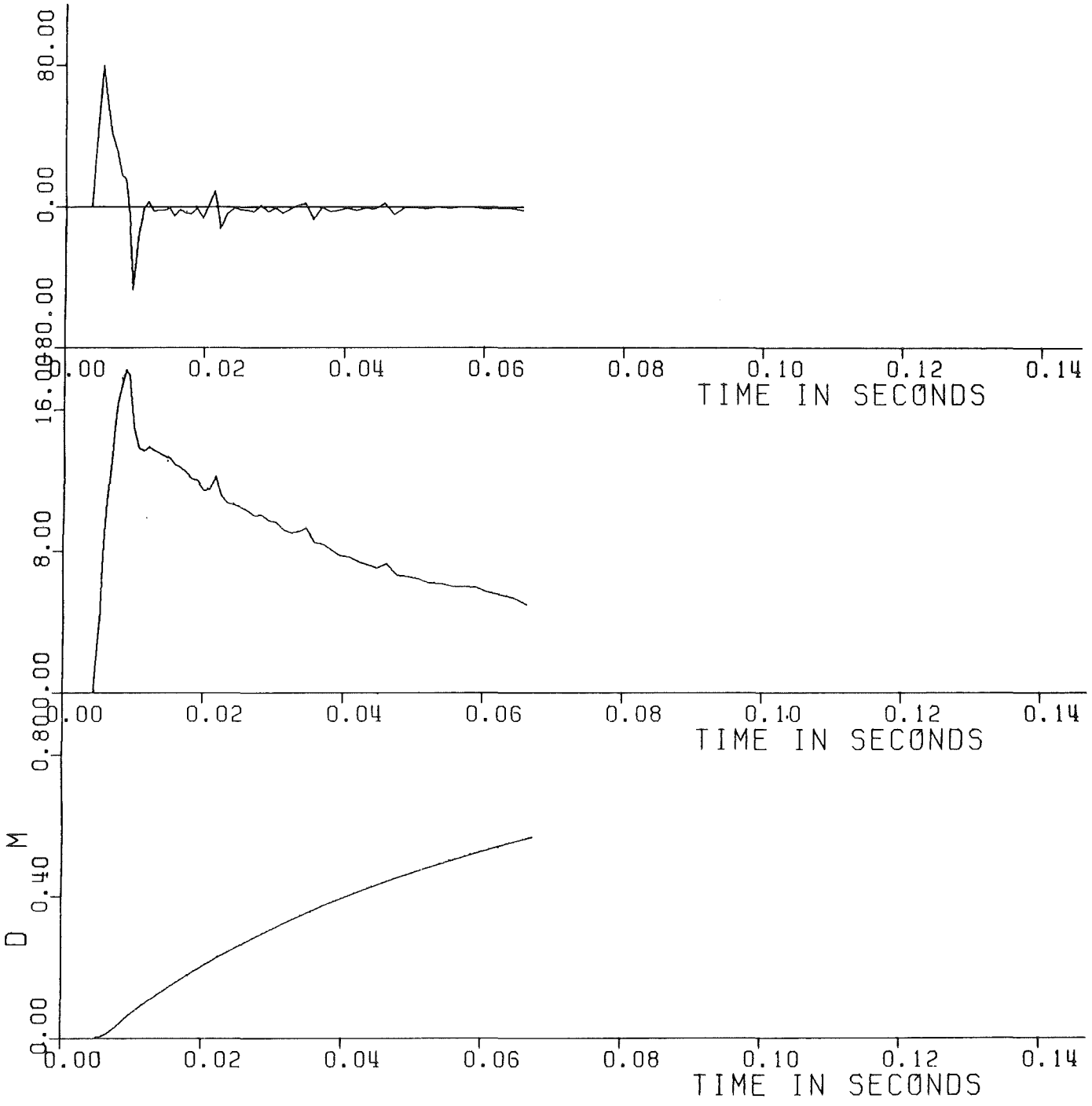

Fig. 6.94 - Experiment Nr. 97 - Displacement, Velocity and Acceleration of the piston.

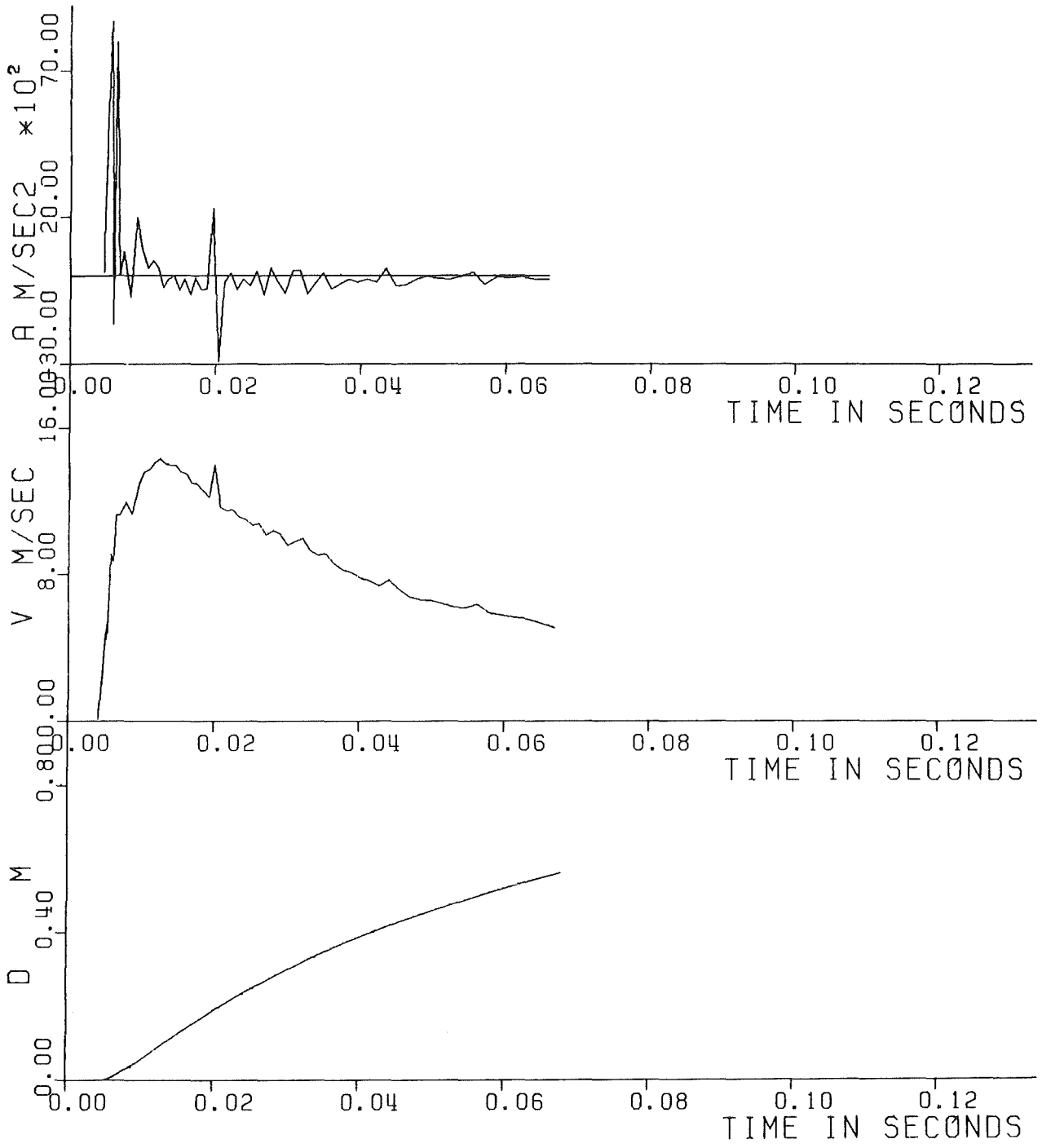

Fig. 6.95 - Experiment Nr. 98 - Displacement, Velocity and Acceleration of the piston.

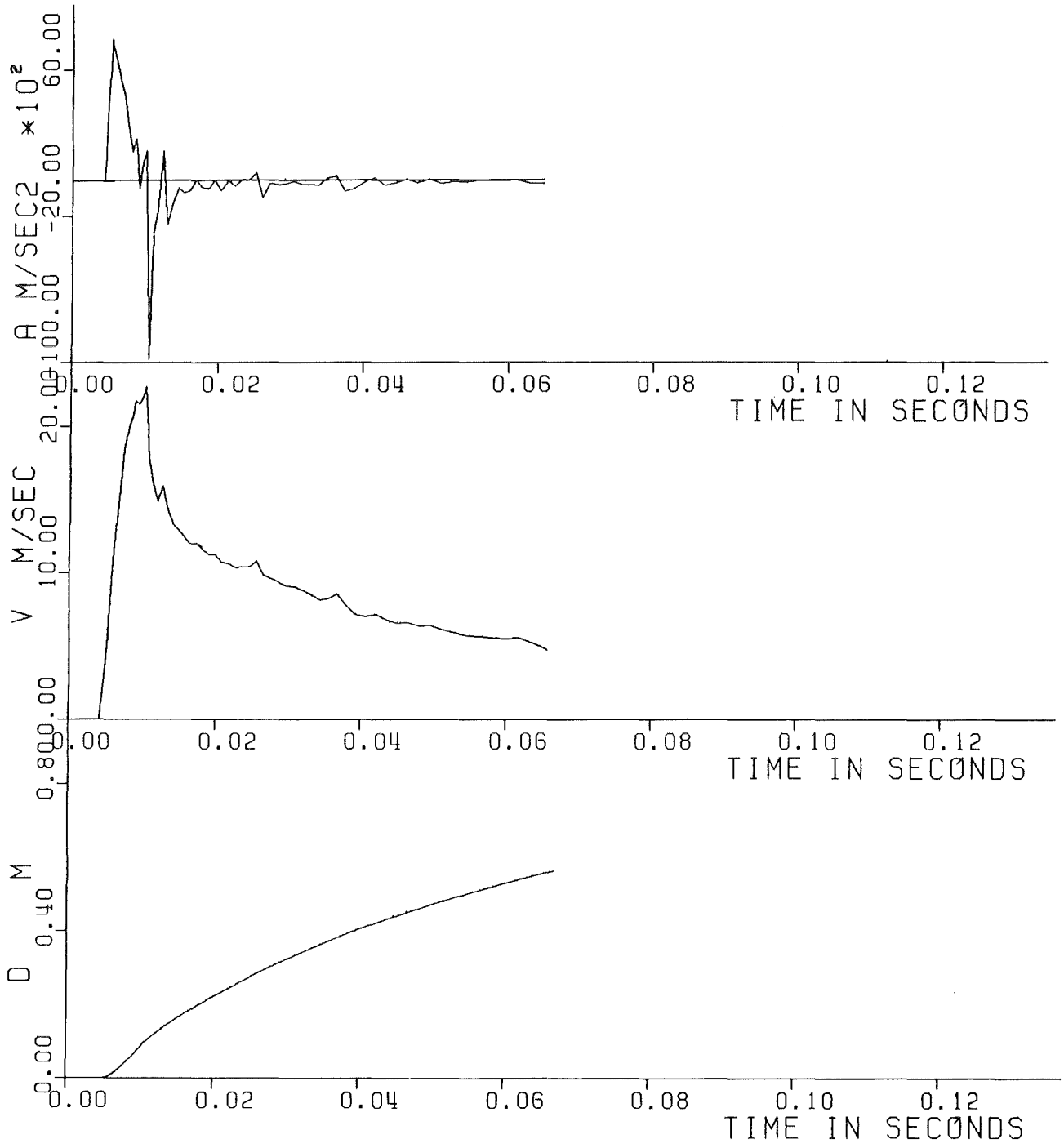

Fig. 6.96 - Experiment Nr. 99 - Displacement, Velocity and Acceleration of the piston.

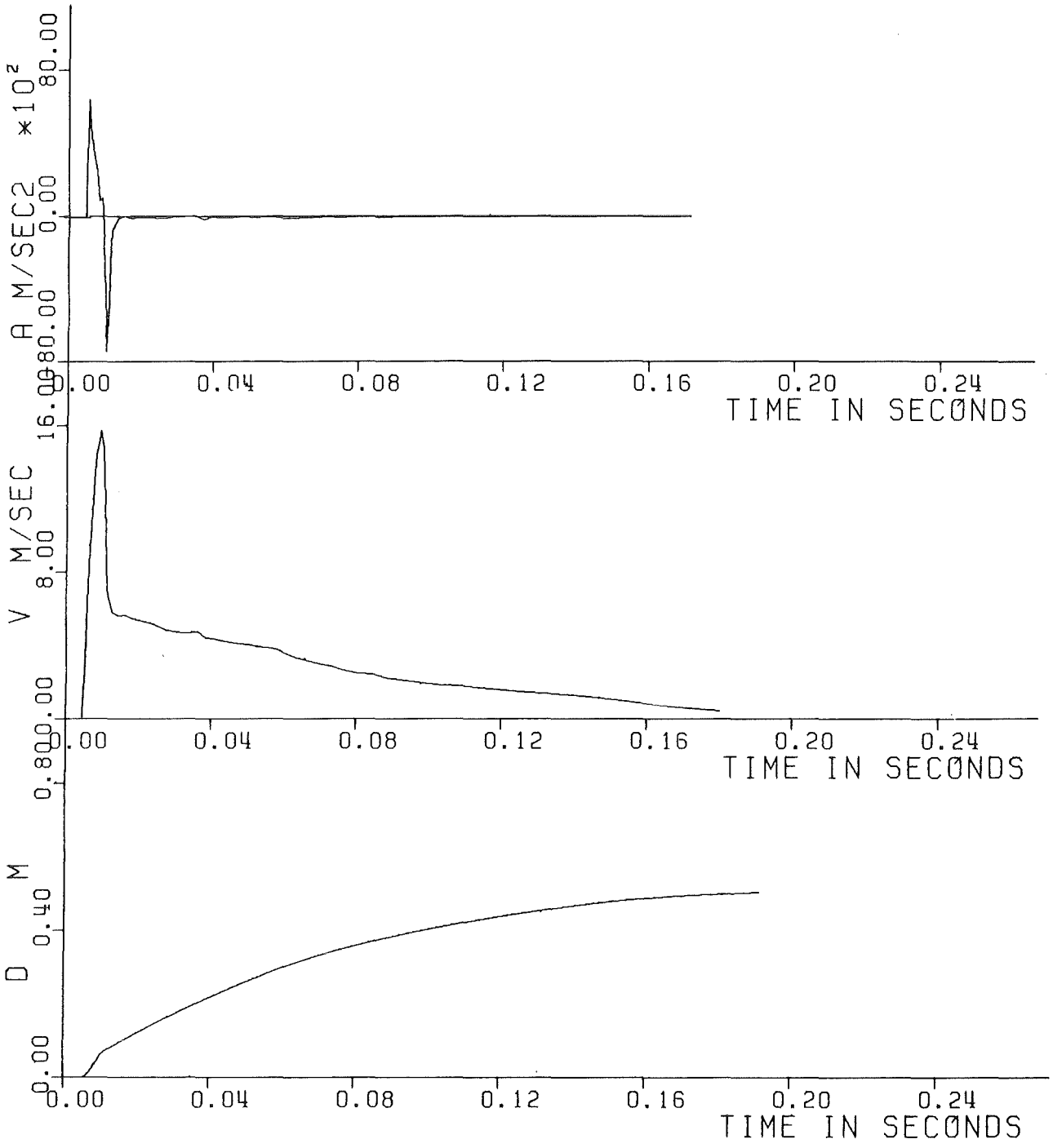

Fig. 6.97- Experiment Nr. 100 - Displacement, Velocity and Acceleration of the piston.

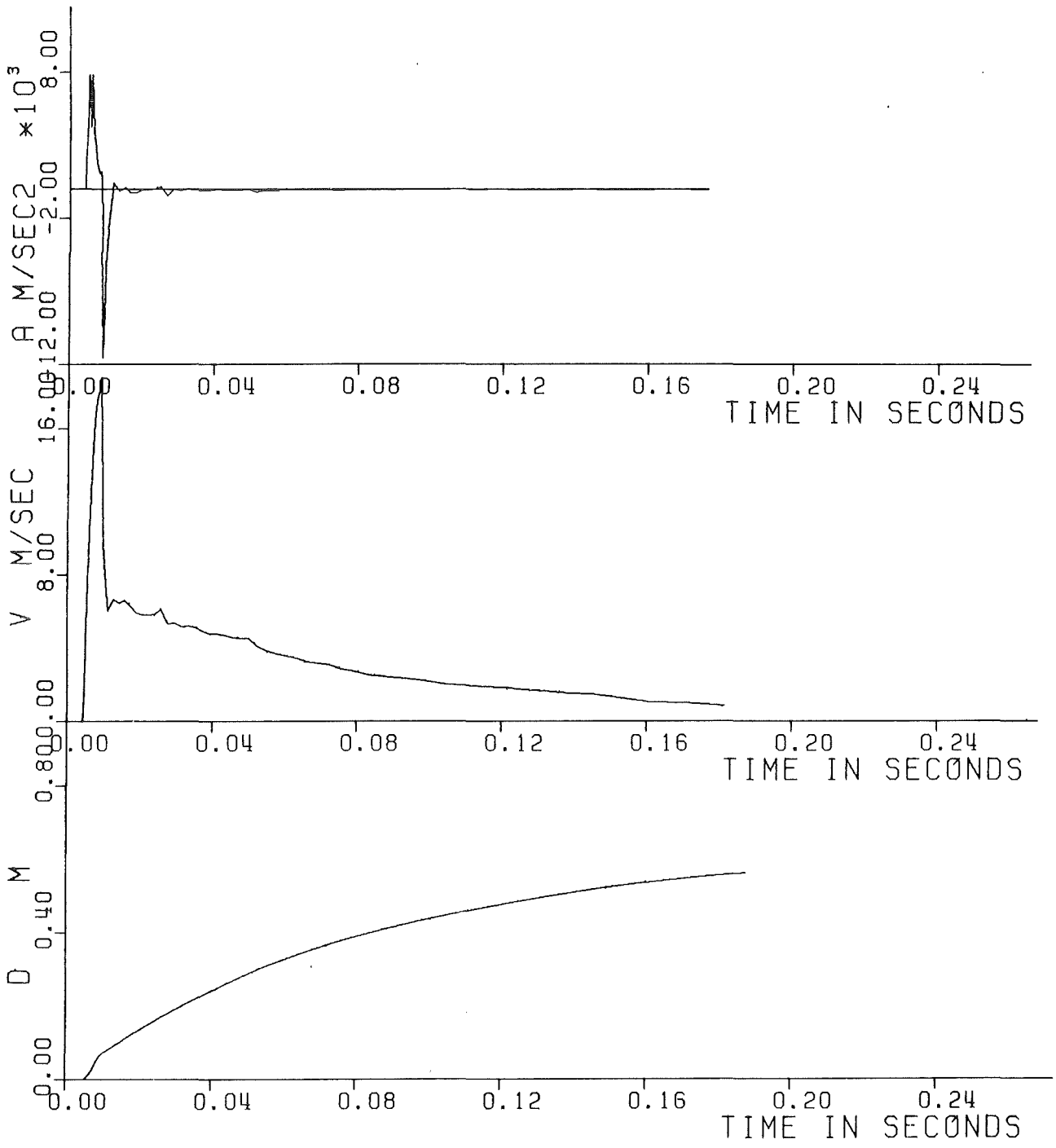

Fig. 6.98 - Experiment Nr. 101 - Displacement, Velocity and Acceleration of the piston.

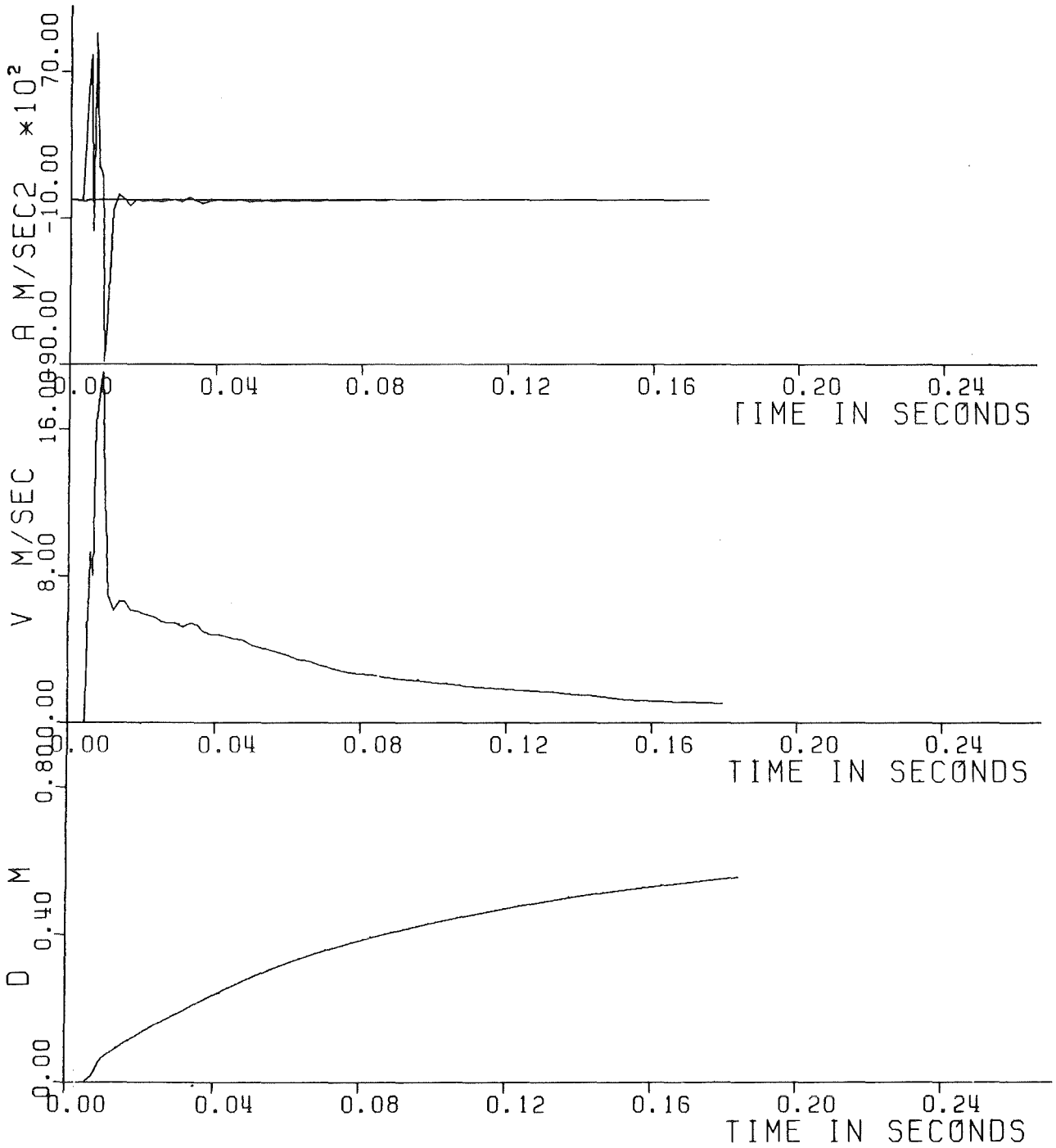

Fig. 6.99 - Experiment Nr. 102 - Displacement, Velocity and Acceleration of the piston.

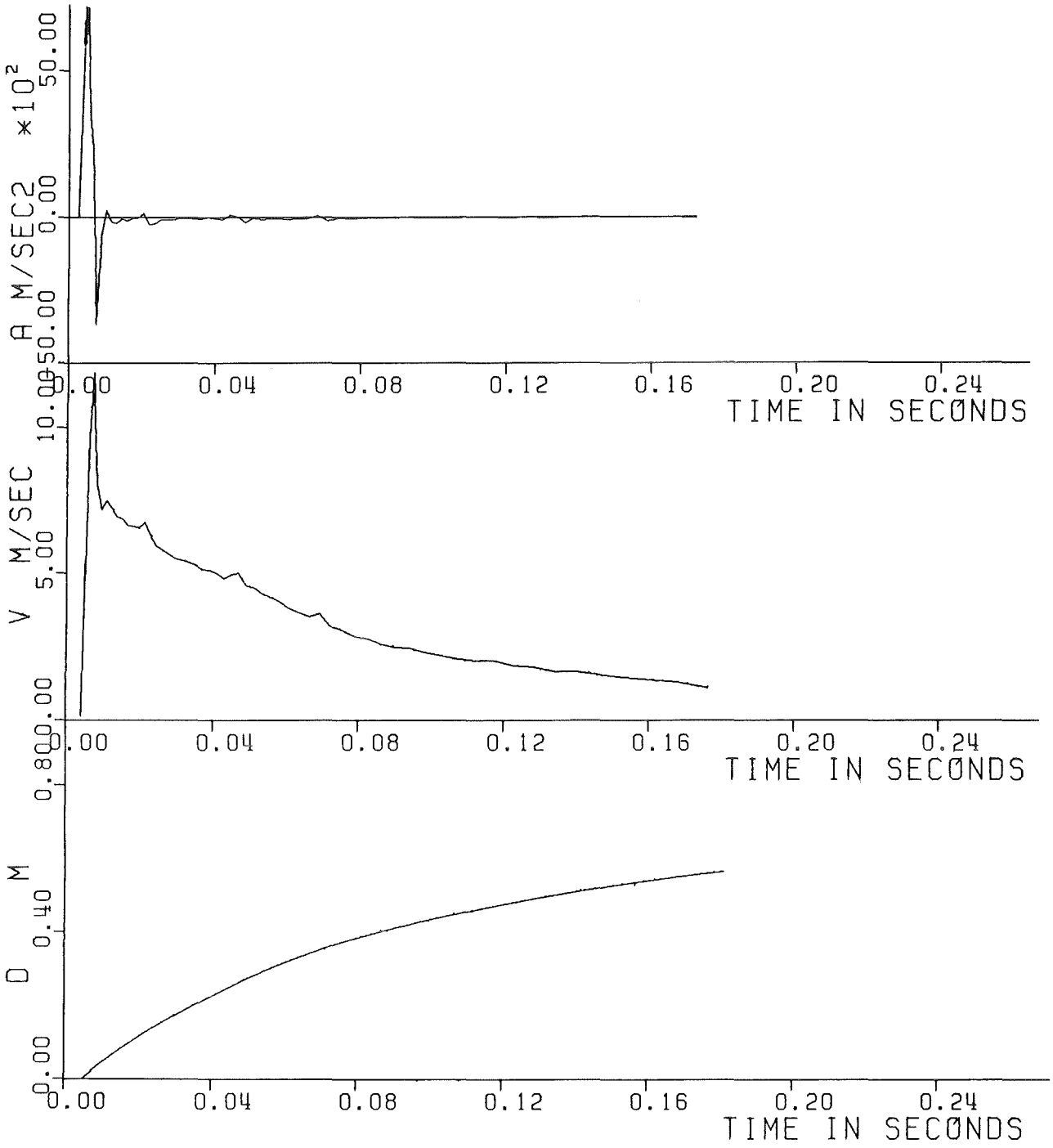

Fig. 6.100- Experiment Nr. 103 - Displacement, Velocity and Acceleration of the piston.

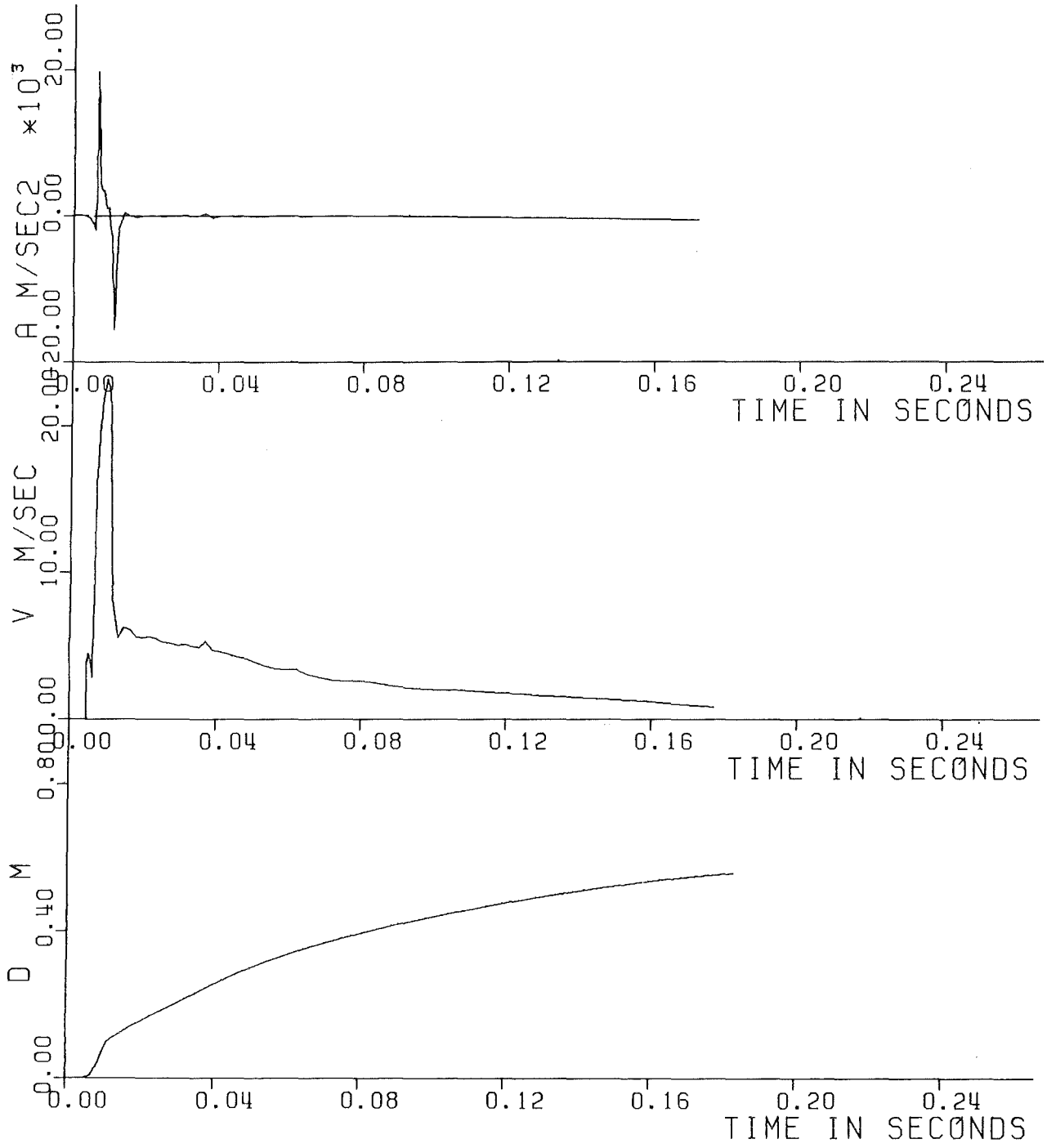

Fig. 6.101 - Experiment Nr. 104 - Displacement, Velocity and Acceleration of the piston.

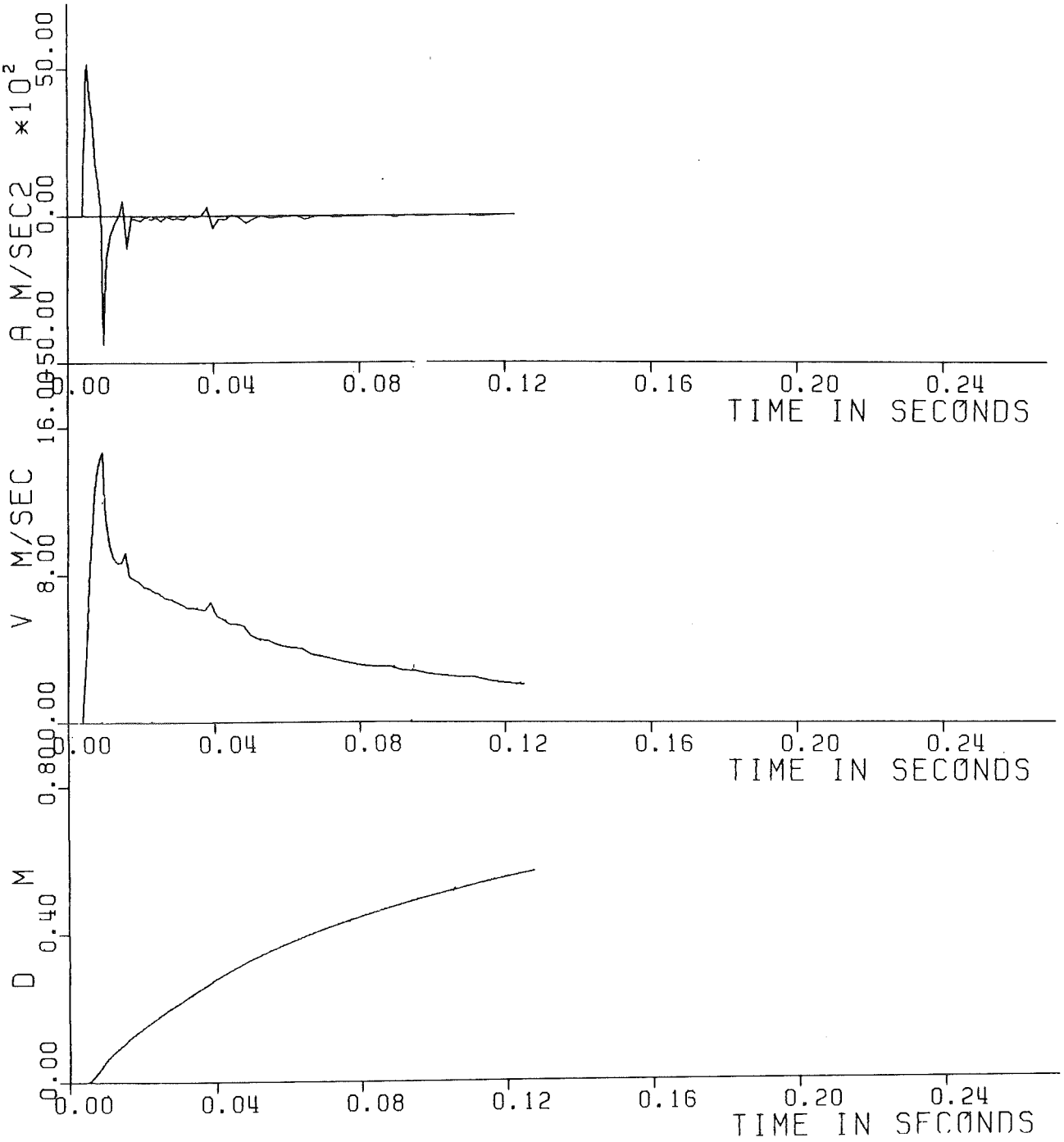

Fig. 6.102- Experiment Nr. 105 - Displacement, Velocity and Acceleration of the piston.

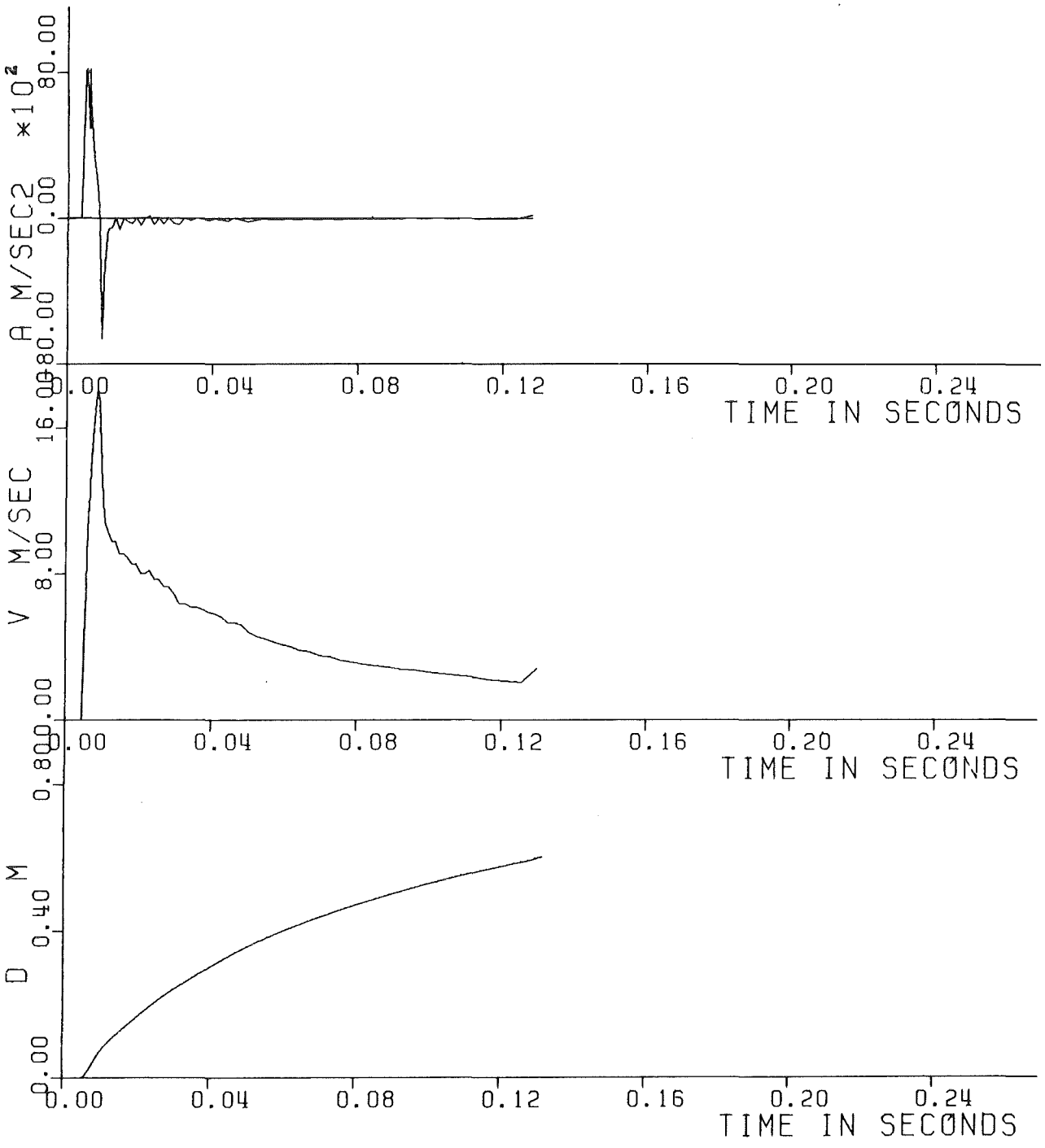

Fig. 6.103 - Experiment Nr. 106 - Displacement, Velocity and Acceleration of the piston.

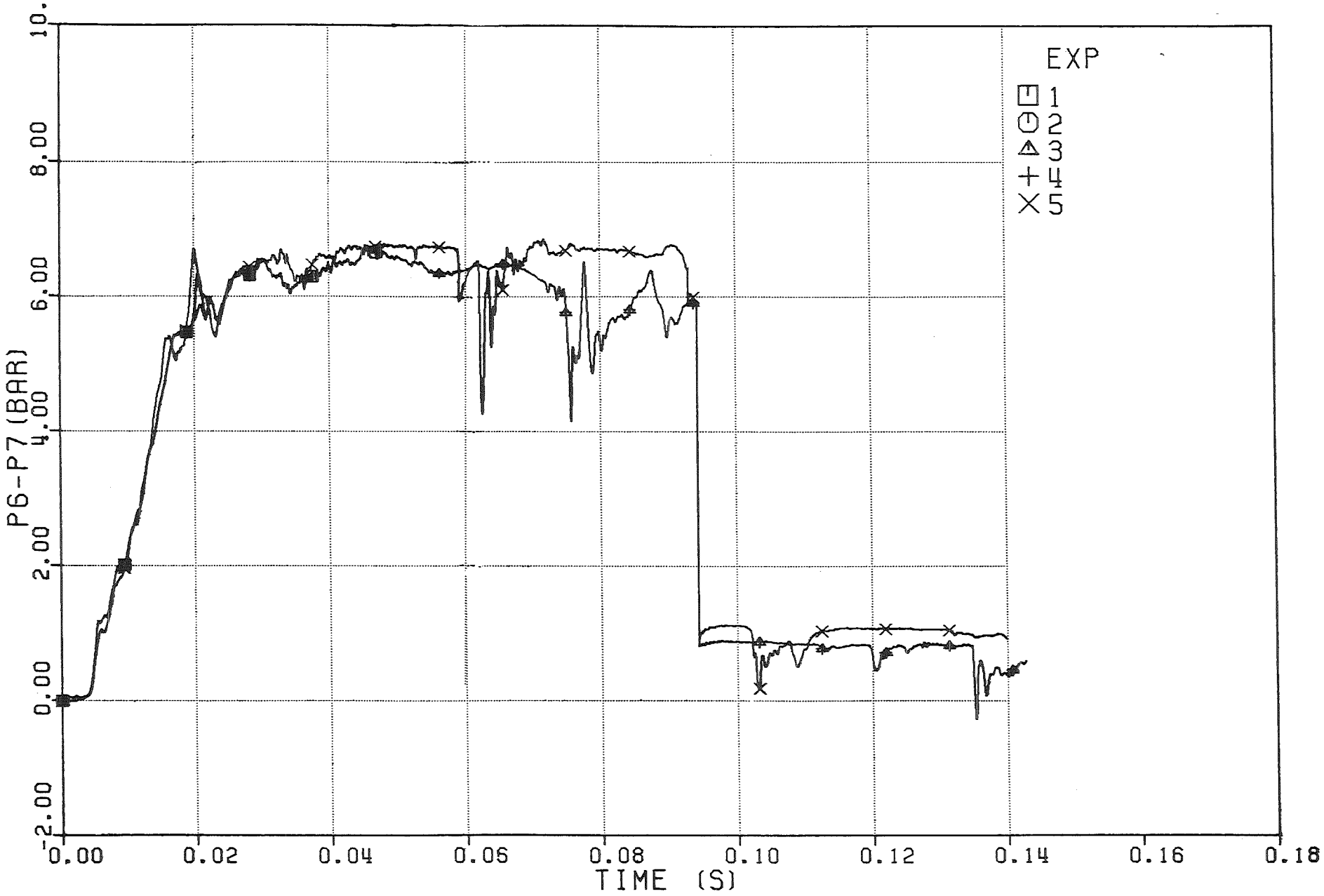

Fig. 6.104 - PRESSURE DROP THROUGH THE DIP-PLATE

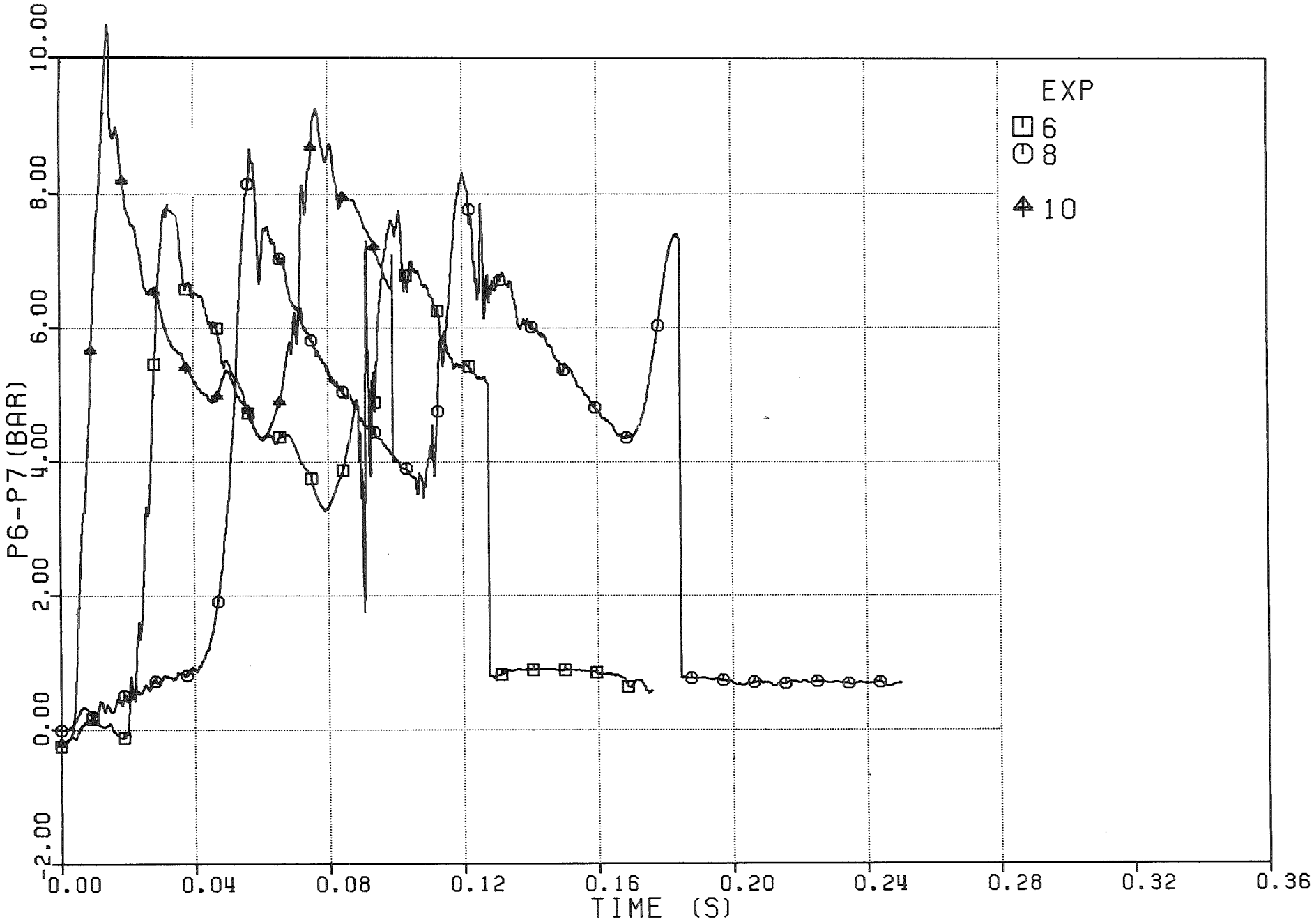

Fig. 6.105 - PRESSURE DROP THROUGH THE DIP-PLATE

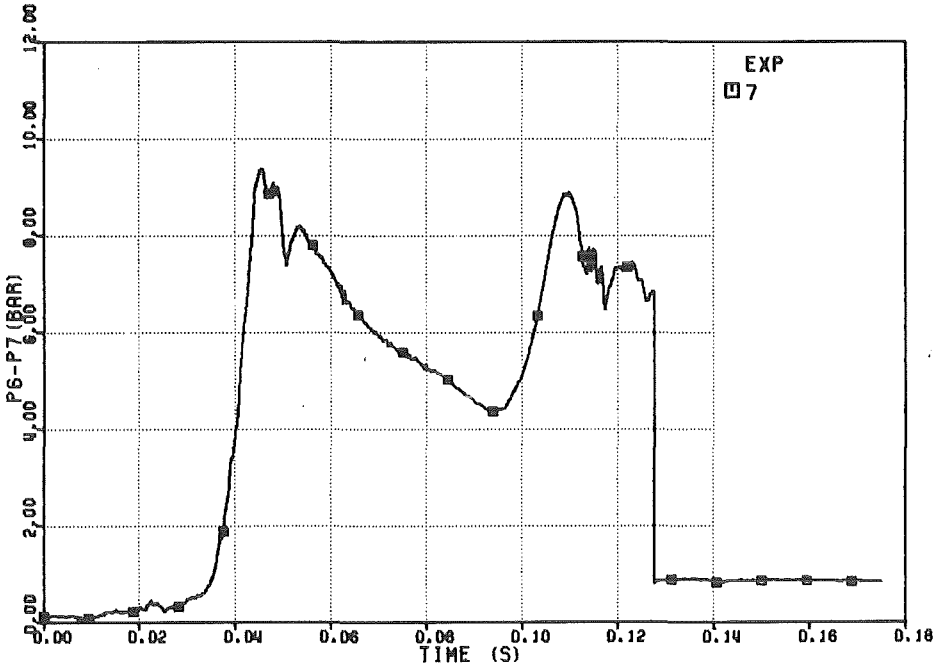

FIG. 6.106 -PRESSURE DROP THROUGH THE DIP-PLATE

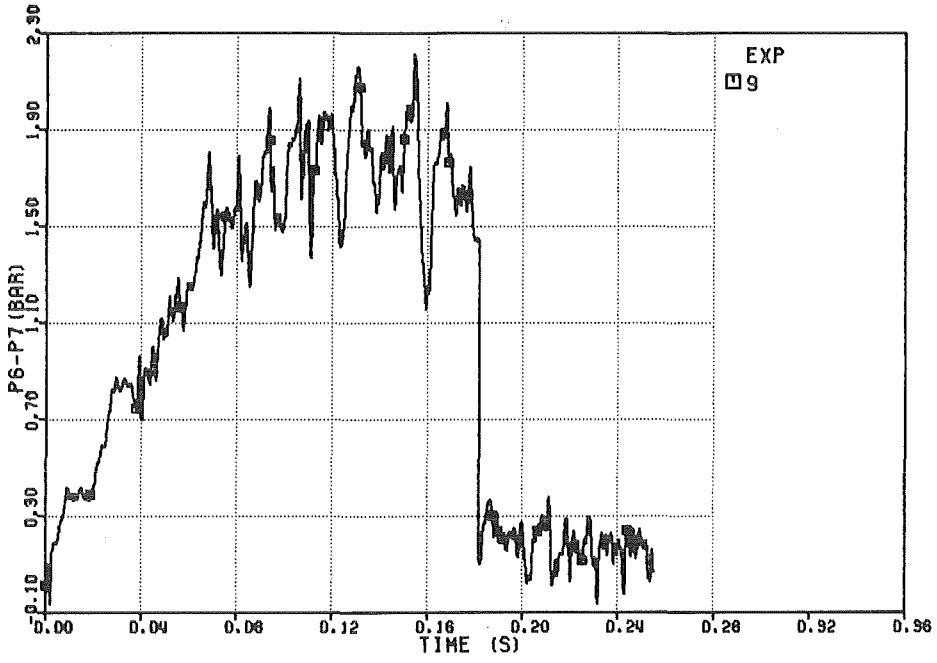

FIG. 6.107 -PRESSURE DROP THROUGH THE DIP-PLATE

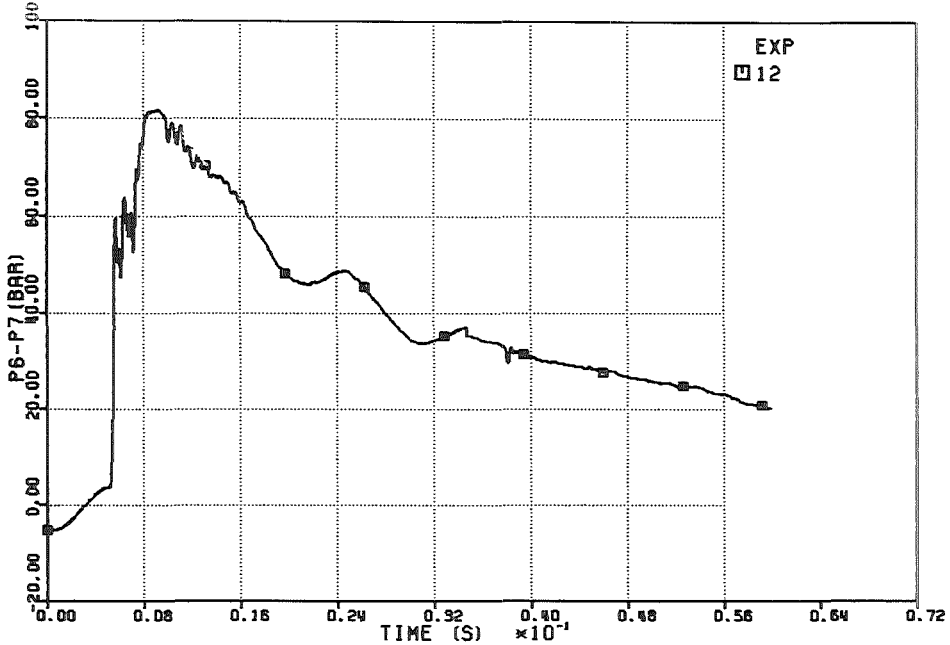

FIG. 6.109 -PRESSURE DROP THROUGH THE DIP-PLATE

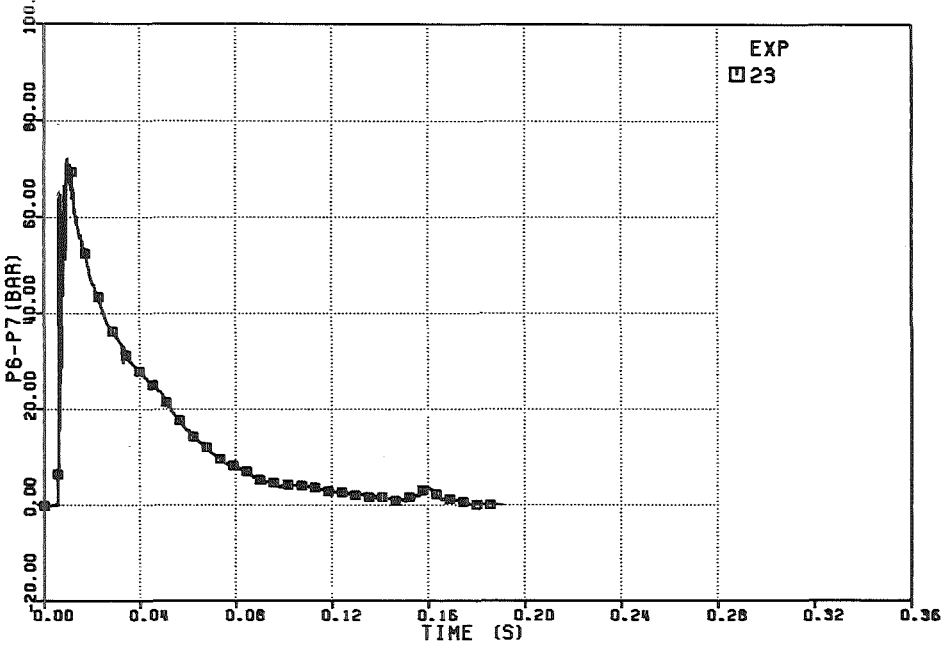

FIG. 6.111 -PRESSURE DROP THROUGH THE DIP-PLATE

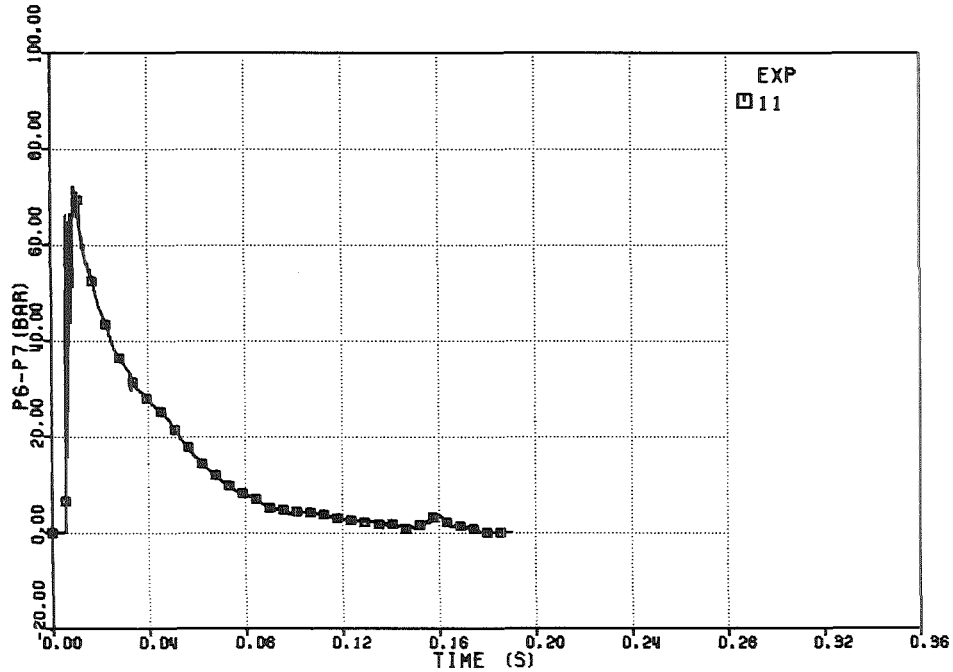

FIG. 6.108 -PRESSURE DROP THROUGH THE DIP-PLATE

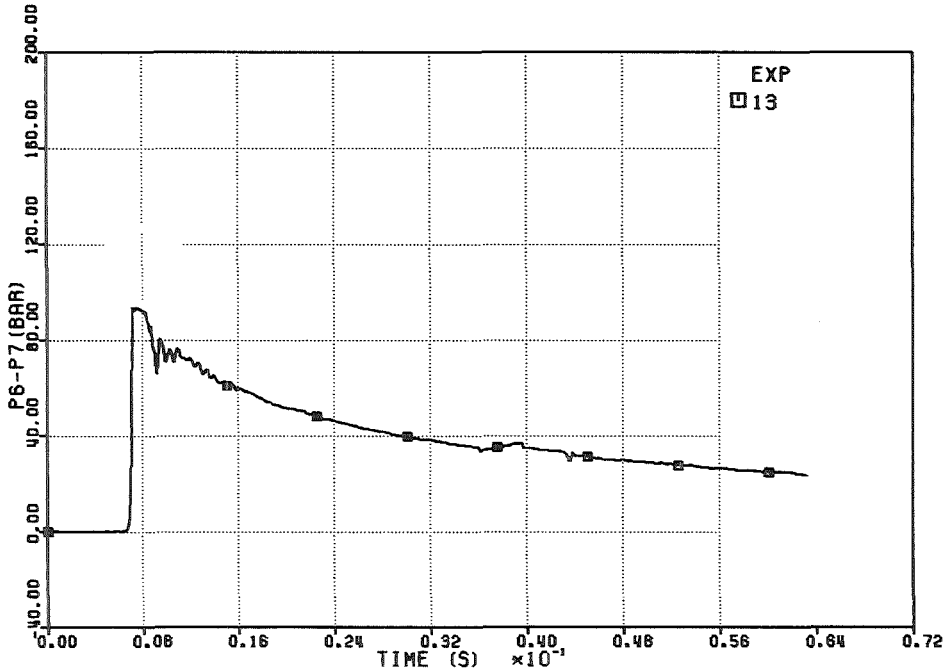

FIG. 6.110 -PRESSURE DROP THROUGH THE DIP-PLATE

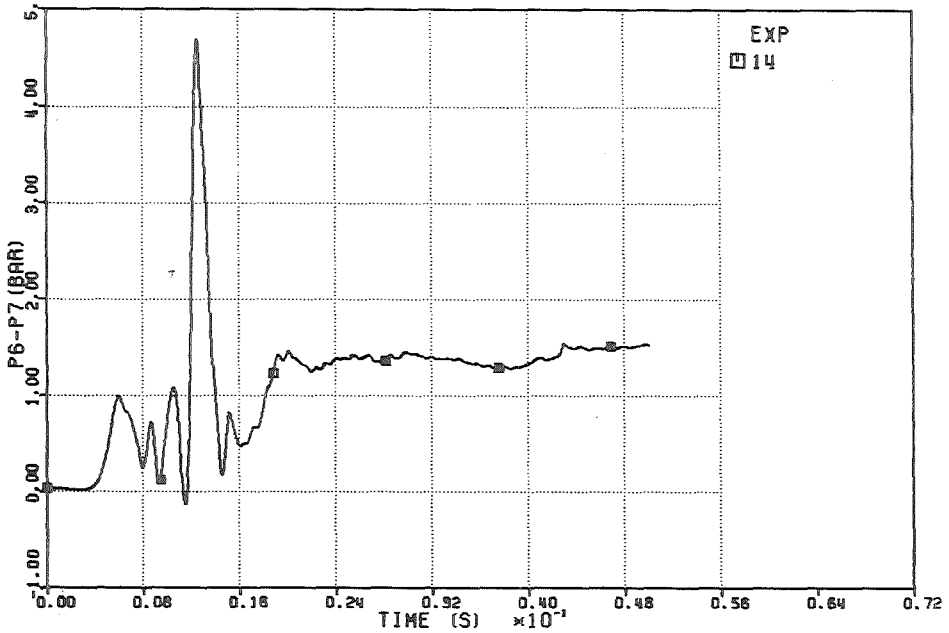

FIG. 6.113 PRESSURE DROP THROUGH THE DIP-PLATE

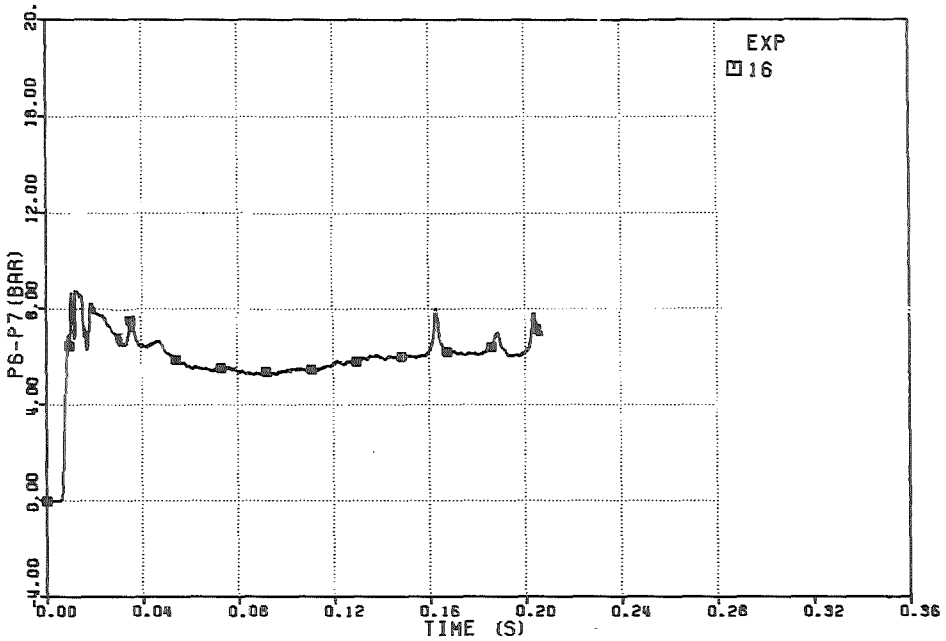

FIG. 6.115 -PRESSURE DROP THROUGH THE DIP-PLATE

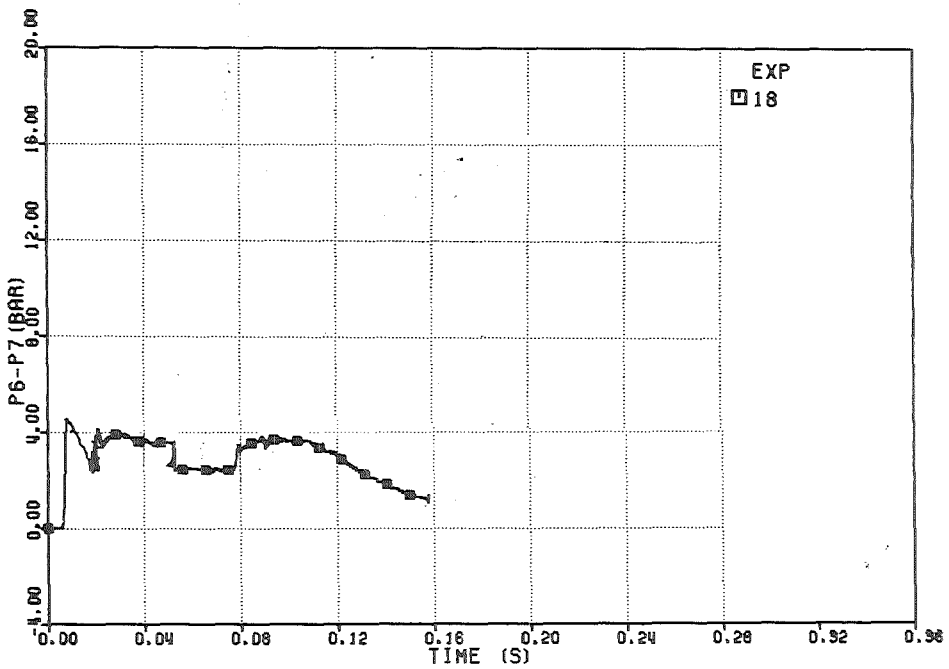

FIG. 6.112 -PRESSURE DROP THROUGH THE DIP-PLATE

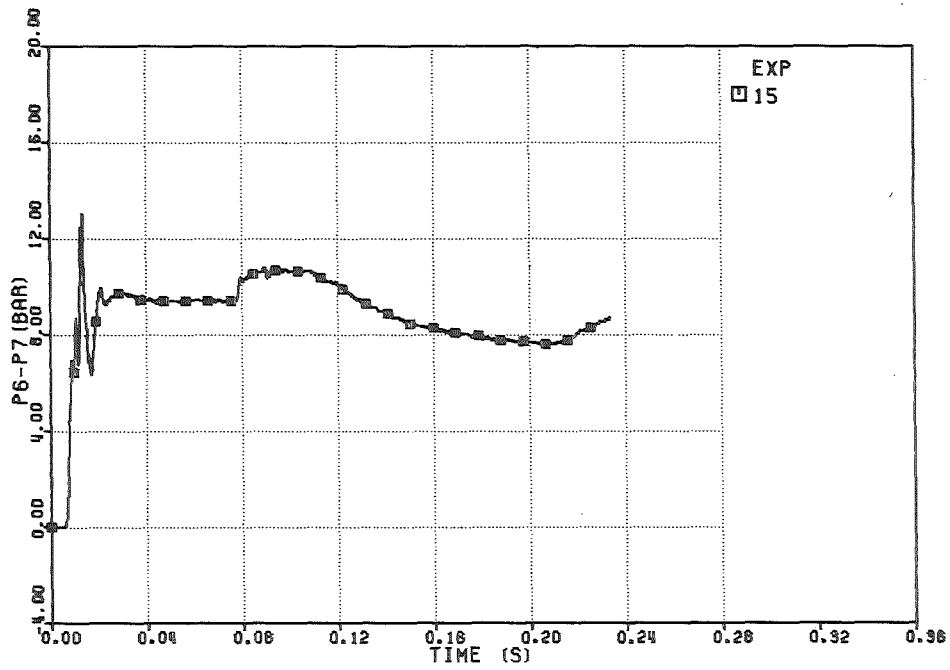

FIG. 6.114 -PRESSURE DROP THROUGH THE DIP-PLATE

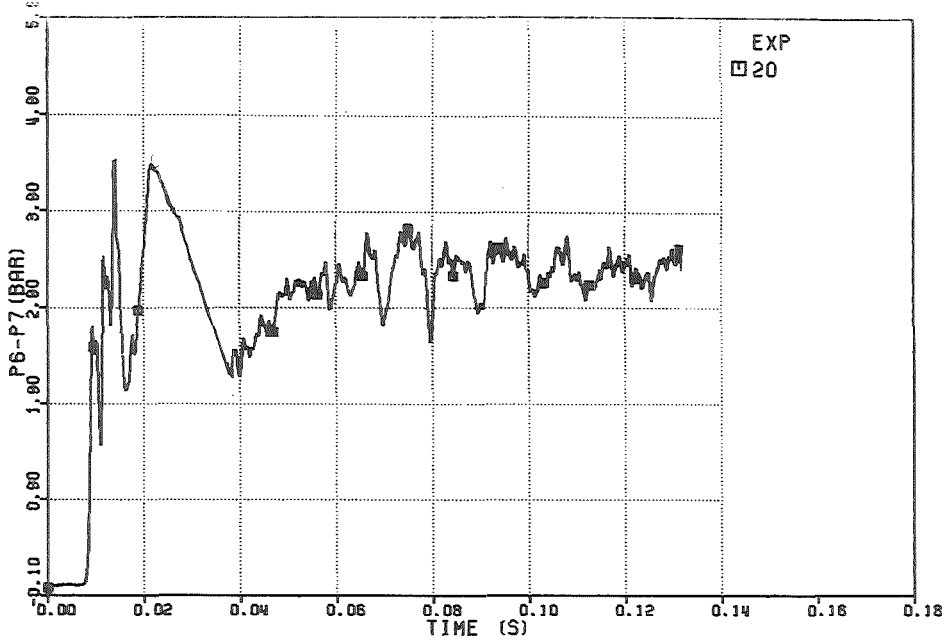

FIG. 6.117 -PRESSURE DROP THROUGH THE DIP-PLATE

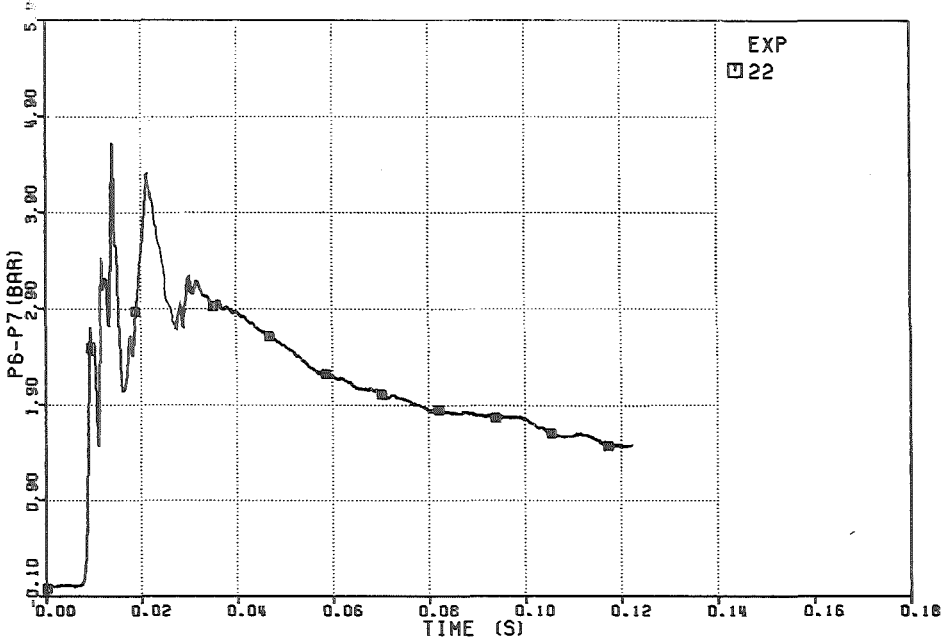

FIG. 6.119 -PRESSURE DROP THROUGH THE DIP-PLATE

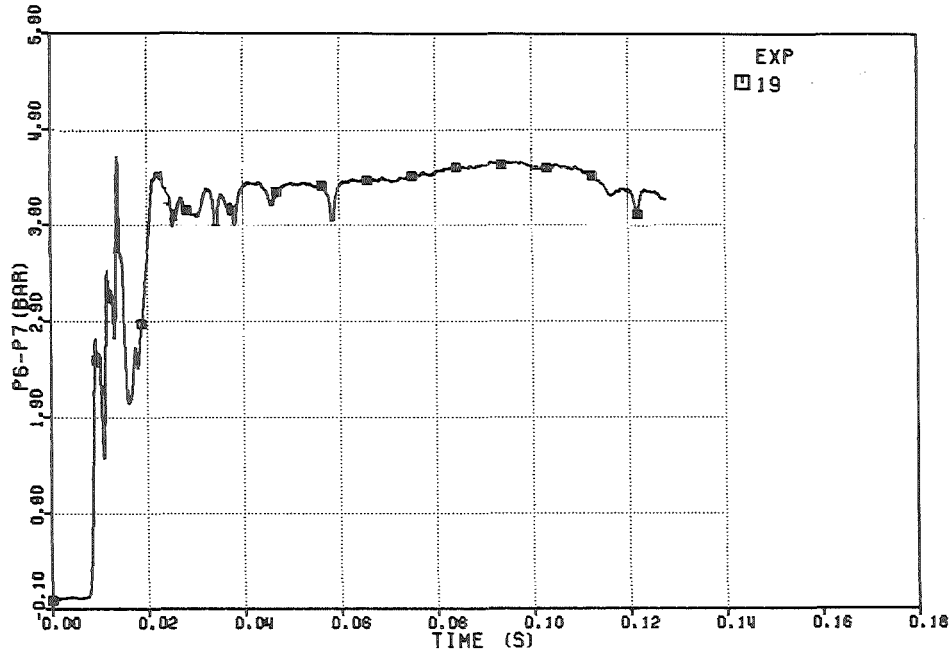

FIG. 6.116 -PRESSURE DROP THROUGH THE DIP-PLATE

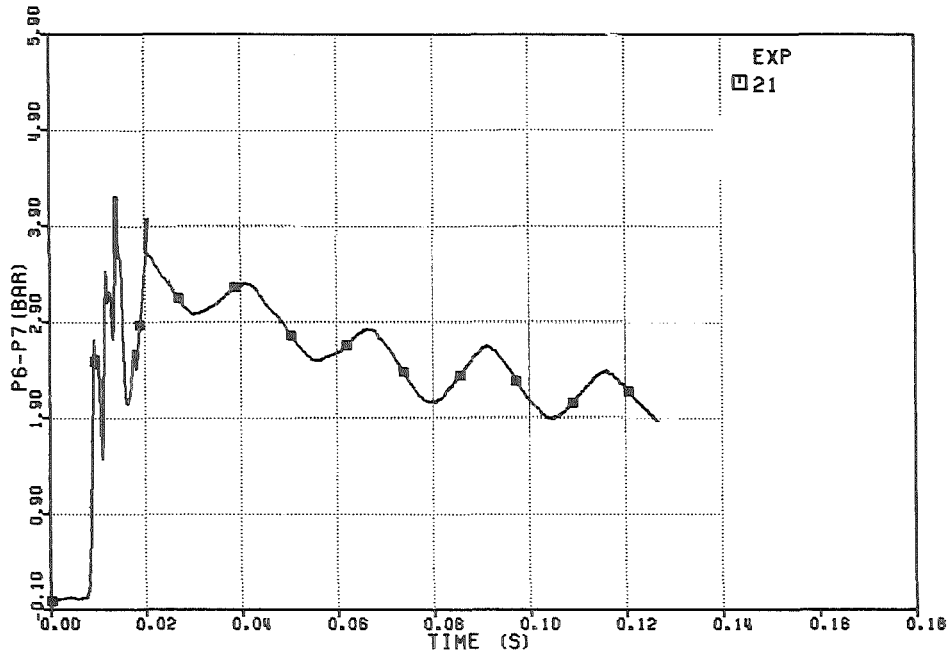

FIG. 6.118 -PRESSURE DROP THROUGH THE DIP-PLATE

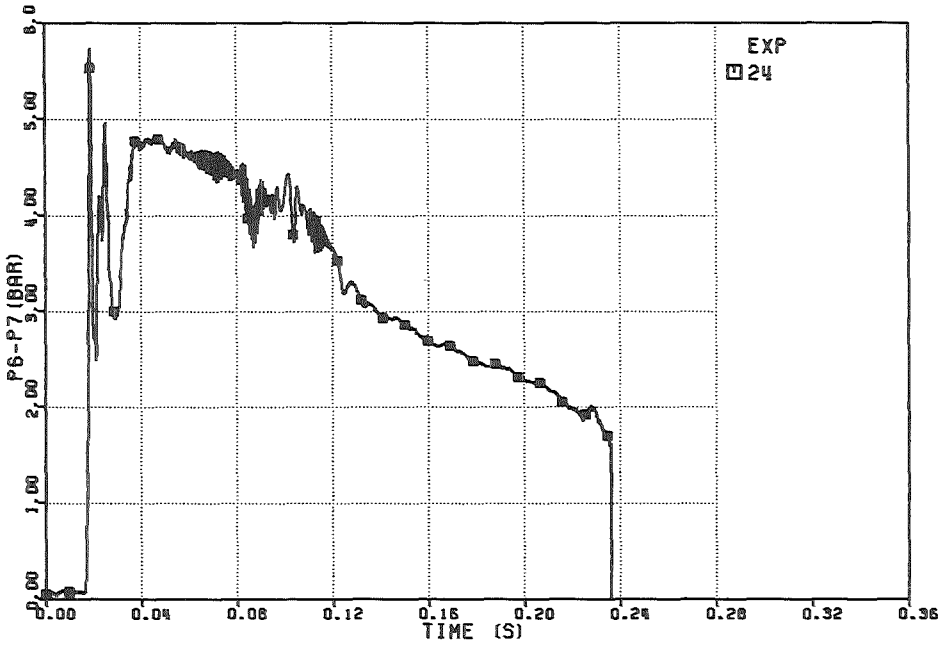

FIG. 6.120 -PRESSURE DROP THROUGH THE DIP-PLATE

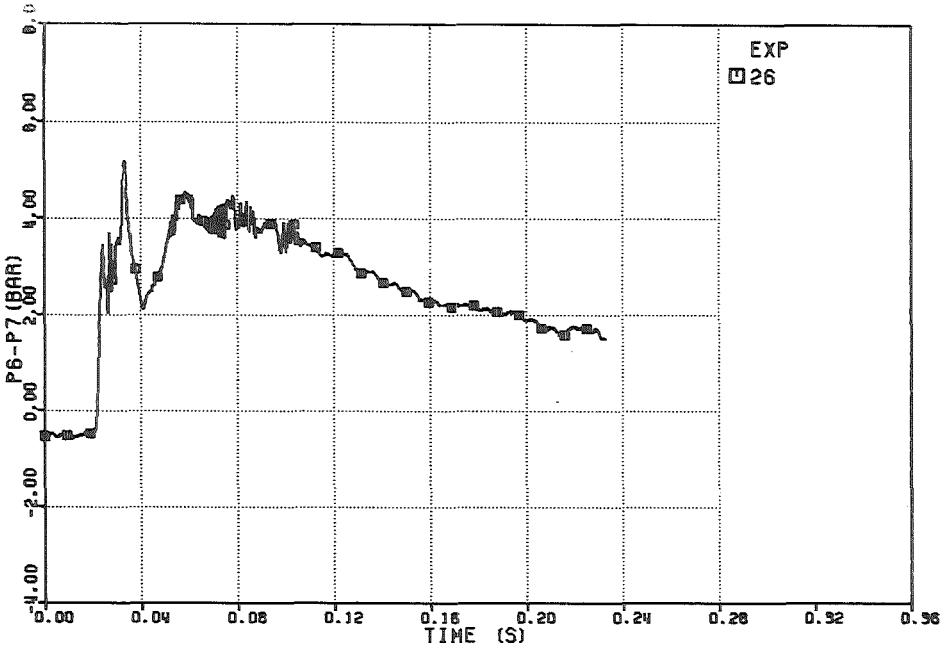

FIG. 6.122-PRESSURE DROP THROUGH THE DIP-PLATE

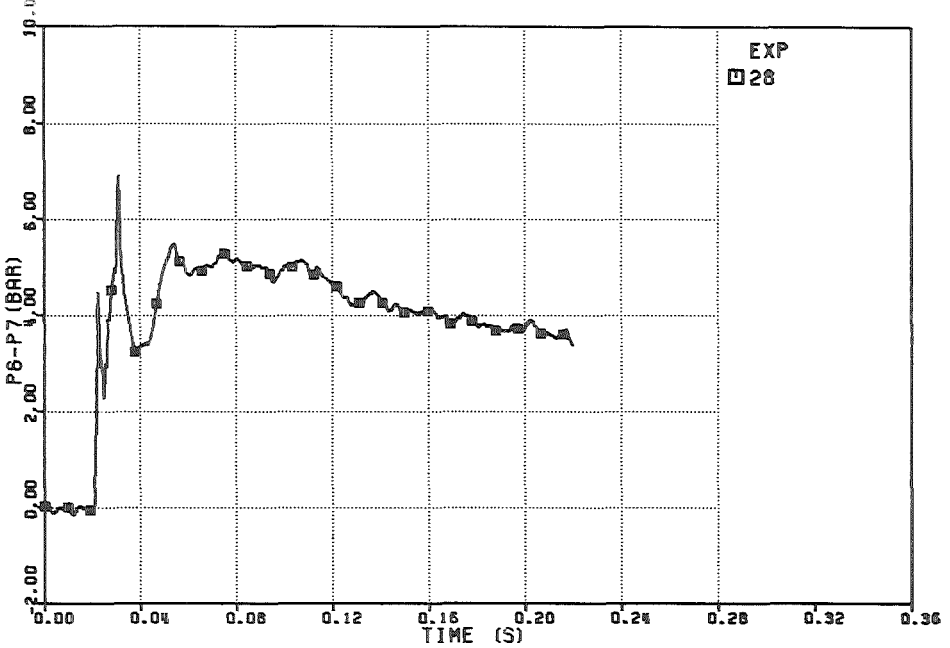

FIG. 6.124 -PRESSURE DROP THROUGH THE DIP-PLATE

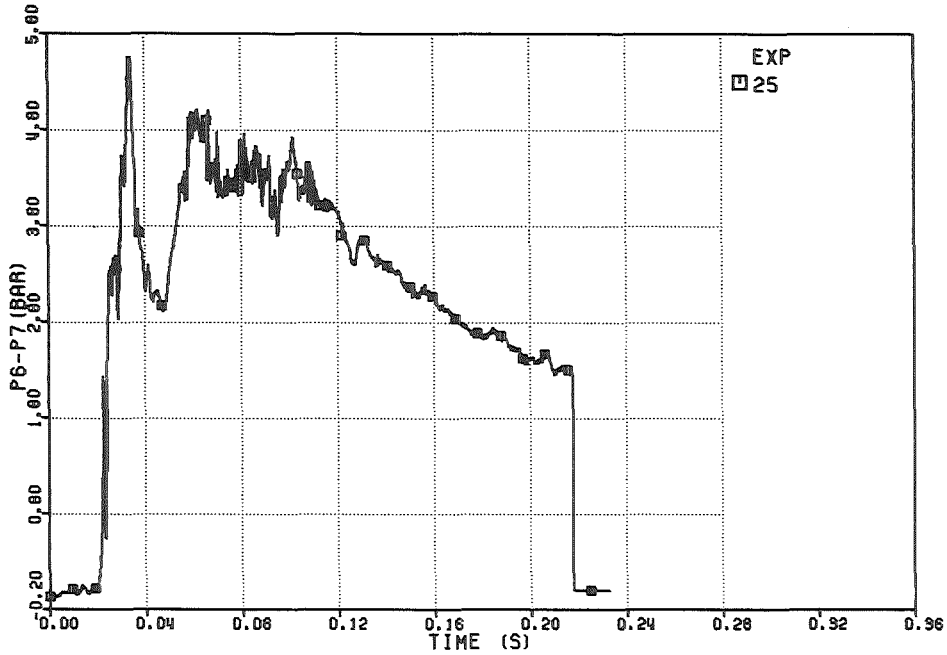

FIG. 6.121 -PRESSURE DROP THROUGH THE DIP-PLATE

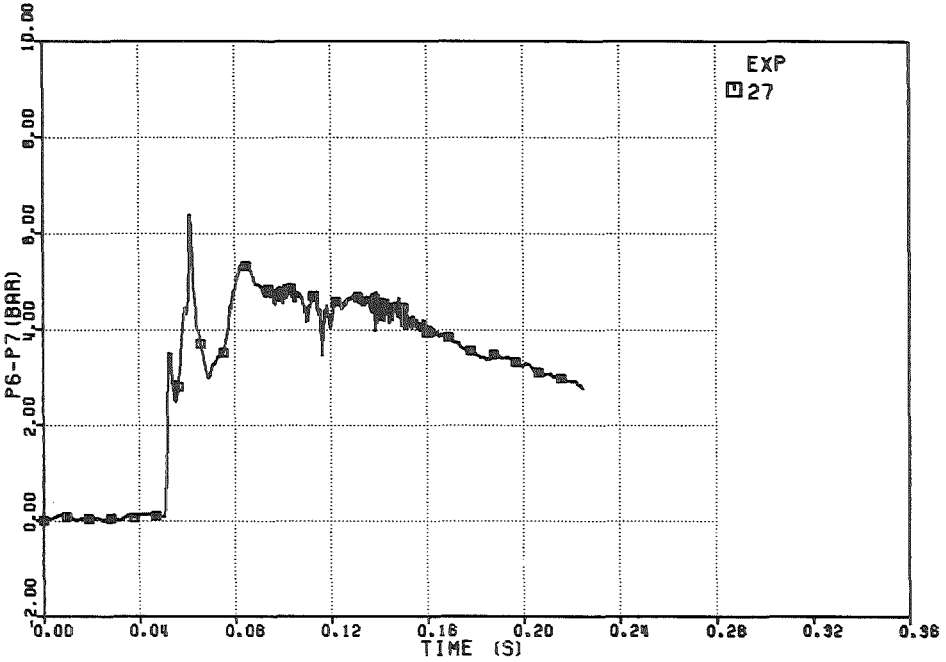

FIG. 6.123 -PRESSURE DROP THROUGH THE DIP-PLATE

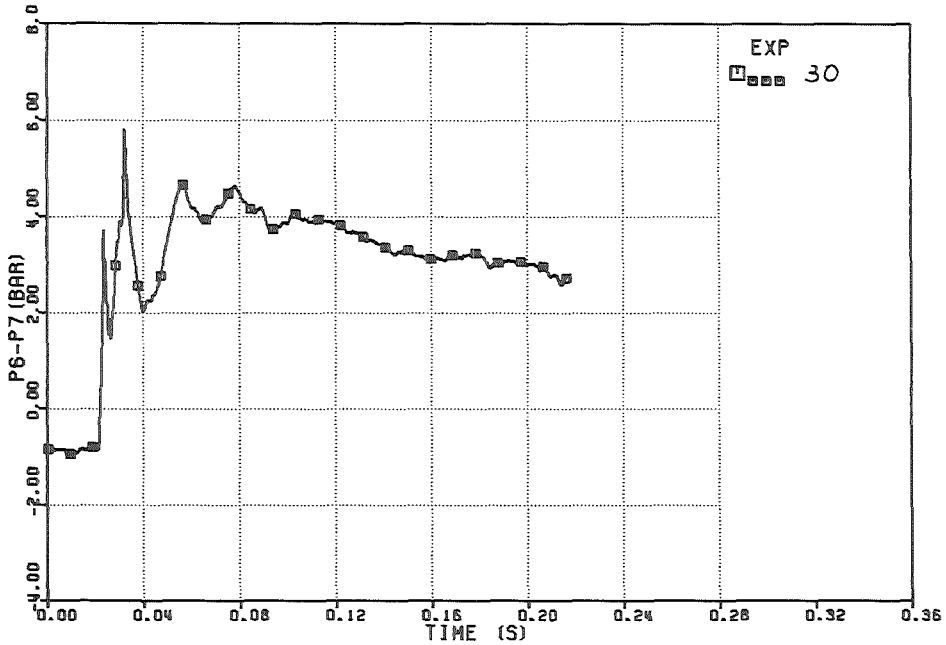

FIG. 6.126-PRESSURE DROP THROUGH THE DIP-PLATE

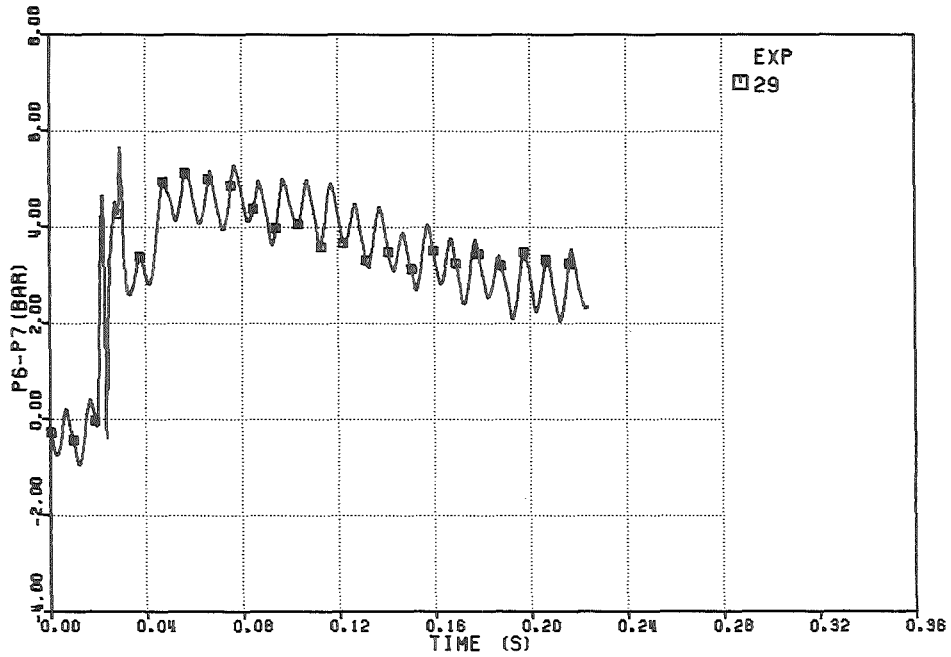

FIG. 6.125 -PRESSURE DROP THROUGH THE DIP-PLATE

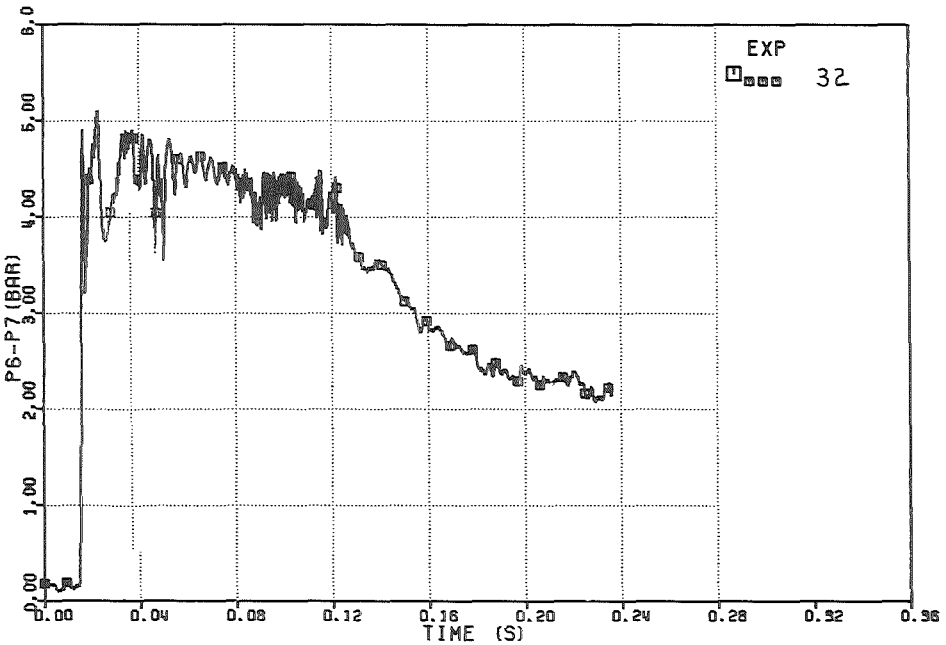

FIG. 6.128 -PRESSURE DROP THROUGH THE DIP-PLATE

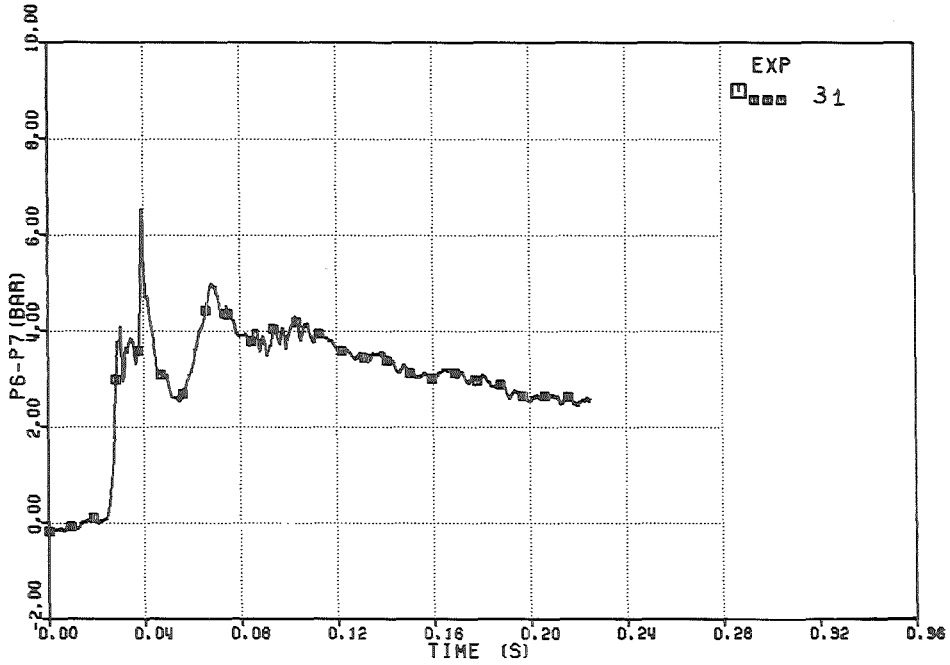

FIG. 6.127 -PRESSURE DROP THROUGH THE DIP-PLATE

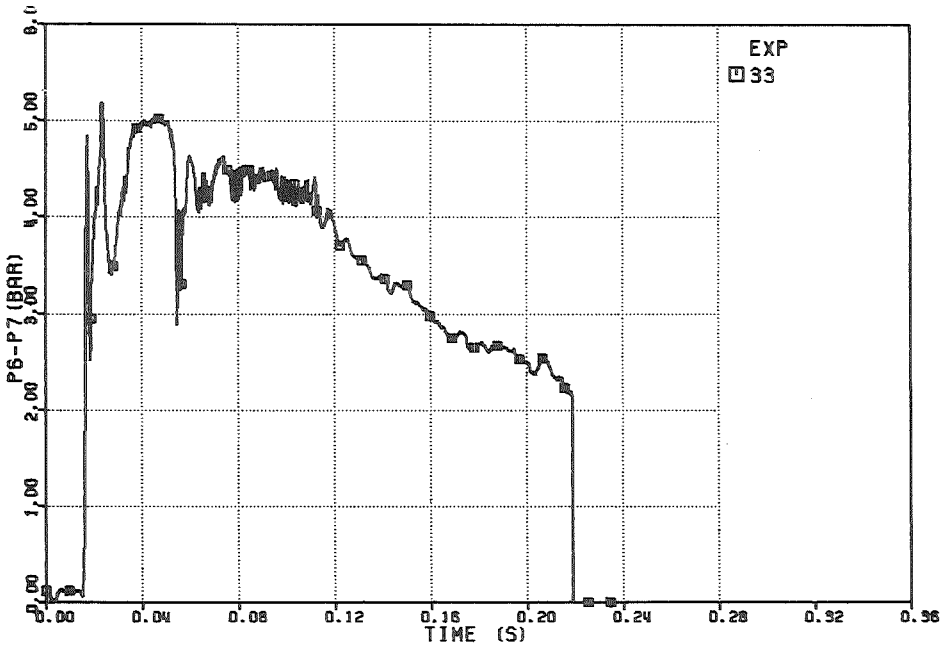

FIG. 6.129-PRESSURE DROP THROUGH THE DIP-PLATE

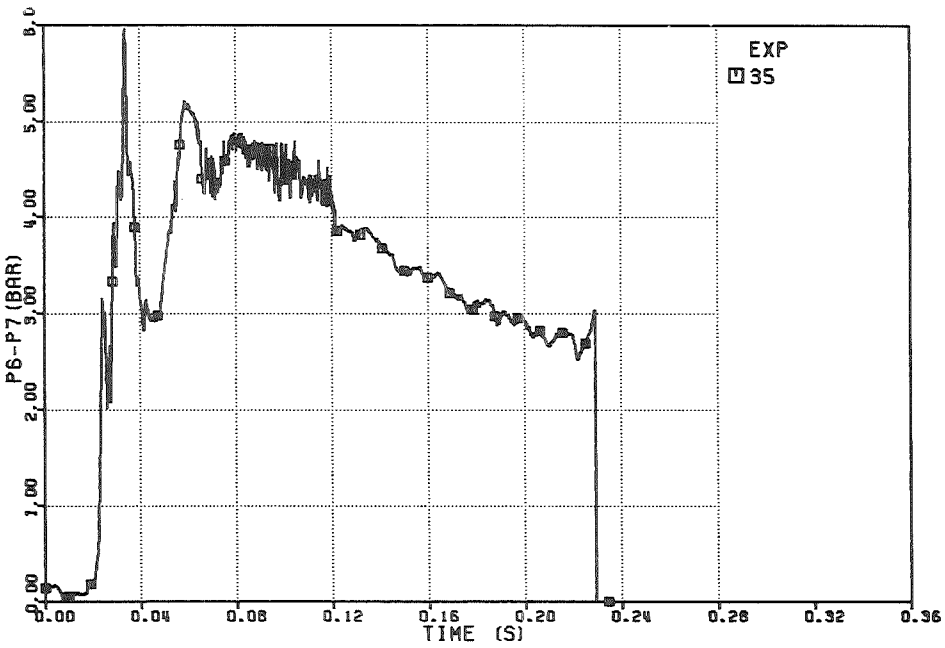

FIG. 6.131 -PRESSURE DROP THROUGH THE DIP-PLATE

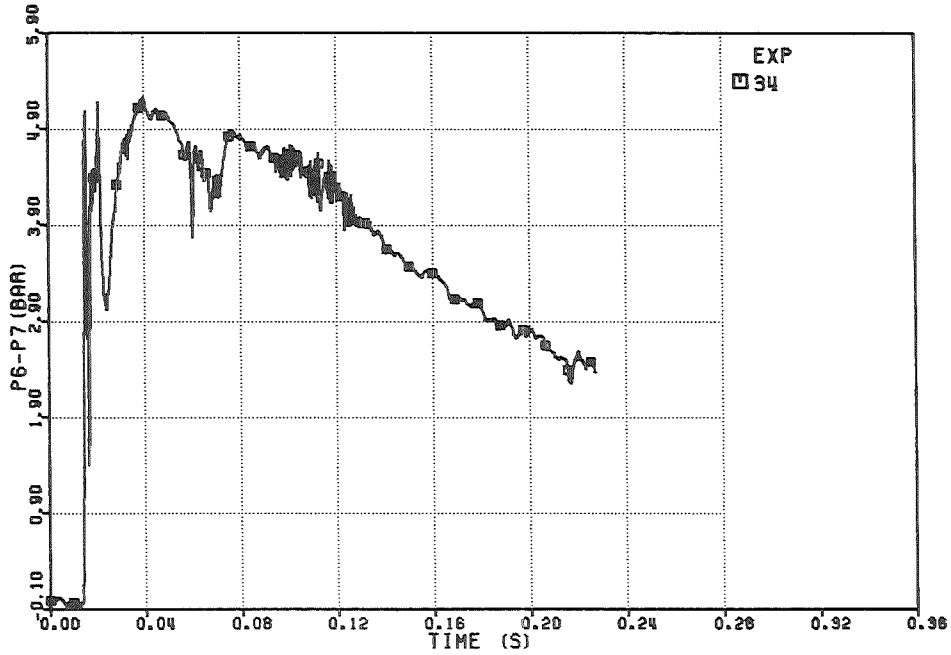

FIG. 6.130 -PRESSURE DROP THROUGH THE DIP-PLATE

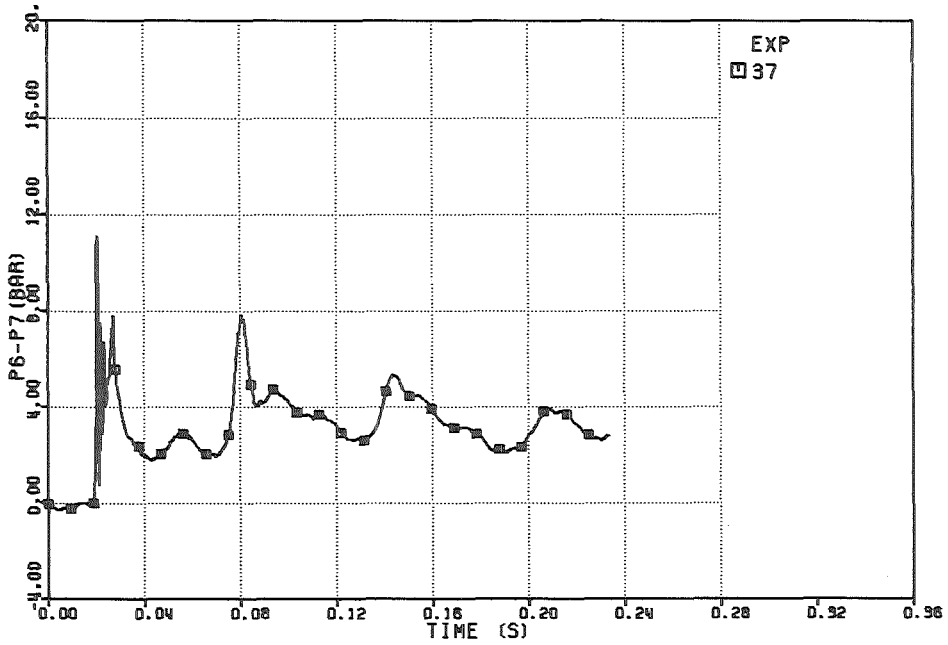

FIG. 6.133 -PRESSURE DROP THROUGH THE DIP-PLATE

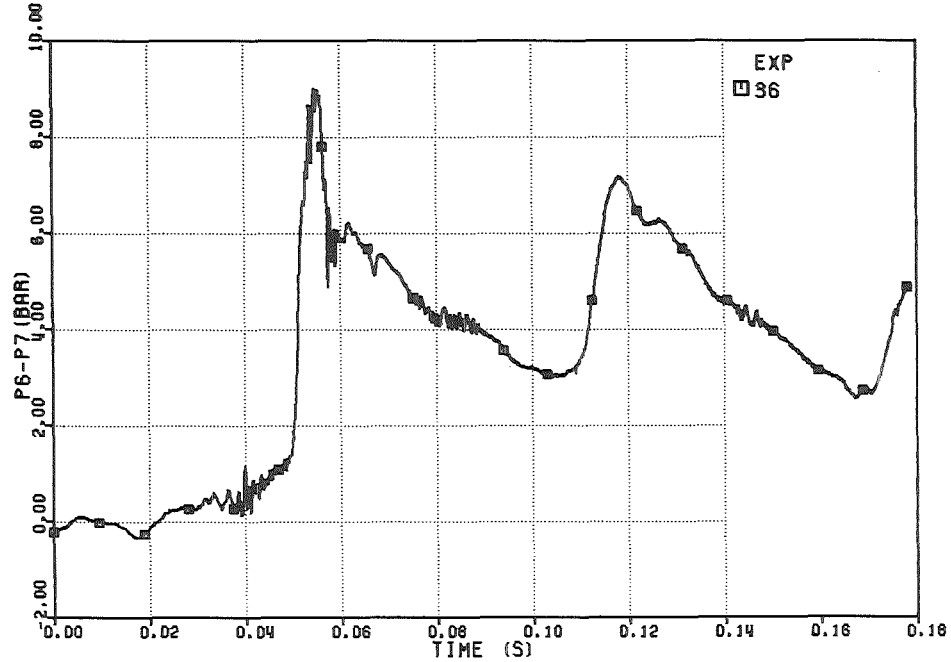

FIG. 6.132 -PRESSURE DROP THROUGH THE DIP-PLATE

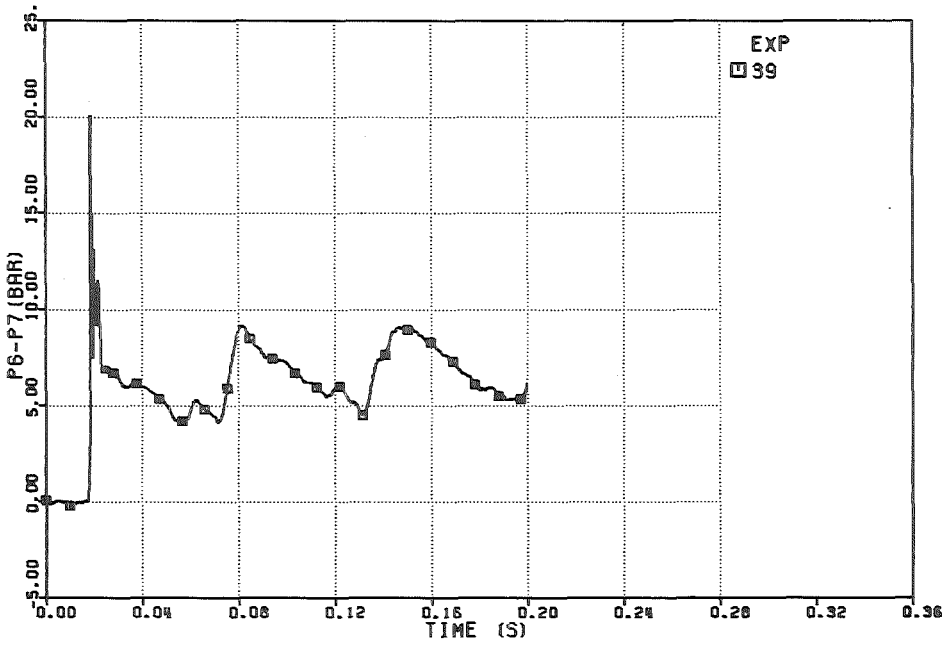

FIG. 6.135 -PRESSURE DROP THROUGH THE DIP-PLATE

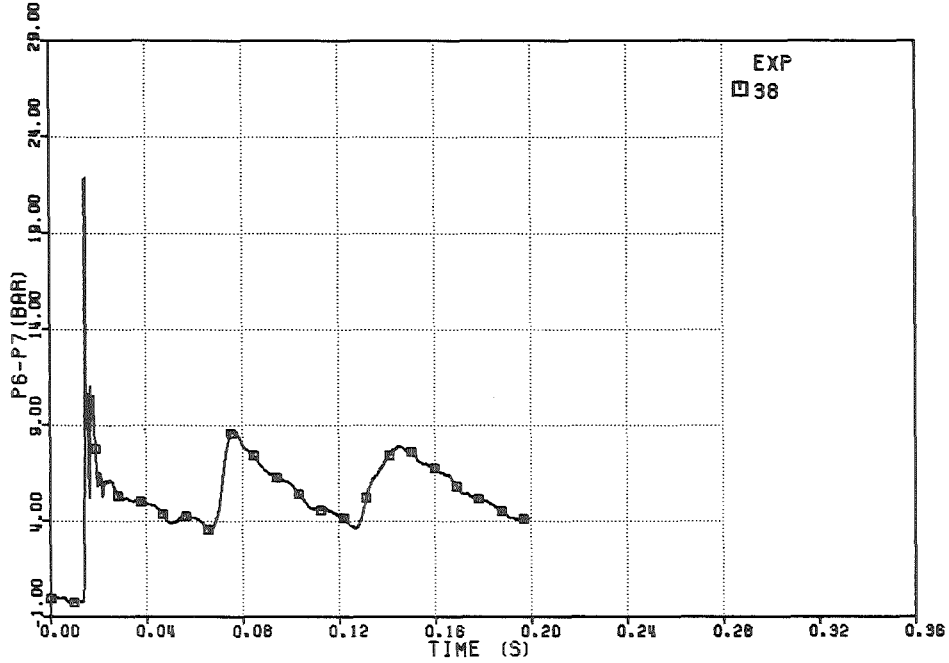

FIG. 6.134 -PRESSURE DROP THROUGH THE DIP-PLATE

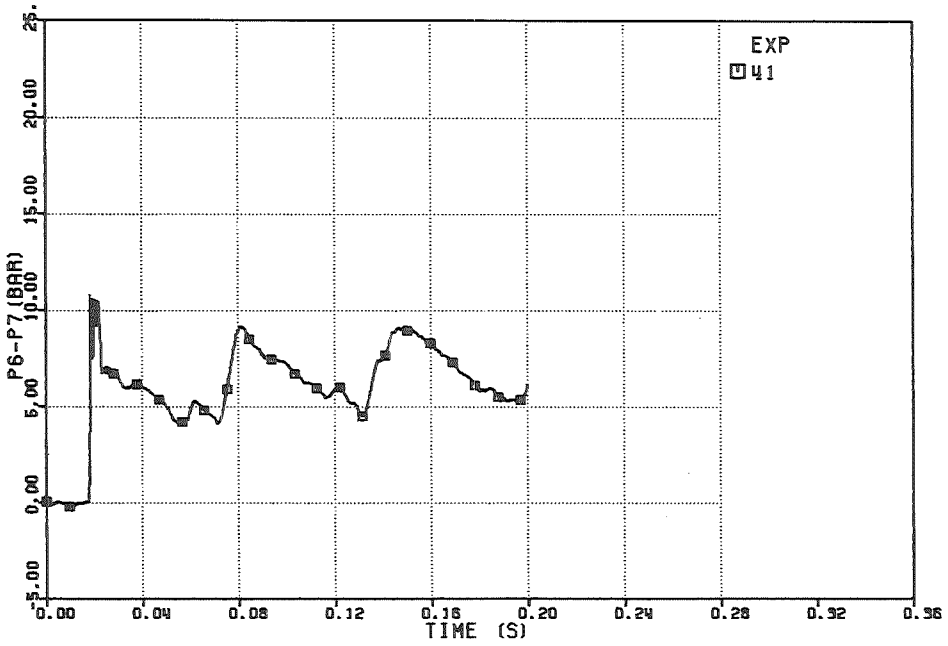

FIG. 6.137 -PRESSURE DROP THROUGH THE DIP-PLATE

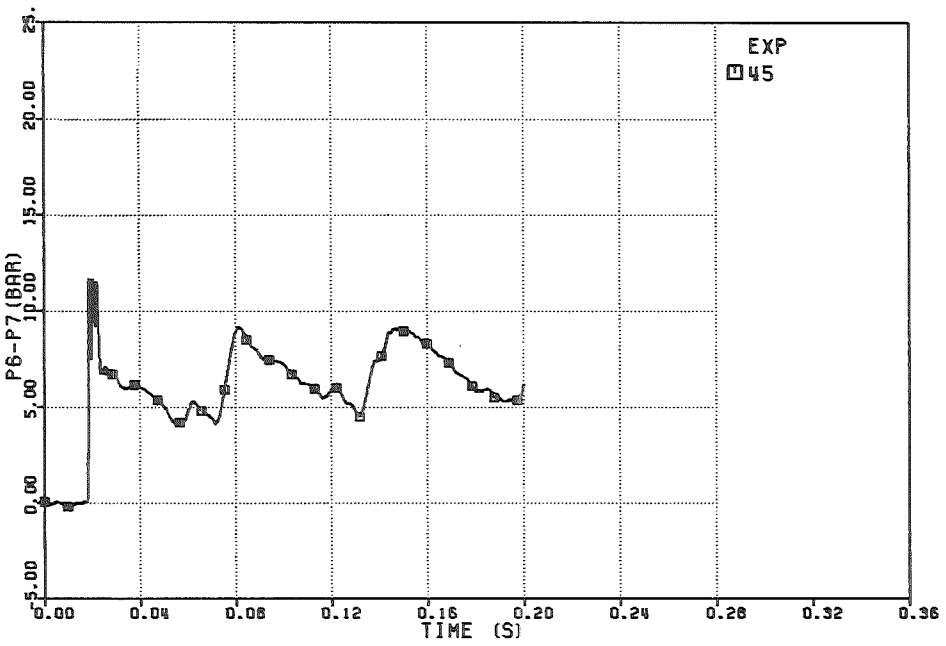

FIG. 6.139 -PRESSURE DROP THROUGH THE DIP-PLATE

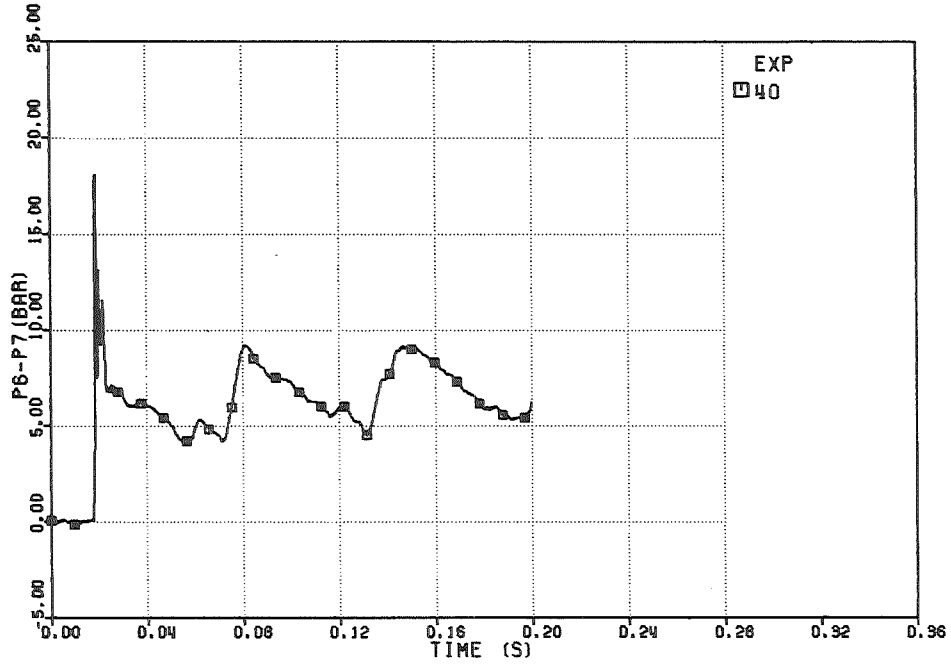

FIG. 6.136 -PRESSURE DROP THROUGH THE DIP-PLATE

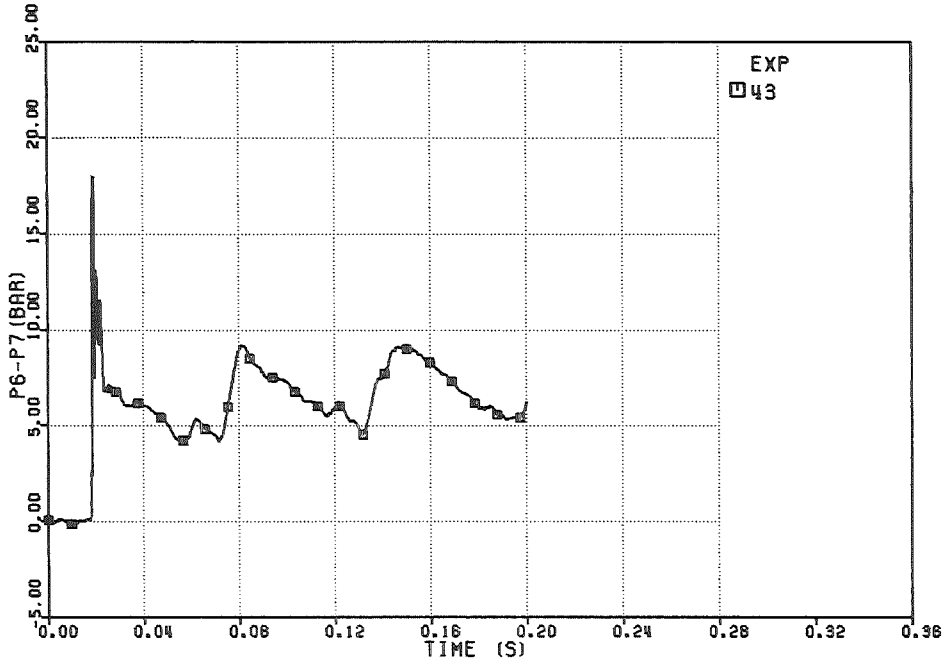

FIG. 6.138 -PRESSURE DROP THROUGH THE DIP-PLATE

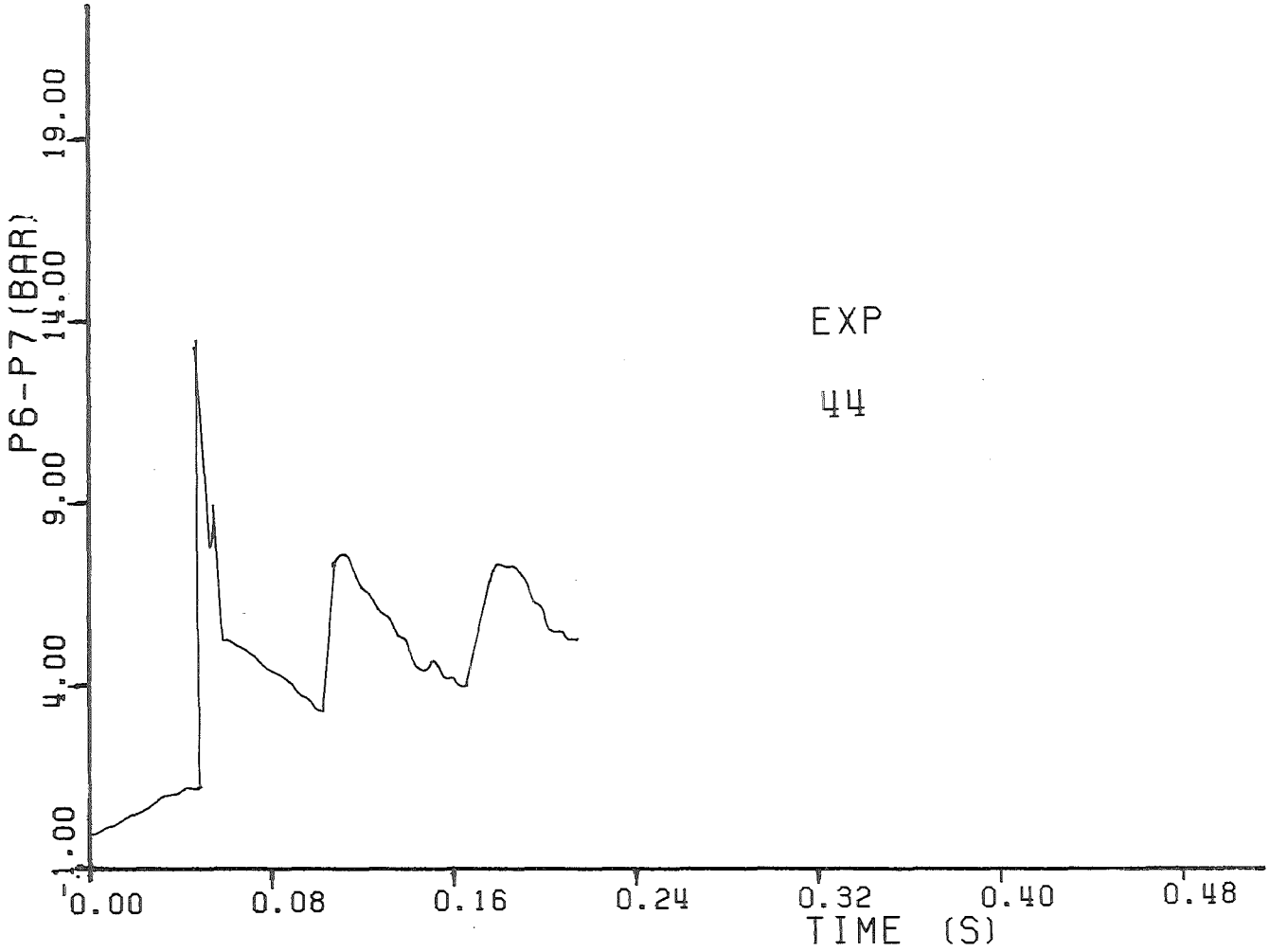

Fig. 6.140 - PRESSURE DROP THROUGH THE DIP-PLATE

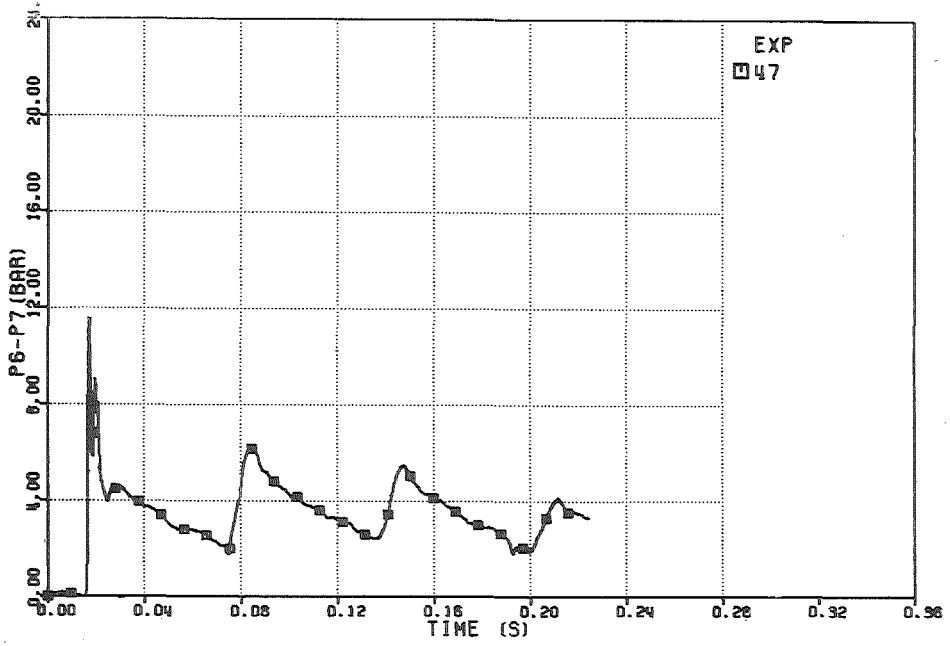

FIG. 6.142 -PRESSURE DROP THROUGH THE DIP-PLATE

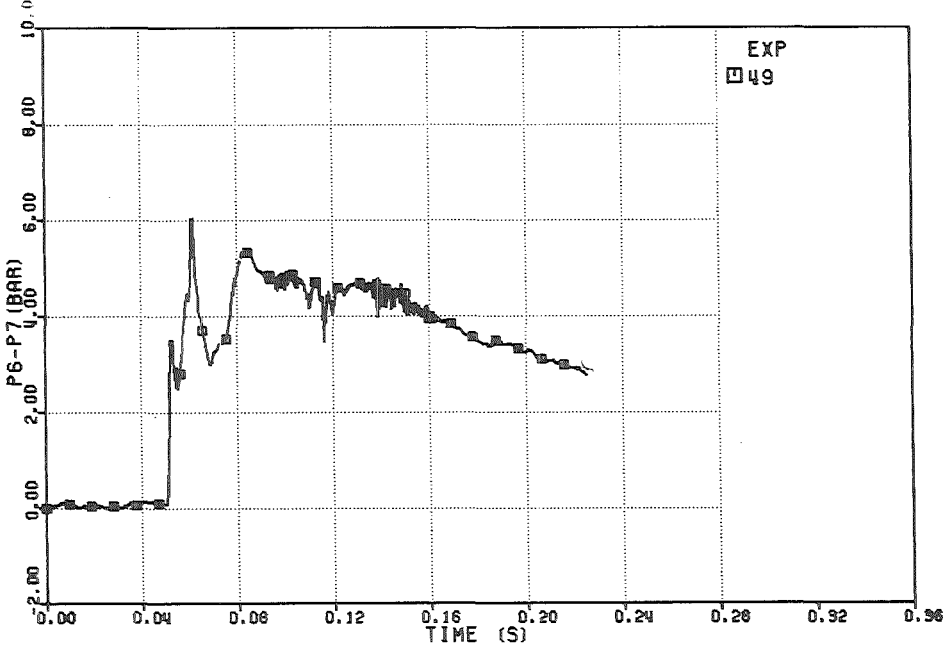

FIG. 6.144 -PRESSURE DROP THROUGH THE DIP-PLATE

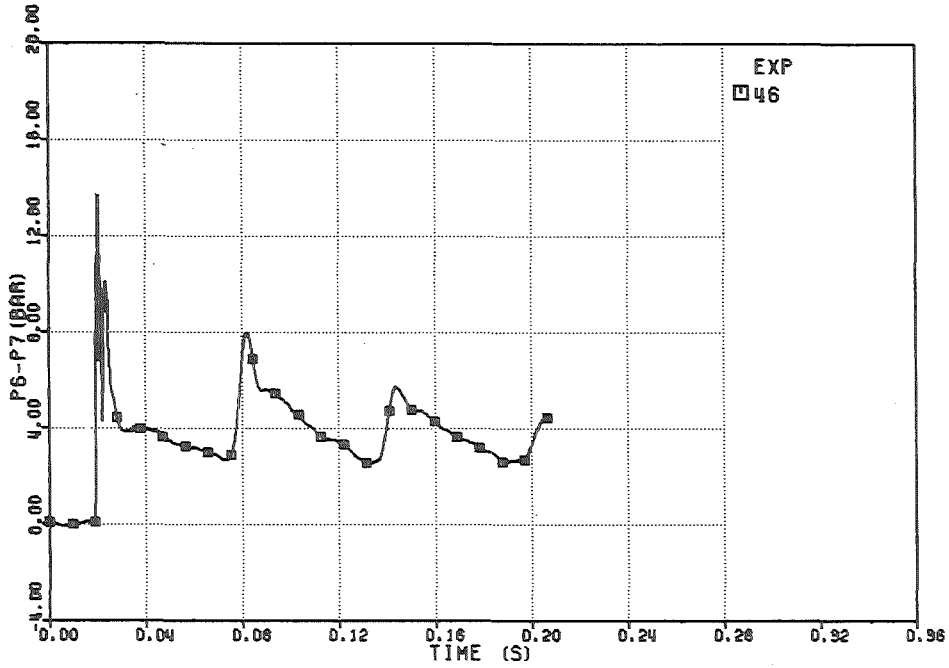

FIG. 6.141 -PRESSURE DROP THROUGH THE DIP-PLATE

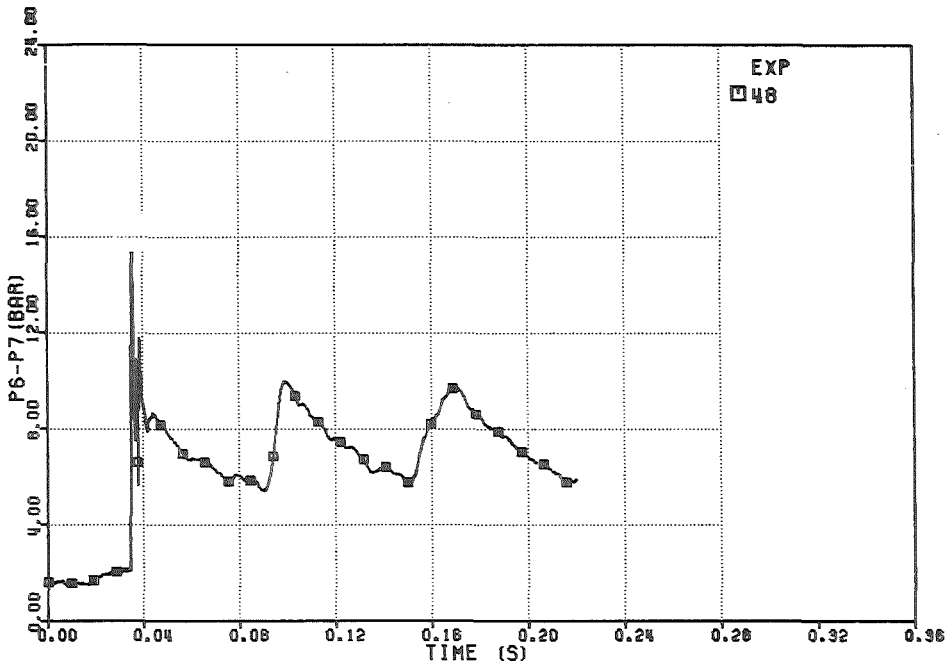

FIG. 6.143 -PRESSURE DROP THROUGH THE DIP-PLATE

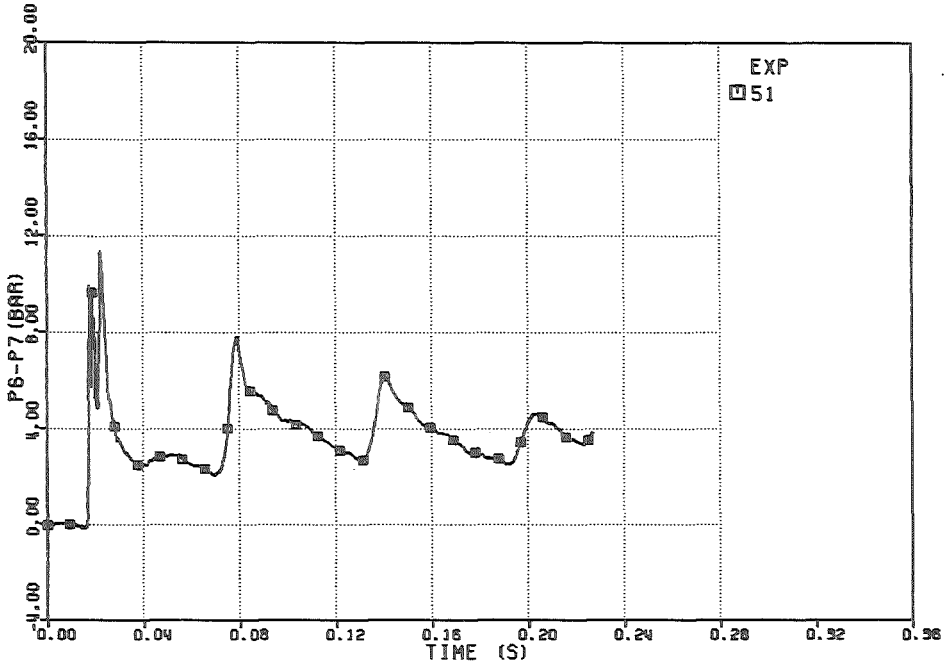

FIG. 6.146 -PRESSURE DROP THROUGH THE DIP-PLATE

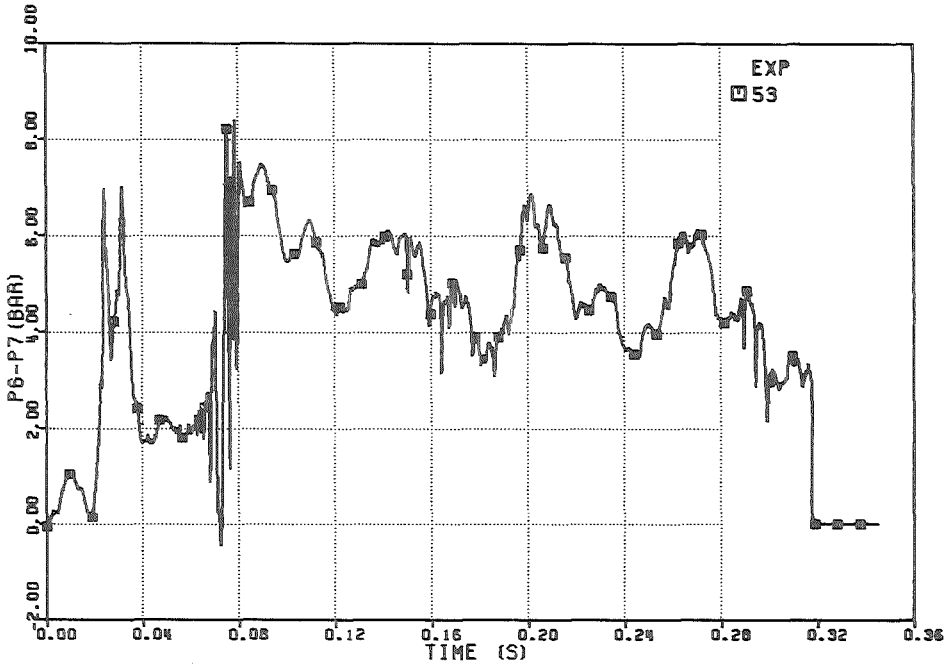

FIG. 6.148 -PRESSURE DROP THROUGH THE DIP-PLATE

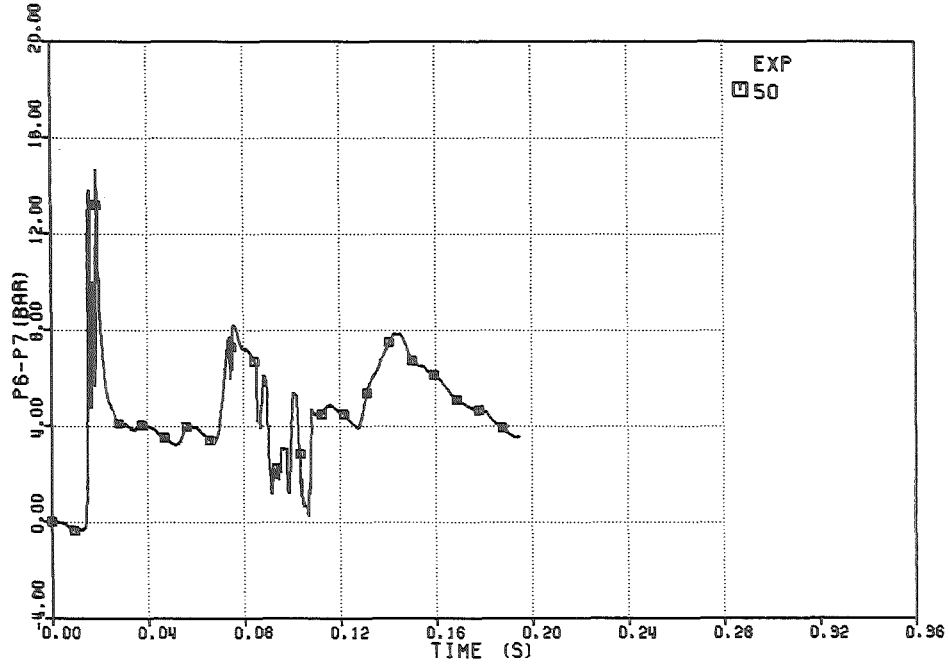

FIG. 6.145 -PRESSURE DROP THROUGH THE DIP-PLATE

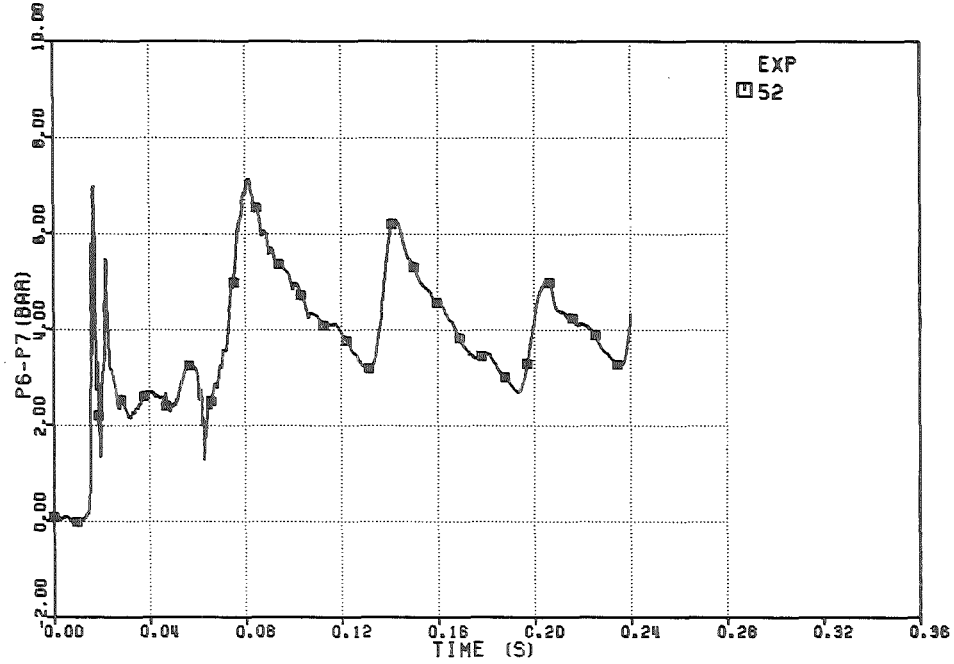

FIG. 6.147 -PRESSURE DROP THROUGH THE DIP-PLATE

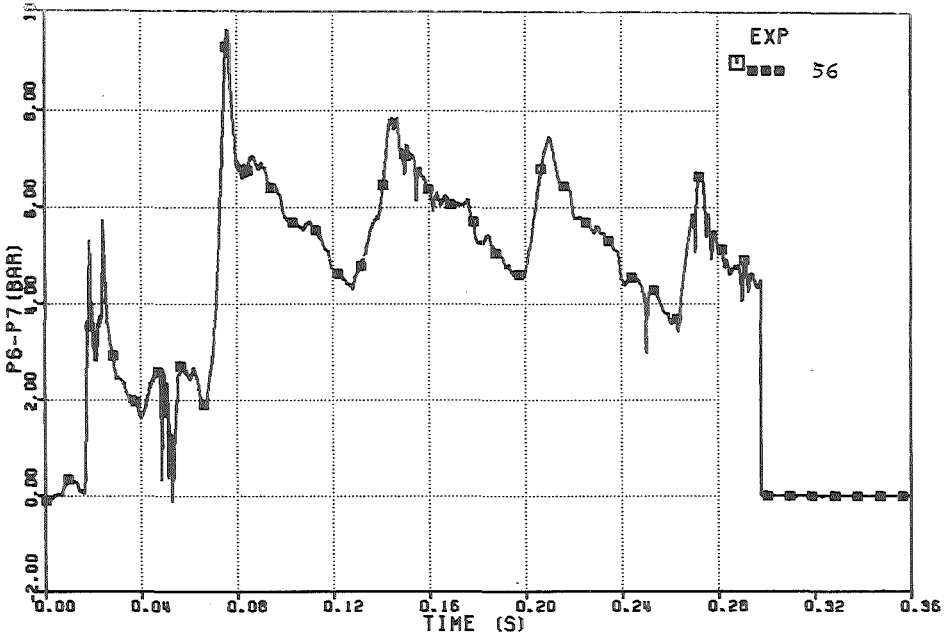

FIG. 6.150 -PRESSURE DROP THROUGH THE DIP-PLATE

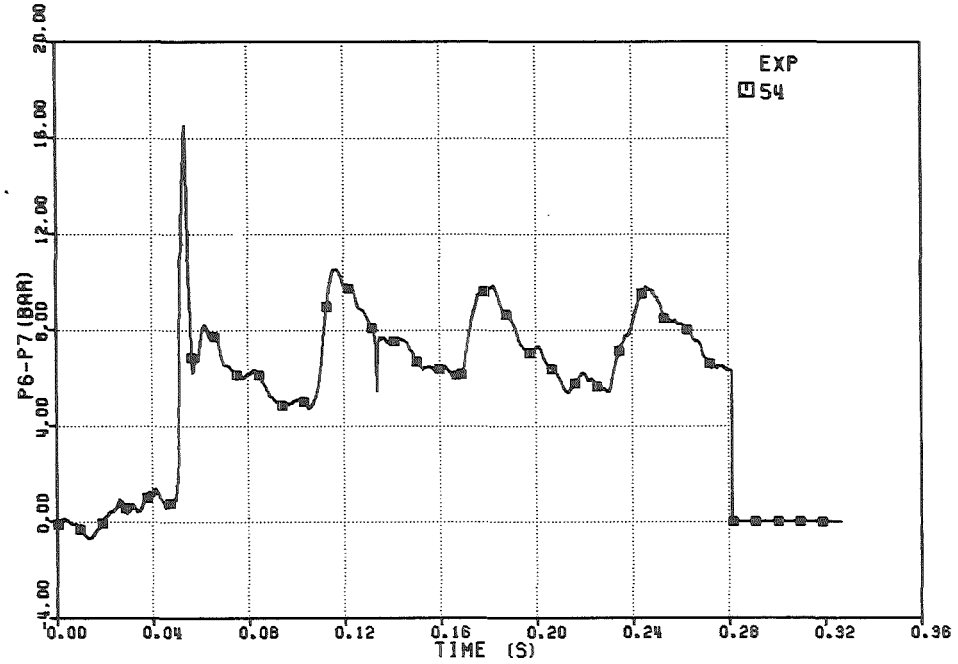

FIG. 6.149 -PRESSURE DROP THROUGH THE DIP-PLATE

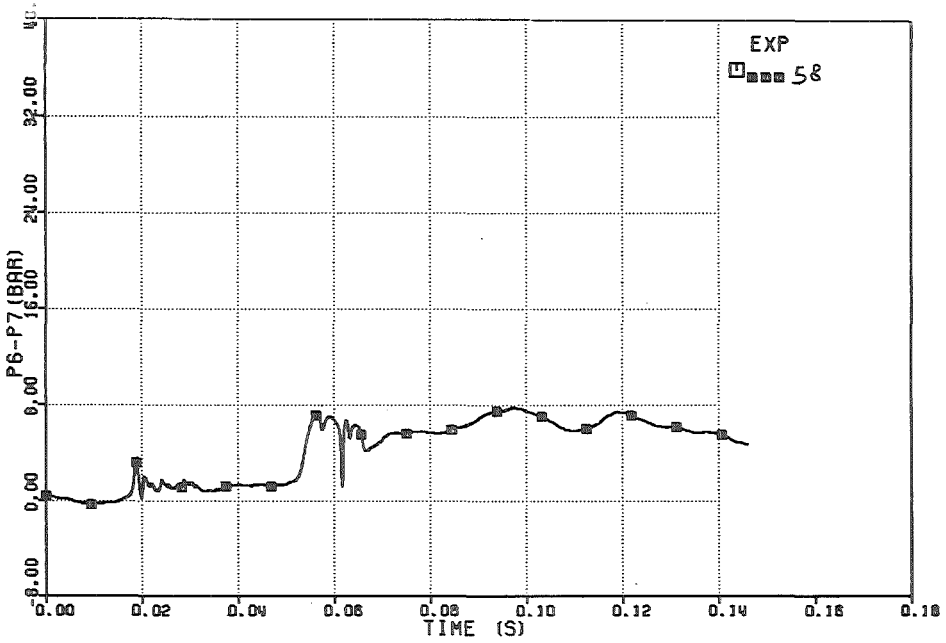

FIG. 6.152-PRESSURE DROP THROUGH THE DIP-PLATE

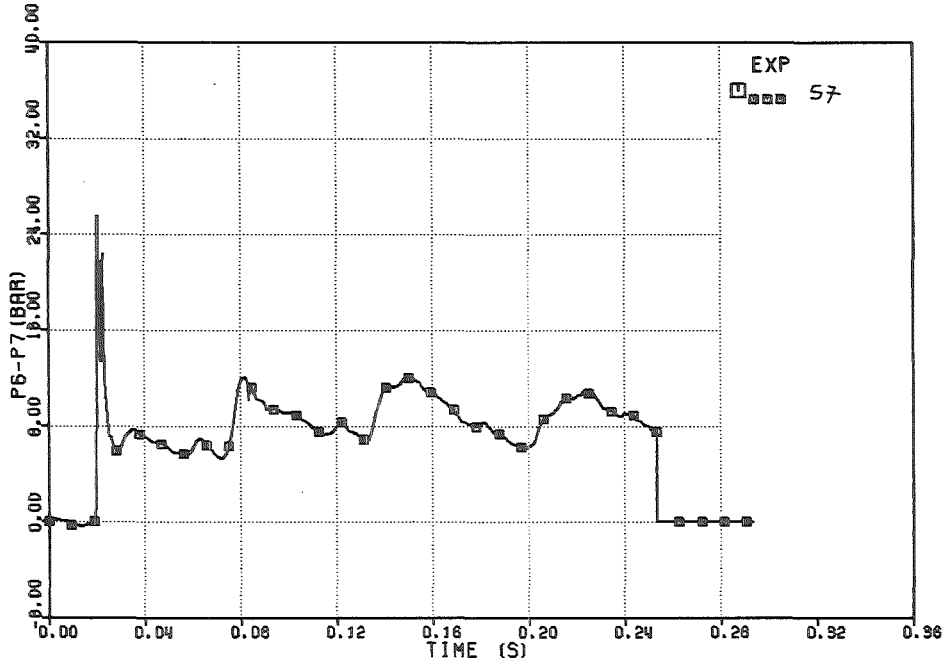

FIG. 6.151 -PRESSURE DROP THROUGH THE DIP-PLATE

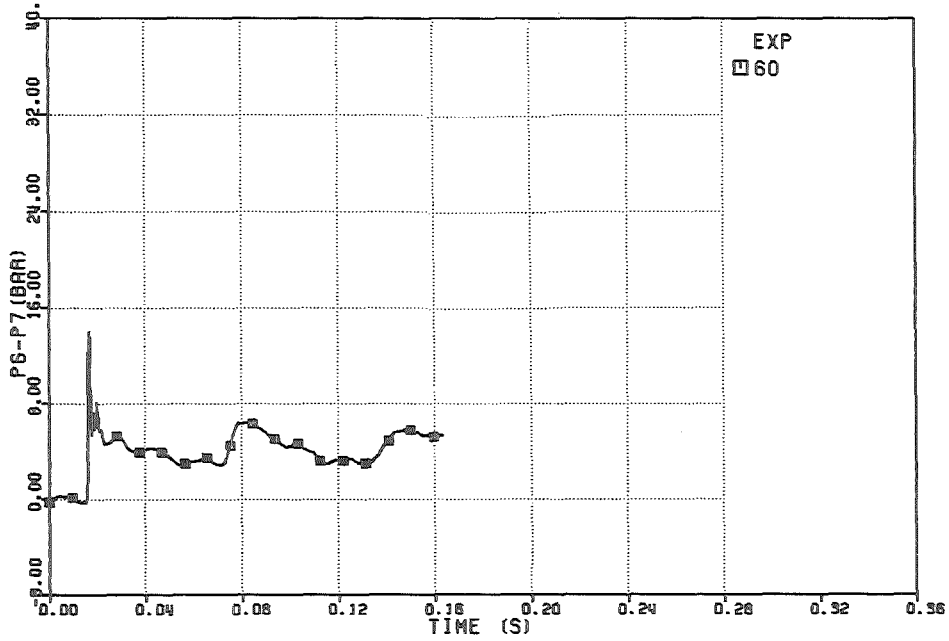

FIG. 6.154 -PRESSURE DROP THROUGH THE DIP-PLATE

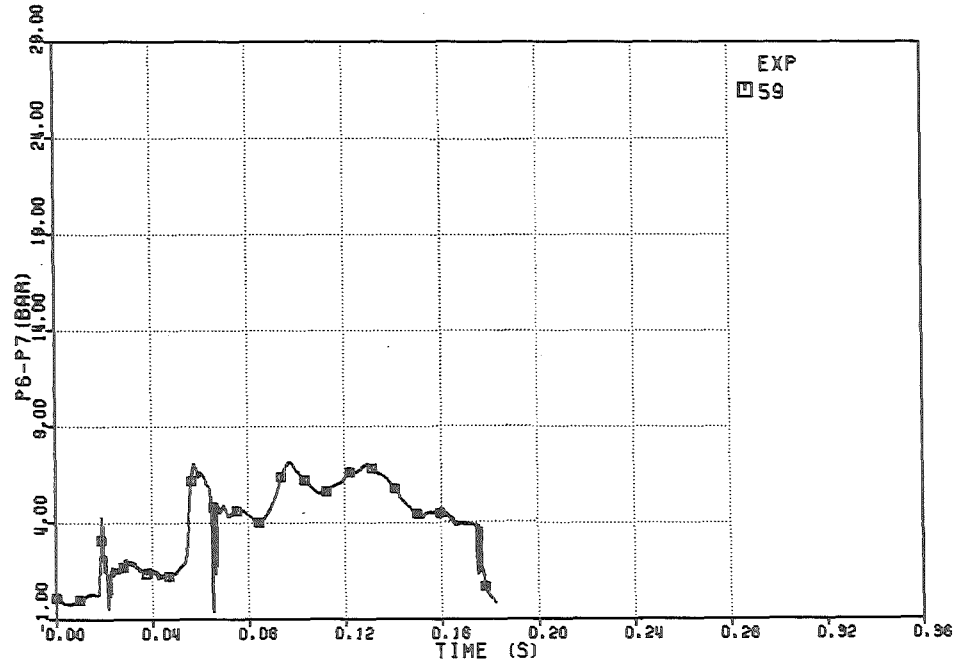

FIG. 6.153 -PRESSURE DROP THROUGH THE DIP-PLATE

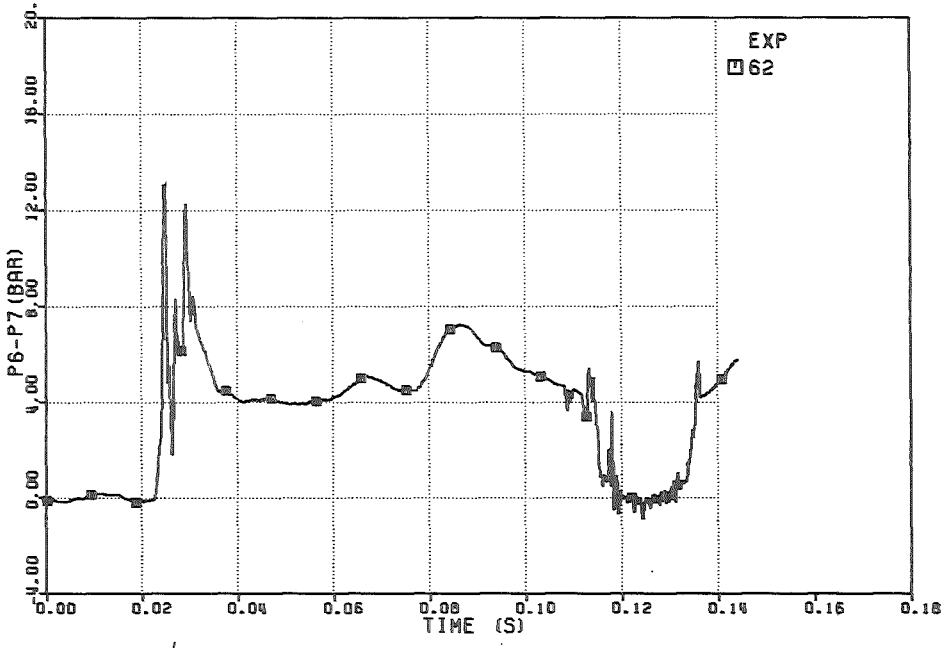

FIG. 6.156 PRESSURE DROP THROUGH THE DIP-PLATE

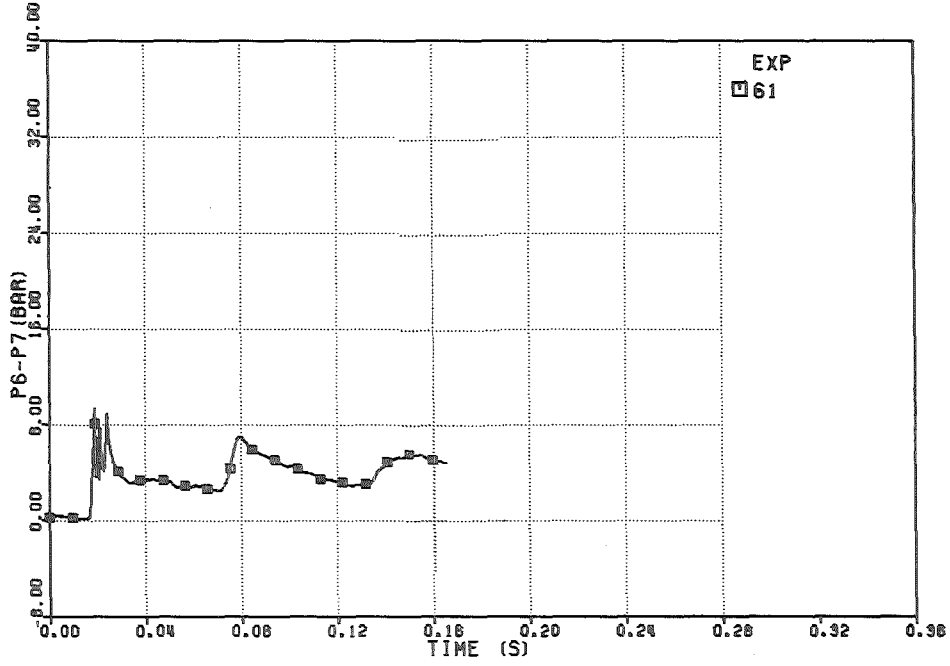

FIG. 6.155 -PRESSURE DROP THROUGH THE DIP-PLATE

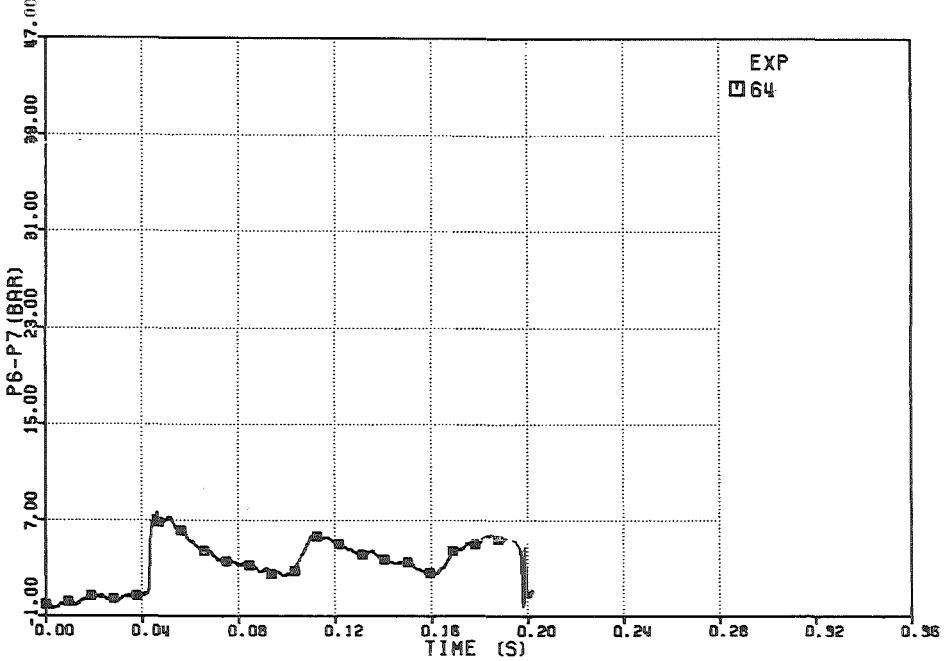

FIG. 6.158 -PRESSURE DROP THROUGH THE DIP-PLATE

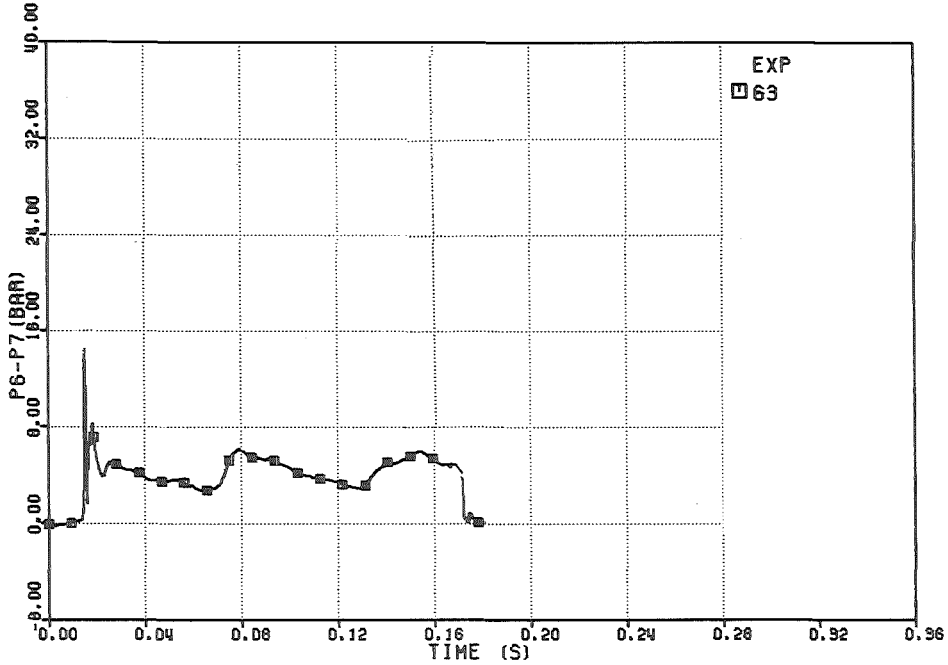

FIG. 6.157 -PRESSURE DROP THROUGH THE DIP-PLATE

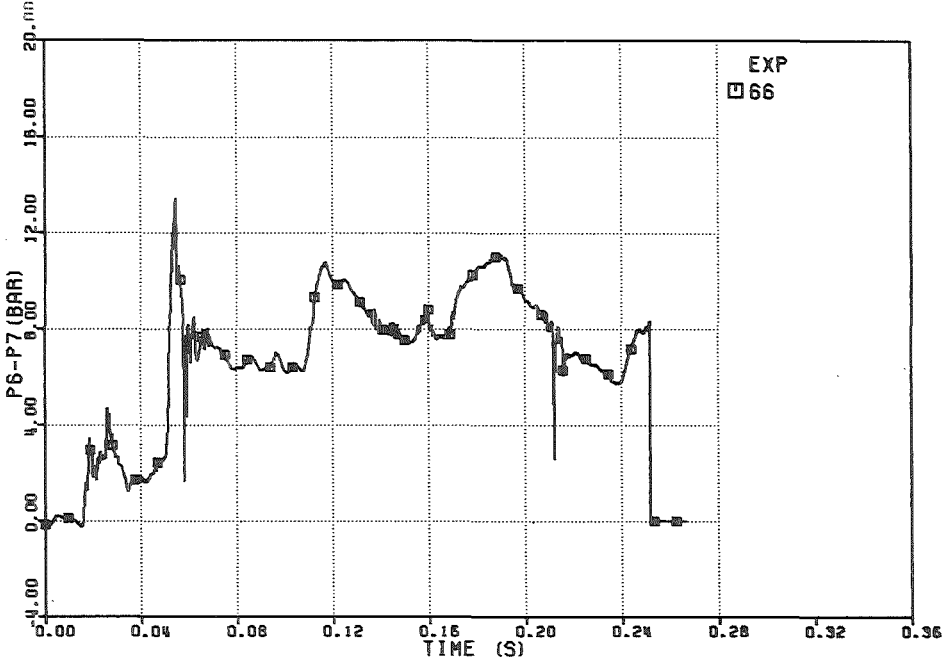

FIG. 6.160 -PRESSURE DROP THROUGH THE DIP-PLATE

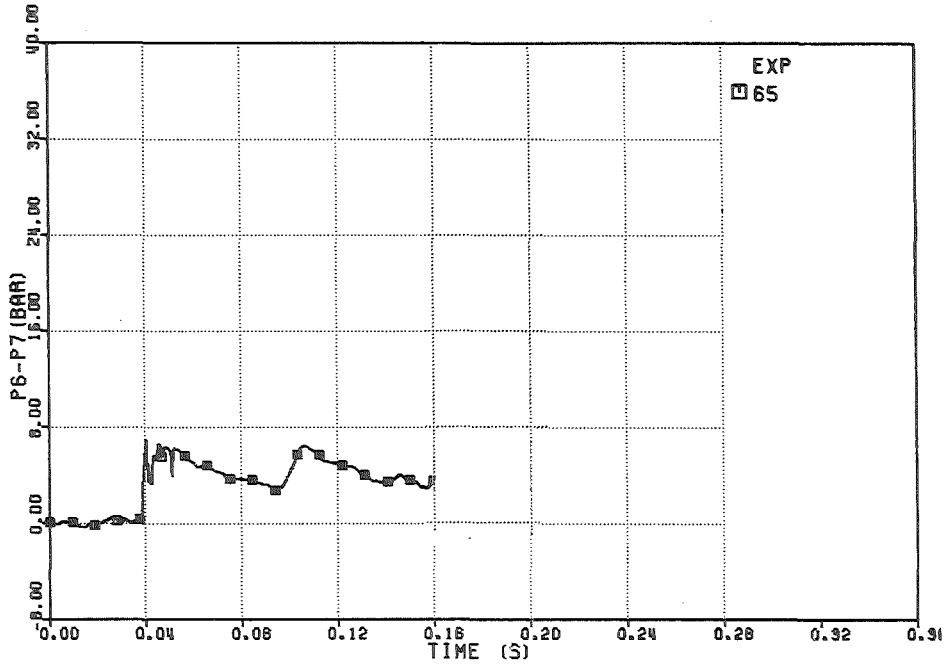

FIG. 6.159 -PRESSURE DROP THROUGH THE DIP-PLATE

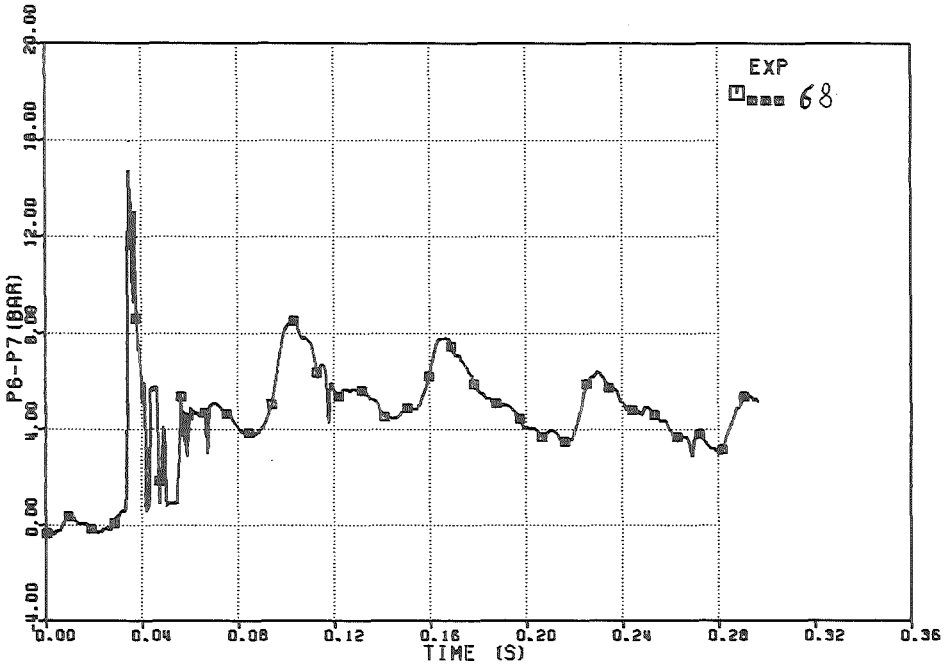

FIG. 6.162-PRESSURE DROP THROUGH THE DIP-PLATE

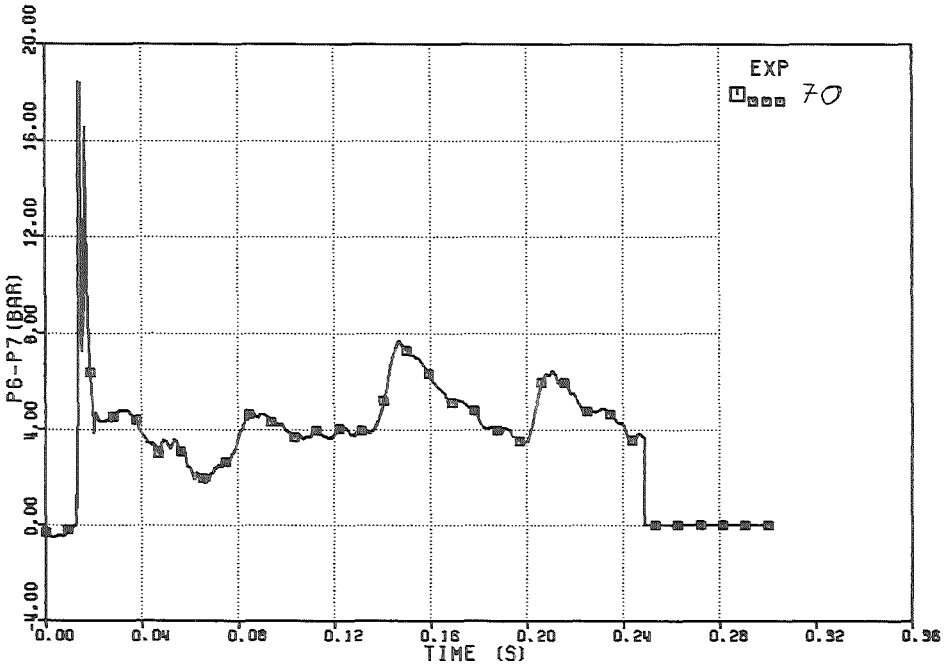

FIG. 6.164-PRESSURE DROP THROUGH THE DIP-PLATE

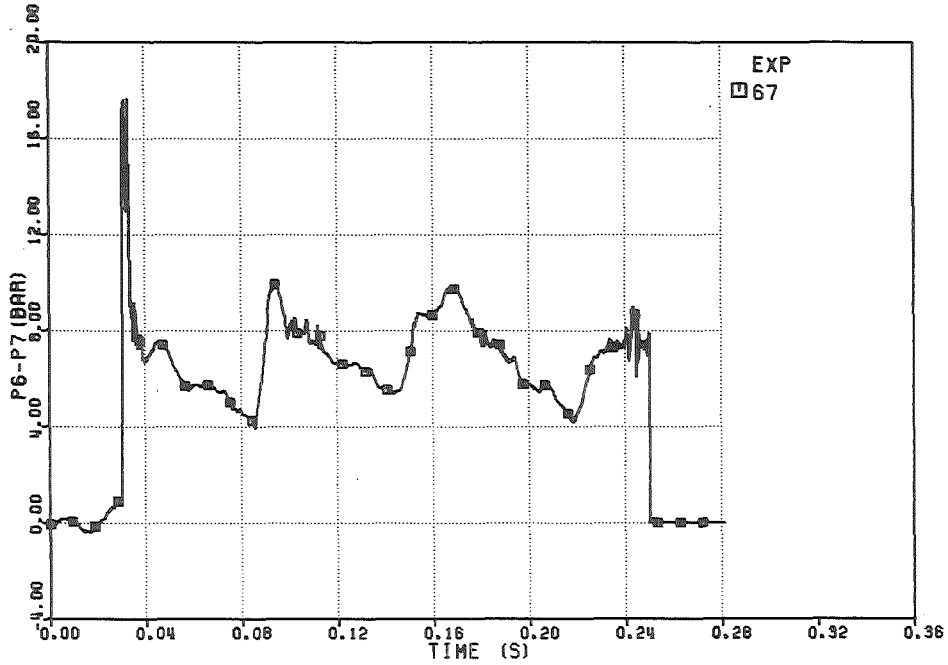

FIG. 6.161-PRESSURE DROP THROUGH THE DIP-PLATE

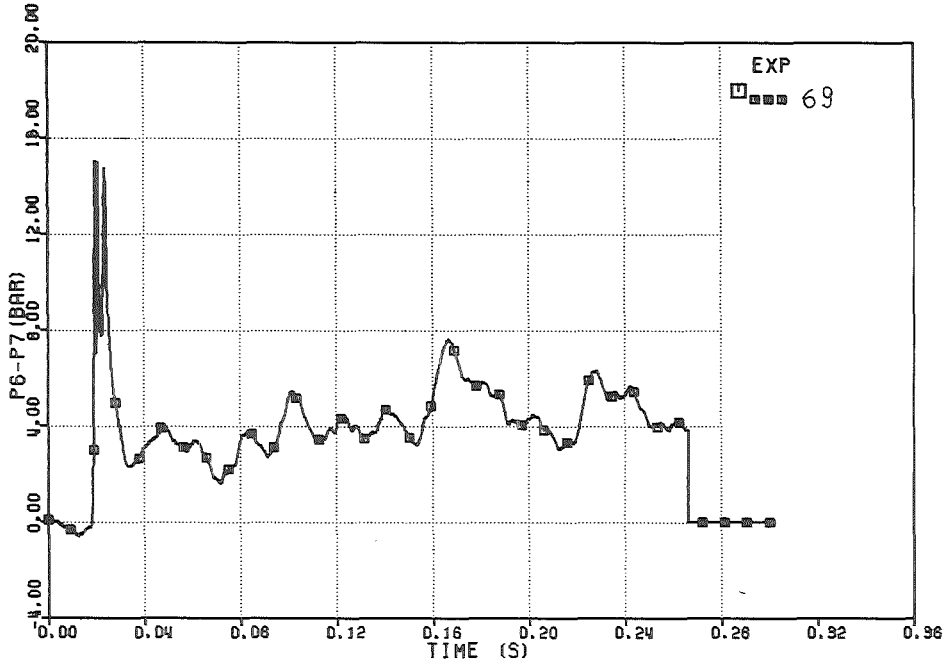

FIG. 6.163-PRESSURE DROP THROUGH THE DIP-PLATE

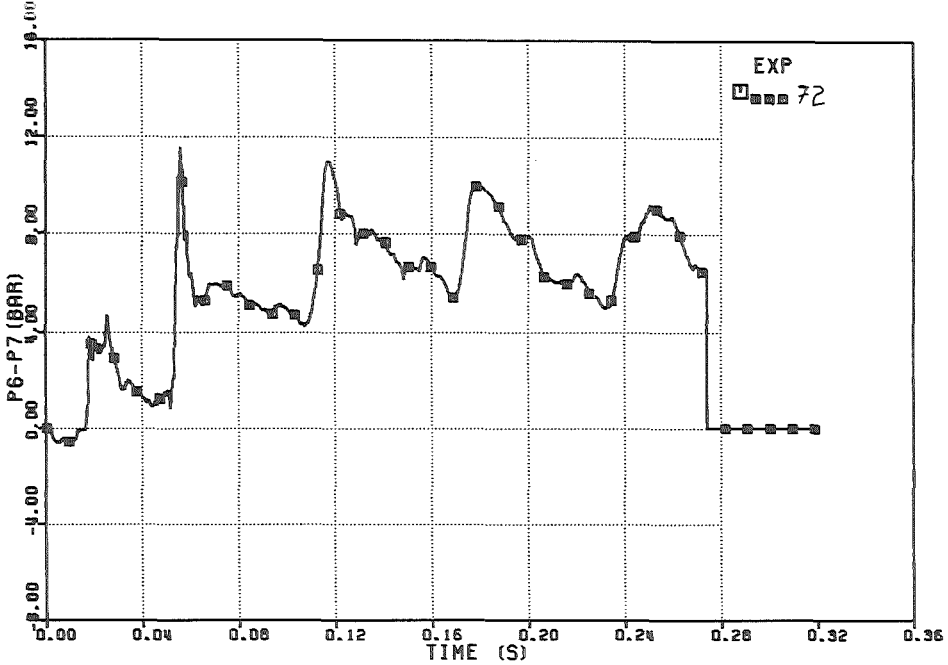

FIG. 6.166 -PRESSURE DROP THROUGH THE DIP-PLATE

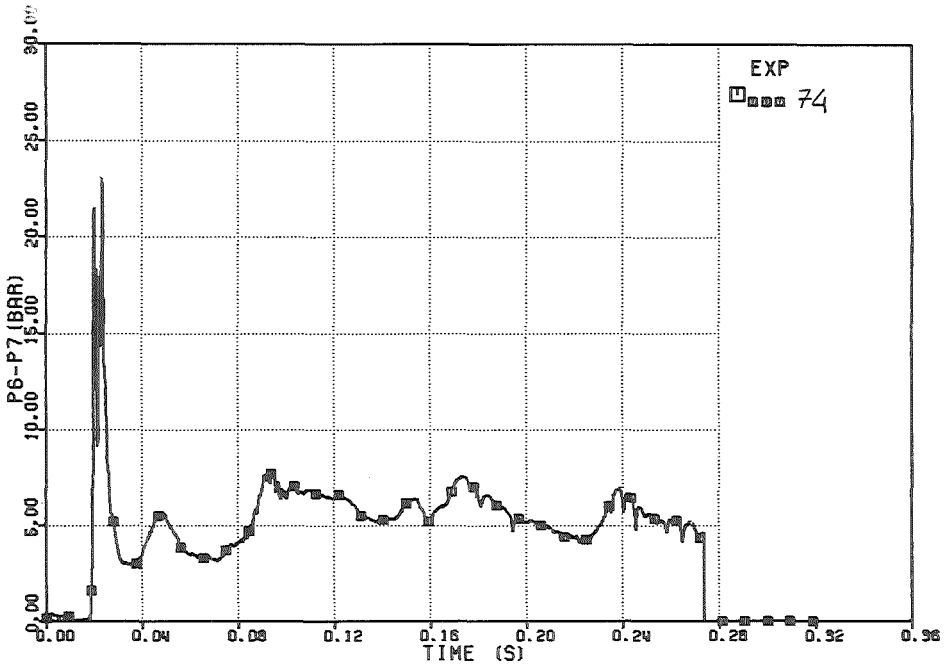

FIG. 6.168 -PRESSURE DROP THROUGH THE DIP-PLATE

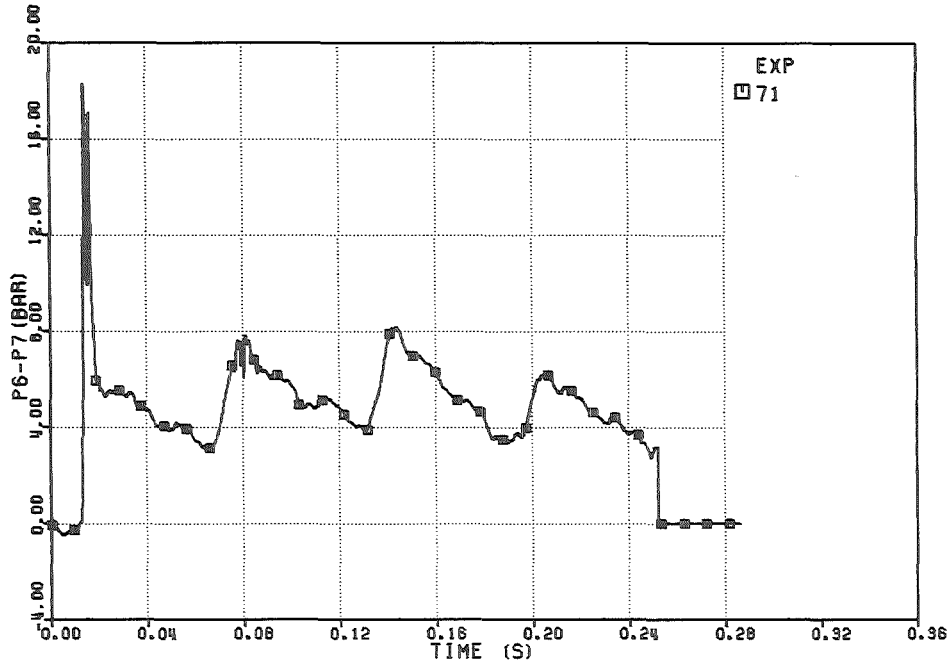

FIG. 6.165 -PRESSURE DROP THROUGH THE DIP-PLATE

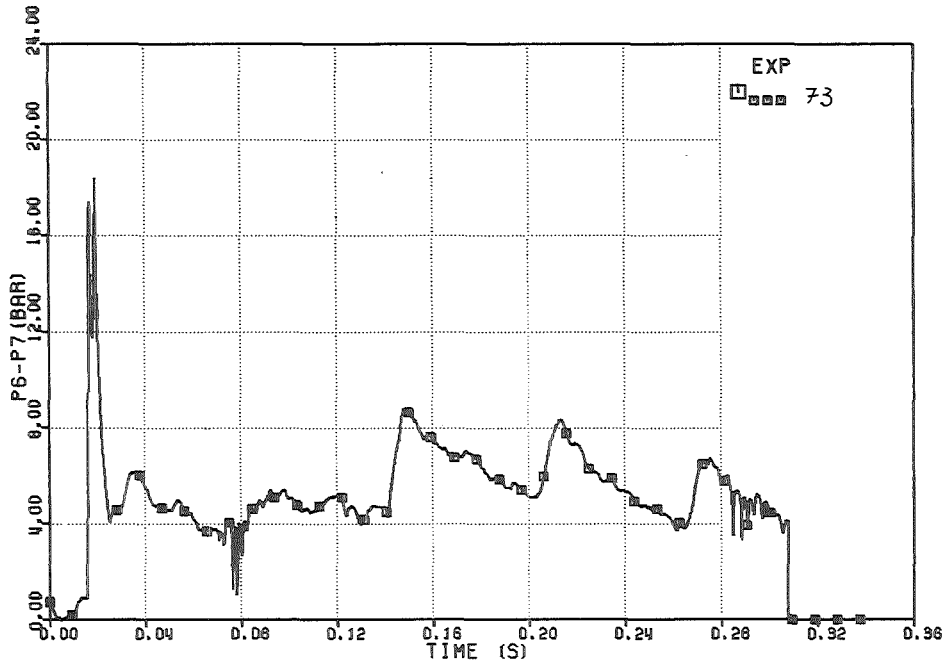

FIG. 6.167 -PRESSURE DROP THROUGH THE DIP-PLATE

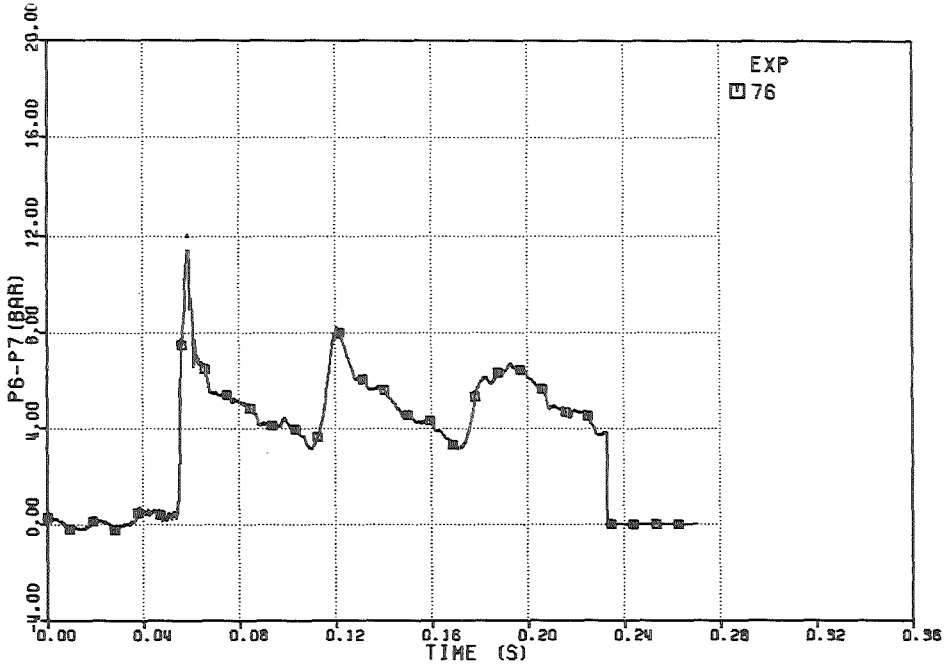

FIG. 6.170 -PRESSURE DROP THROUGH THE DIP-PLATE

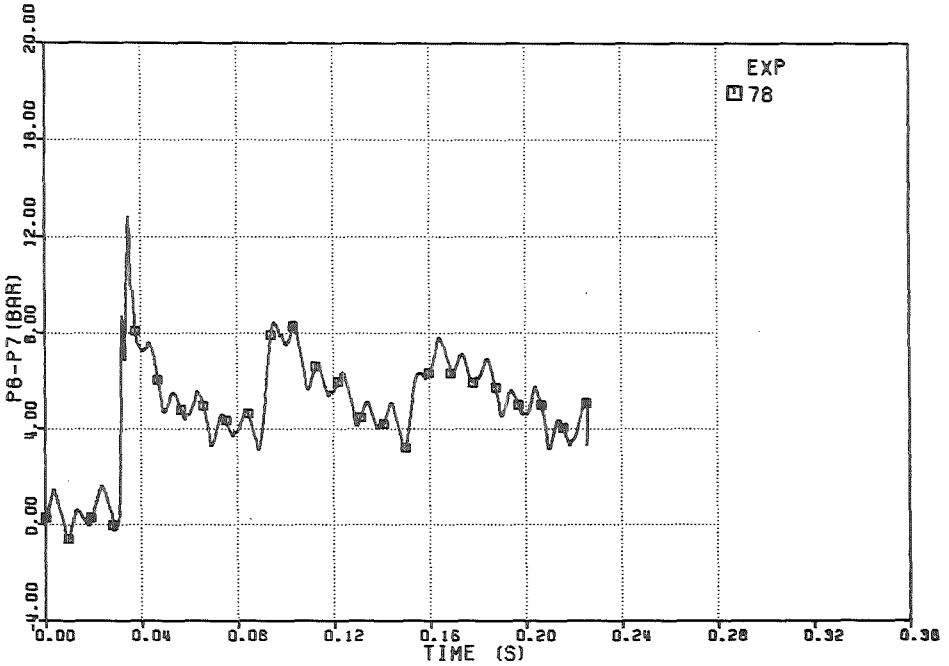

FIG. 6.172 -PRESSURE DROP THROUGH THE DIP-PLATE

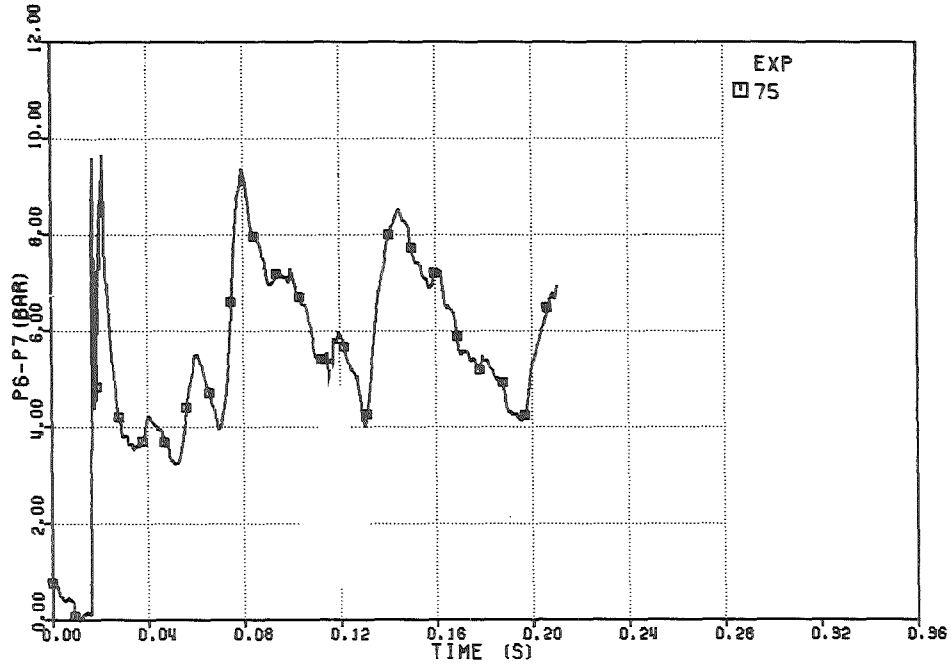

FIG. 6.169 -PRESSURE DROP THROUGH THE DIP-PLATE

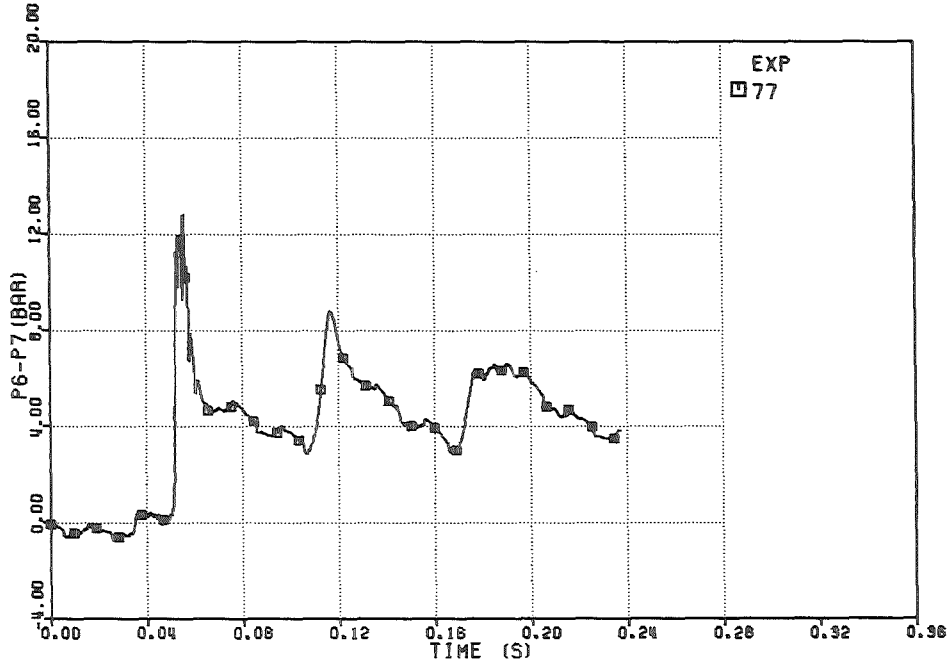

FIG. 6.171 -PRESSURE DROP THROUGH THE DIP-PLATE

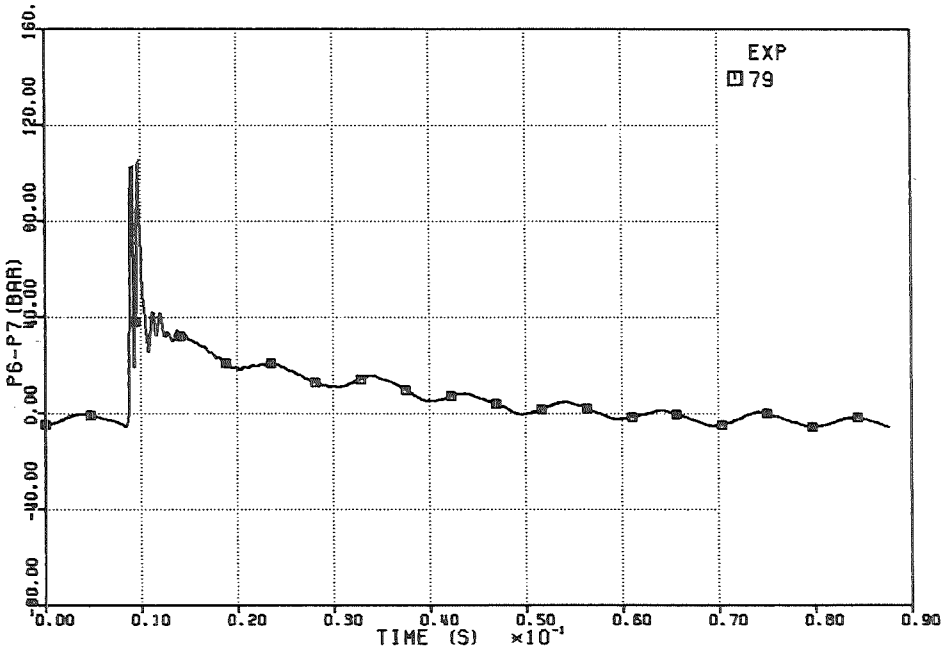

FIG. 6.173 -PRESSURE DROP THROUGH THE DIP-PLATE

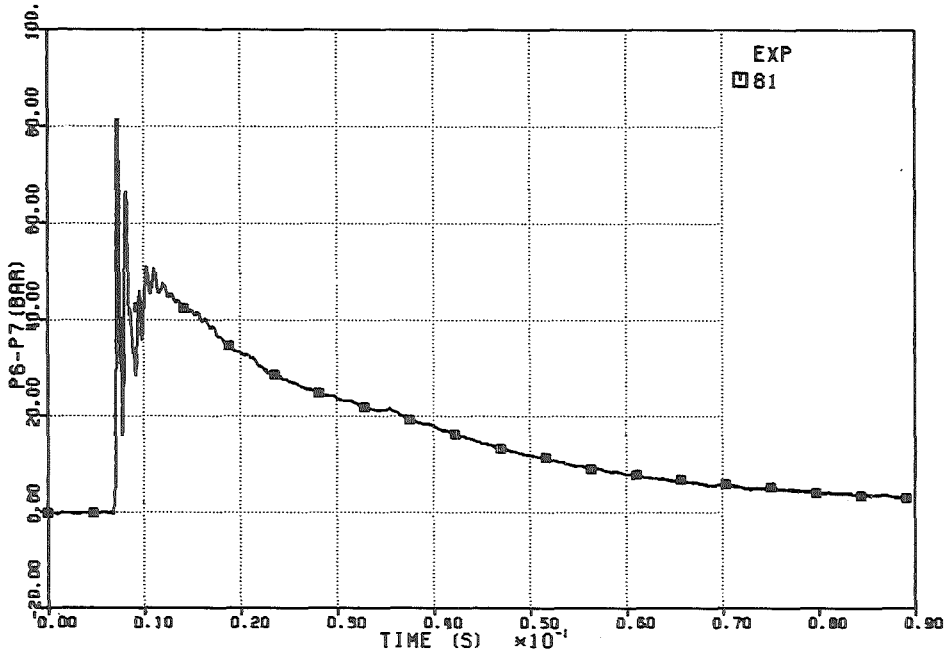

FIG. 6.175 -PRESSURE DROP THROUGH THE DIP-PLATE

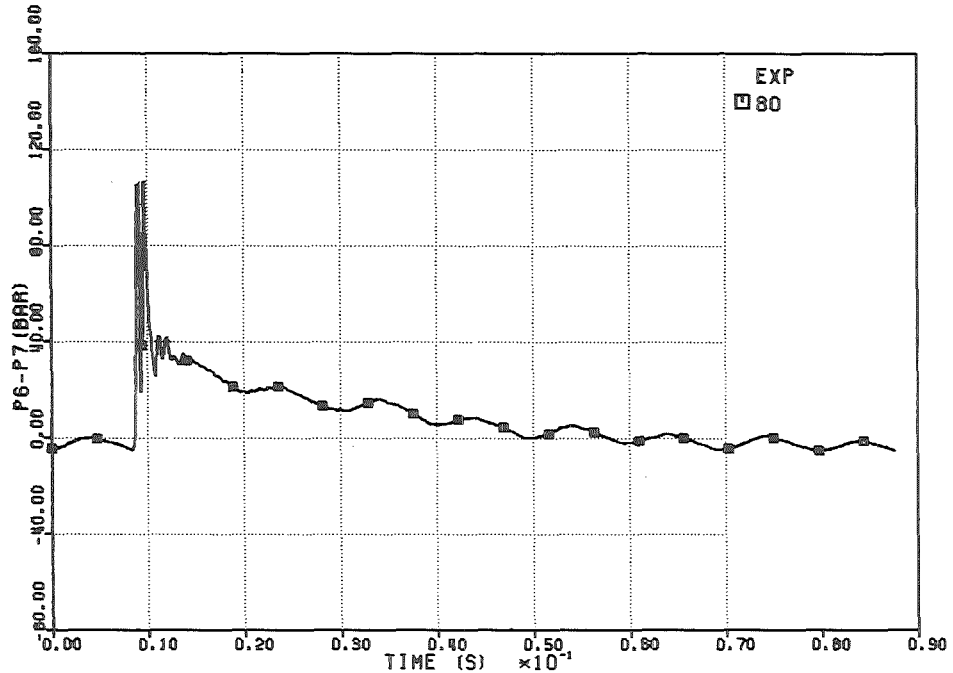

FIG. 6.174 -PRESSURE DROP THROUGH THE DIP-PLATE

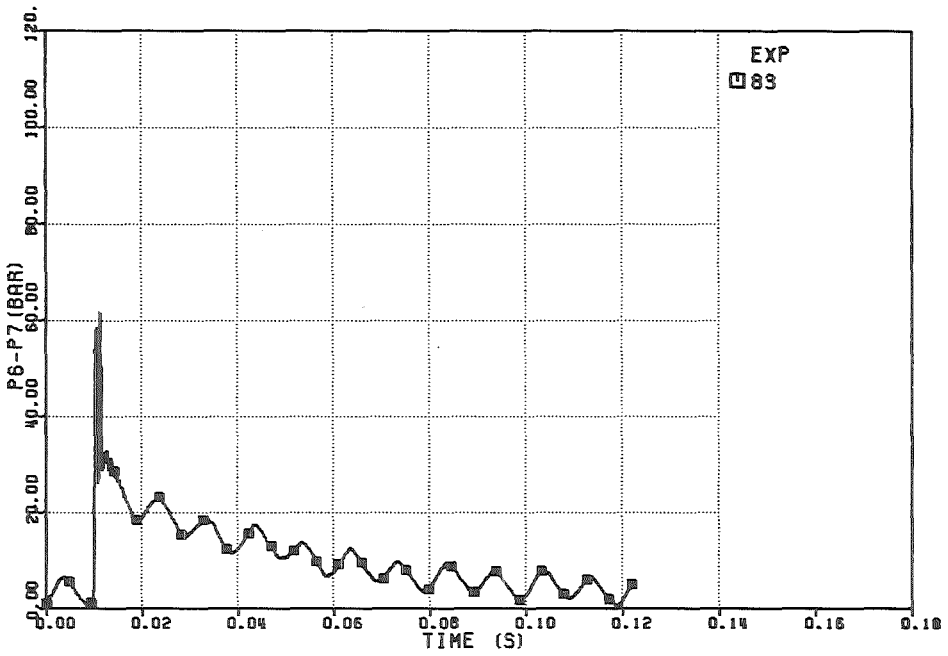

FIG. 6.177-PRESSURE DROP THROUGH THE DIP-PLATE

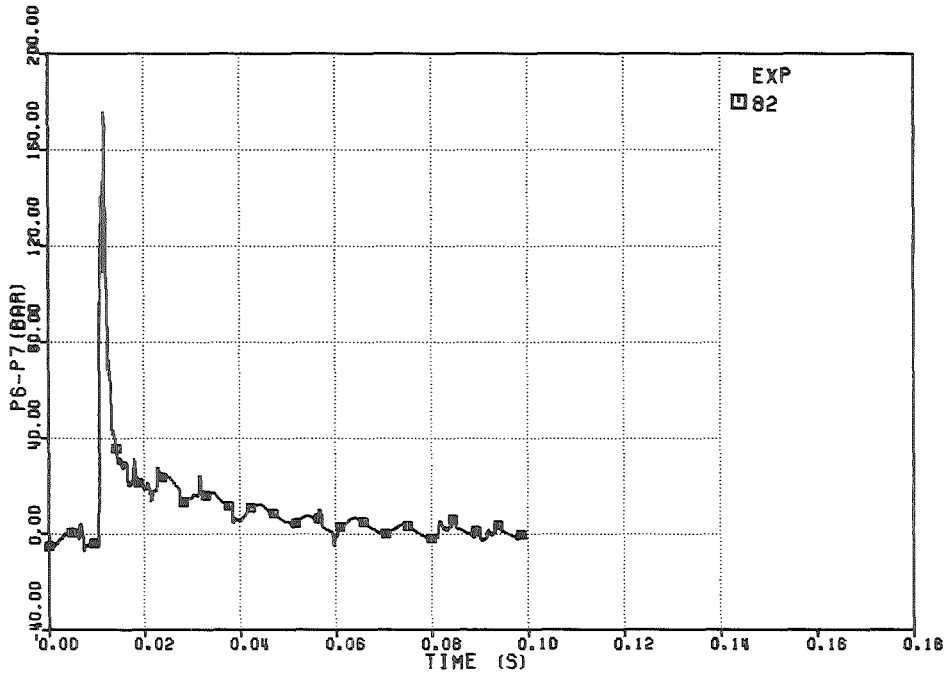

FIG. 6.176 -PRESSURE DROP THROUGH THE DIP-PLATE

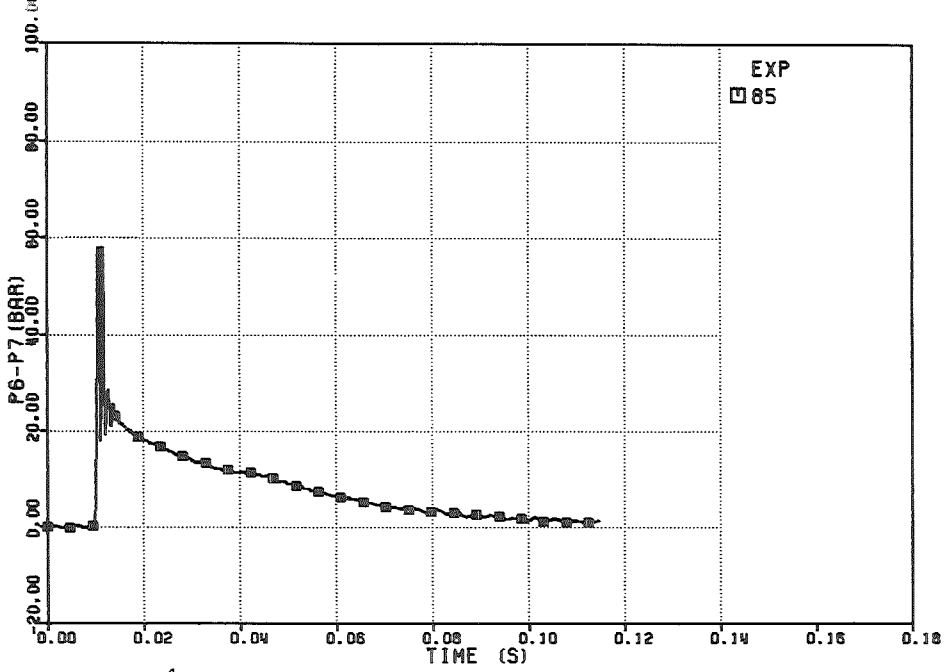

FIG. 6.179 -PRESSURE DROP THROUGH THE DIP-PLATE

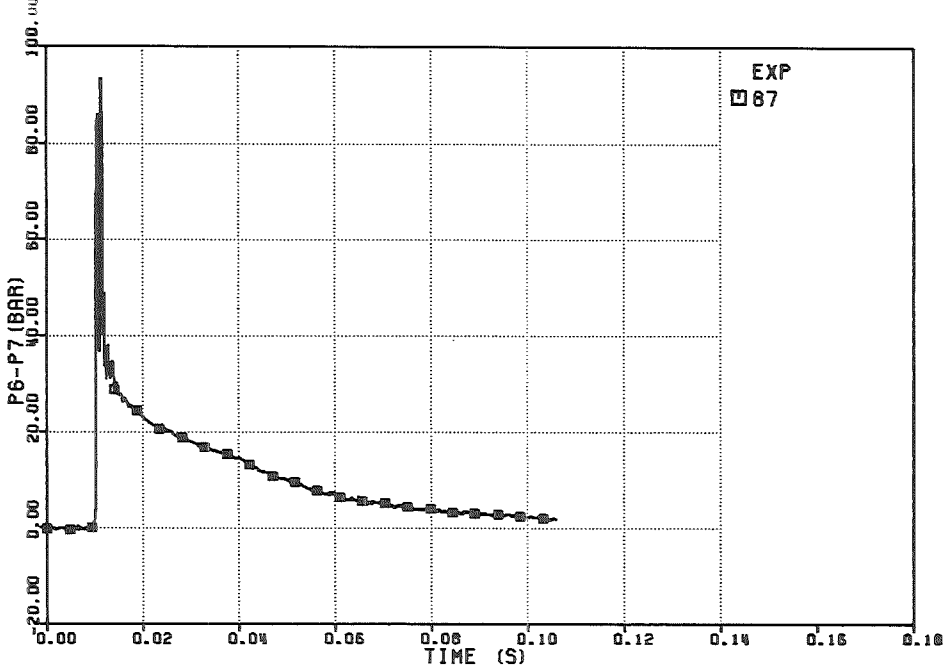

FIG. 6.181-PRESSURE DROP THROUGH THE DIP-PLATE

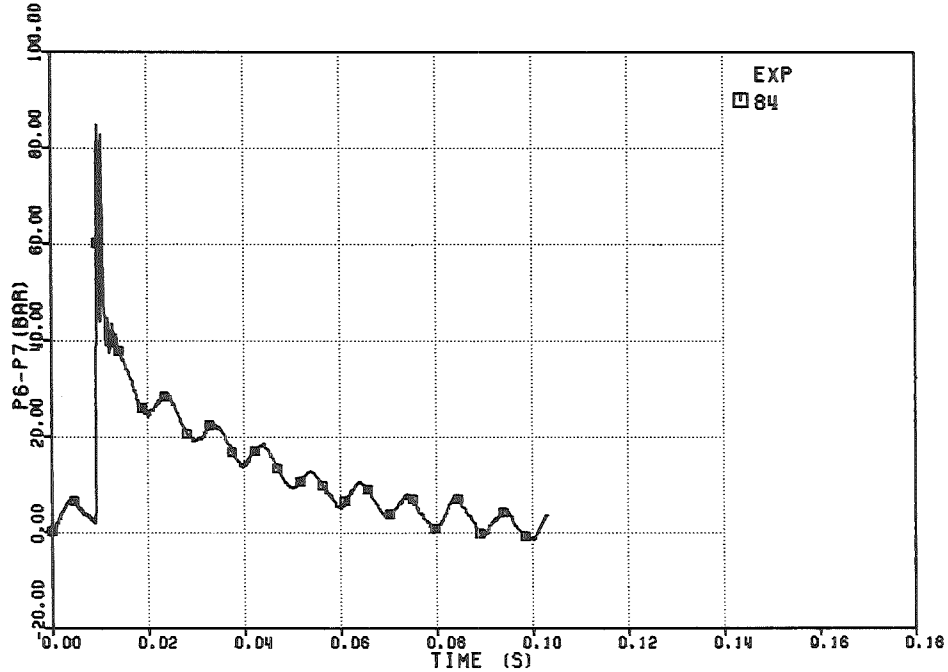

FIG. 6.178 -PRESSURE DROP THROUGH THE DIP-PLATE

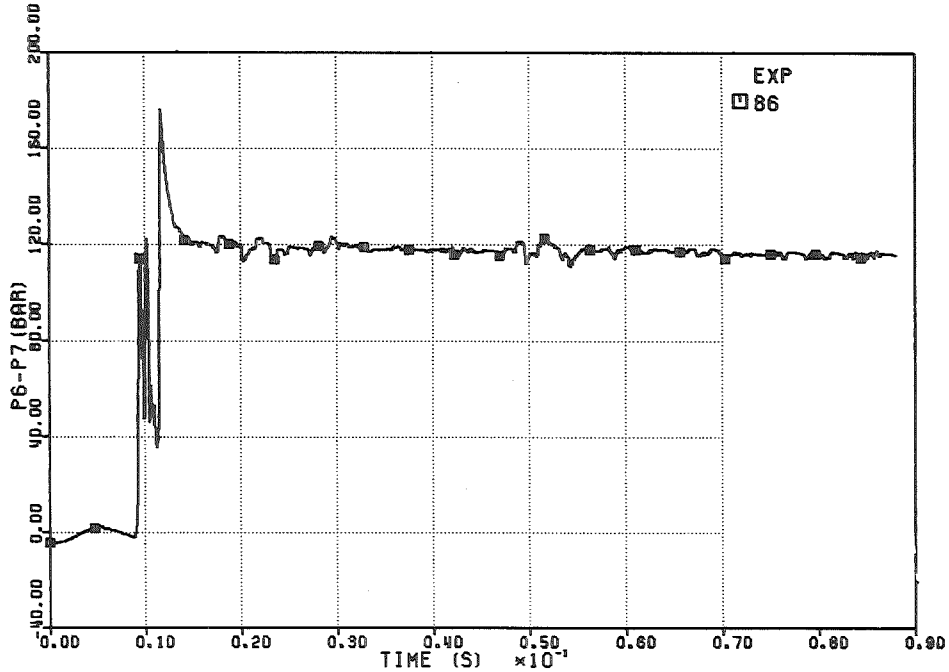

FIG. 6.180-PRESSURE DROP THROUGH THE DIP-PLATE

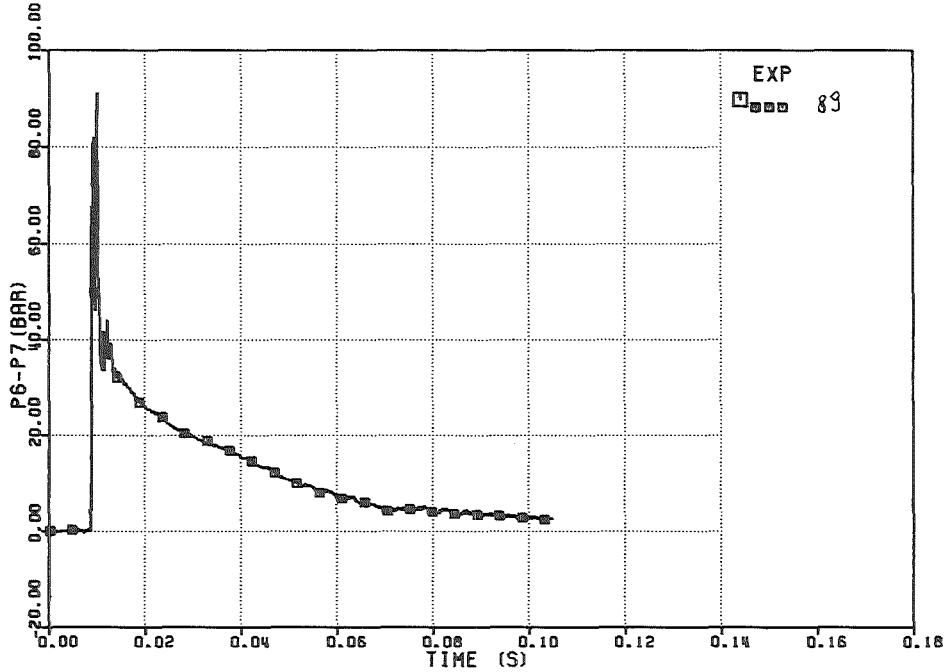

FIG. 6.183 -PRESSURE DROP THROUGH THE DIP-PLATE

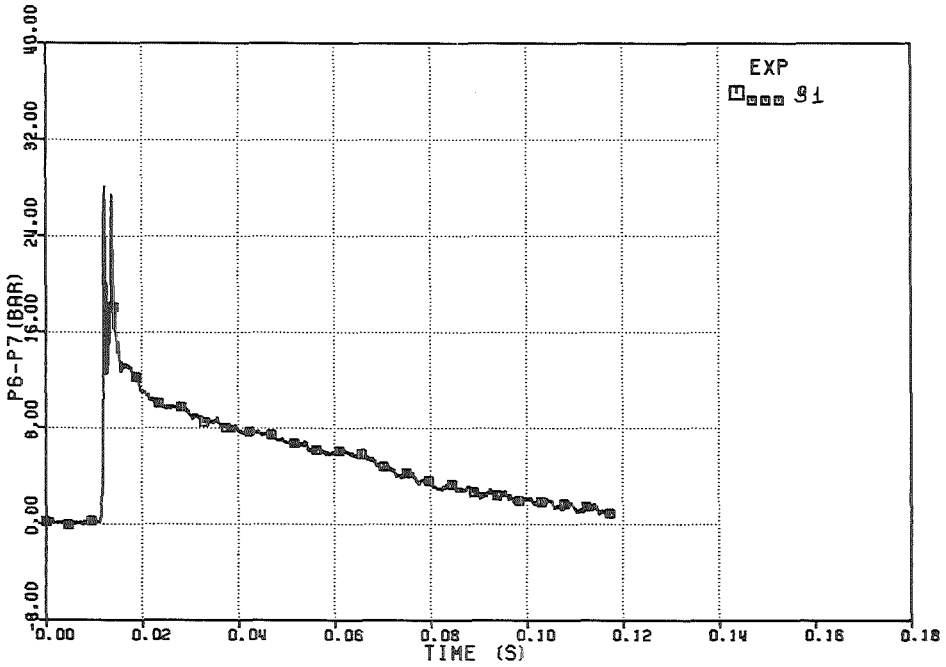

FIG. 6.185-PRESSURE DROP THROUGH THE DIP-PLATE

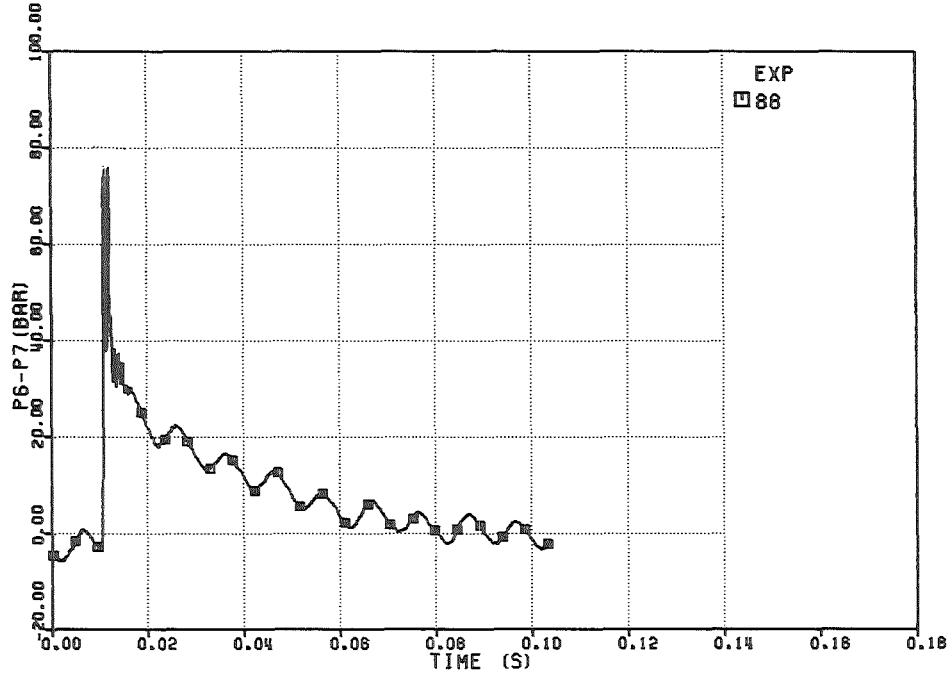

FIG. 6.182 -PRESSURE DROP THROUGH THE DIP-PLATE

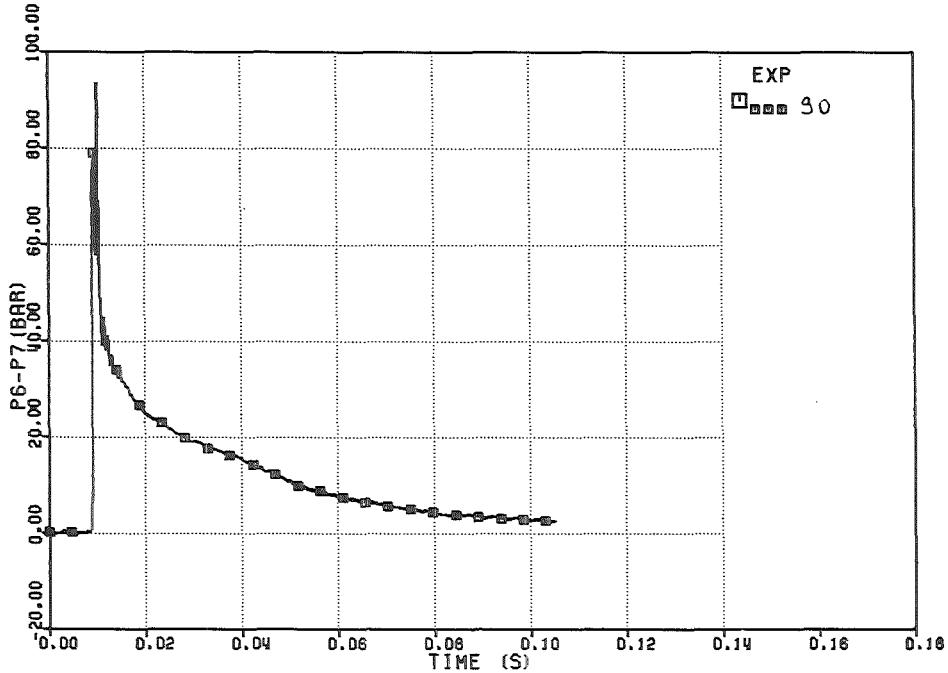

FIG. 6.184 -PRESSURE DROP THROUGH THE DIP-PLATE

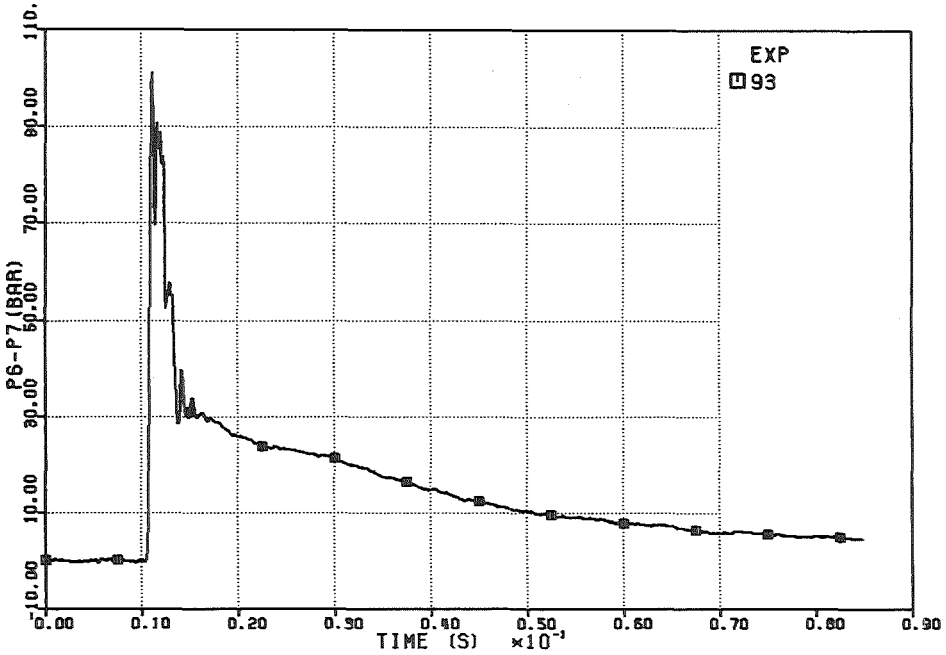

FIG. 6.187 -PRESSURE DROP THROUGH THE DIP-PLATE

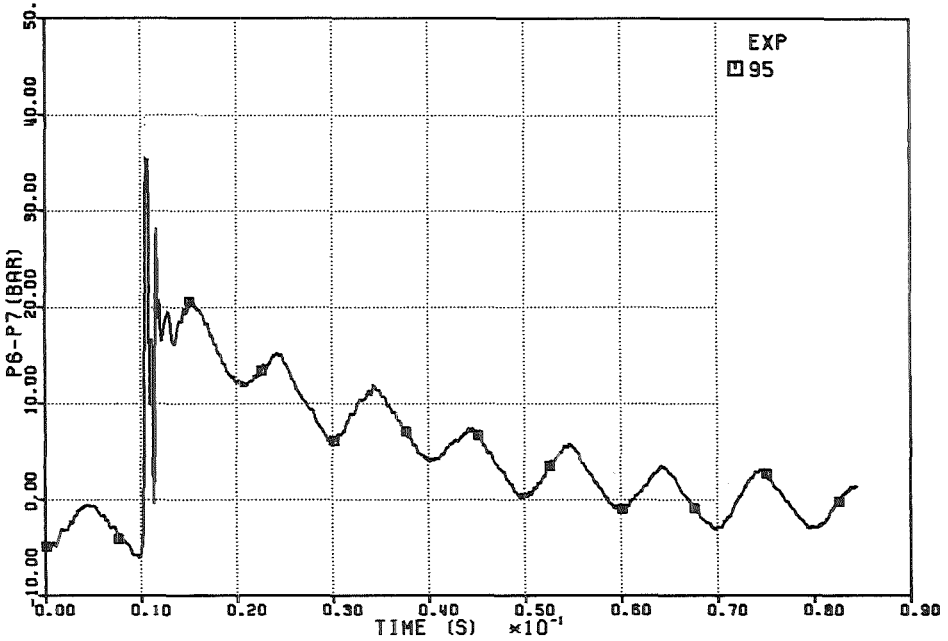

FIG. 6.189 -PRESSURE DROP THROUGH THE DIP-PLATE

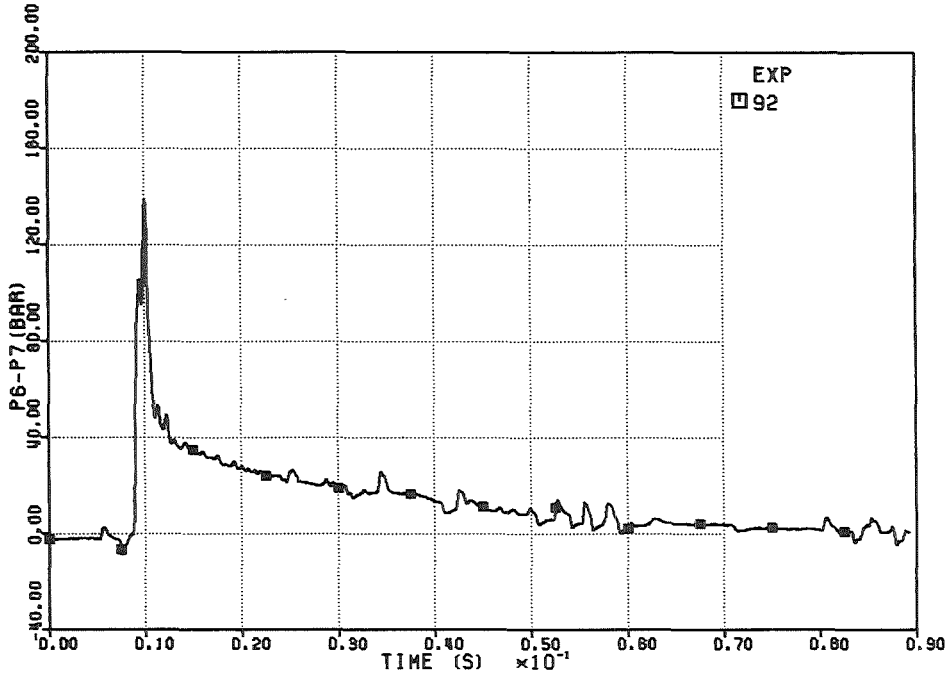

FIG. 6.186 -PRESSURE DROP THROUGH THE DIP-PLATE

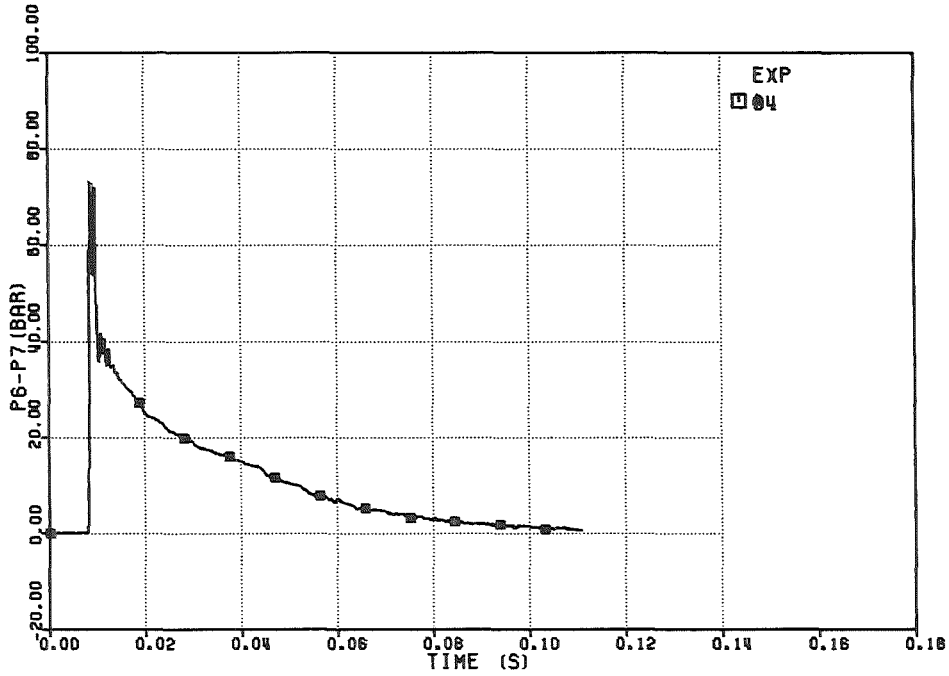

FIG. 6.188 -PRESSURE DROP THROUGH THE DIP-PLATE

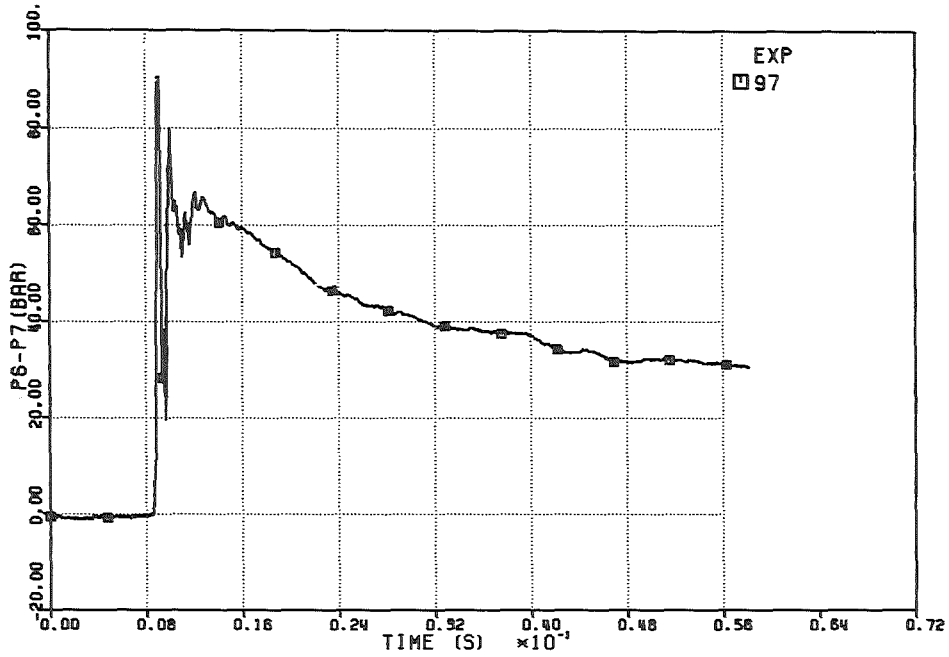

FIG. 6.191 -PRESSURE DROP THROUGH THE DIP-PLATE

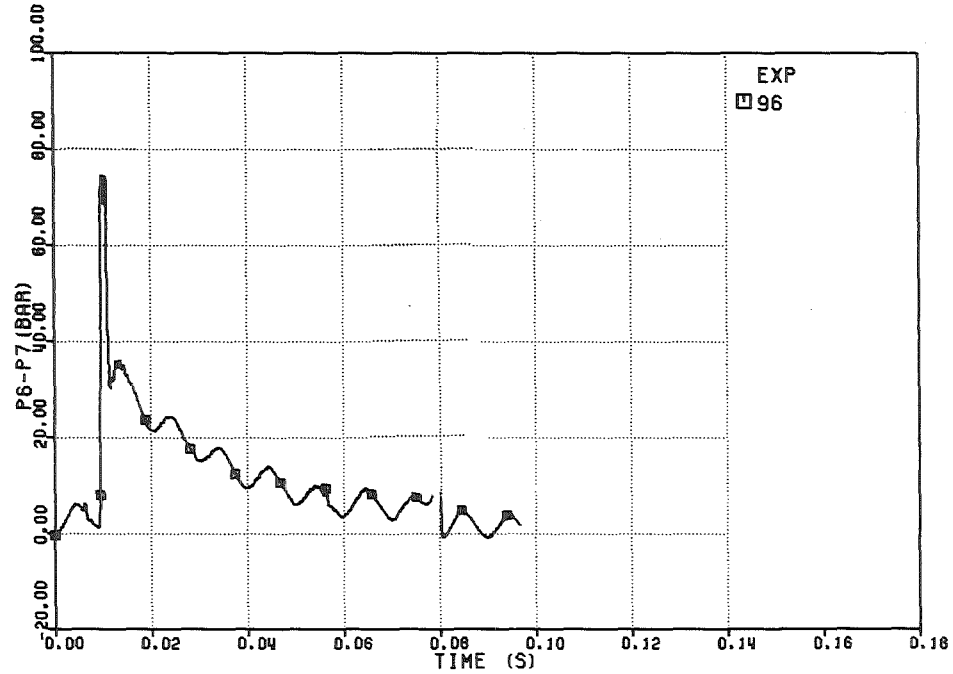

FIG. 6.190 -PRESSURE DROP THROUGH THE DIP-PLATE

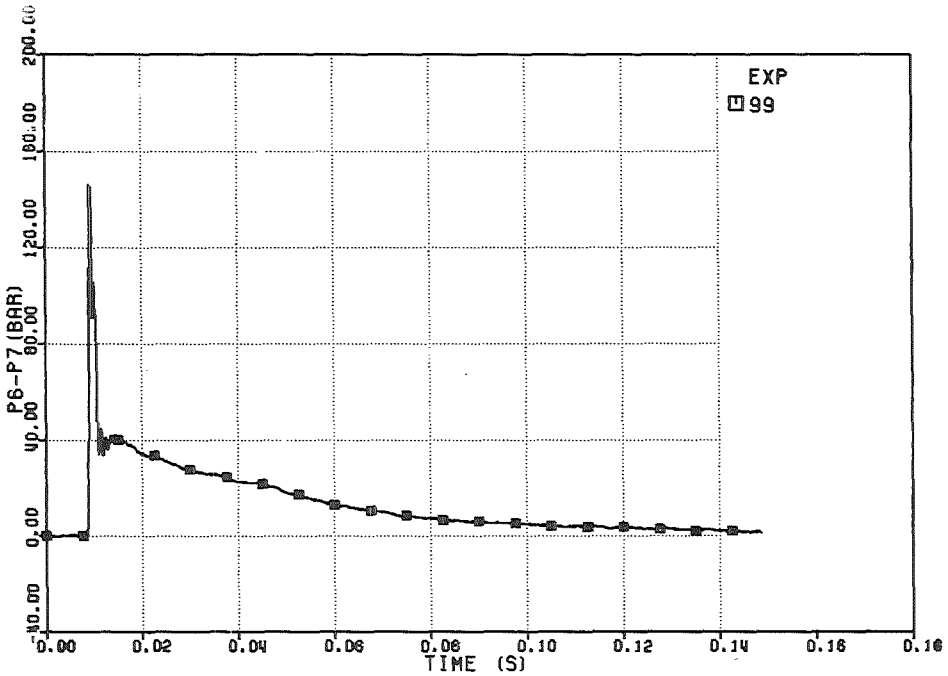

FIG. 6.193 -PRESSURE DROP THROUGH THE DIP-PLATE

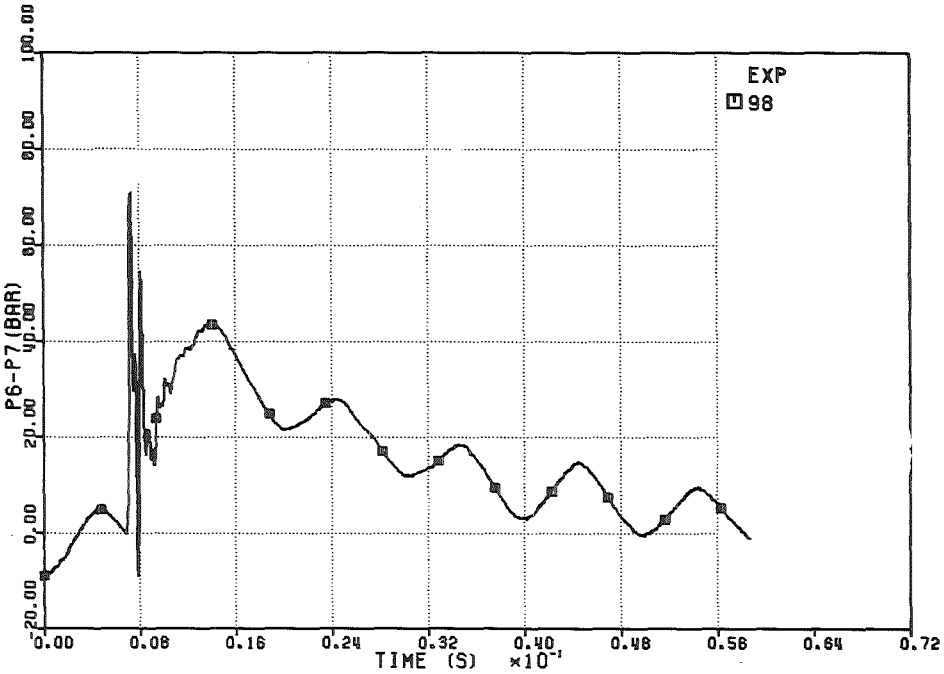

FIG. 6.192 -PRESSURE DROP THROUGH THE DIP-PLATE

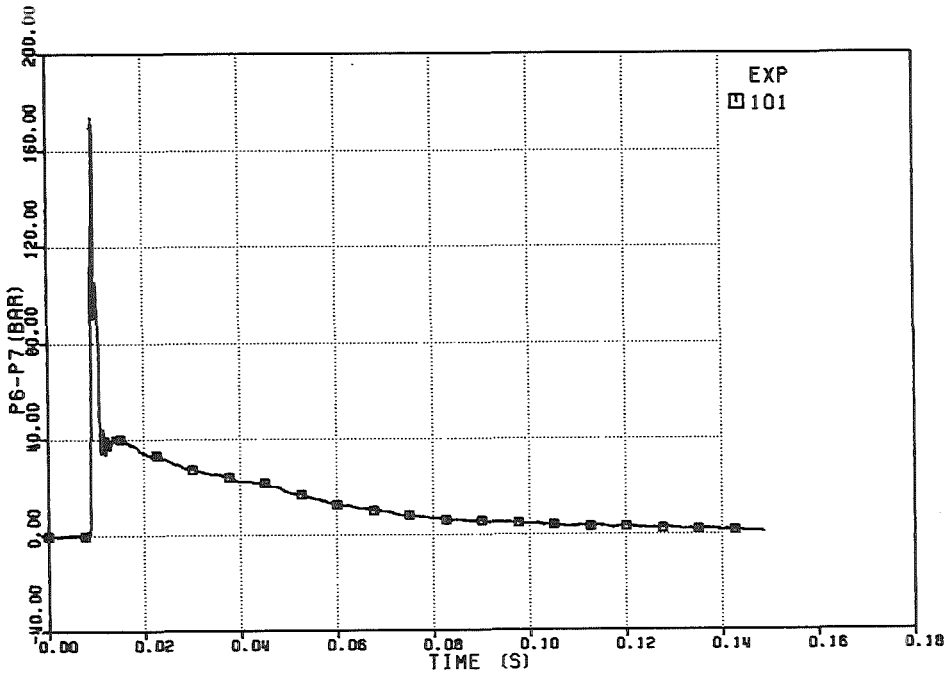

FIG. 6.195 -PRESSURE DROP THROUGH THE DIP-PLATE

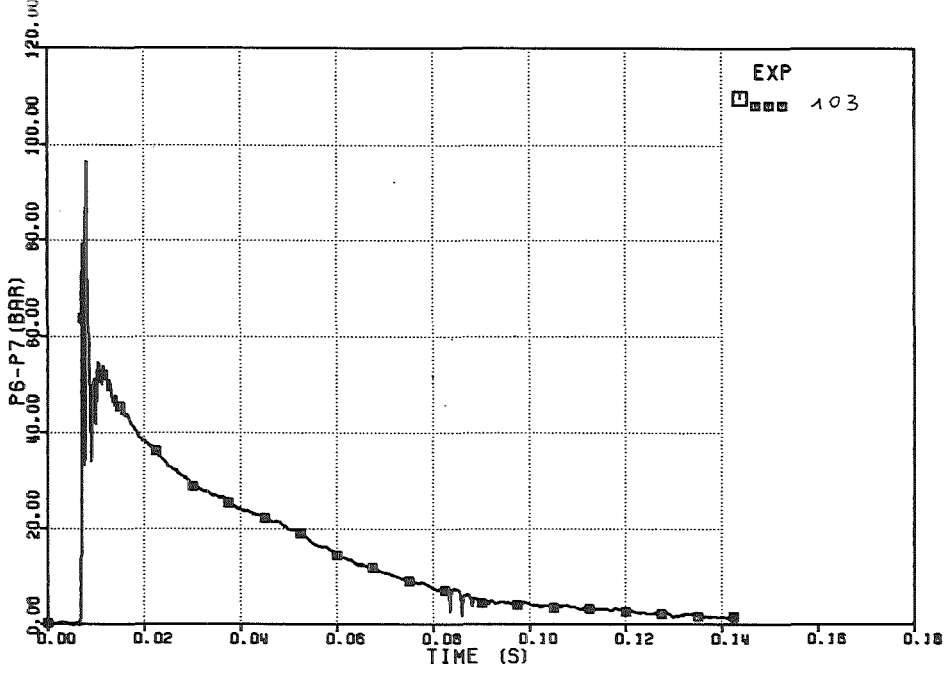

FIG. 6.197 -PRESSURE DROP THROUGH THE DIP-PLATE

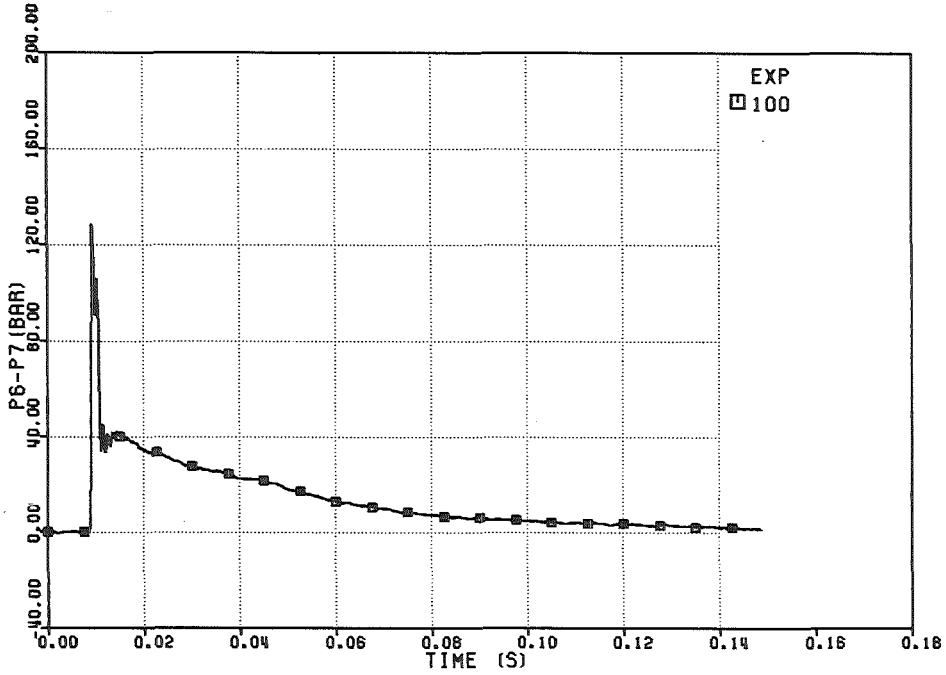

FIG. 6.194 -PRESSURE DROP THROUGH THE DIP-PLATE

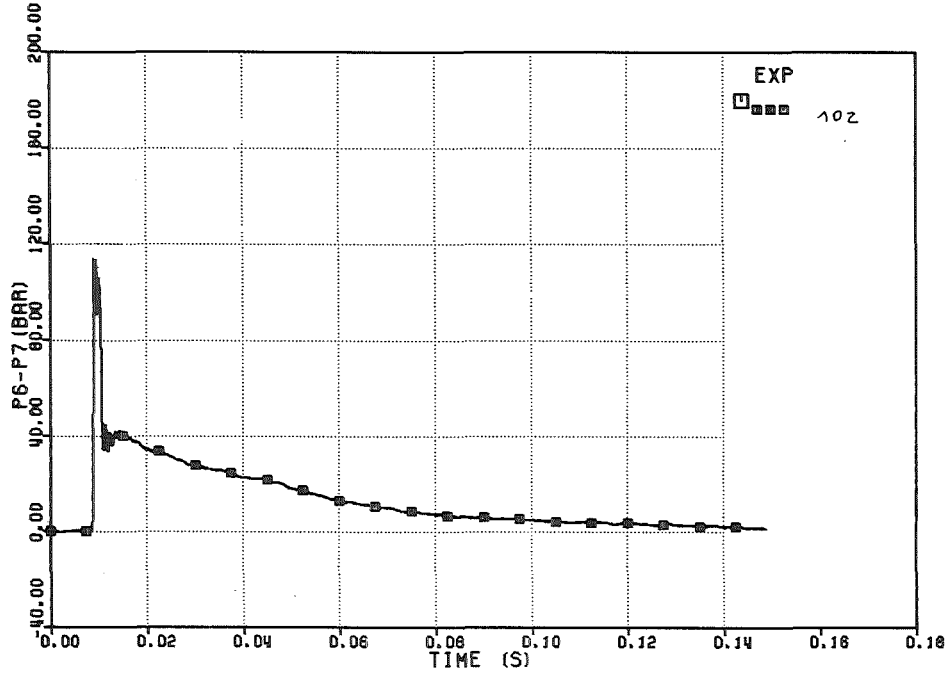

FIG. 6.196 -PRESSURE DROP THROUGH THE DIP-PLATE

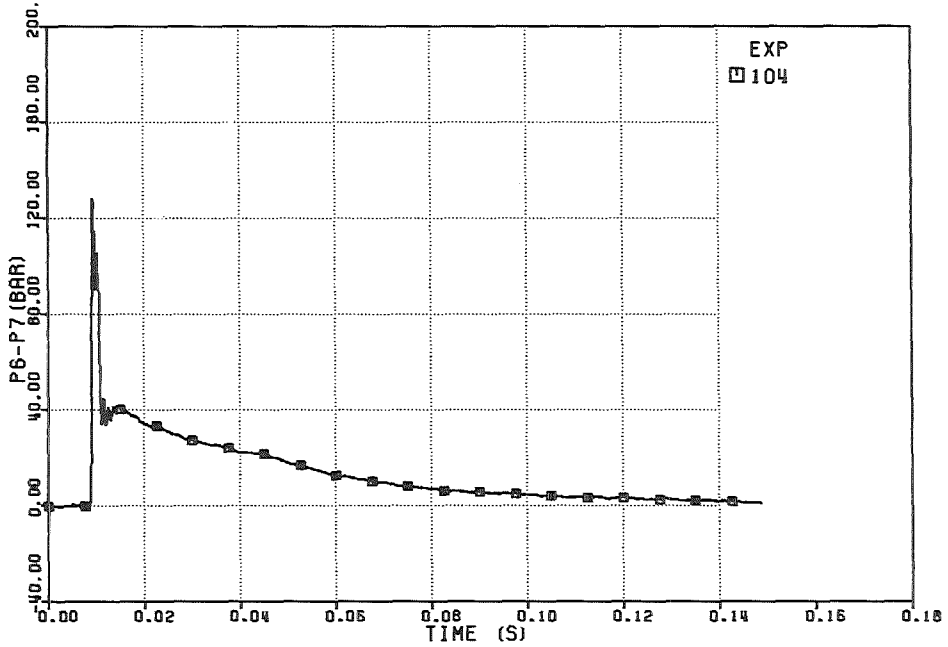

FIG. 6.197 b -PRESSURE DROP THROUGH THE DIP-PLATE

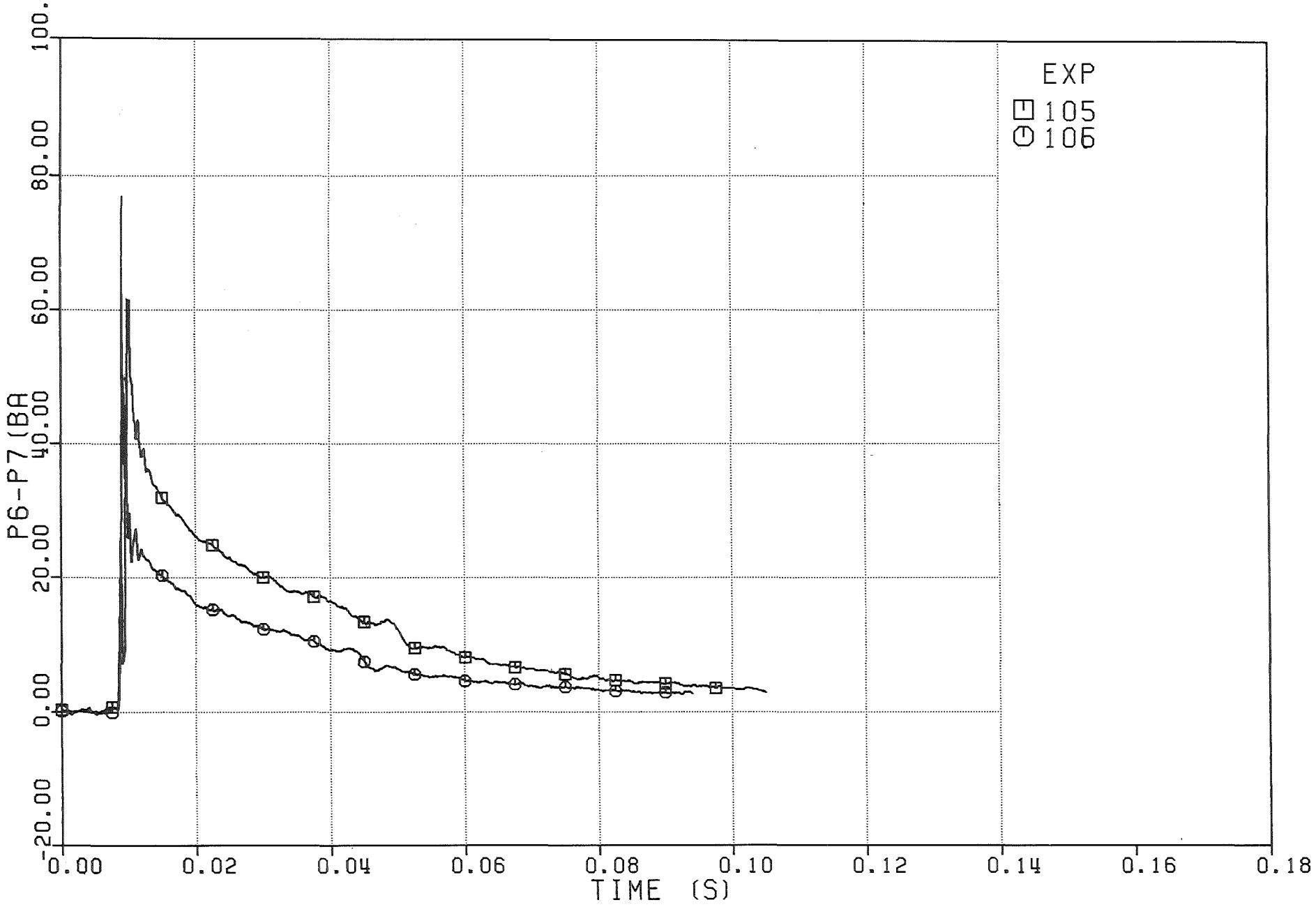

Fig. 6.198 - PRESSURE DROP THROUGH THE DIP-PLATE

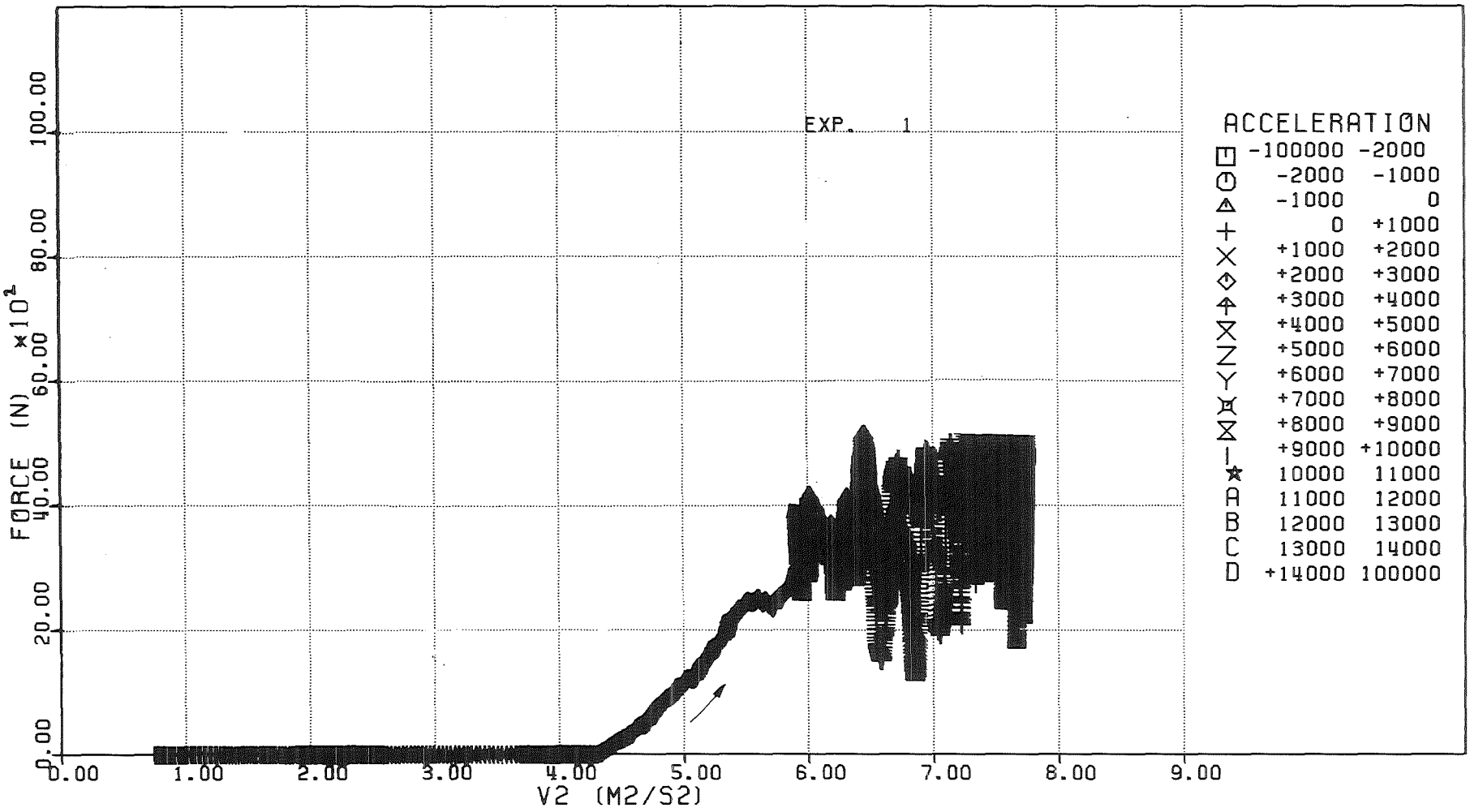

FIG. 6.199 - FORCE ACTING ON THE DIP-PLATE VERSUS THE SQUARE OF THE PISTON VELOCITY

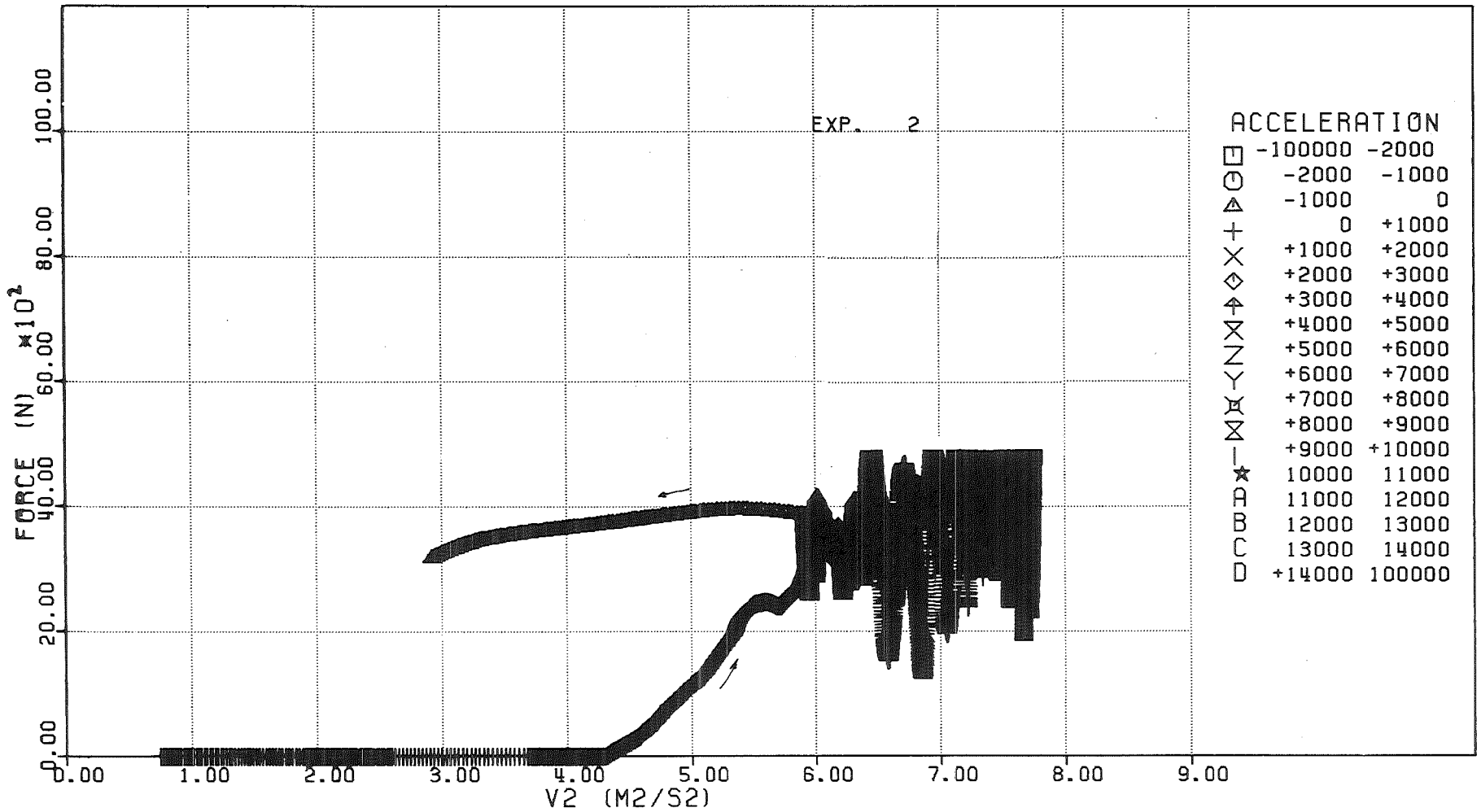

FIG. 6.200 - FORCE ACTING ON THE DIP-PLATE VERSUS THE SQUARE OF THE PISTON VELOCITY

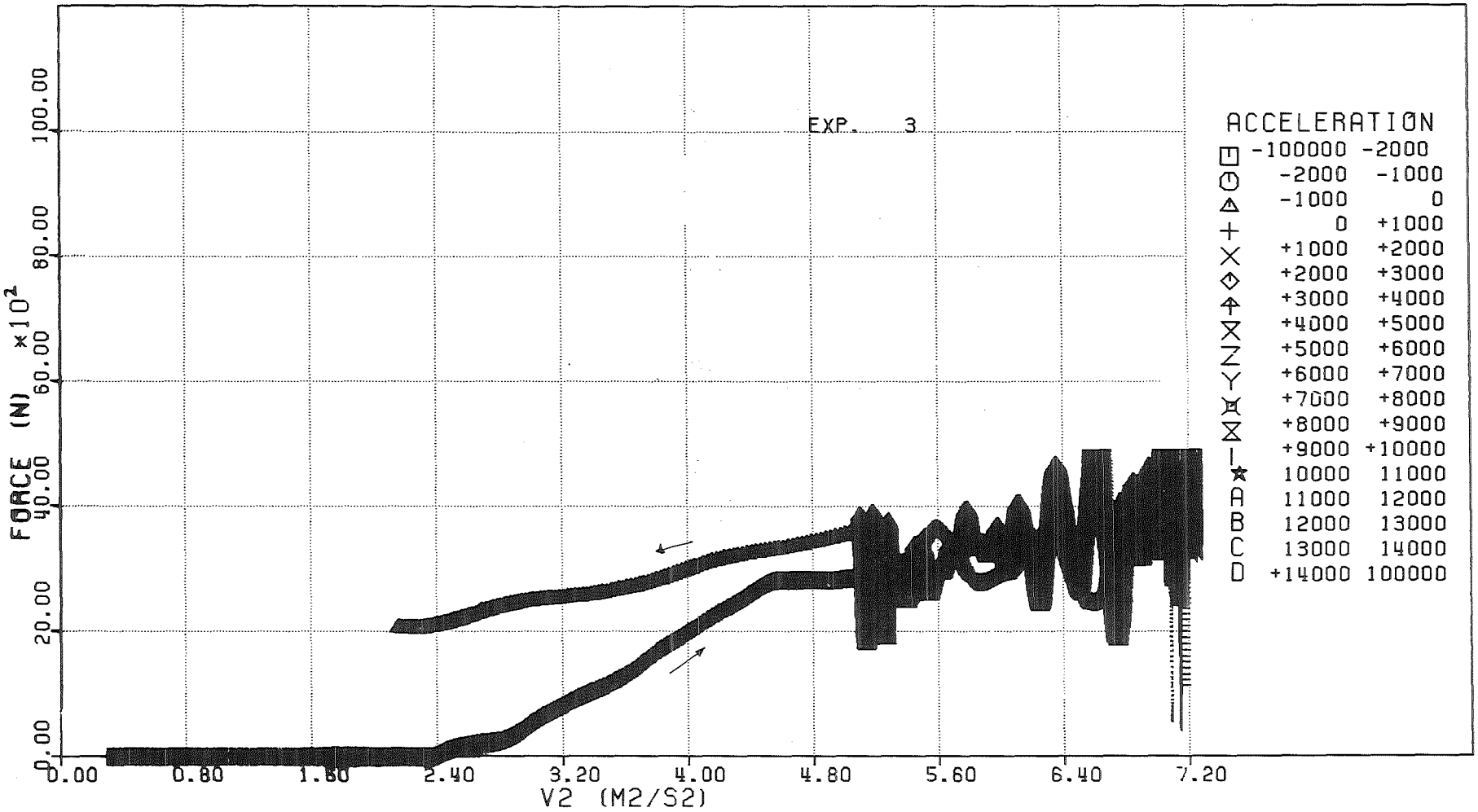

FIG. 6.201 - FORCE ACTING ON THE DIP-PLATE VERSUS THE SQUARE OF THE PISTON VELOCITY

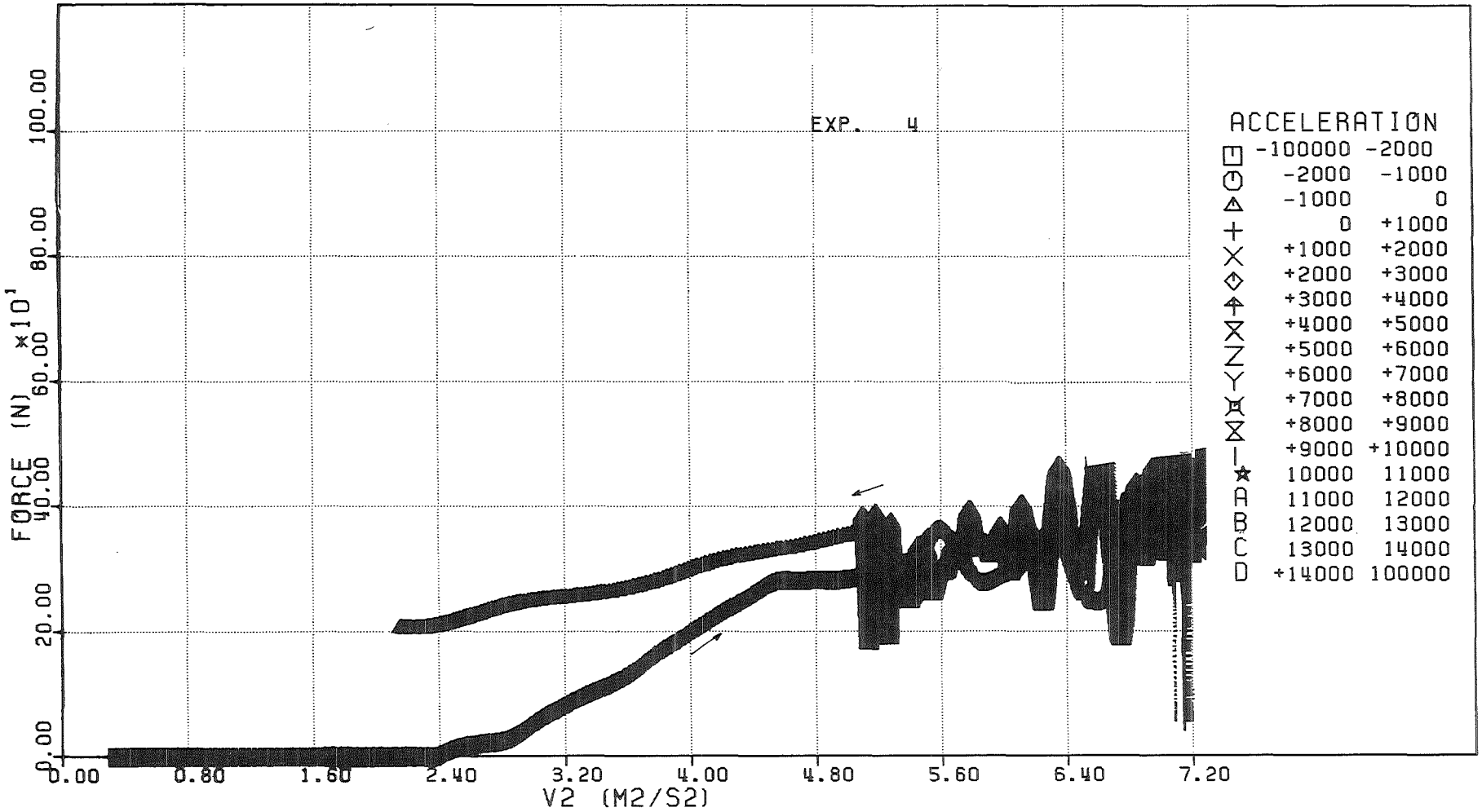

FIG. 6.202 - FORCE ACTING ON THE DIP-PLATE VERSUS THE SQUARE OF THE PISTON VELOCITY

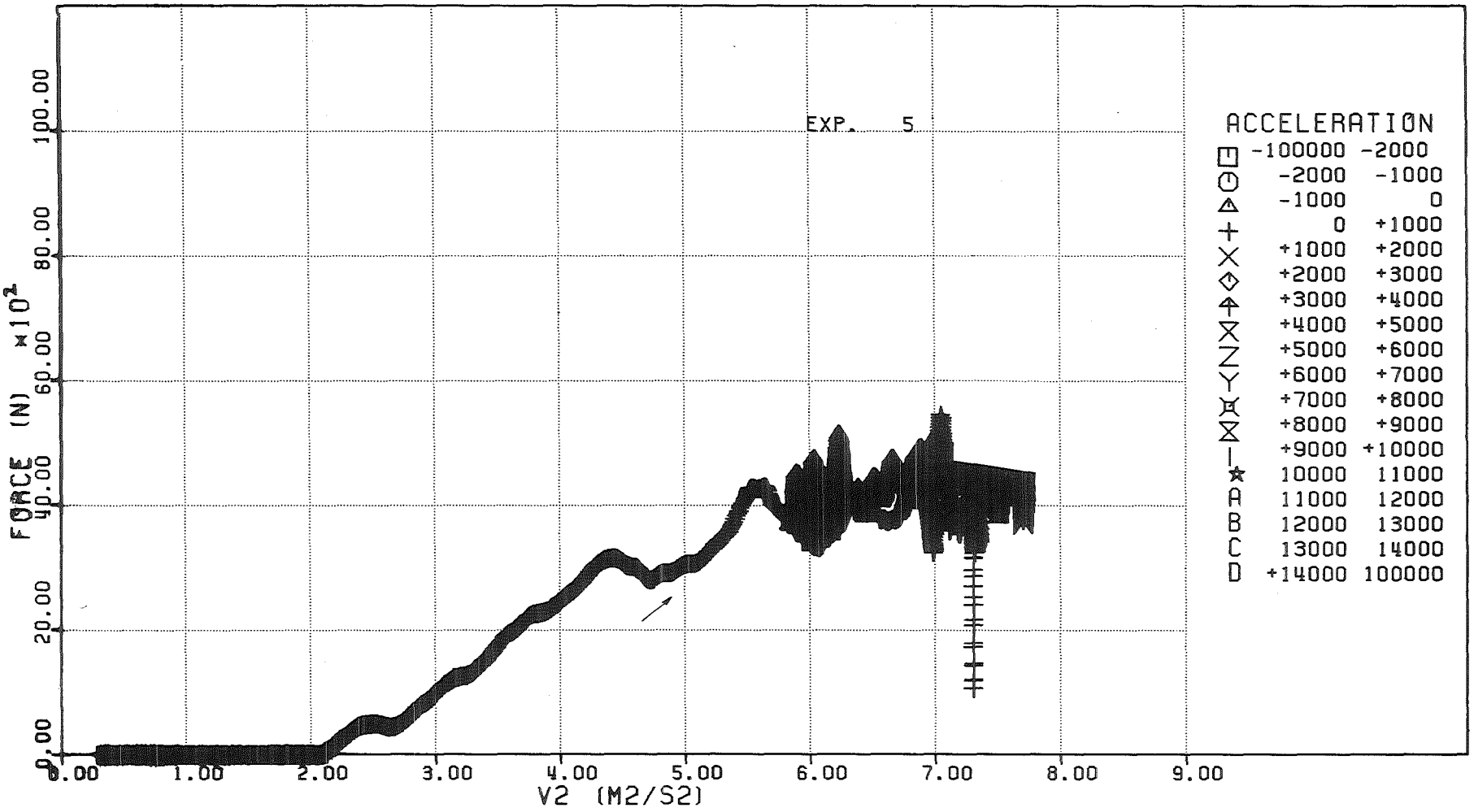

FIG. 6.203 - FORCE ACTING ON THE DIP-PLATE VERSUS THE SQUARE OF THE PISTON VELOCITY

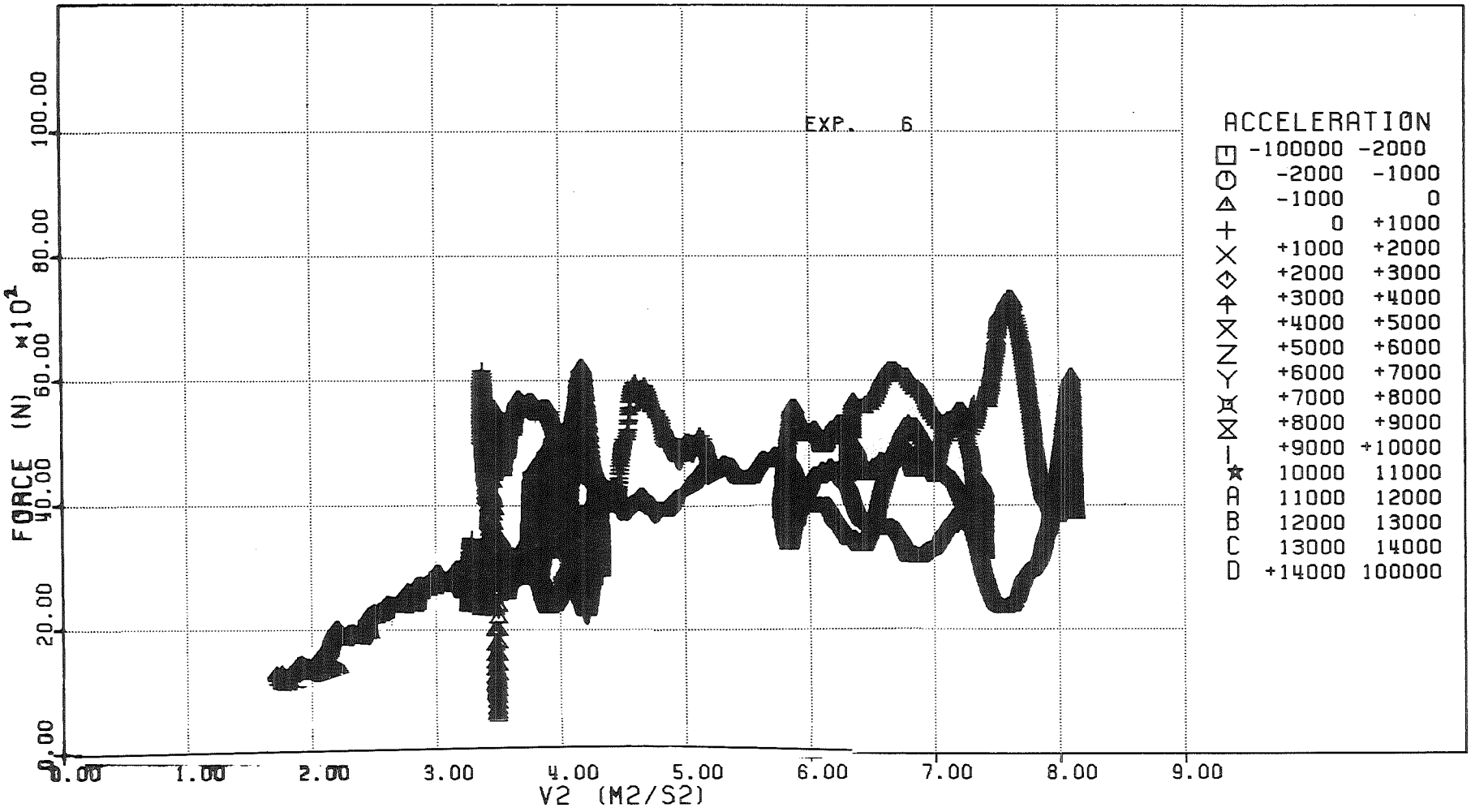

FIG. 6.204 -FORCE ACTING ON THE DIP-PLATE VERSUS THE SQUARE OF THE PISTON VELOCITY

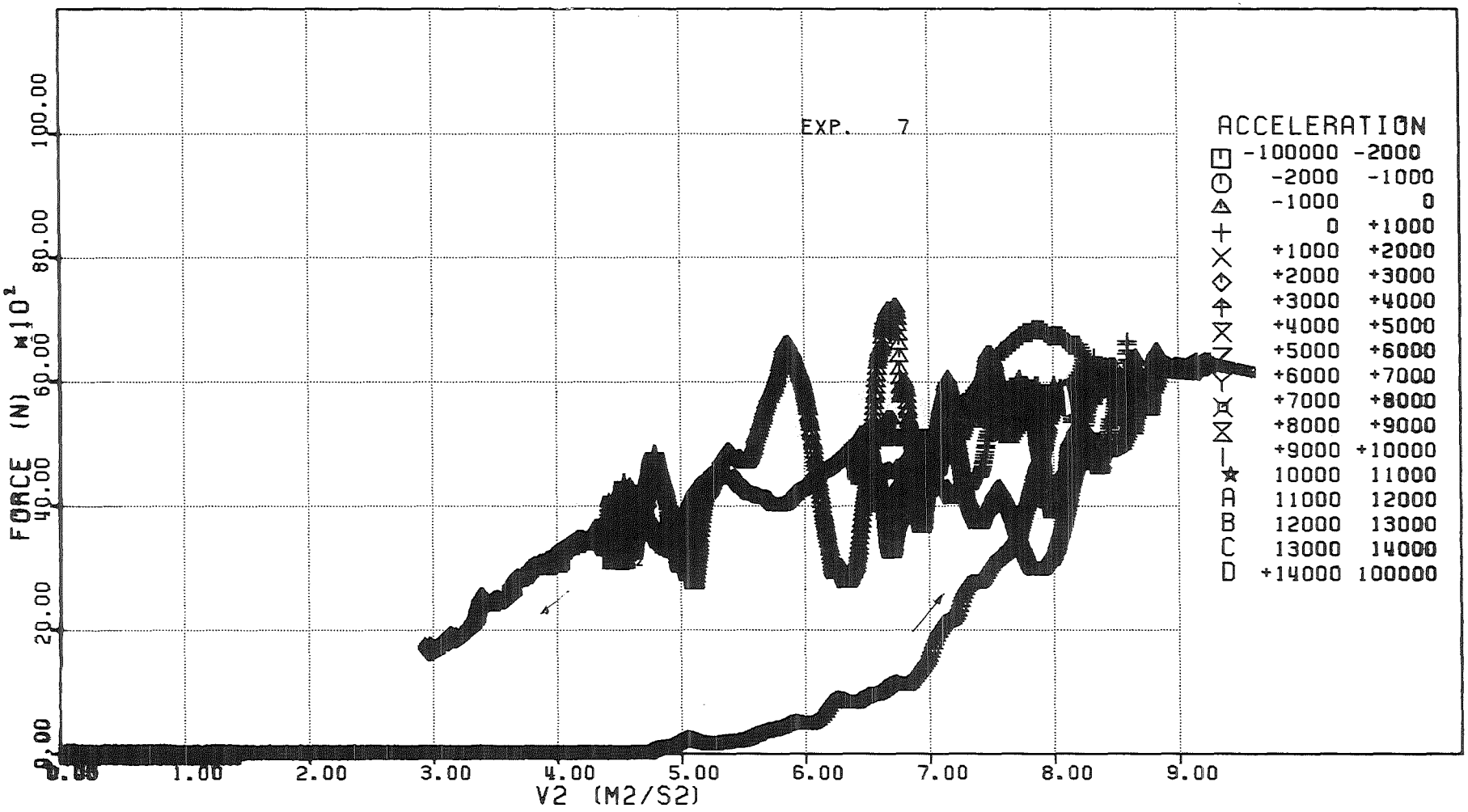

FIG. 6.205 -FORCE ACTING ON THE DIP-PLATE VERSUS THE SQUARE OF THE PISTON VELOCITY

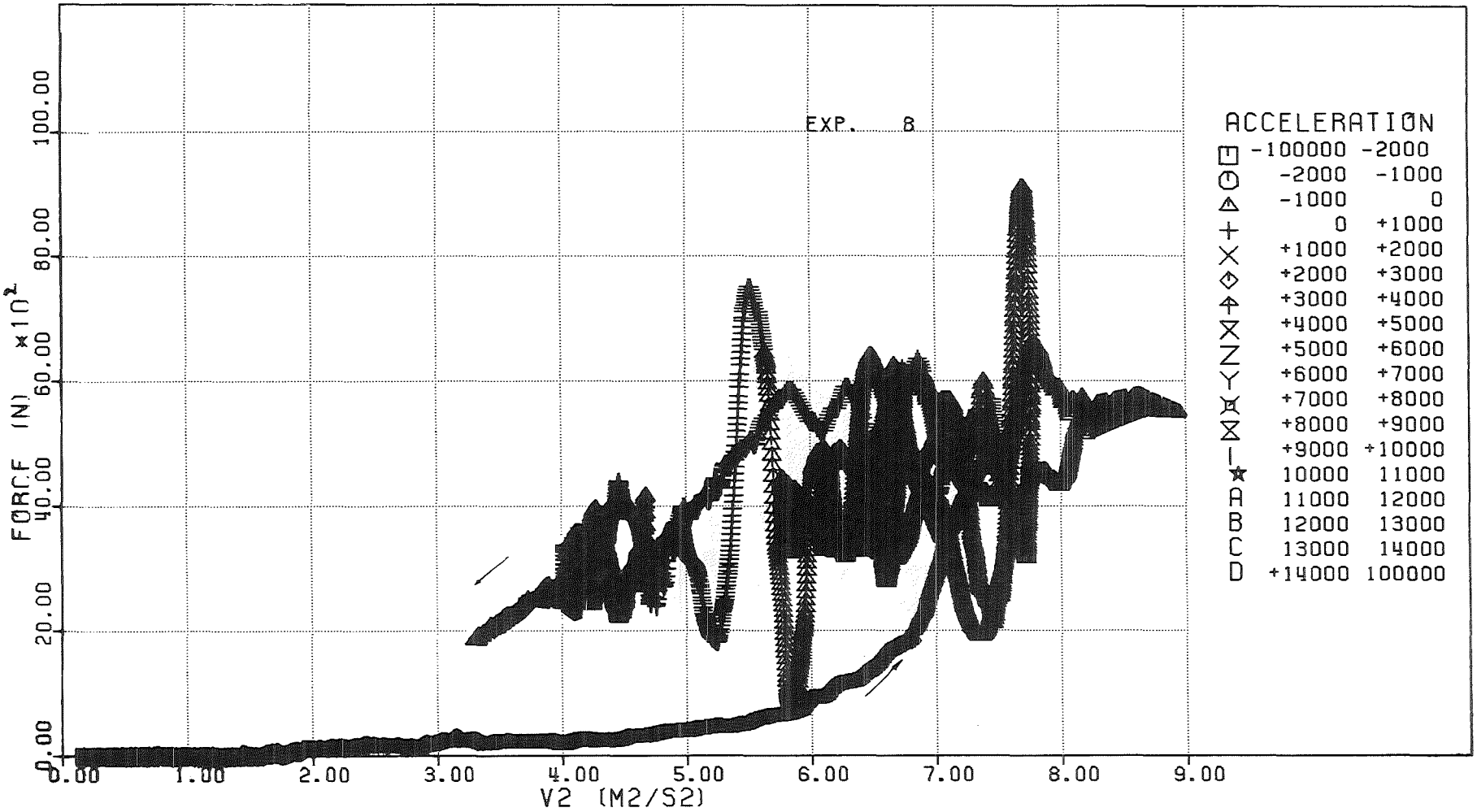

FIG. 6.206 - FORCE ACTING ON THE DIP-PLATE VERSUS THE SQUARE OF THE PISTON VELOCITY

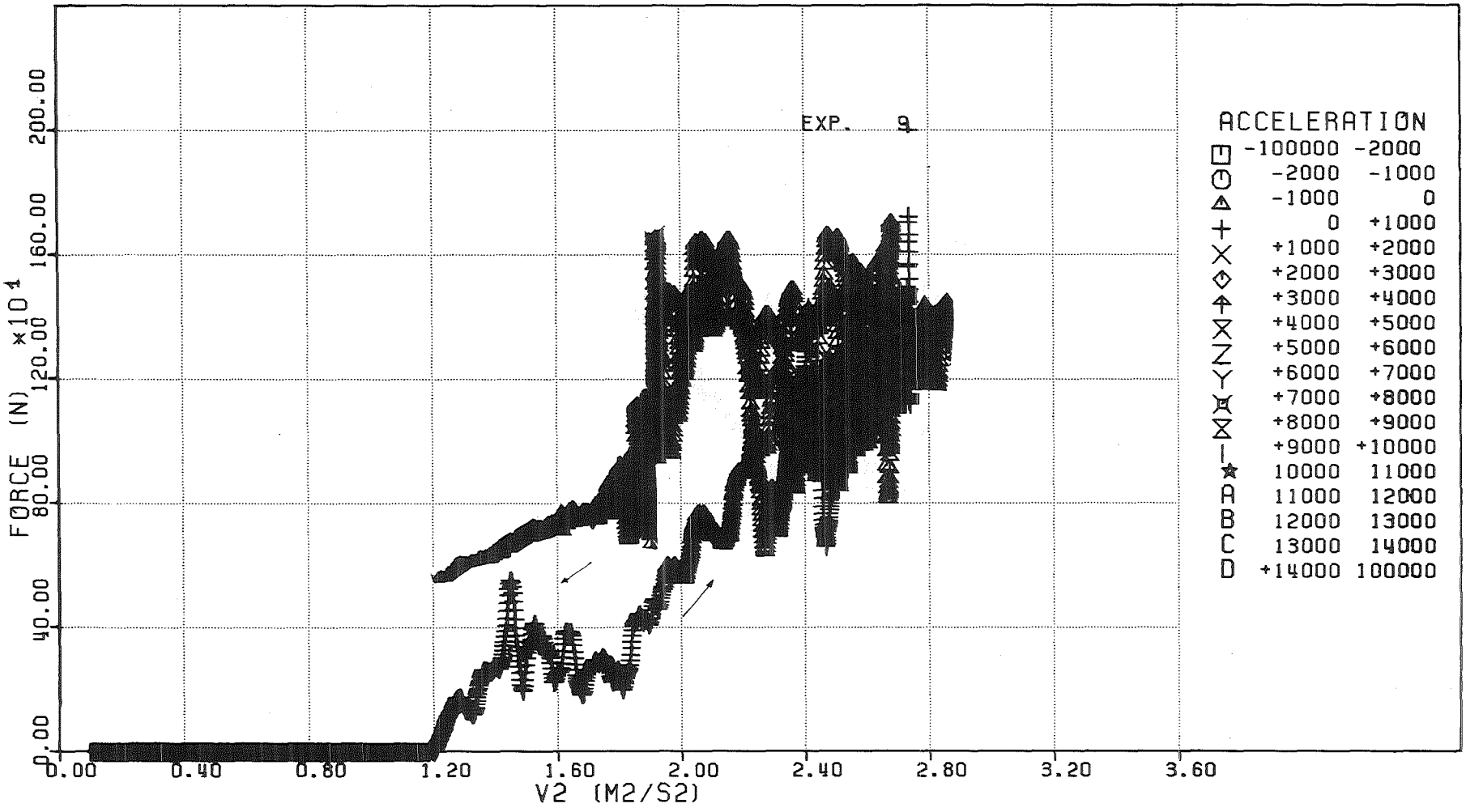

FIG. 6.207 - FORCE ACTING ON THE DIP-PLATE VERSUS THE SQUARE OF THE PISTON VELOCITY

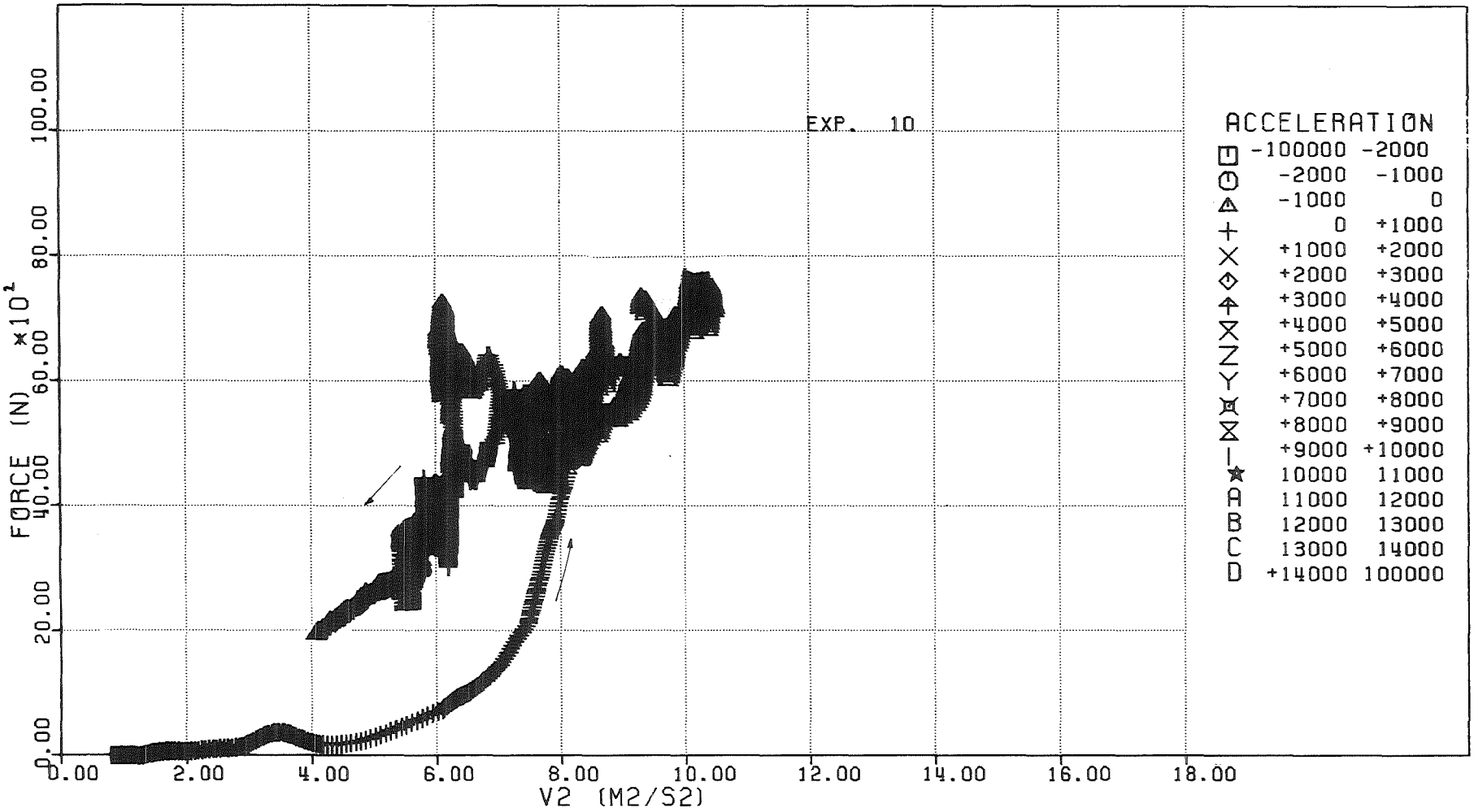

FIG. 6.208 - FORCE ACTING ON THE DIP-PLATE VERSUS THE SQUARE OF THE PISTON VELOCITY

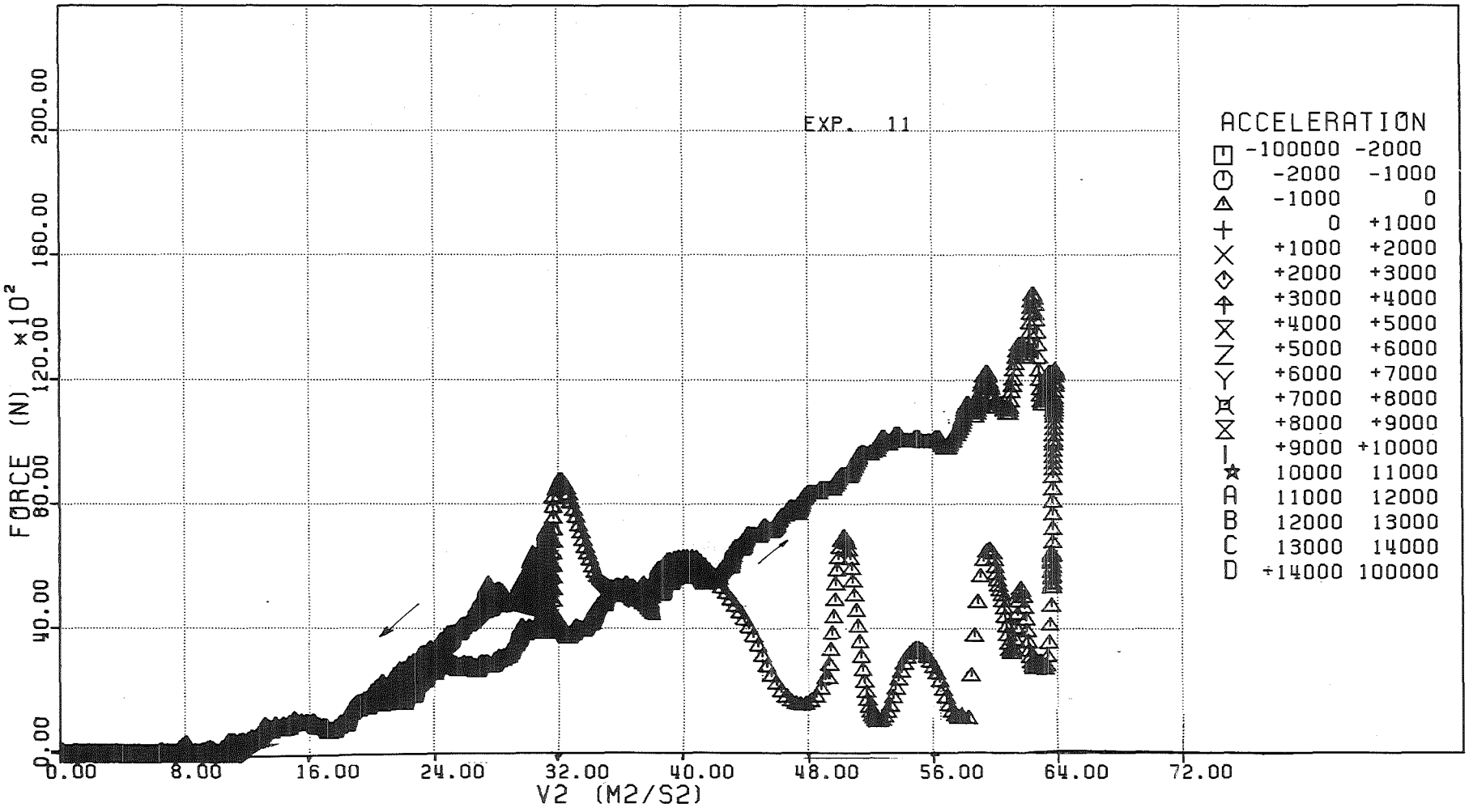

FIG. 6.209 -FORCE ACTING ON THE DIP-PLATE VERSUS THE SQUARE OF THE PISTON VELOCITY

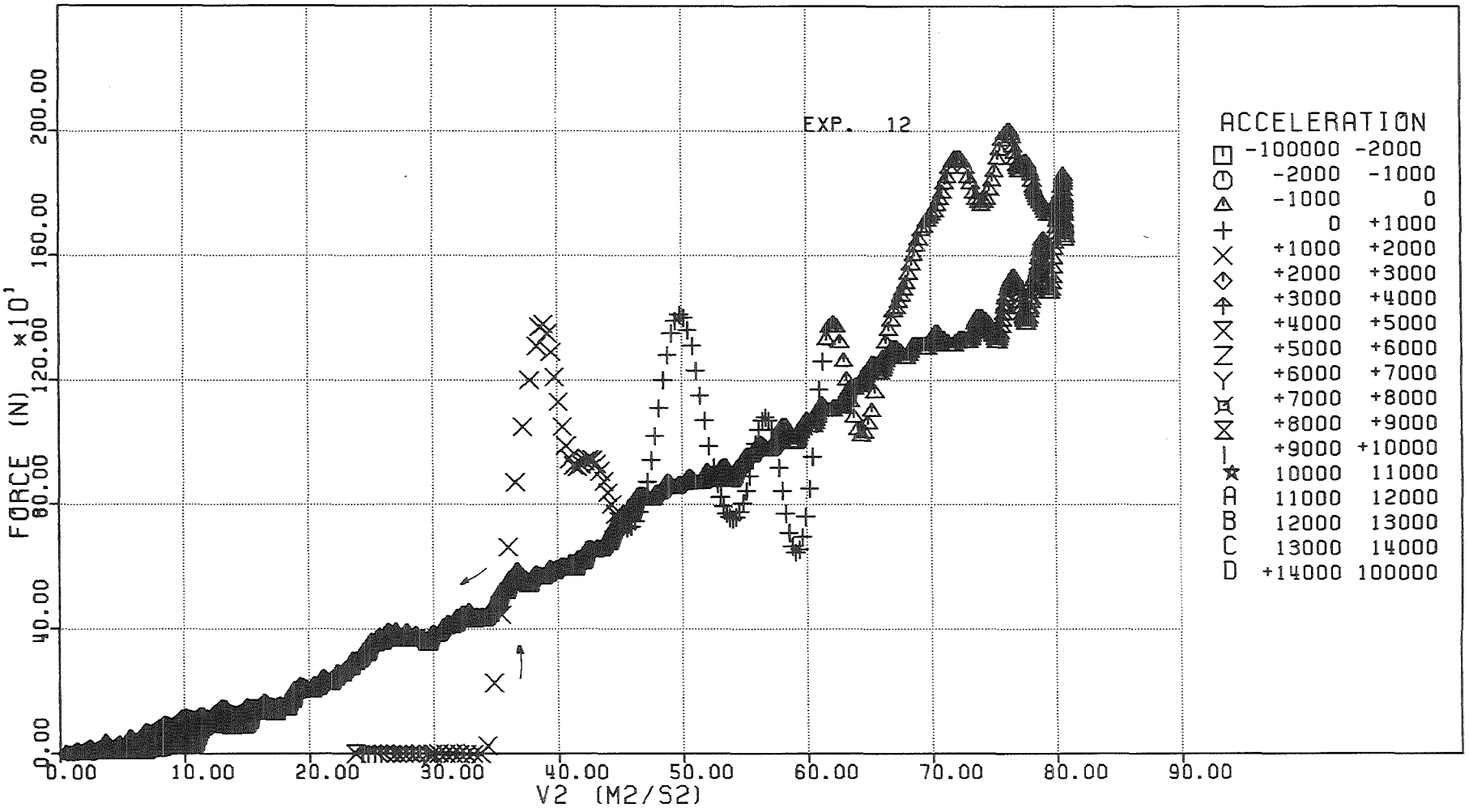

FIG. 6.210 - FORCE ACTING ON THE DIP-PLATE VERSUS THE SQUARE OF THE PISTON VELOCITY

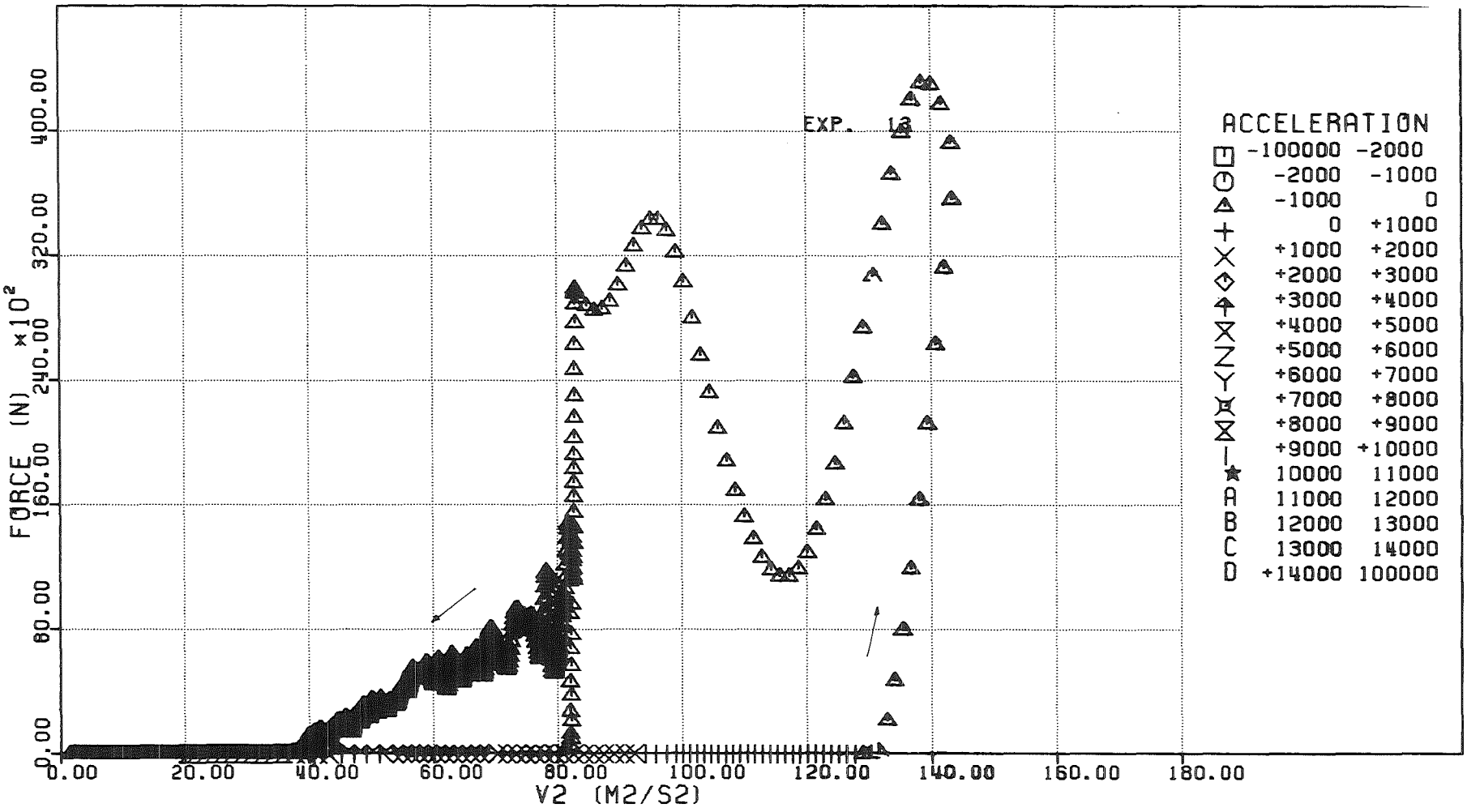

FIG. 6.211 - FORCE ACTING ON THE DIP-PLATE VERSUS THE SQUARE OF THE PISTON VELOCITY

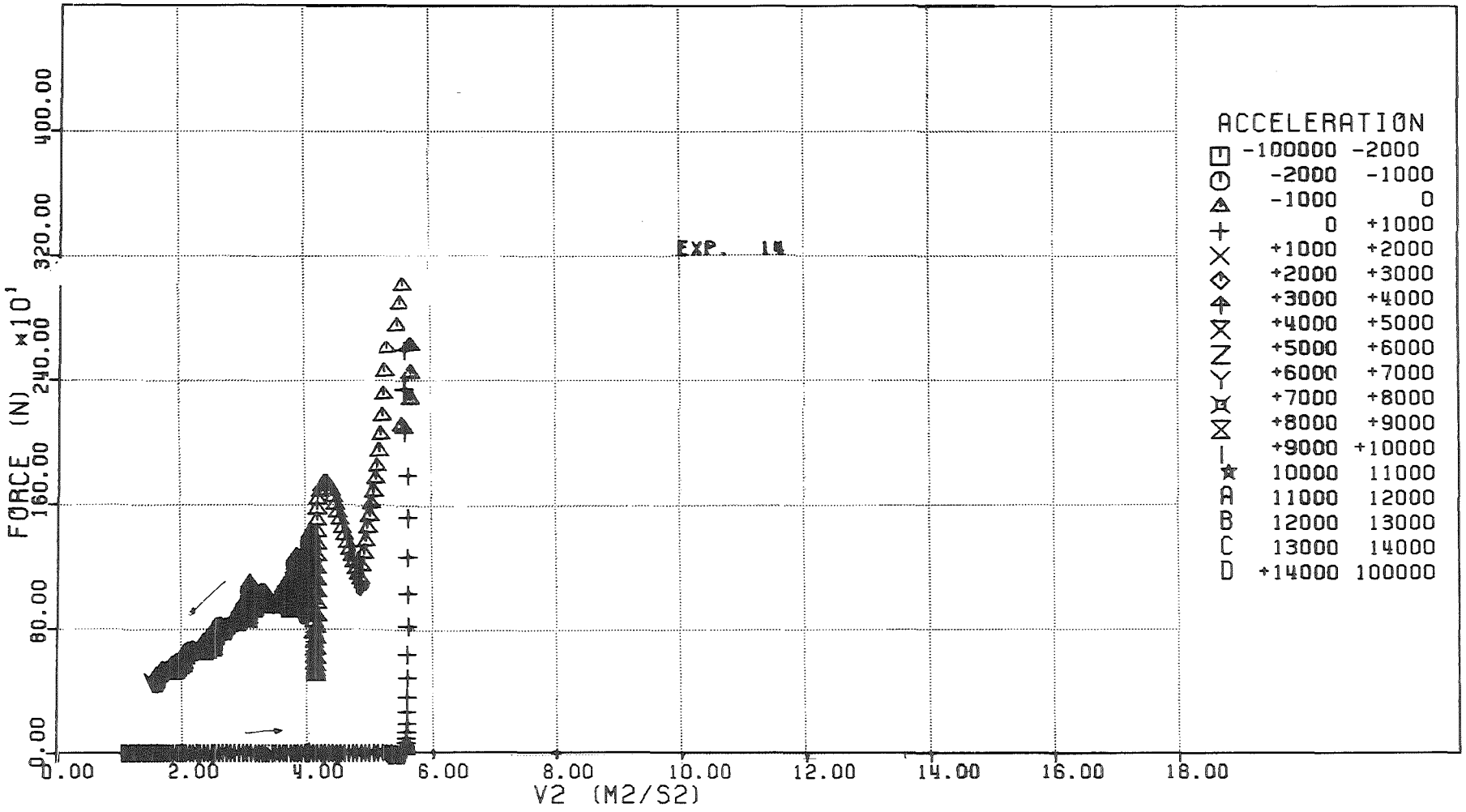

FIG. 6.212 -FORCE ACTING ON THE DIP-PLATE VERSUS THE SQUARE OF THE PISTON VELOCITY

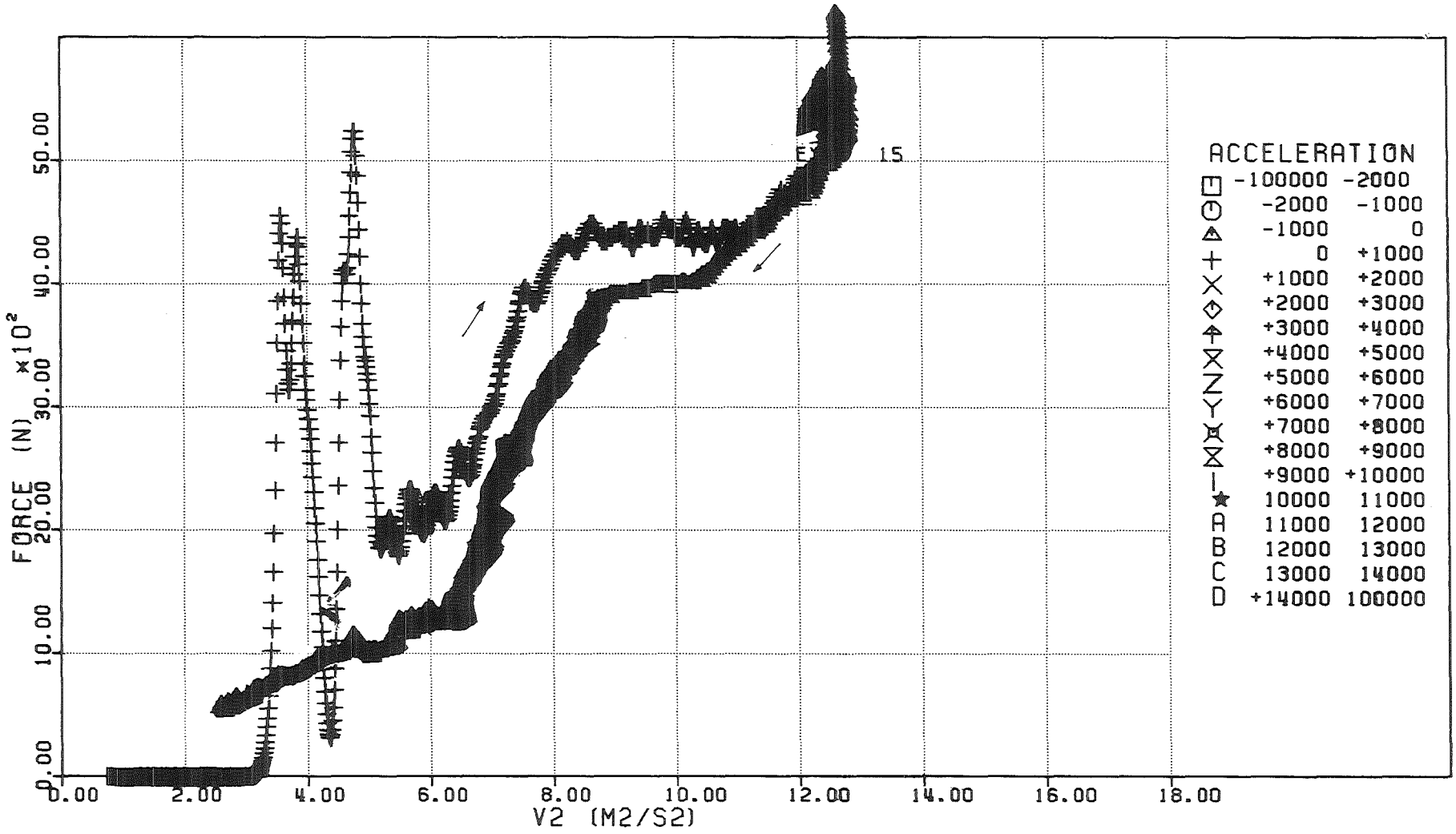

FIG. 6.213 - FORCE ACTING ON THE DIP-PLATE VERSUS THE SQUARE OF THE PISTON VELOCITY

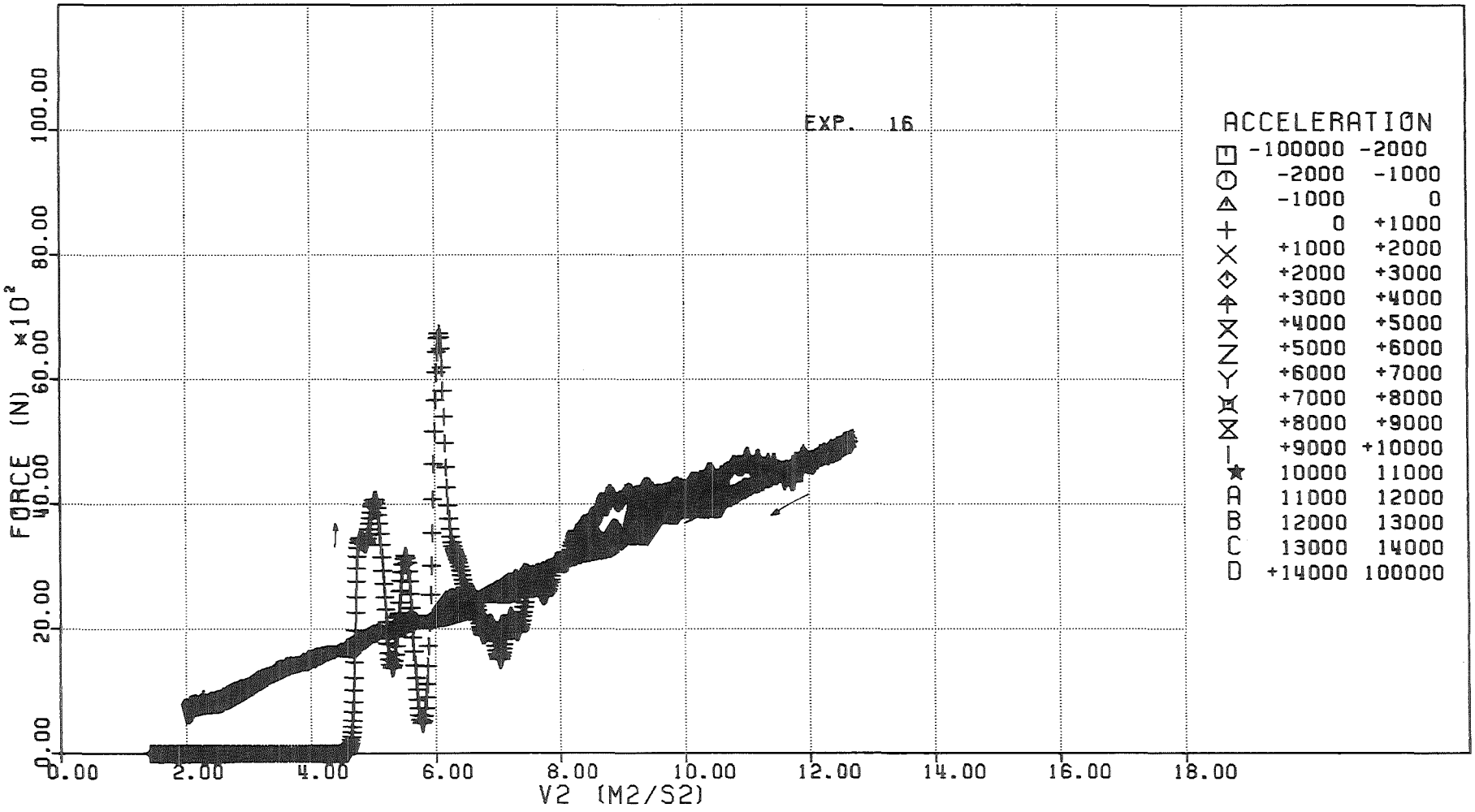

FIG. 6.214 - FORCE ACTING ON THE DIP-PLATE VERSUS THE SQUARE OF THE PISTON VELOCITY

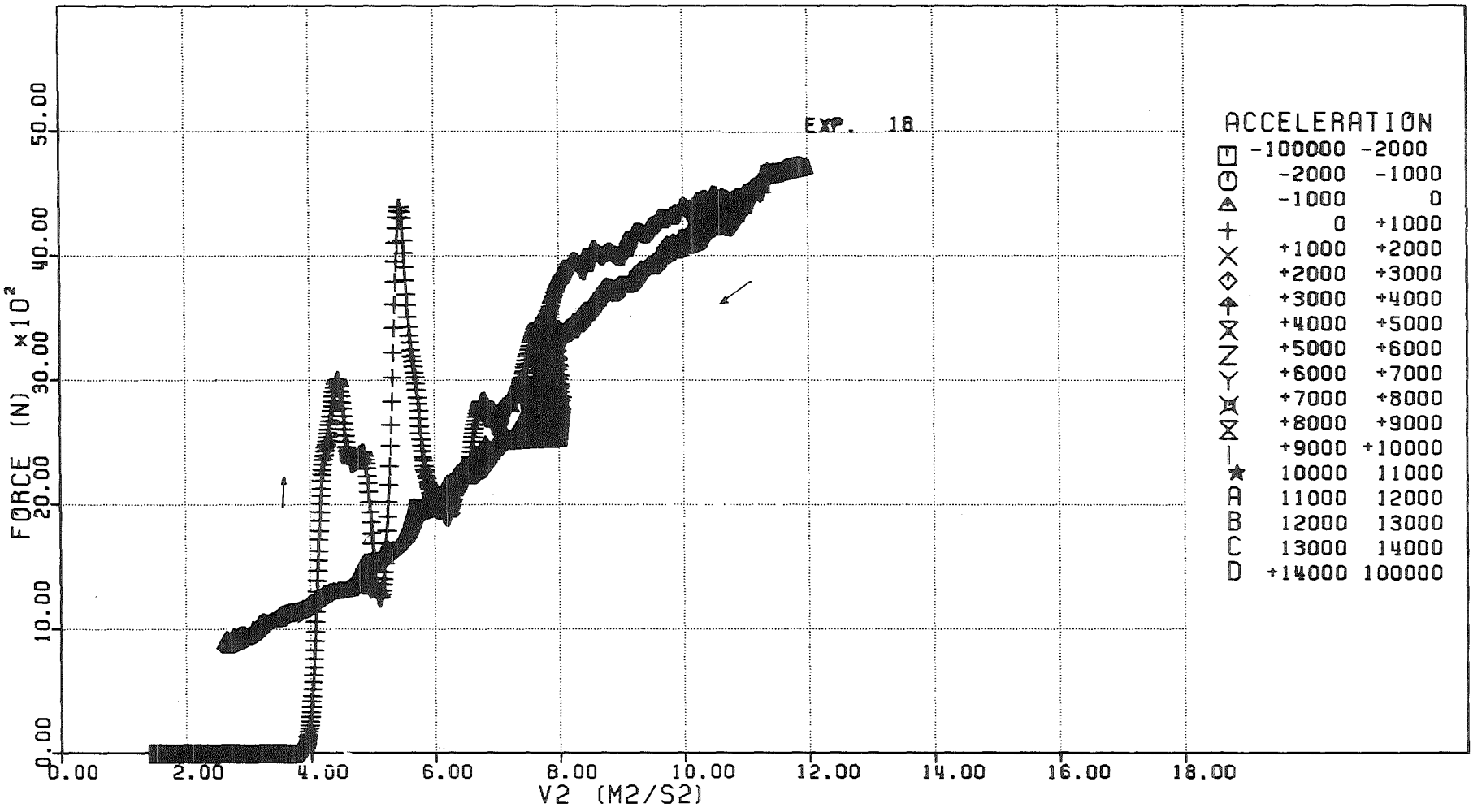

FIG. 6.215 - FORCE ACTING ON THE DIP-PLATE VERSUS THE SQUARE OF THE PISTON VELOCITY

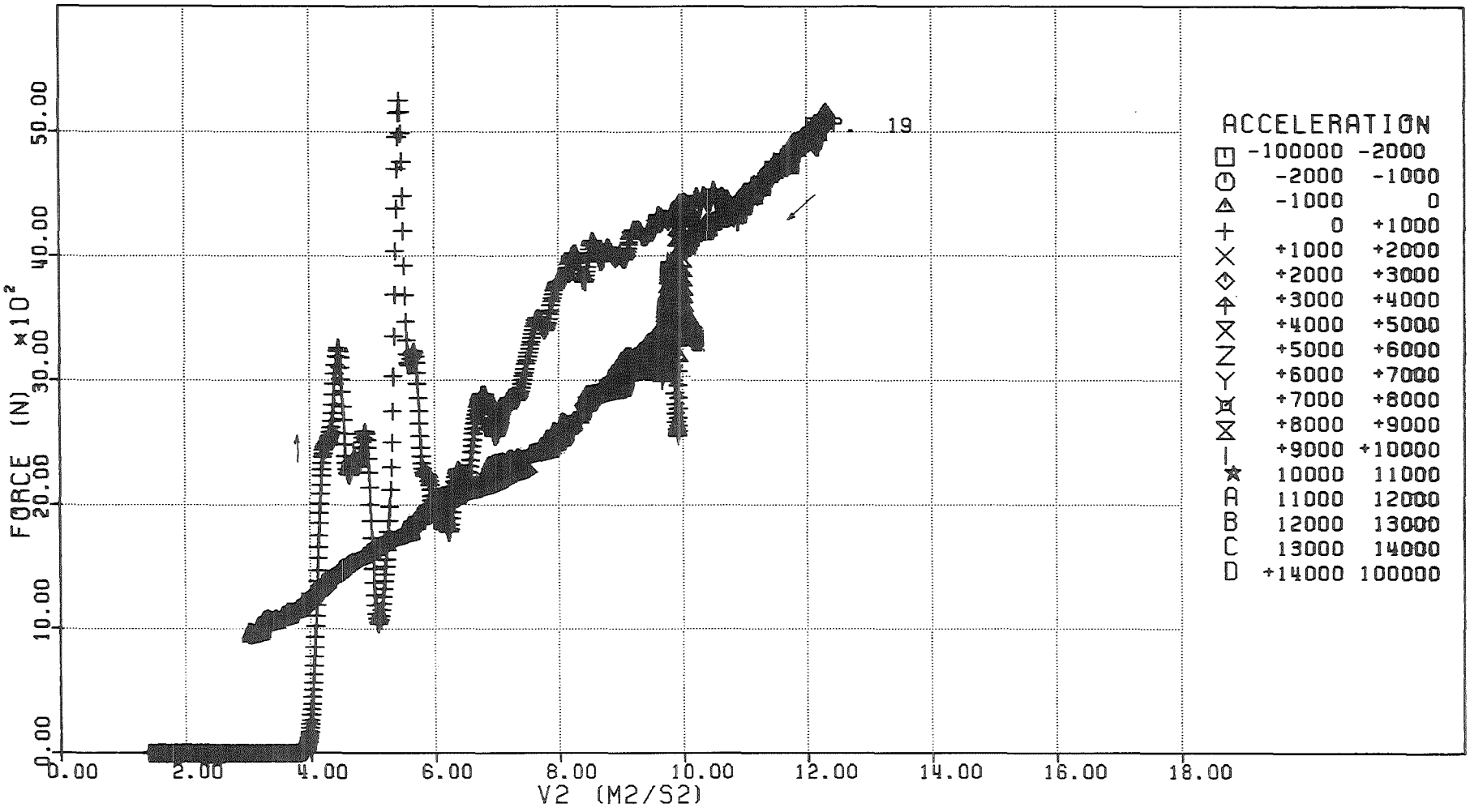

FIG. 6.216 - FORCE ACTING ON THE DIP-PLATE \ERSUS THE SQUARE OF THE PISTON VELOCITY

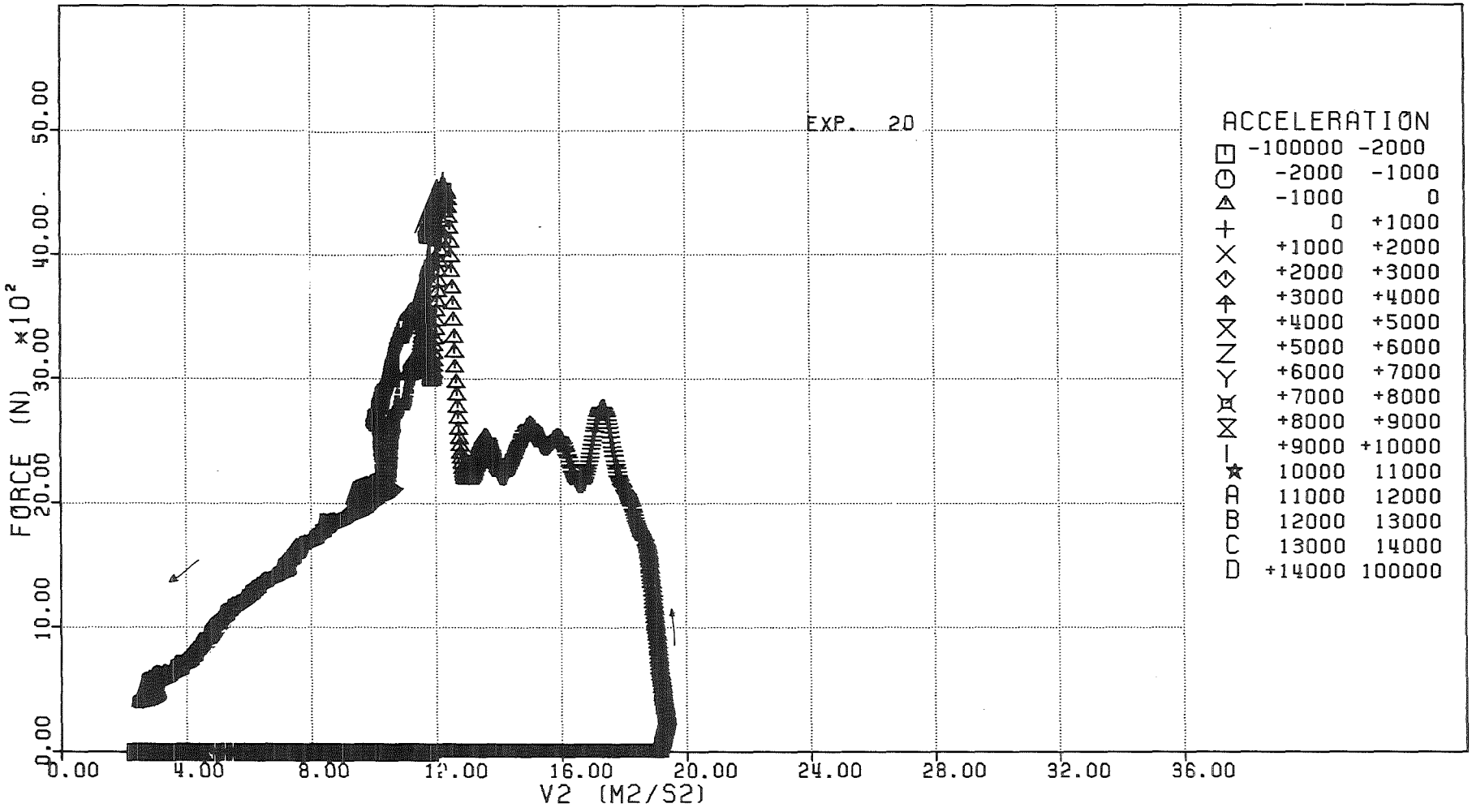

FIG. 6.217 - FORCE ACTING ON THE DIP-PLATE VERSUS THE SQUARE OF THE PISTON VELOCITY

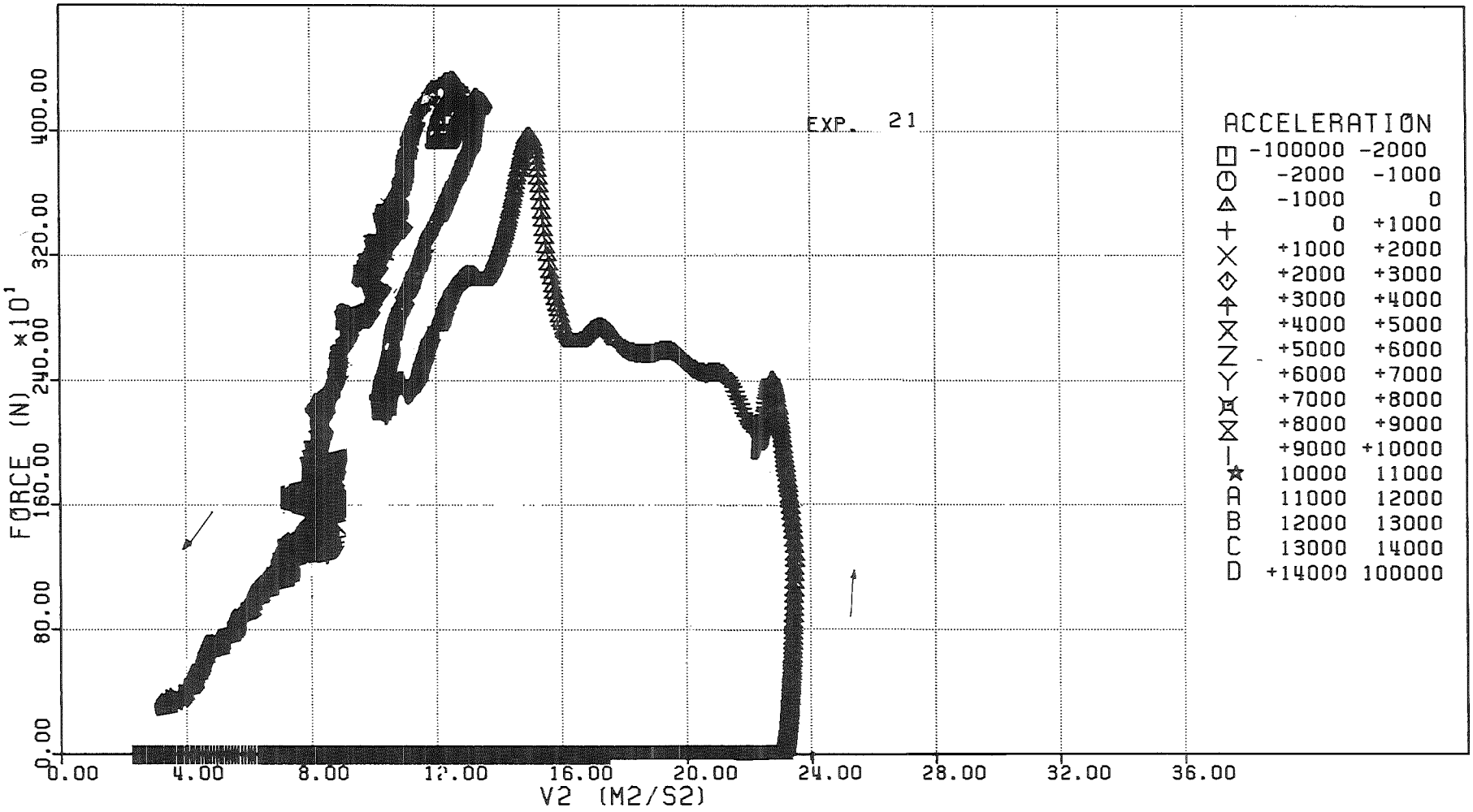

FIG. 6.218 - FORCE ACTING ON THE DIP-PLATE VERSUS THE SQUARE OF THE PISTON VELOCITY

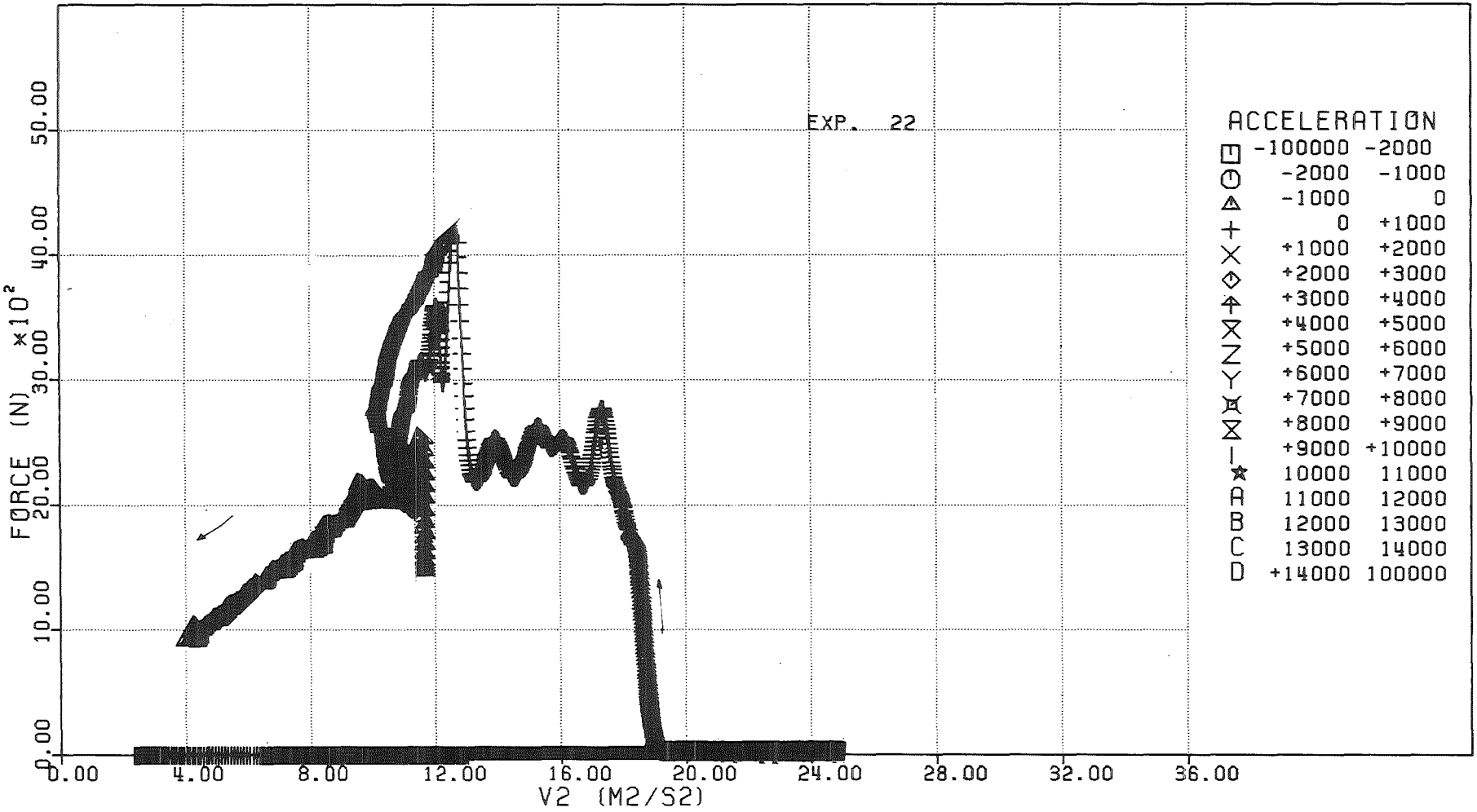

FIG. 6.219 - FORCE ACTING ON THE DIP-PLATE VERSUS THE SQUARE OF THE PISTON VELOCITY

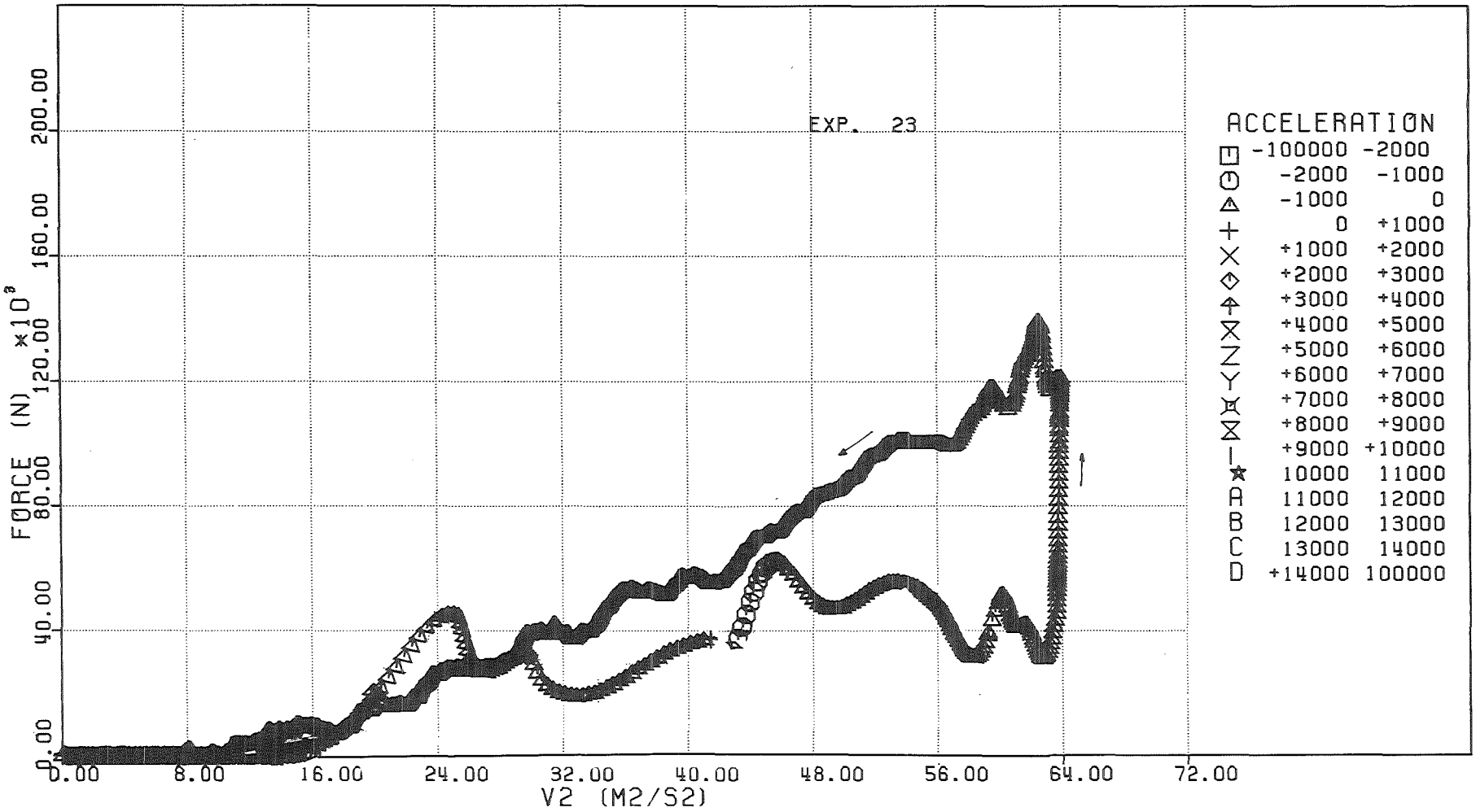

FIG. 6.220 - FORCE ACTING ON THE DIP-PLATE VERSUS THE SQUARE OF THE PISTON VELOCITY

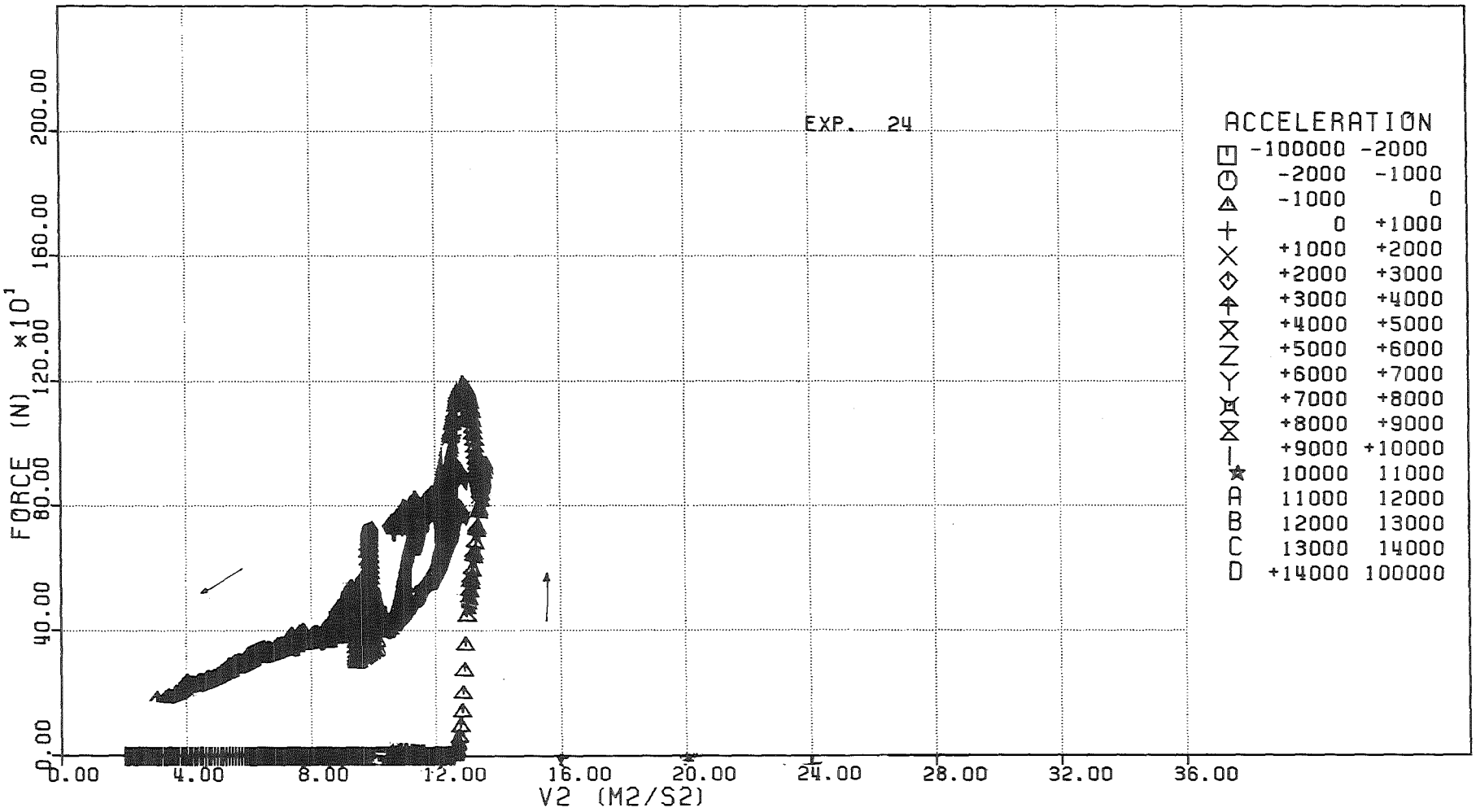

FIG. 6.221 - FORCE ACTING ON THE DIP-PLATE VERSUS THE SQUARE OF THE PISTON VELOCITY

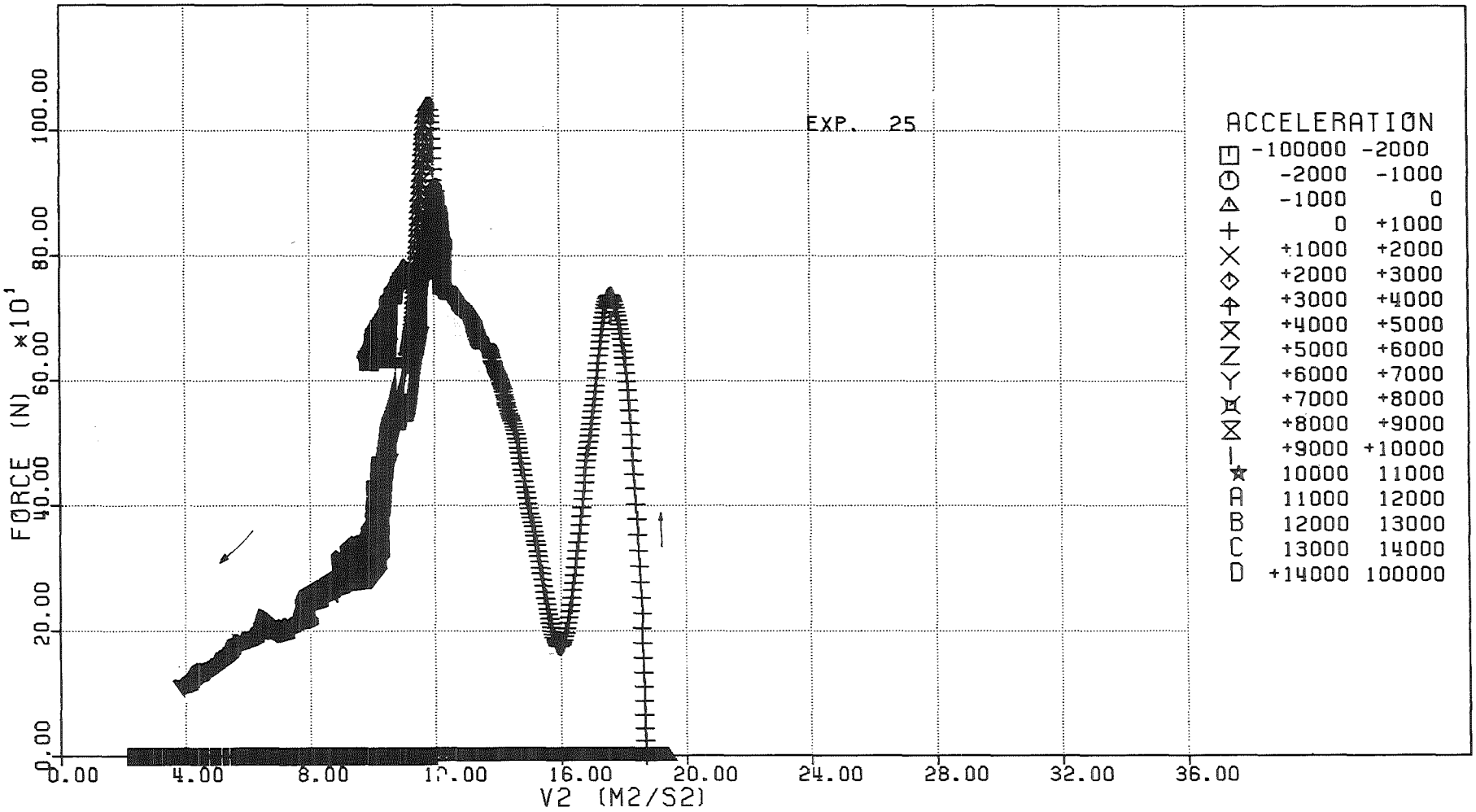

FIG. 6.222 - FORCE ACTING ON THE DIP-PLATE VERSUS THE SQUARE OF THE PISTON VELOCITY

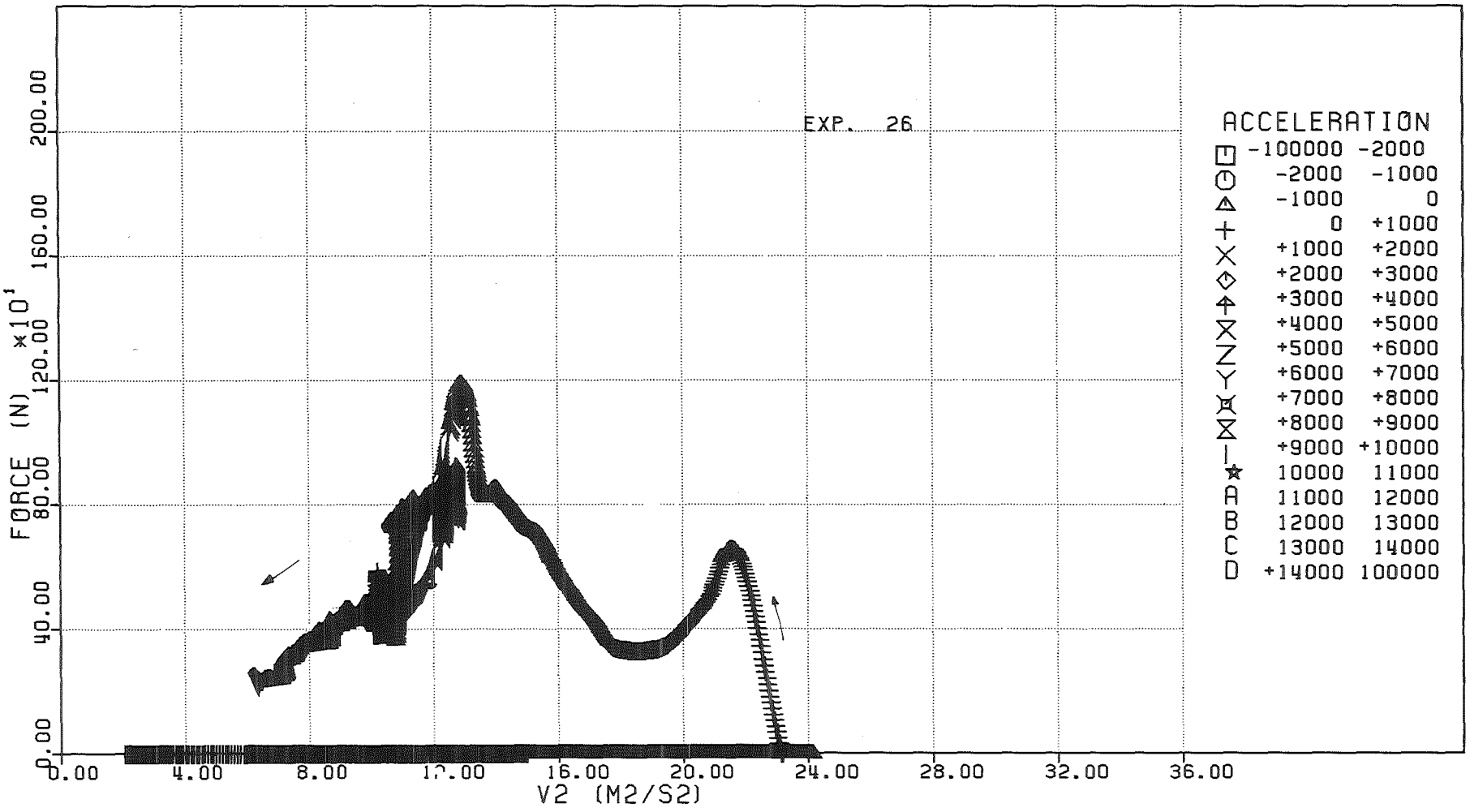

FIG. 6.223 - FORCE ACTING ON THE DIP-PLATE VERSUS THE SQUARE OF THE PISTON VELOCITY

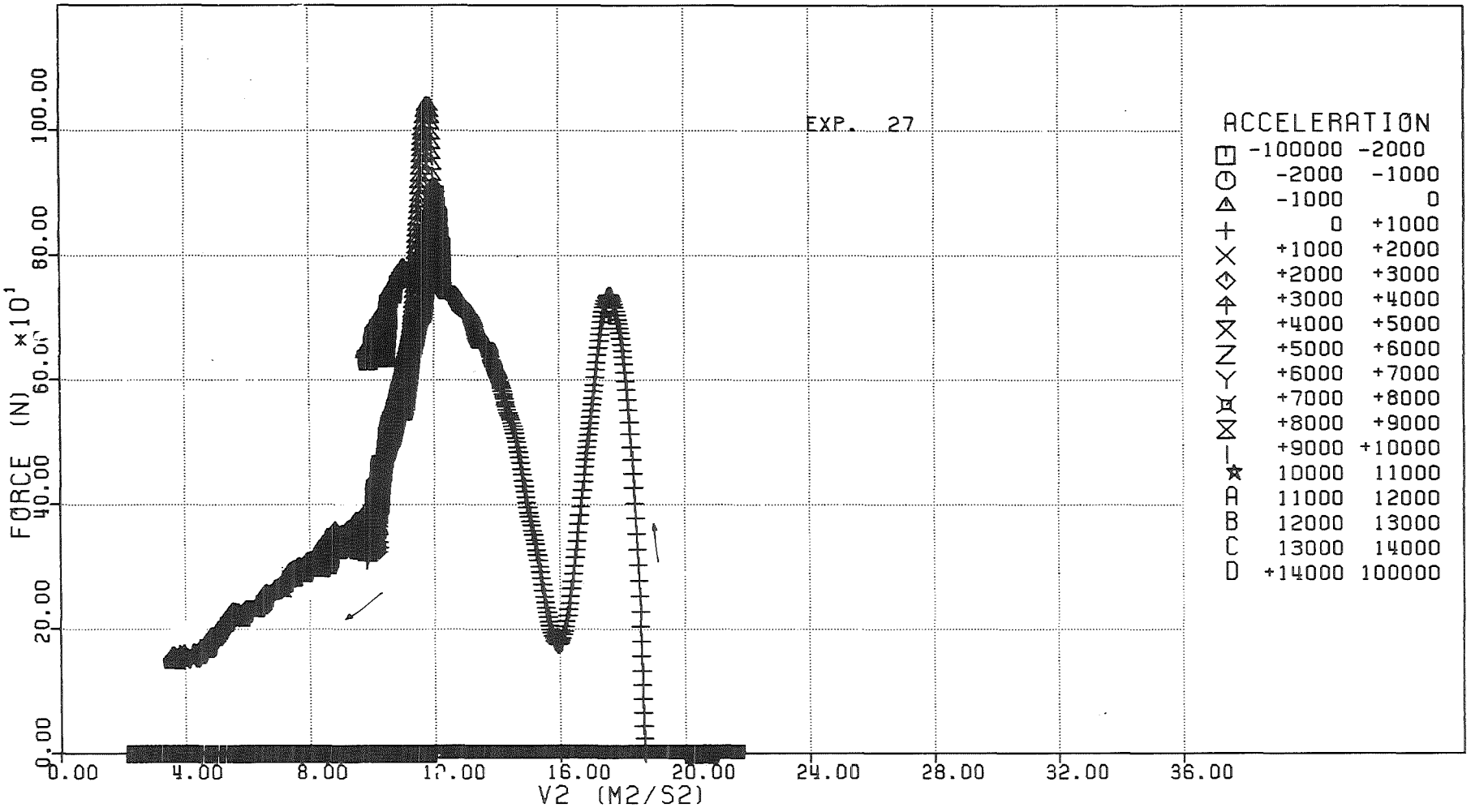

FIG. 6.224 - FORCE ACTING ON THE DIP-PLATE VERSUS THE SQUARE OF THE PISTON VELOCITY

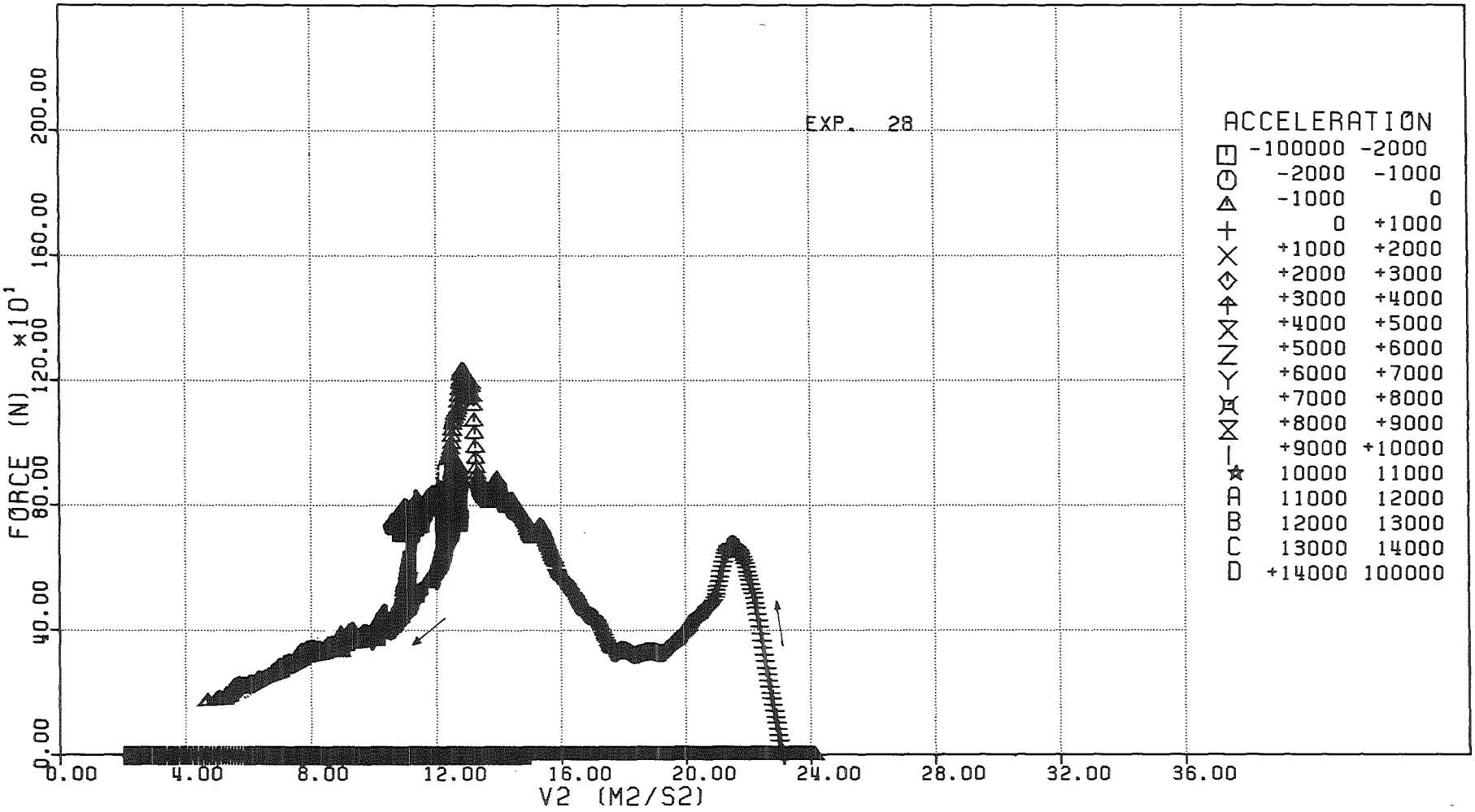

FIG. 6.225 - FORCE ACTING ON THE DIP-PLATE VERSUS THE SQUARE OF THE PISTON VELOCITY

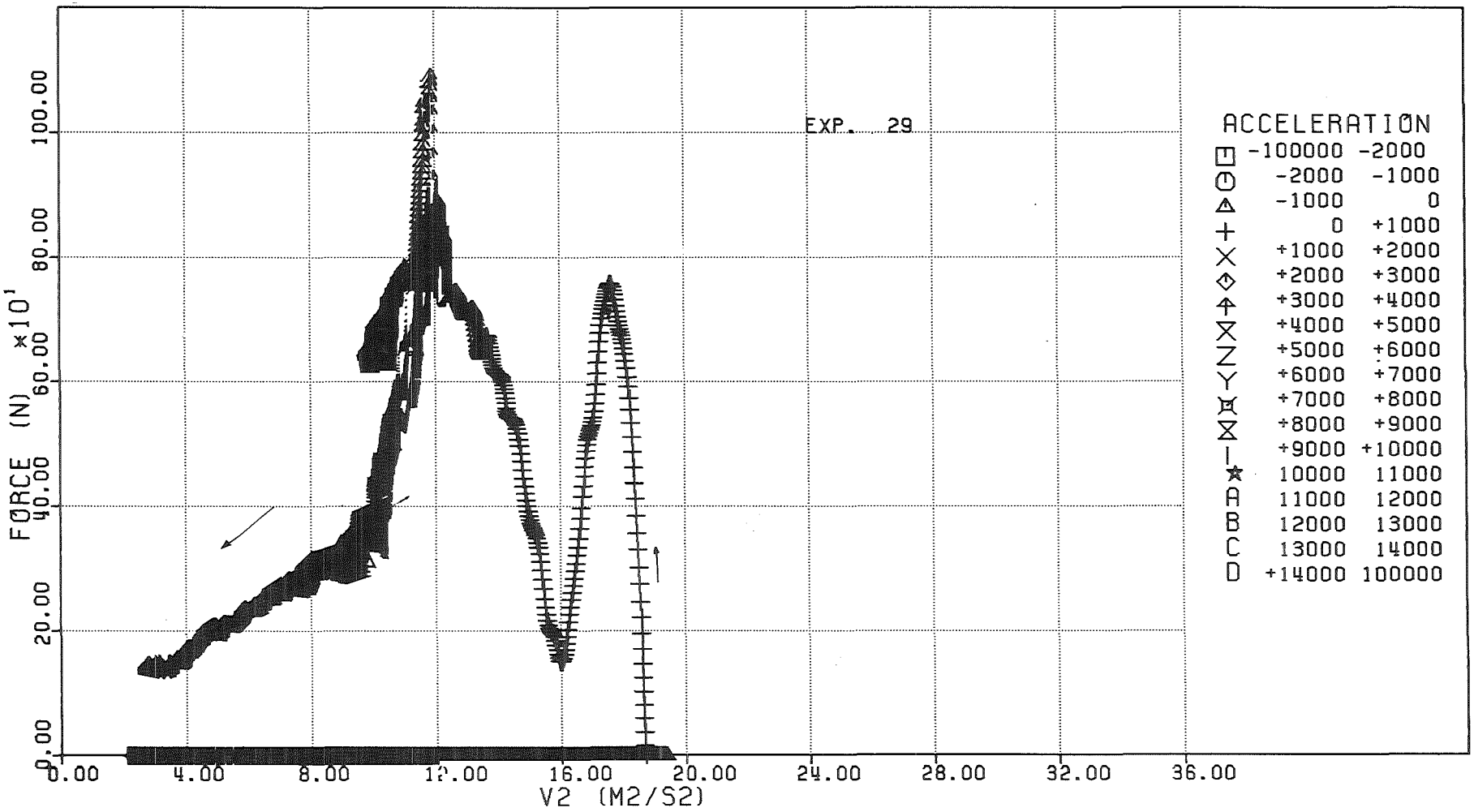

FIG. 6.226 - FORCE ACTING ON THE DIP-PLATE VERSUS THE SQUARE OF THE PISTON VELOCITY

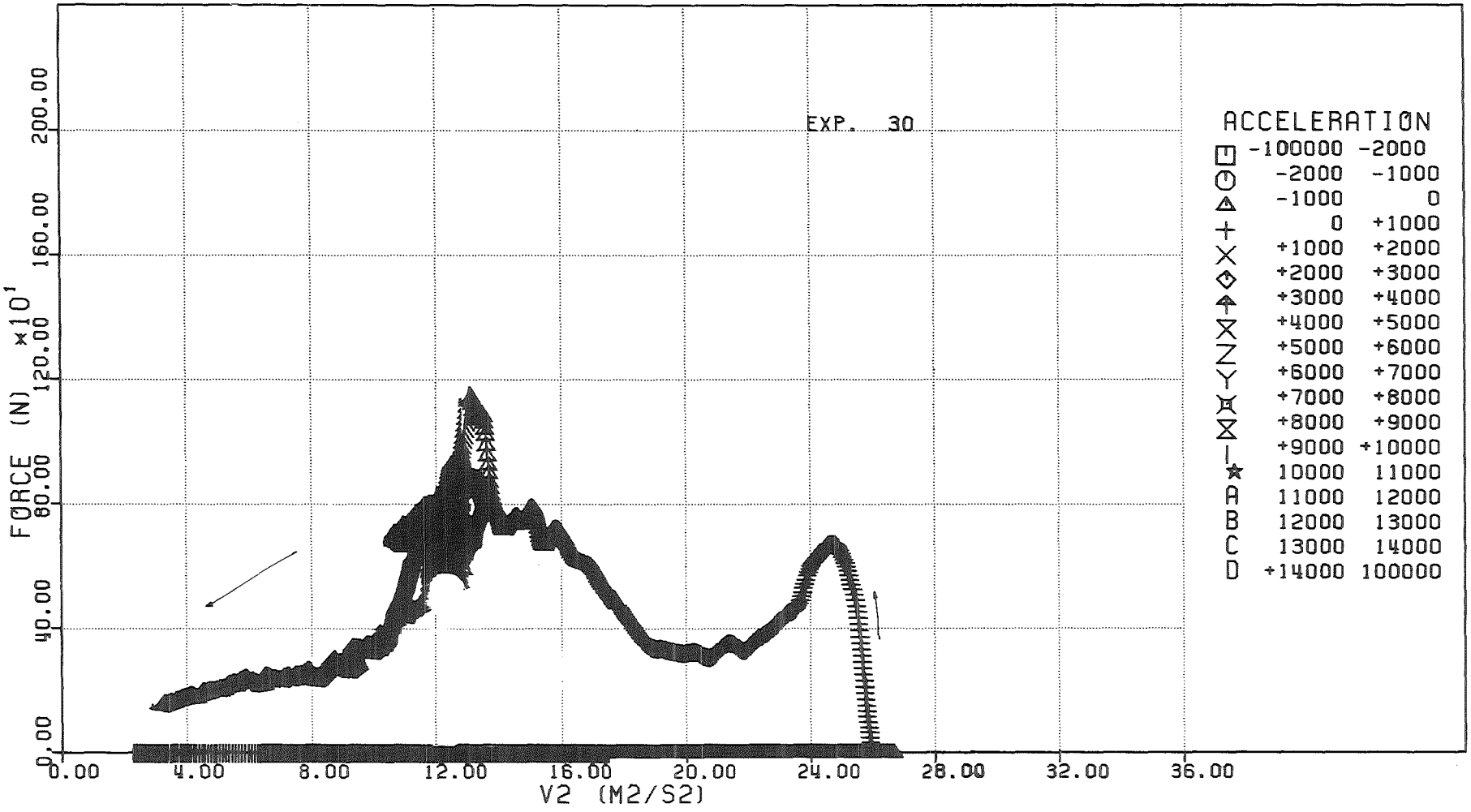

FIG. 6.227 - FORCI ACTING ON THE DIP-PLATE VERSUS THE SQUARE OF THE PISTON VELOCITY

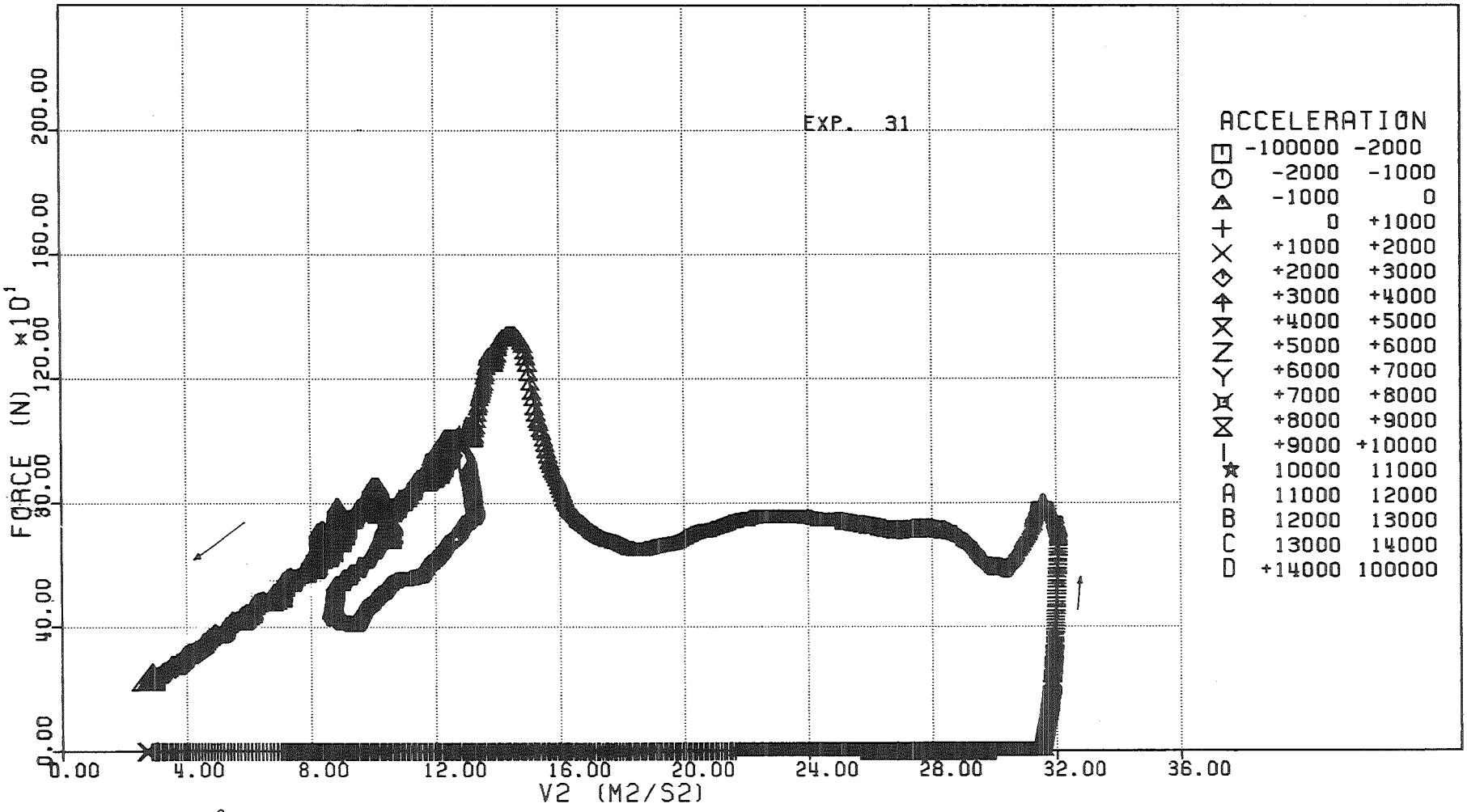

FIG. 6.228 - FORCE ACTING ON THE DIP-PLATE VERSUS THE SQUARE OF THE PISTON VELOCITY

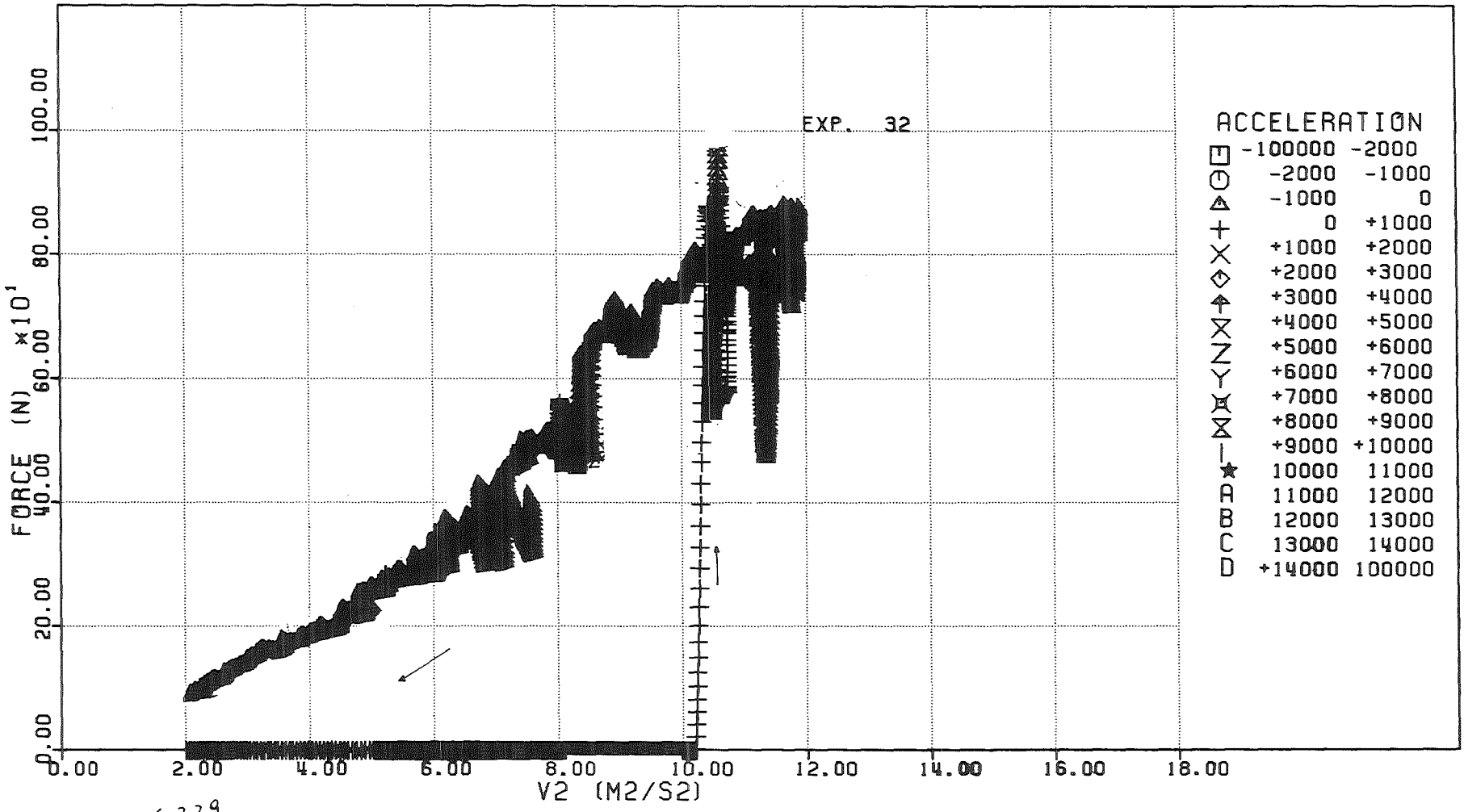

FIG. 6.229 -FORCE ACTING ON THE DIP-PLATE VERSUS THE SQUARE OF THE PISTON VELOCITY

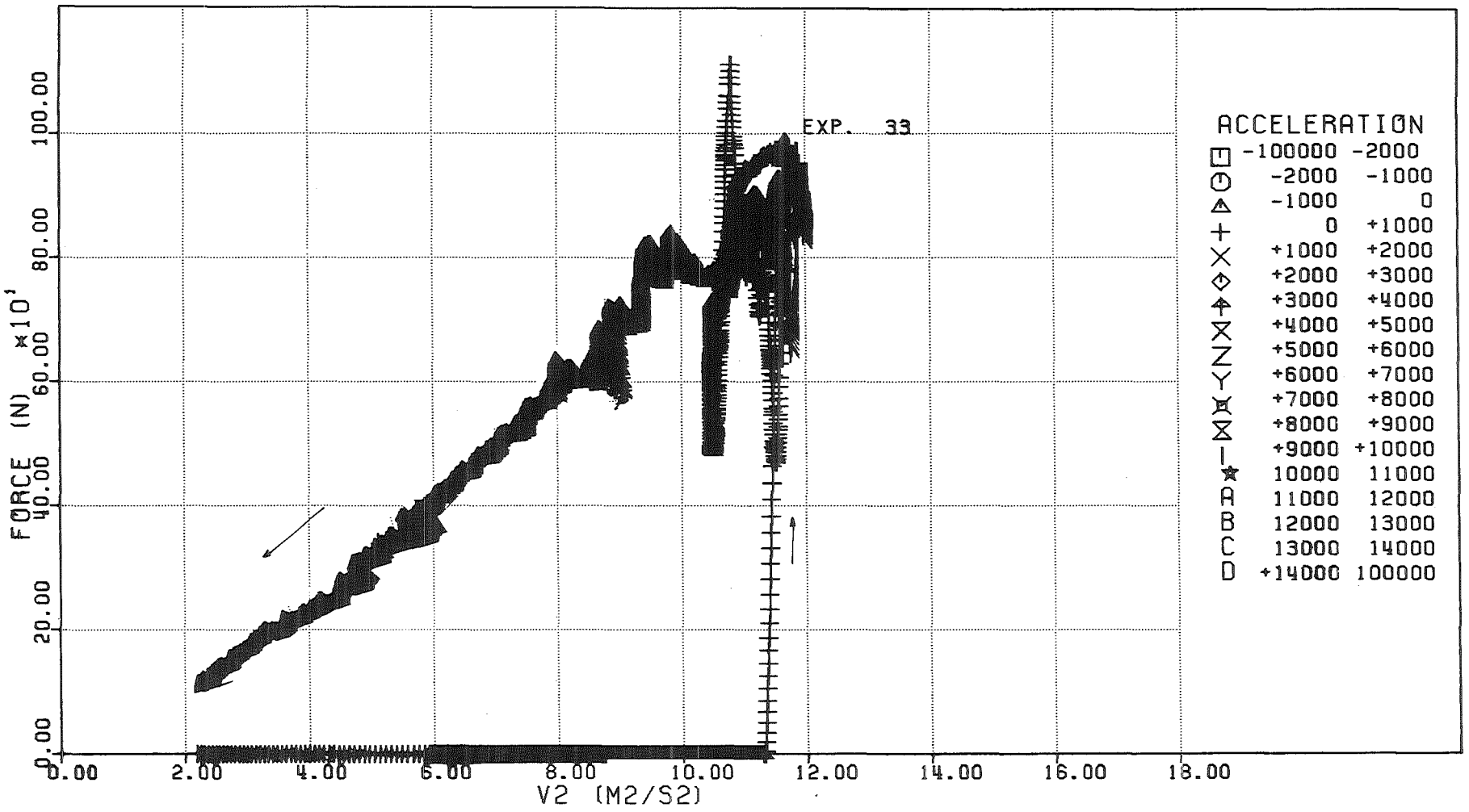

FIG. 6.230 - FORCE ACTING ON THE DIP-PLATE VERSUS THE SQUARE OF THE PISTON VELOCITY

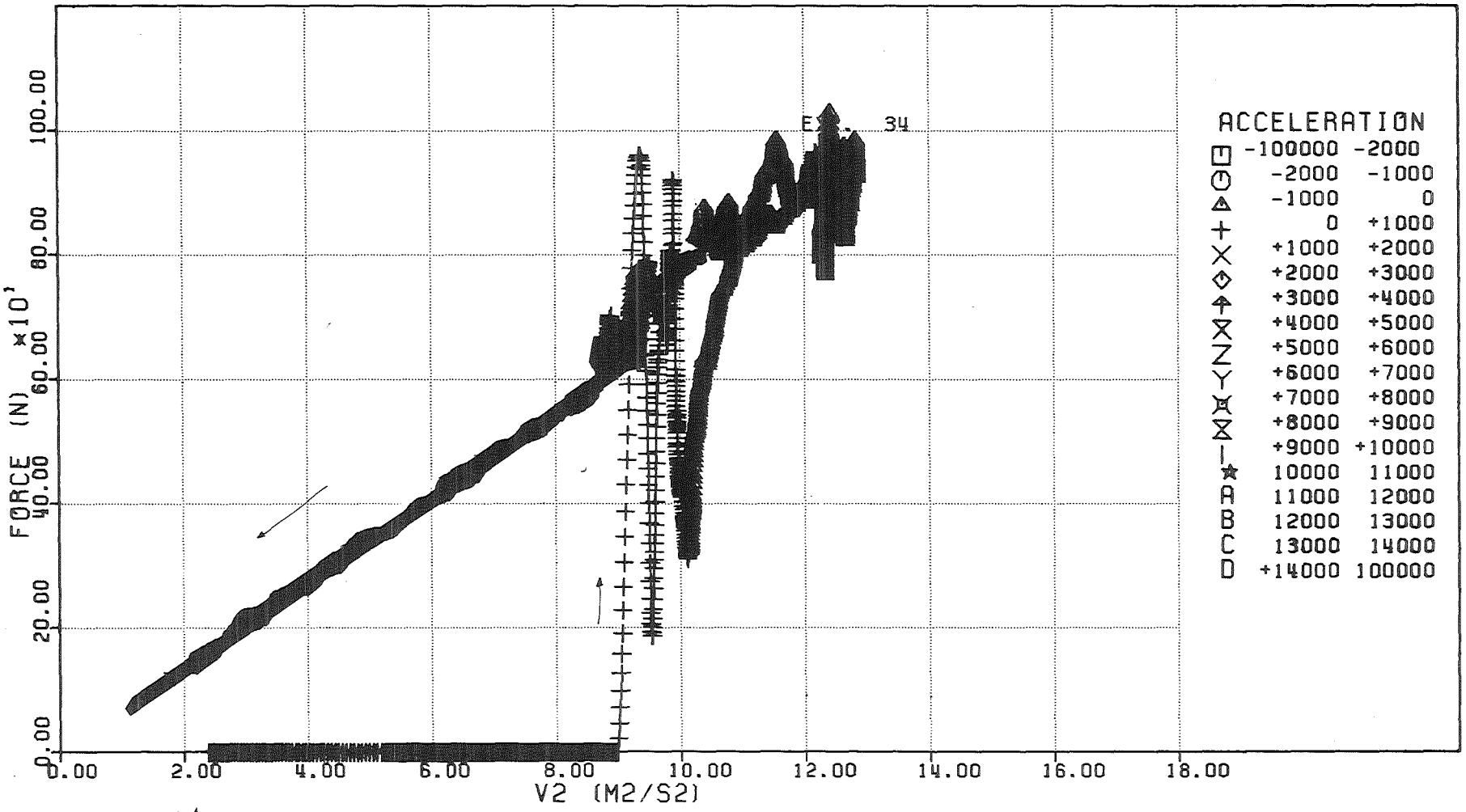

FIG. 6.23 - FORCE ACTING ON THE DIP-PLATE VERSUS THE SQUARE OF THE PISTON VELOCITY

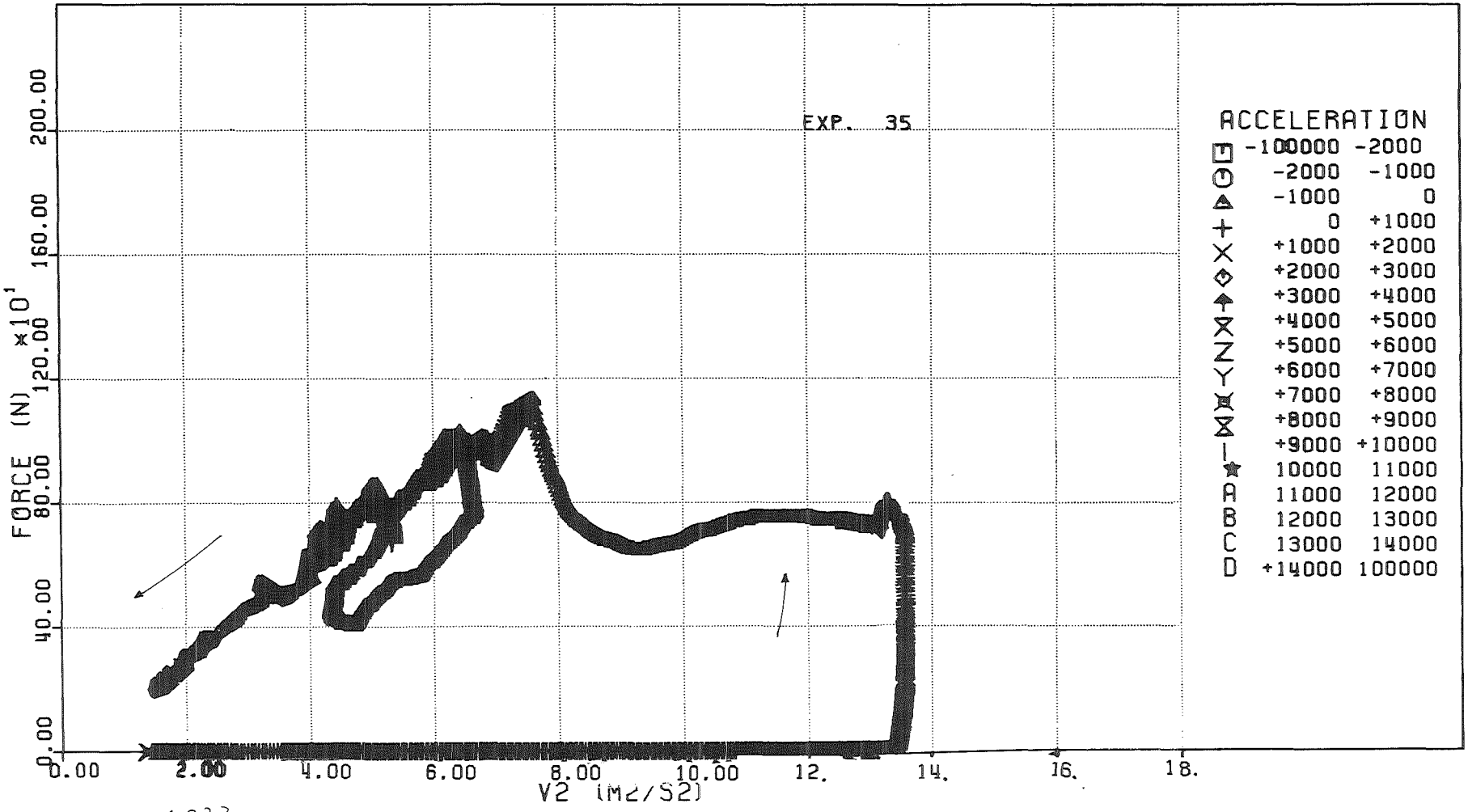

6.232

FIG. -FORCE ACTING ON THE DIP-PLATE VERSUS THE SQUARE OF THE PISTON VELOCITY

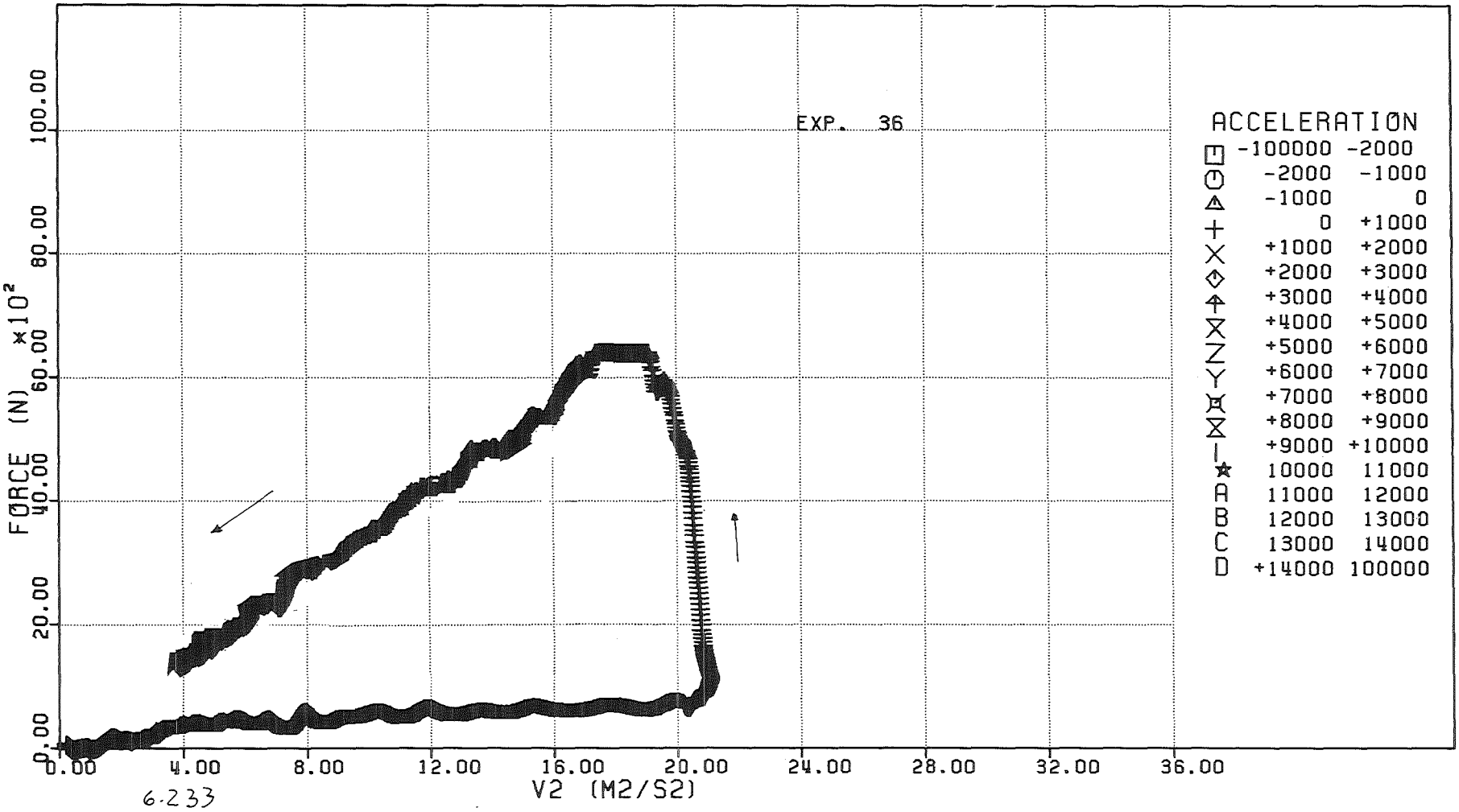

6.233

FIG. -FORCE ACTING ON THE DIP-PLATE VERSUS THE SQUARE OF THE PISTON VELOCITY

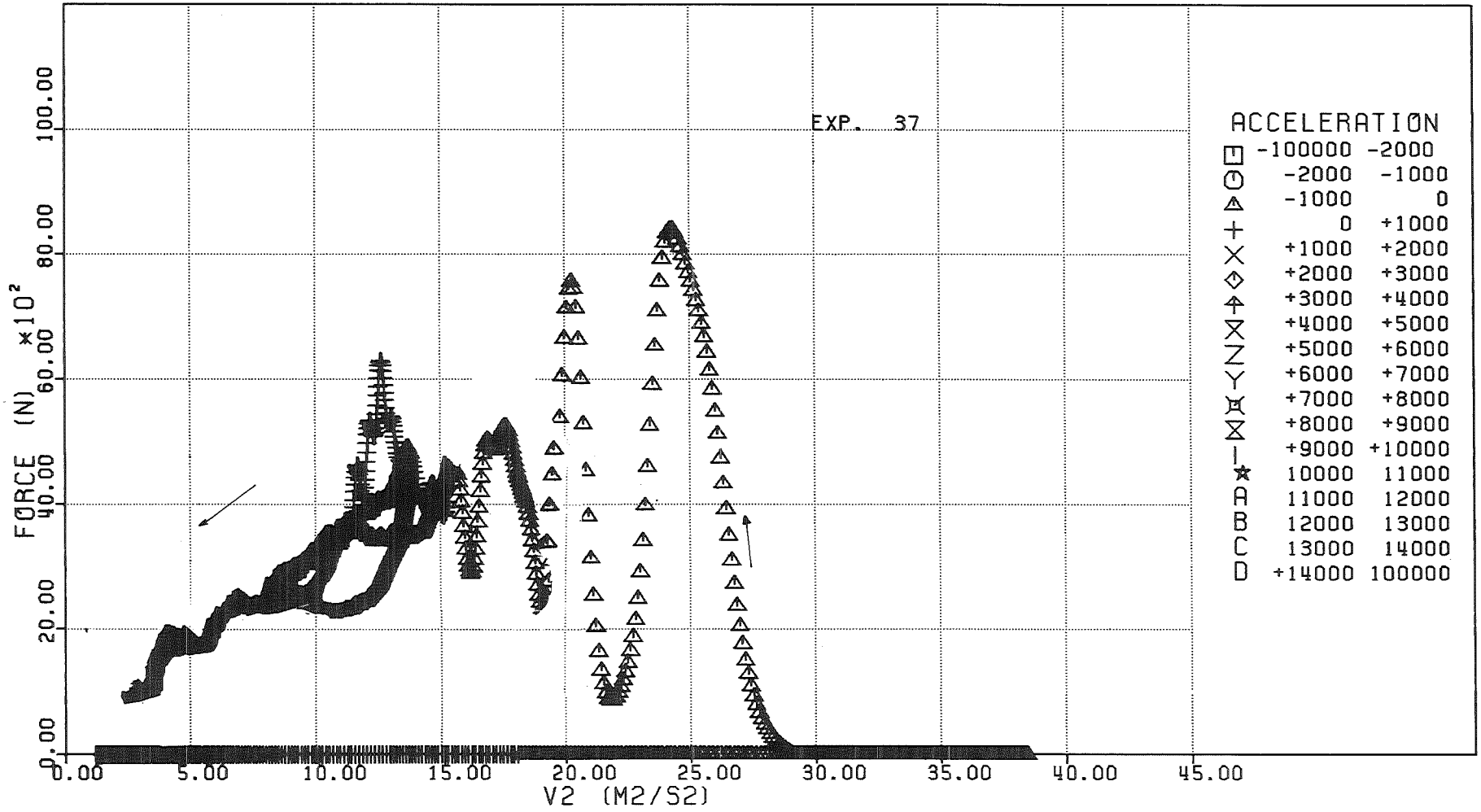

FIG. 6.234 - FORCE ACTING ON THE DIP-PLATE VERSUS THE SQUARE OF THE PISTON VELOCITY

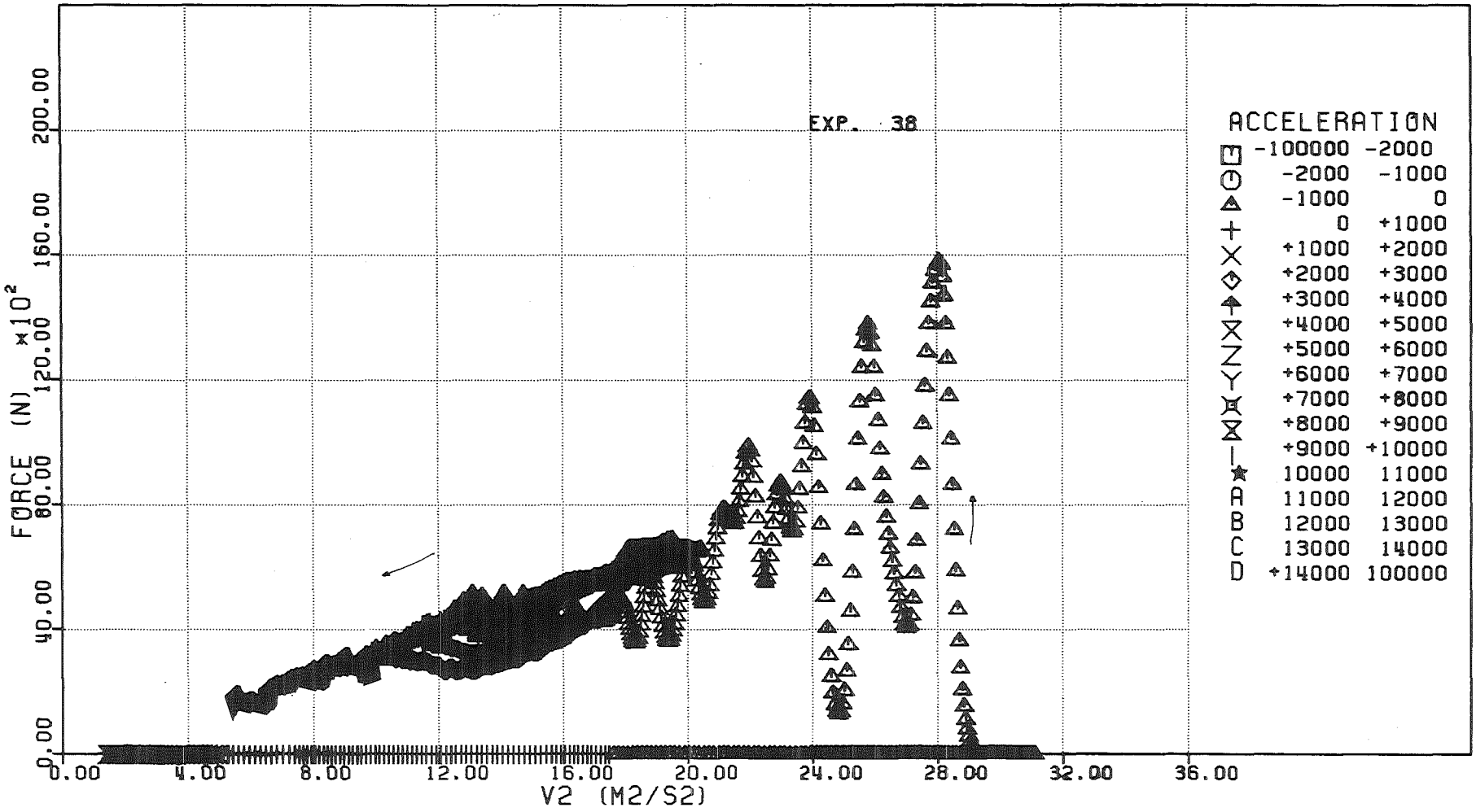

FIG. 6.235 - FORCE ACTING ON THE DIP-PLATE VERSUS THE SQUARE OF THE PISTON VELOCITY

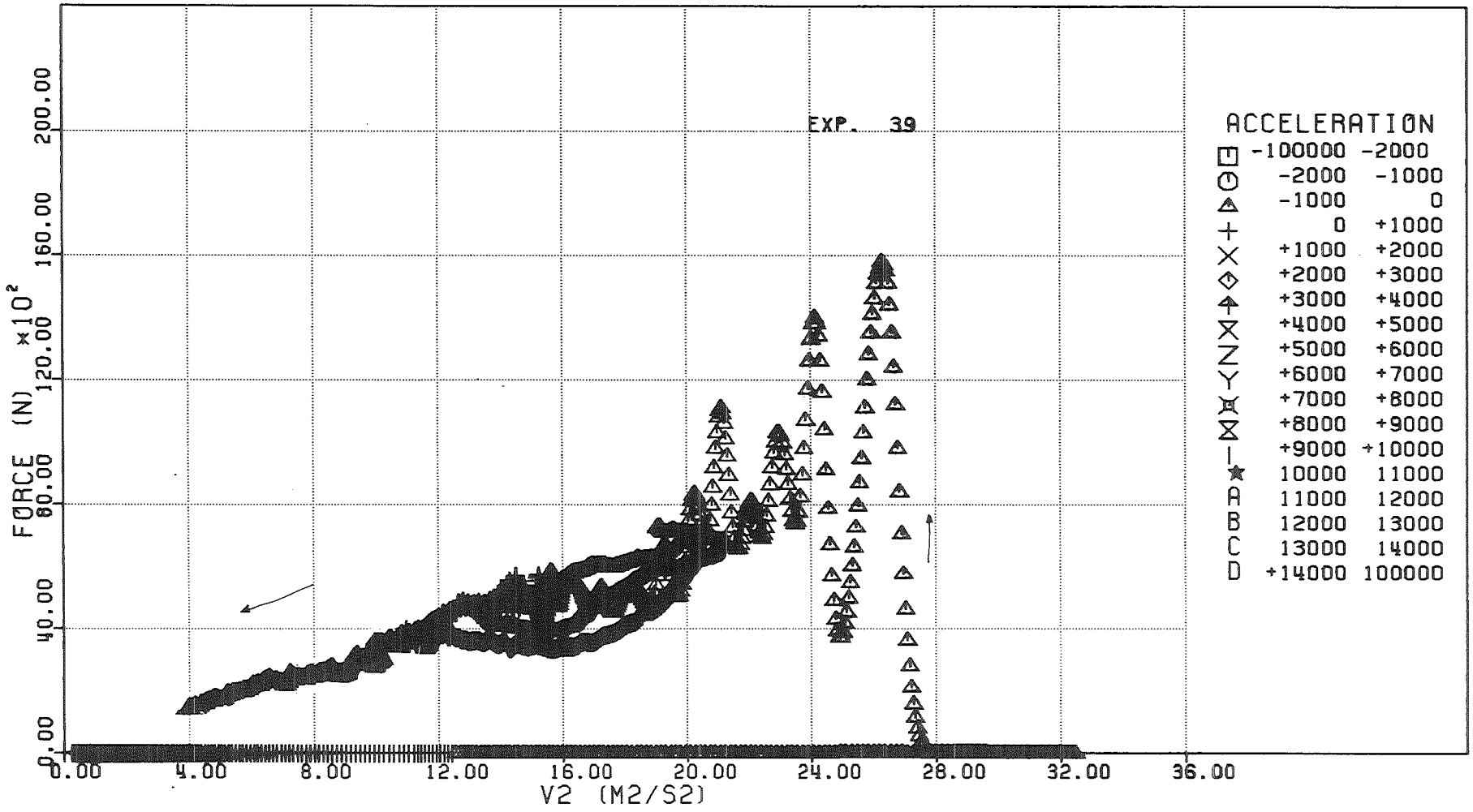

FIG. 6.236 - FORCE ACTING ON THE DIP-PLATE VERSUS THE SQUARE OF THE PISTON VELOCITY

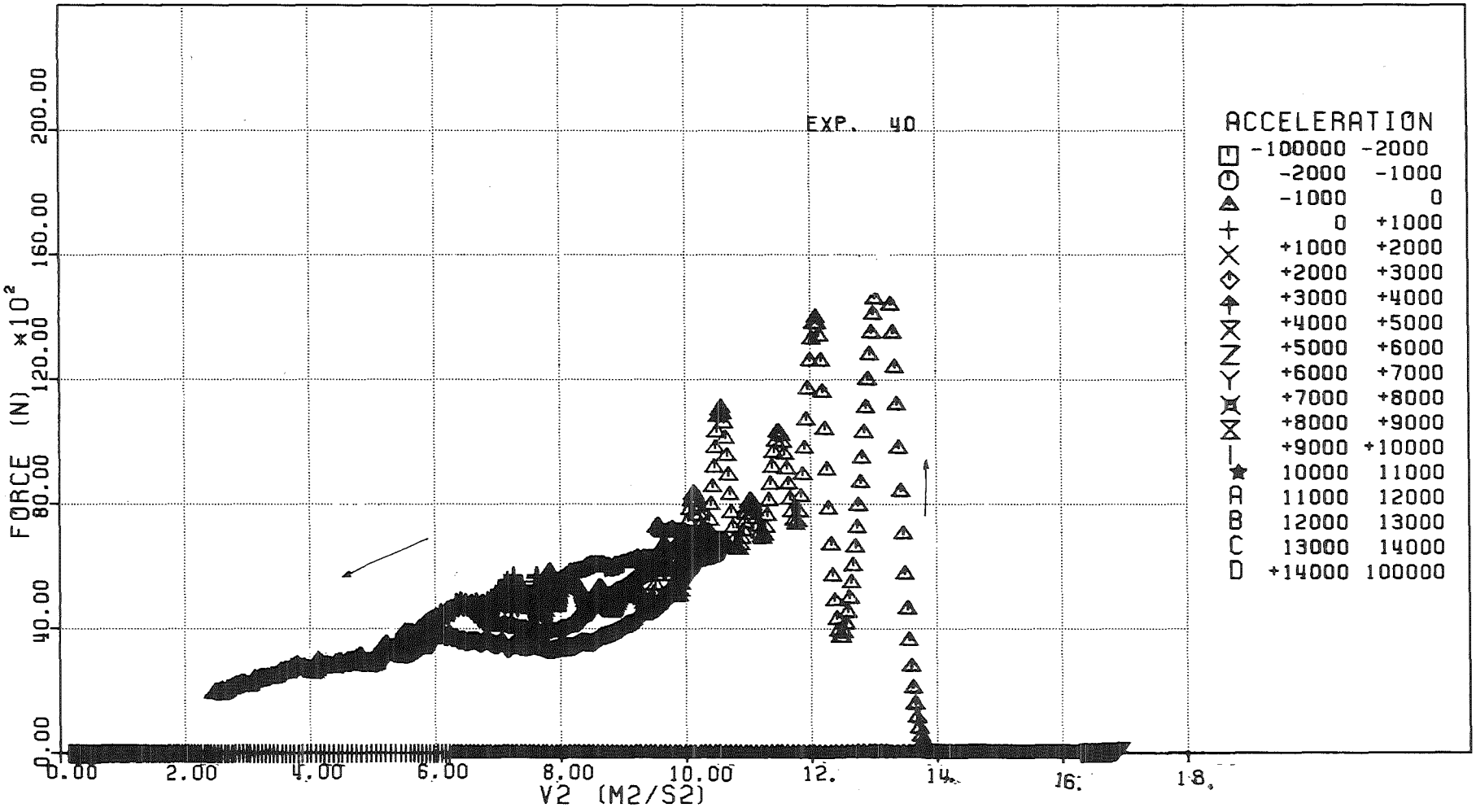

FIG. 6.237 - FORCE ACTING ON THE DIP-PLATE VERSUS THE SQUARE OF THE PISTON VELOCITY

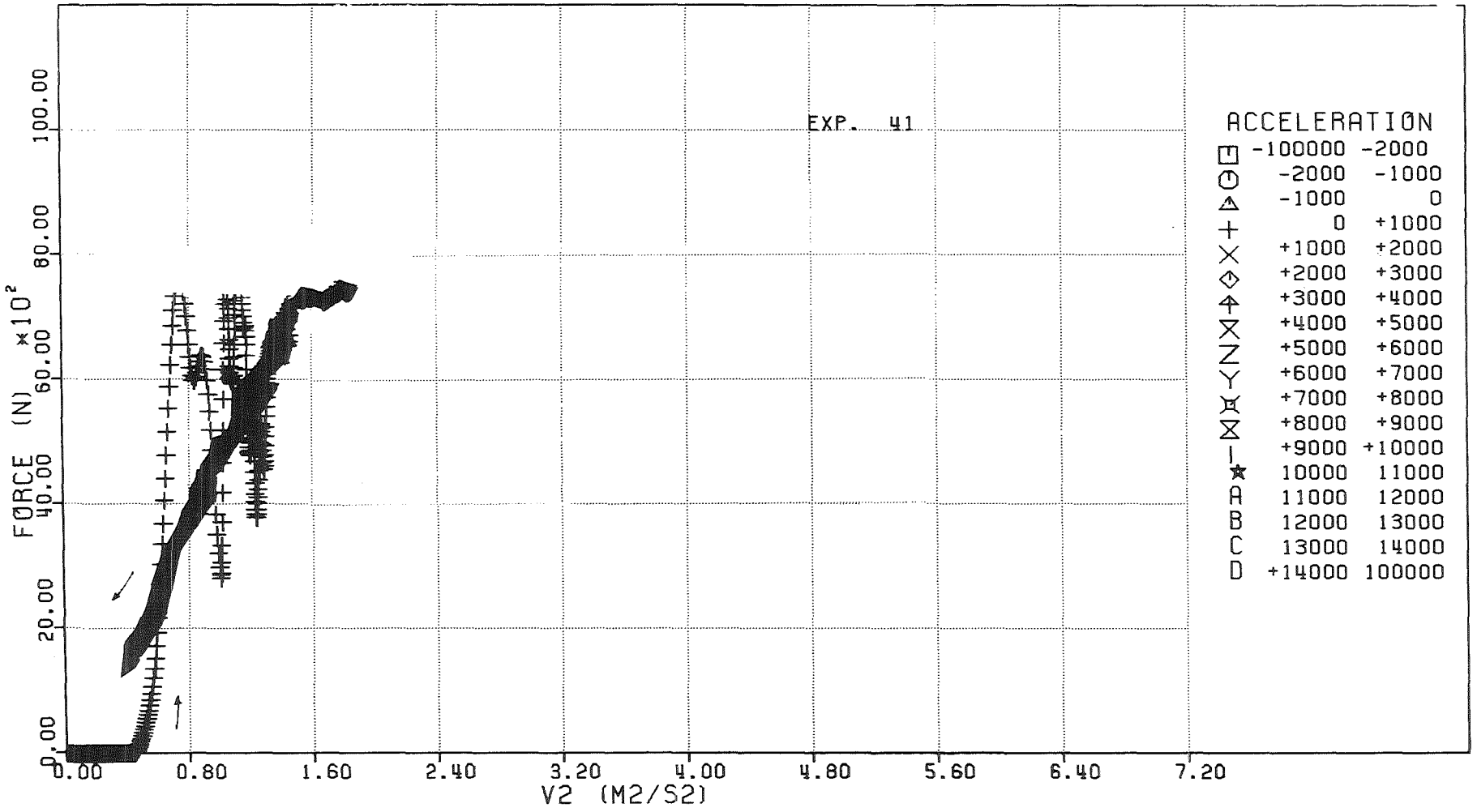

FIG. 6.238 - FORCE ACTING ON THE DIP-PLATE VERSUS THE SQUARE OF THE PISTON VELOCITY

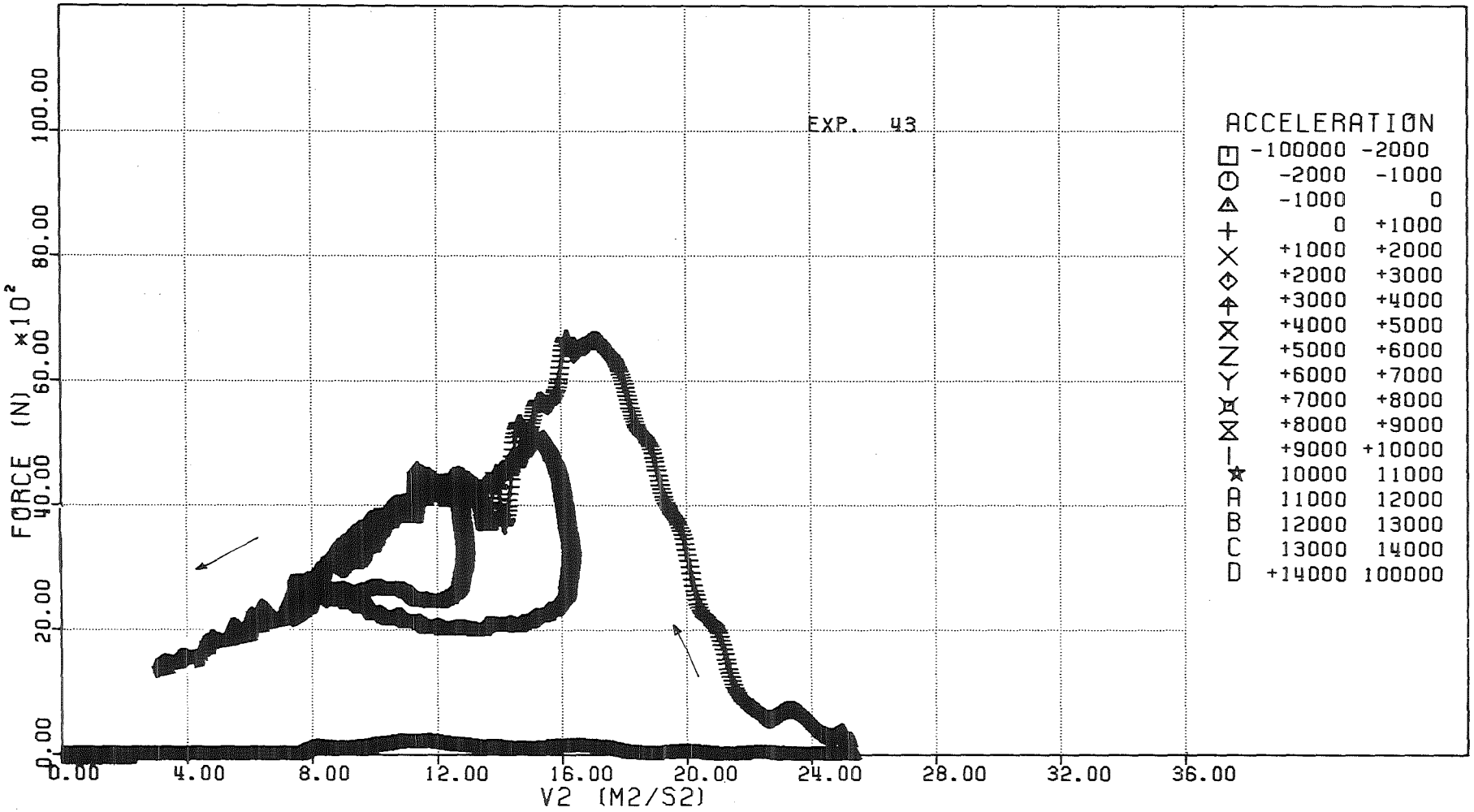

FIG. 6.239 - FORCE ACTING ON THE DIP-PLATE VERSUS THE SQUARE OF THE PISTON VELOCITY

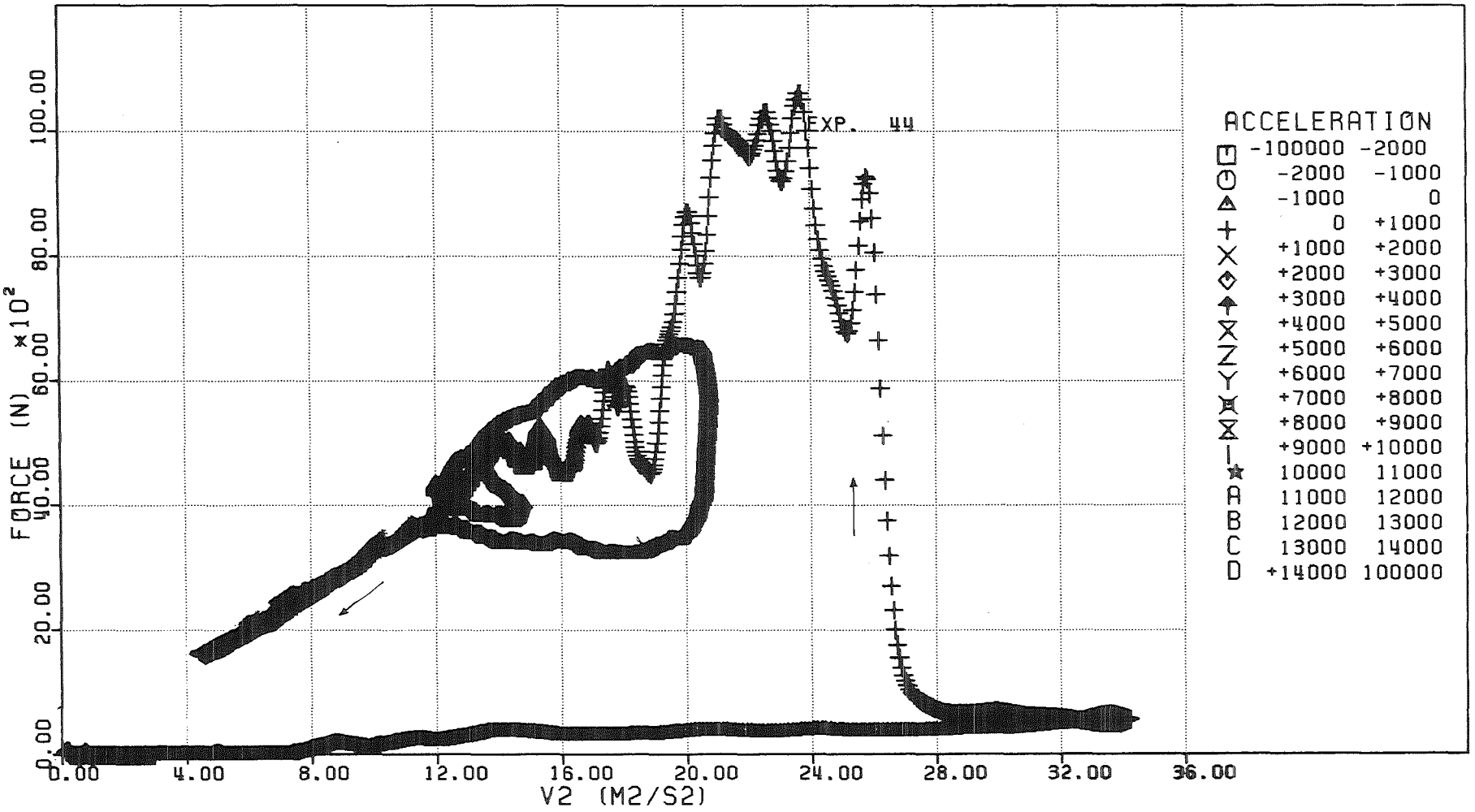

FIG. 6.240 - FORCE ACTING ON THE DIP-PLATE VERSUS THE SQUARE OF THE PISTON VELOCITY

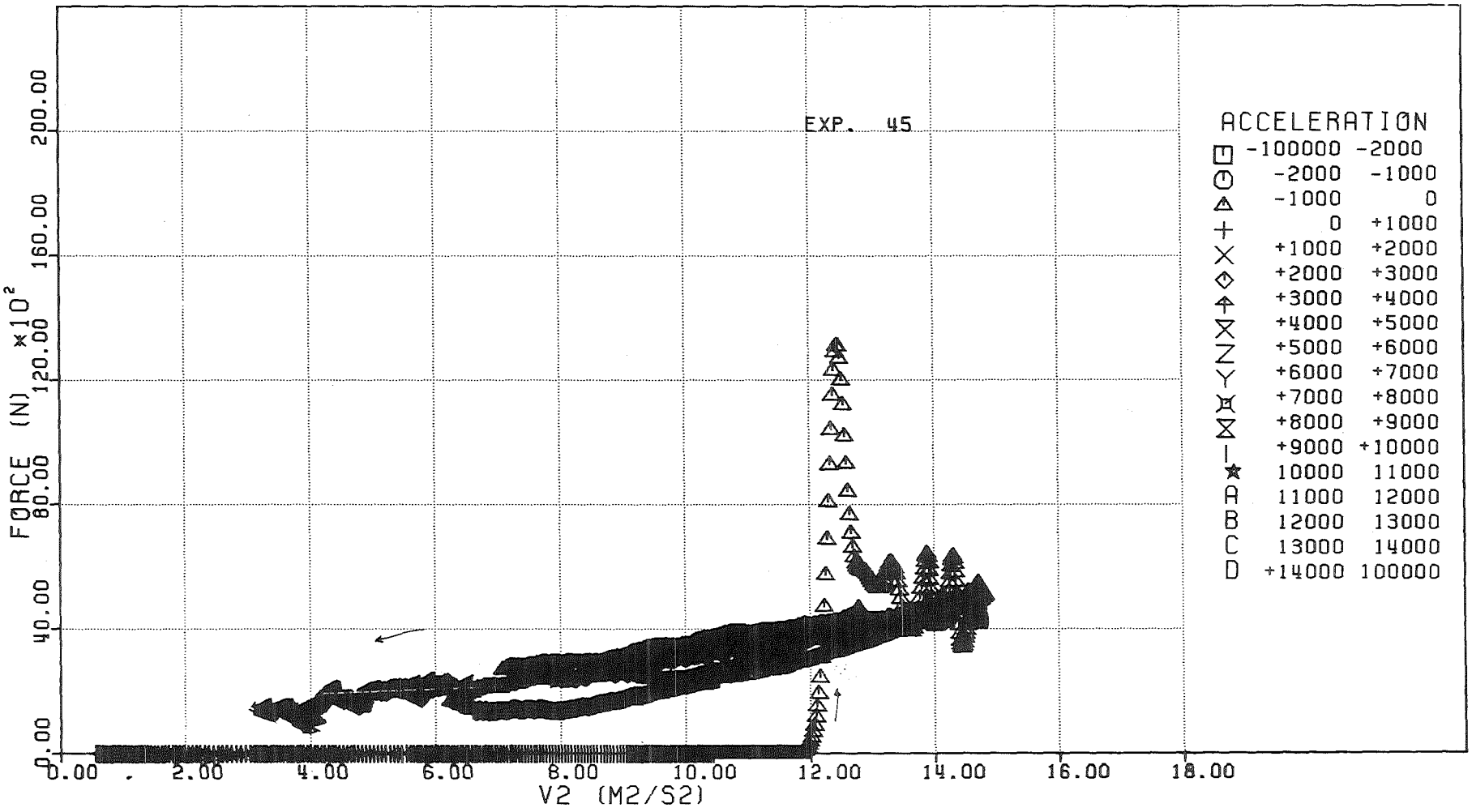

FIG. 6.241 - FORCE ACTING ON THE DIP-PLATE VERSUS THE SQUARE OF THE PISTON VELOCITY

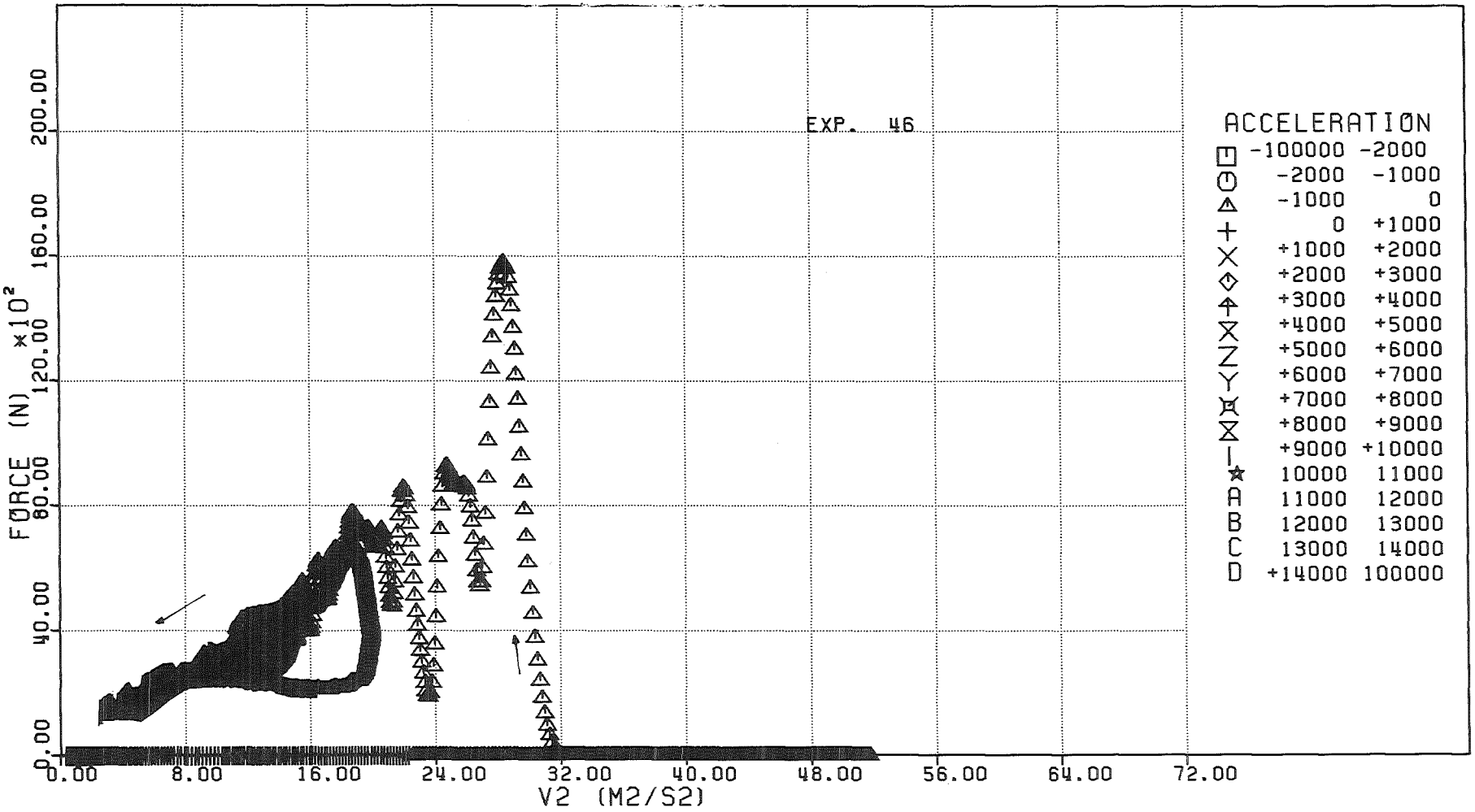

FIG. 6,242 - FORCE ACTING ON THE DIP-PLATE VERSUS THE SQUARE OF THE PISTON VELOCITY

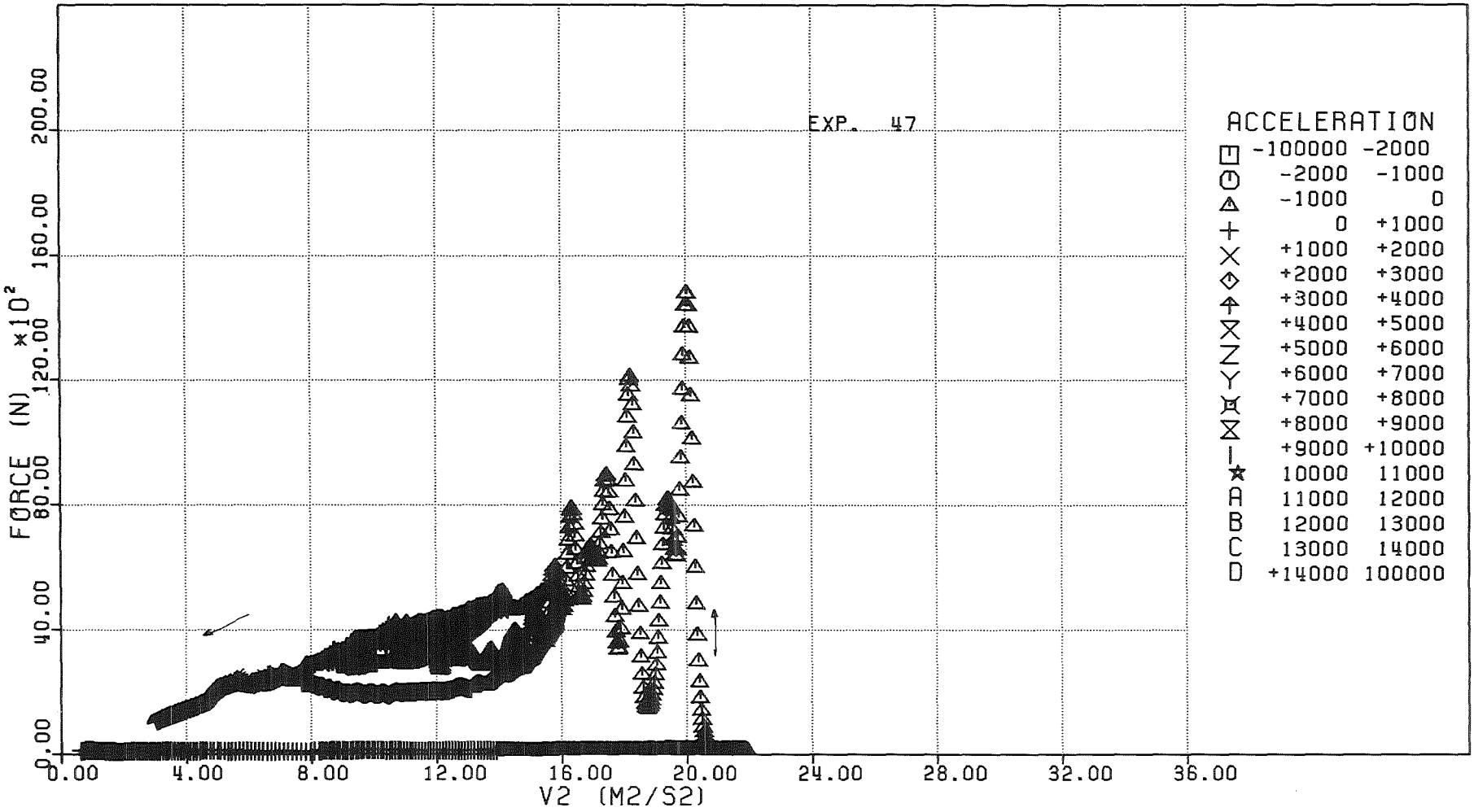

FIG. 6.243 - FORCE ACTING ON THE DIP-PLATE VERSUS THE SQUARE OF THE PISTON VELOCITY

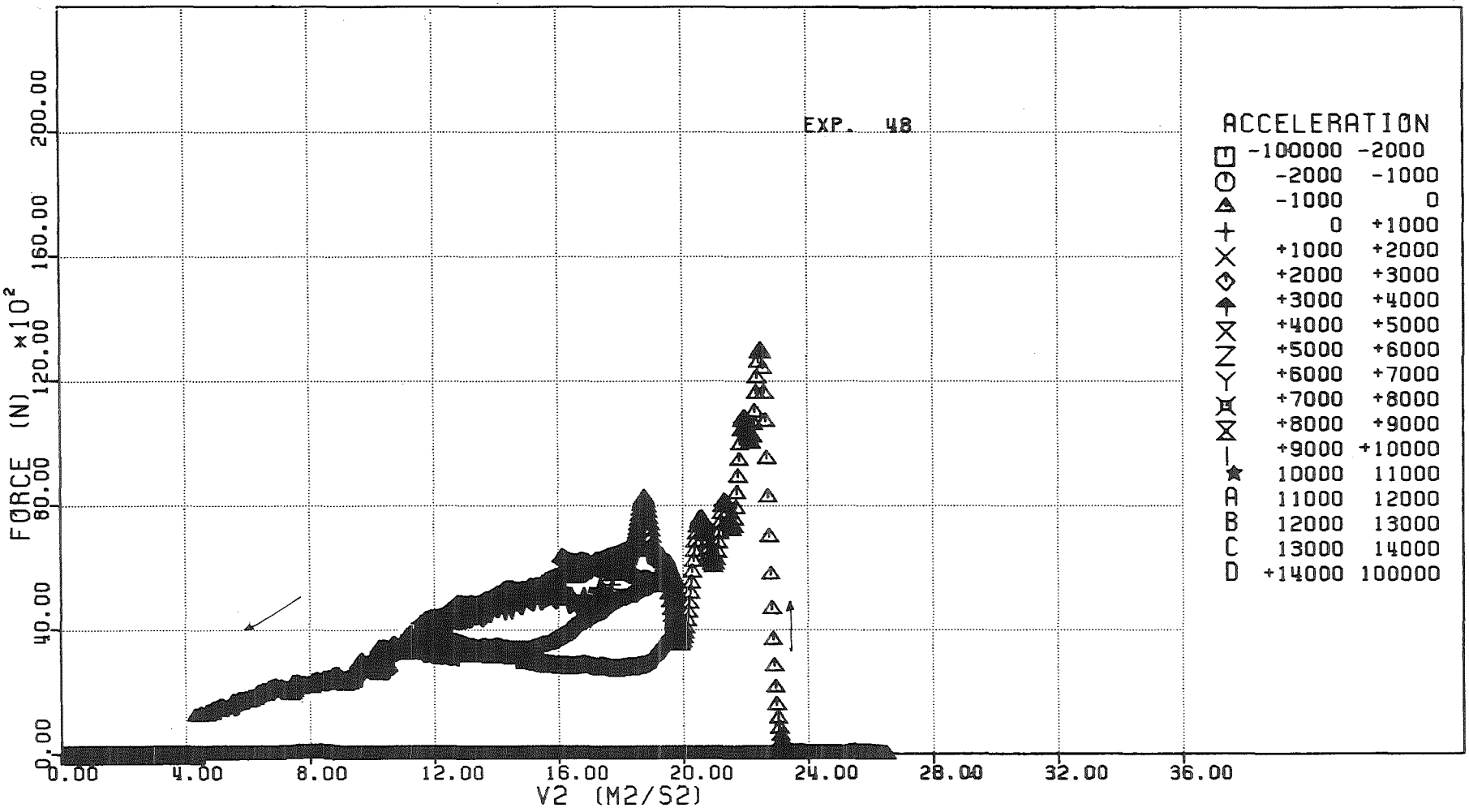

FIG. 6.244 -FORCE ACTING ON THE DIP-PLATE VERSUS THE SQUARE OF THE PISTON VELOCITY

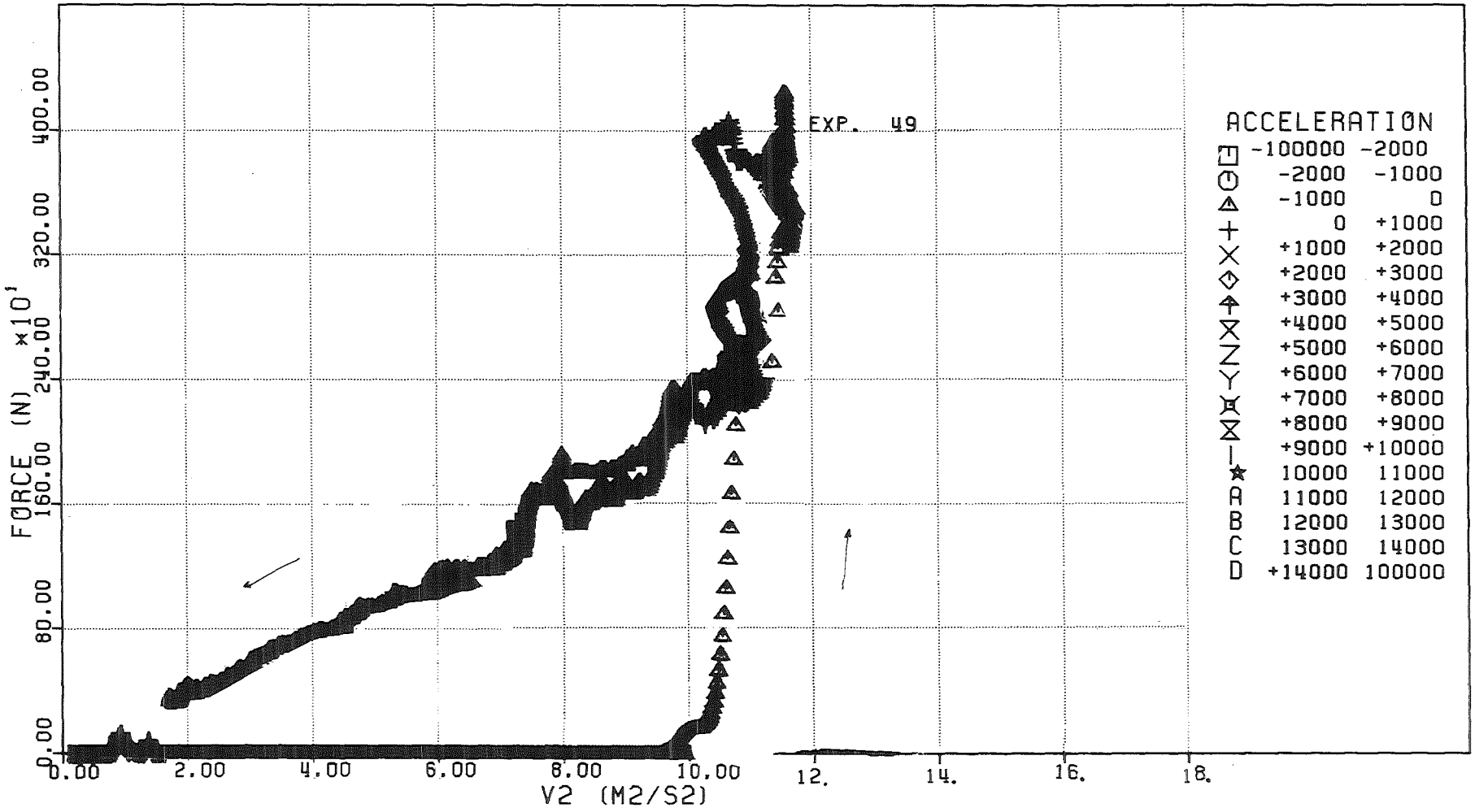

FIG. 6.245 - FORCE ACTING ON THE DIP-PLATE VERSUS THE SQUARE OF THE PISTON VELOCITY

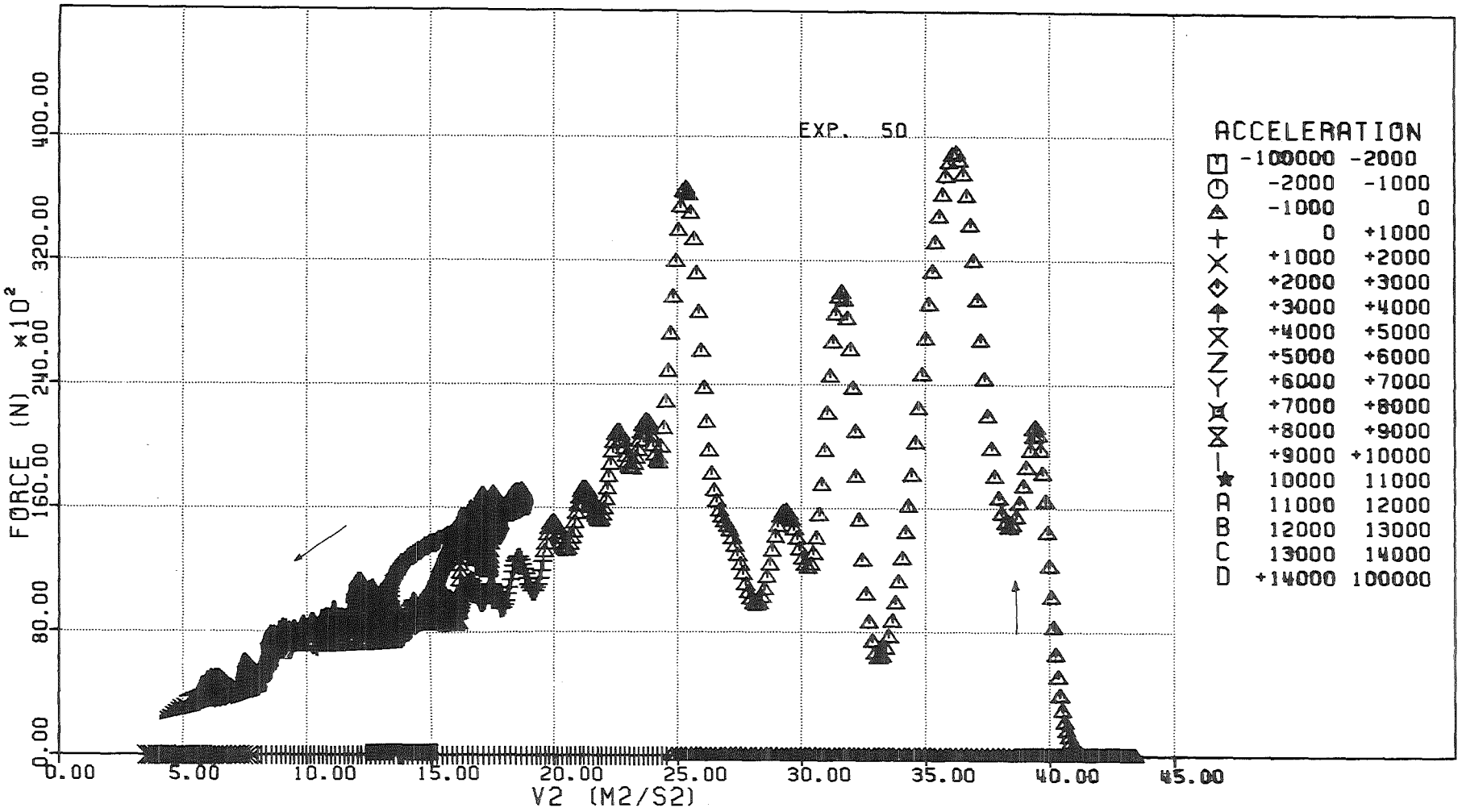

FIG. 6.246 - FORCE ACTING ON THE DIP-PLATE VERSUS THE SQUARE OF THE PISTON VELOCITY

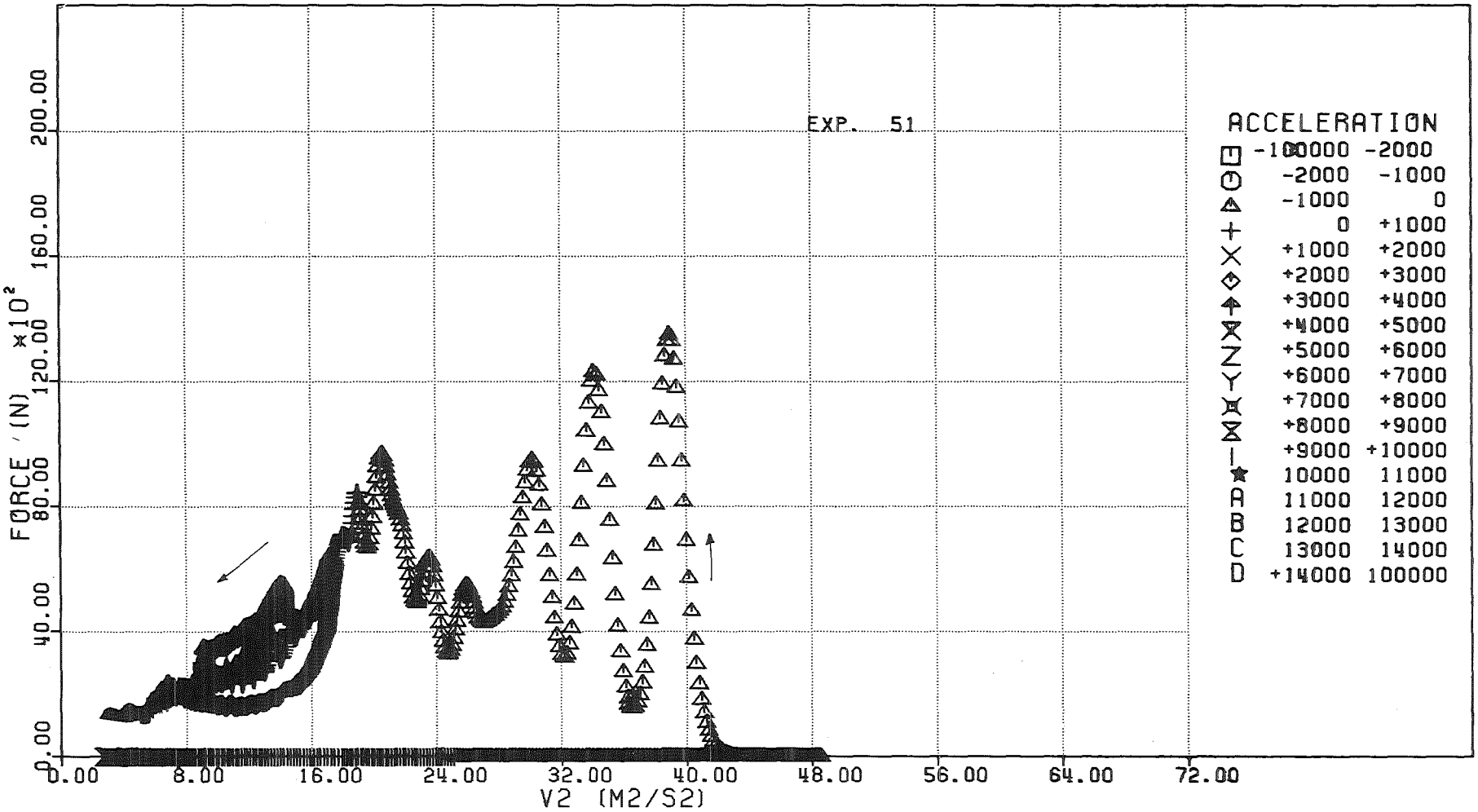

FIG. 6.247 - FORCE ACTING ON THE DIP-PLATE VERSUS THE SQUARE OF THE PISTON VELOCITY

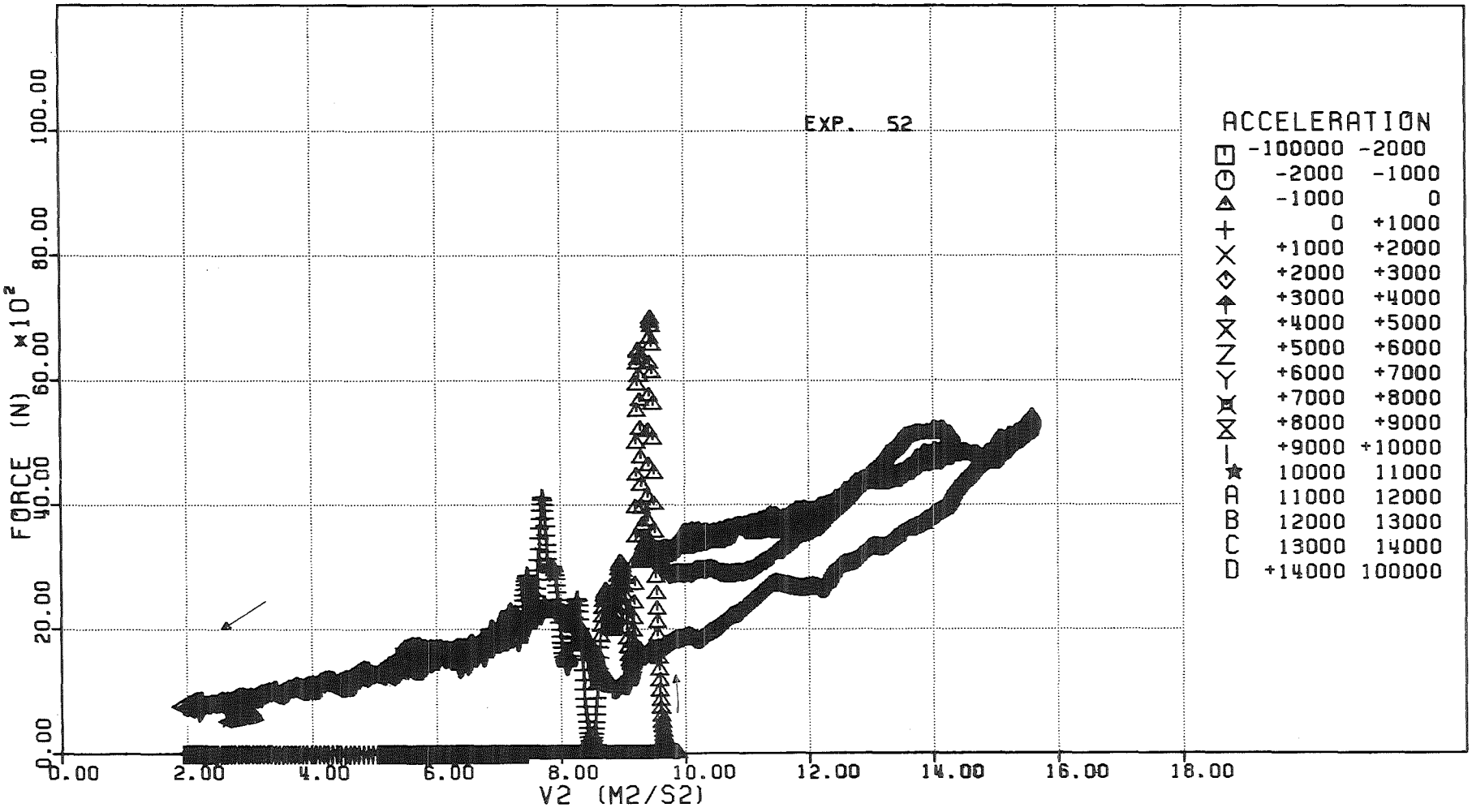

FIG. 6.24 - FORCE ACTING ON THE DIP-PLATE VERSUS THE SQUARE OF THE PISTON VELOCITY

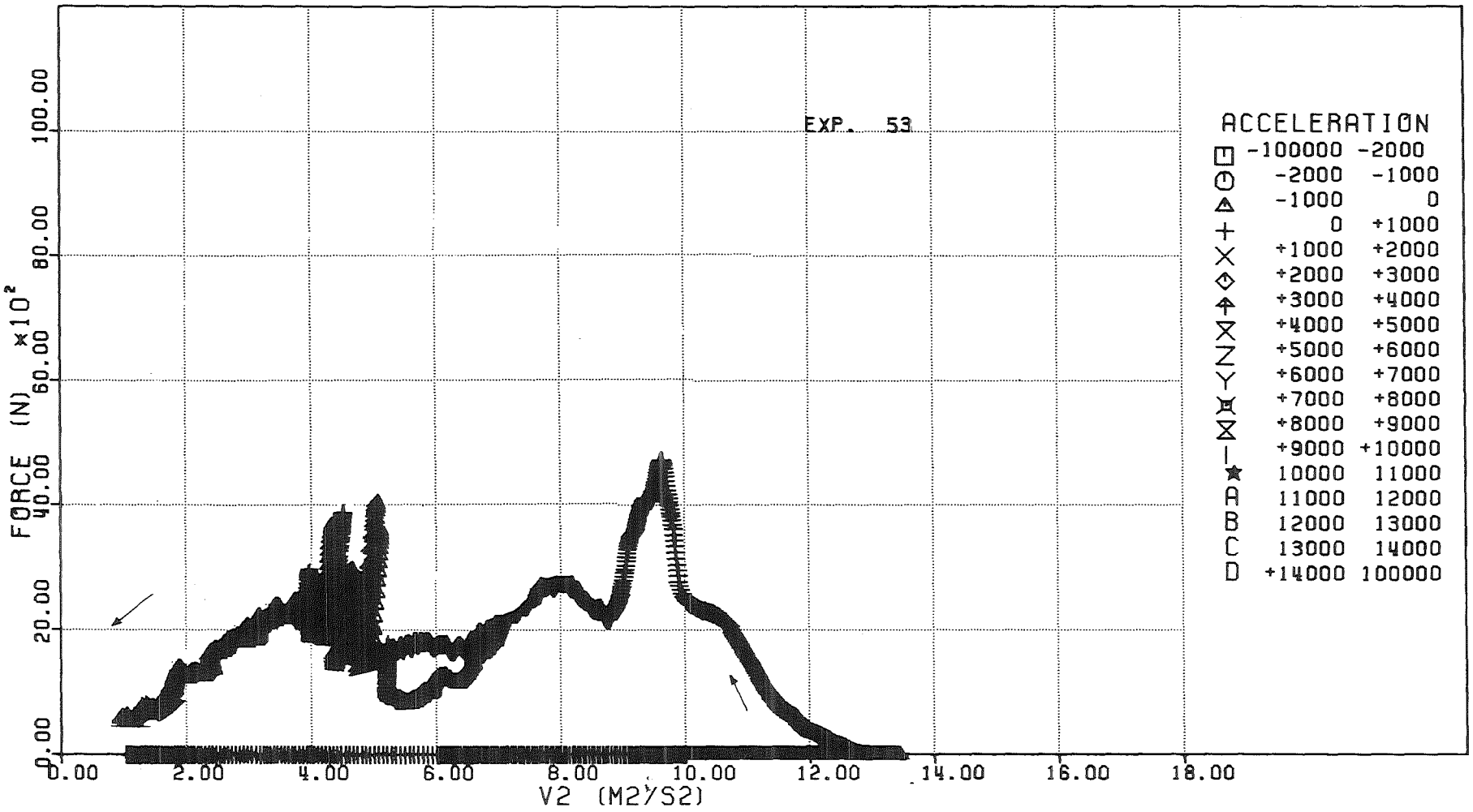

FIG. 6.249 - FORCE ACTING ON THE DIP-PLATE VERSUS THE SQUARE OF THE PISTON VELOCITY

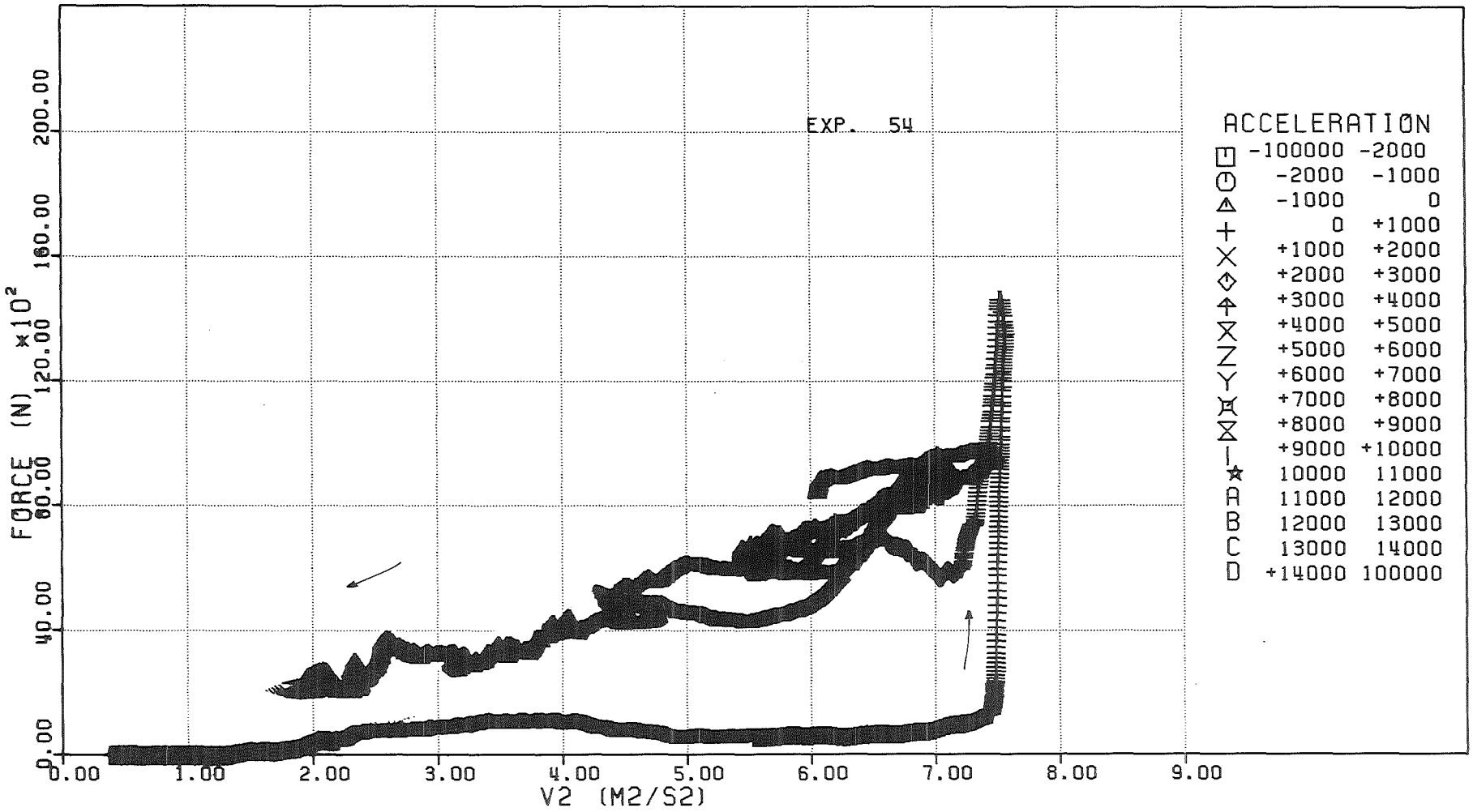

FIG. 6.250 - FORCE ACTING ON THE DIP-PLATE VERSUS THE SQUARE OF THE PISTON VELOCITY

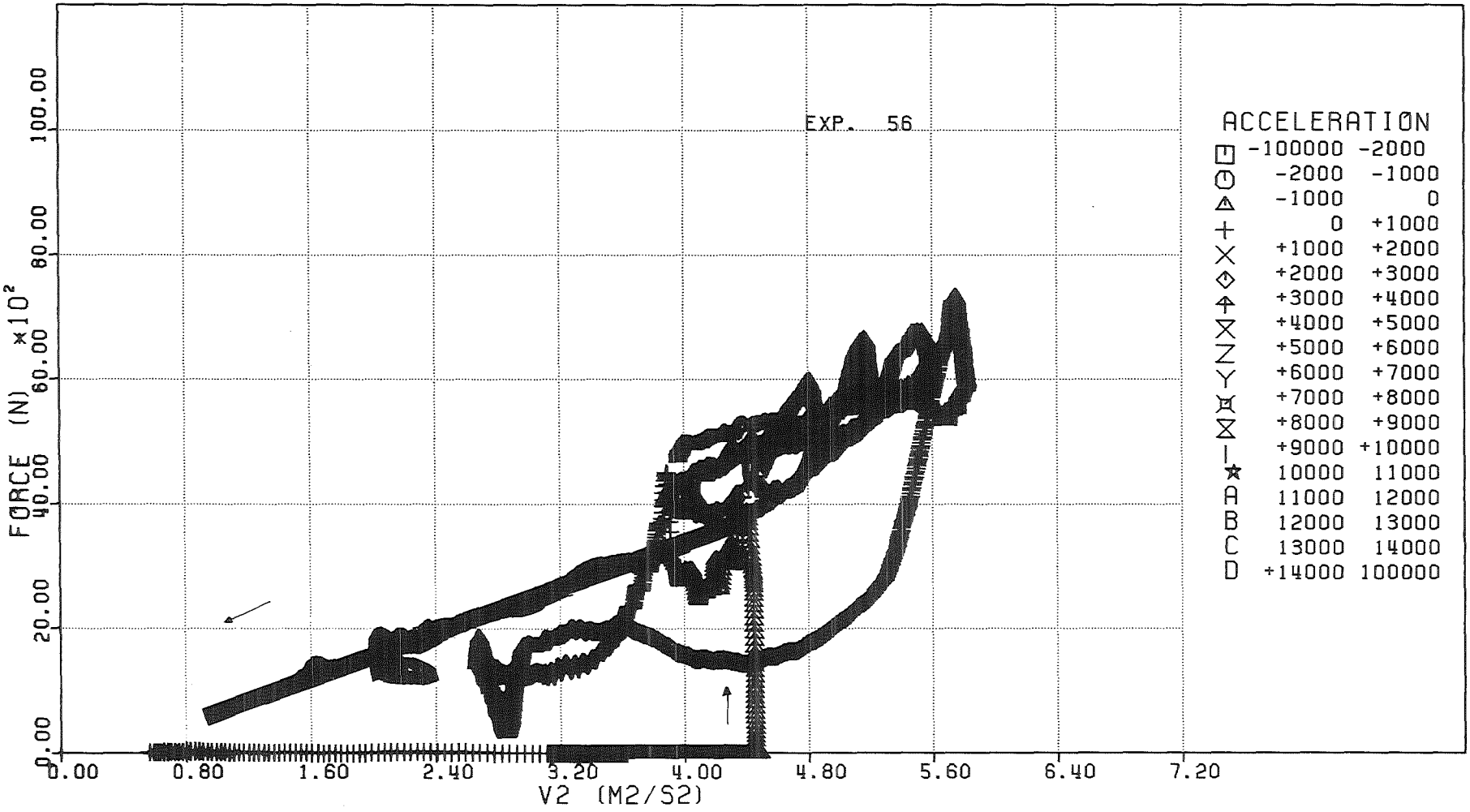

FIG. 6.251 - FORCE ACTING ON THE DIP-PLATE VERSUS THE SQUARE OF THE PISTON VELOCITY

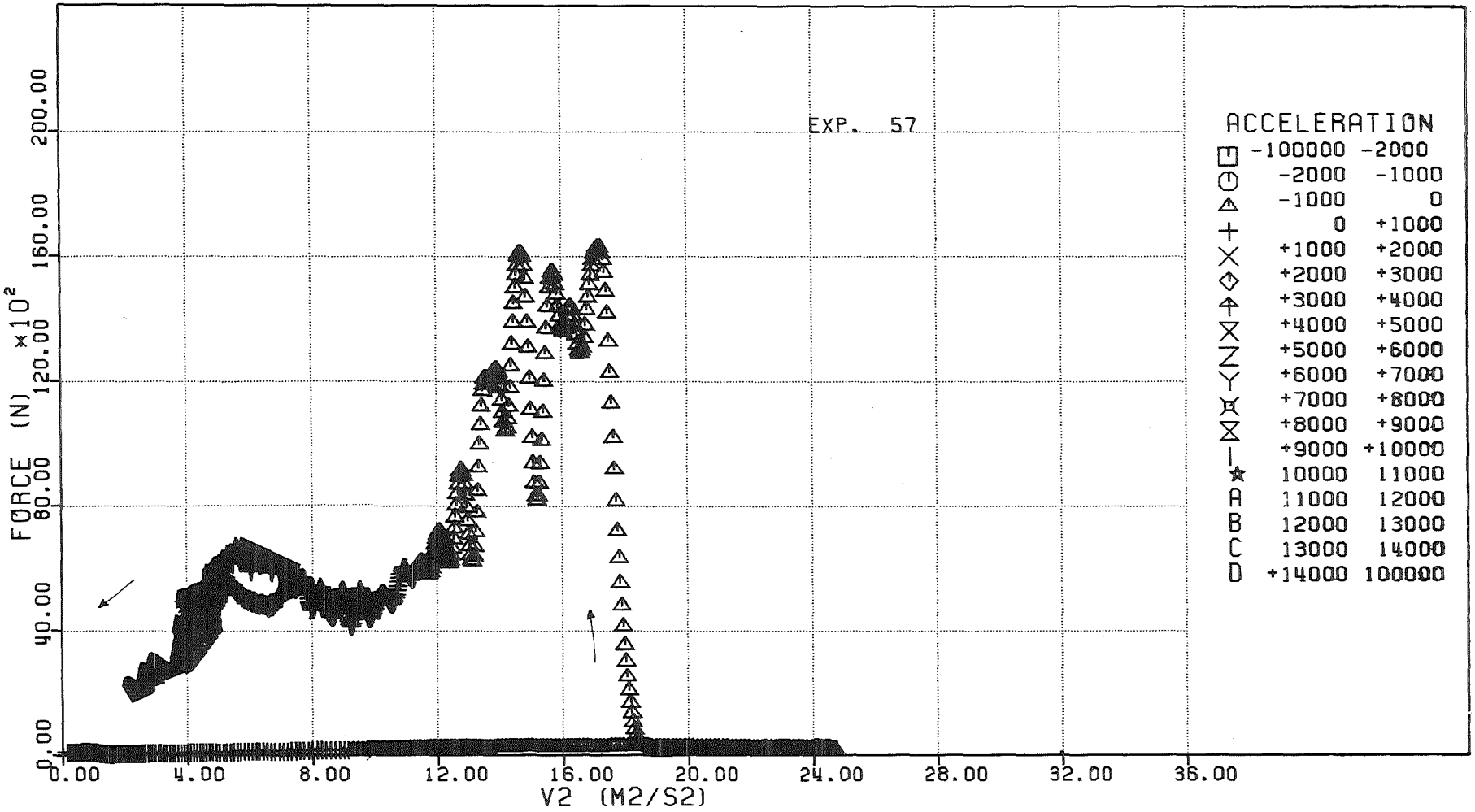

FIG. 6.252 - FORCE ACTING ON THE DIP-PLATE VERSUS THE SQUARE OF THE PISTON VELOCITY

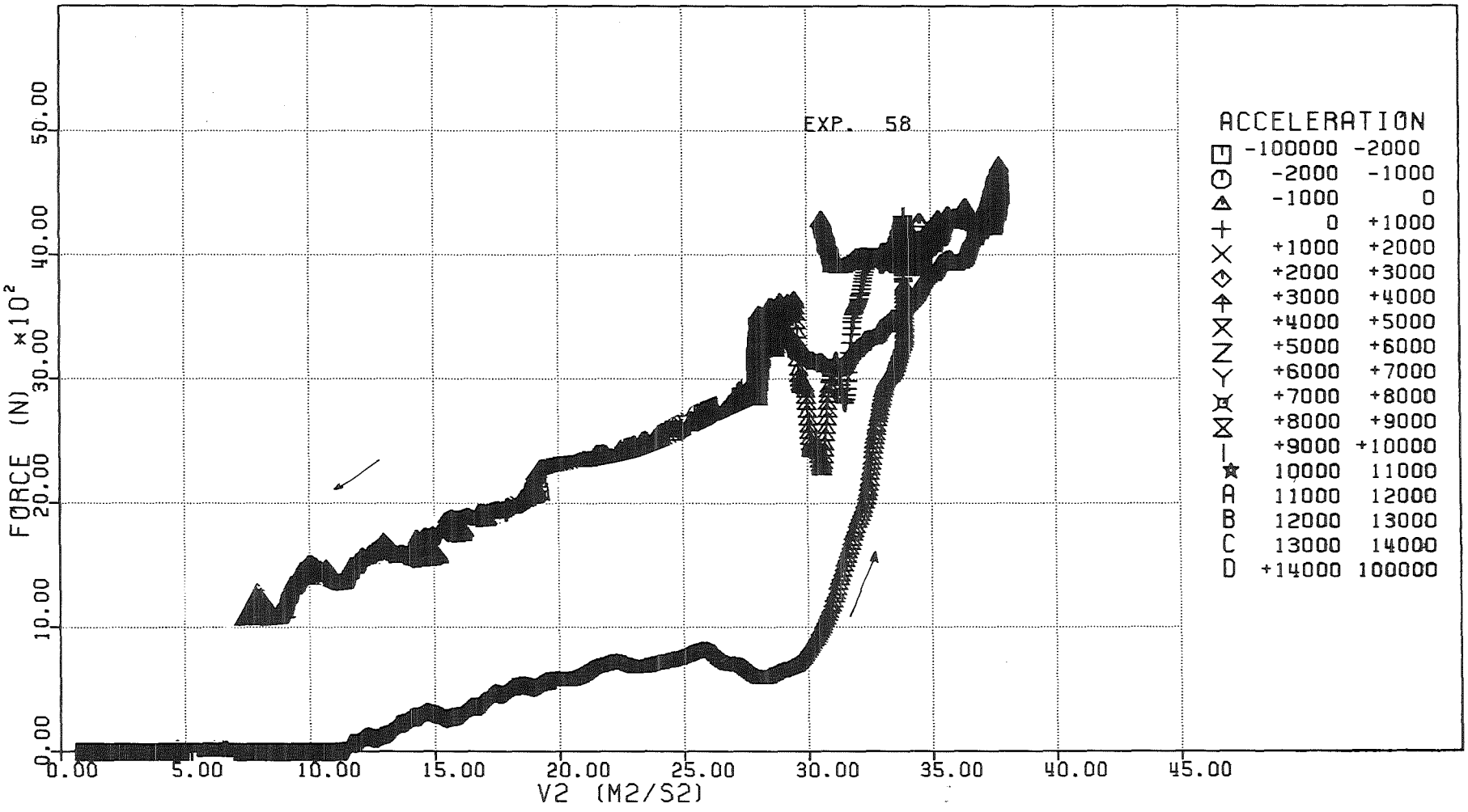

FIG. 6.253 - FORCE ACTING ON THE DIP-PLATE VERSUS THE SQUARE OF THE PISTON VELOCITY

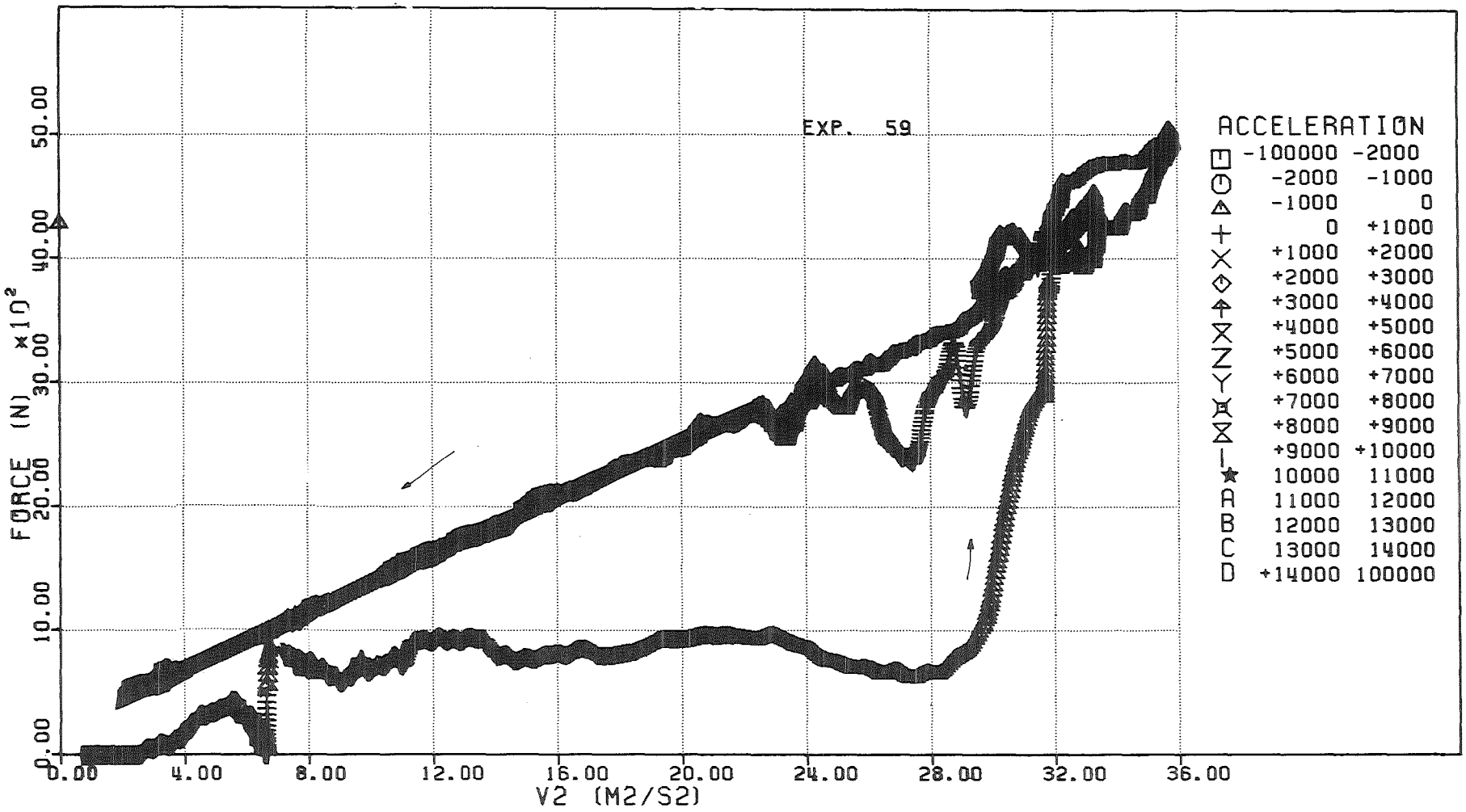

FIG. 6.254 - FORCE ACTING ON THE DIP-PLATE VERSUS THE SQUARE OF THE PISTON VELOCITY

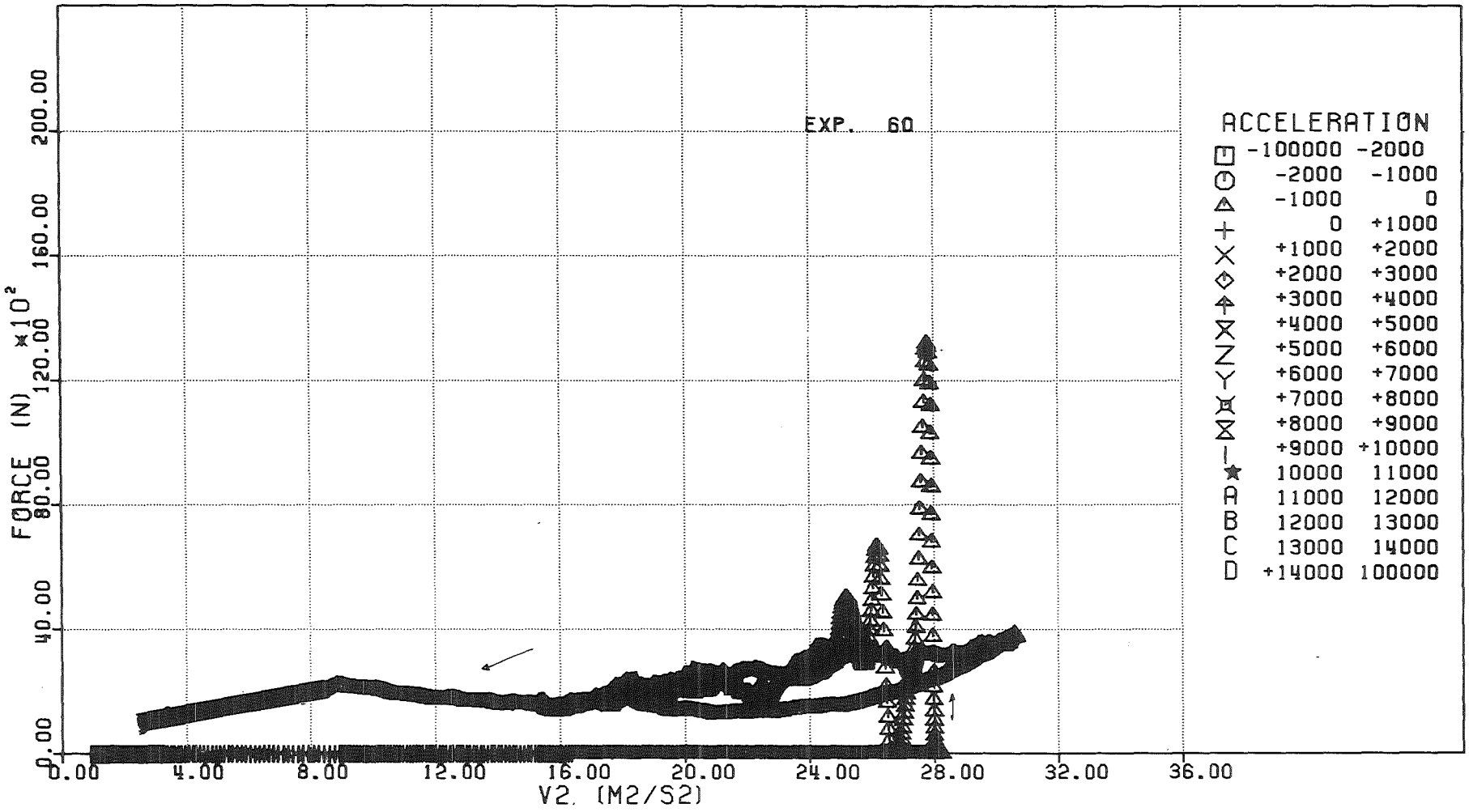

FIG. 6.255 - FORCE ACTING ON THE DIP-PLATE VERSUS THE SQUARE OF THE PISTON VELOCITY

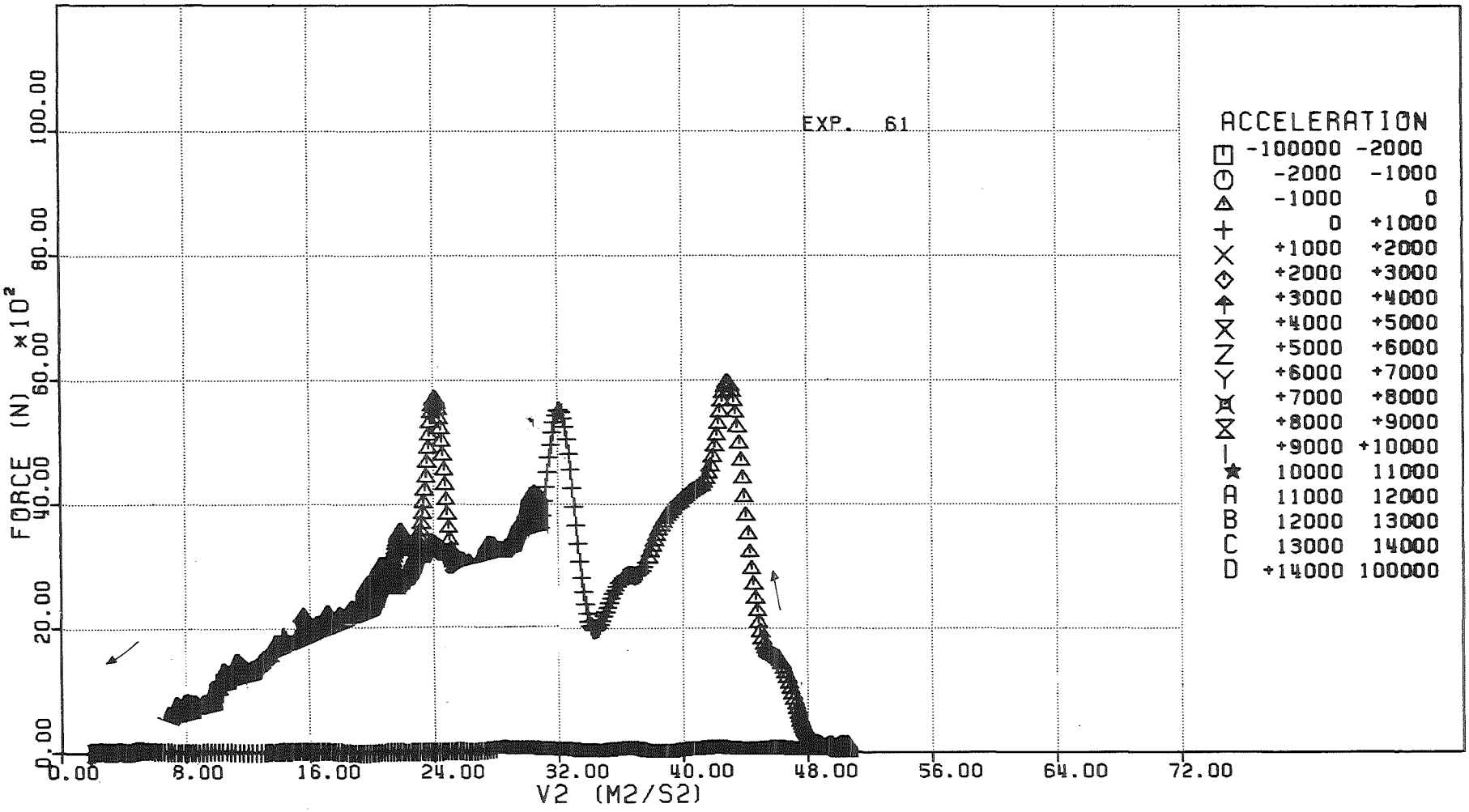

FIG. 6.256 - FORCE ACTING ON THE DIP-PLATE VERSUS THE SQUARE OF THE PISTON VELOCITY

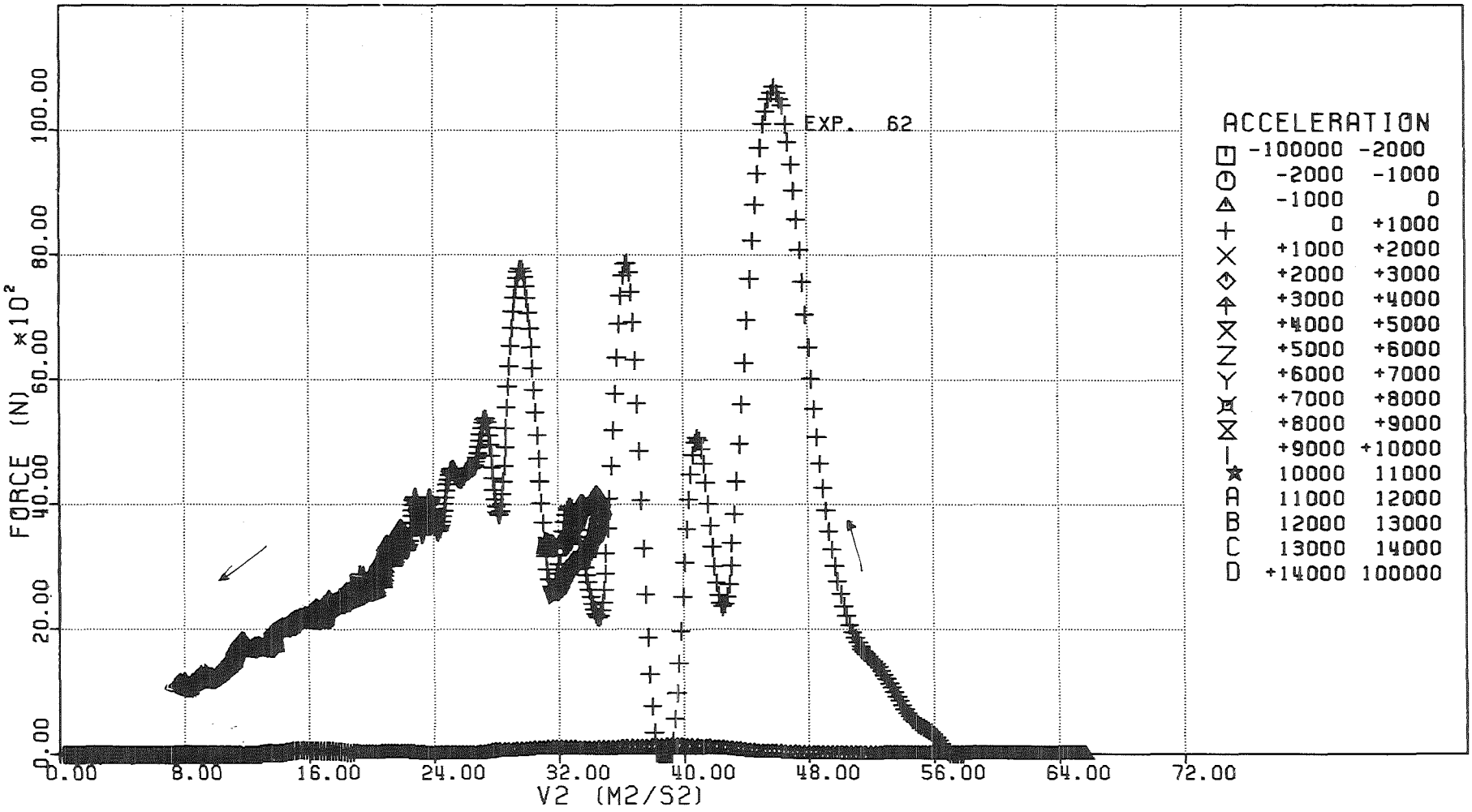

FIG. 6.257 - FORCE ACTING ON THE DIP-PLATE VERSUS THE SQUARE OF THE PISTON VELOCITY

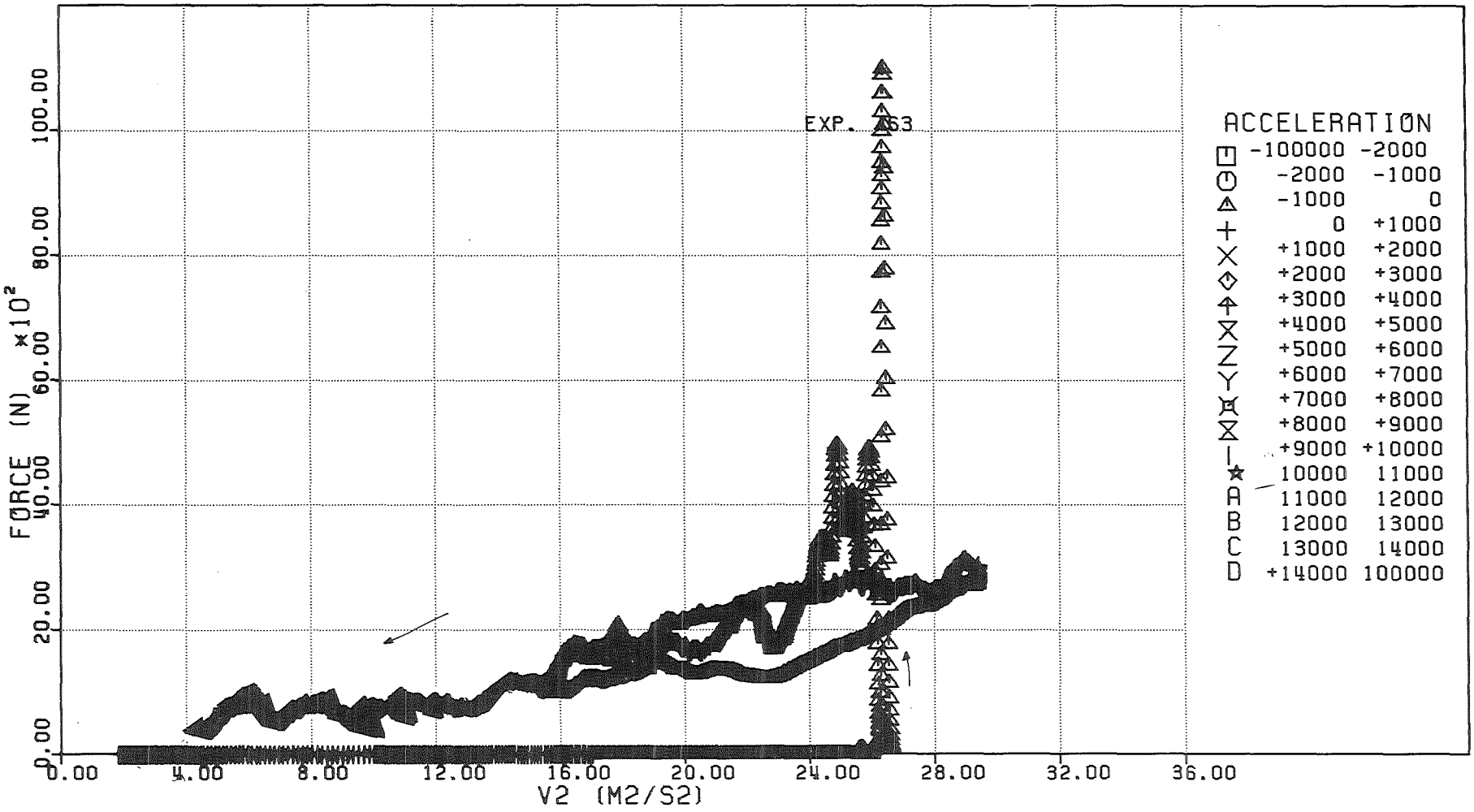

FIG. 6.258 - FORCE ACTING ON THE DIP-PLATE VERSUS THE SQUARE OF THE PISTON VELOCITY

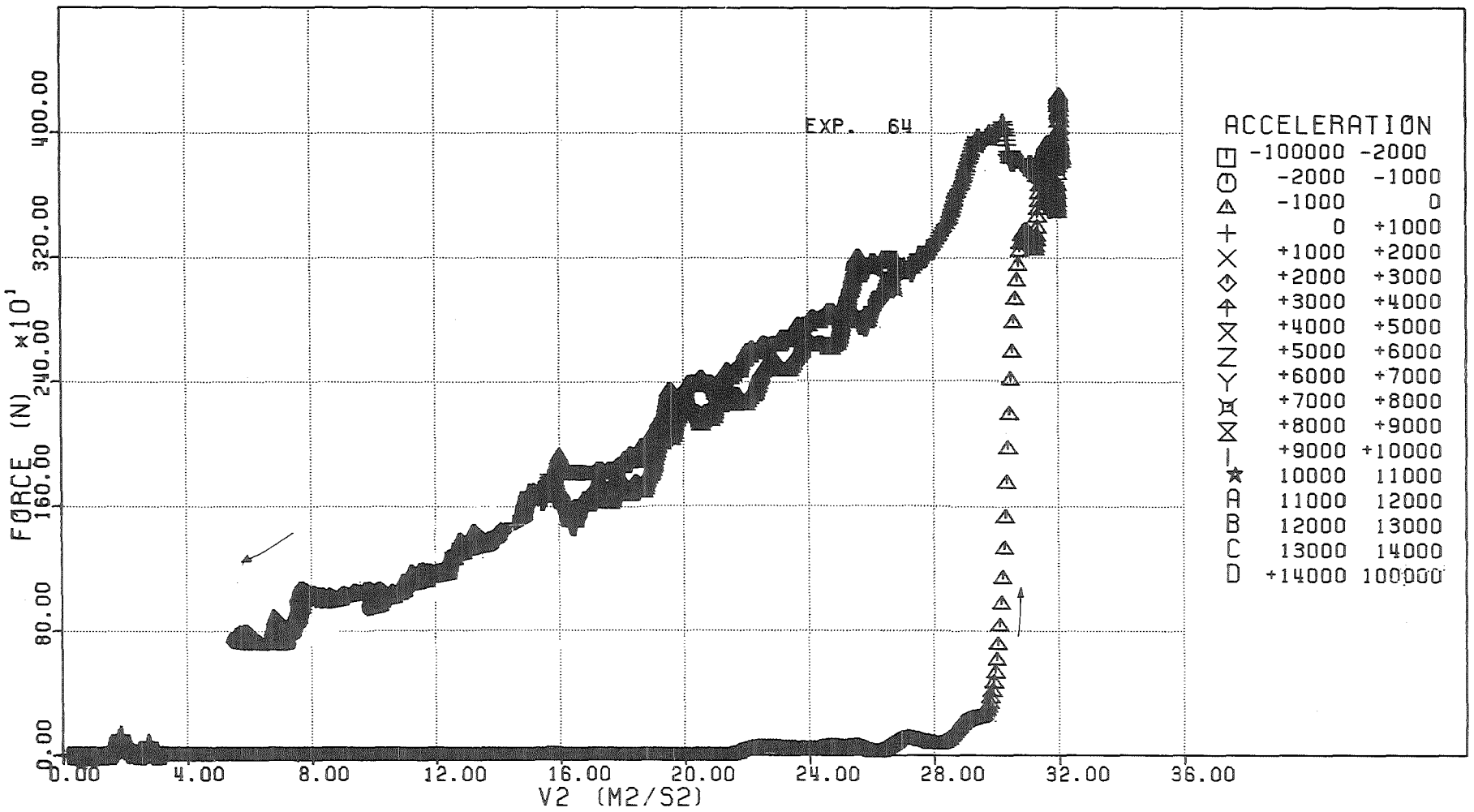

FIG. 6.259 - FORCE ACTING ON THE DIP-PLATE VERSUS THE SQUARE OF THE PISTON VELOCITY

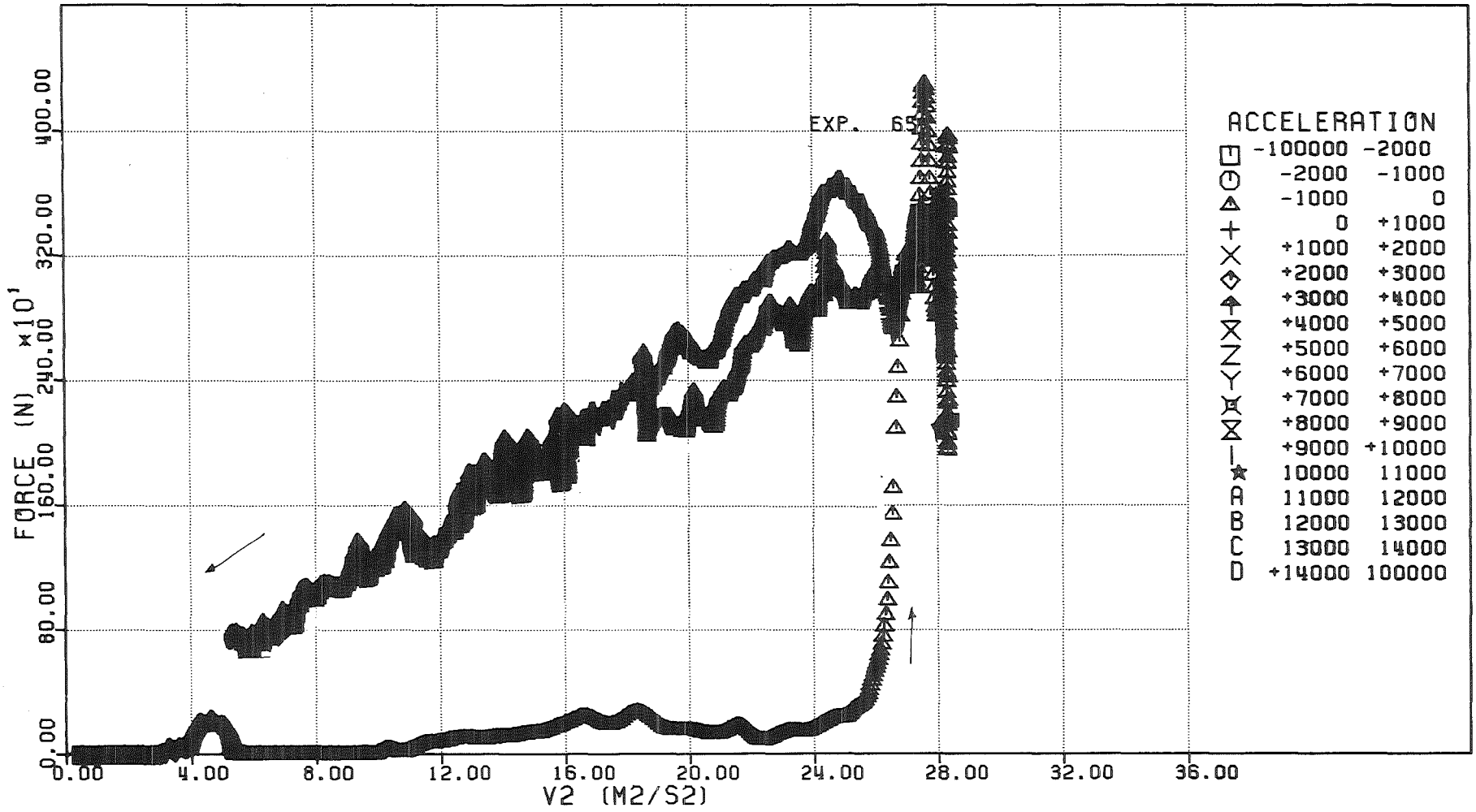

FIG. 6.260 - FORCE ACTING ON THE DIP-PLATE VERSUS THE SQUARE OF THE PISTON VELOCITY

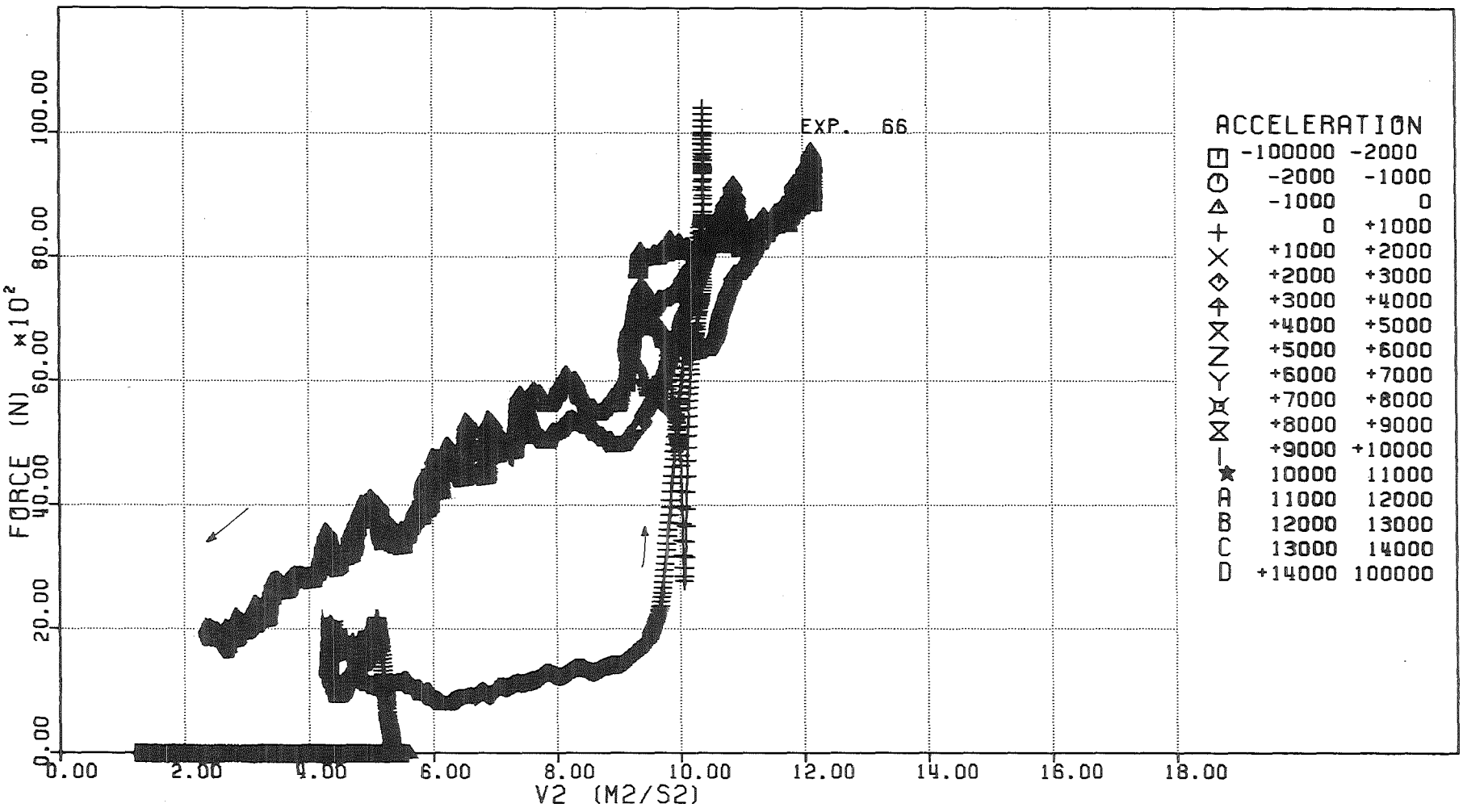

FIG. 6.261 - FORCE ACTING ON THE DIP-PLATE VERSUS THE SQUARE OF THE PISTON VELOCITY

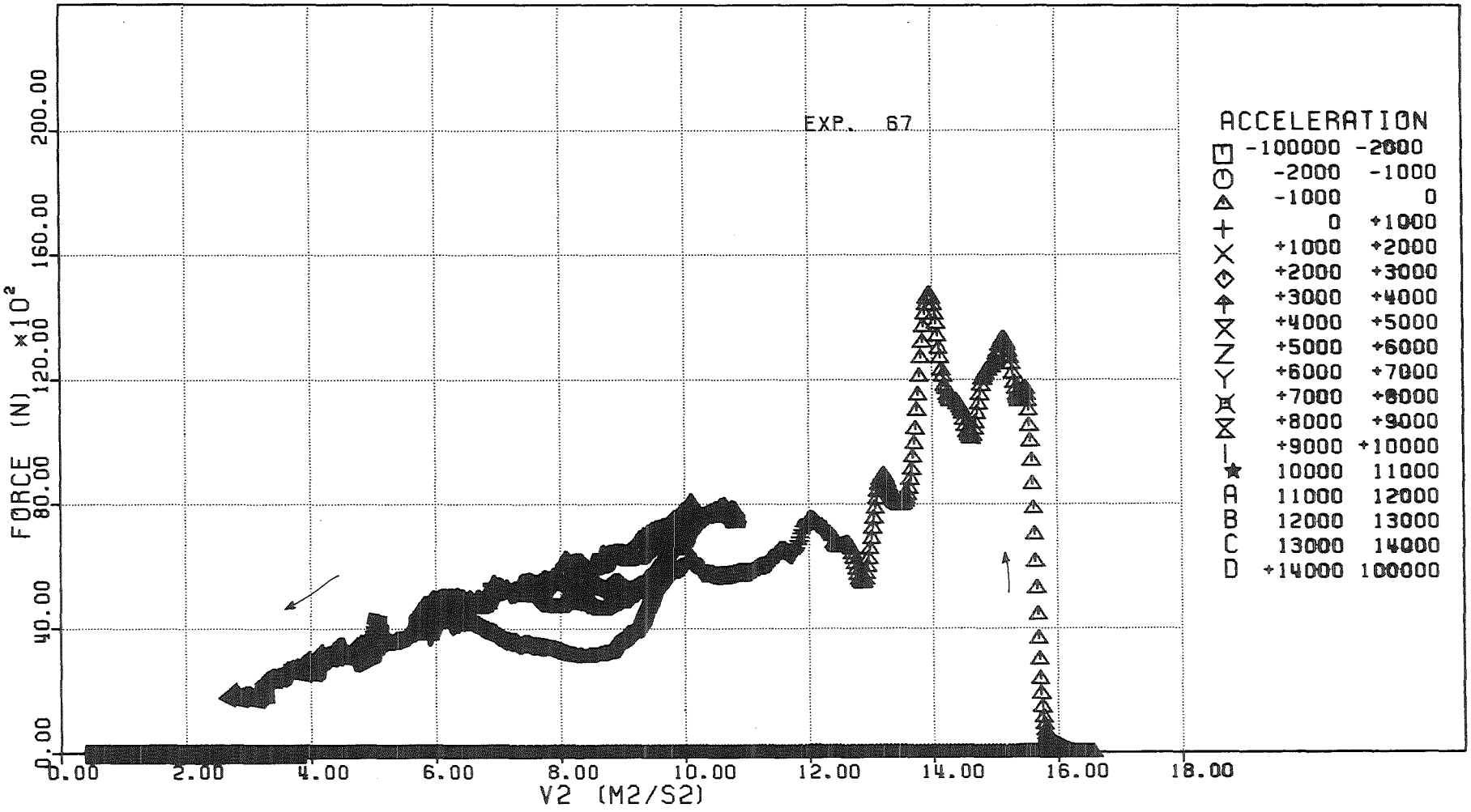

FIG. 6.262 - FORCE ACTING ON THE DIP-PLATE VERSUS THE SQUARE OF THE PISTON VELOCITY

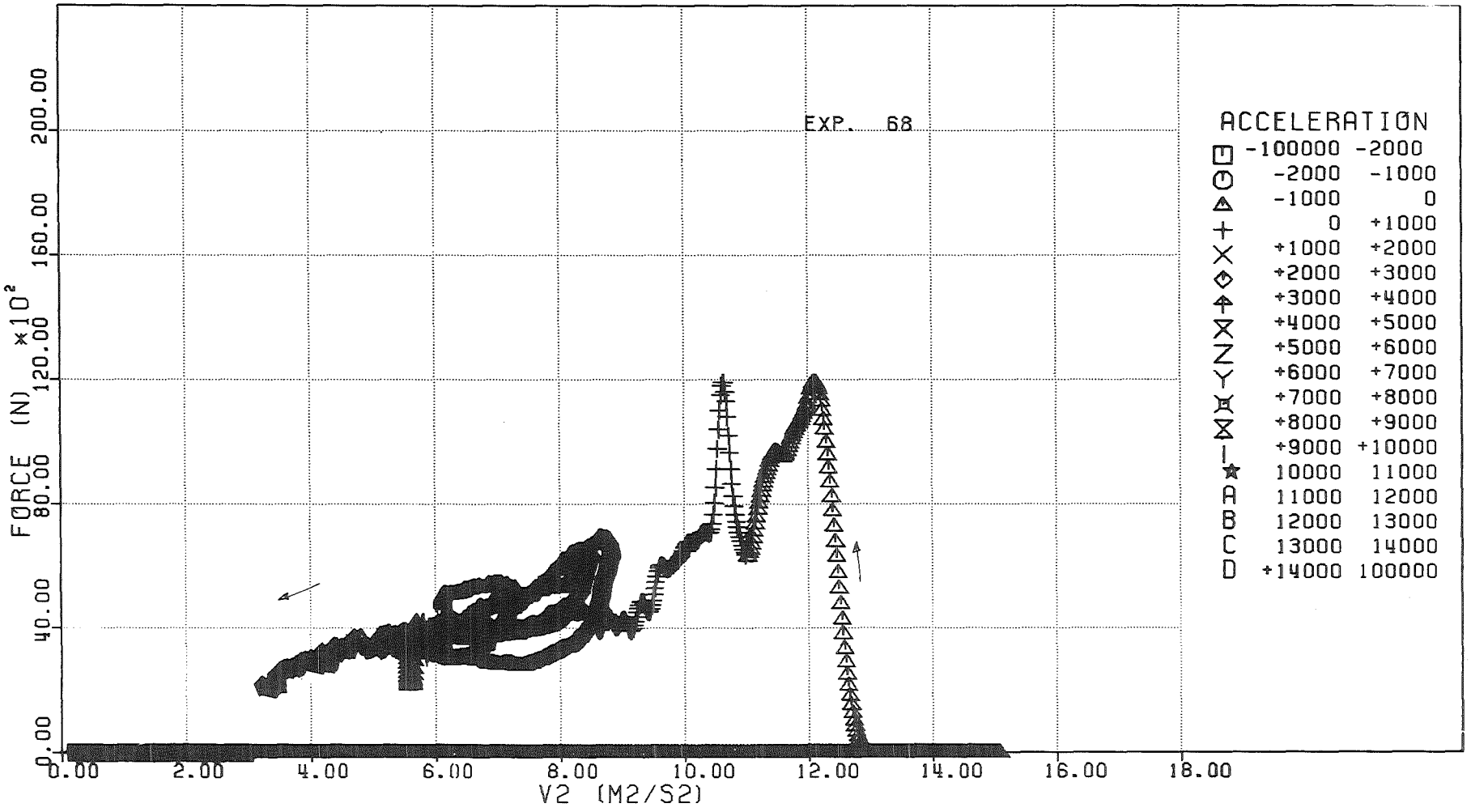

FIG. 6.263 - FORCE ACTING ON THE DIP-PLATE VERSUS THE SQUARE OF THE PISTON VELOCITY

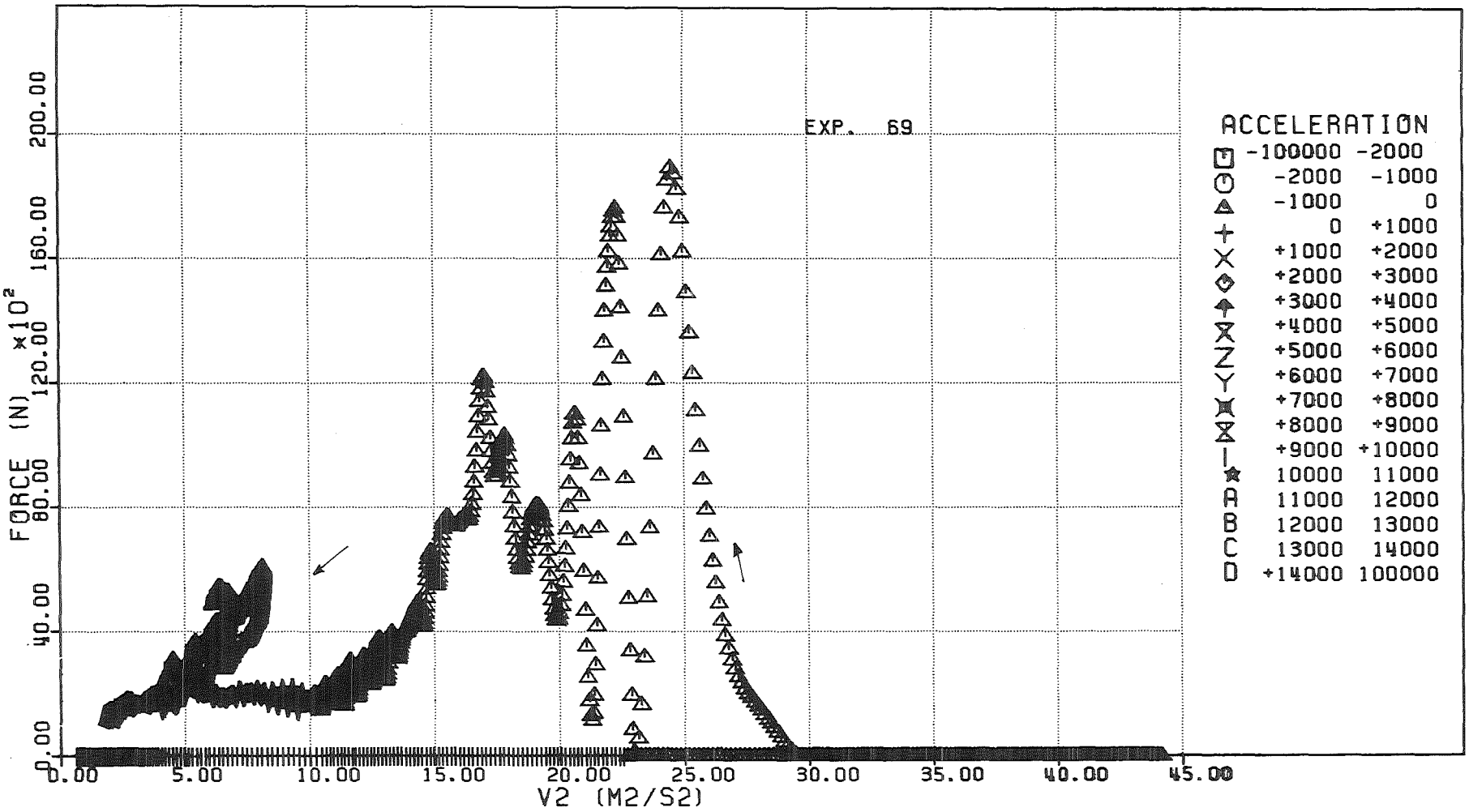

FIG. 6.264 - FORCE ACTING ON THE DIP-PLATE VERSUS THE SQUARE OF THE PISTON VELOCITY

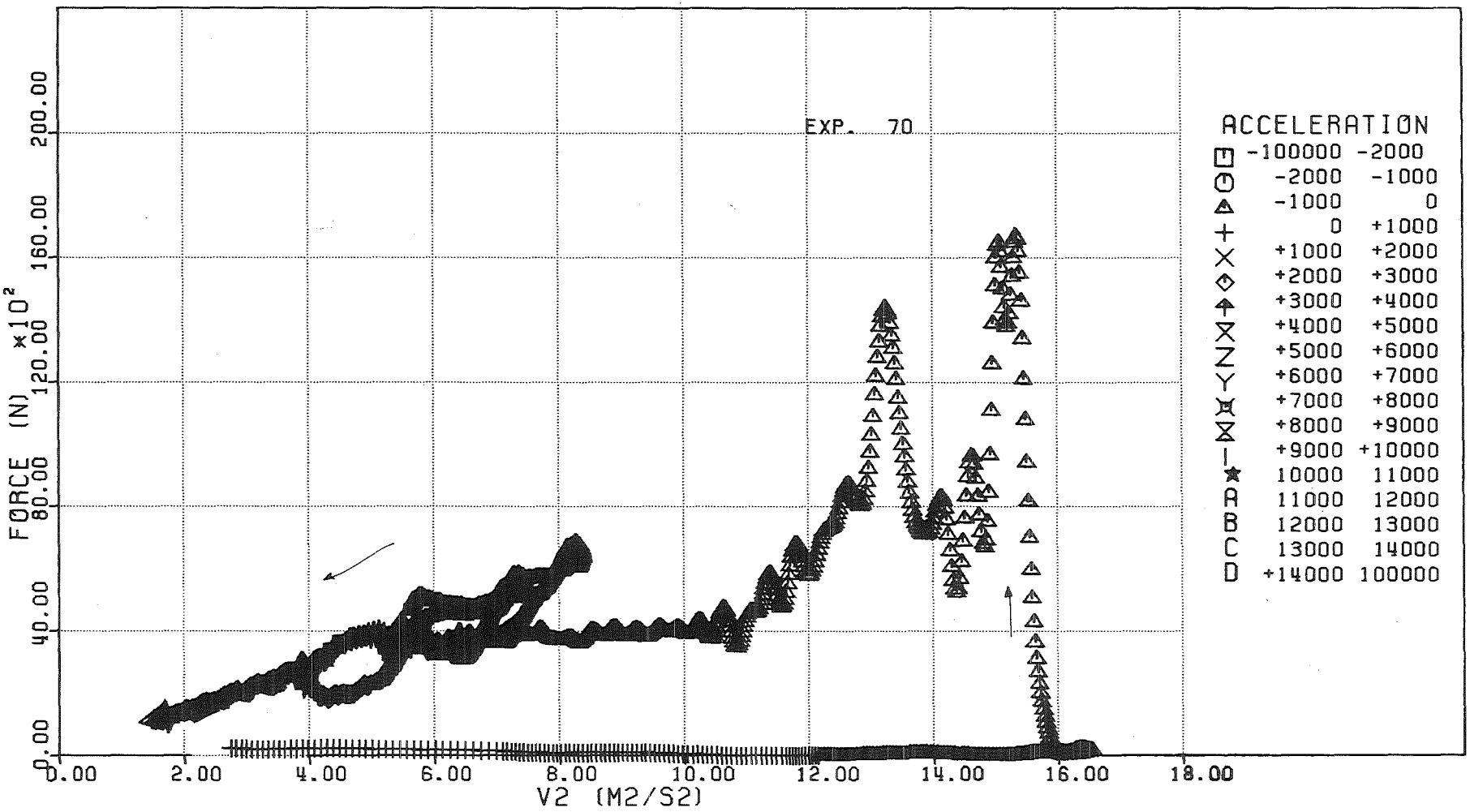

FIG. 6.265 - FORCE ACTING ON THE DIP-PLATE VERSUS THE SQUARE OF THE PISTON VELOCITY

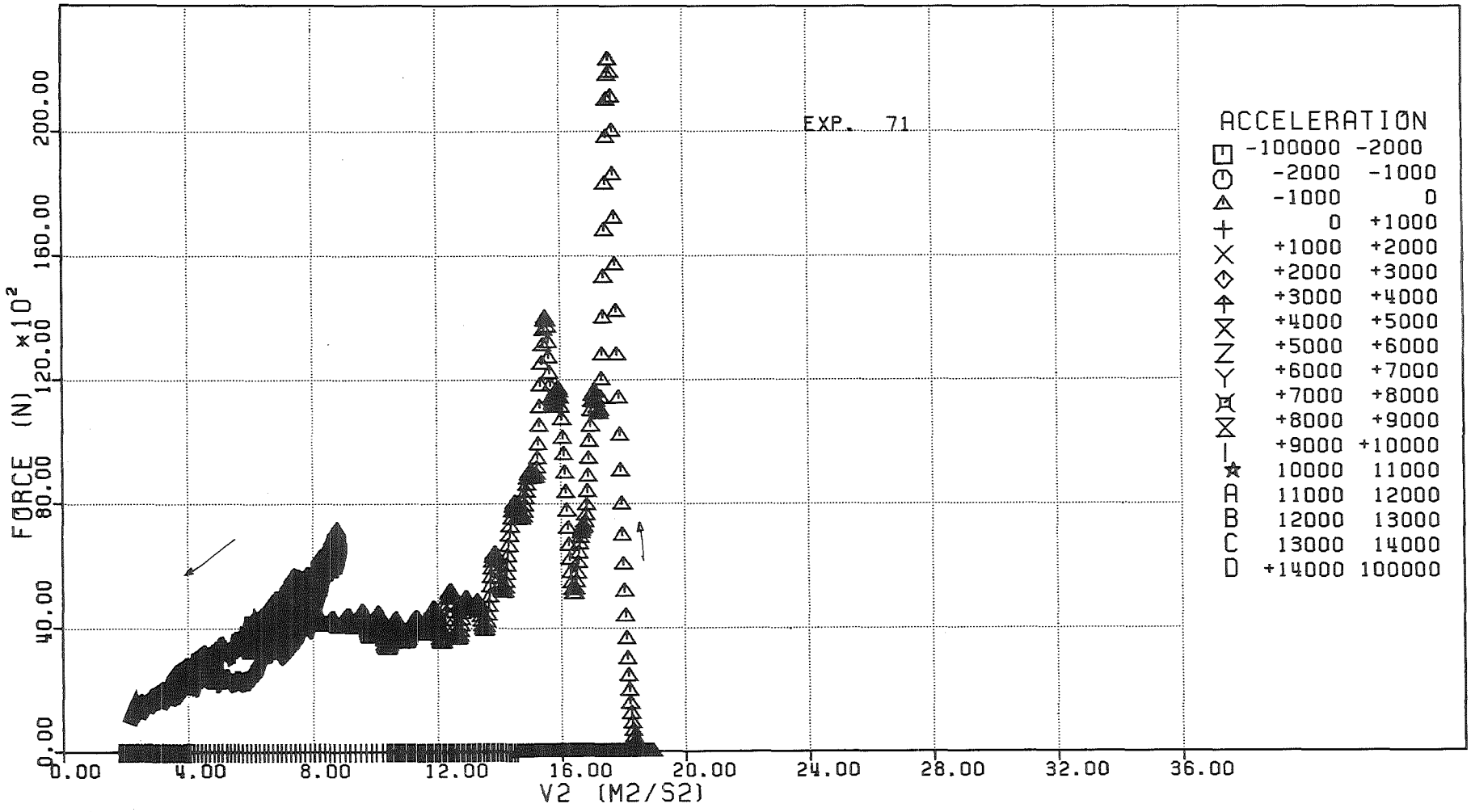

FIG. 6.266 -FORCE ACTING ON THE DIP-PLATE VERSUS THE SQUARE OF THE PISTON VELOCITY

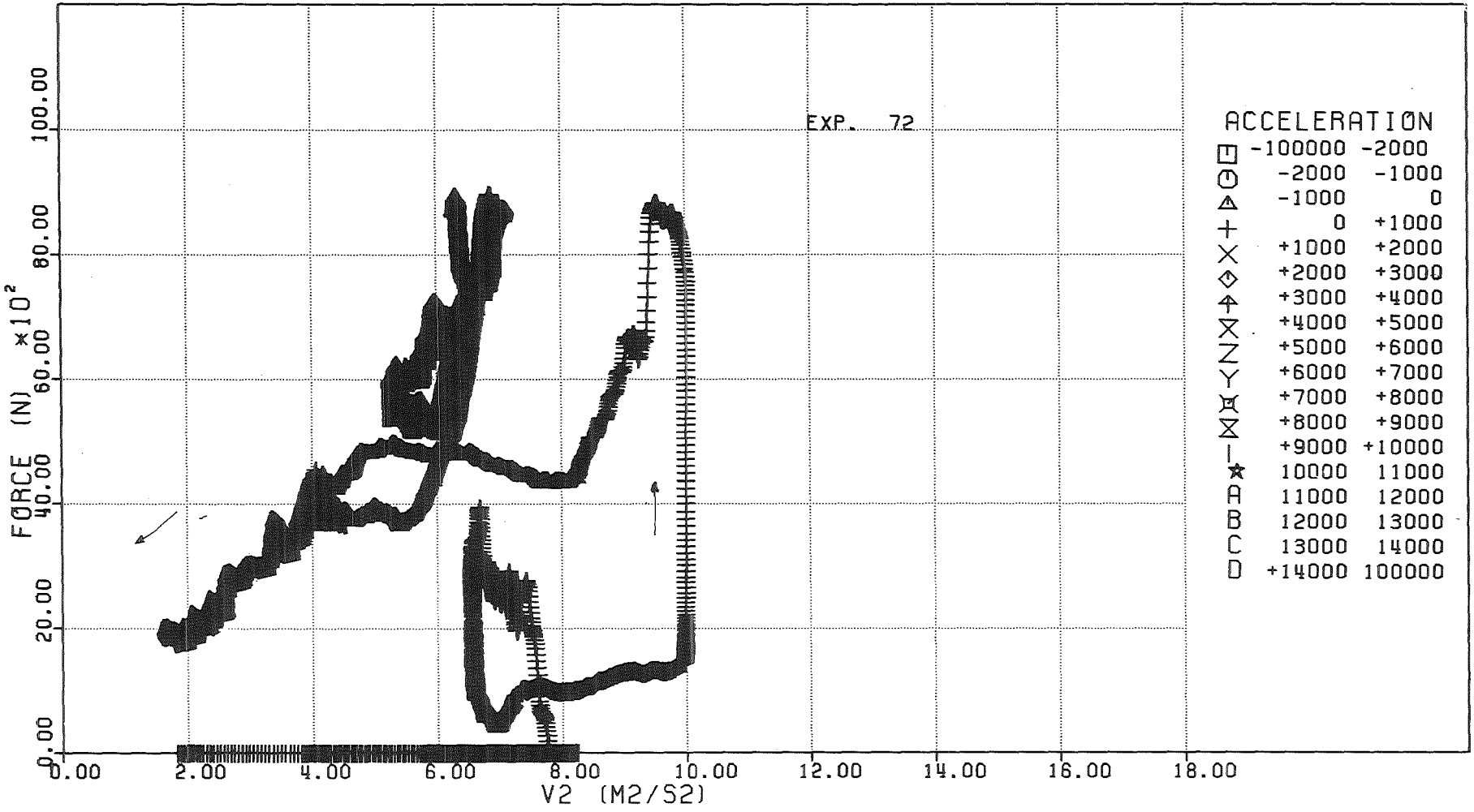

FIG. 6.267 - FORCE ACTING ON THE DIP-PLATE VERSUS THE SQUARE OF THE PISTON VELOCITY

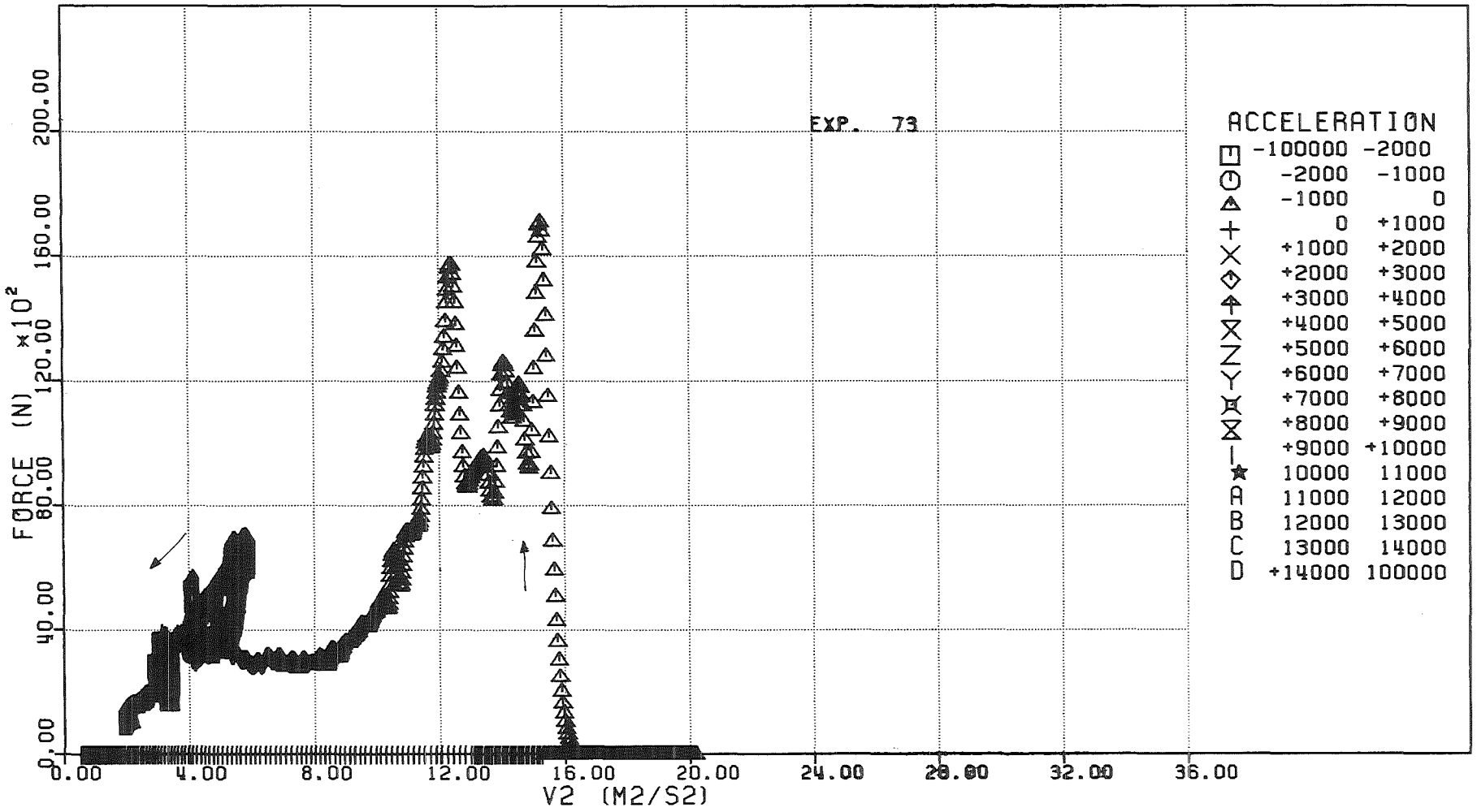

FIG. 6-26B - FORCE ACTING ON THE DIP-PLATE VERSUS THE SQUARE OF THE PISTON VELOCITY

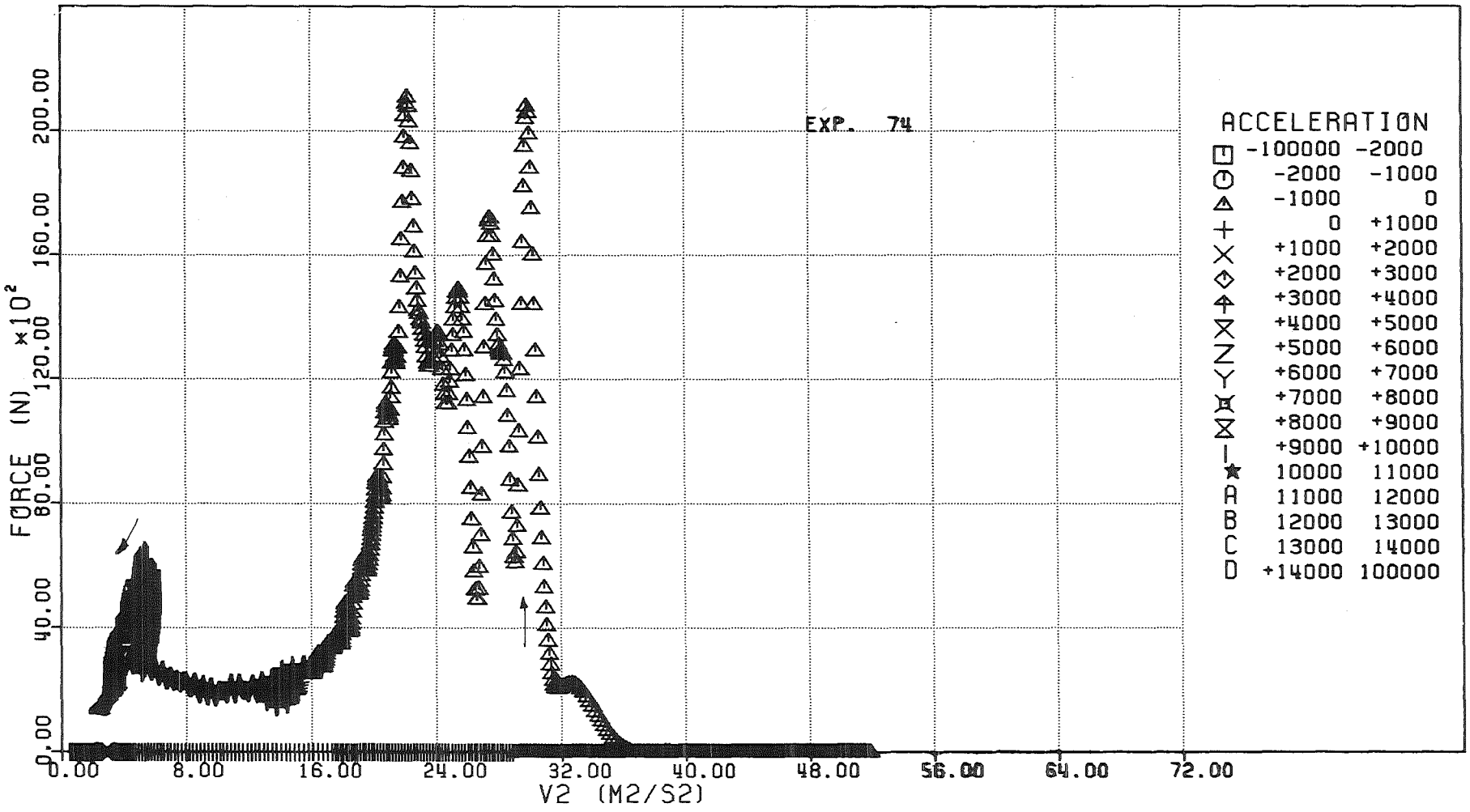

FIG. 6.269 - FORCE ACTING ON THE DIP-PLATE VERSUS THE SQUARE OF THE PISTON VELOCITY

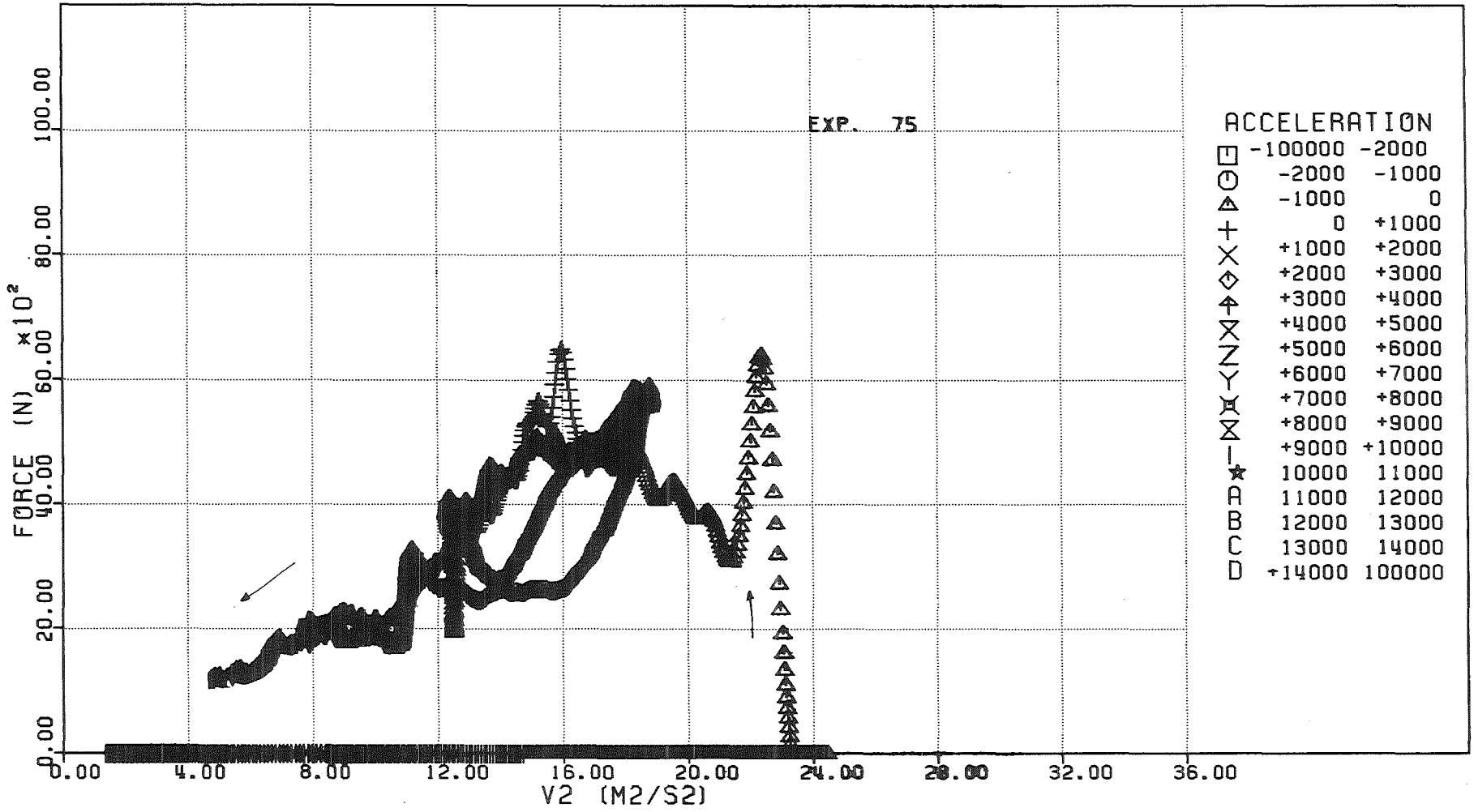

FIG. 6.270 - FORCE ACTING ON THE DIP-PLATE VERSUS THE SQUARE OF THE PISTON VELOCITY

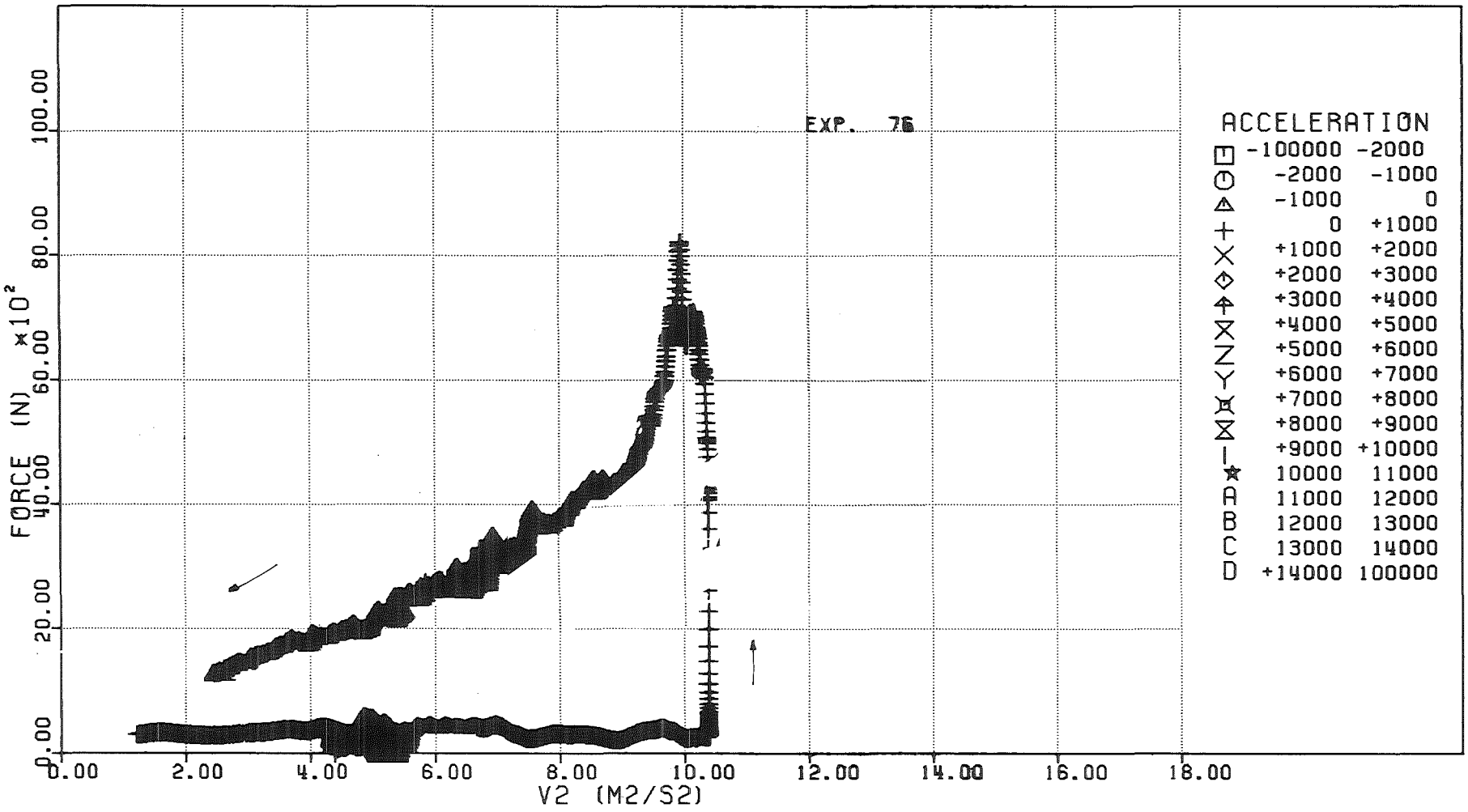

FIG. 6.271 - FORCE ACTING ON THE DIP-PLATE VERSUS THE SQUARE OF THE PISTON VELOCITY

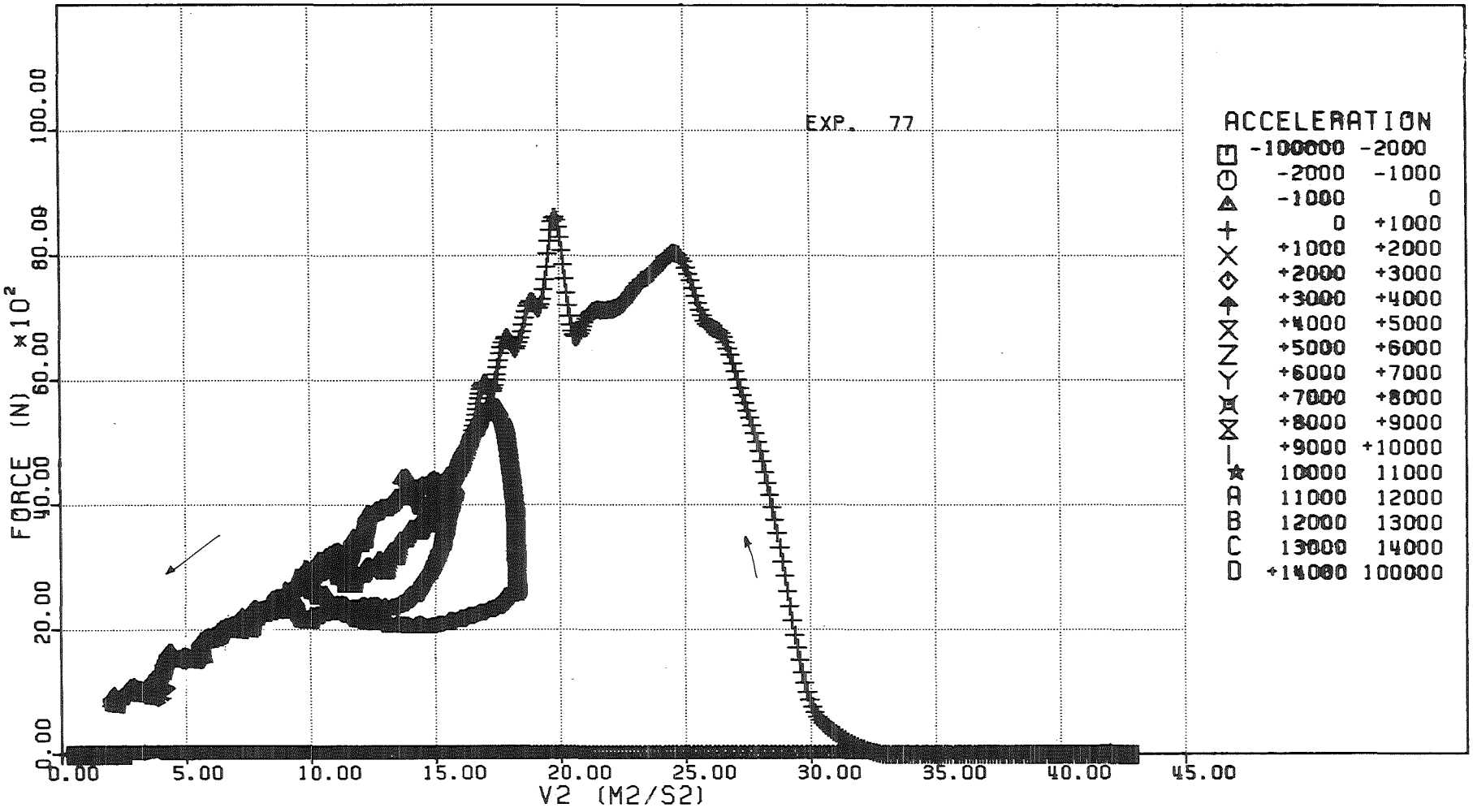

FIG. 6.272 - FORCE ACTING ON THE DIP-PLATE VERSUS THE SQUARE OF THE PISTON VELOCITY

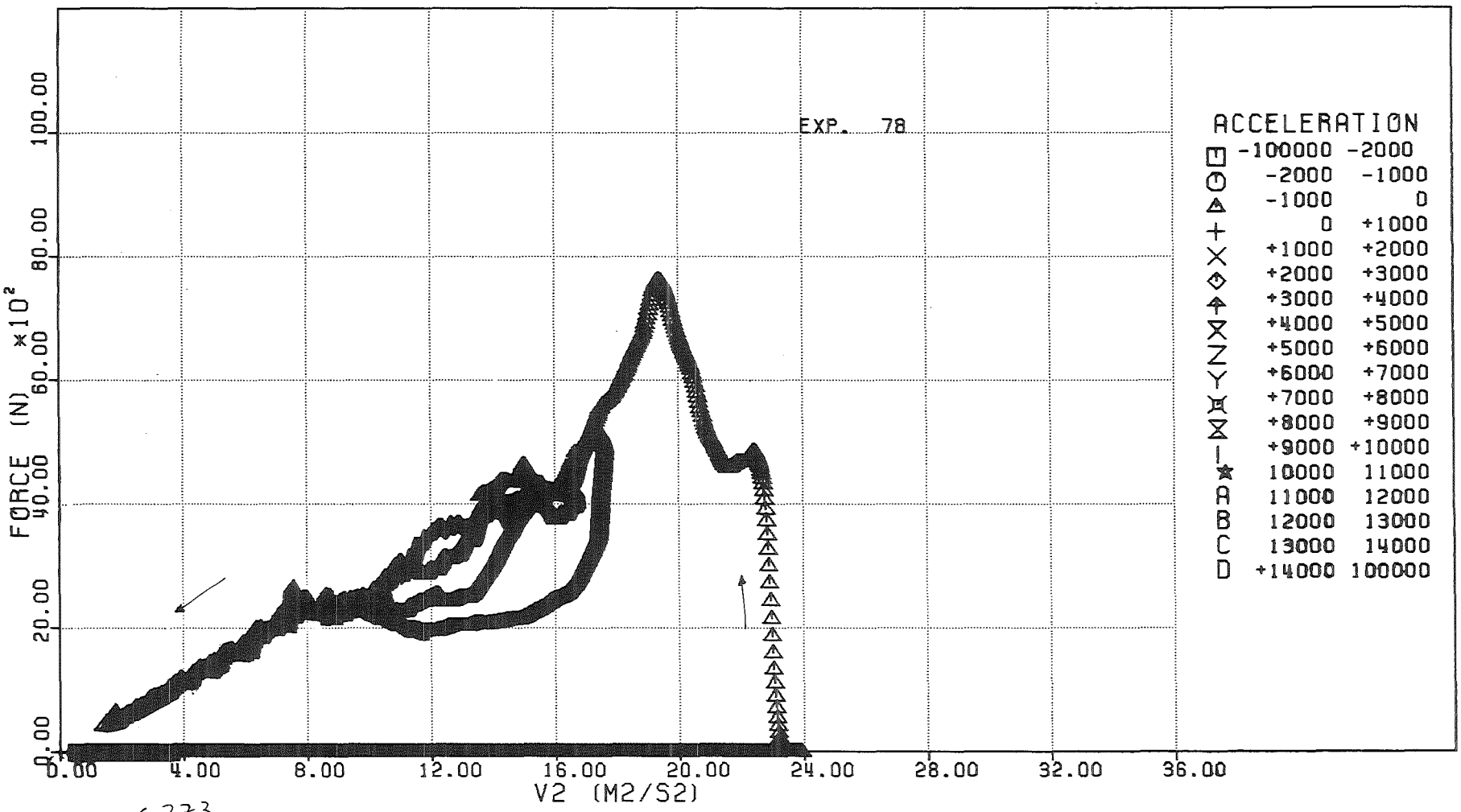

6.273

FIG. - FORCE ACTING ON THE DIP-PLATE VERSUS THE SQUARE OF THE PISTON VELOCITY

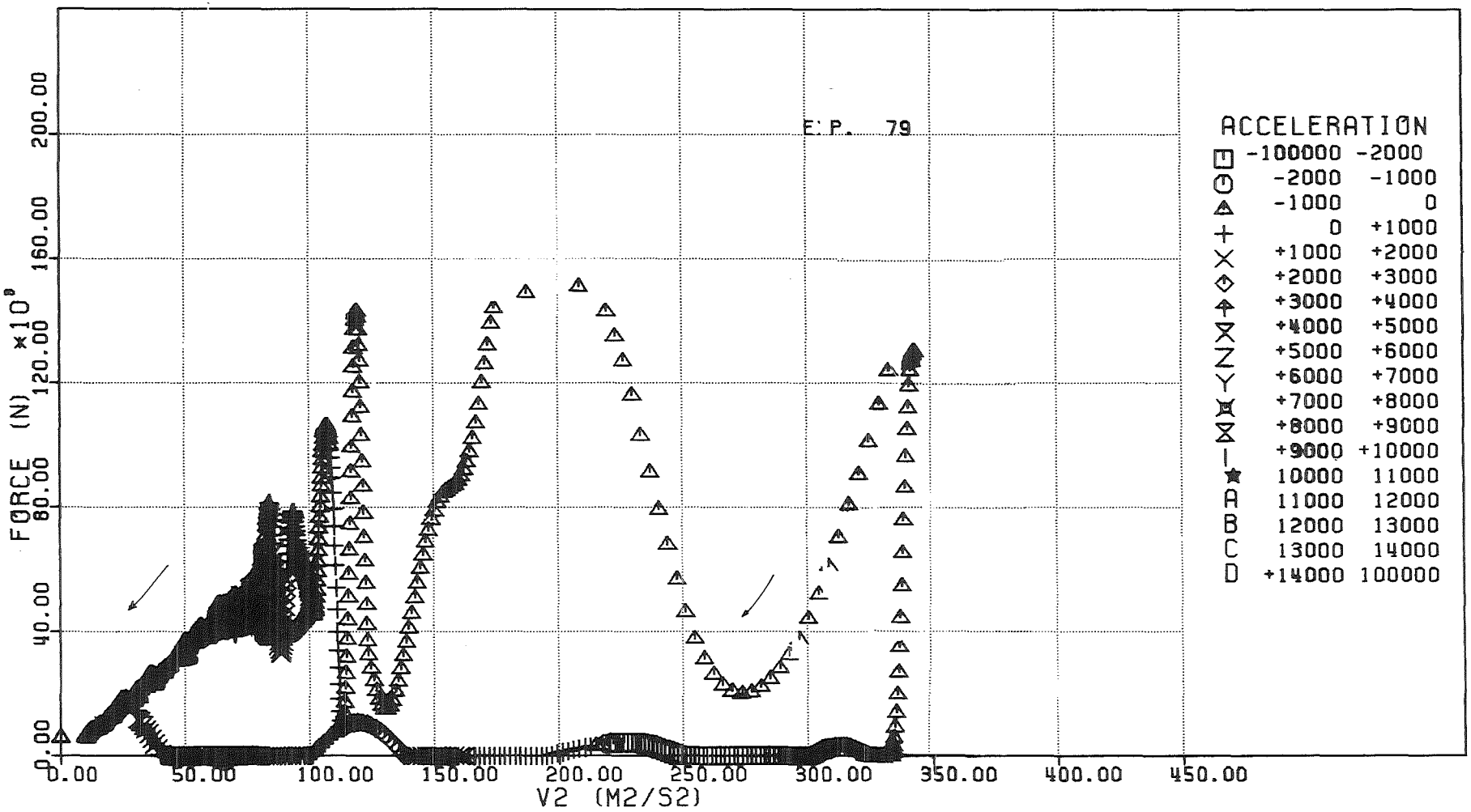

FIG. 6.274 - FORCE ACTING ON THE DIP-PLATE VERSUS THE SQUARE OF THE PISTON VELOCITY

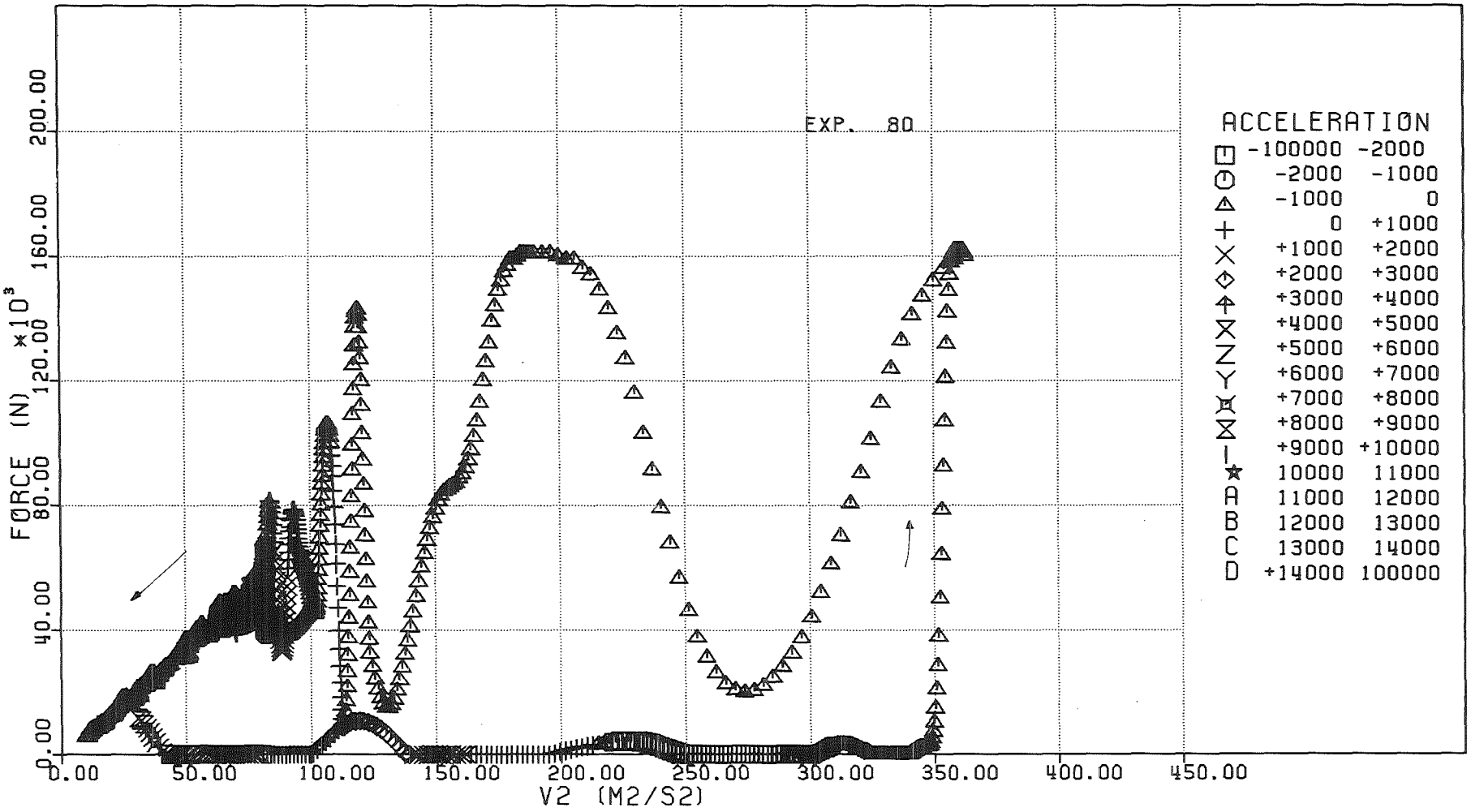

FIG. 6.275 - FORCE ACTING ON THE DIP-PLATE VERSUS THE SQUARE OF THE PISTON VELOCITY

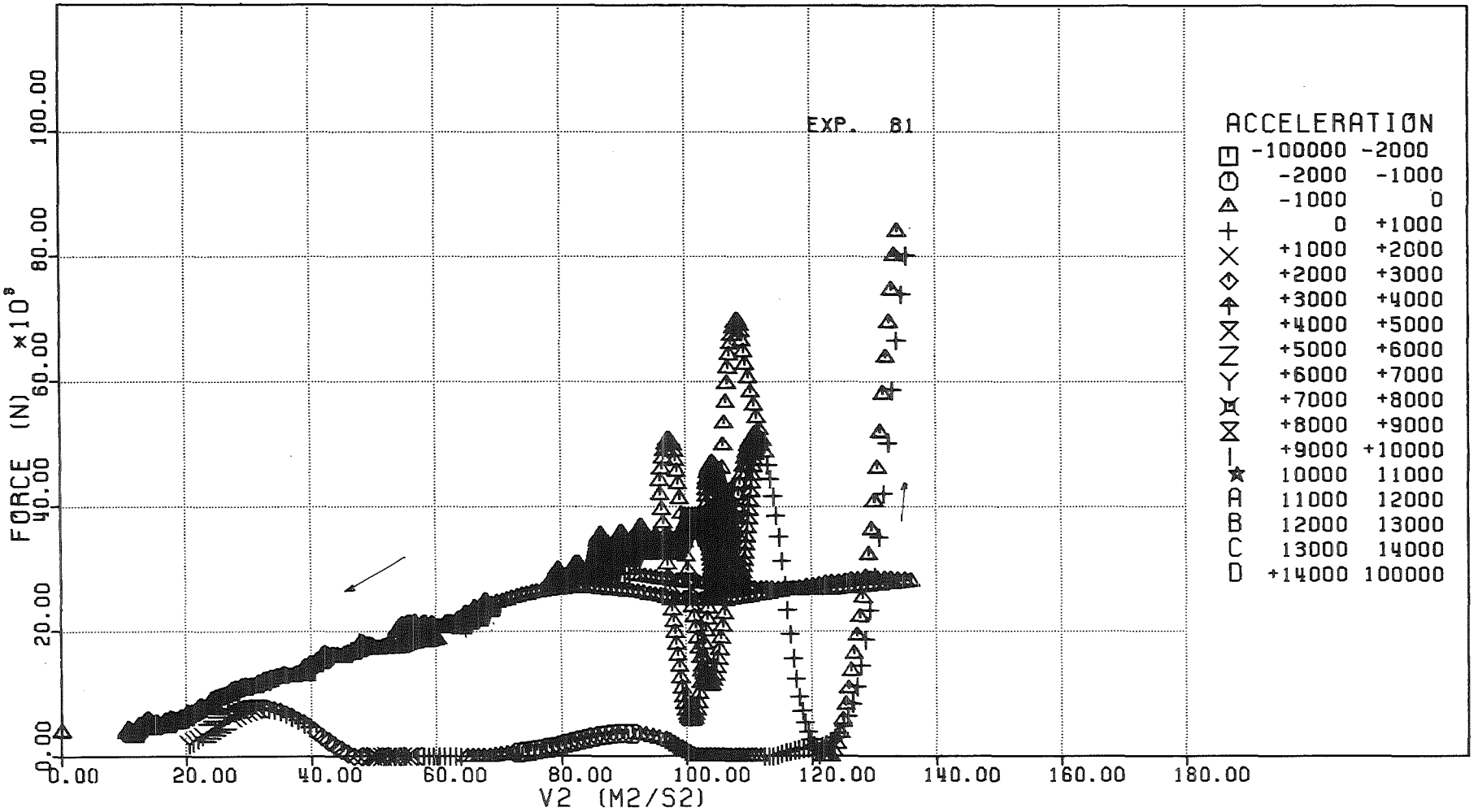

FIG. 6.276 - FORCE ACTING ON THE DIP-PLATE VERSUS THE SQUARE OF THE PISTON VELOCITY

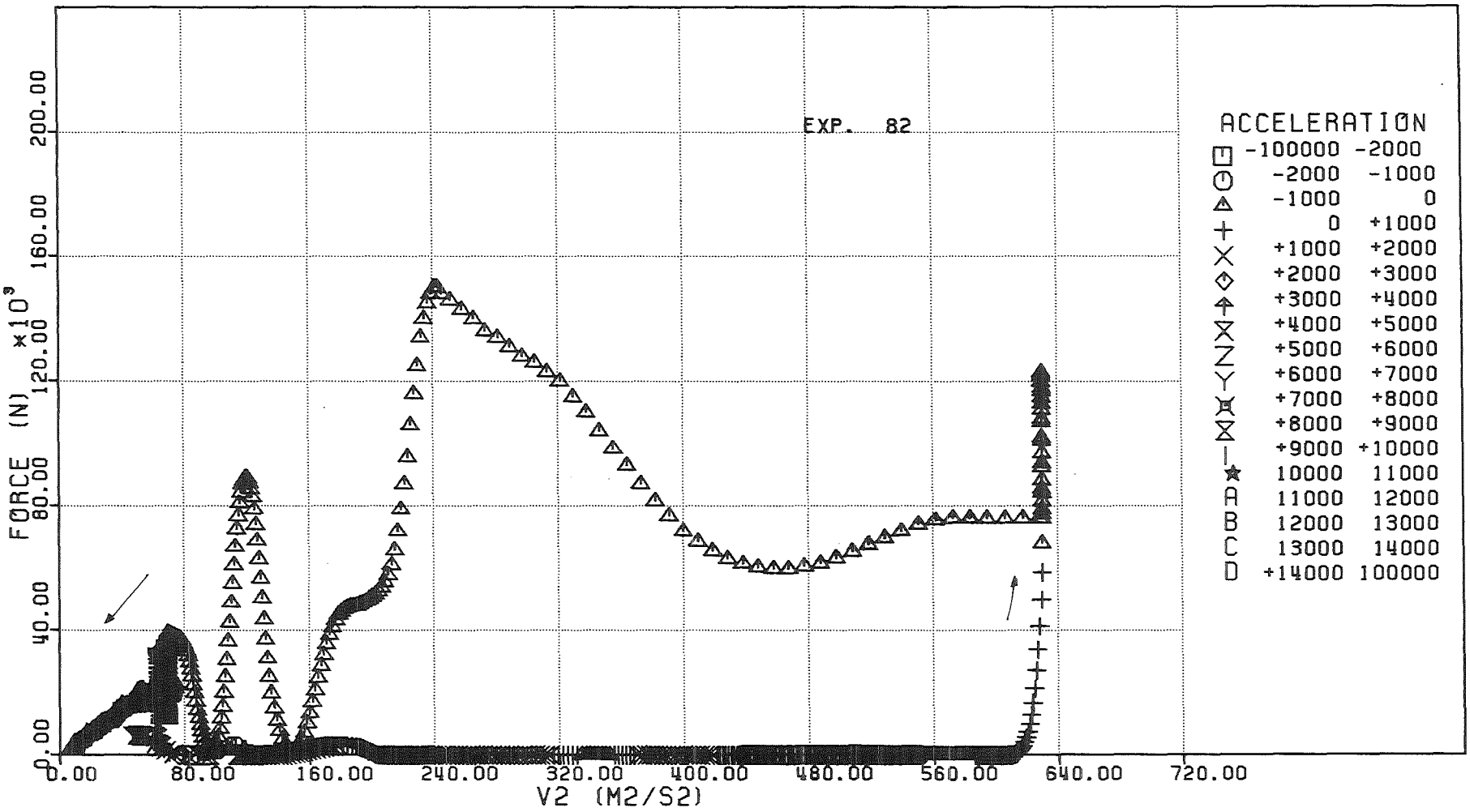

FIG. 6.277 - FORCE ACTING ON THE DIP-PLATE VERSUS THE SQUARE OF THE PISTON VELOCITY

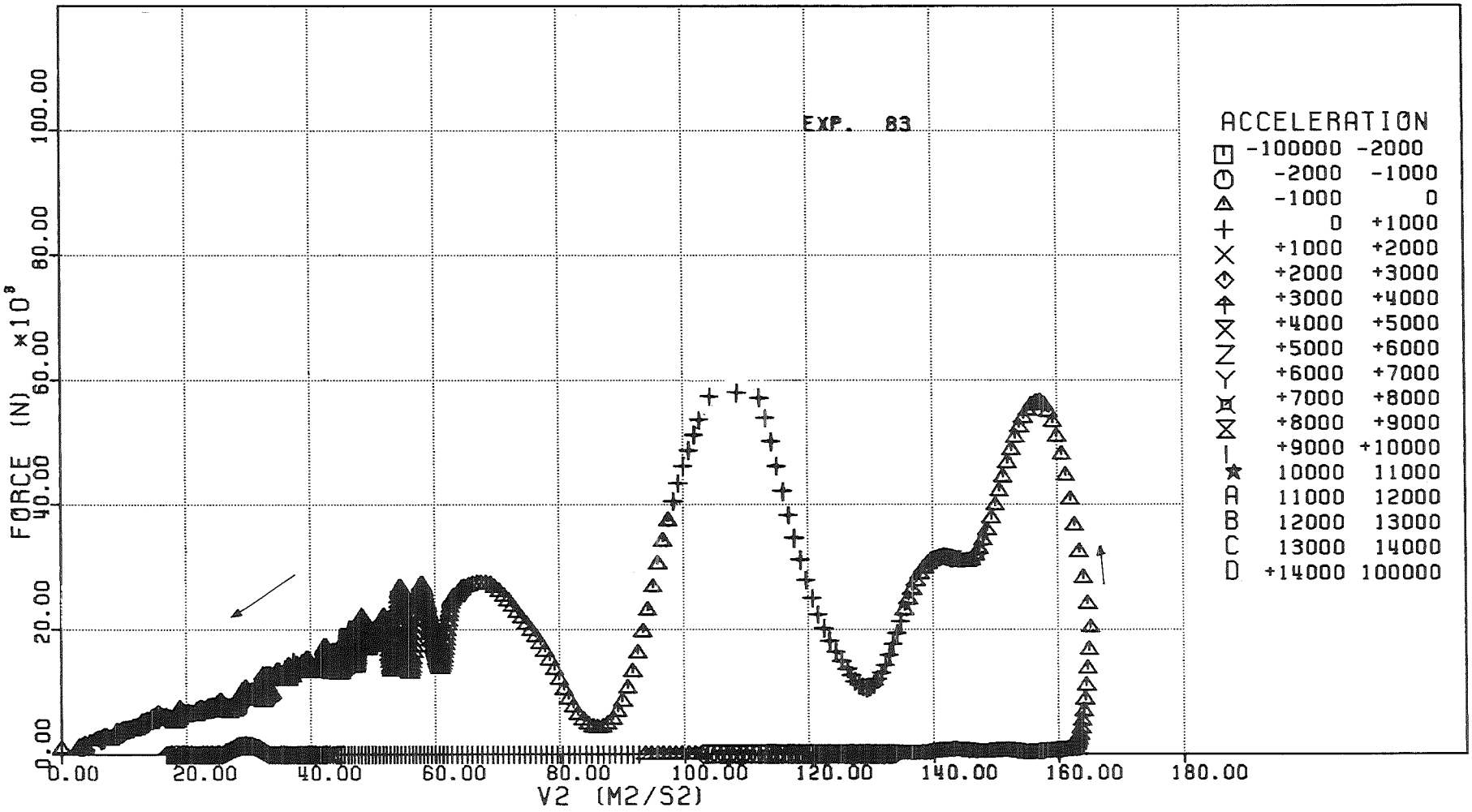

FIG. 6.278 - FORCE ACTING ON THE DIP-PLATE VERSUS THE SQUARE OF THE PISTON VELOCITY

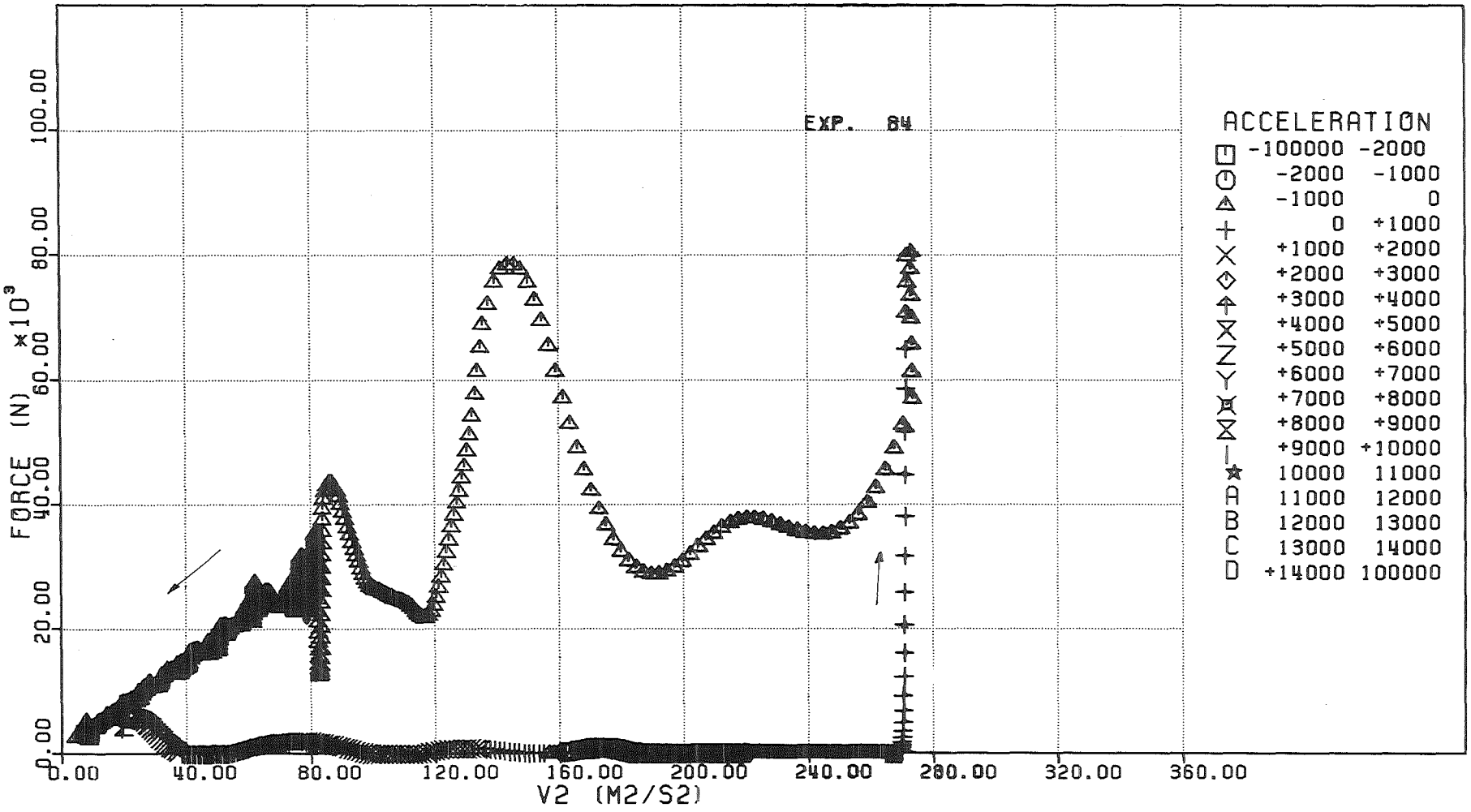

FIG. 6.279 - FORCE ACTING ON THE DIP-PLATE VERSUS THE SQUARE OF THE PISTON VELOCITY

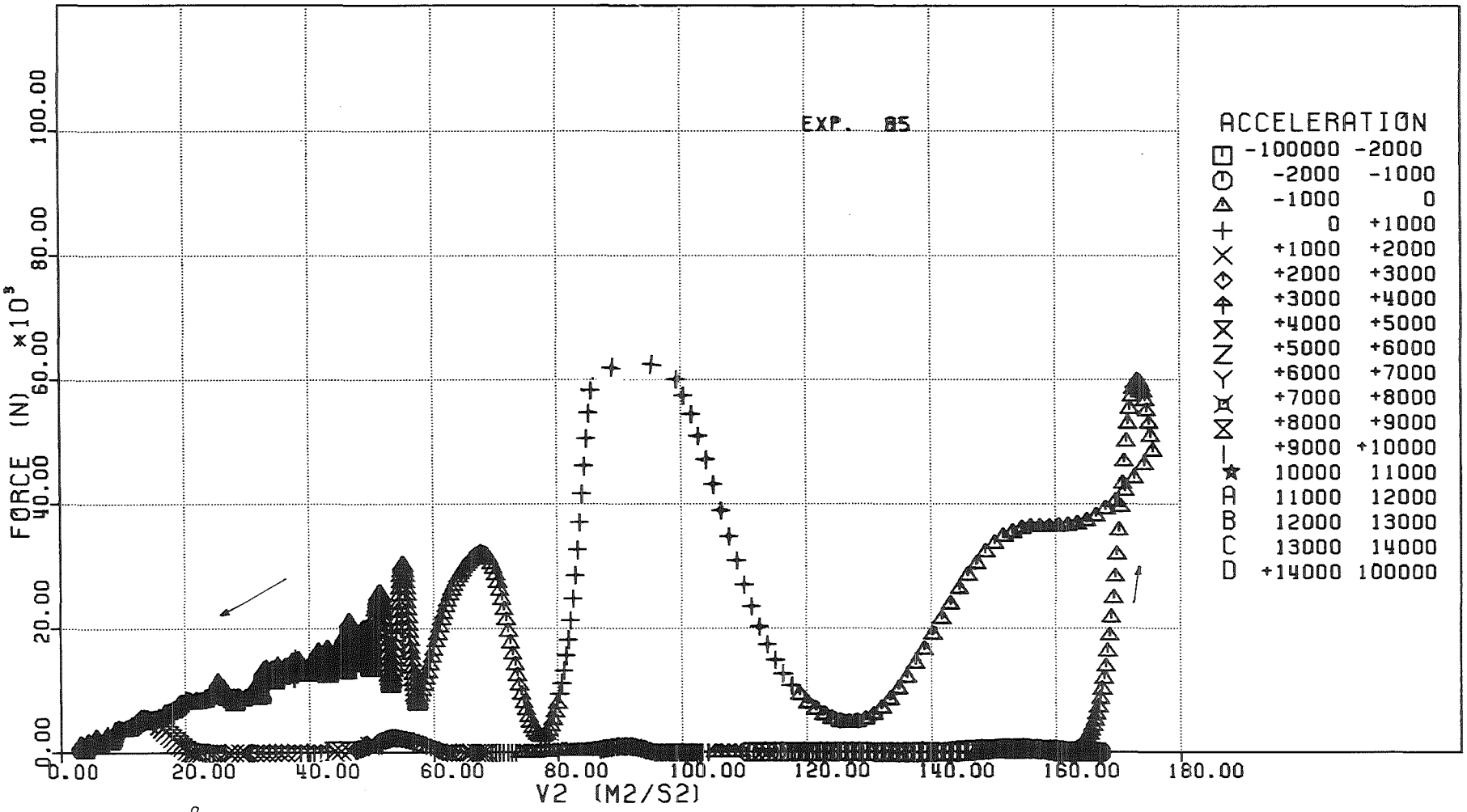

FIG. 6.280 - FORCE ACTING ON THE DIP-PLATE VERSUS THE SQUARE OF THE PISTON VELOCITY

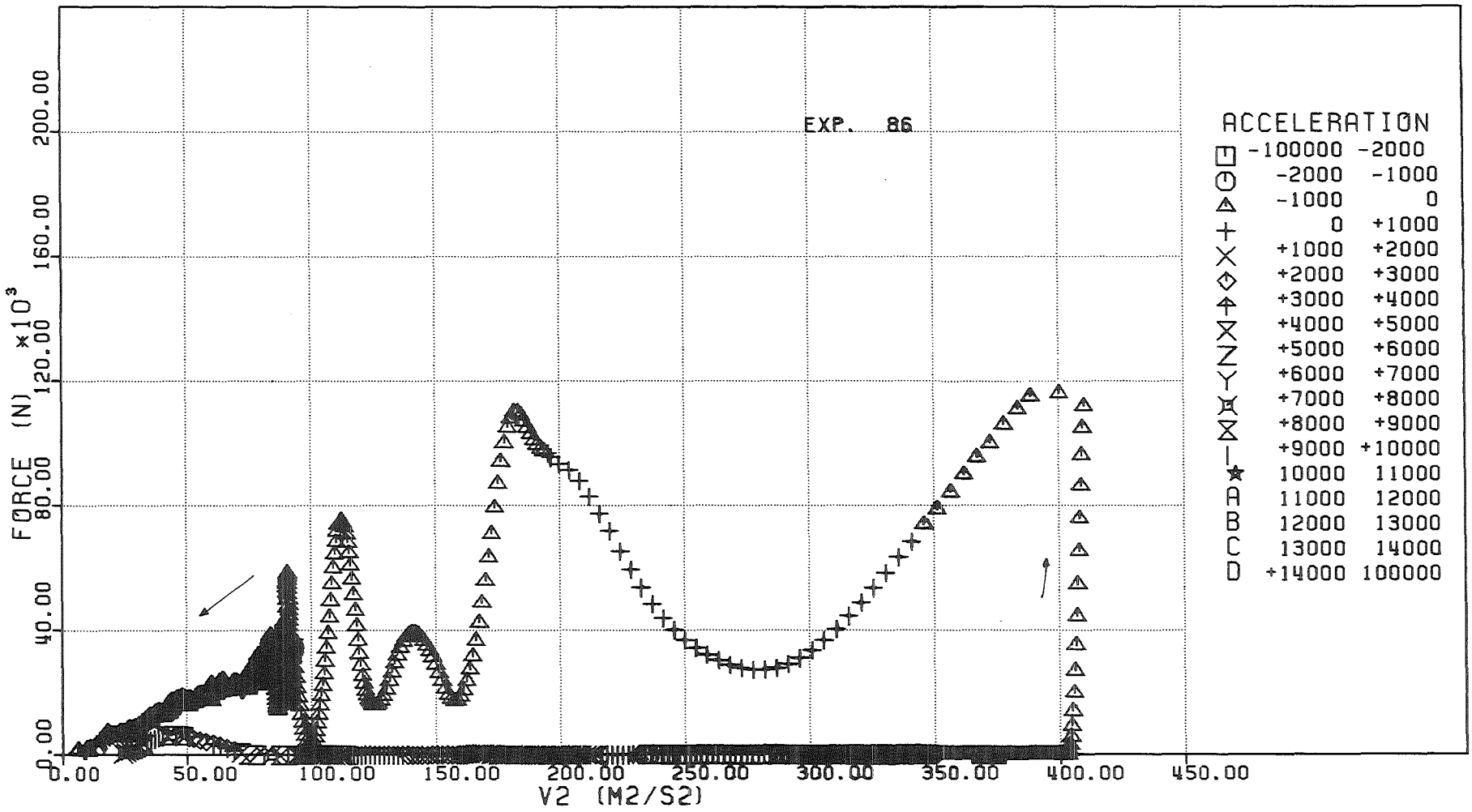

FIG. 6.281 - FORCE ACTING ON THE DIP-PLATE VERSUS THE SQUARE OF THE PISTON VELOCITY

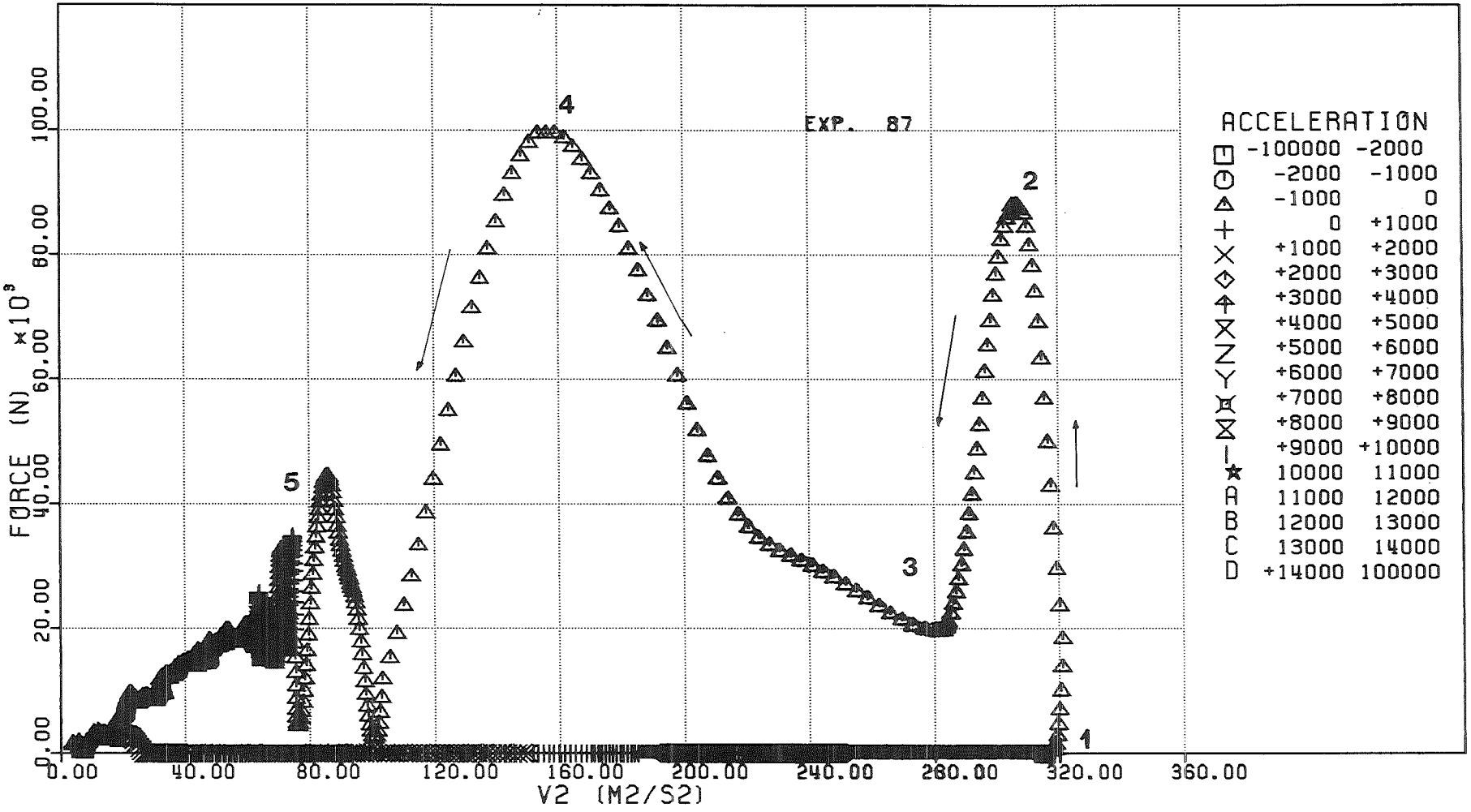

FIG. 6.282 - FORCE ACTING ON THE DIP-PLATE VERSUS THE SQUARE OF THE PISTON VELOCITY

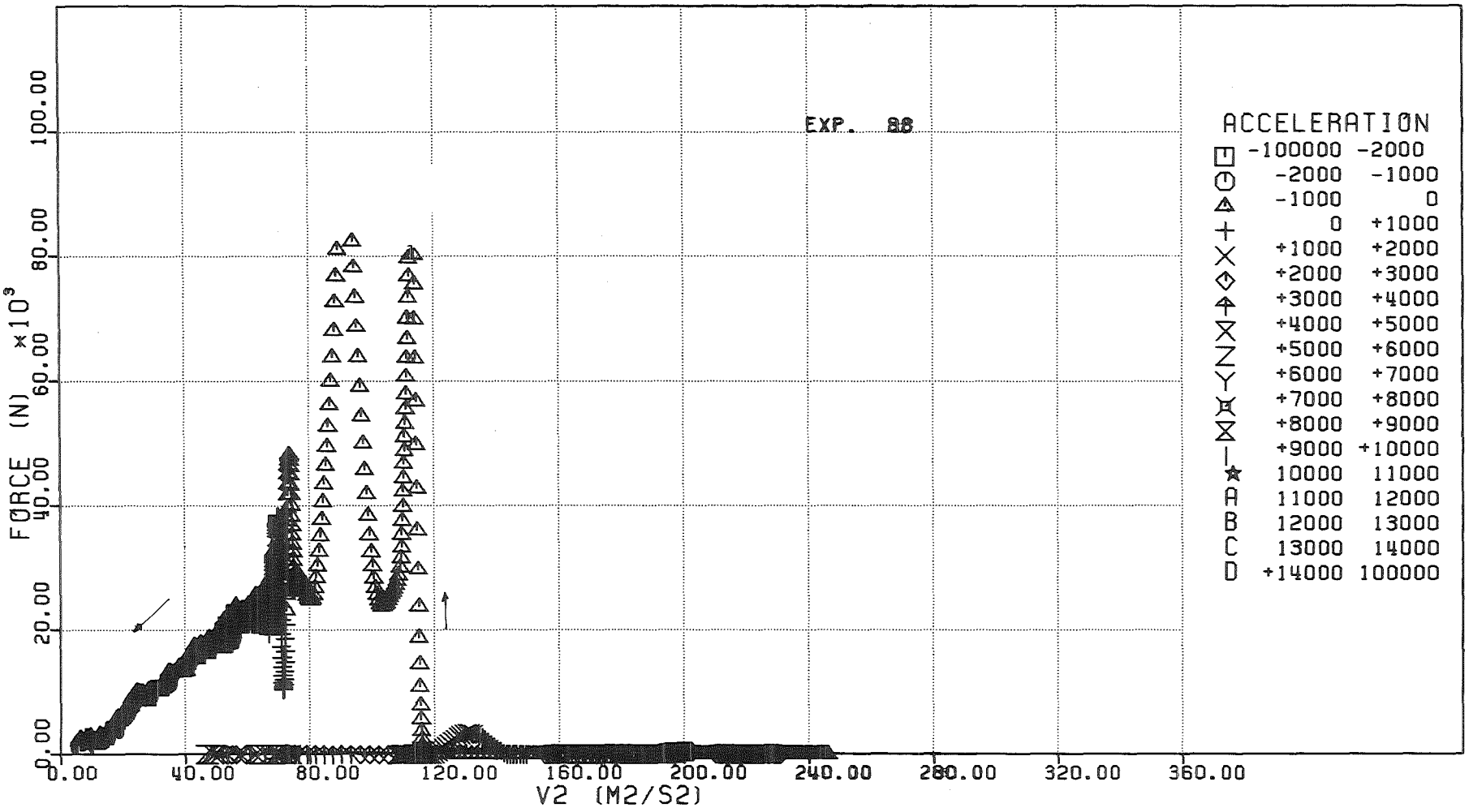

FIG. 6.283 - FORCE ACTING ON THE DIP-PLATE VERSUS THE SQUARE OF THE PISTON VELOCITY

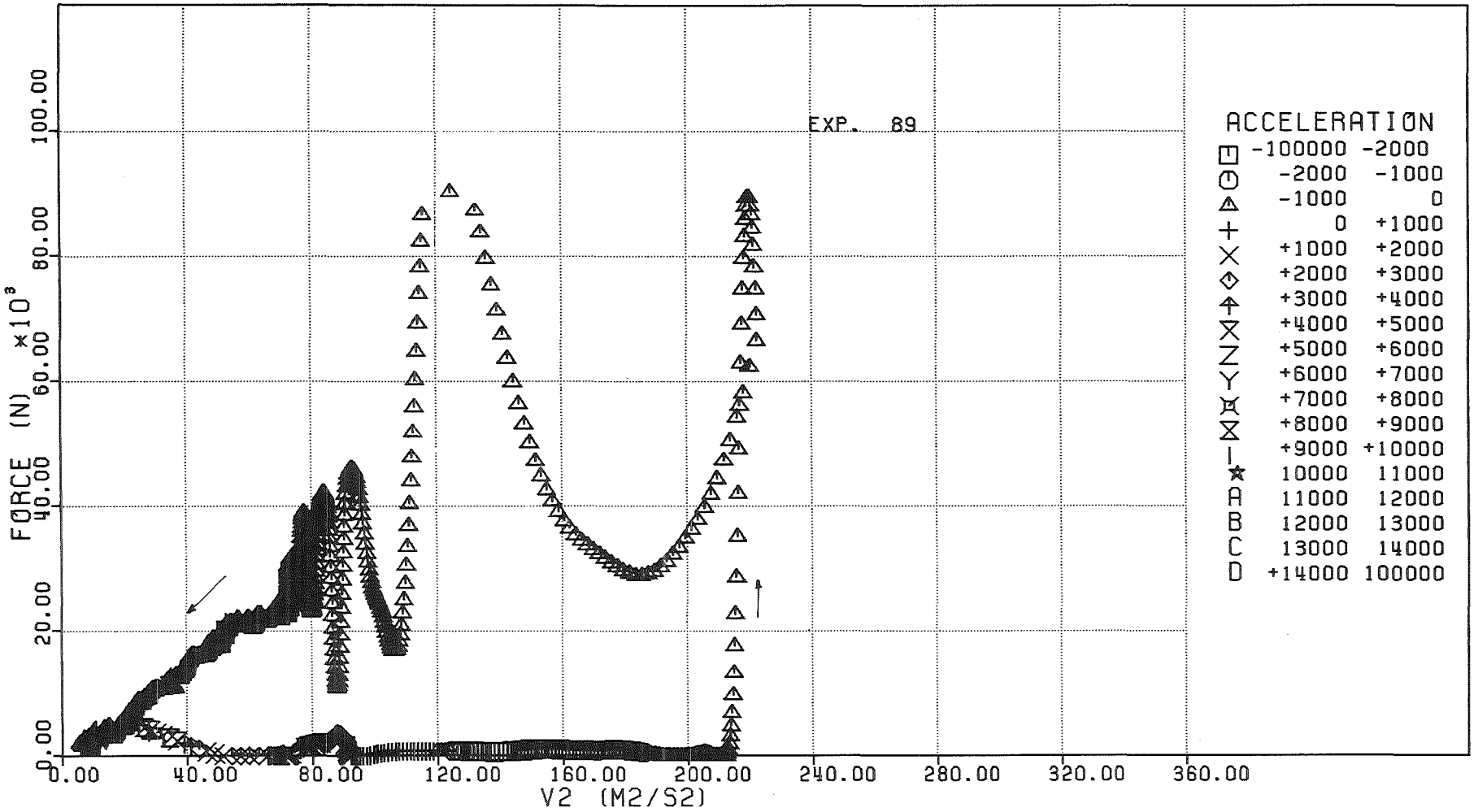

FIG. 6.284 - FORCE ACTING ON THE DIP-PLATE VERSUS THE SQUARE OF THE PISTON VELOCITY

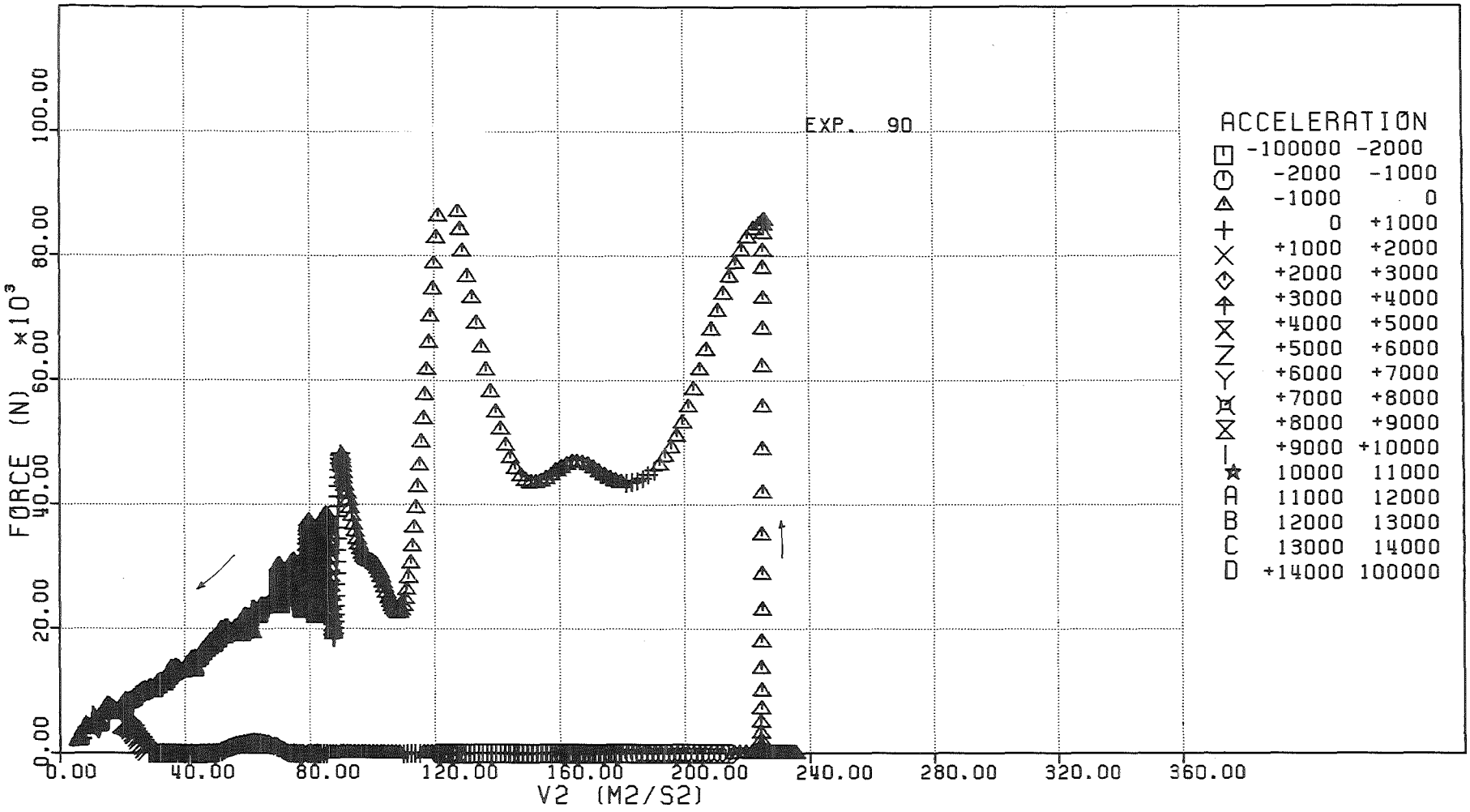

FIG. 6.285 - FORCE ACTING ON THE DIP-PLATE VERSUS THE SQUARE OF THE PISTON VELOCITY

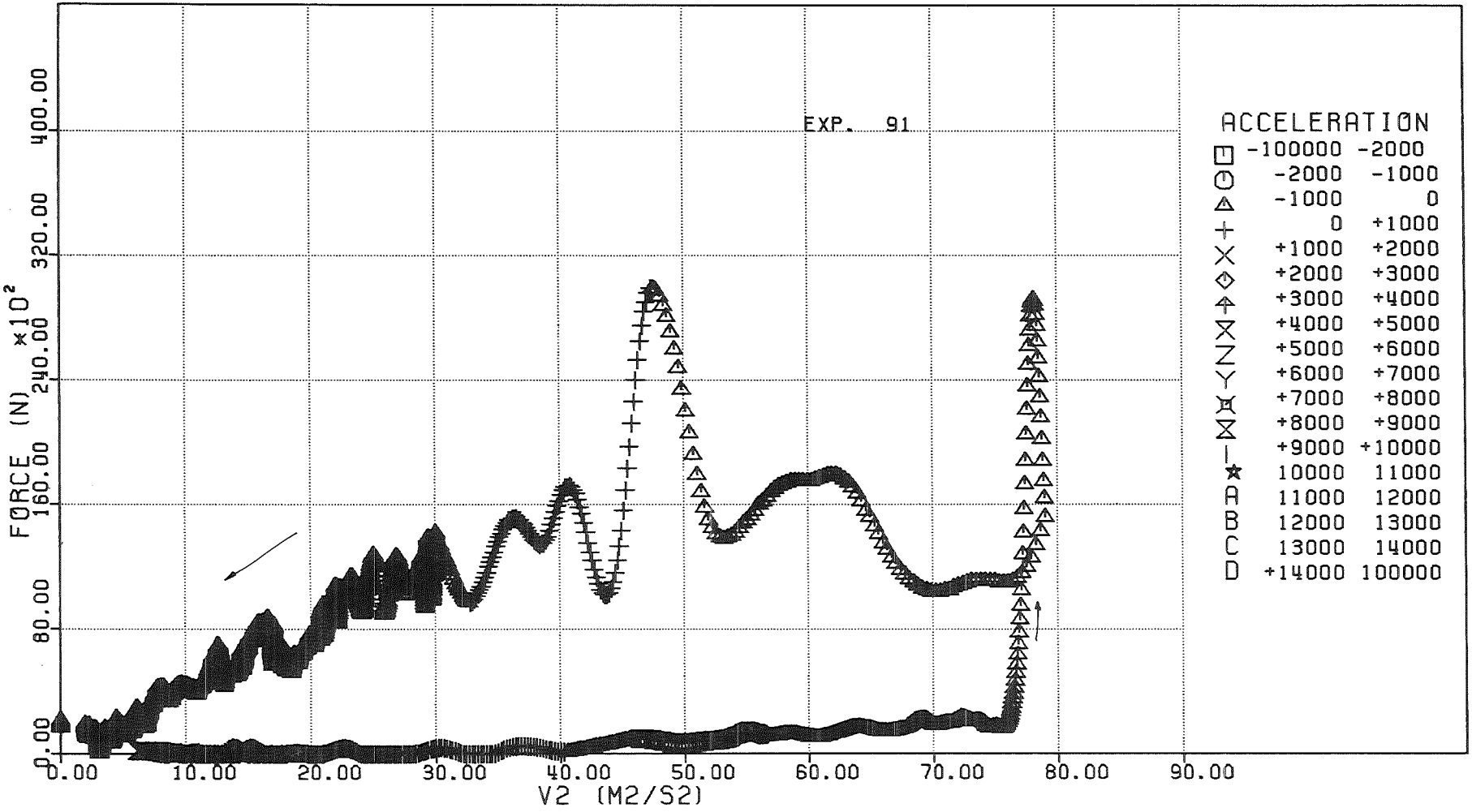

FIG. 6.286 -FORCE ACTING ON THE DIP-PLATE VERSUS THE SQUARE OF THE PISTON VELOCITY

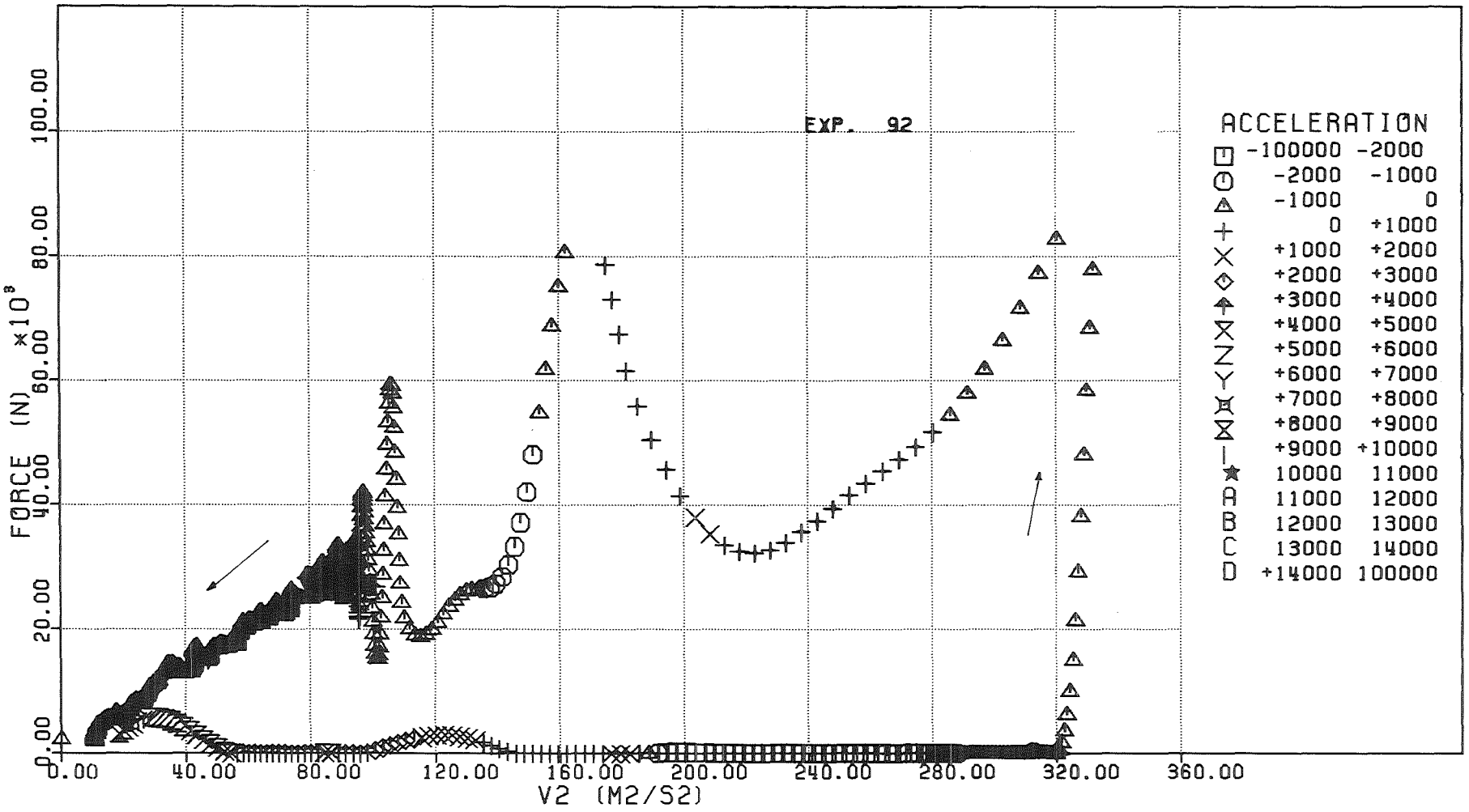

FIG. 6.287 - FORCE ACTING ON THE DIP-PLATE VERSUS THE SQUARE OF THE PISTON VELOCITY

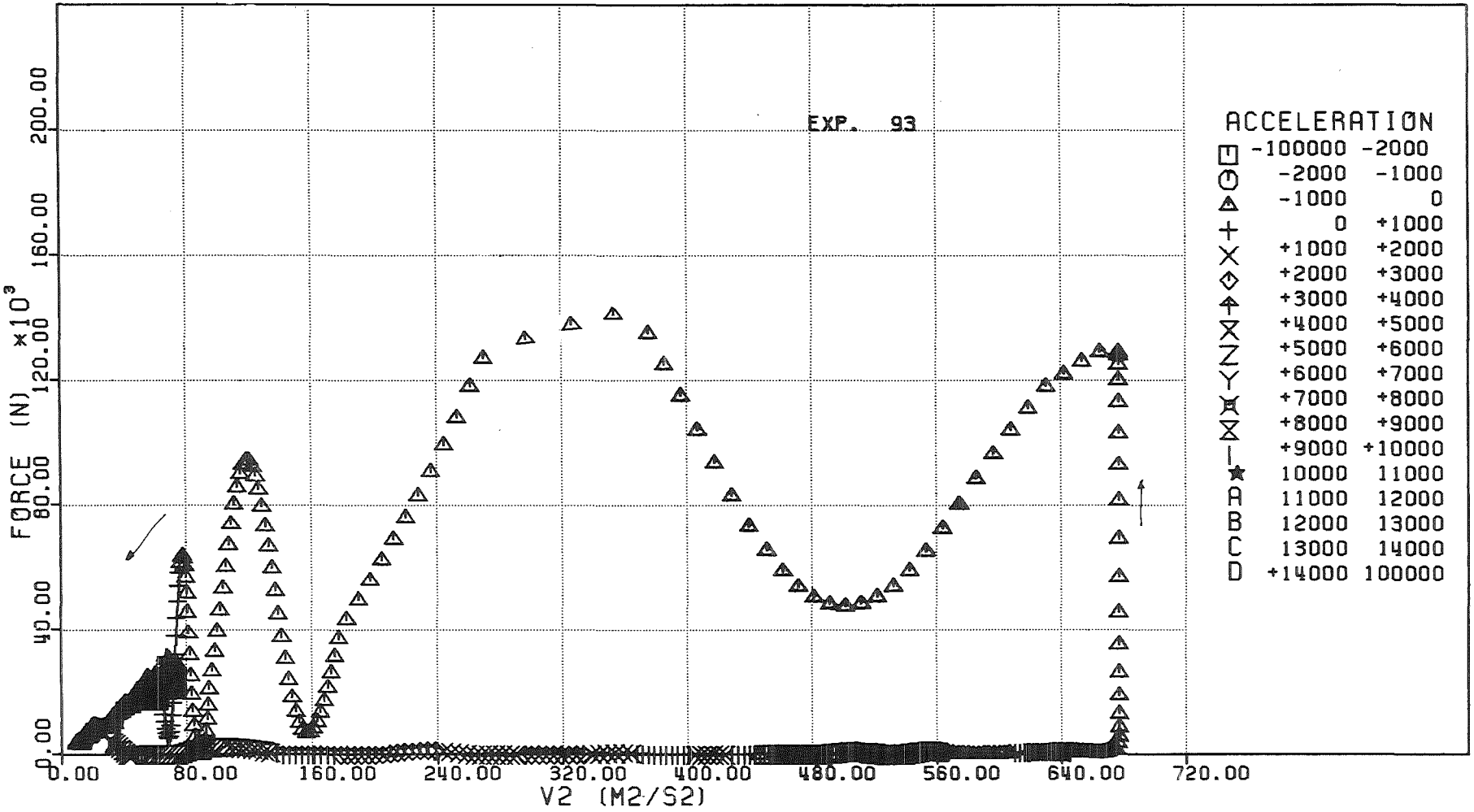

FIG. 6.288 - FORCE ACTING ON THE DIP-PLATE VERSUS THE SQUARE OF THE PISTON VELOCITY

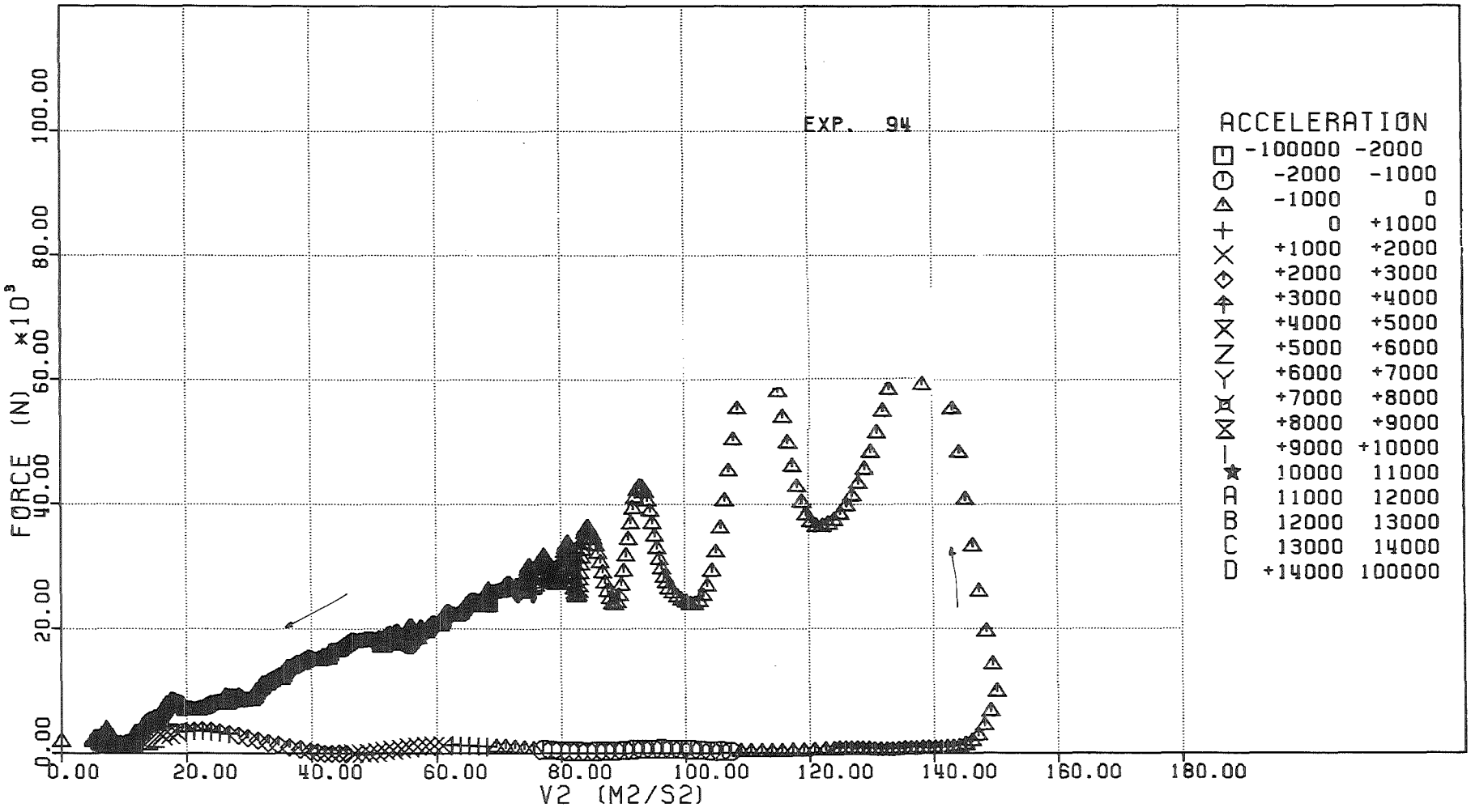

FIG. 6.289 - FORCE ACTING ON THE DIP-PLATE VERSUS THE SQUARE OF THE PISTON VELOCITY

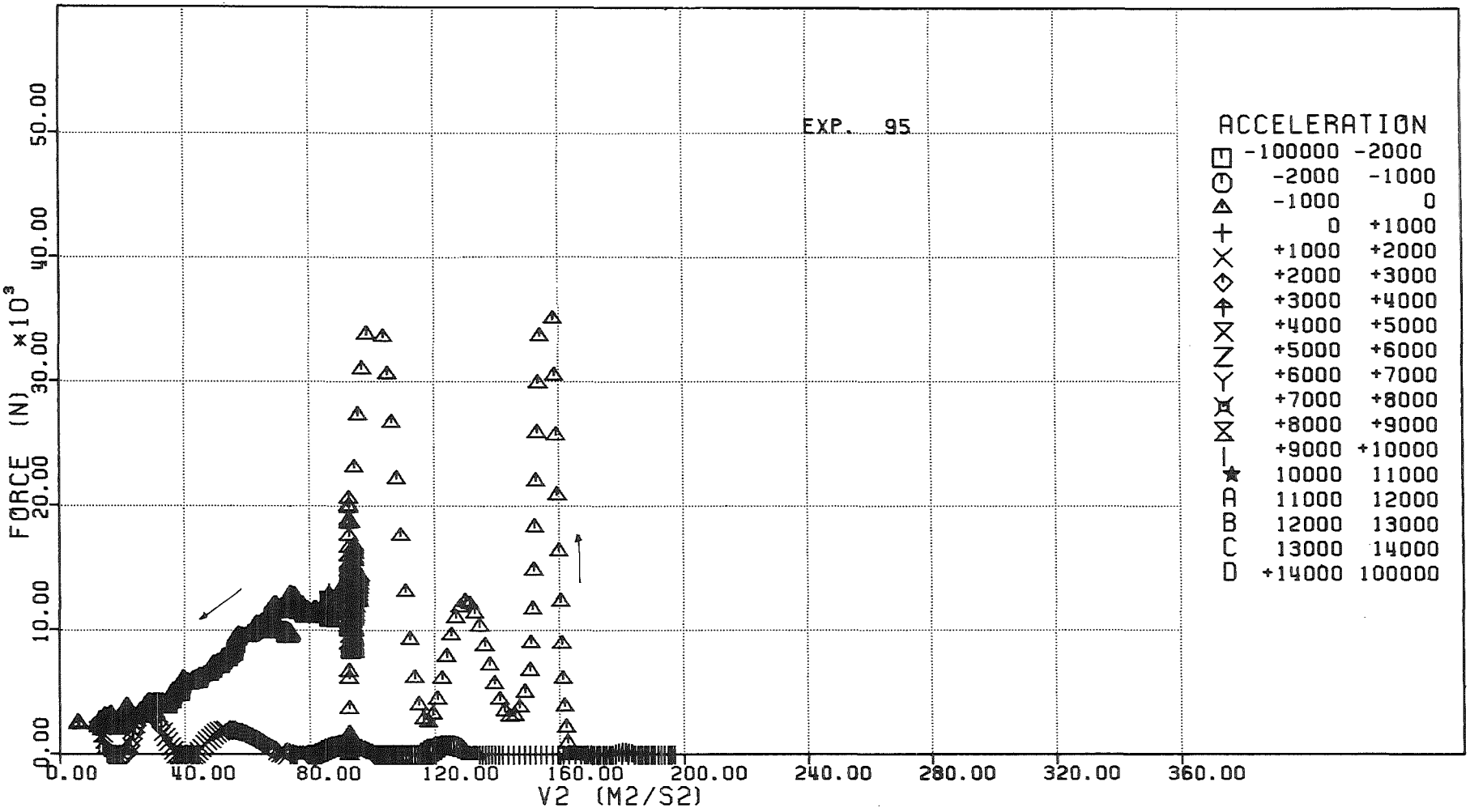

FIG. 6.290 - FORCE ACTING ON THE DIP-PLATE VERSUS THE SQUARE OF THE PISTON VELOCITY

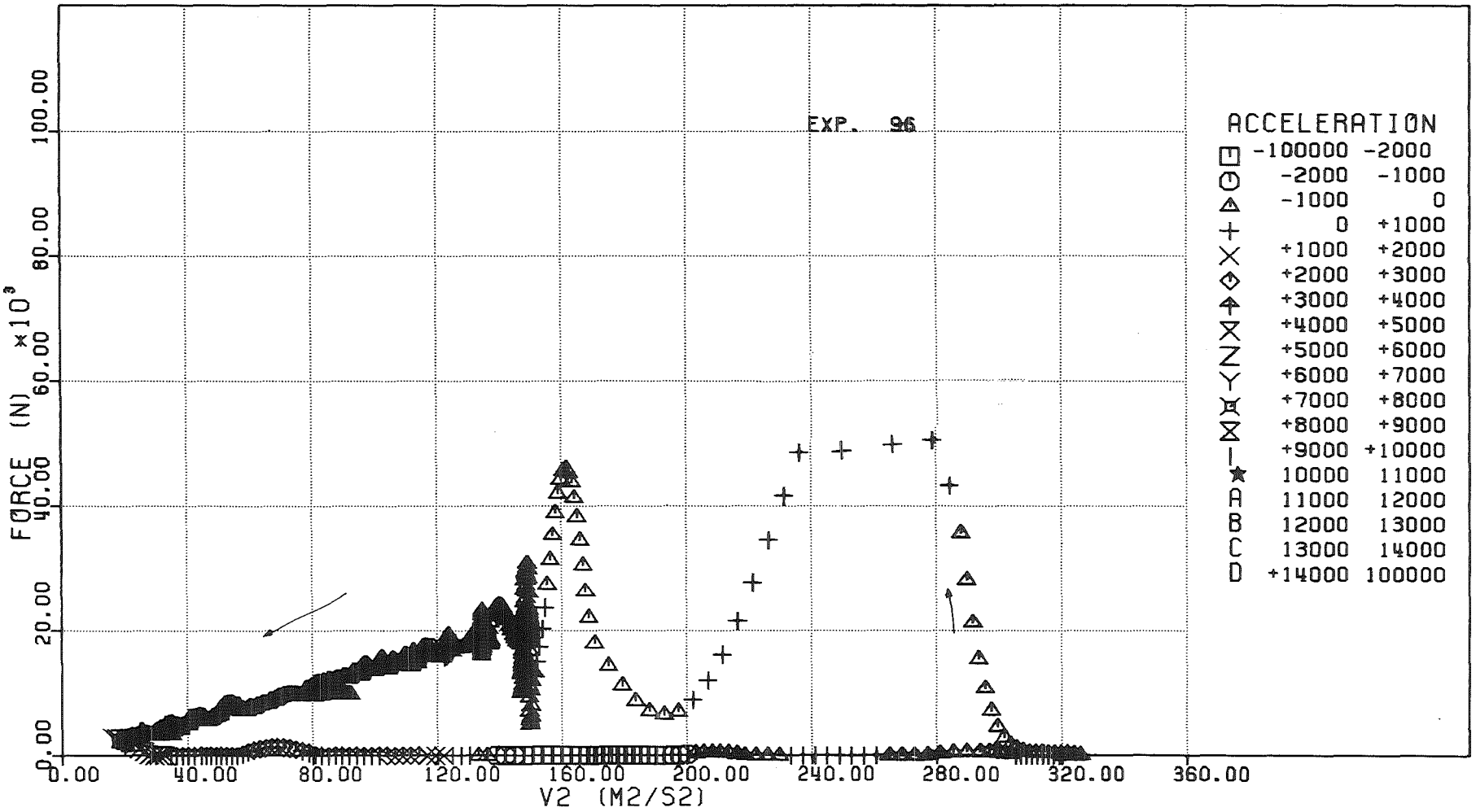

FIG. 6.291 - FORCE ACTING ON THE DIP-PLATE VERSUS THE SQUARE OF THE PISTON VELOCITY

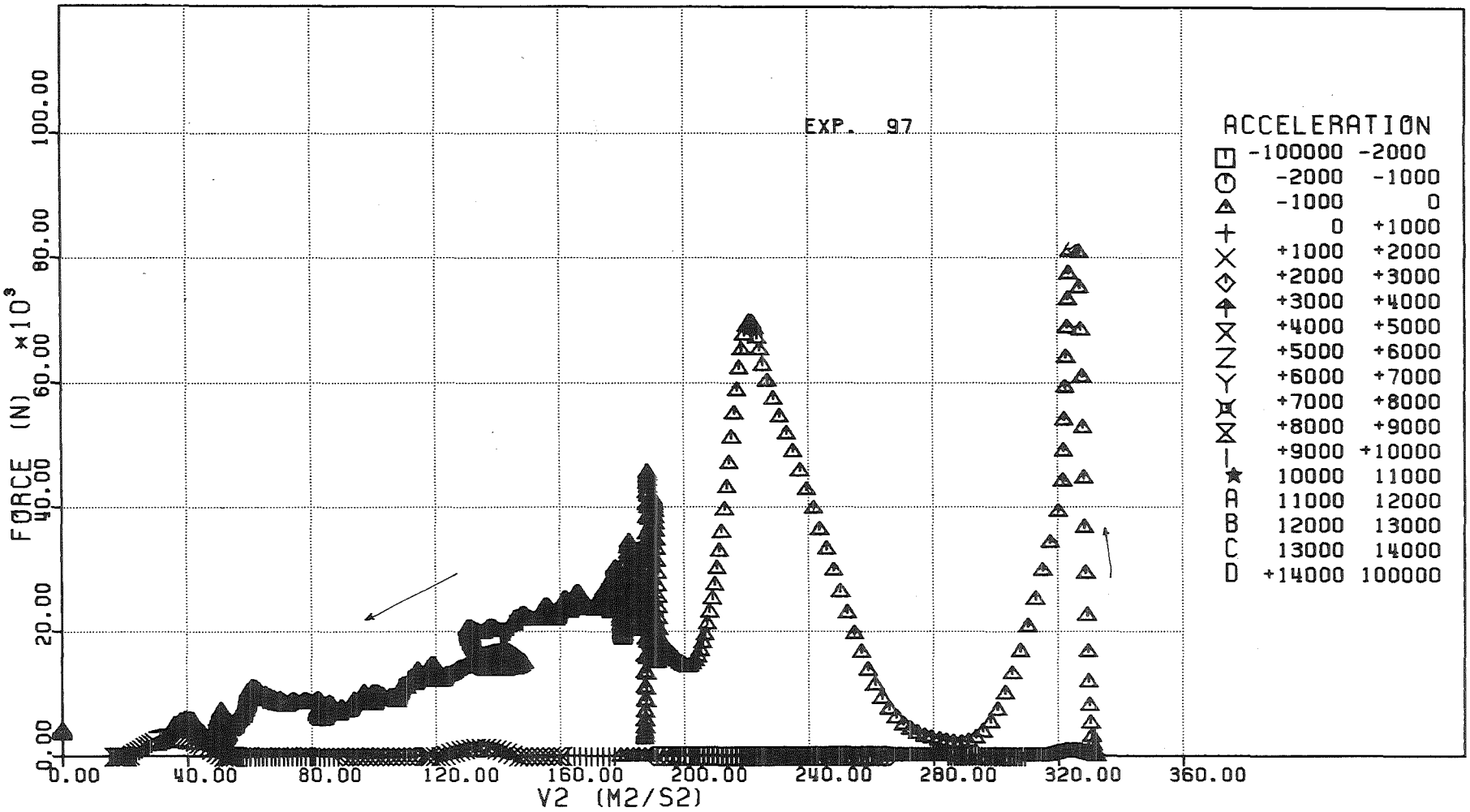

FIG. 6.292 - FORCE ACTING ON THE DIP-PLATE VERSUS THE SQUARE OF THE PISTON VELOCITY

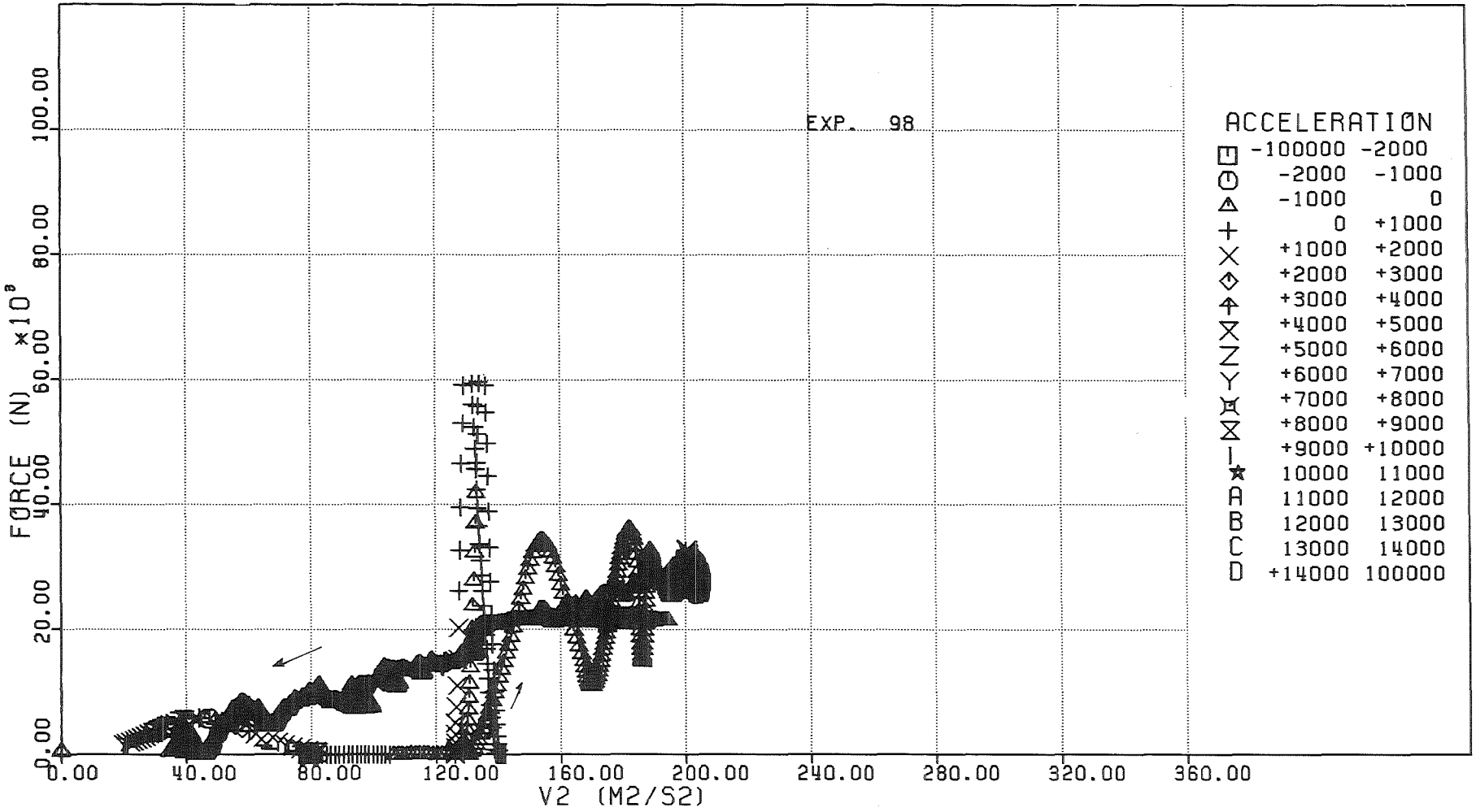

FIG. 6.293 -FORCE ACTING ON THE DIP-PLATE VERSUS THE SQUARE OF THE PISTON VELOCITY

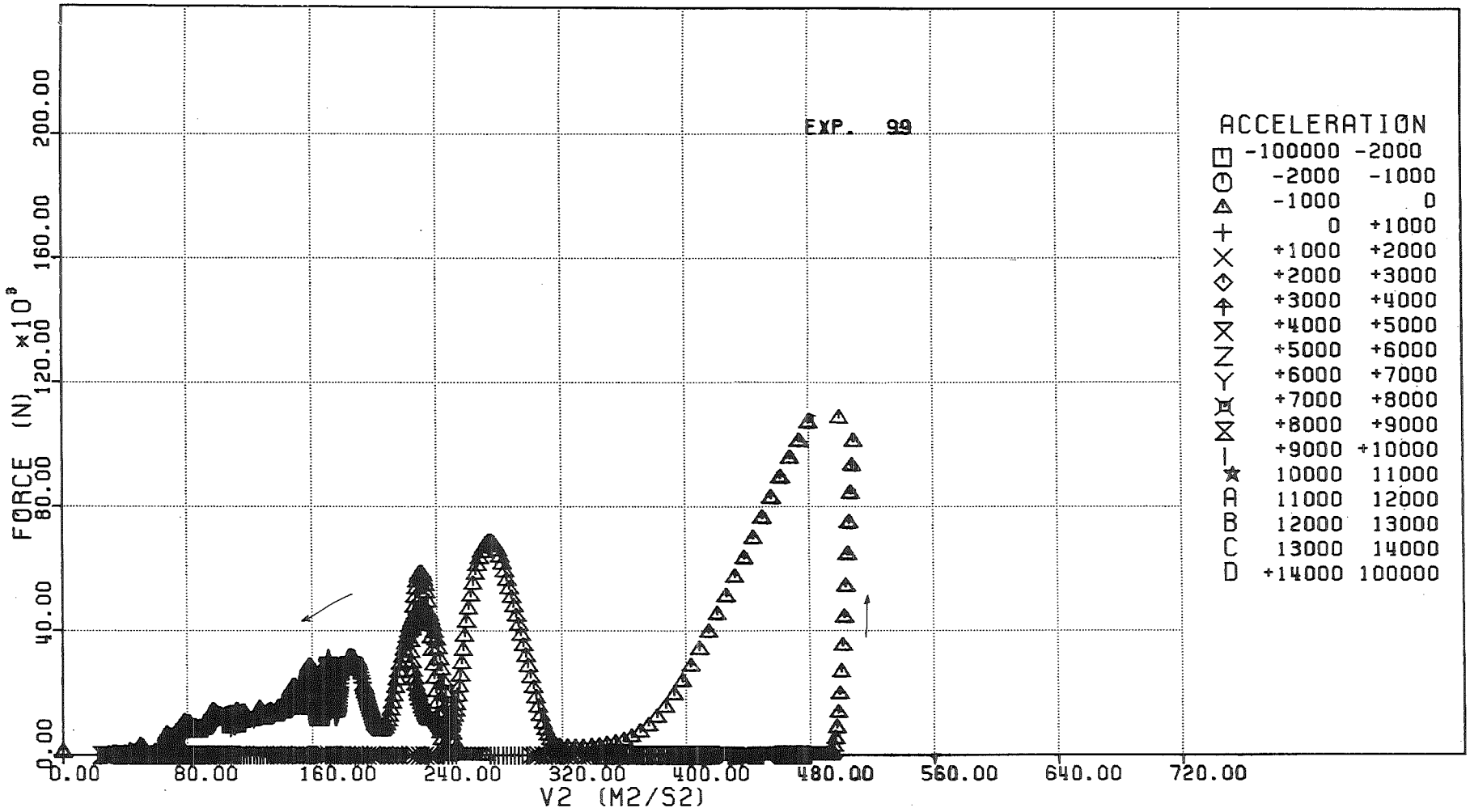

FIG. 6-294 - FORCE ACTING ON THE DIP-PLATE VERSUS THE SQUARE OF THE PISTON VELOCITY

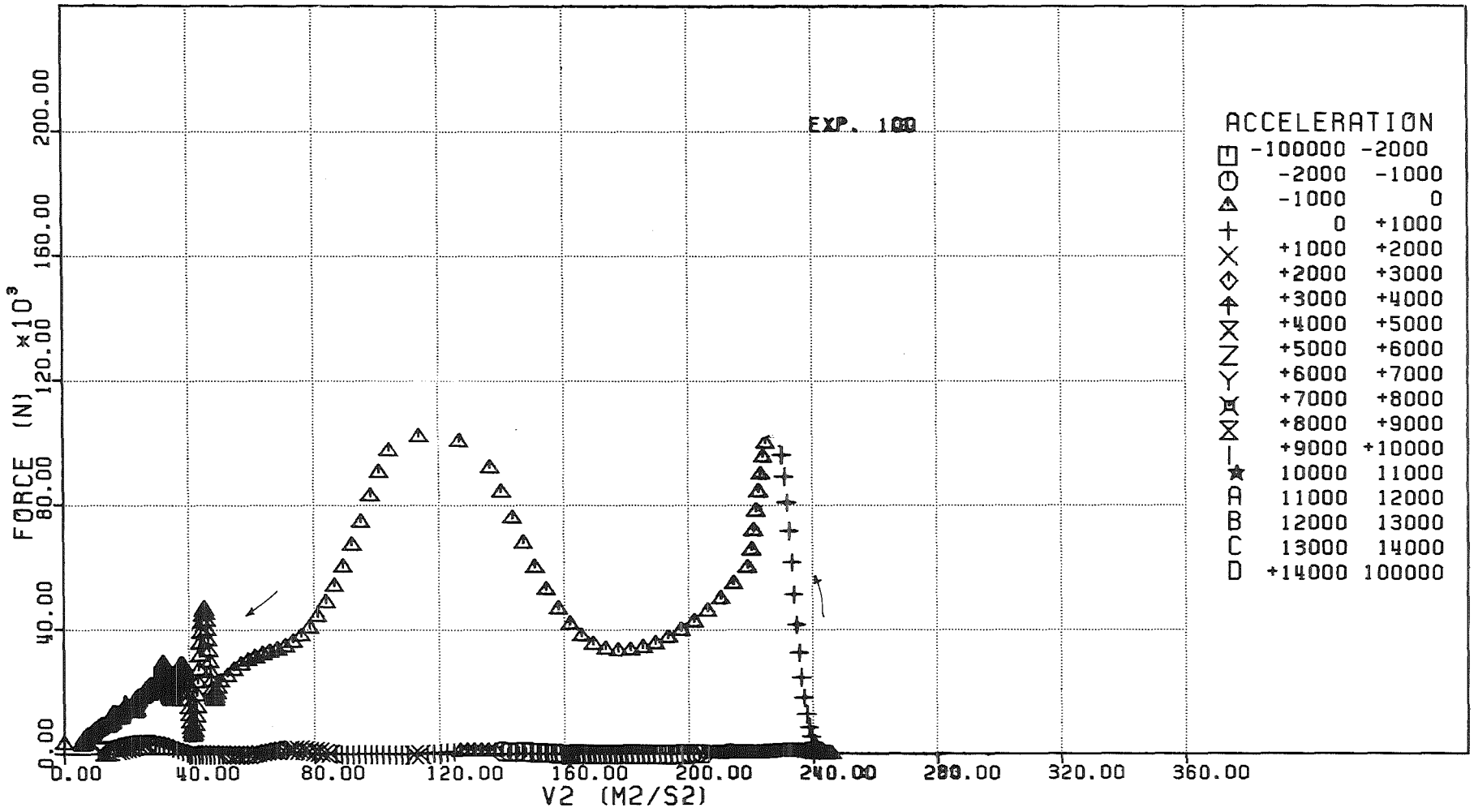

FIG. 6.295 - FORCE ACTING ON THE DIP-PLATE VERSUS THE SQUARE OF THE PISTON VELOCITY

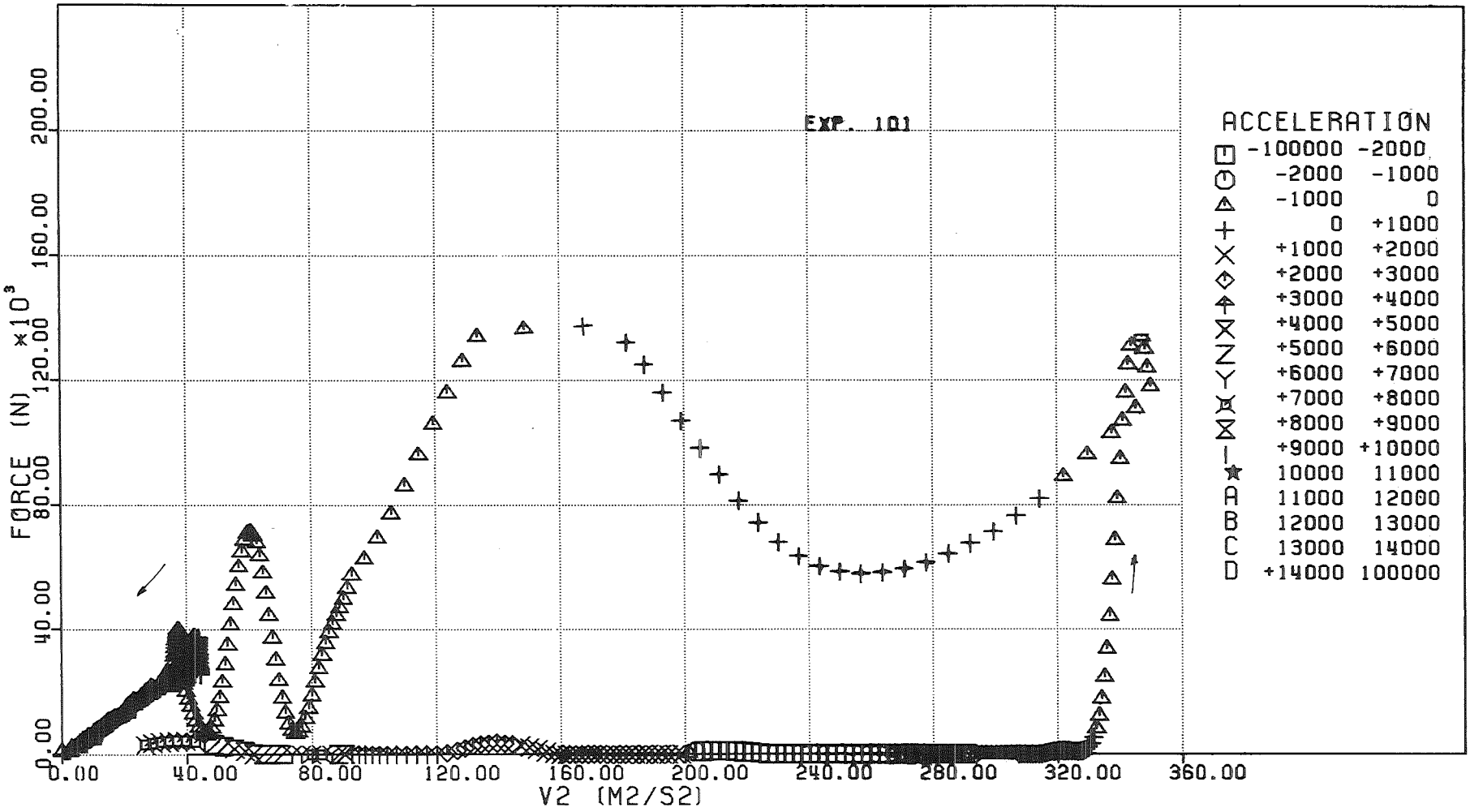

FIG. 6.296 - FORCE ACTING ON THE DIP-PLATE VERSUS THE SQUARE OF THE PISTON VELOCITY

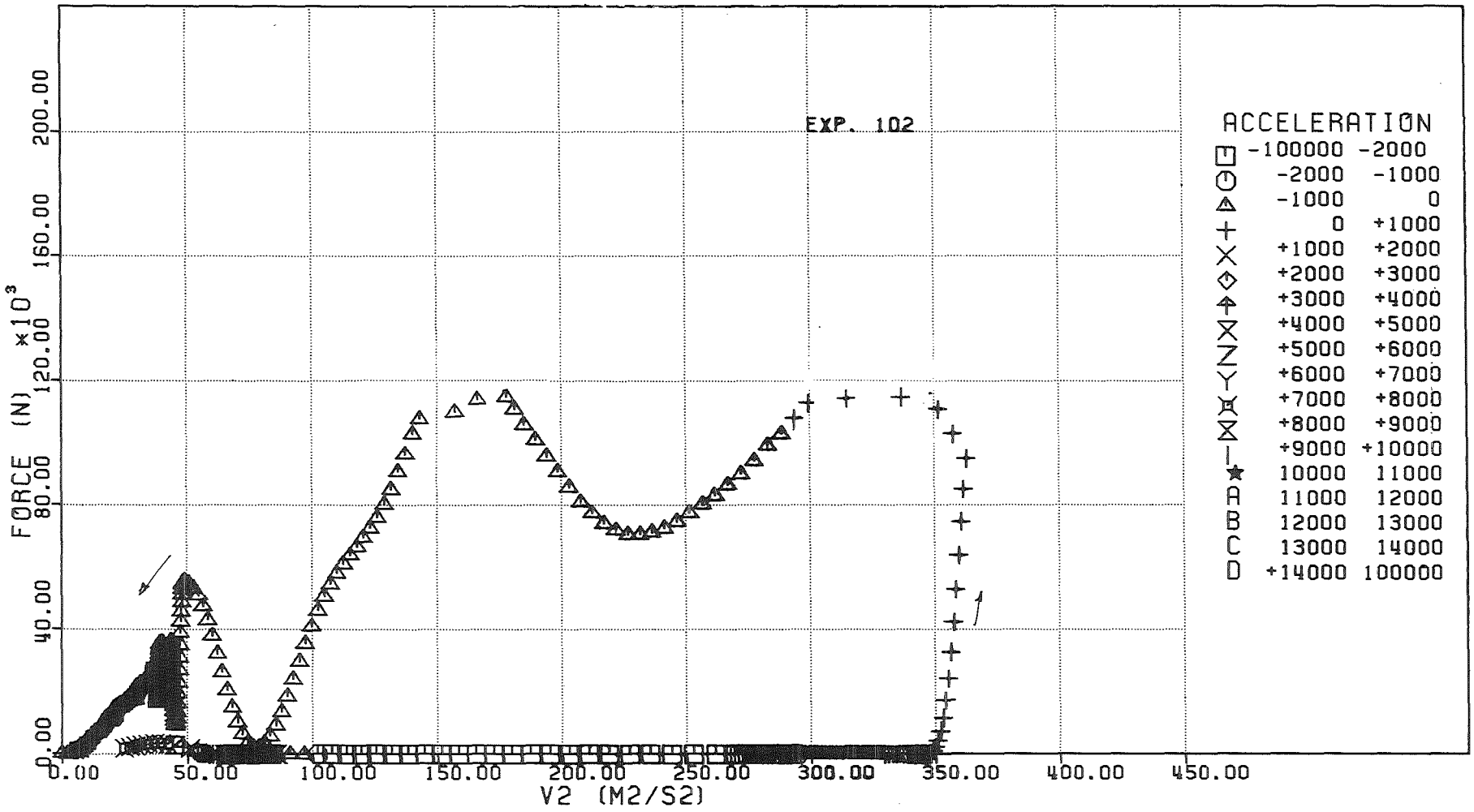

FIG. 6.297 - FORCE ACTING ON THE DIP-PLATE VERSUS THE SQUARE OF THE PISTON VELOCITY

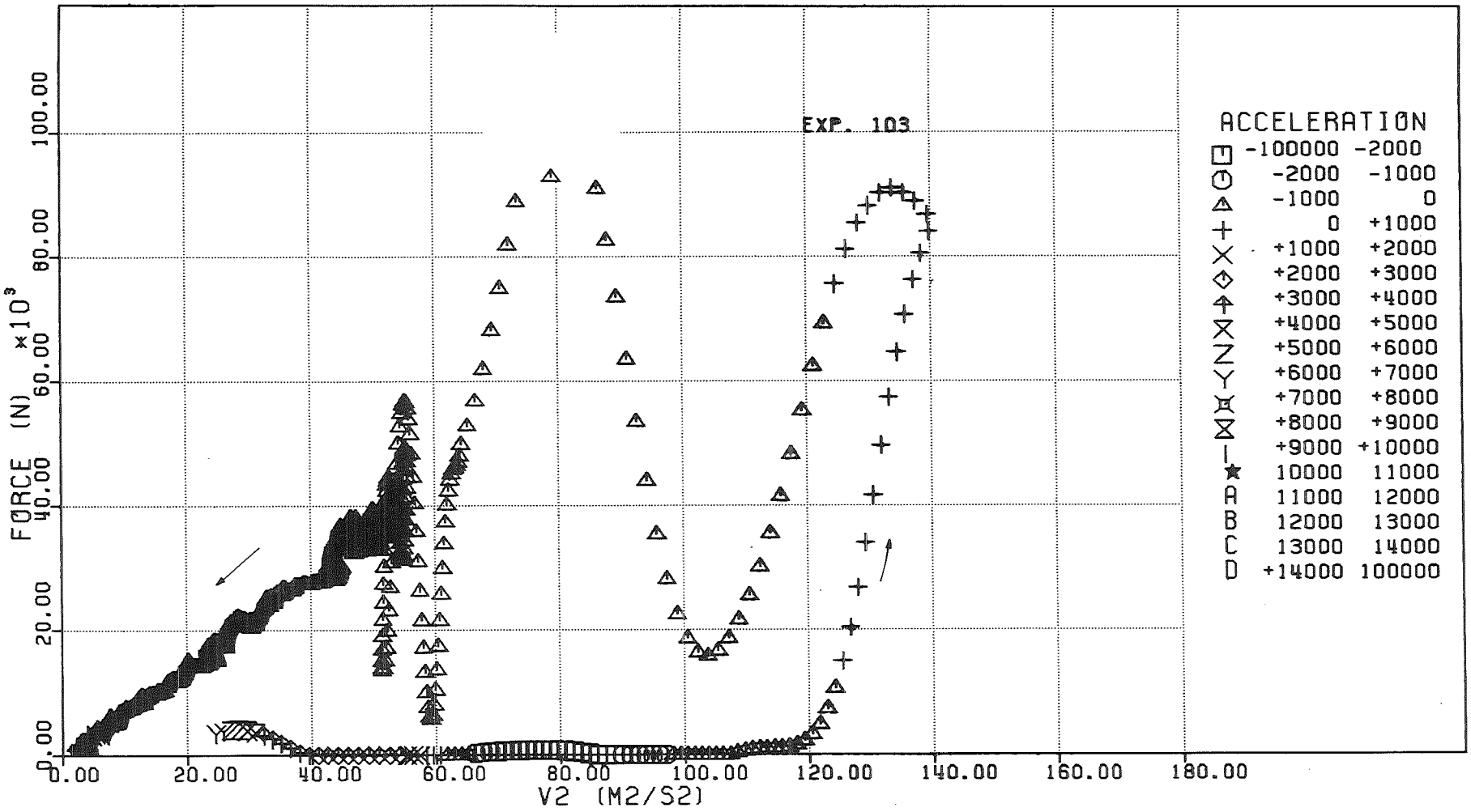

FIG. 6.298 - FORCE ACTING ON THE DIP-PLATE VERSUS THE SQUARE OF THE PISTON VELOCITY

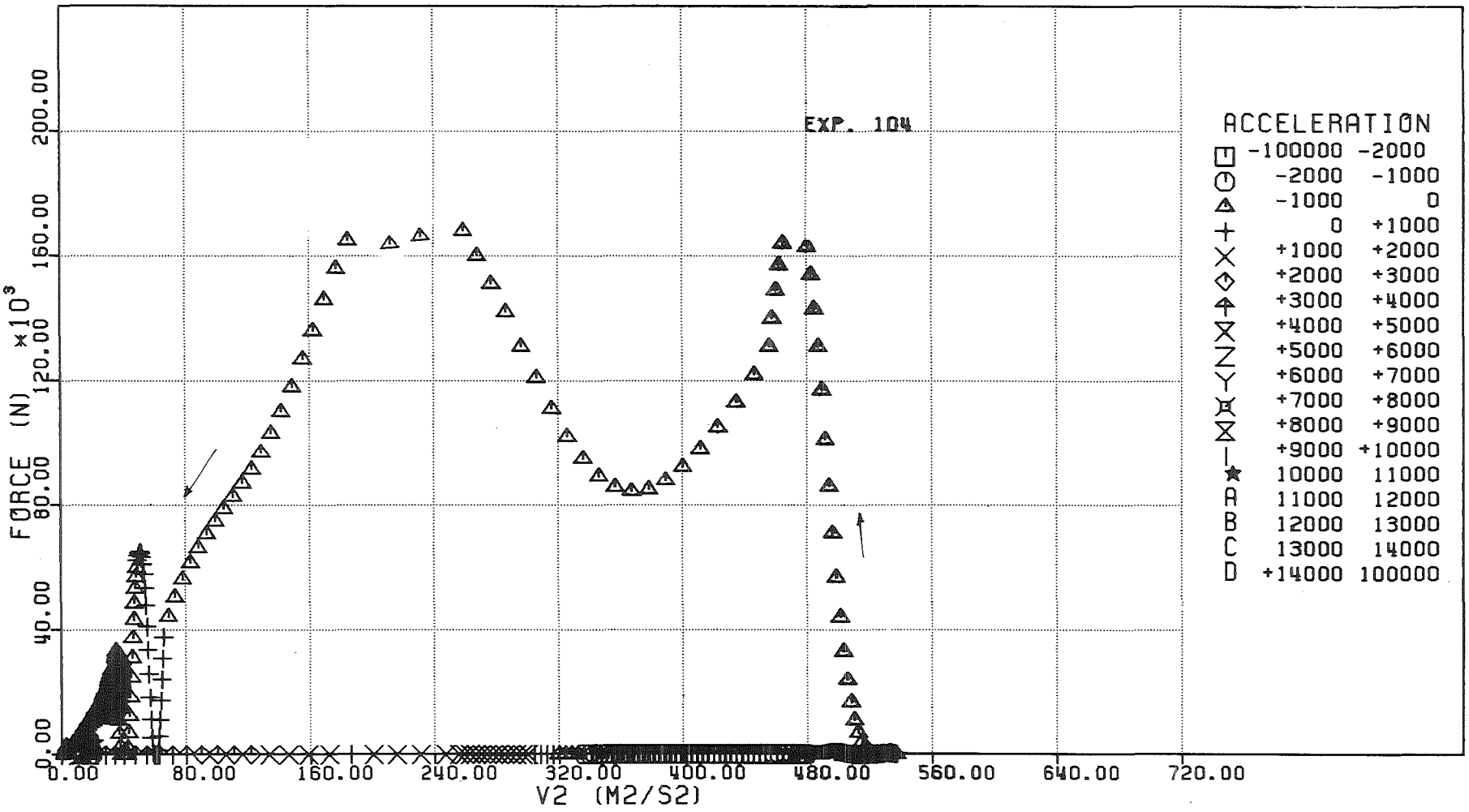

FIG. 6.299 - FORCE ACTING ON THE DIP-PLATE VERSUS THE SQUARE OF THE PISTON VELOCITY

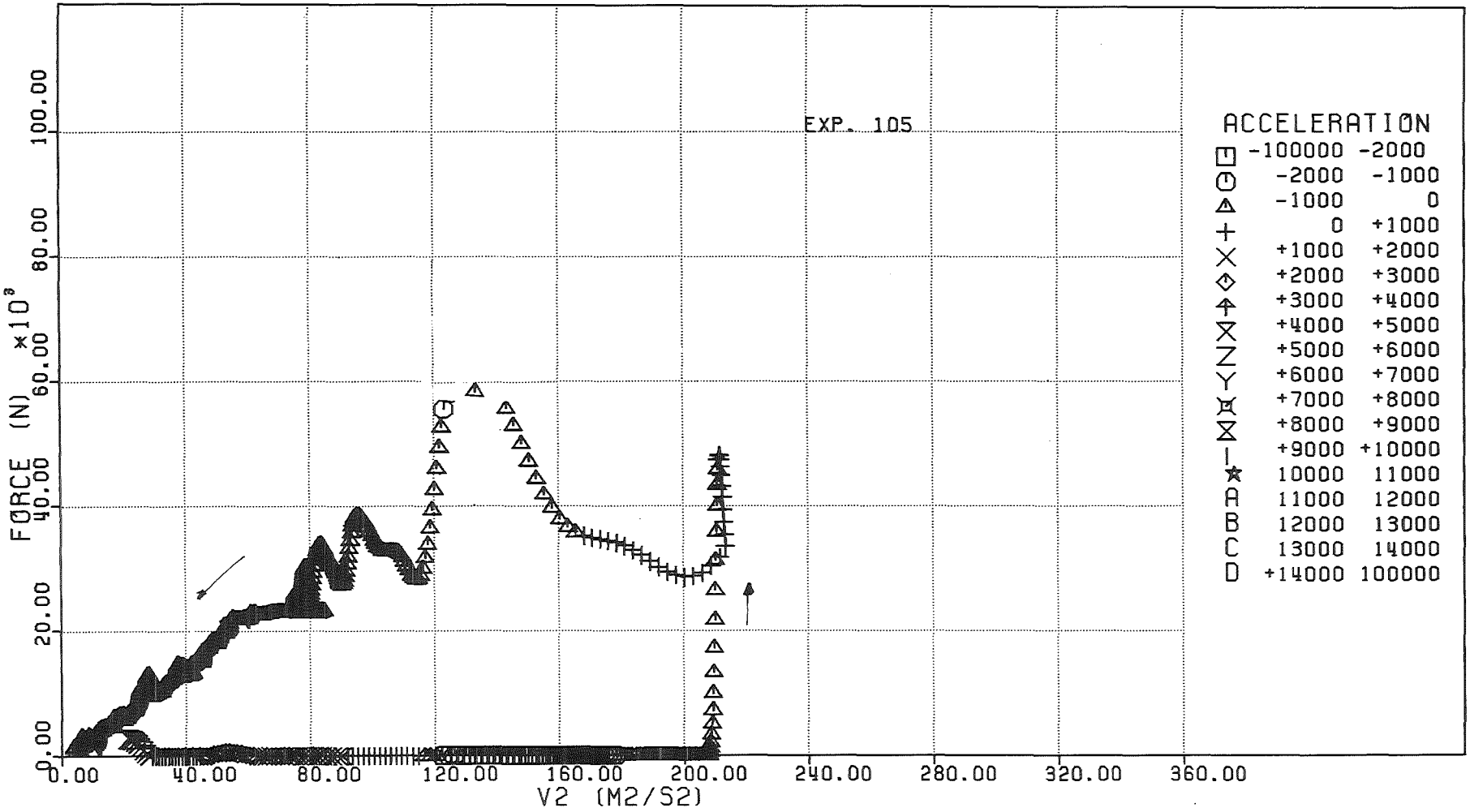

FIG. 6.300 - FORCE ACTING ON THE DIP-PLATE VERSUS THE SQUARE OF THE PISTON VELOCITY

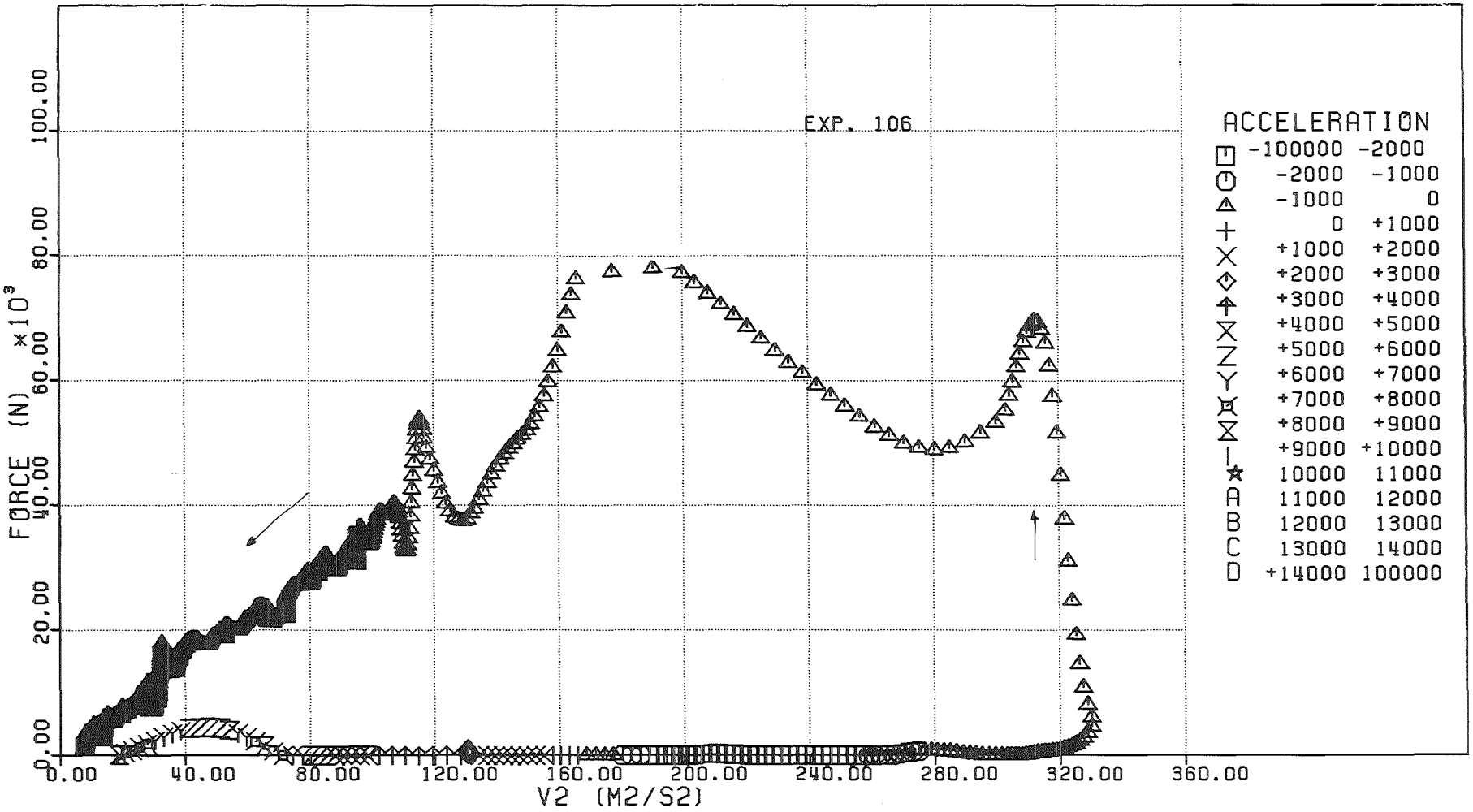

FIG. 6.301 - FORCE ACTING ON THE DIP-PLATE VERSUS THE SQUARE OF THE PISTON VELOCITY

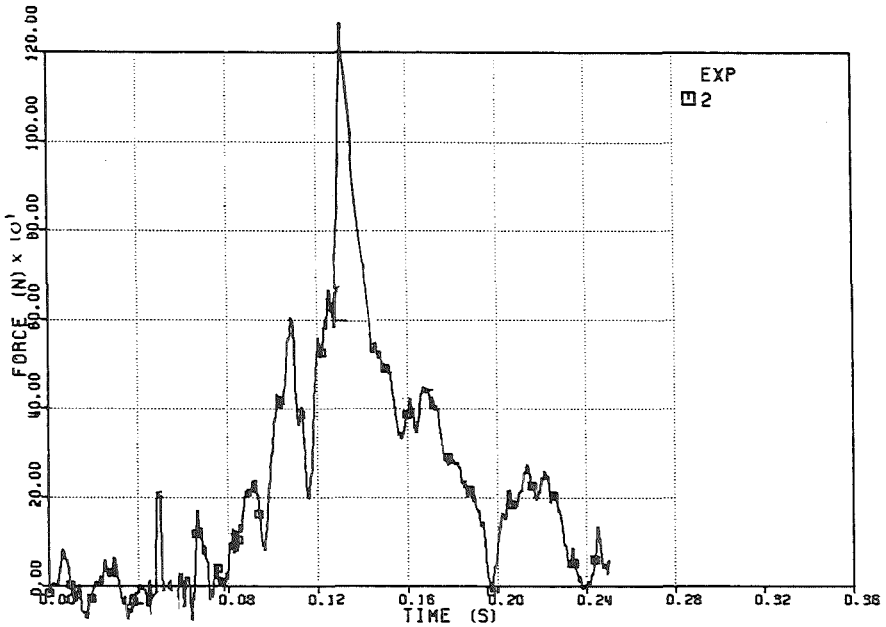

FIG. 6.303 FORCE ON THE UPPER PLATE

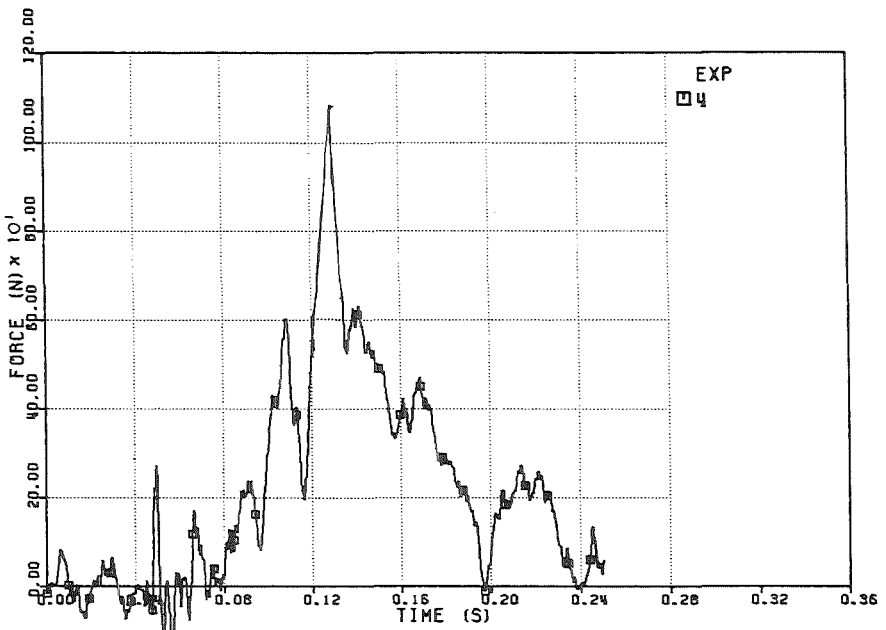

FIG. 6.305 FORCE ON THE UPPER PLATE

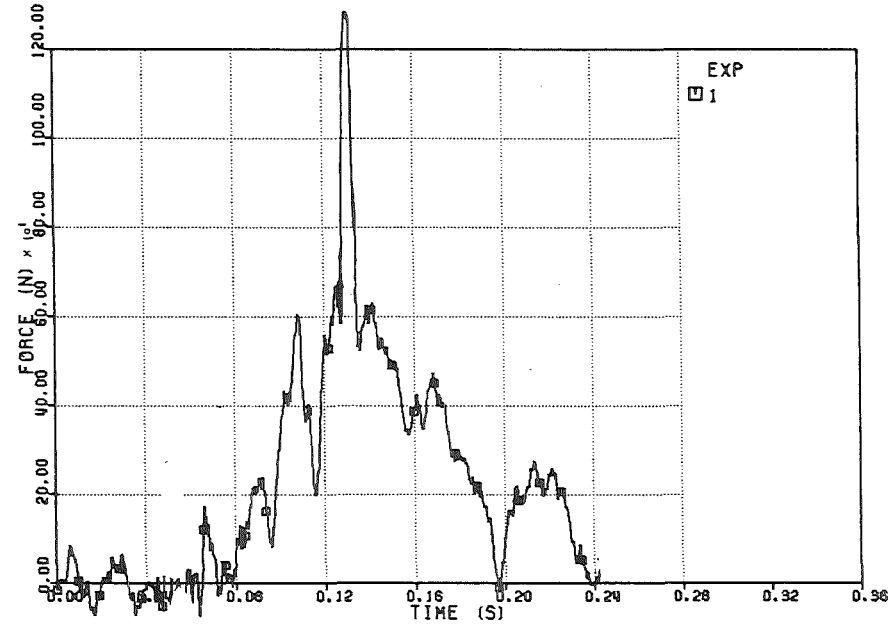

FIG. 6.302 FORCE ON THE UPPER PLATE

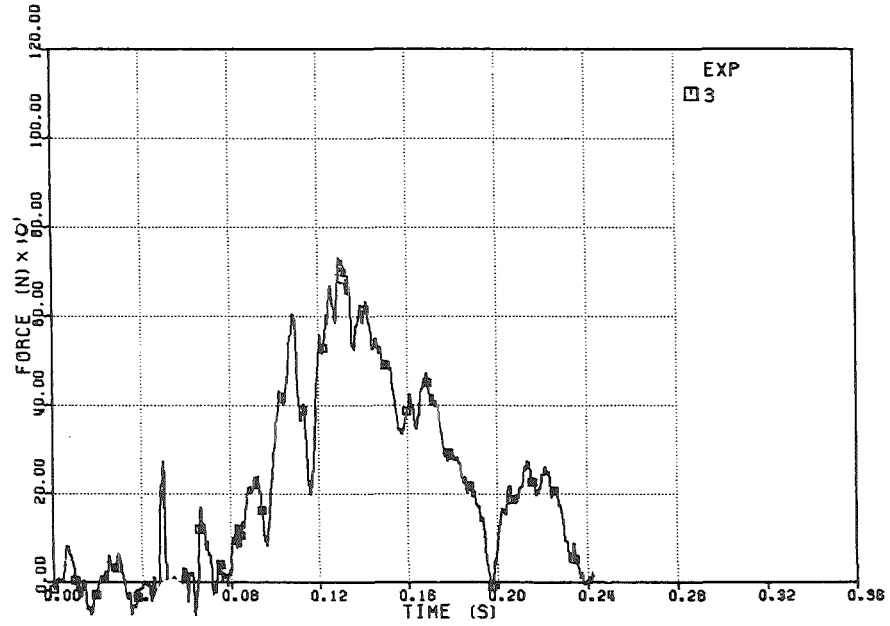

FIG. 6.304 FORCE ON THE UPPER PLATE

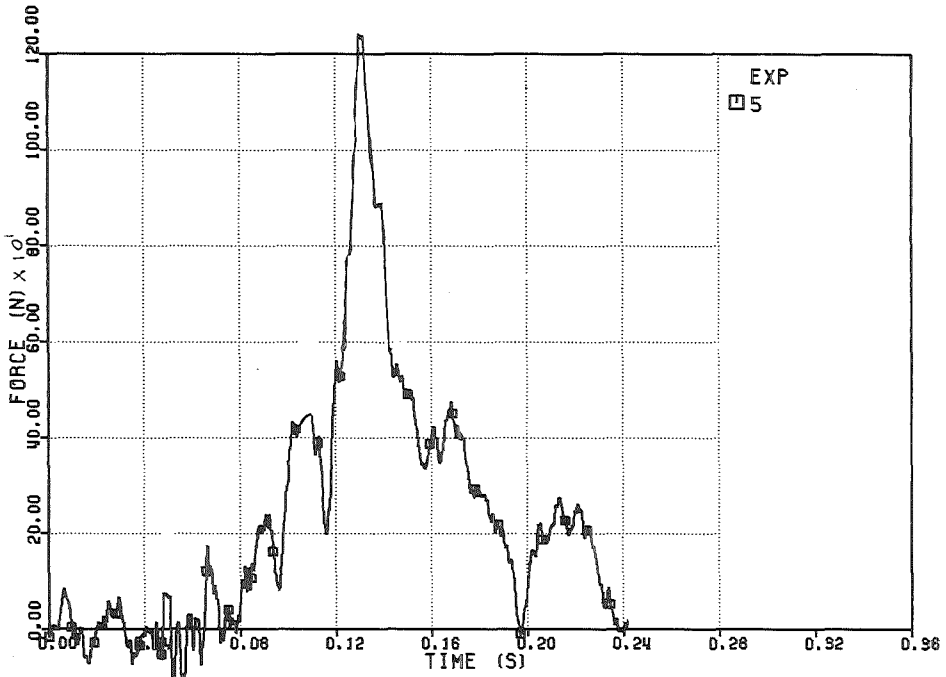

FIG. 6.306 FORCE ON THE UPPER PLATE

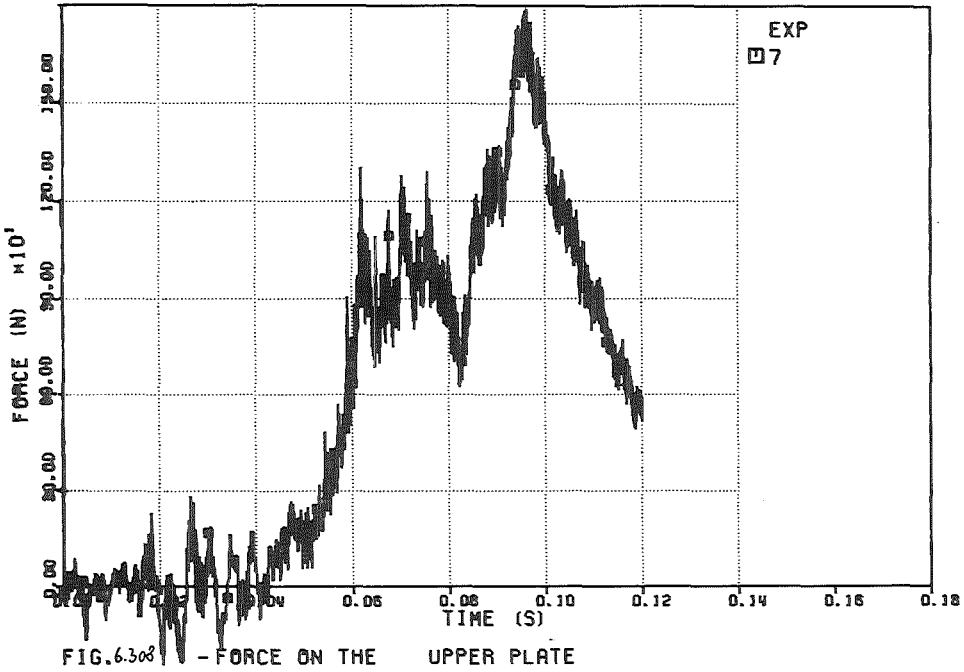

FIG.6.308 - FORCE ON THE UPPER PLATE

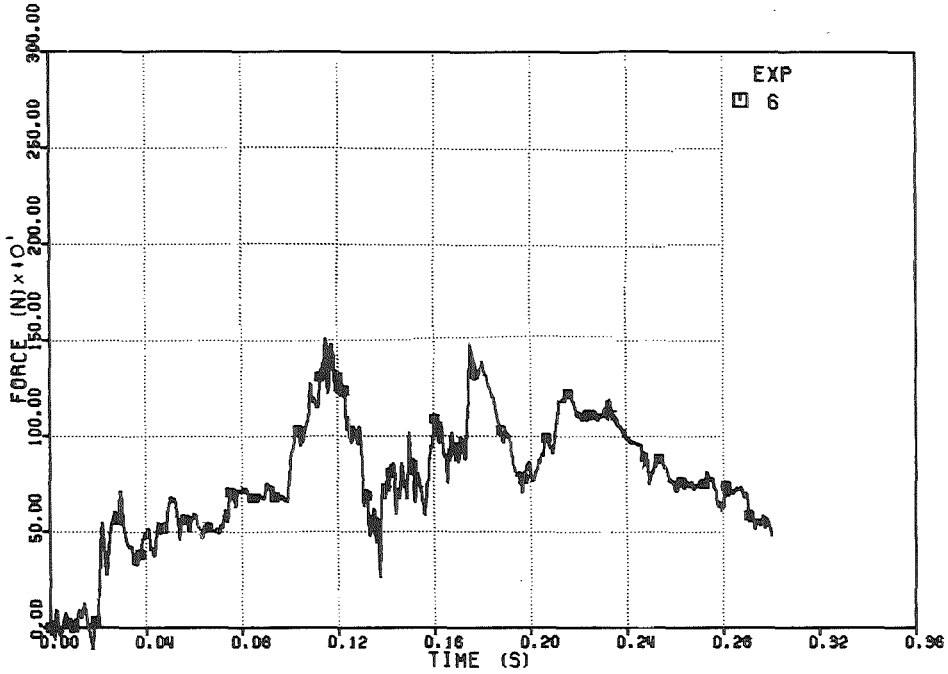

FIG. 6.307- FORCE ON THE UPPER PLATE

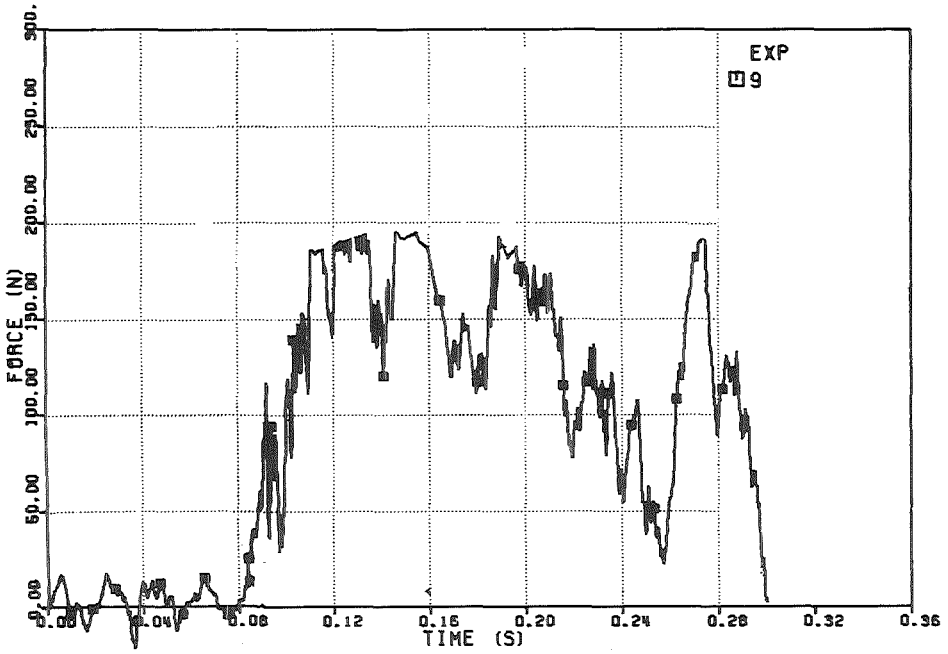

FIG. 6.310 - FORCE ON THE UPPER PLATE

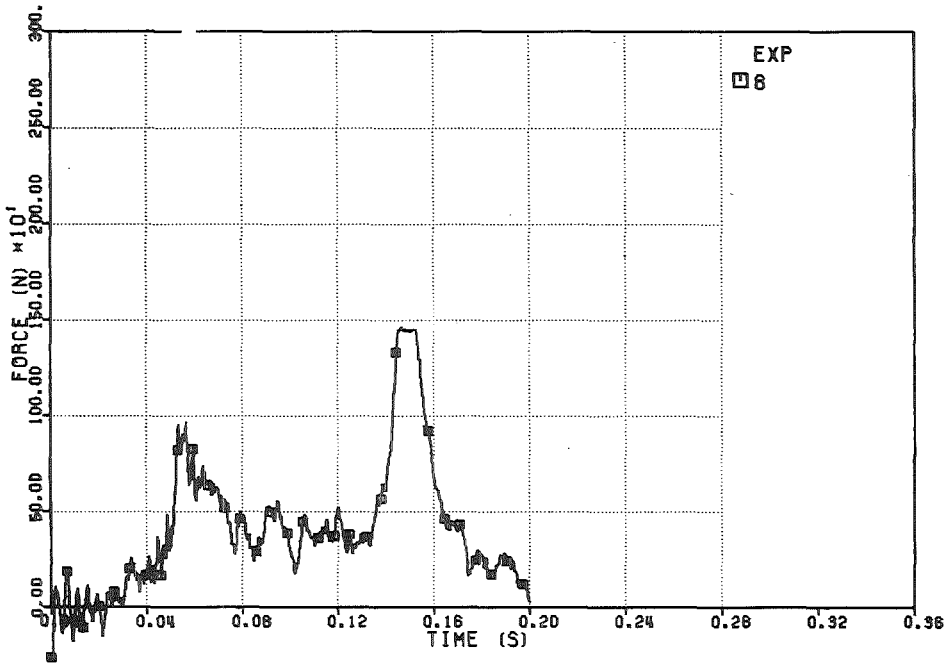

FIG. 6.309 - FORCE ON THE UPPER PLATE

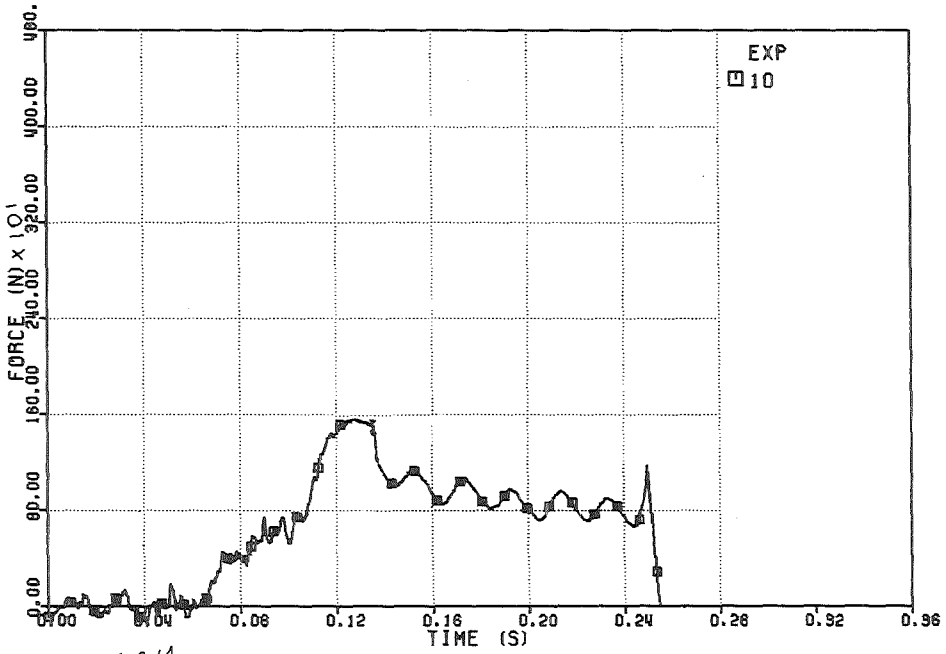

FIG. 6.311 - FORCE ON THE UPPER PLATE

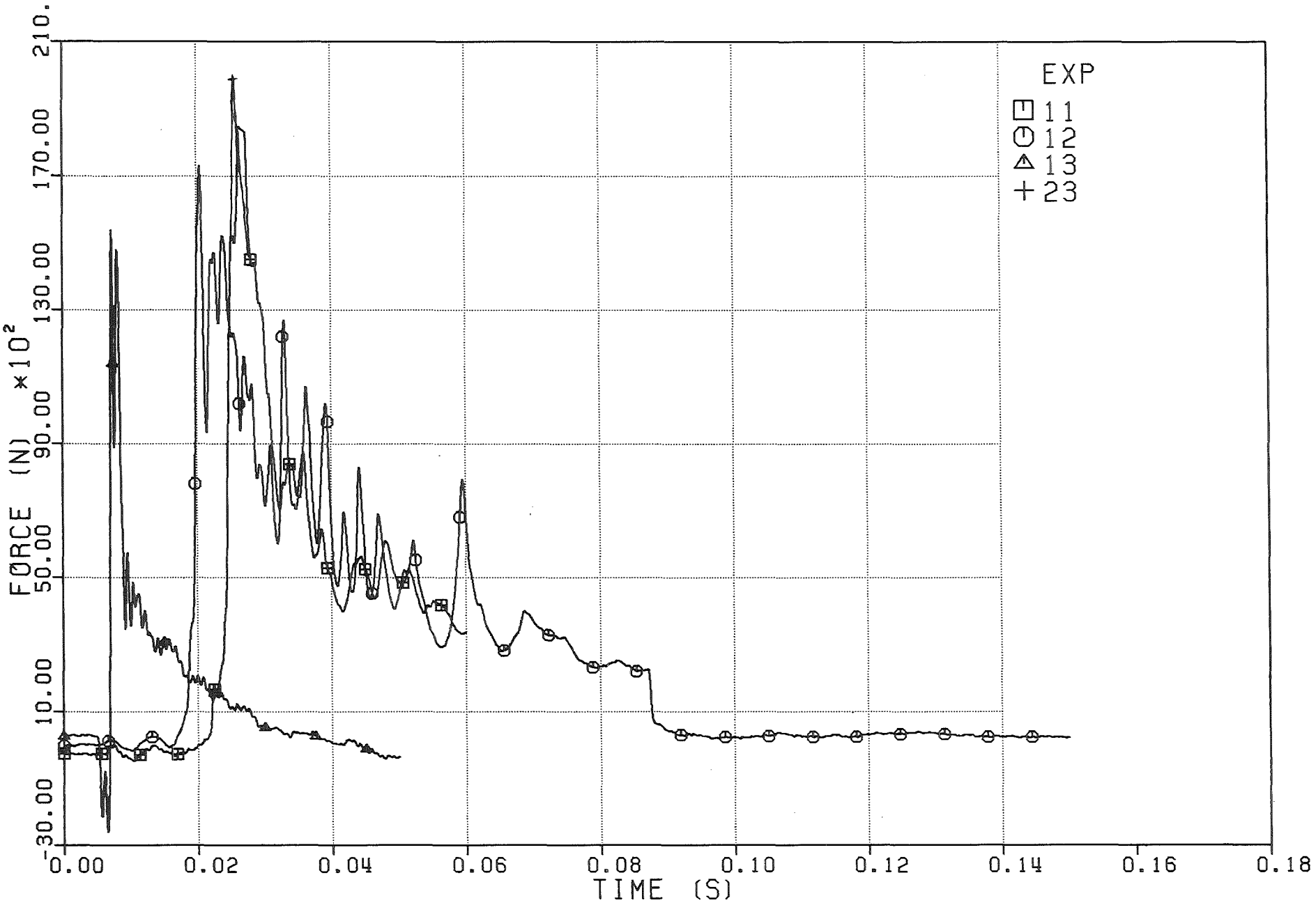

Fig. 6.312 - Force on the upper plate

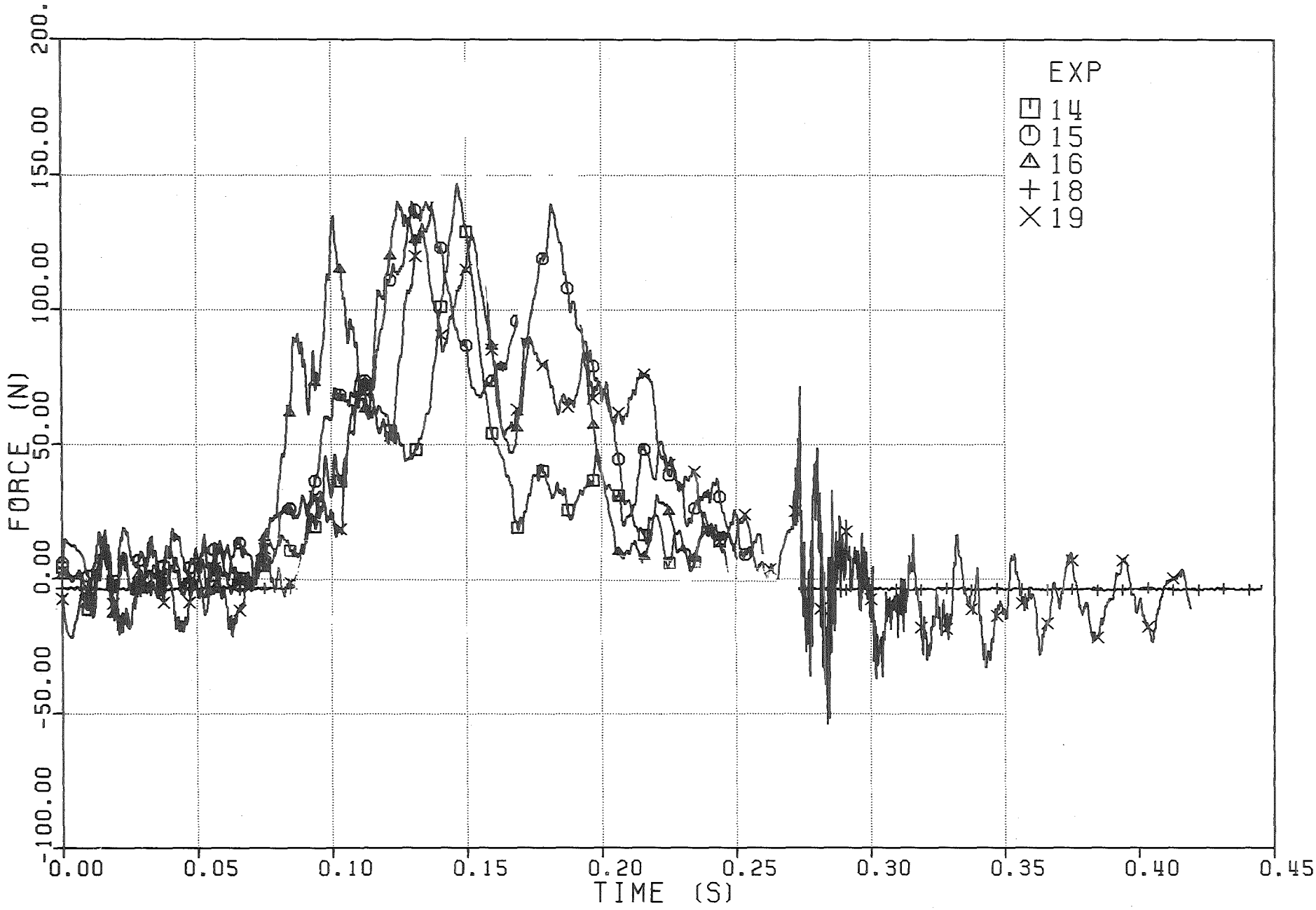

Fig. 6.313 - Force on the upper plate

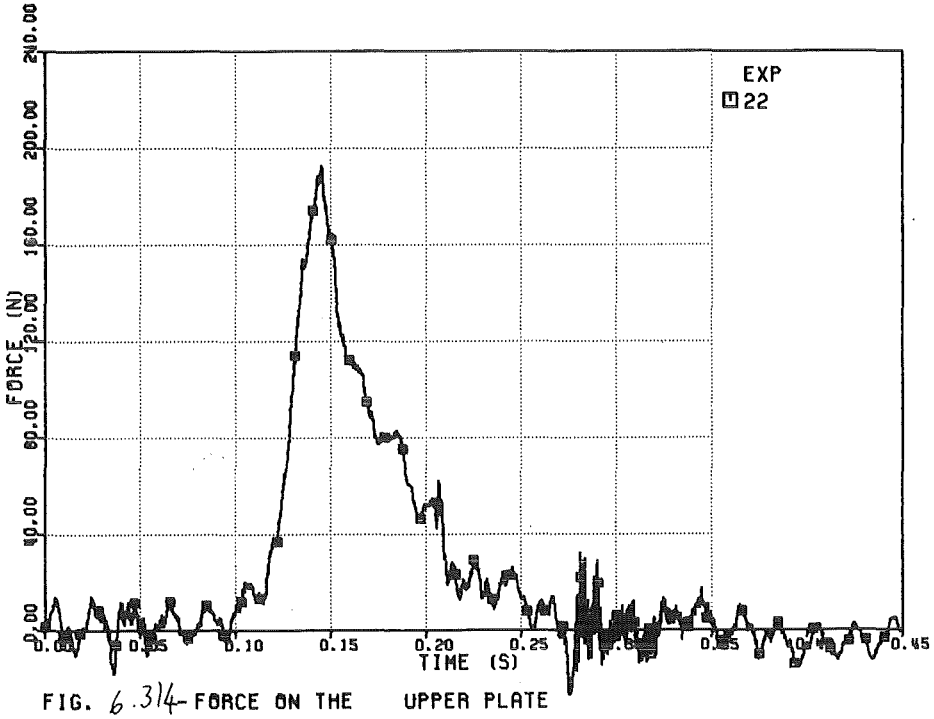

FIG. 6.314- FORCE ON THE UPPER PLATE

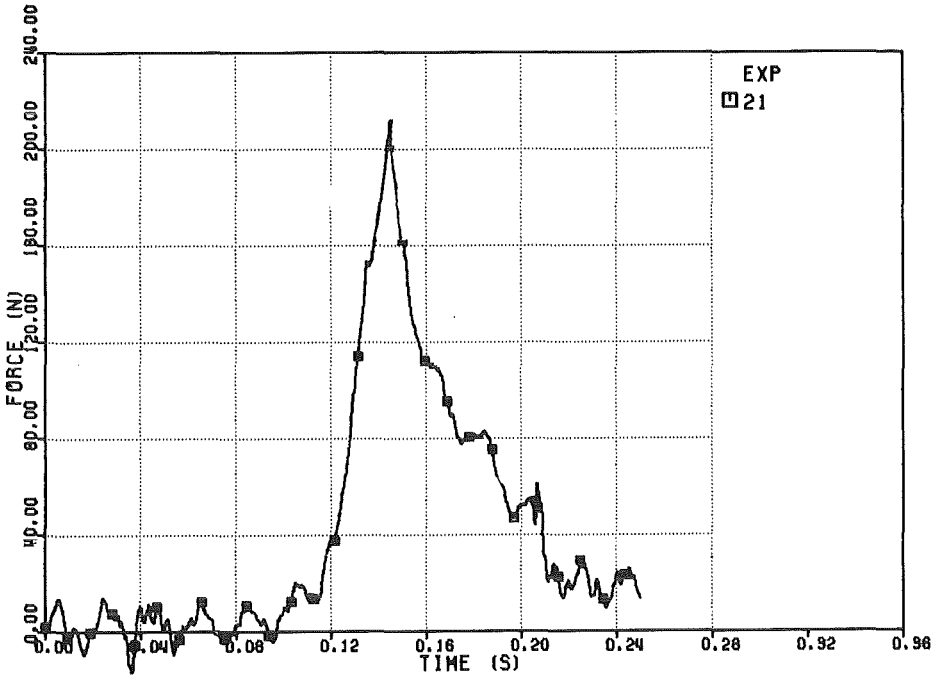

FIG. 6.315- FORCE ON THE UPPER PLATE

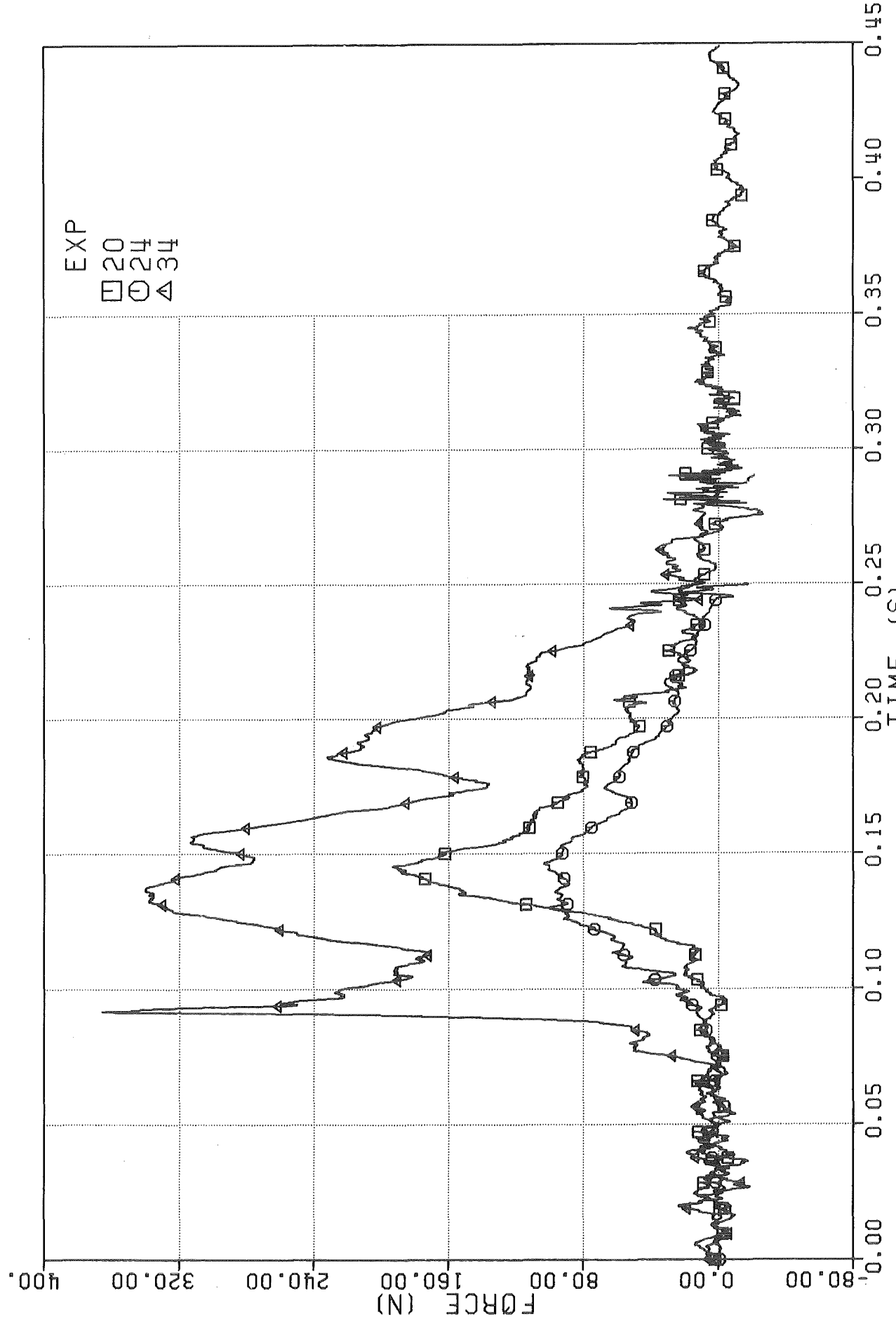

Fig. 6.316 - Force on the upper plate

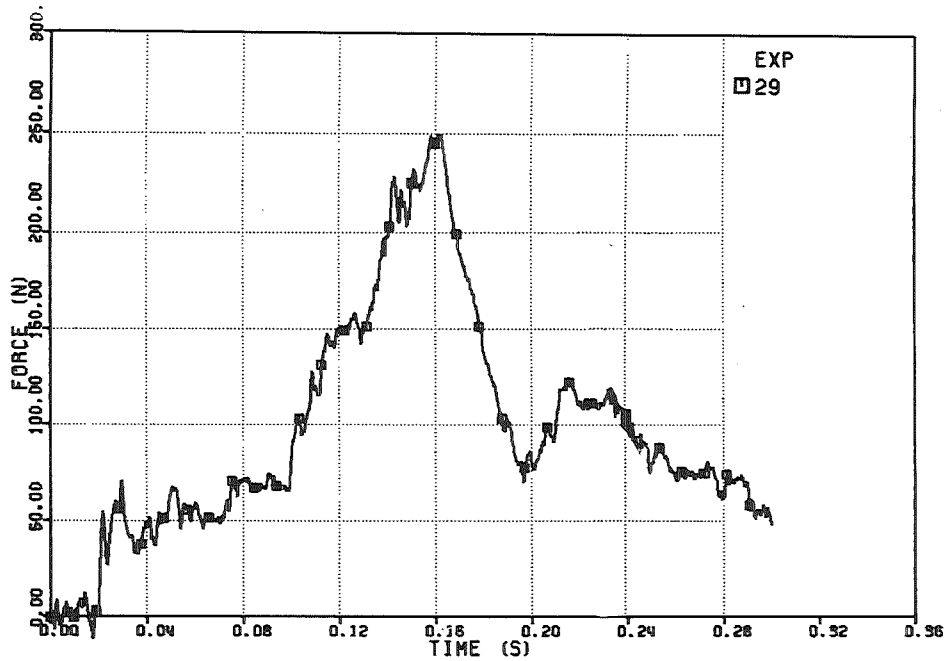

FIG. 6.316 - FORCE ON THE UPPER PLATE

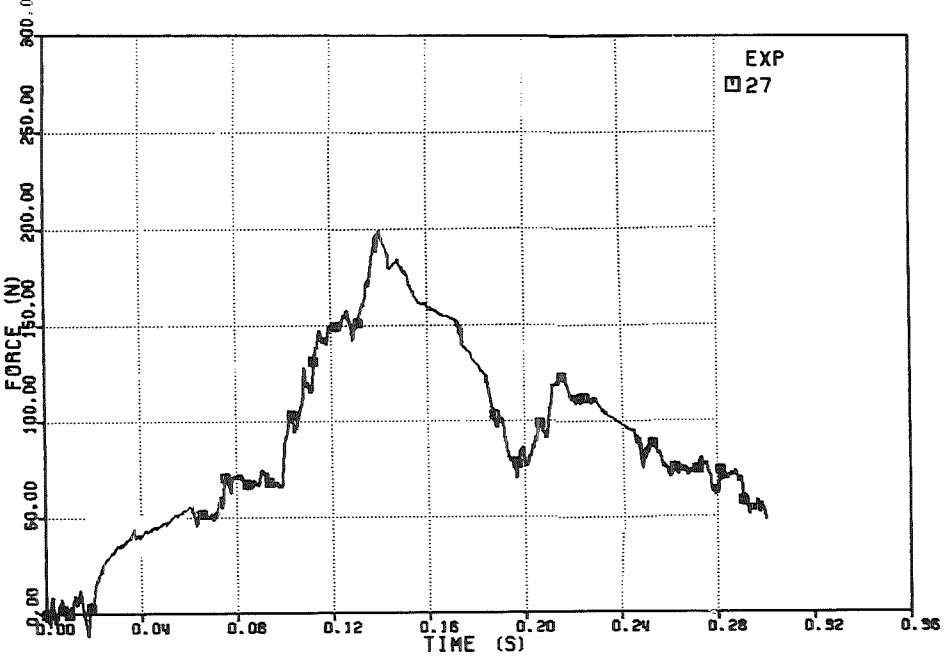

FIG. 6.320 - FORCE ON THE UPPER PLATE

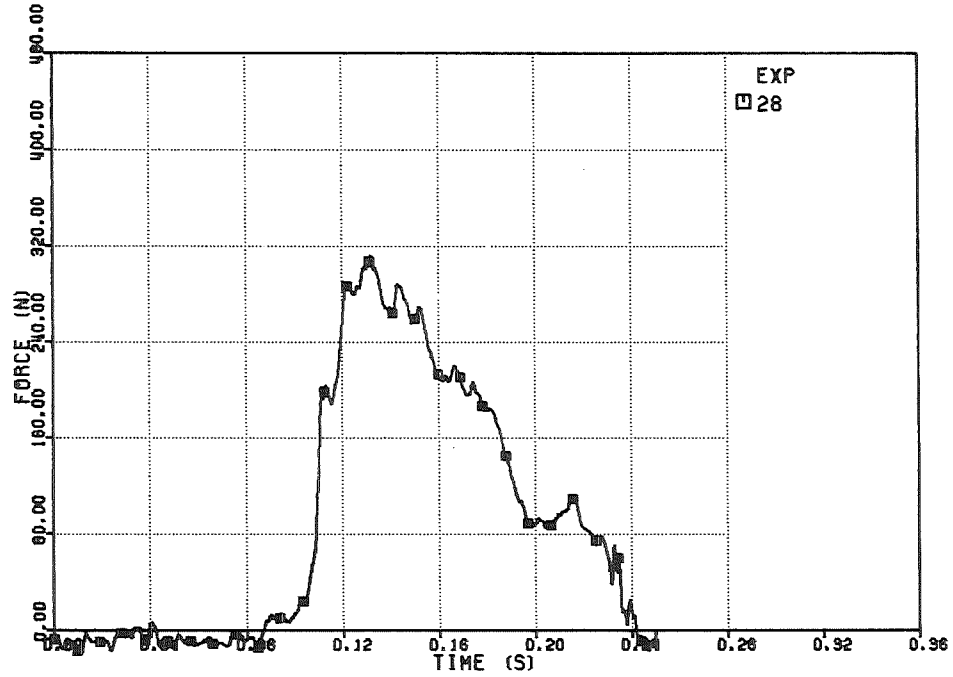

FIG. 6.317 - FORCE ON THE UPPER PLATE

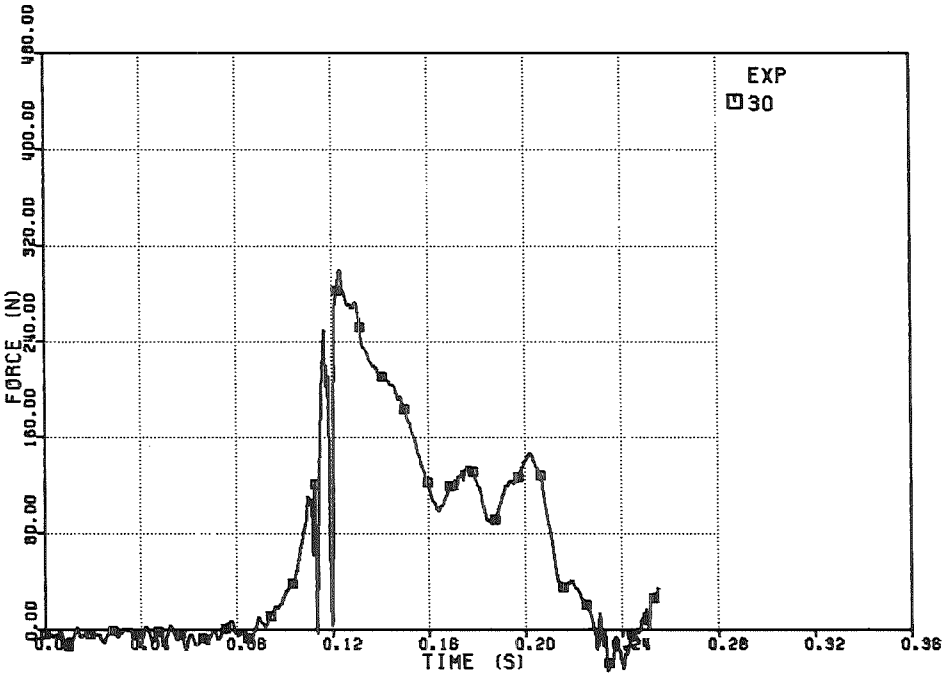

FIG. 6.319 - FORCE ON THE UPPER PLATE

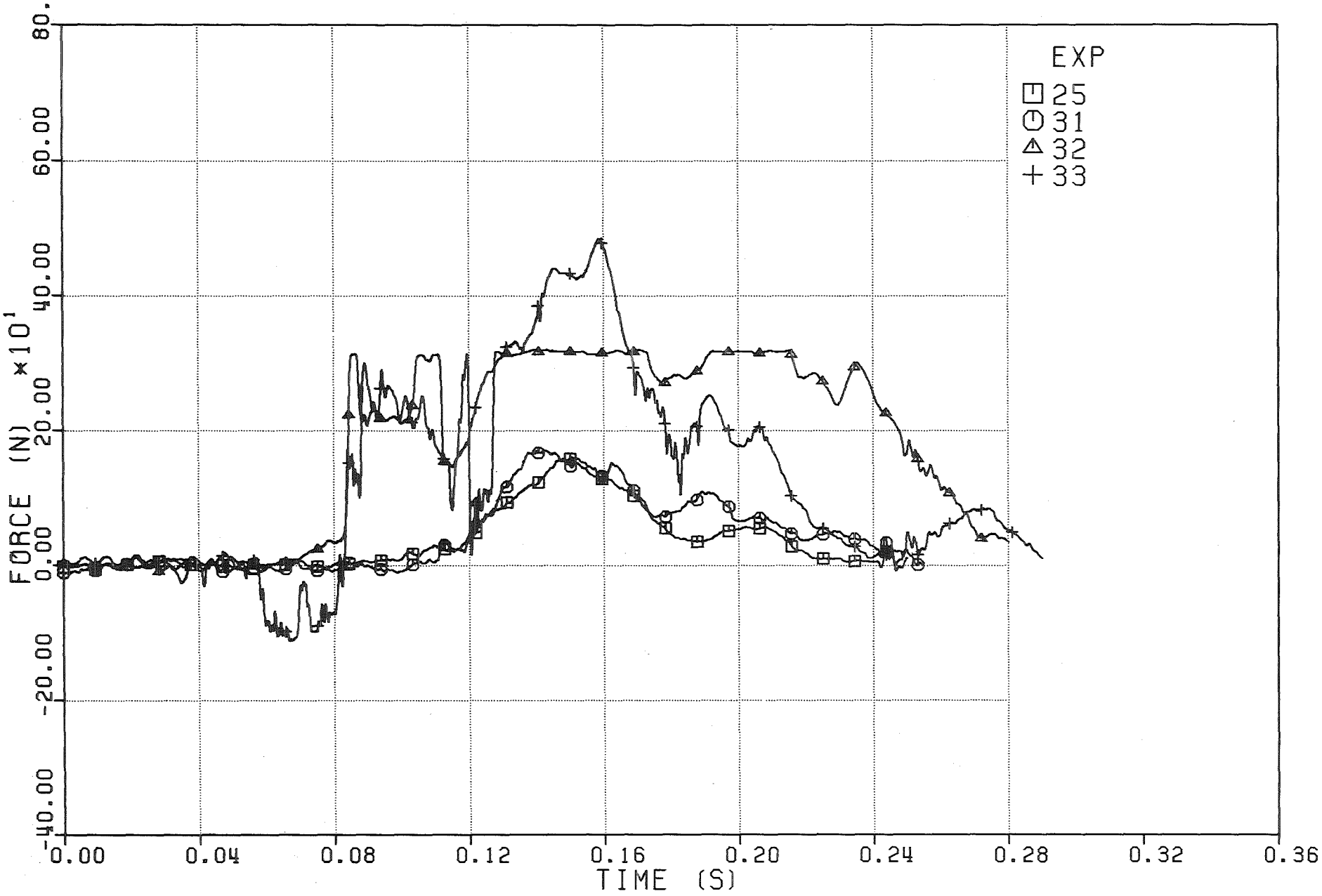

Fig. 6.321 - Force on the upper plate

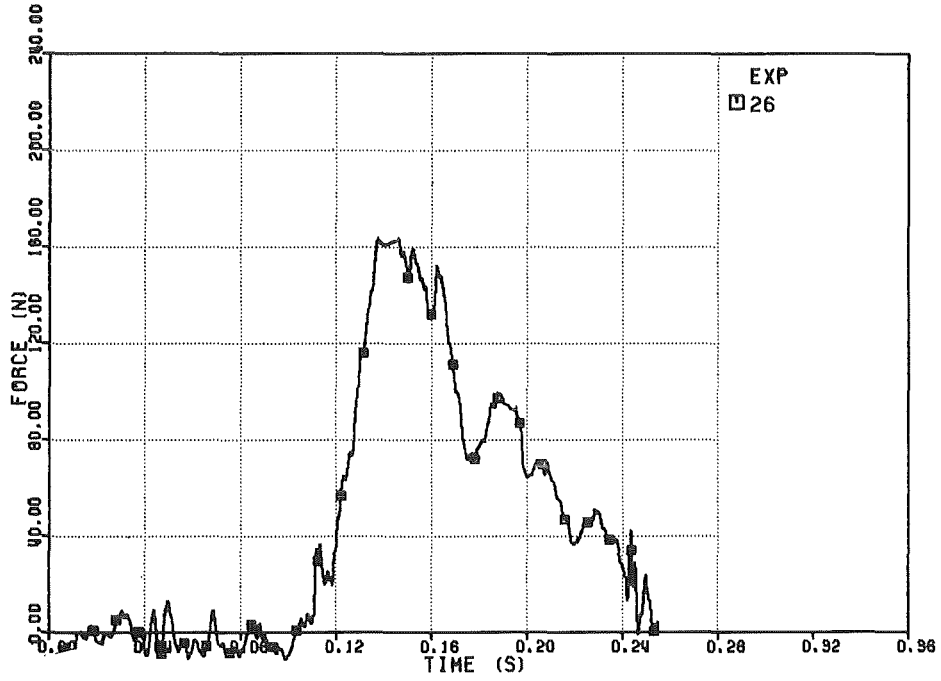

FIG.6322 - FORCE ON THE UPPER PLATE

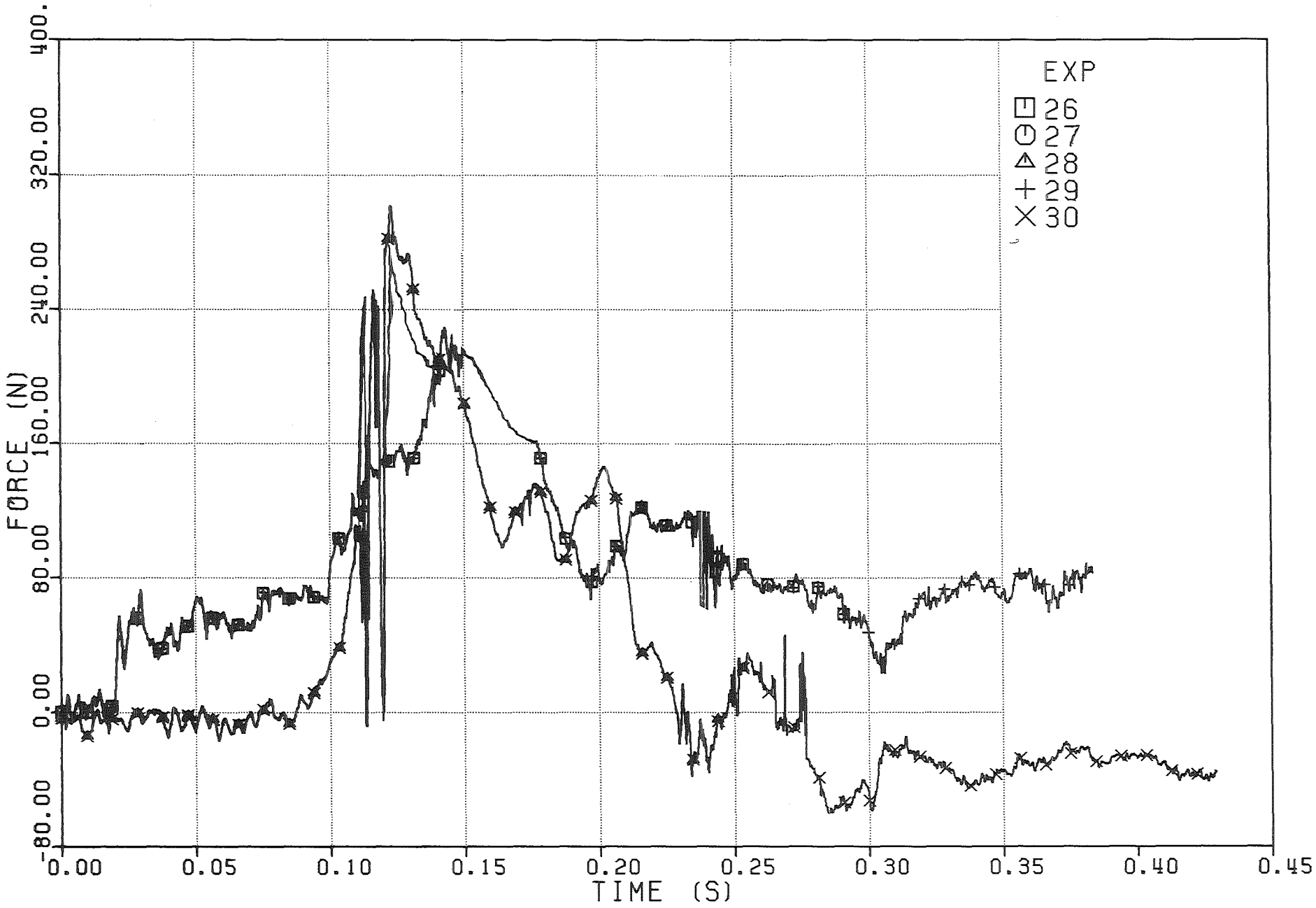

Fig. 6.323 - Force on the upper plate

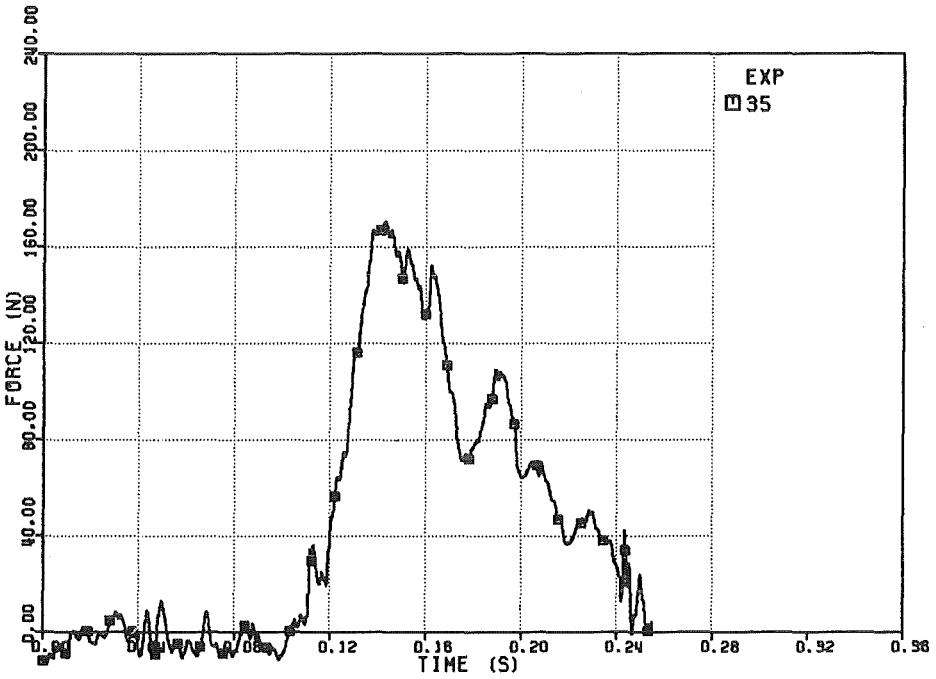

FIG. 6.324 - FORCE ON THE UPPER PLATE

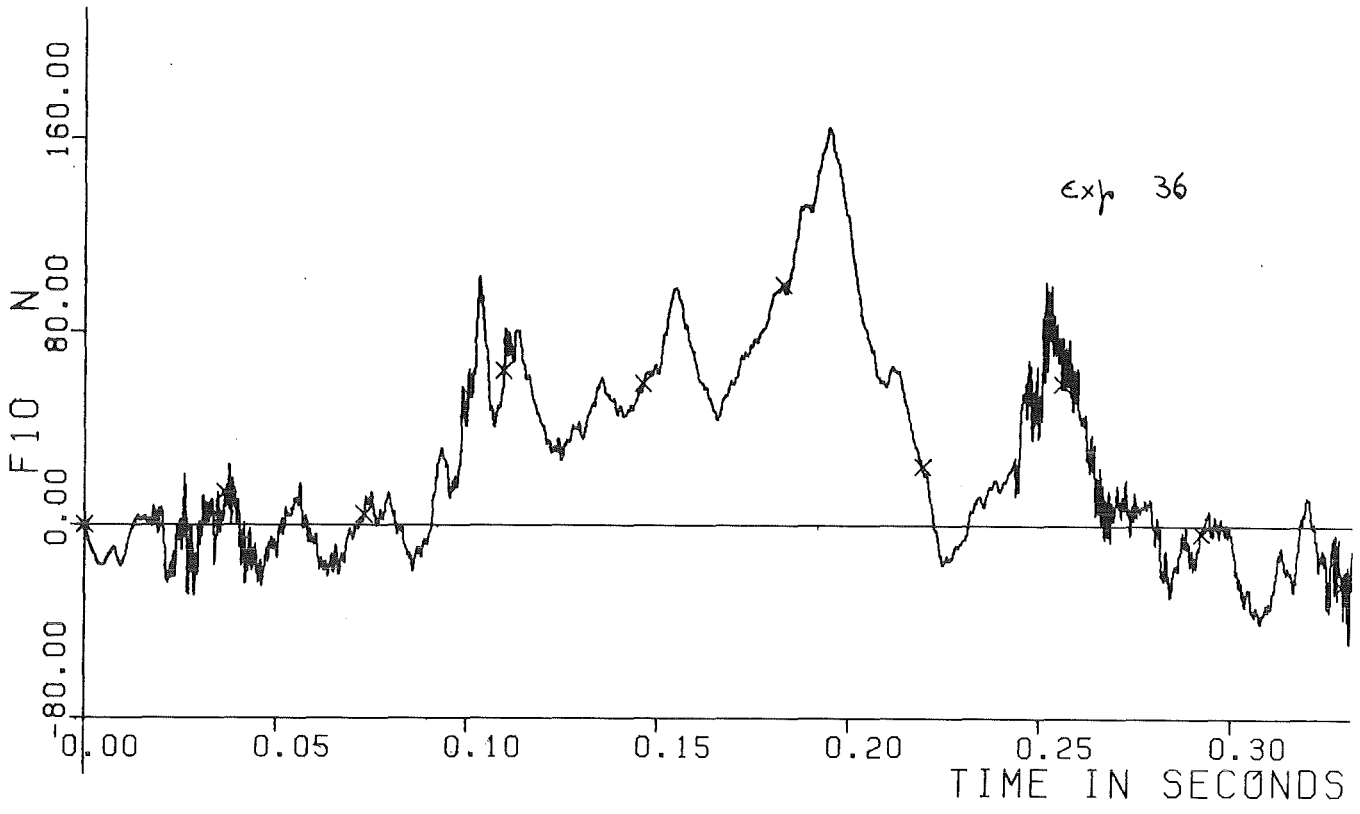

Fig. 6.325 - Force on the upper plate

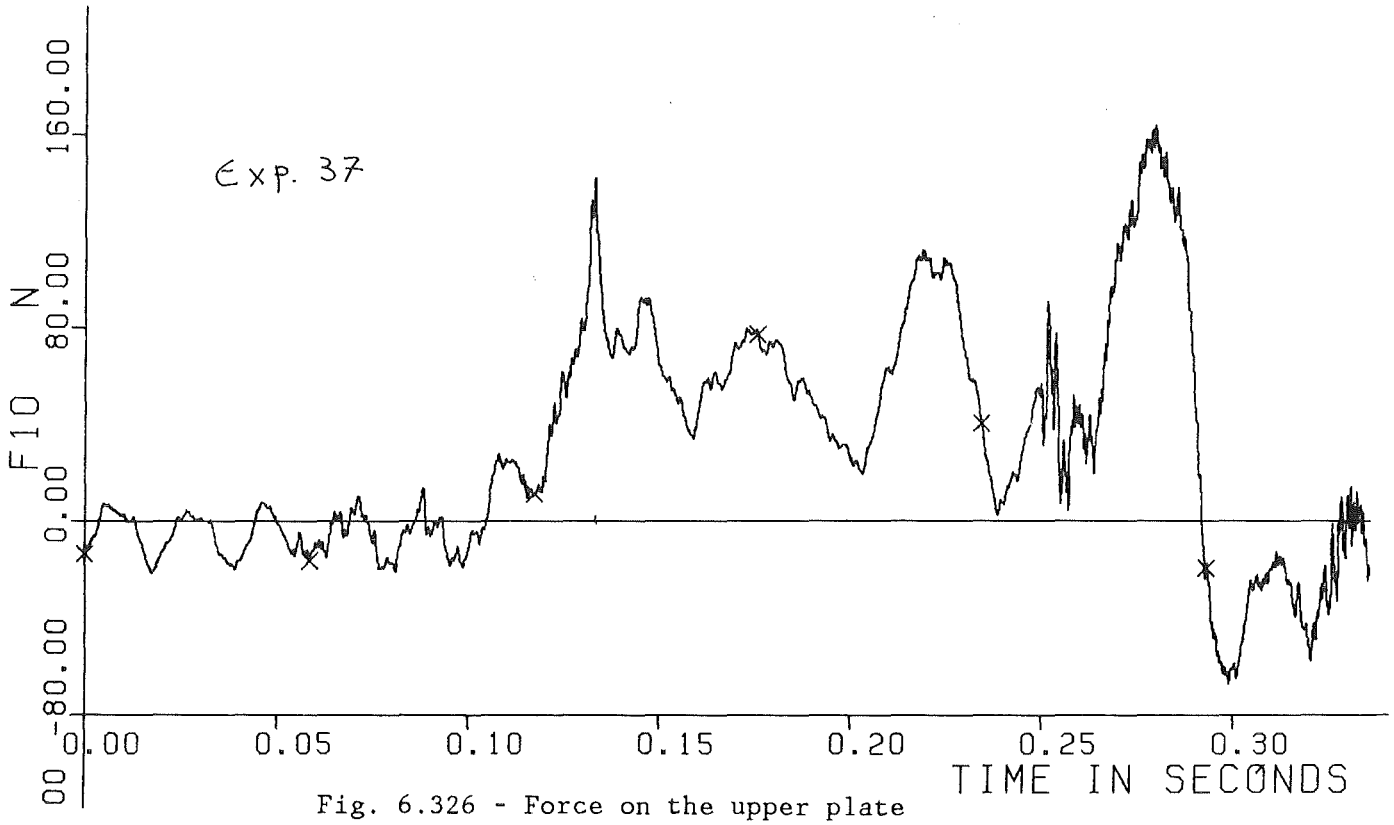

Fig. 6.326 - Force on the upper plate

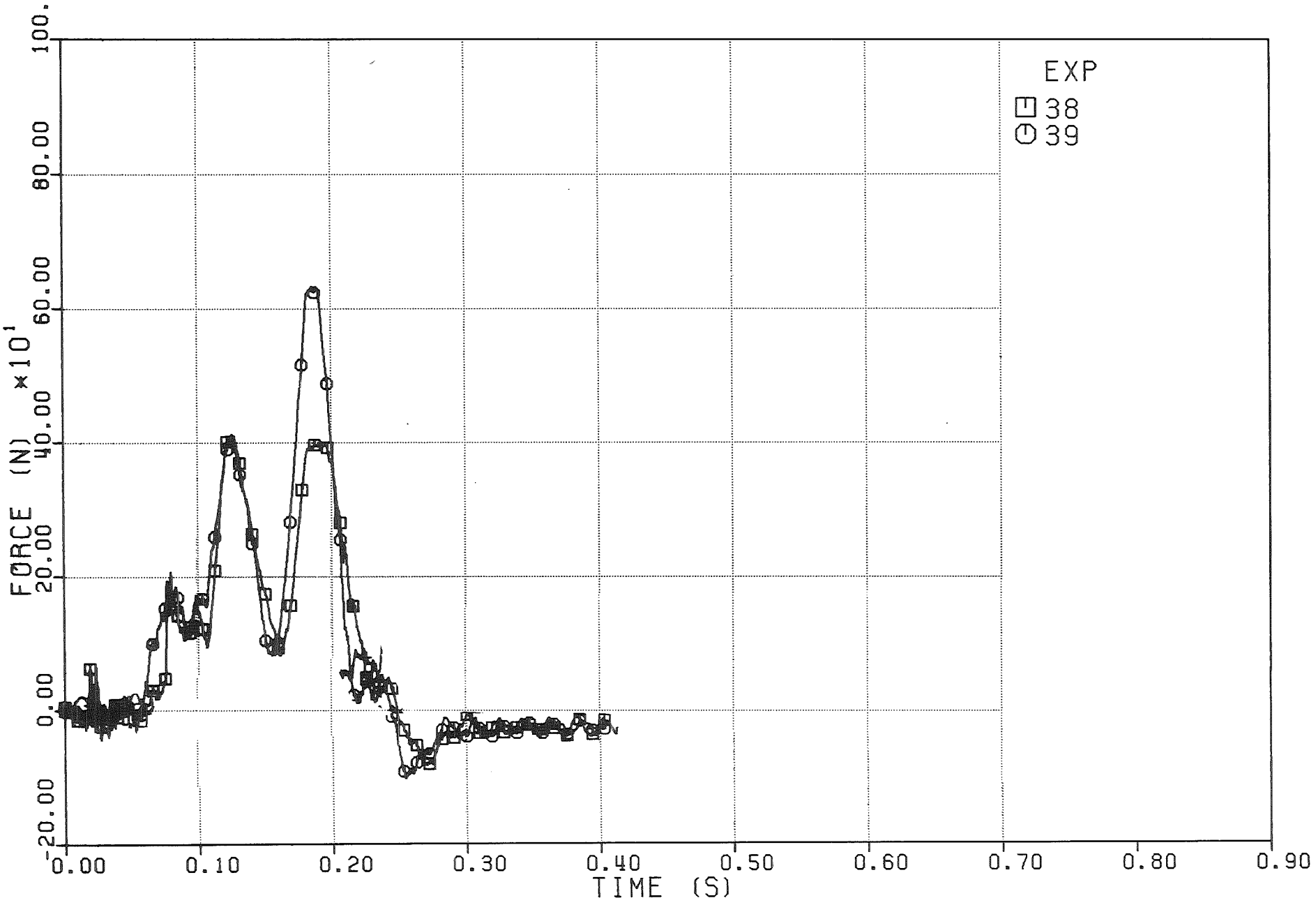

Fig. 6.327 - Force on the upper plate

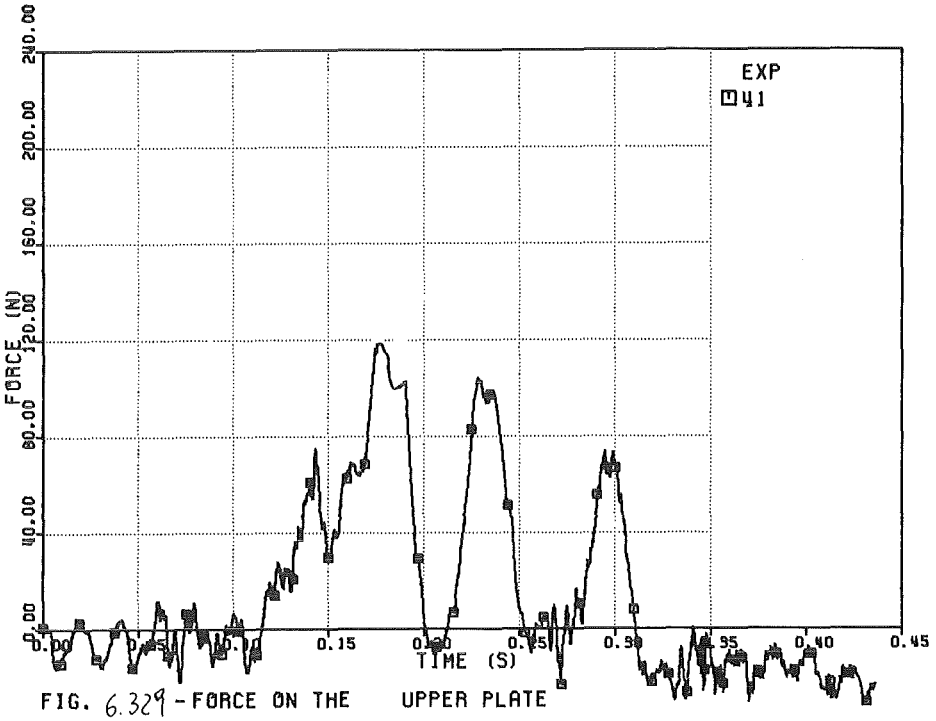

FIG. 6.329 - FORCE ON THE UPPER PLATE

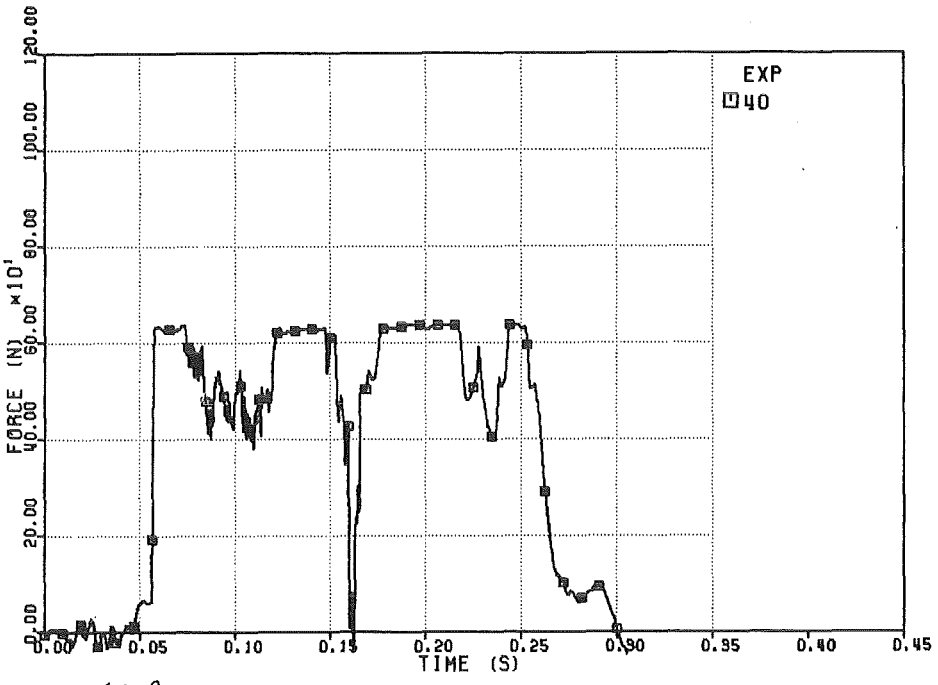

FIG. 6.328 - FORCE ON THE UPPER PLATE

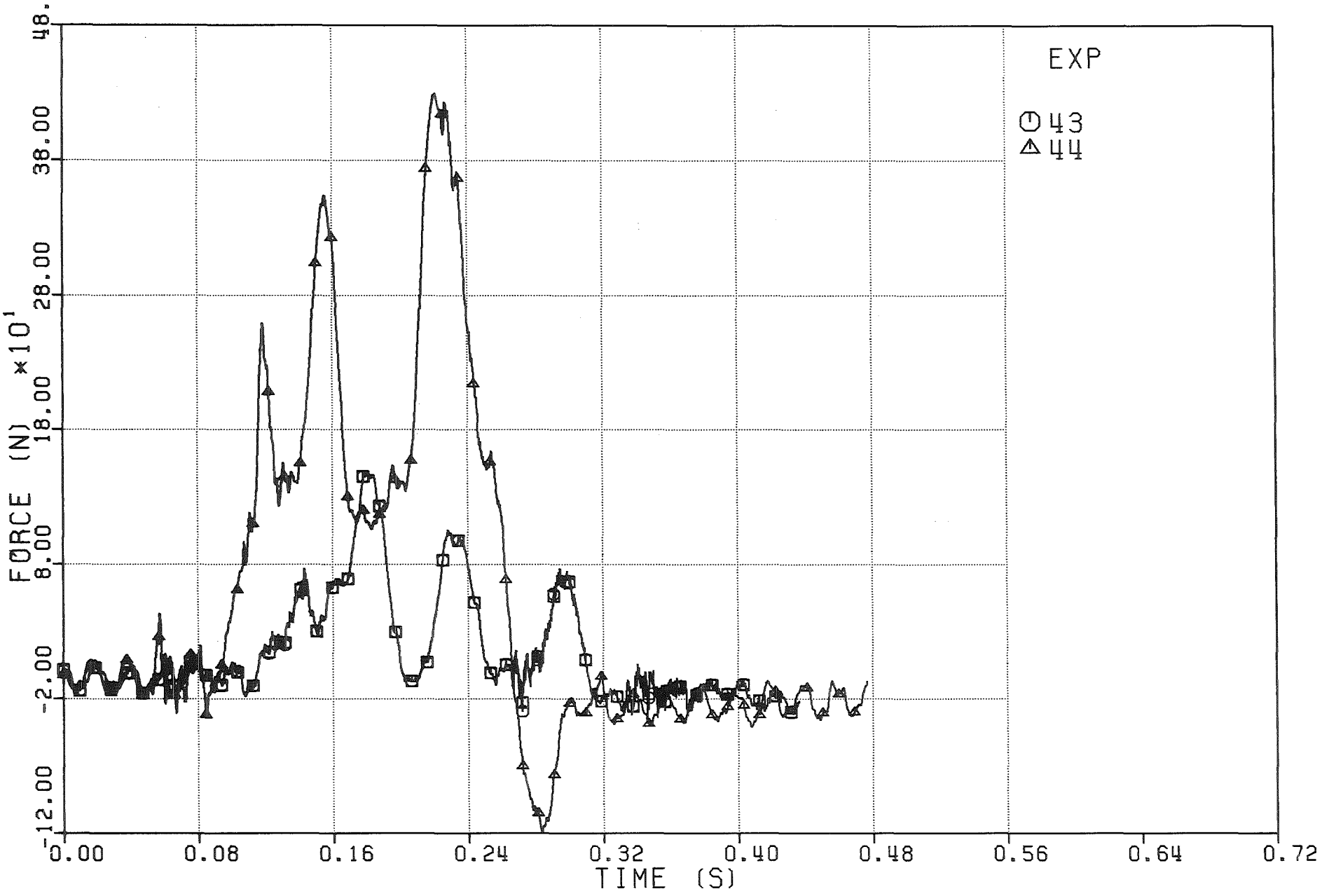

Fig. 6.330 - Force on the upper plate

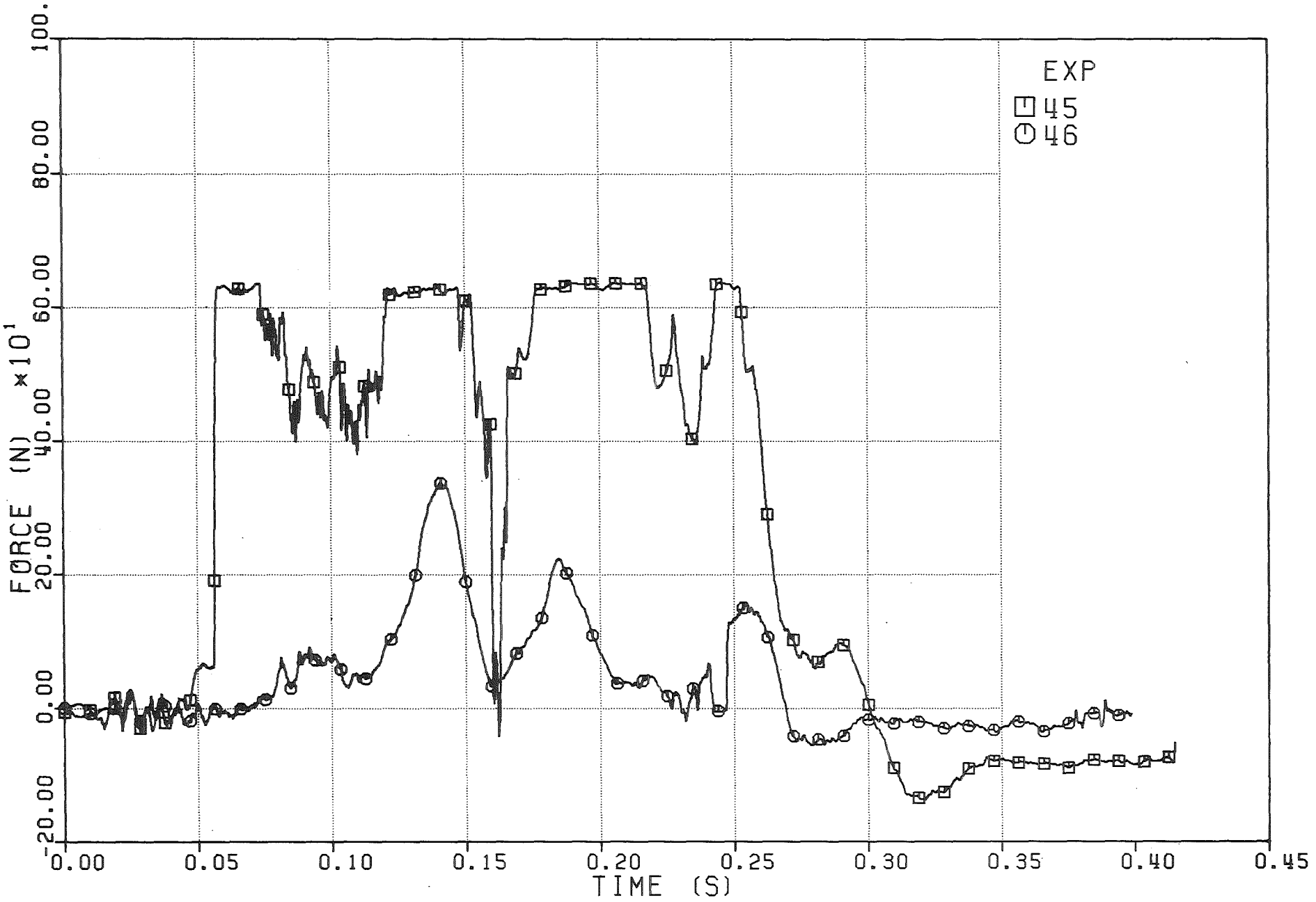

Fig. 6.331 - Force on the upper plate

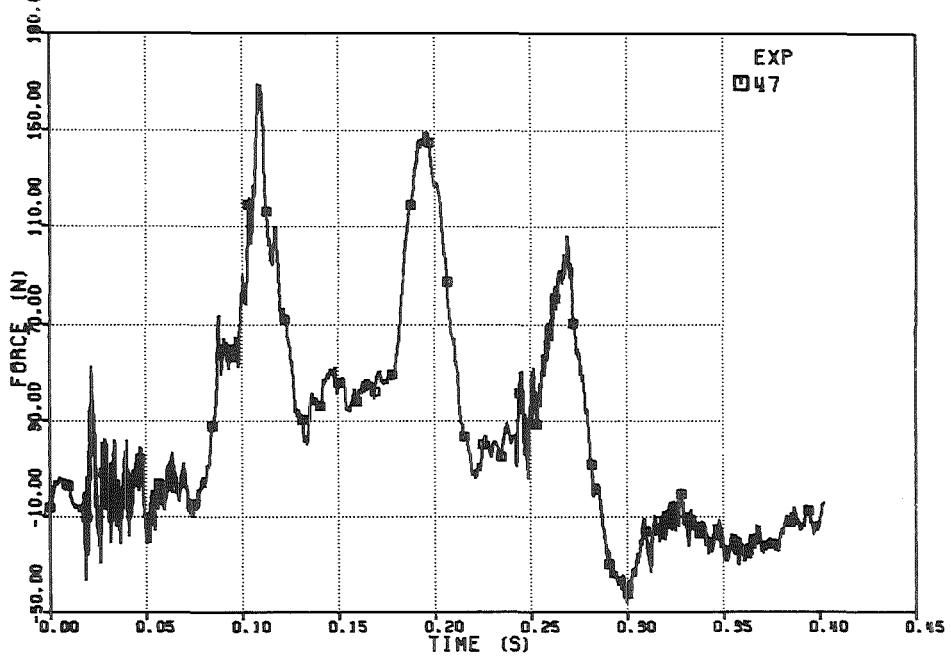

FIG. 6.333 - FORCE ON THE UPPER PLATE

IMRS36F1 01.06.85 00.54.40

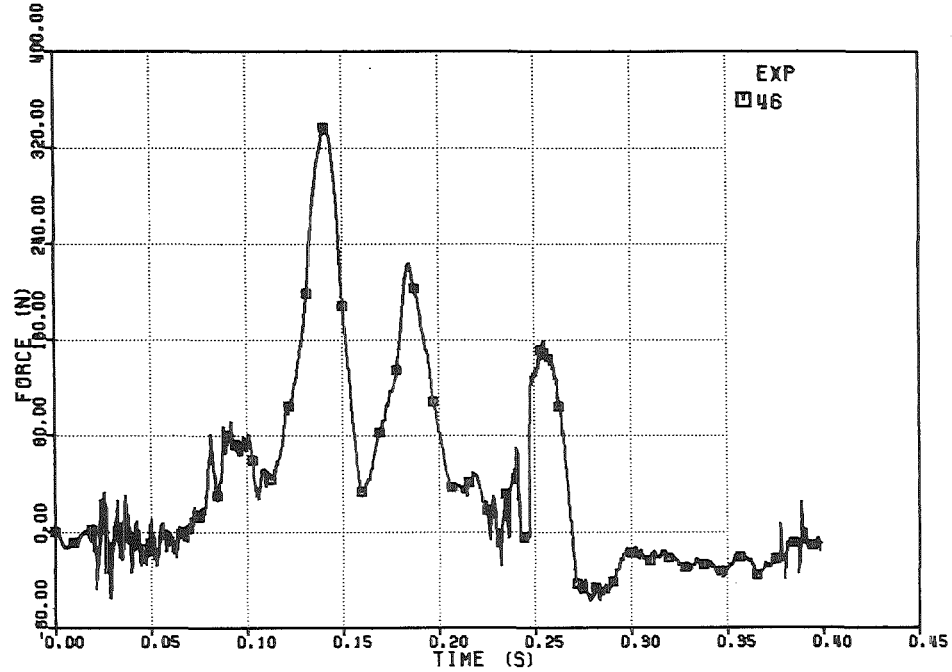

FIG. 6.332 - FORCE ON THE UPPER PLATE

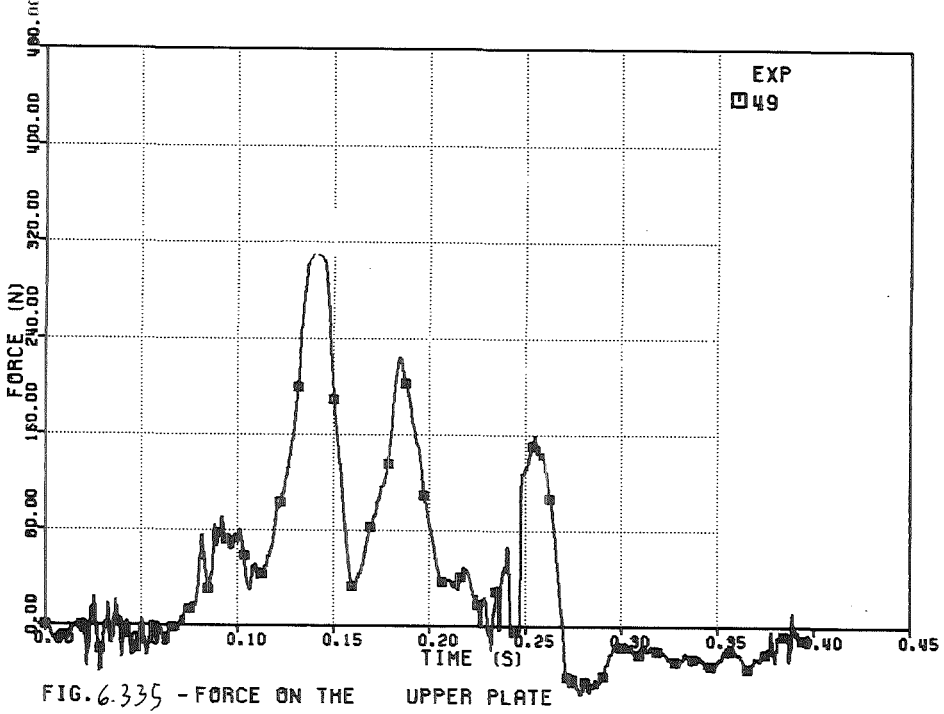

FIG. 6.335 - FORCE ON THE UPPER PLATE

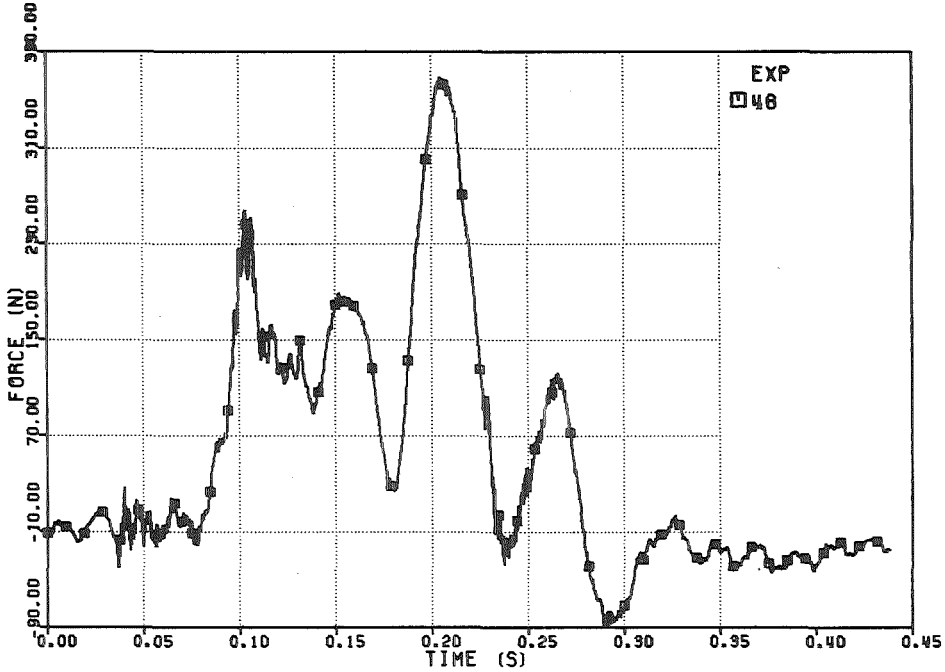

FIG. 6.334 - FORCE ON THE UPPER PLATE

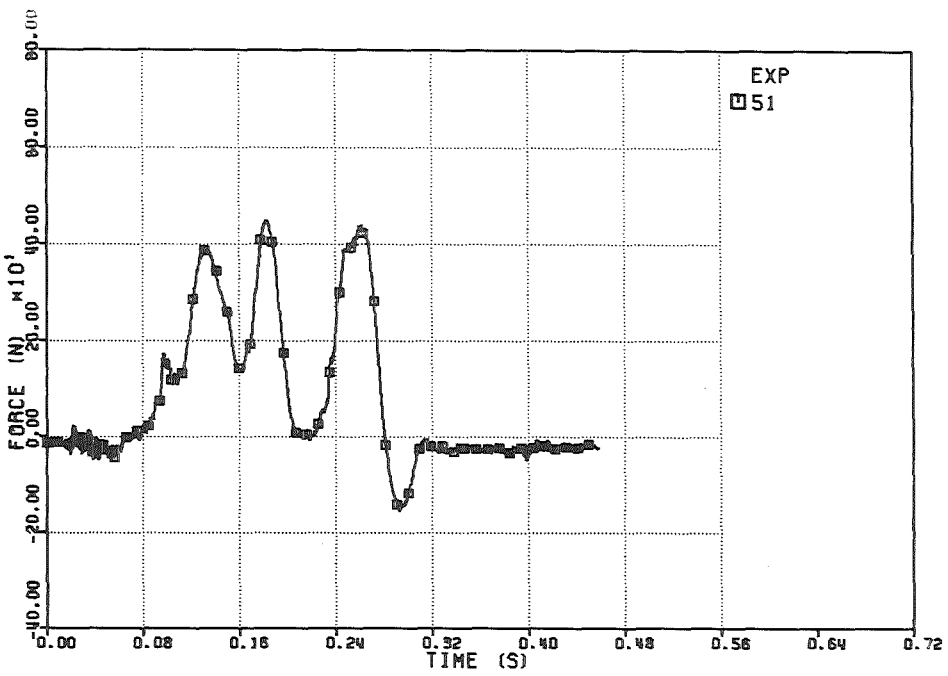

FIG. 6.337 - FORCE ON THE UPPER PLATE
INR538F1 01.06.85 00.54.40

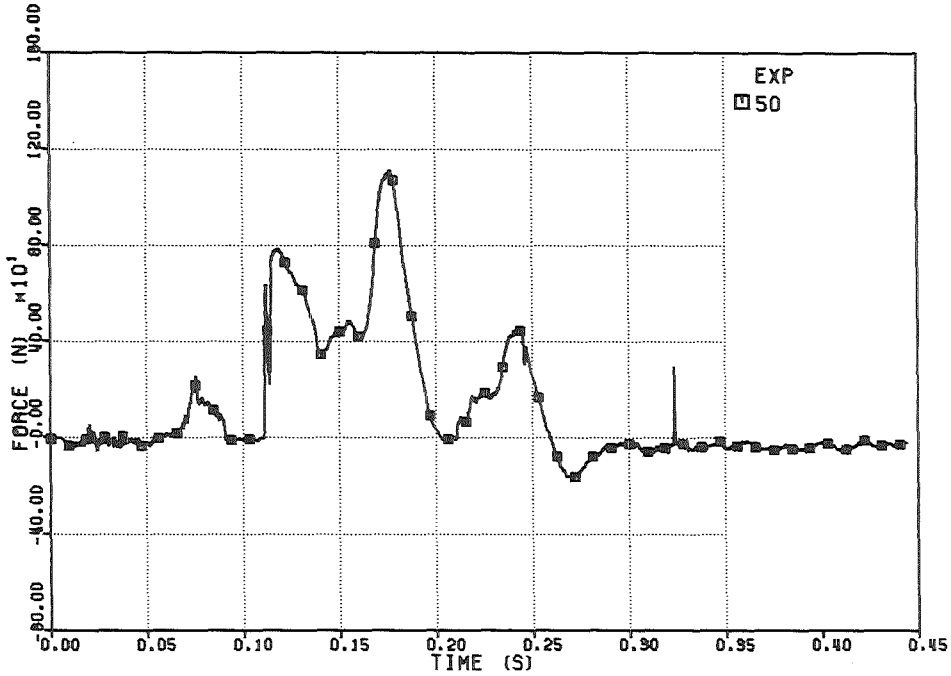

FIG. 6.336 - FORCE ON THE UPPER PLATE

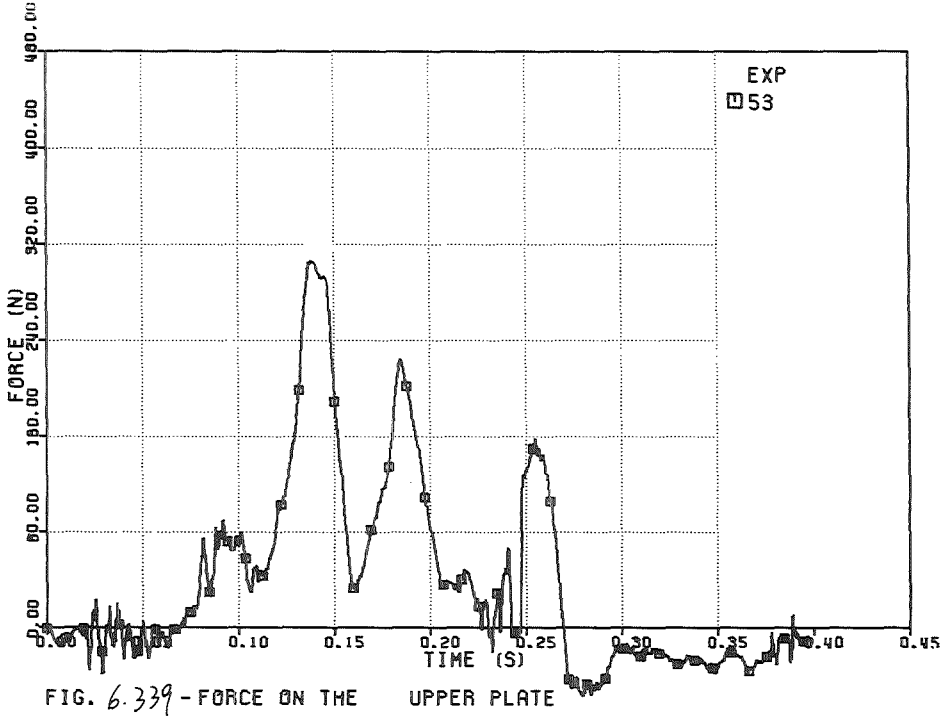

FIG. 6.339 - FORCE ON THE UPPER PLATE

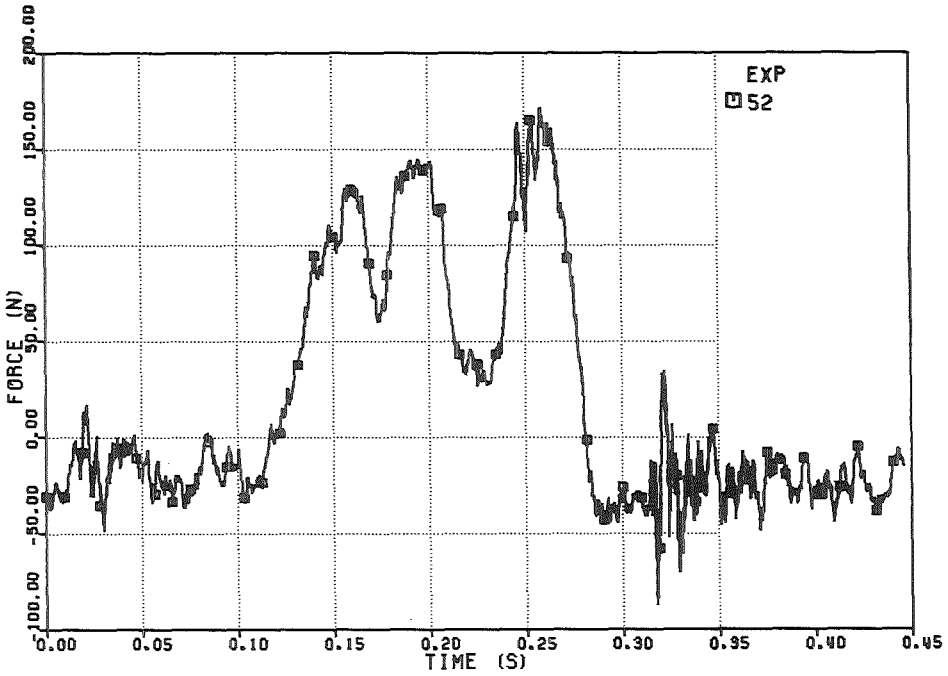

FIG. 6.338 - FORCE ON THE UPPER PLATE

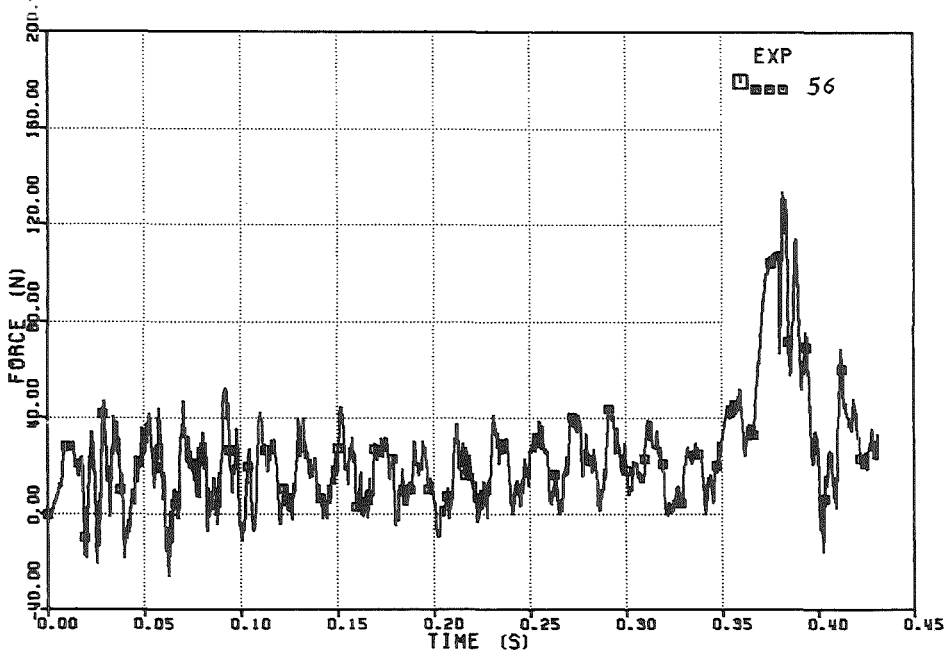

FIG. 6.341 - FORCE ON THE UPPER PLATE
INR596F1 01.06.85 00.54.40

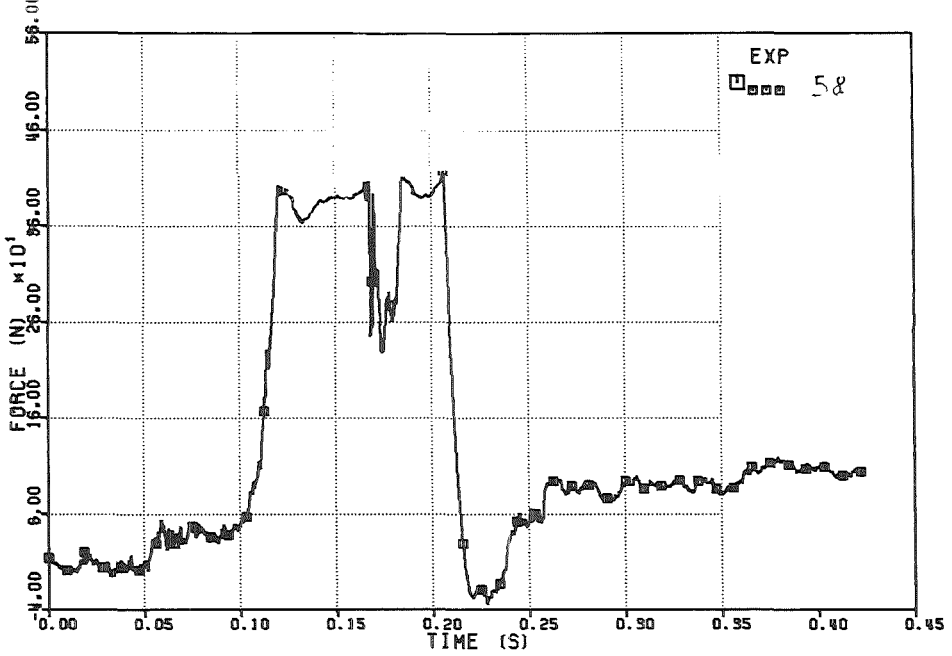

FIG. 6.343 - FORCE ON THE UPPER PLATE
INR596F1 01.06.85 00.54.40

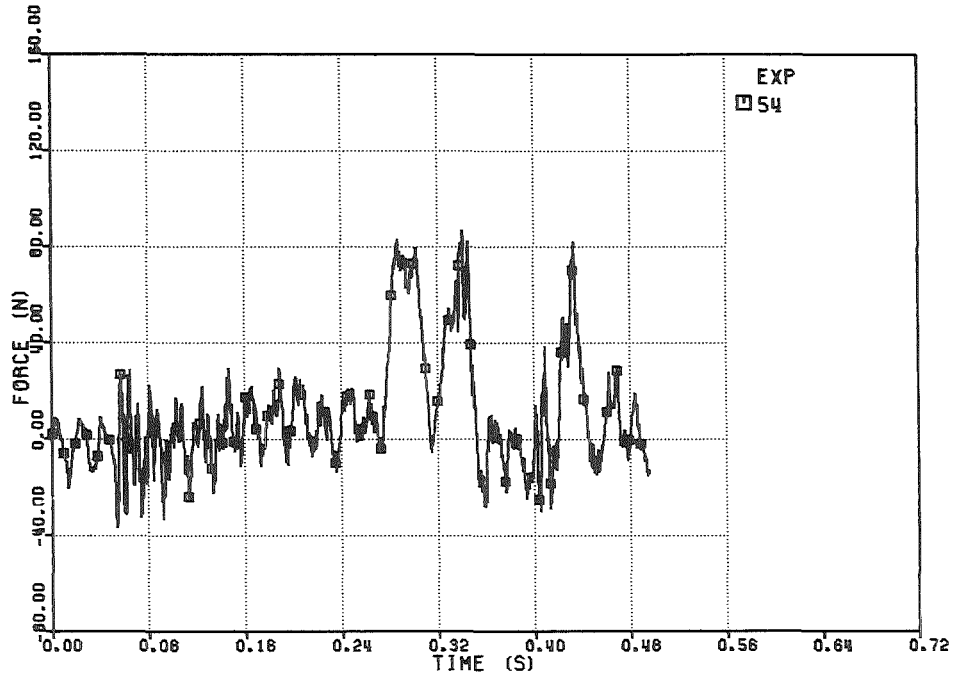

FIG. 6.340 - FORCE ON THE UPPER PLATE

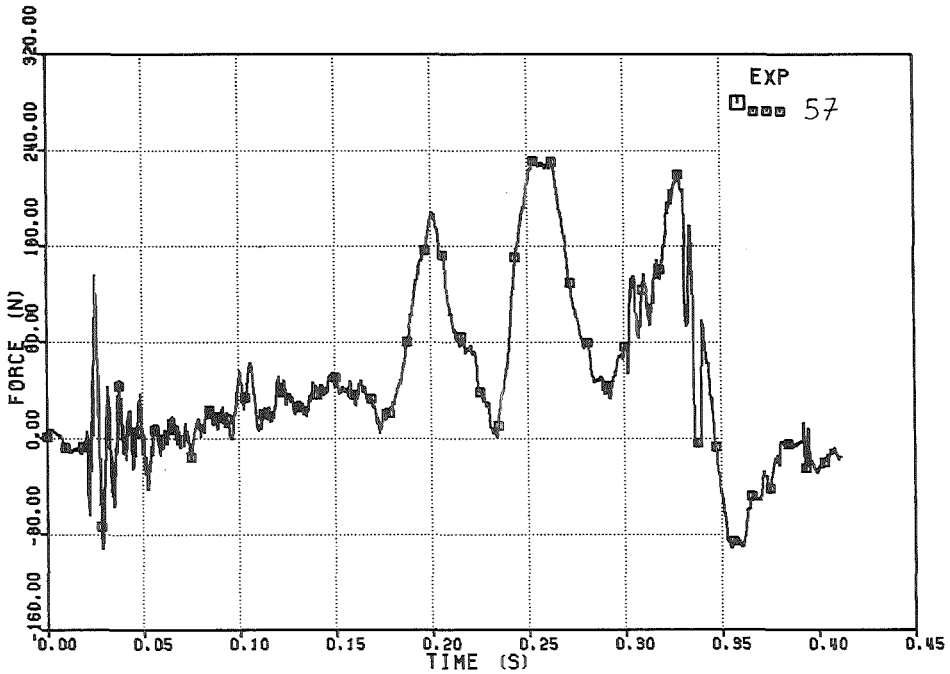

FIG. 6.342 - FORCE ON THE UPPER PLATE

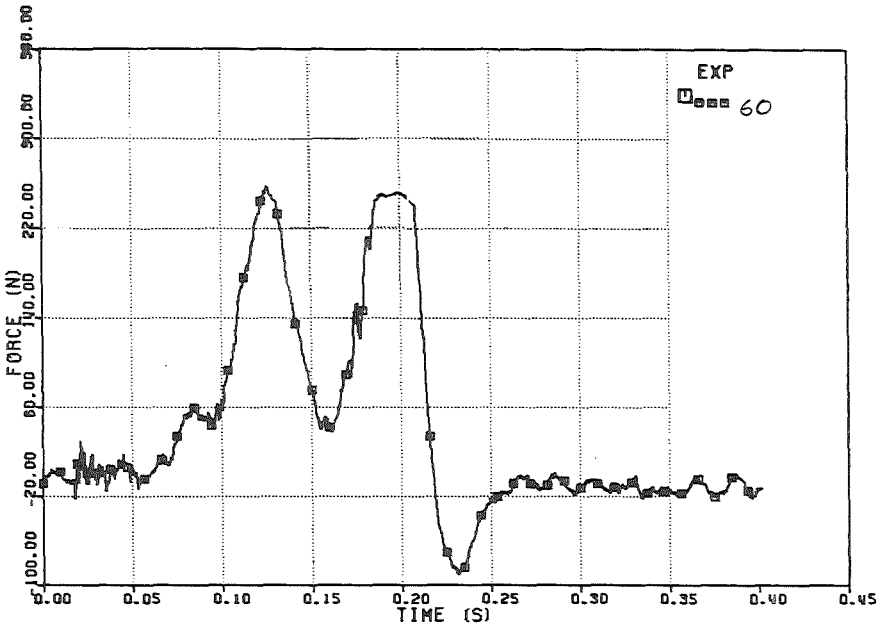

FIG. 6.345 - FORCE ON THE UPPER PLATE
INRS38F1 01.06.85 00.37.45

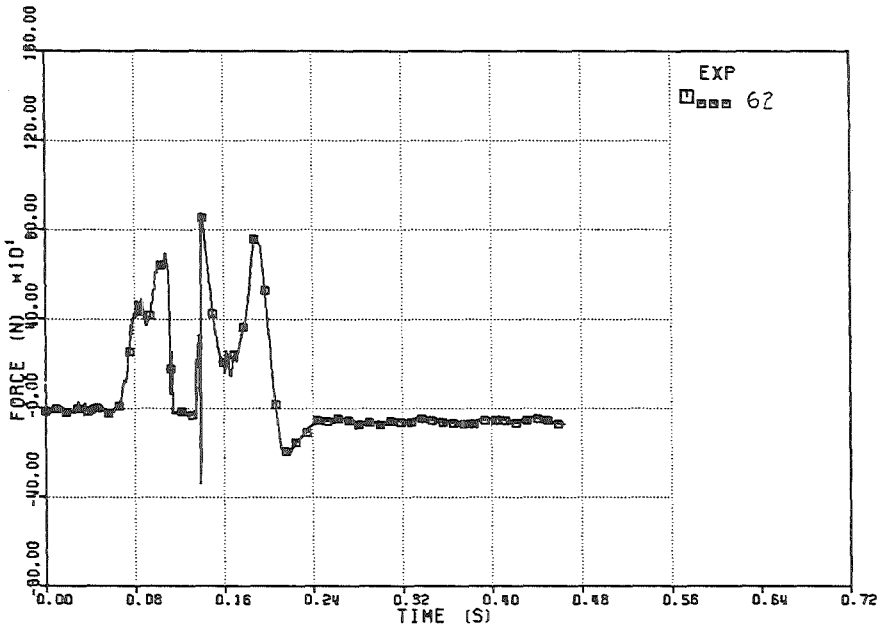

FIG. 6.347 - FORCE ON THE UPPER PLATE
INRS38F1 01.06.85 00.37.45

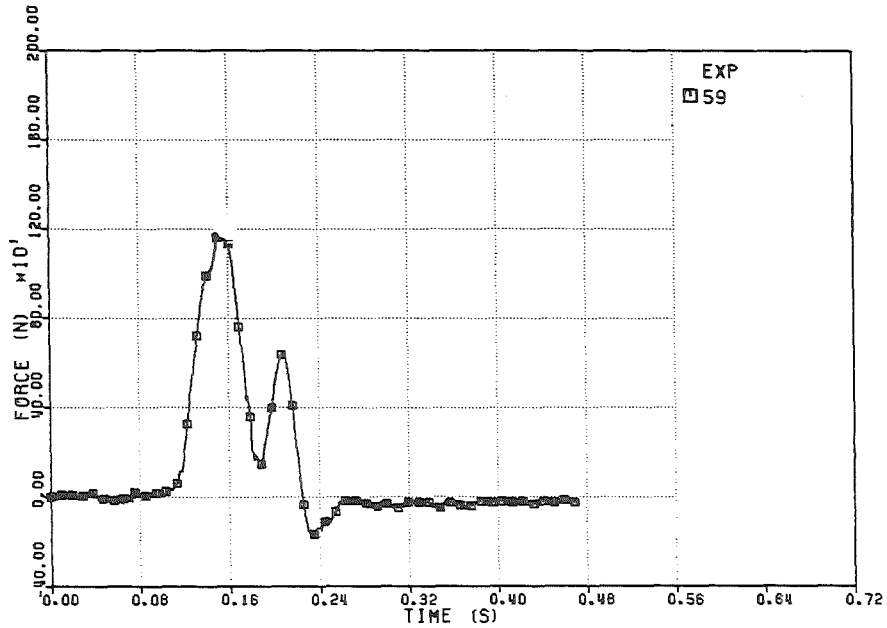

FIG. 6.344 - FORCE ON THE UPPER PLATE

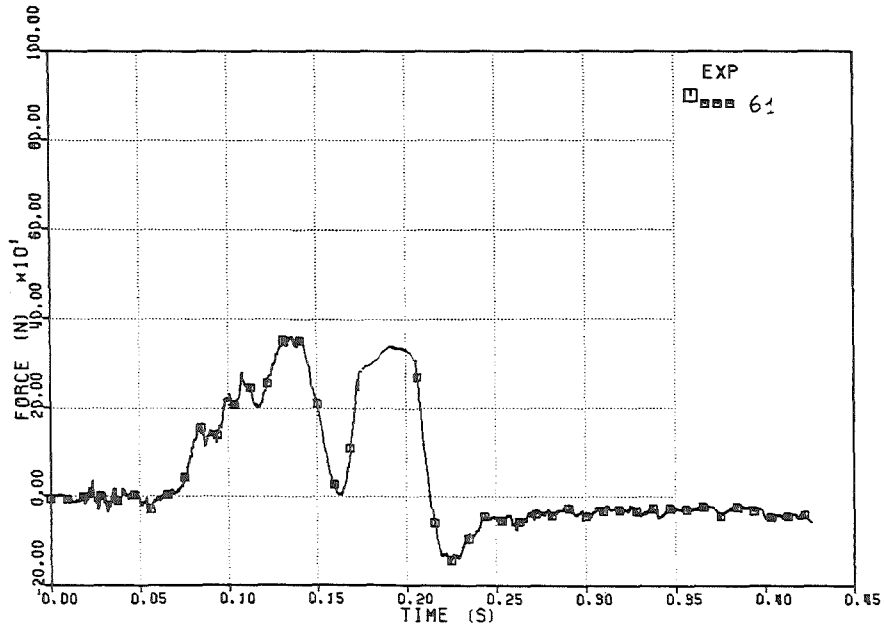

FIG. 6.346 - FORCE ON THE UPPER PLATE

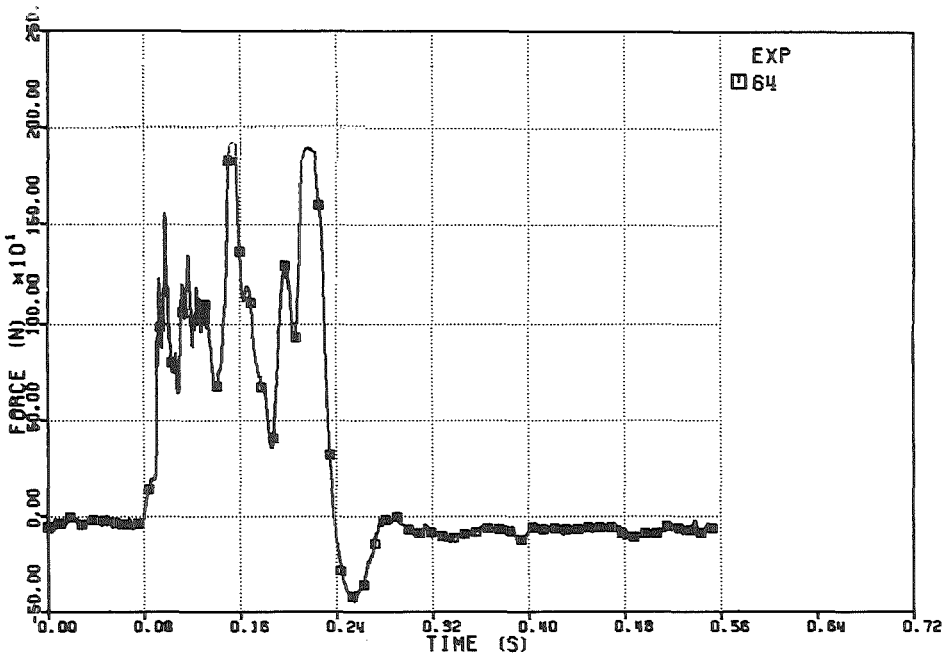

FIG. 6.349 - FORCE ON THE UPPER PLATE
INR536F1 01.06.85 00.37.45

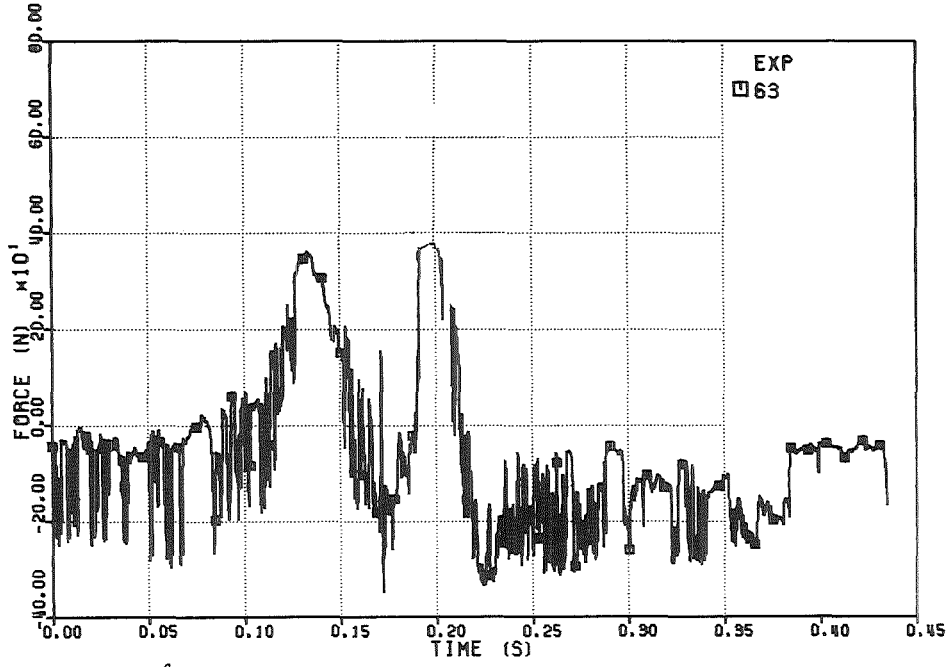

FIG. 6.348 - FORCE ON THE UPPER PLATE

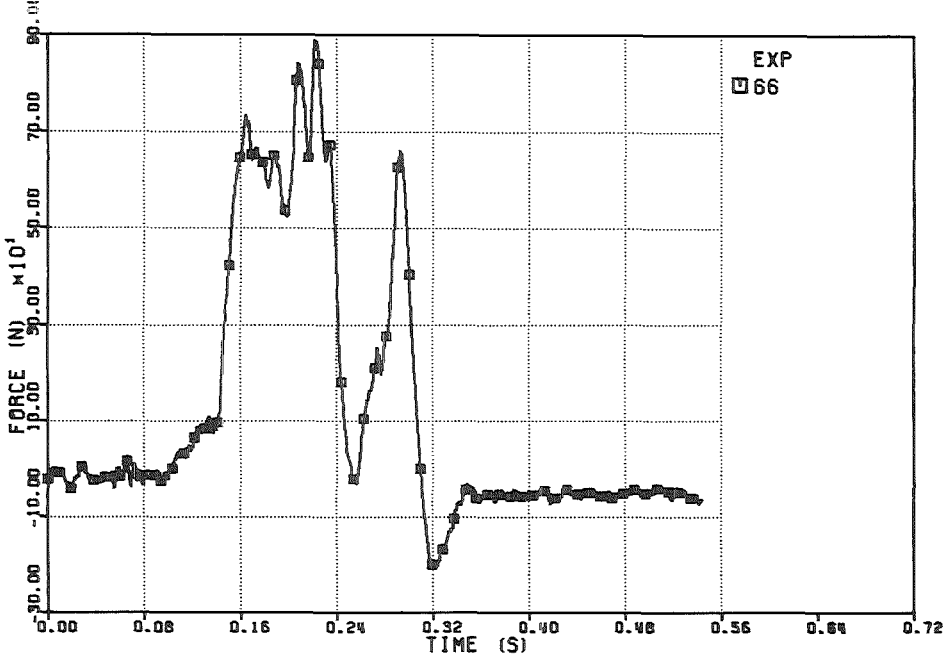

FIG. 6.351 - FORCE ON THE UPPER PLATE
INR536F1 01.06.85 00.37.45

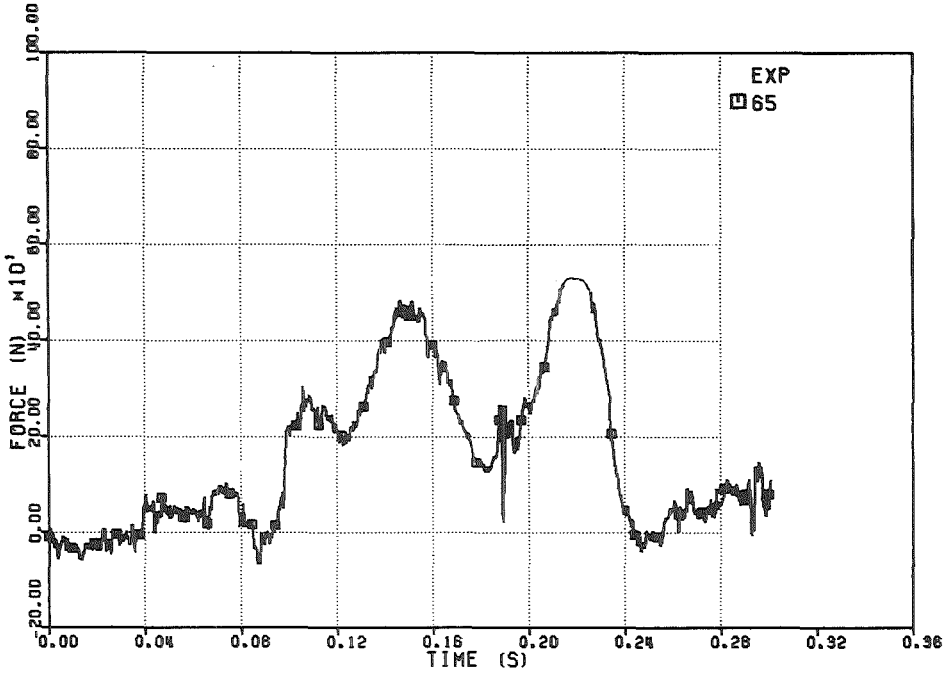

FIG. 6.350 - FORCE ON THE UPPER PLATE

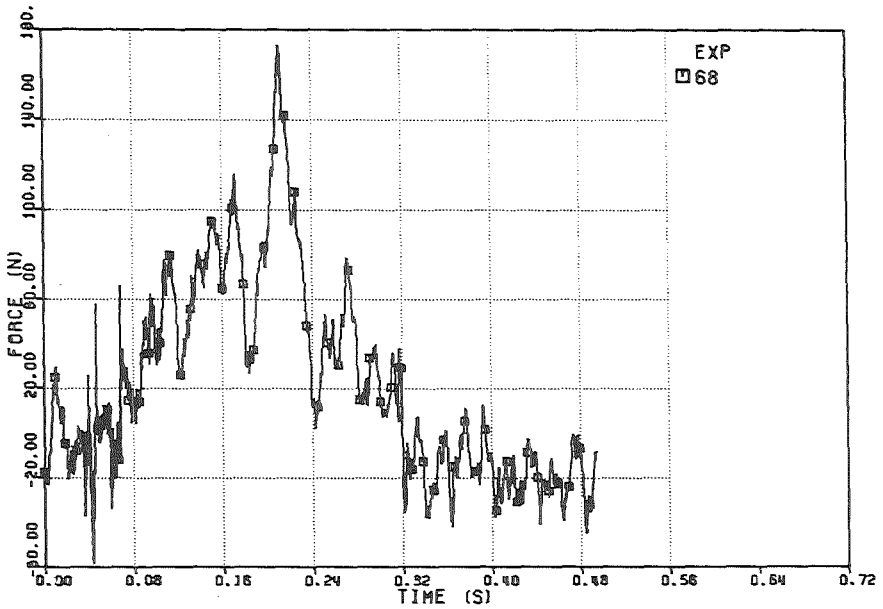

FIG. 6.353 - FORCE ON THE UPPER PLATE

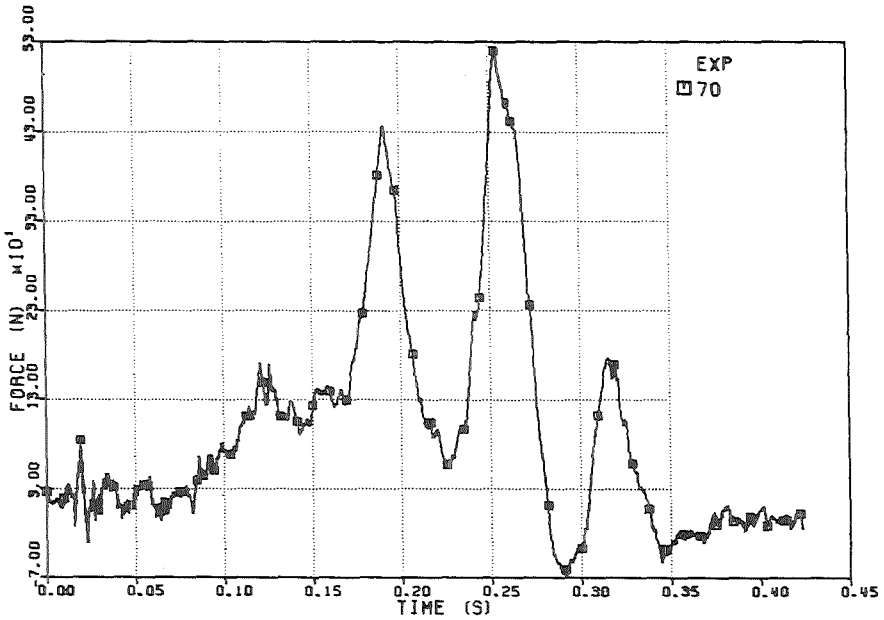

FIG. 6.355 - FORCE ON THE UPPER PLATE

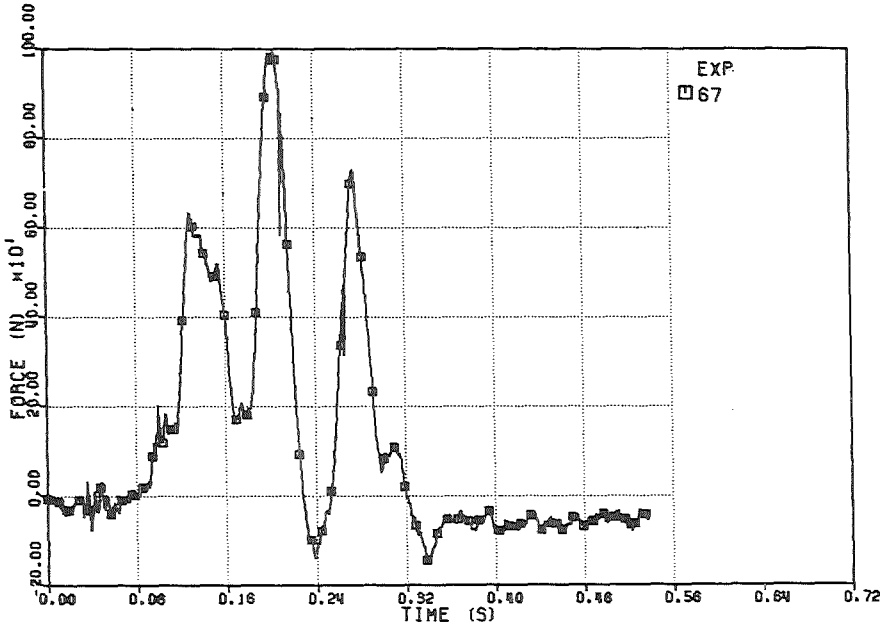

FIG. 6.352 - FORCE ON THE UPPER PLATE

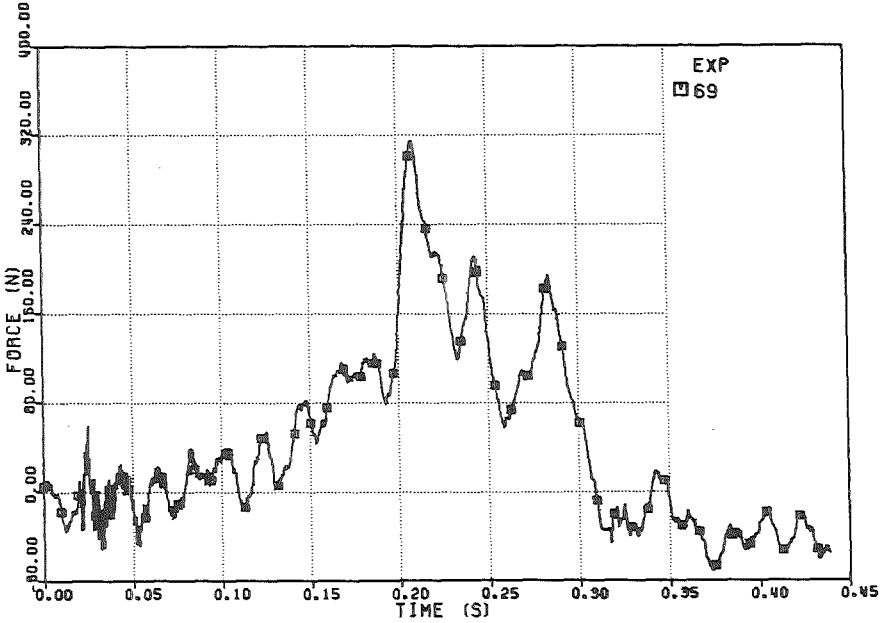

FIG. 6.354 - FORCE ON THE UPPER PLATE

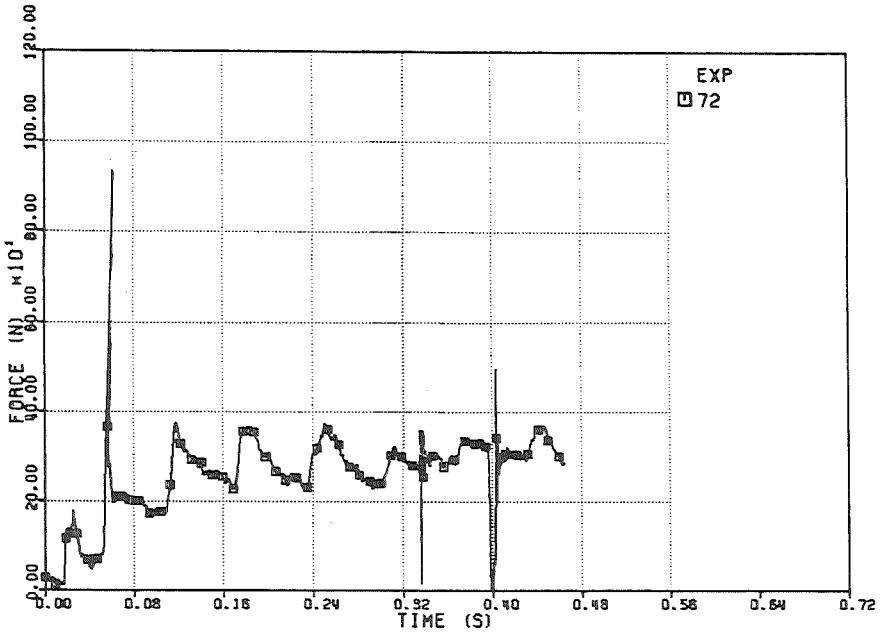

FIG. 6.357 - FORCE ON THE UPPER PLATE
INR536F1 01.06.85 00.16.58

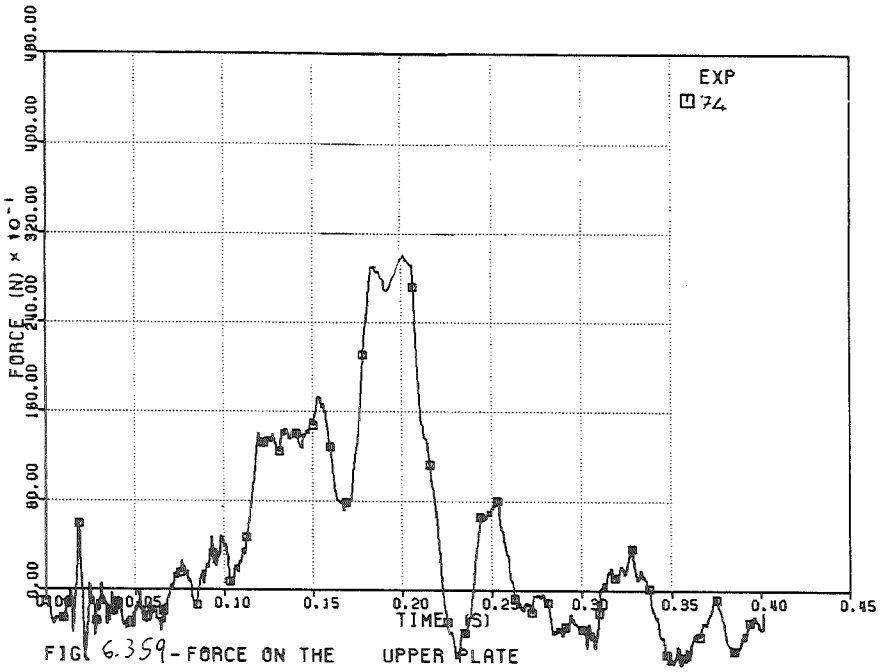

FIG. 6.359 - FORCE ON THE UPPER PLATE

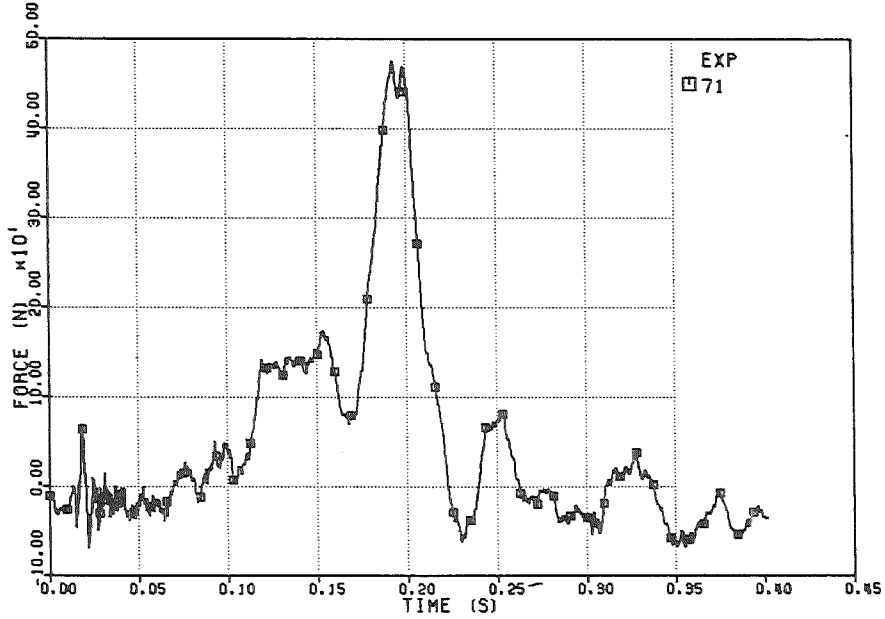

FIG. 6.356 - FORCE ON THE UPPER PLATE

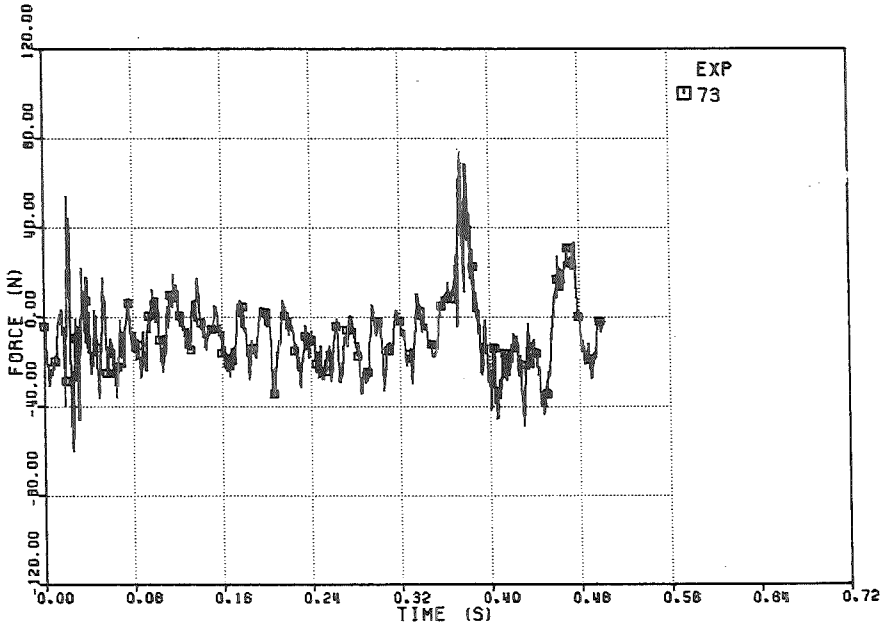

FIG. 6.358 - FORCE ON THE UPPER PLATE

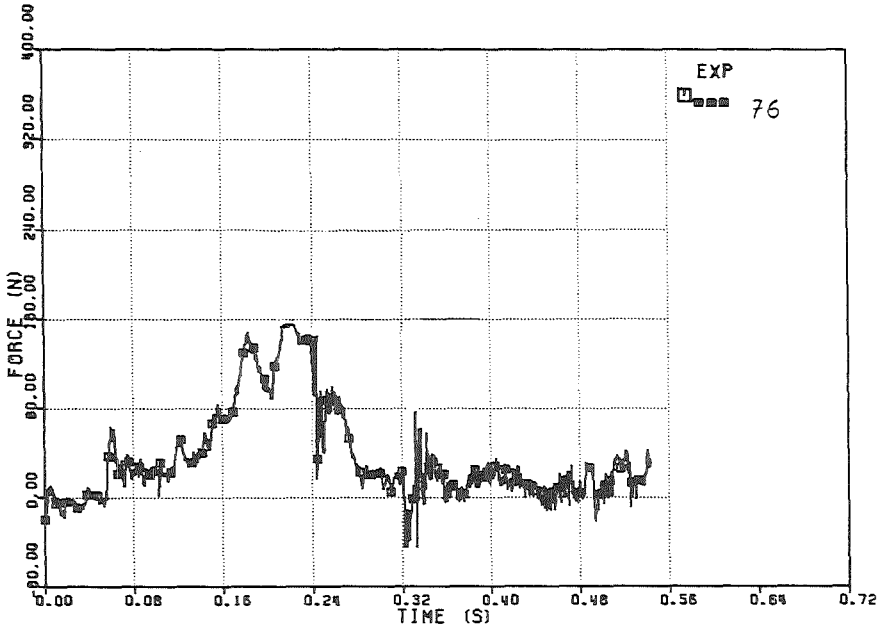

FIG. 6.361 - FORCE ON THE UPPER PLATE
INRS36F1 01.06.85 00.16.58

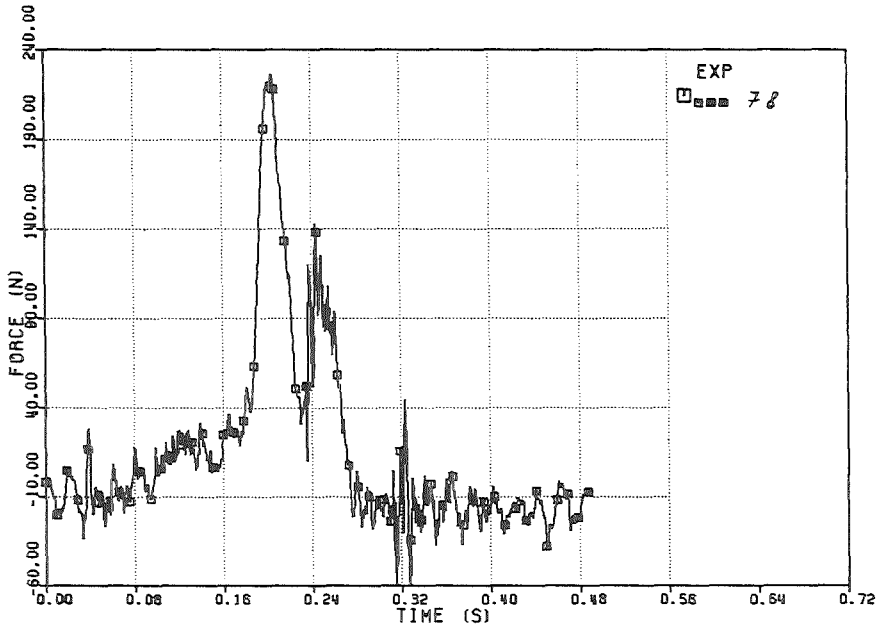

FIG. 6.363 - FORCE ON THE UPPER PLATE
INRS36F1 01.06.85 00.16.58

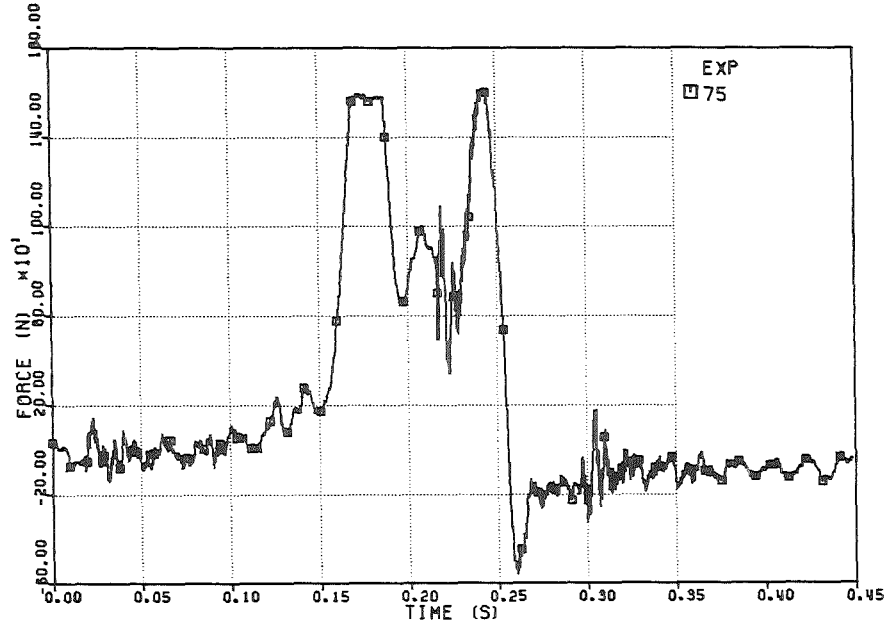

FIG. 6.360 - FORCE ON THE UPPER PLATE

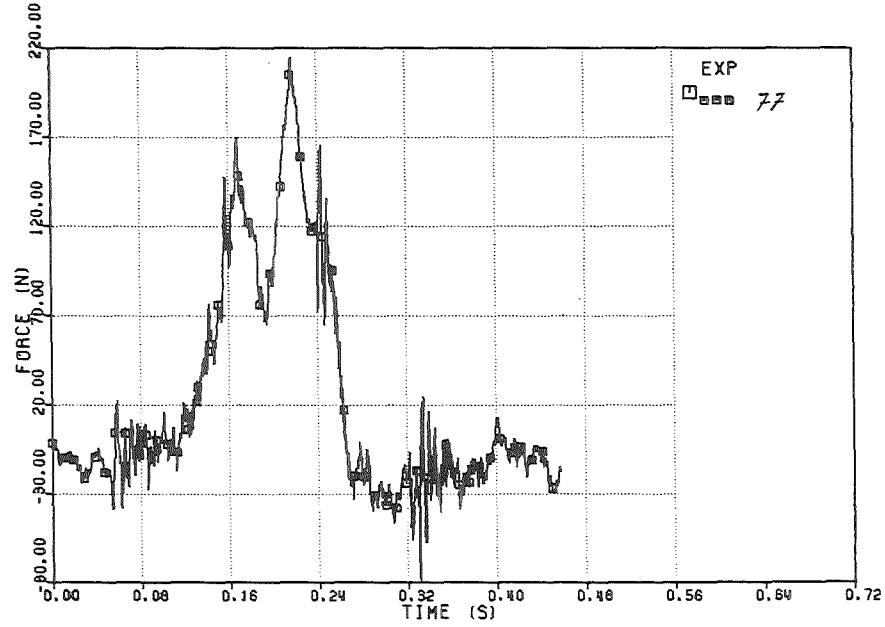

FIG. 6.362 - FORCE ON THE UPPER PLATE

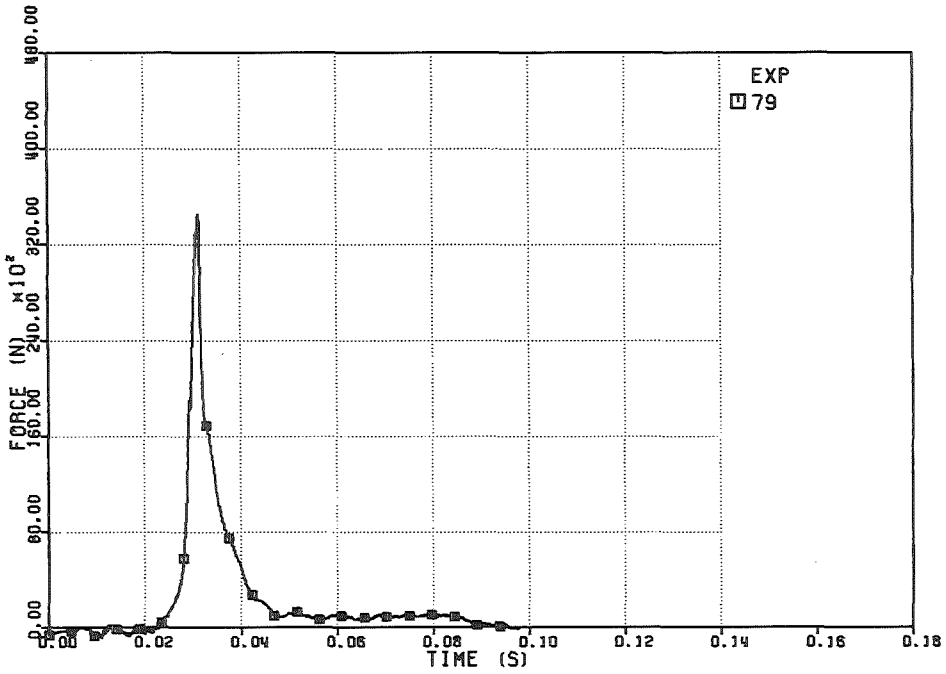

FIG. 6.364 - FORCE ON THE UPPER PLATE

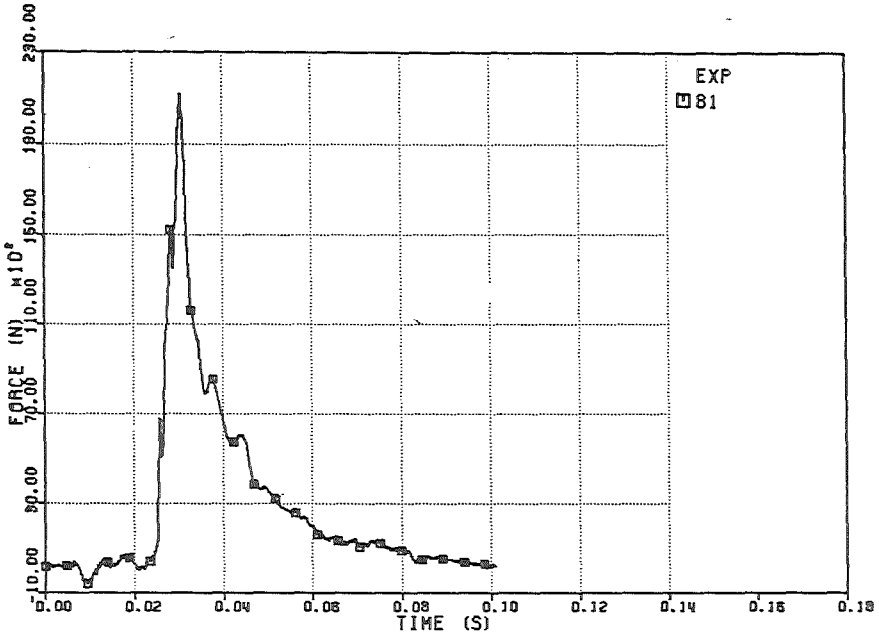

FIG. 6.366 - FORCE ON THE UPPER PLATE
INRS36F1 31.05.85 23.42.05

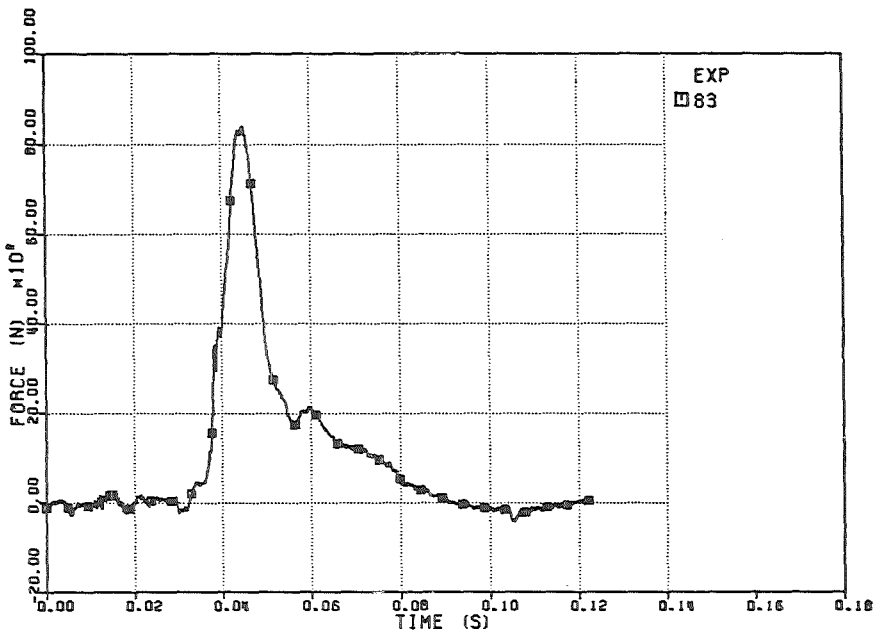

FIG. 6.368 - FORCE ON THE UPPER PLATE
INRS36F1 31.05.85 23.42.05

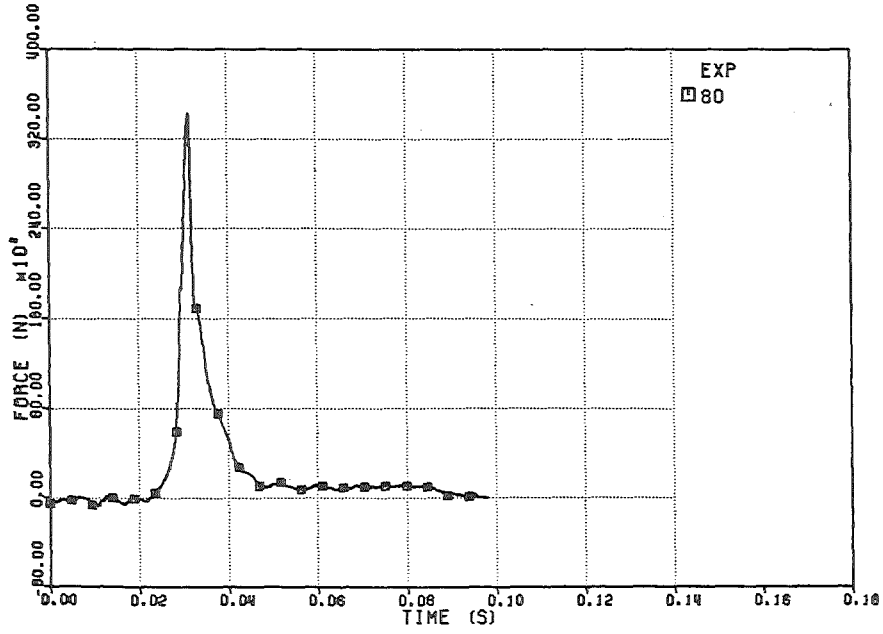

FIG. 6.365 - FORCE ON THE UPPER PLATE

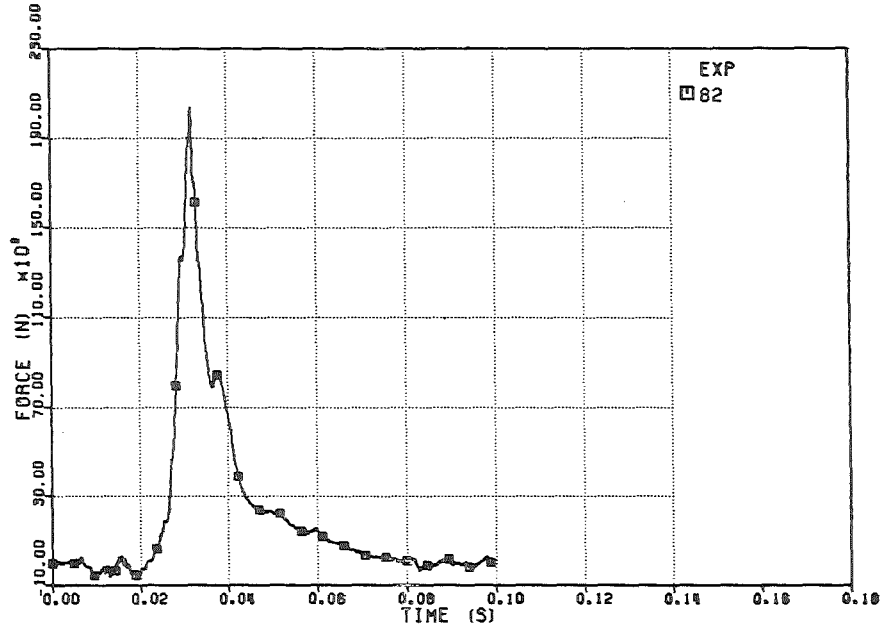

FIG. 6.367 - FORCE ON THE UPPER PLATE

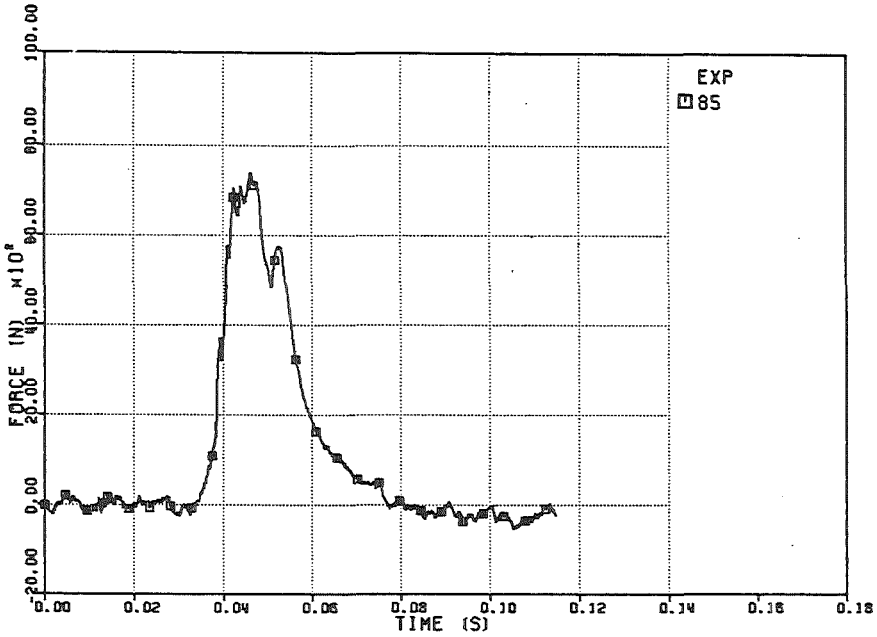

FIG. 6.370 - FORCE ON THE UPPER PLATE
INR536F1 31.05.85 29.42.05

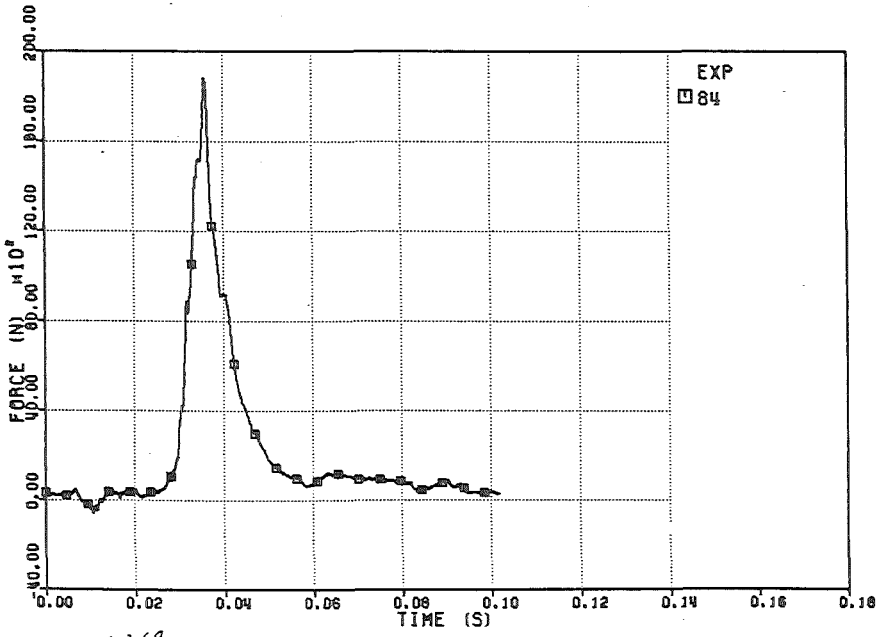

FIG. 6.369 - FORCE ON THE UPPER PLATE

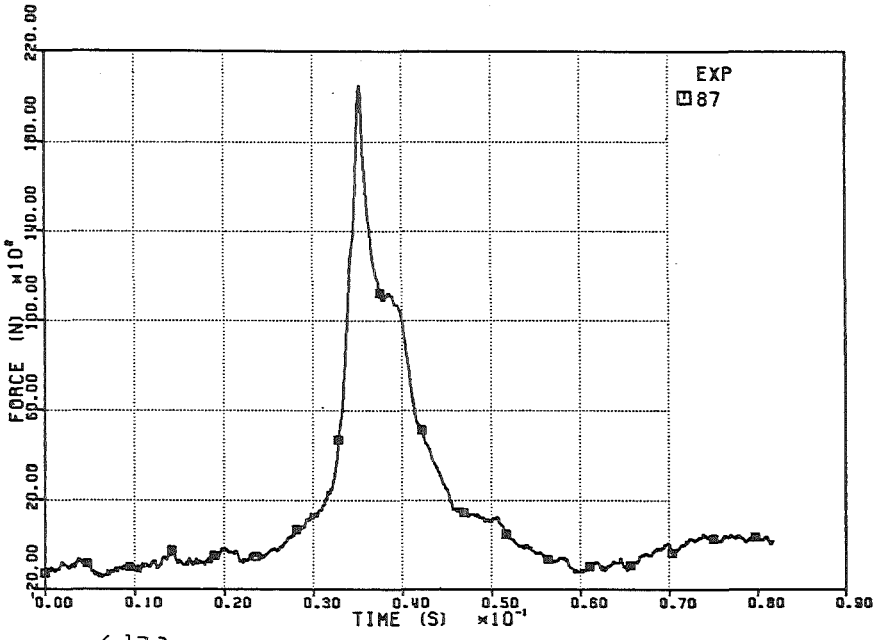

FIG. 6.372 - FORCE ON THE UPPER PLATE
INR536F1 31.05.85 29.42.05

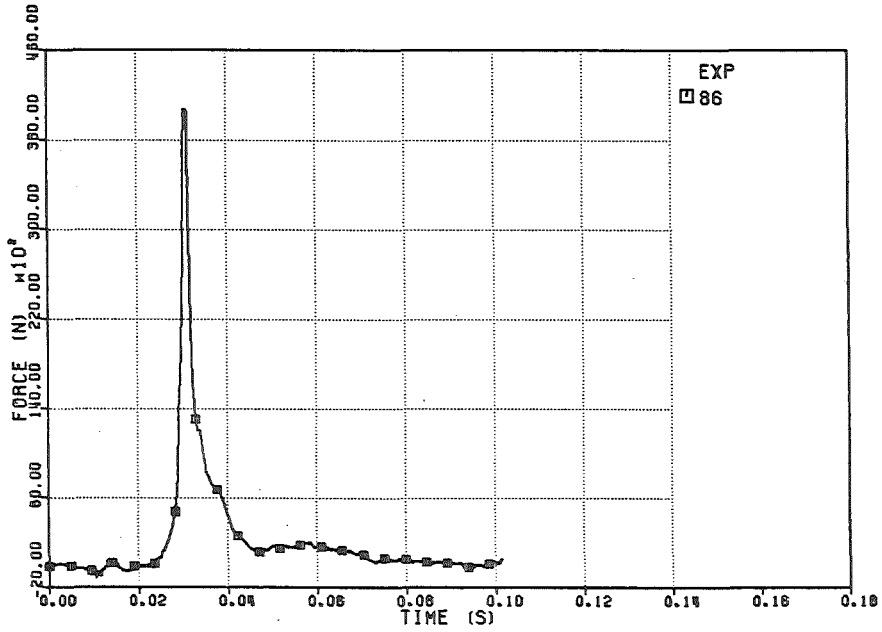

FIG. 6.371 - FORCE ON THE UPPER PLATE

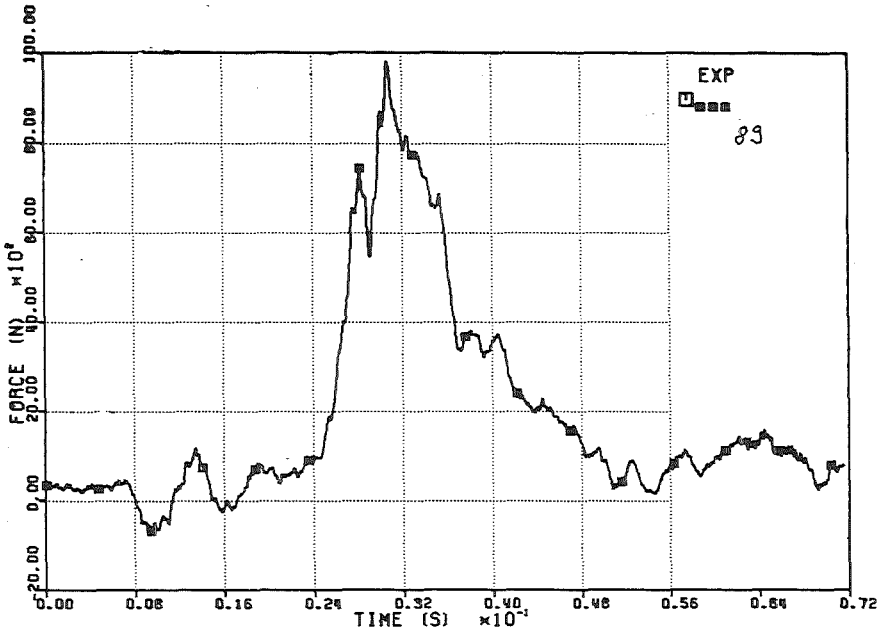

FIG. 6.374 - FORCE ON THE UPPER PLATE
IWR536F1 31.05.85 23.42.05

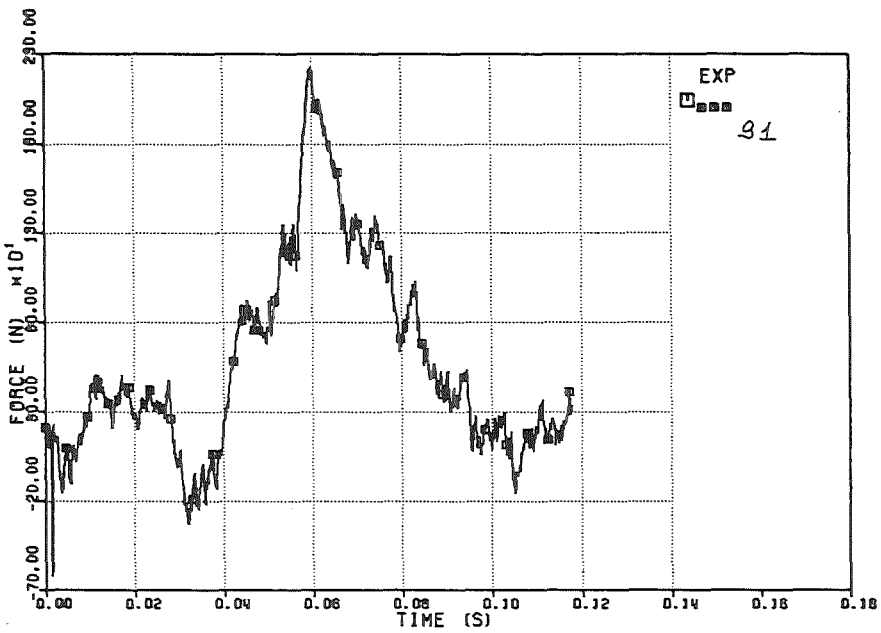

FIG. 6.376 - FORCE ON THE UPPER PLATE
IWR536F1 31.05.85 23.42.05

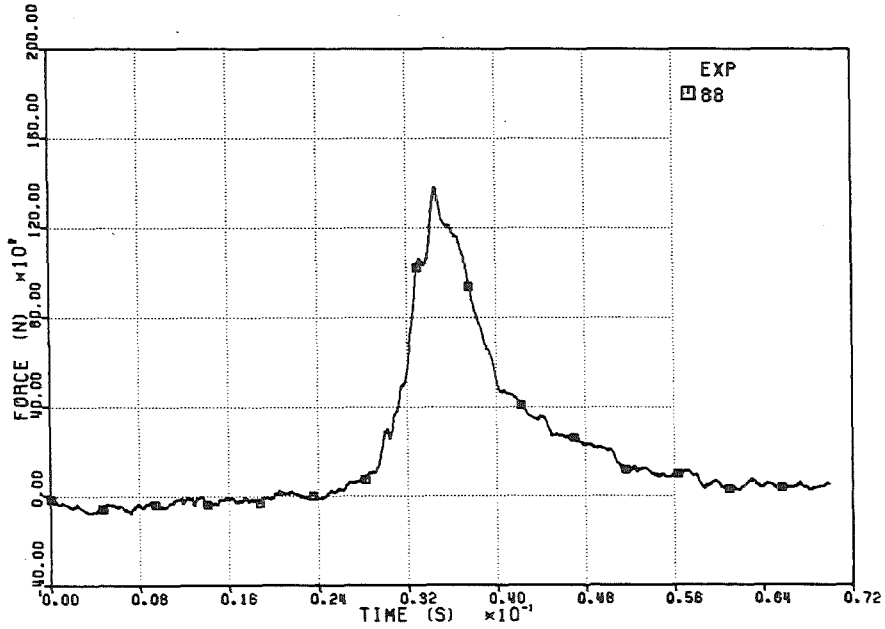

FIG. 6.373 - FORCE ON THE UPPER PLATE

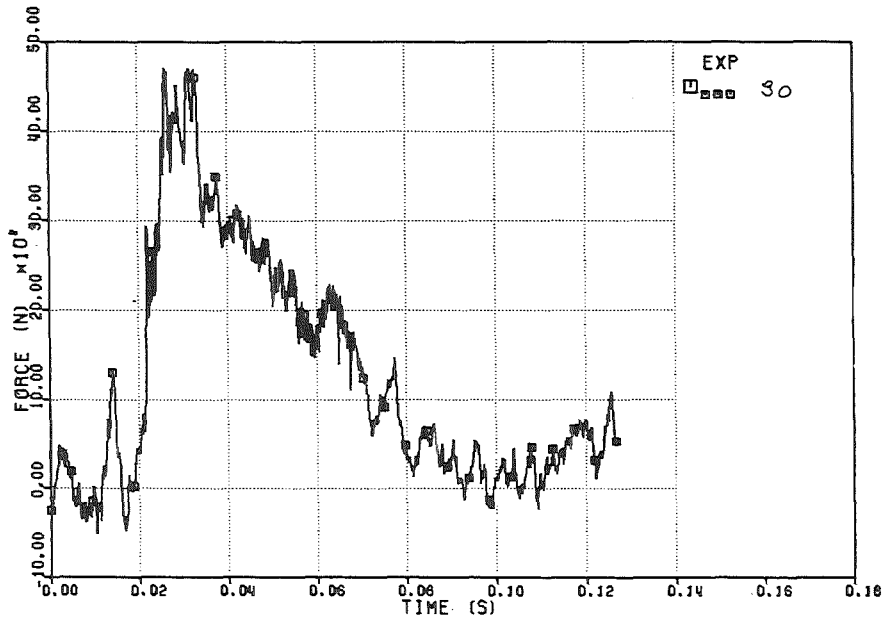

FIG. 6.375 - FORCE ON THE UPPER PLATE

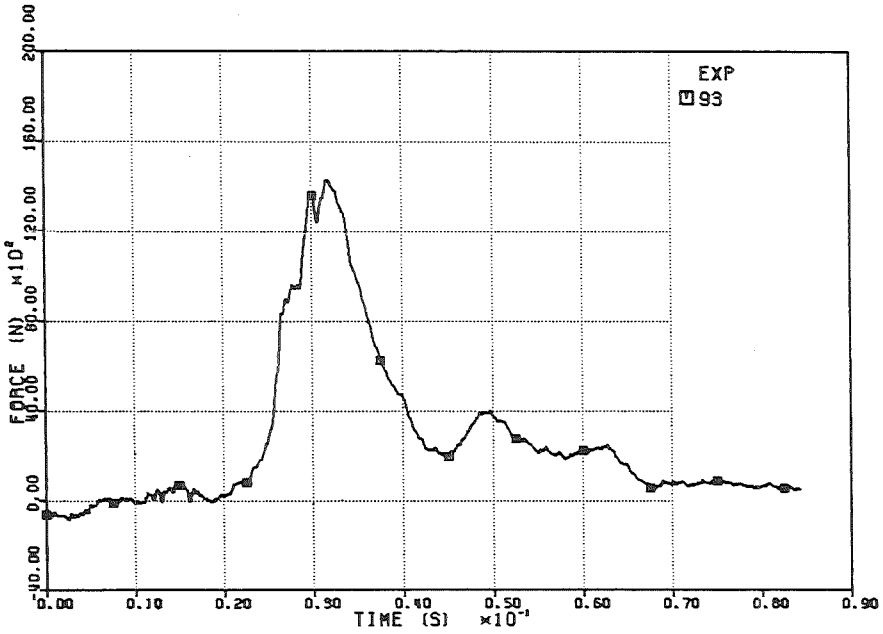

FIG. 6.378 - FORCE ON THE UPPER PLATE
INR536F1 31.05.85 23.53.05

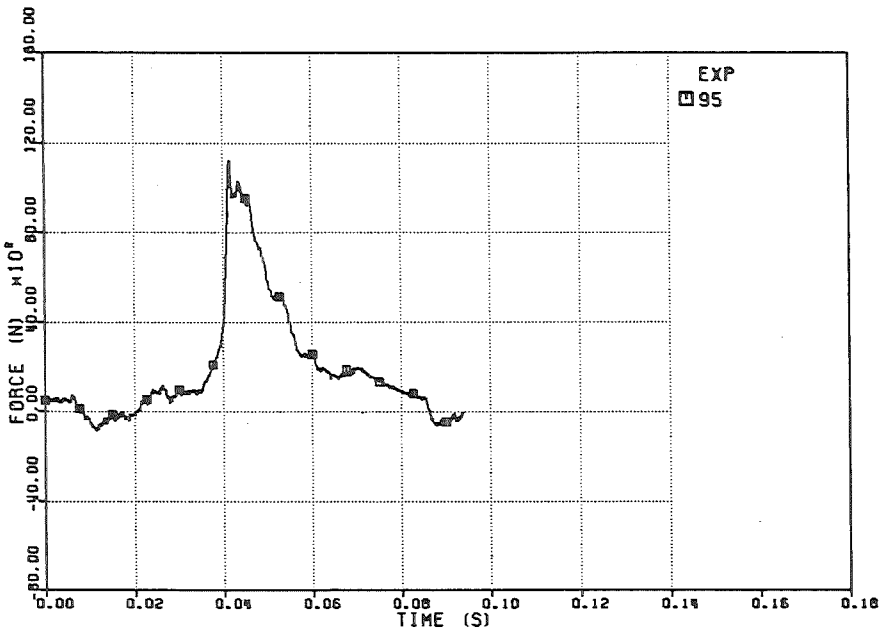

FIG. 6.380 - FORCE ON THE UPPER PLATE
INR536F1 31.05.85 23.53.05

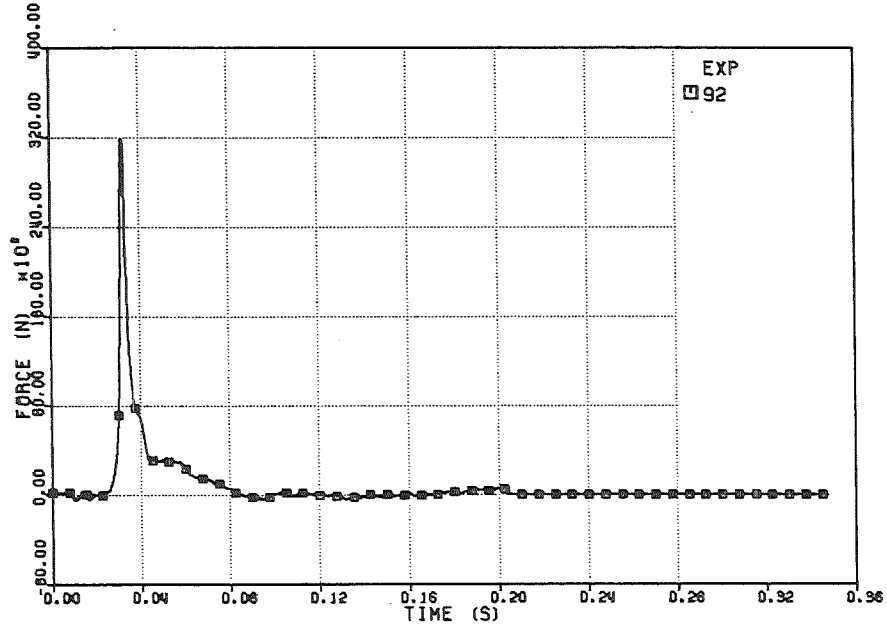

FIG. 6.377 - FORCE ON THE UPPER PLATE

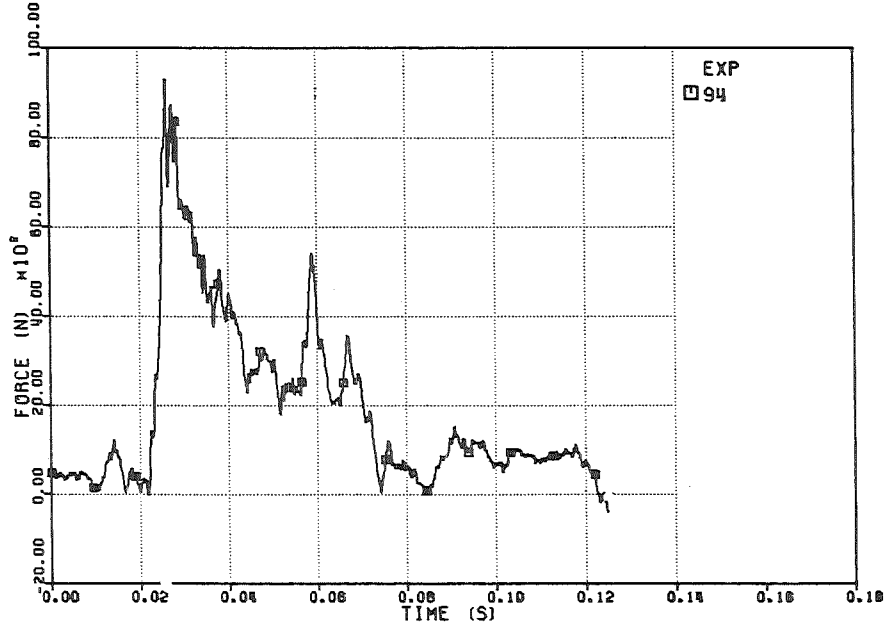

FIG. 6.379 - FORCE ON THE UPPER PLATE

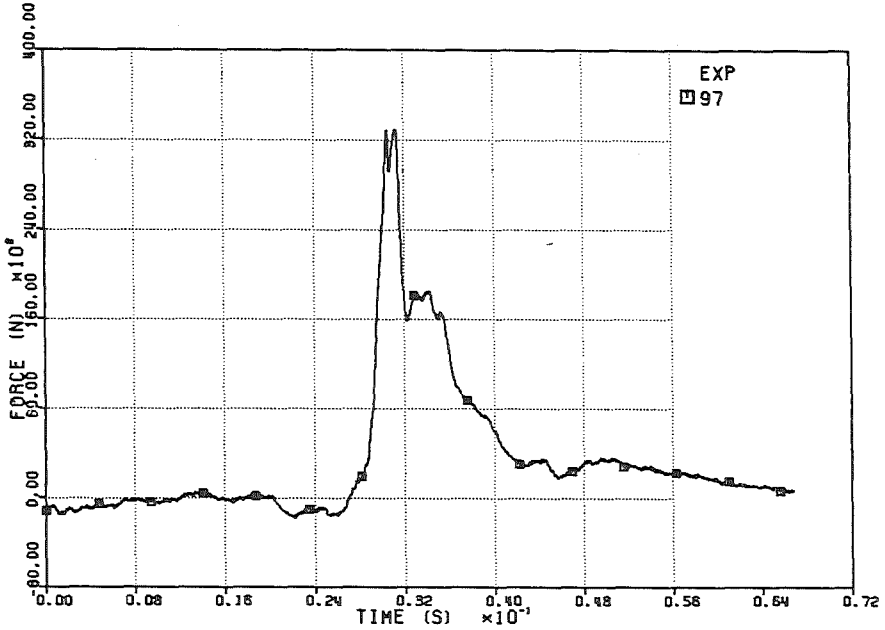

FIG. 6.382 - FORCE ON THE UPPER PLATE
IWR538F1 31.05.85 23.53.05

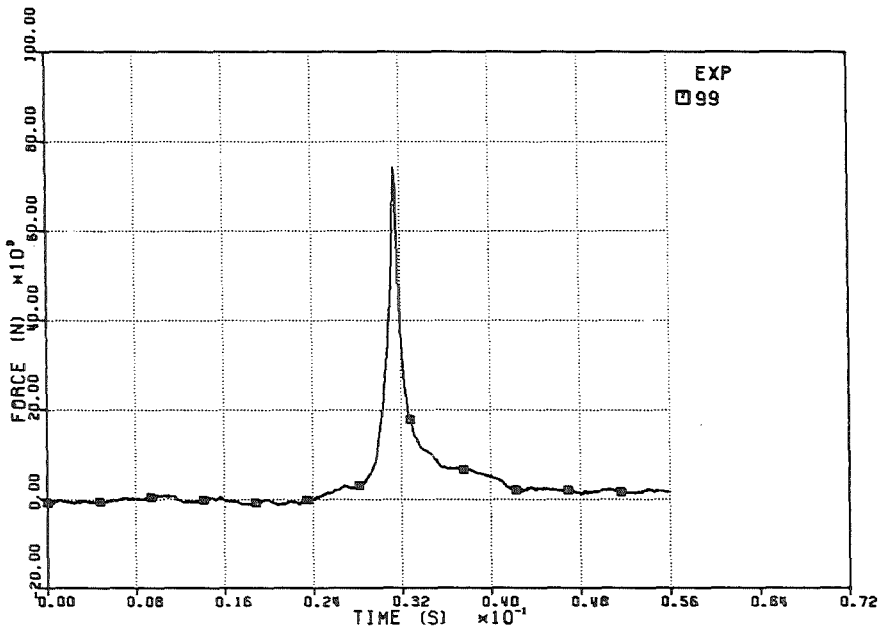

FIG. 6.384 - FORCE ON THE UPPER PLATE
IWR536F1 31.05.85 23.53.05

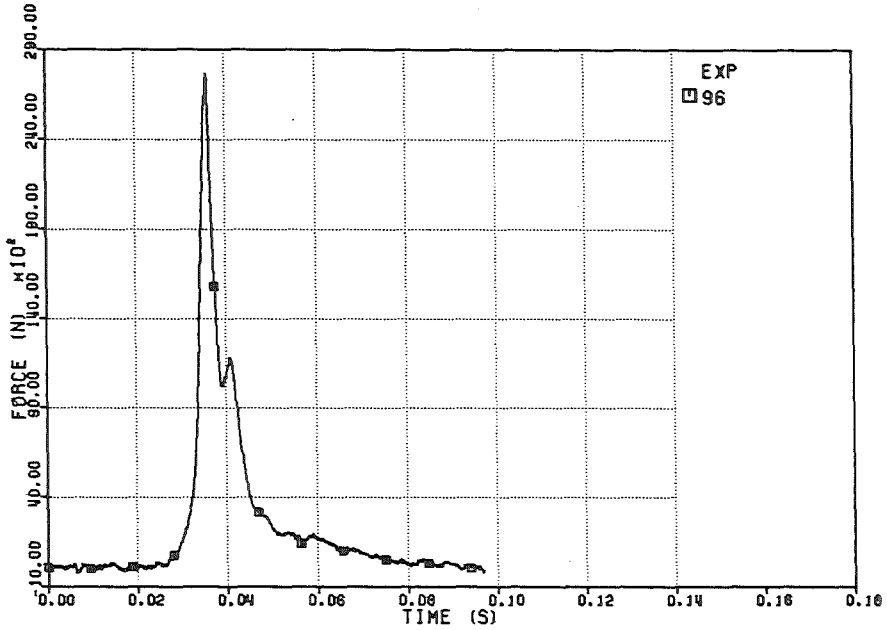

FIG. 6.381 - FORCE ON THE UPPER PLATE

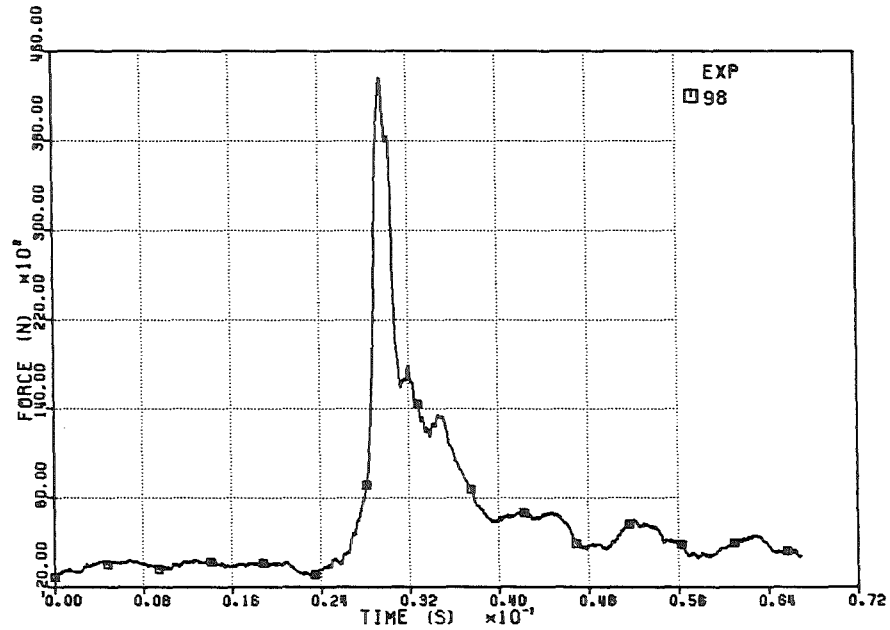

FIG. 6.383 - FORCE ON THE UPPER PLATE

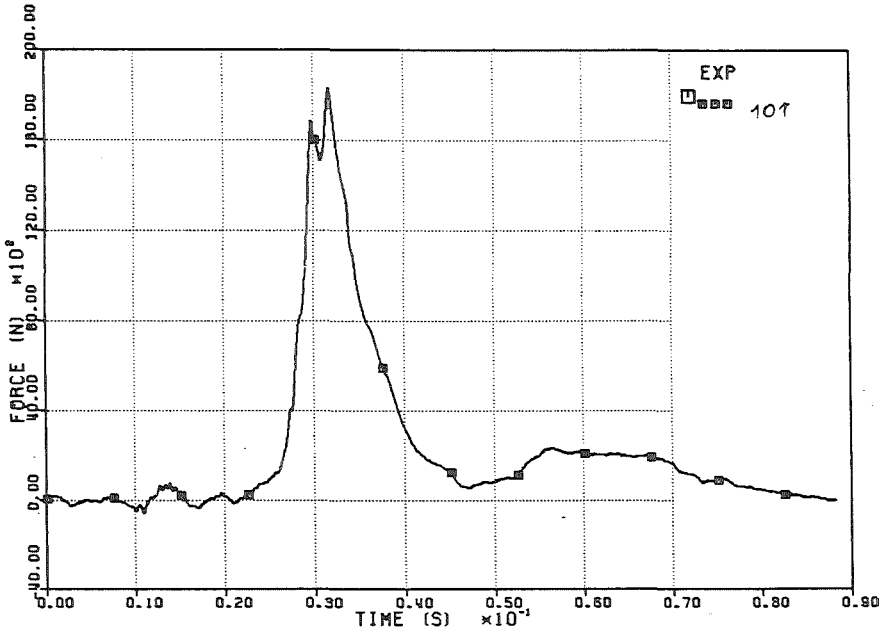

FIG. 6.386 - FORCE ON THE UPPER PLATE
INRS36F1 31.05.85 23.53.05

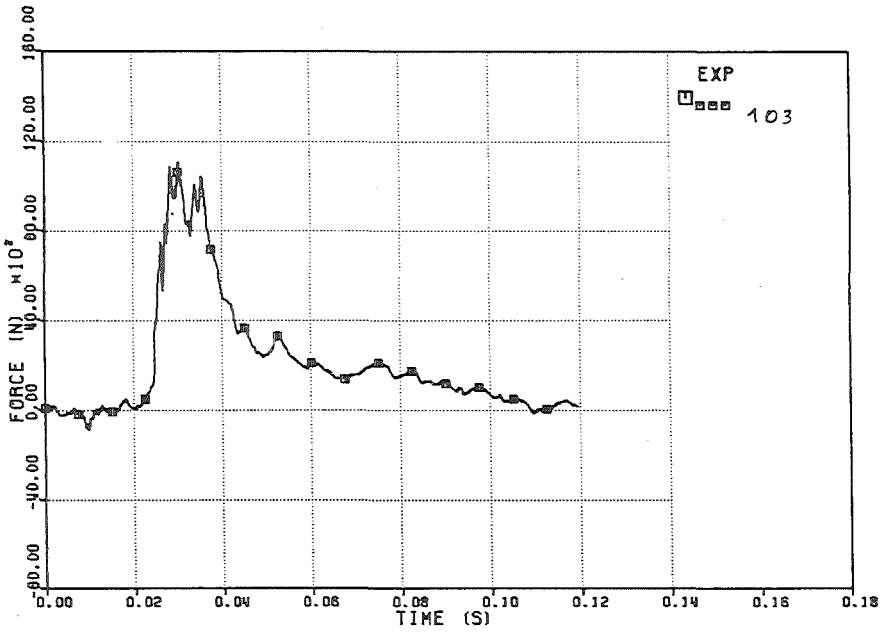

FIG. 6.388 - FORCE ON THE UPPER PLATE
INRS36F1 31.05.85 23.53.05

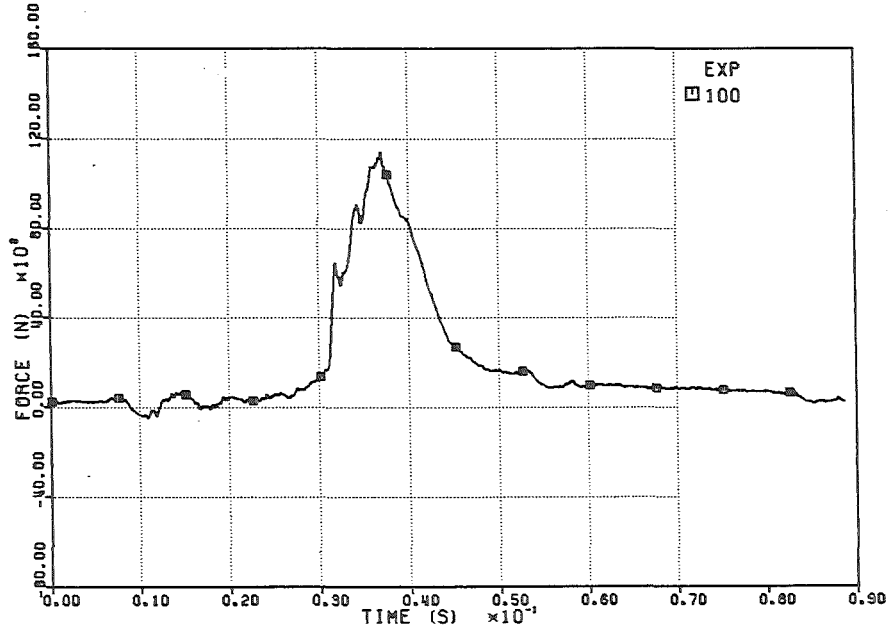

FIG. 6.385 - FORCE ON THE UPPER PLATE

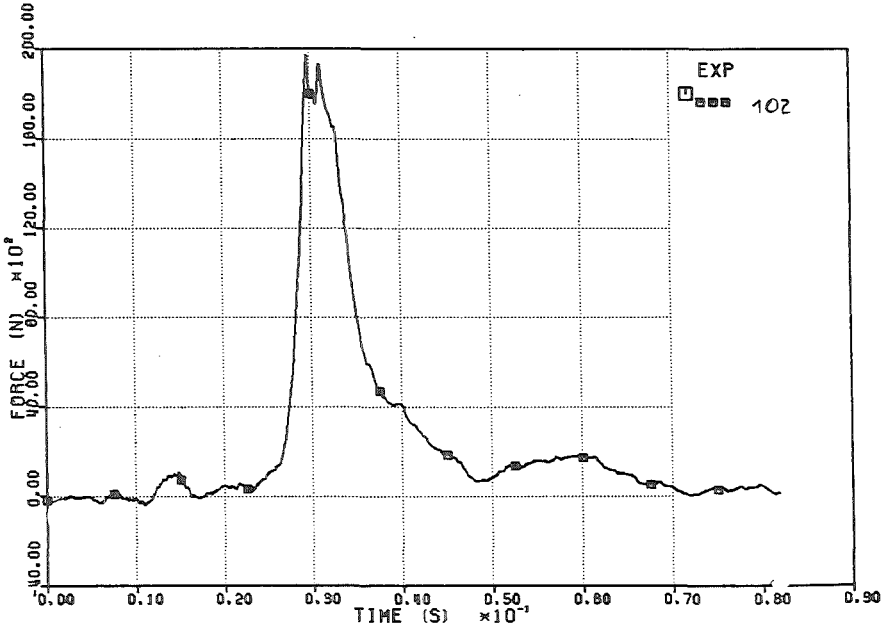

FIG. 6.387 - FORCE ON THE UPPER PLATE

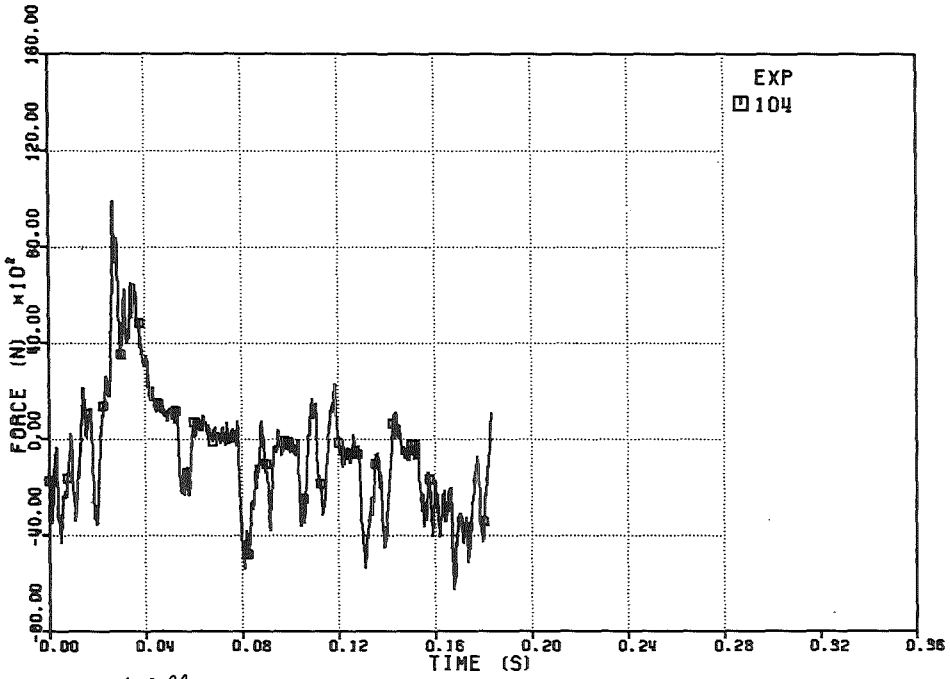

FIG. 6.389- FORCE ON THE UPPER PLATE

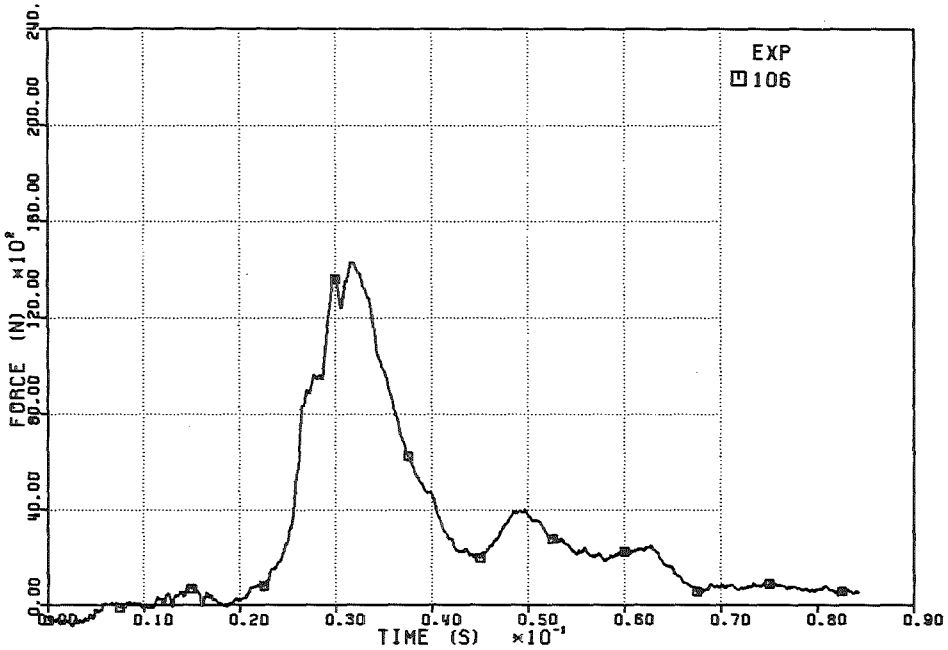

FIG. 6.391- FORCE ON THE UPPER PLATE

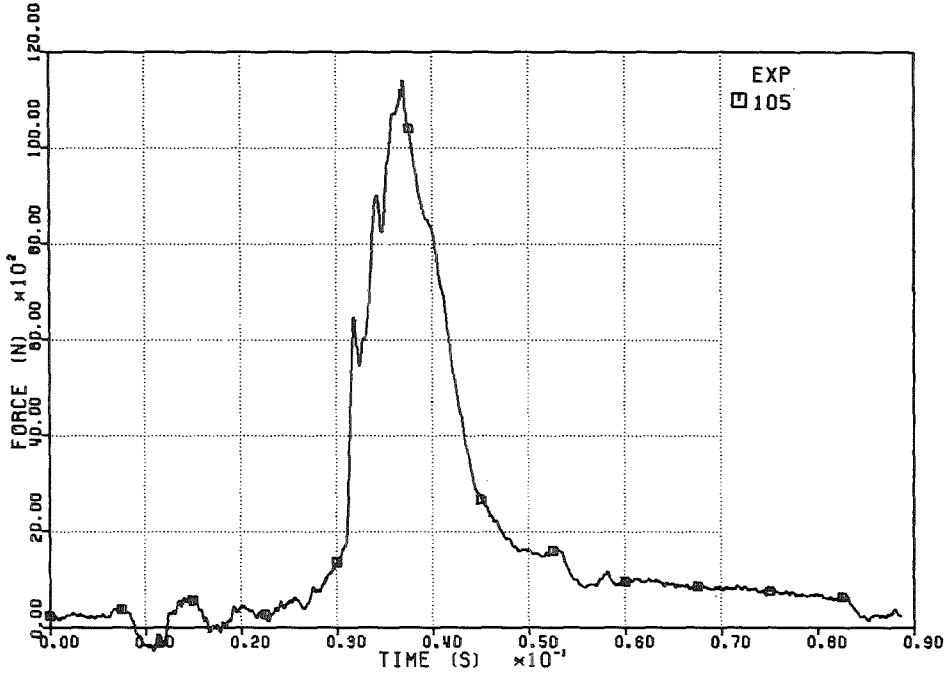

FIG. 6.390- FORCE ON THE UPPER PLATE

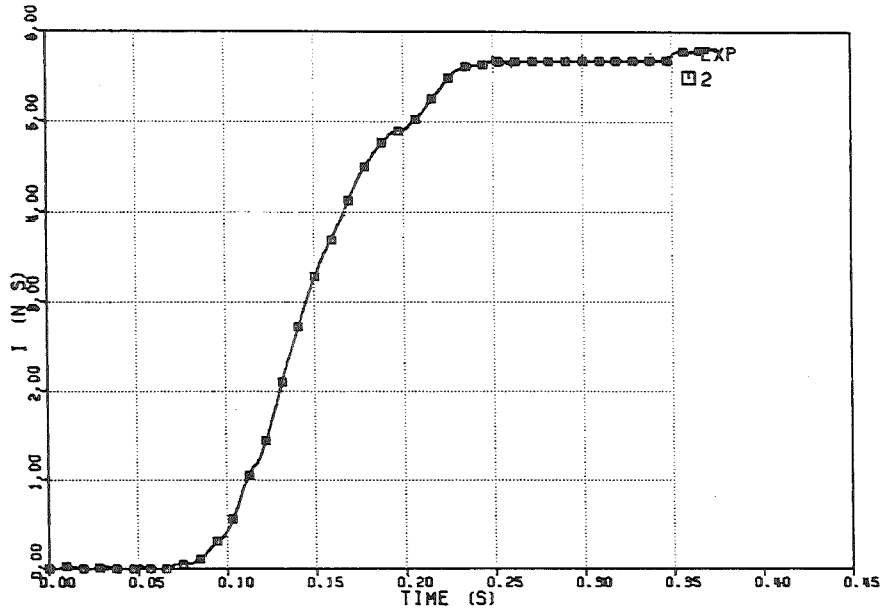

FIG. 6.393 IMPULSE ON THE UPPER PLATE

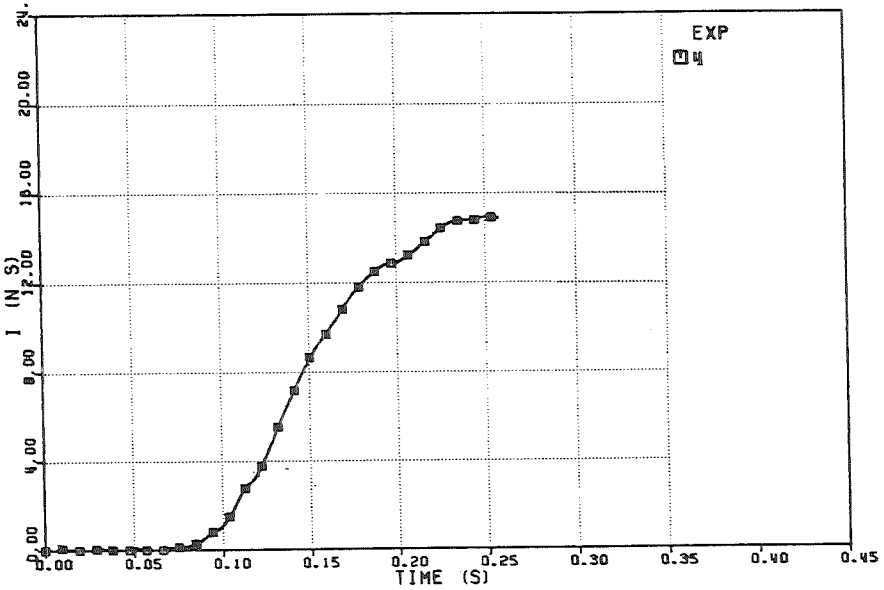

FIG. 6.395 IMPULSE ON THE UPPER PLATE

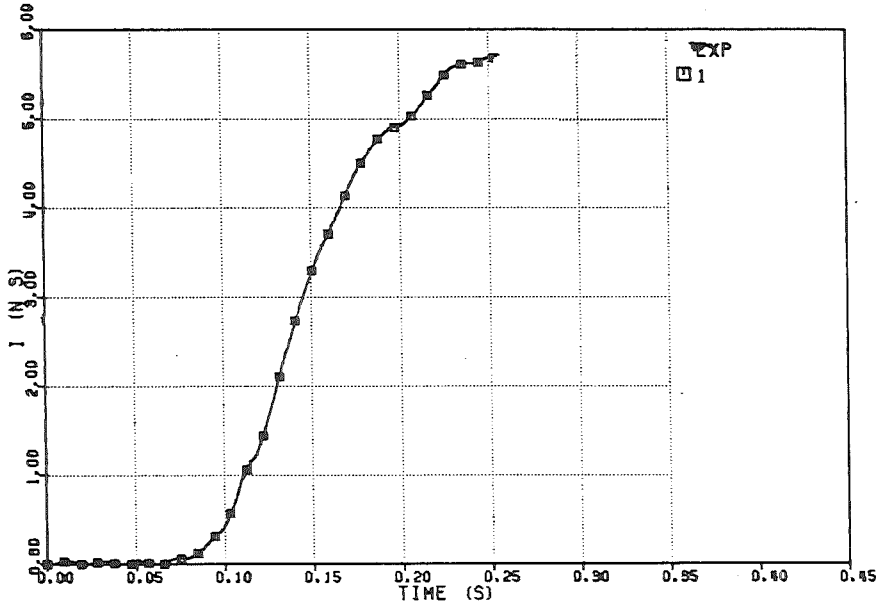

FIG. 6.392 IMPULSE ON THE UPPER PLATE

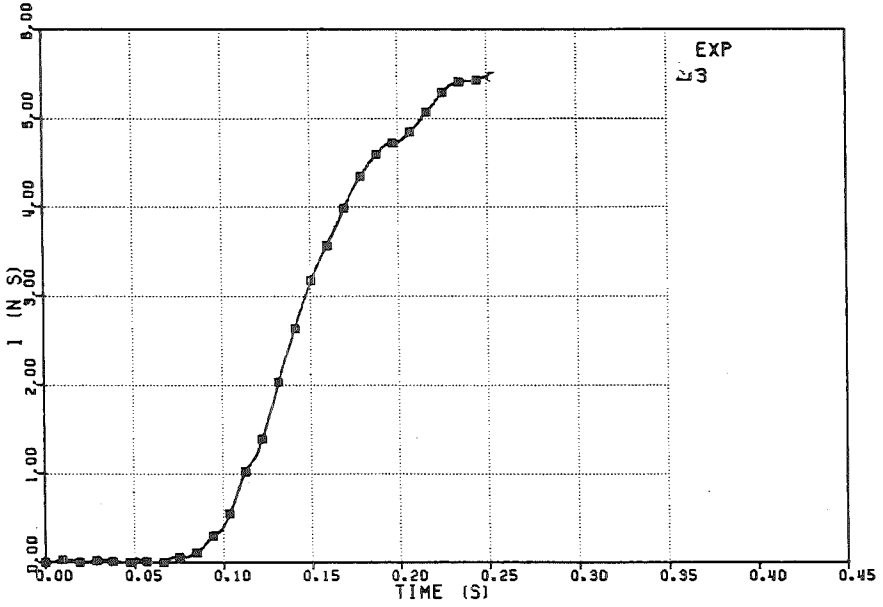

FIG. 6.394 IMPULSE ON THE UPPER PLATE

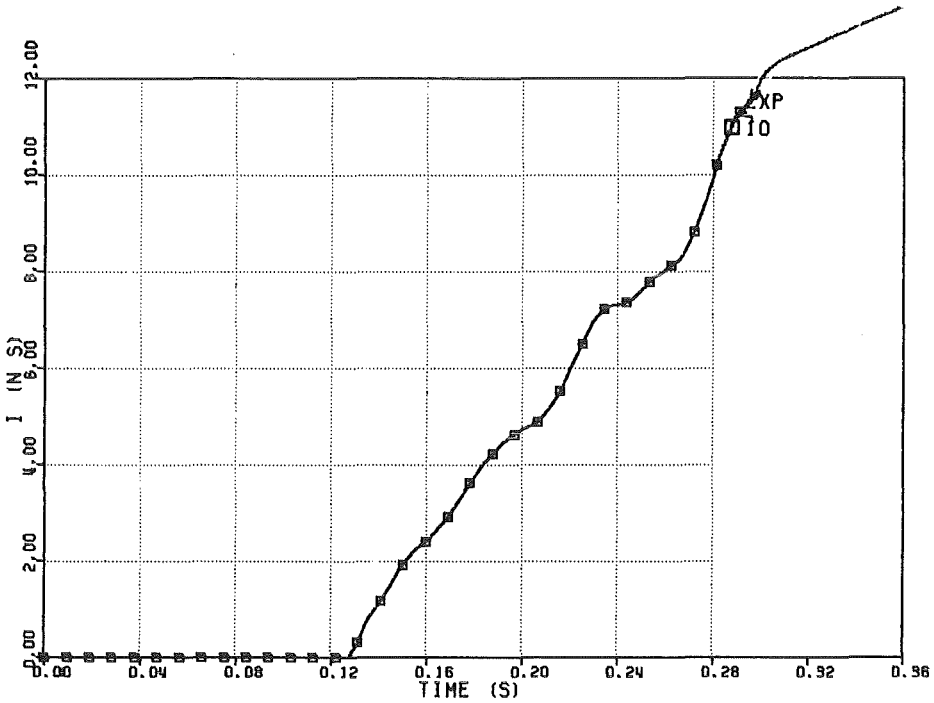

FIG. 6.397 IMPULSE ON THE UPPER PLATE

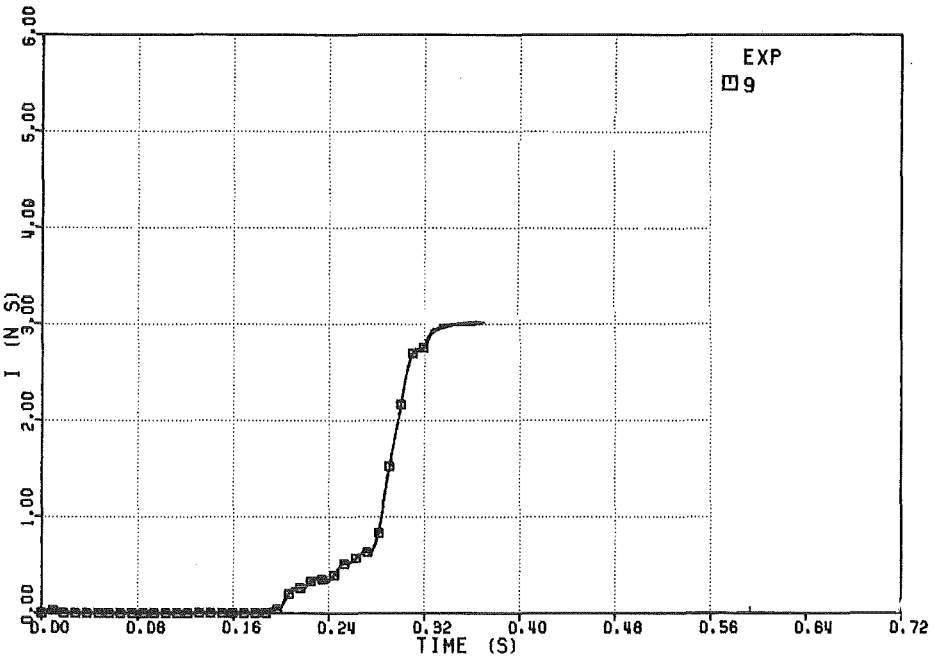

FIG. 6.396 IMPULSE ON THE UPPER PLATE

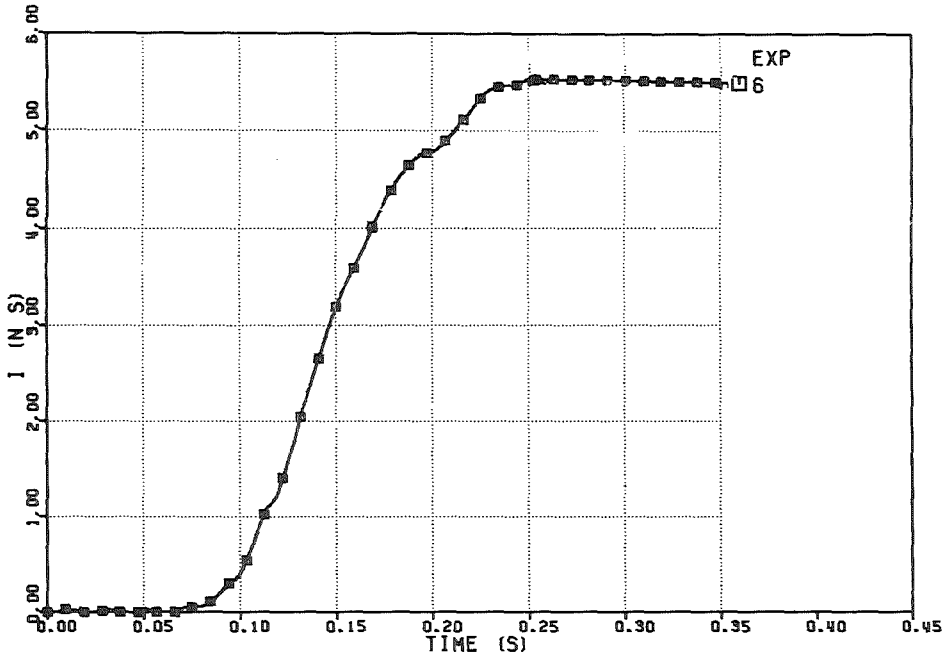

FIG. 6.399 IMPULSE ON THE UPPER PLATE

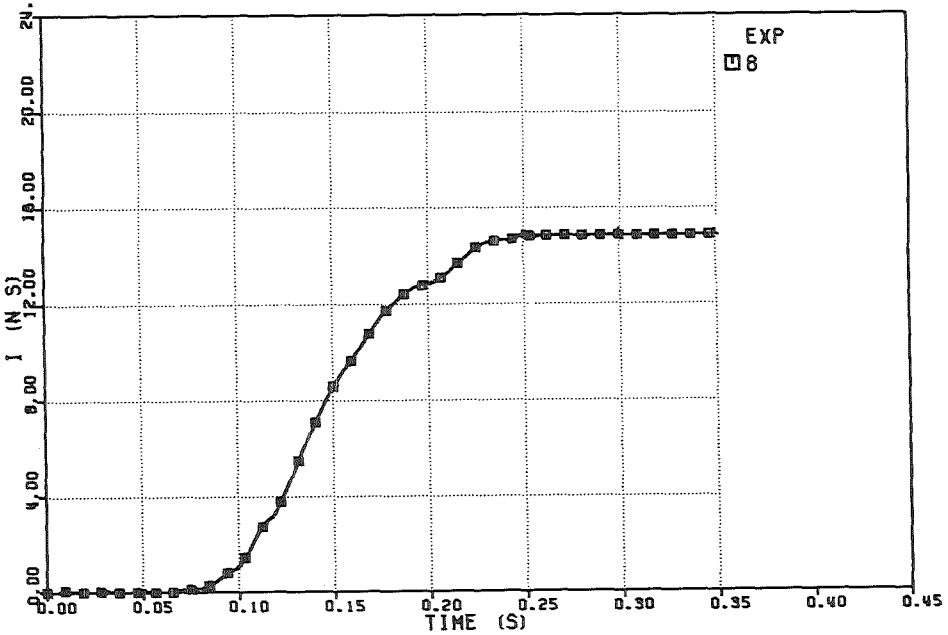

FIG. 6.401 IMPULSE ON THE UPPER PLATE

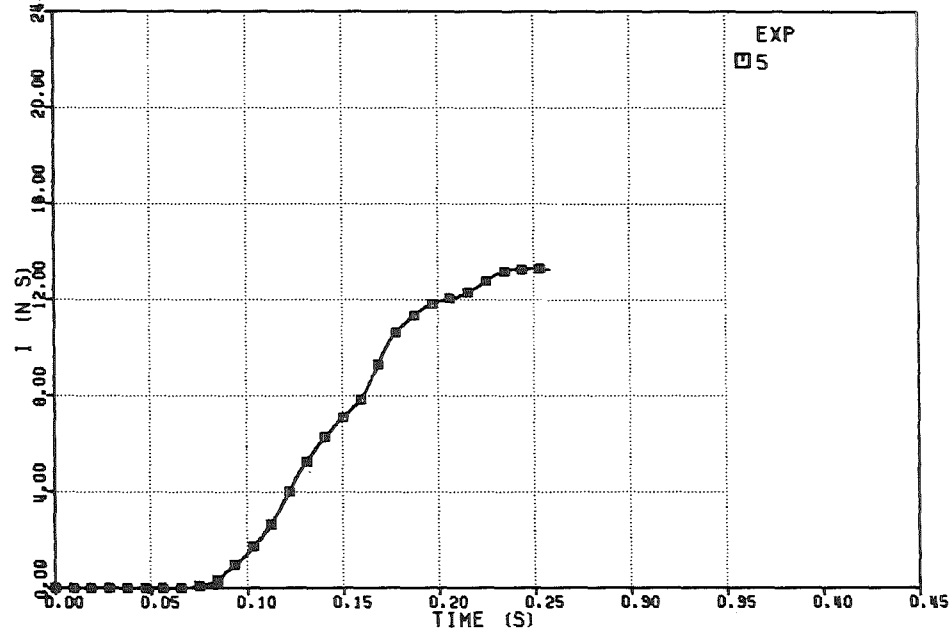

FIG. 6398 IMPULSE ON THE UPPER PLATE

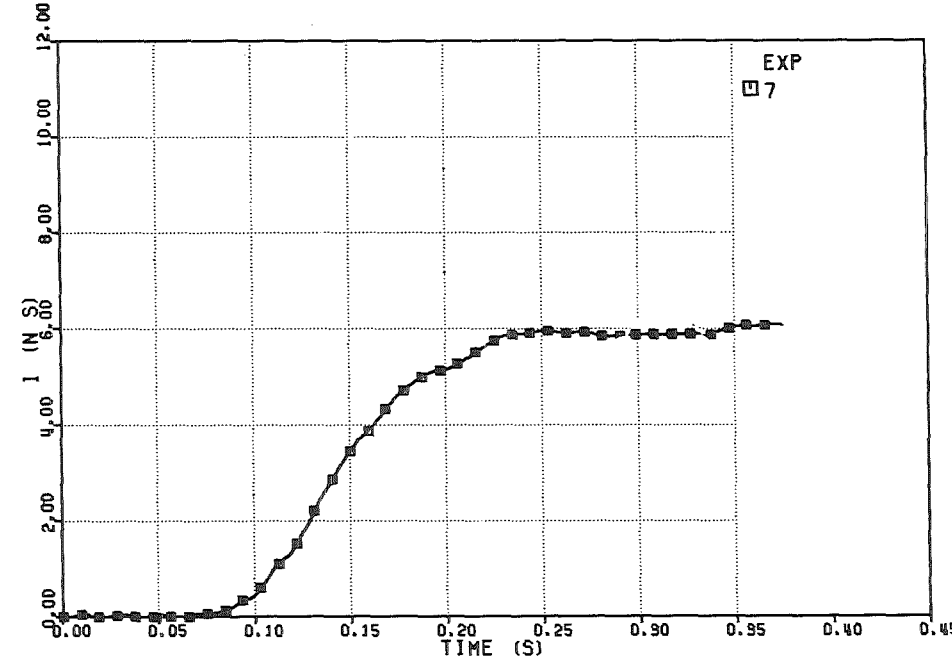

FIG. 6.400 IMPULSE ON THE UPPER PLATE

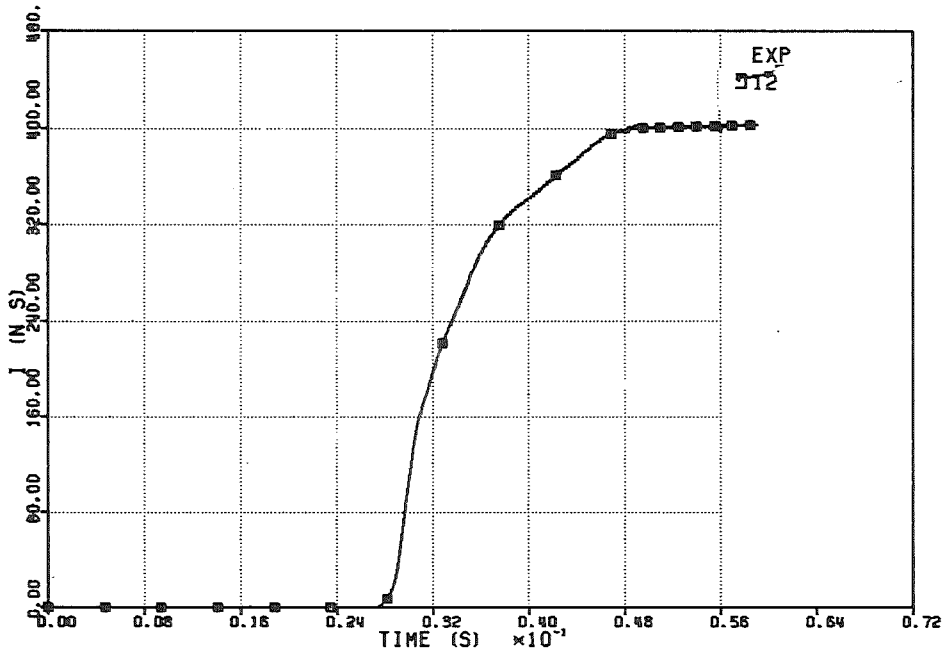

FIG. 6.403 -IMPULSE ON THE UPPER PLATE

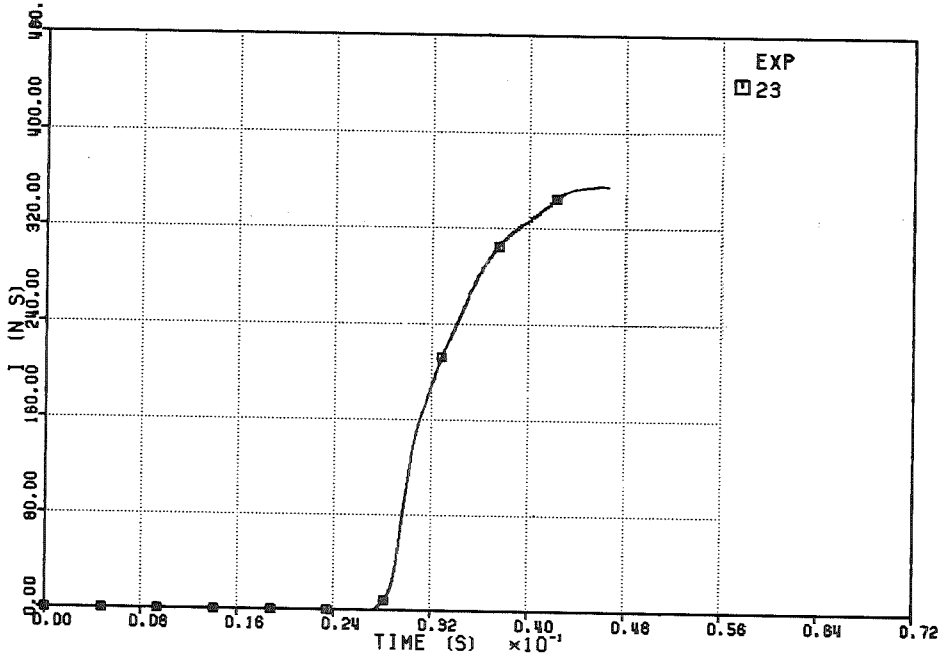

FIG. 6.405-IMPULSE ON THE UPPER PLATE

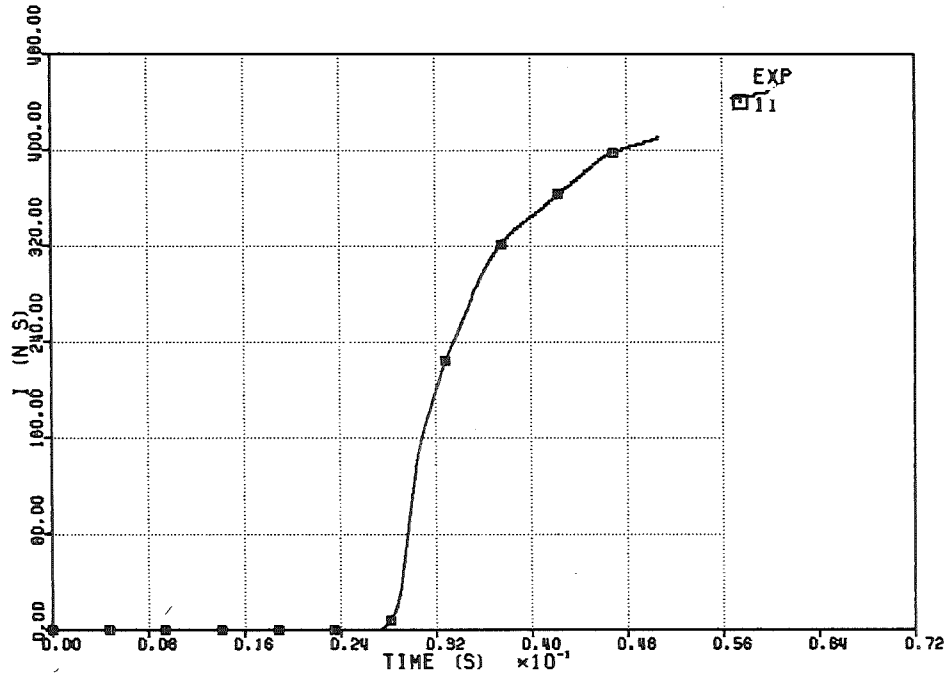

FIG. 6.402 -IMPULSE ON THE UPPER PLATE

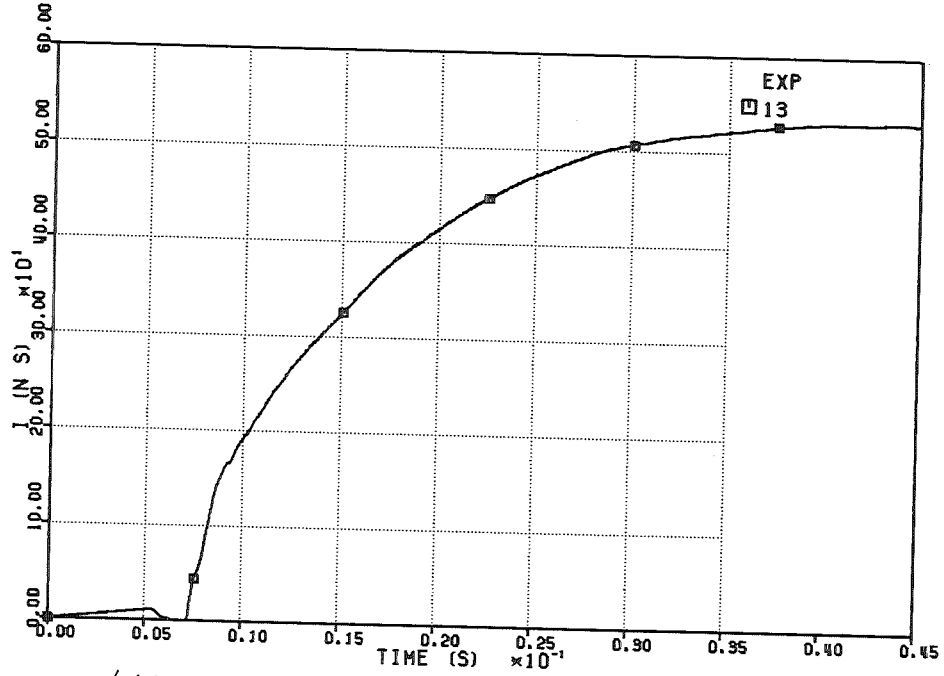

FIG. 6.404-IMPULSE ON THE UPPER PLATE

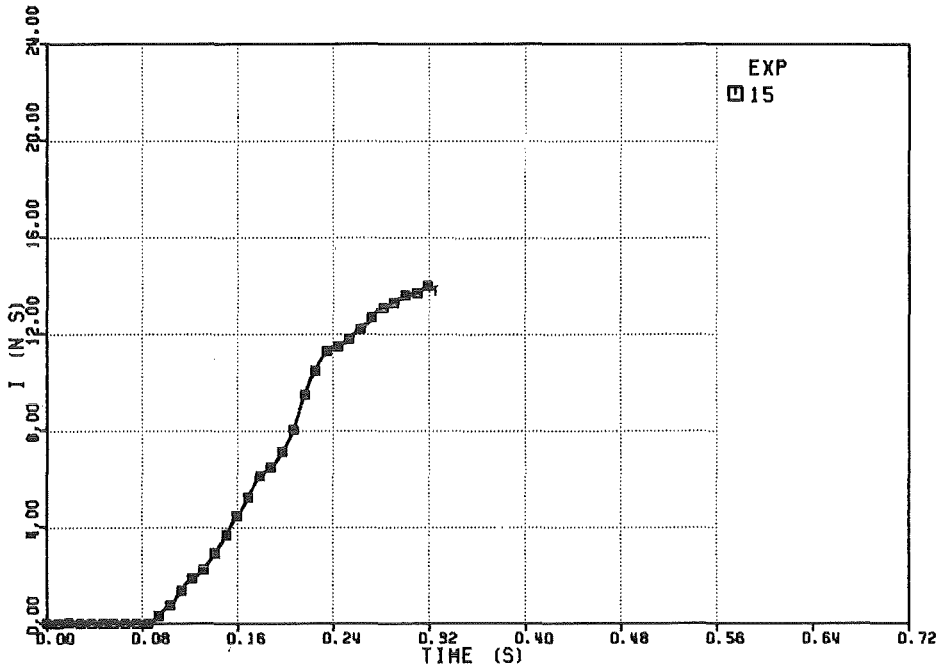

FIG. 6.407 IMPULSE ON THE UPPER PLATE

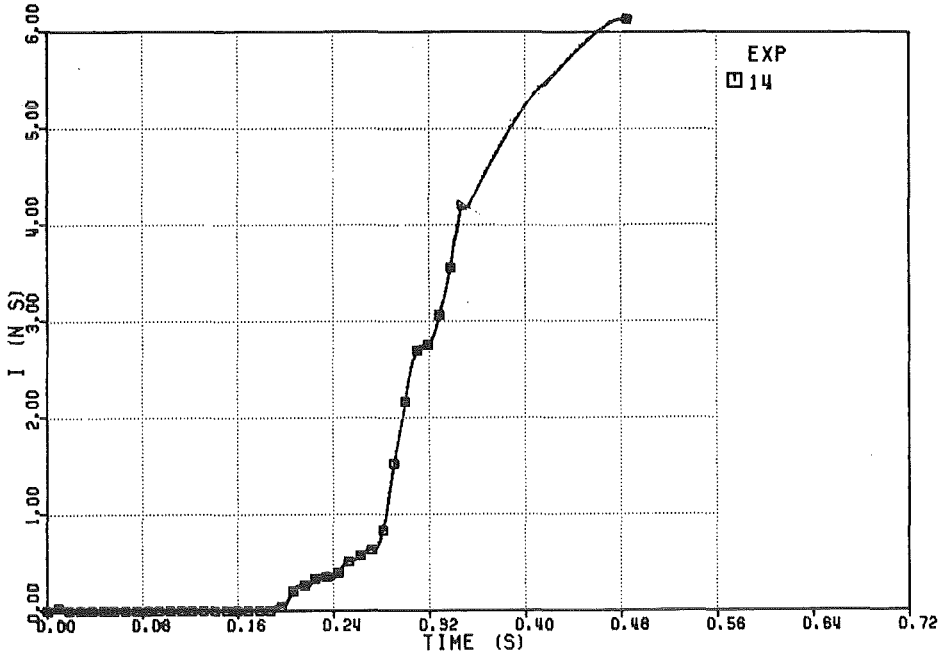

FIG. 6.406 IMPULSE ON THE UPPER PLATE

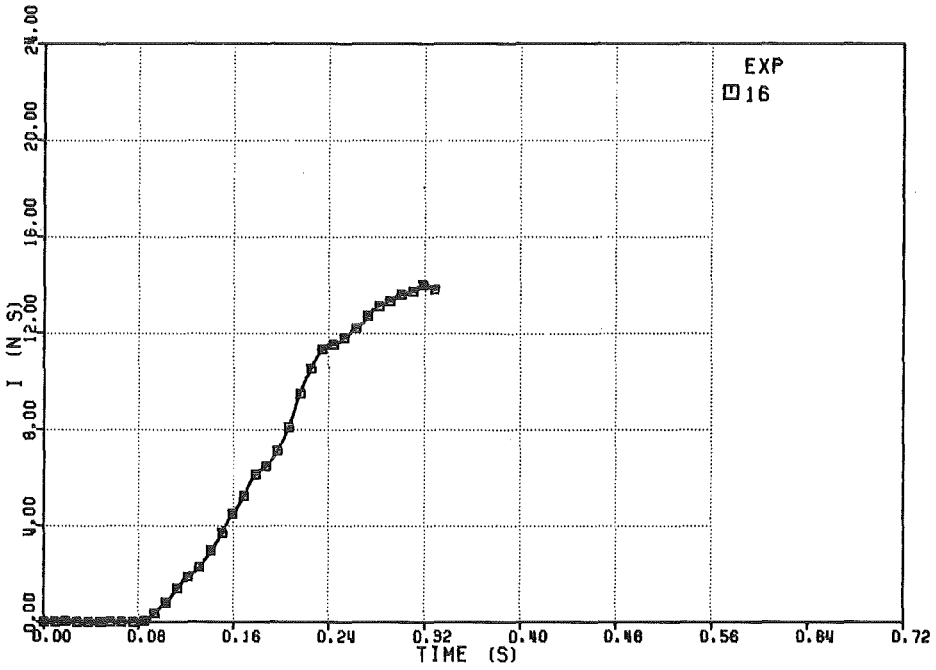

FIG. 6.408 IMPULSE ON THE UPPER PLATE

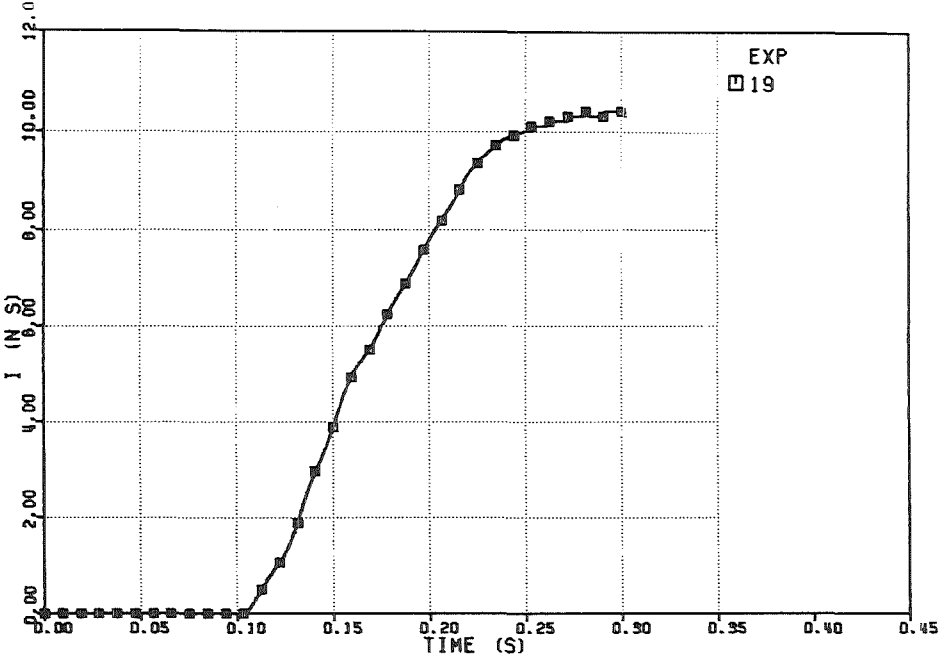

FIG. 6.410 IMPULSE ON THE UPPER PLATE

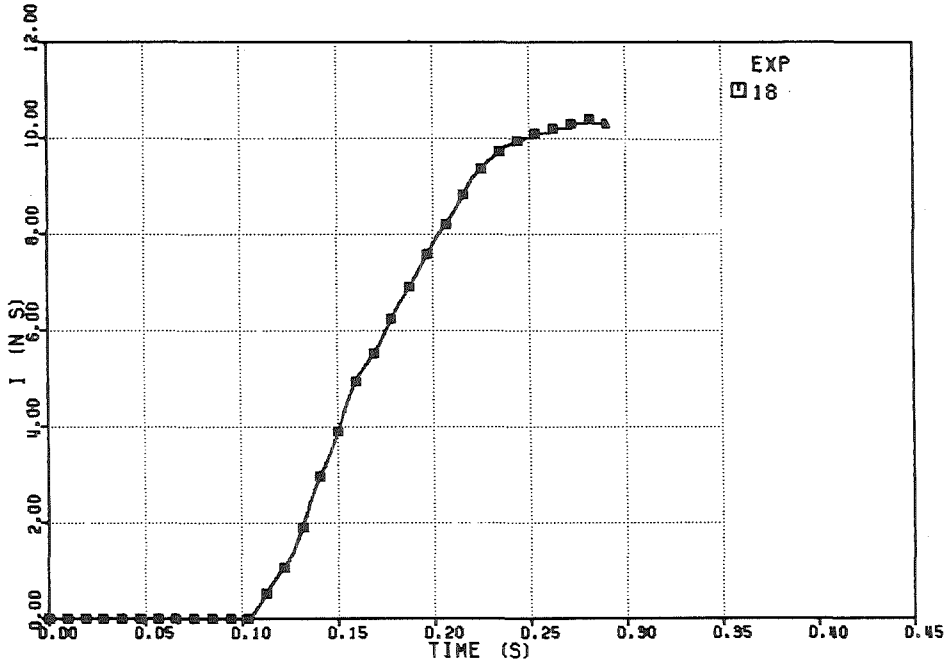

FIG. 6.409 IMPULSE ON THE UPPER PLATE

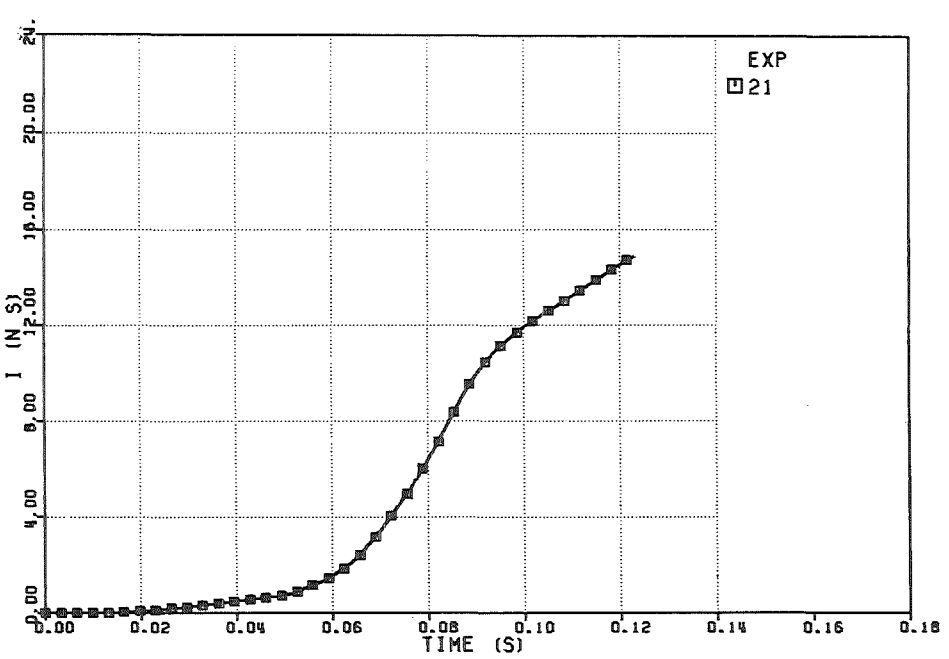

FIG. 6.412 IMPULSE ON THE UPPER PLATE

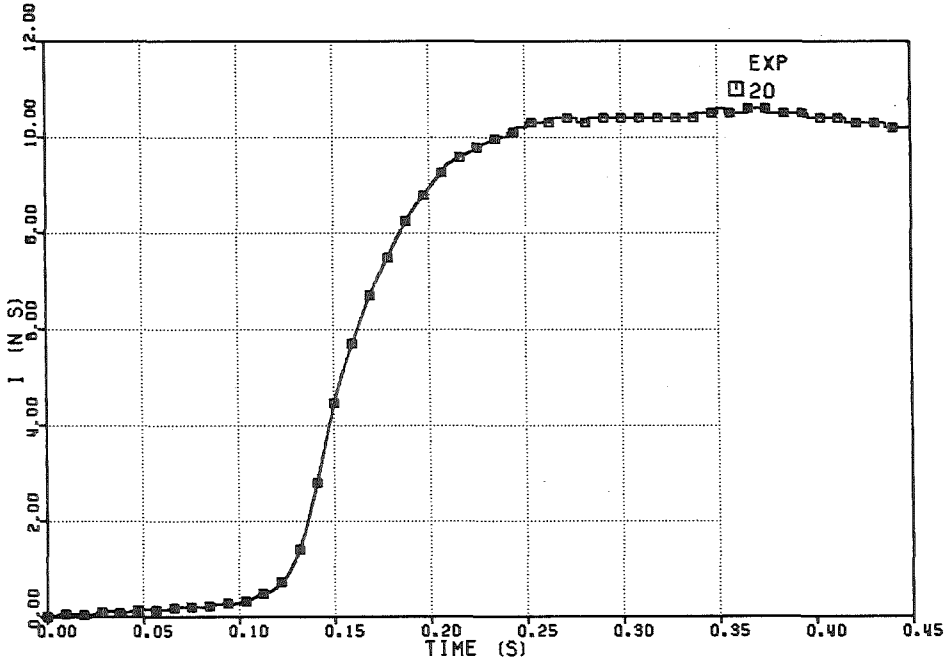

FIG. 6.411 IMPULSE ON THE UPPER PLATE

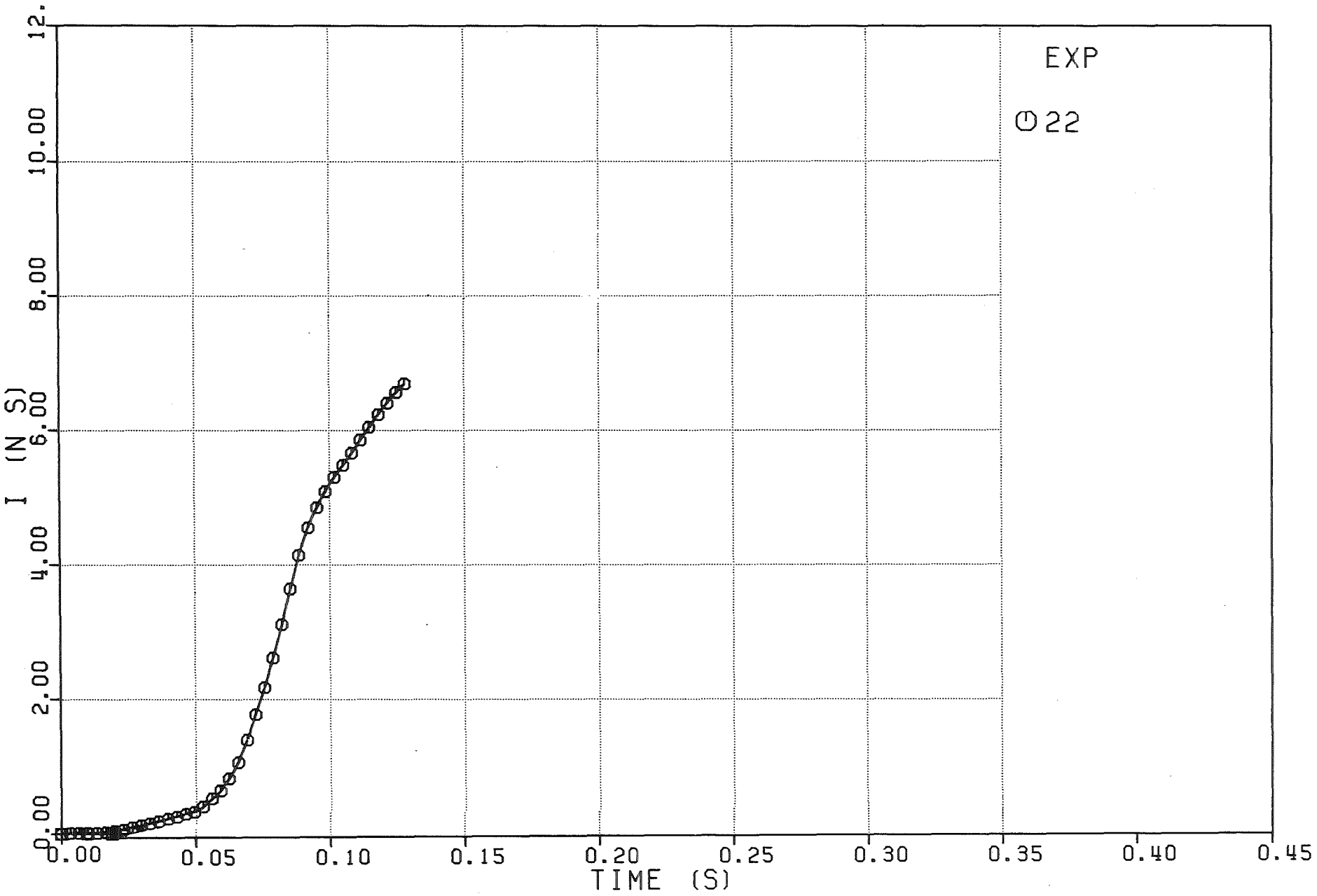

Fig. 6.413 - Impulse on the upper plate

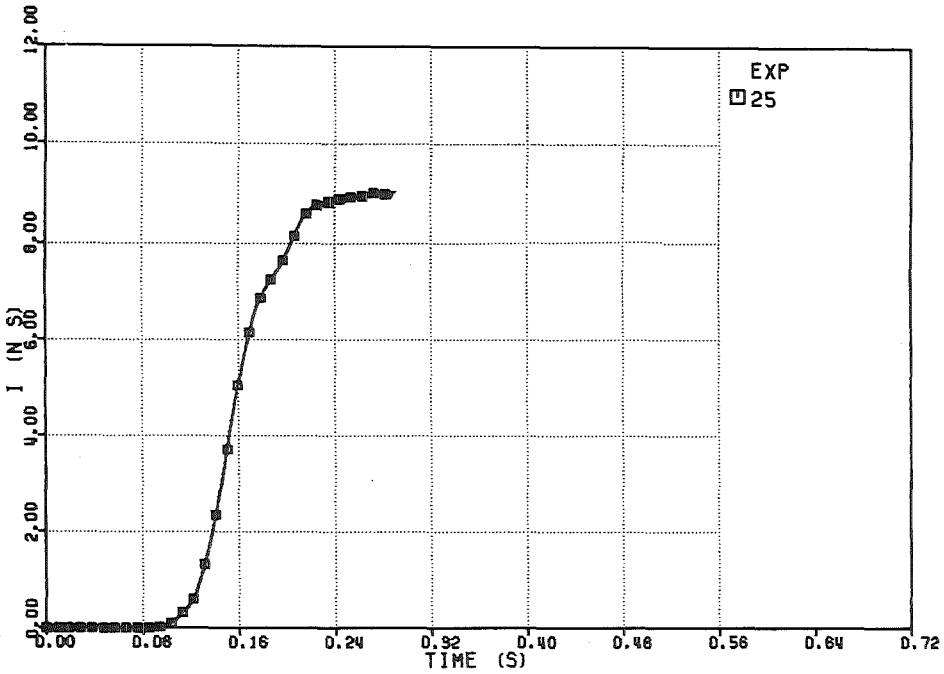

FIG. 6.415 IMPULSE ON THE UPPER PLATE

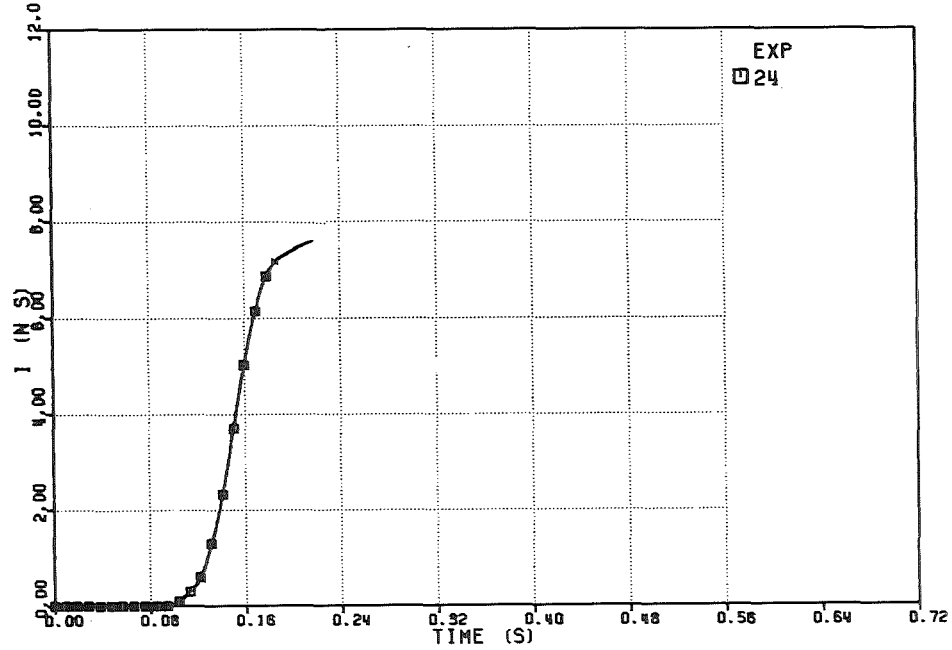

FIG. 6.414 IMPULSE ON THE UPPER PLATE

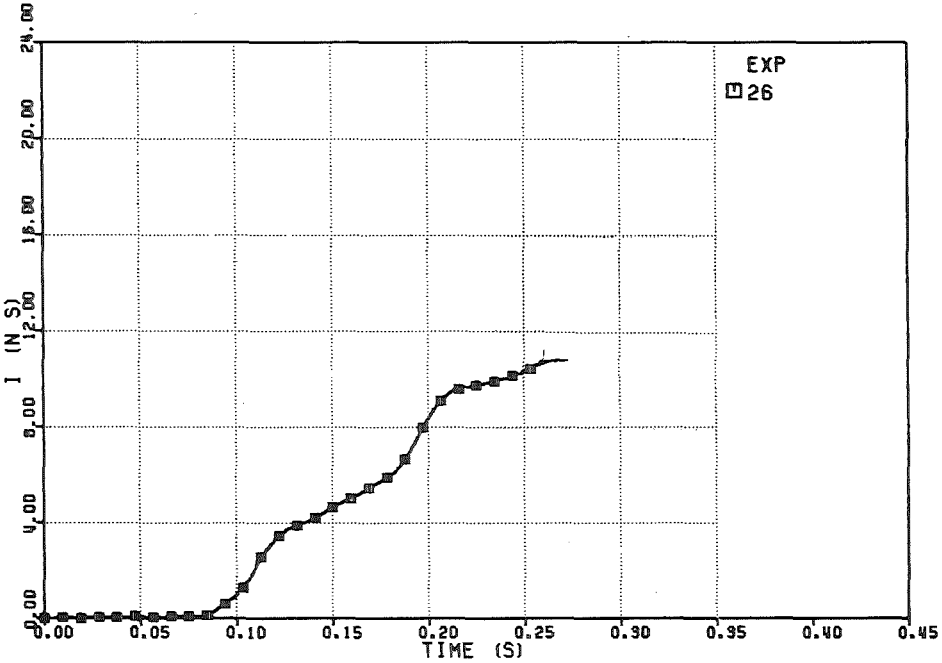

FIG. 6.416 IMPULSE ON THE UPPER PLATE

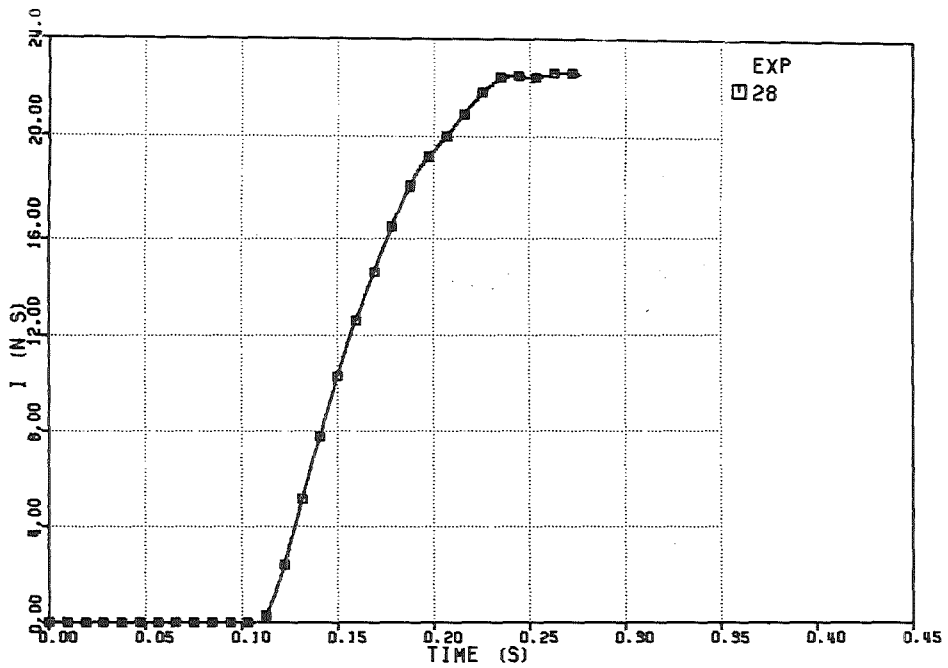

FIG. 6.418 IMPULSE ON THE UPPER PLATE

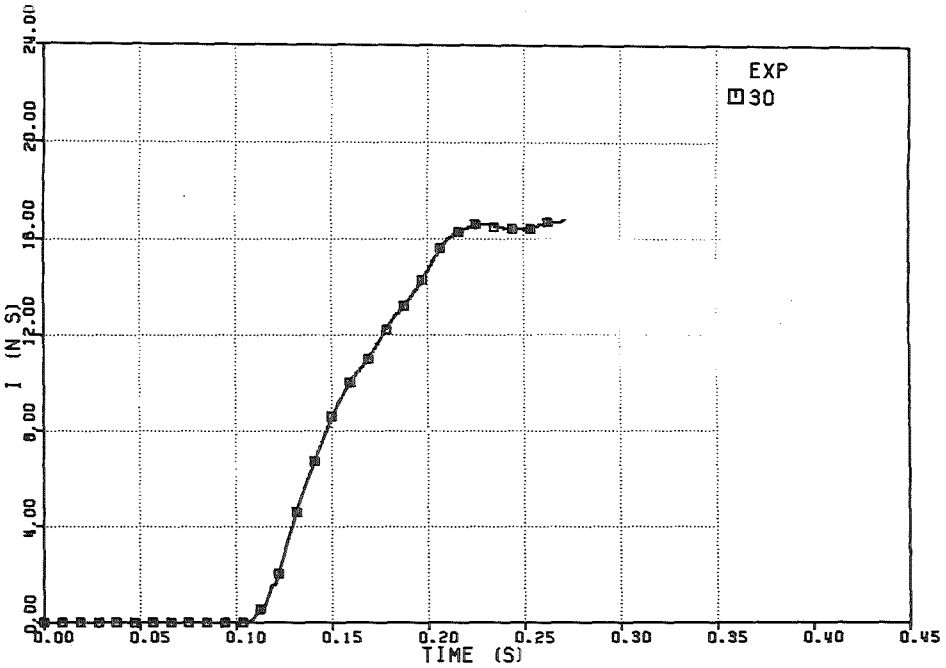

FIG. 6.420 IMPULSE ON THE UPPER PLATE

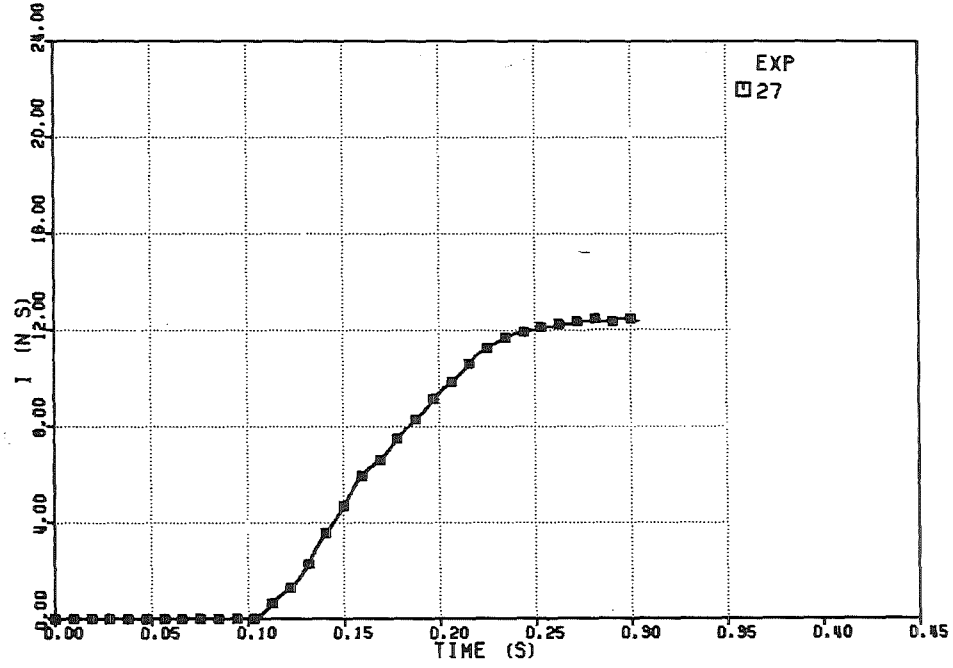

FIG. 6.417 IMPULSE ON THE UPPER PLATE

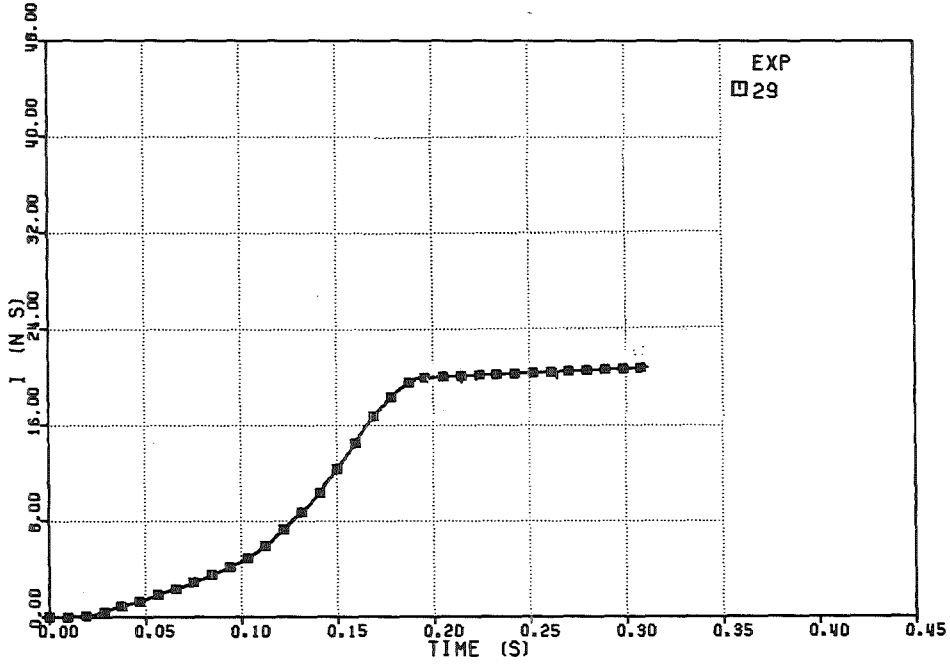

FIG. 6.419 IMPULSE ON THE UPPER PLATE

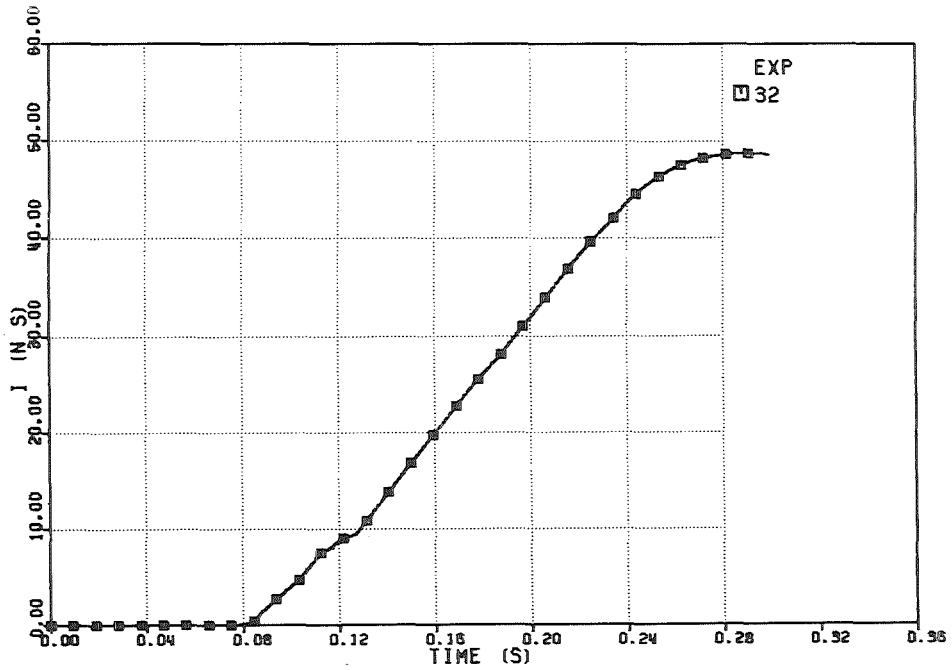

FIG. 6.422 IMPULSE ON THE UPPER PLATE

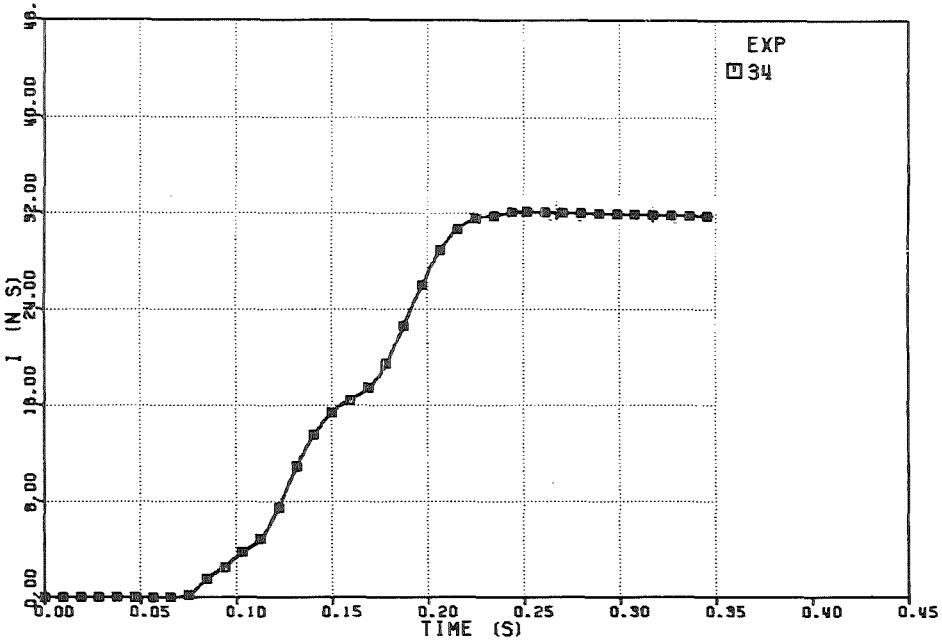

FIG. 6.424 IMPULSE ON THE UPPER PLATE

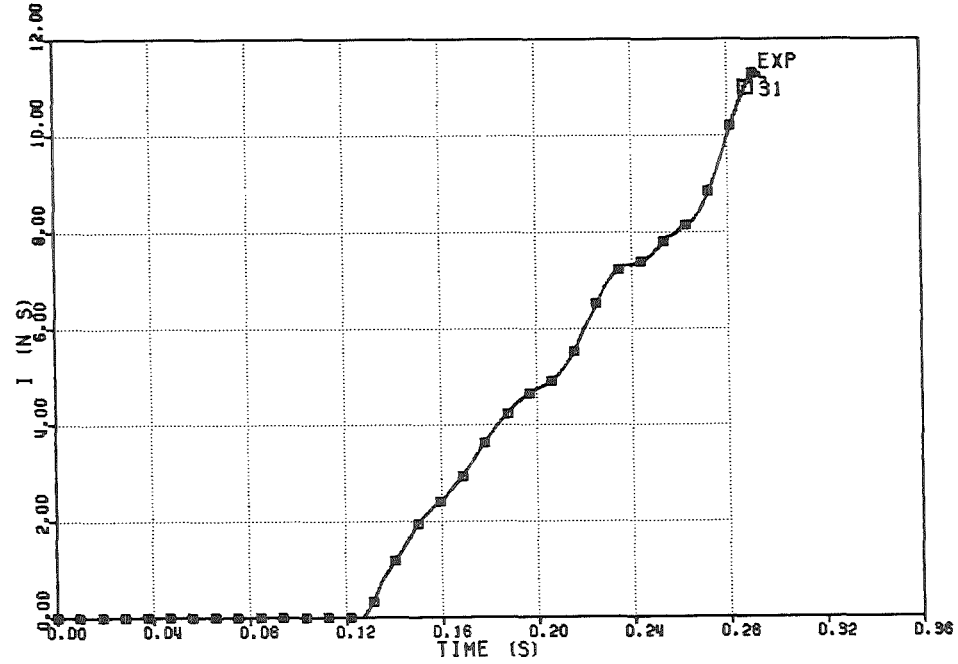

FIG. 6.421 IMPULSE ON THE UPPER PLATE

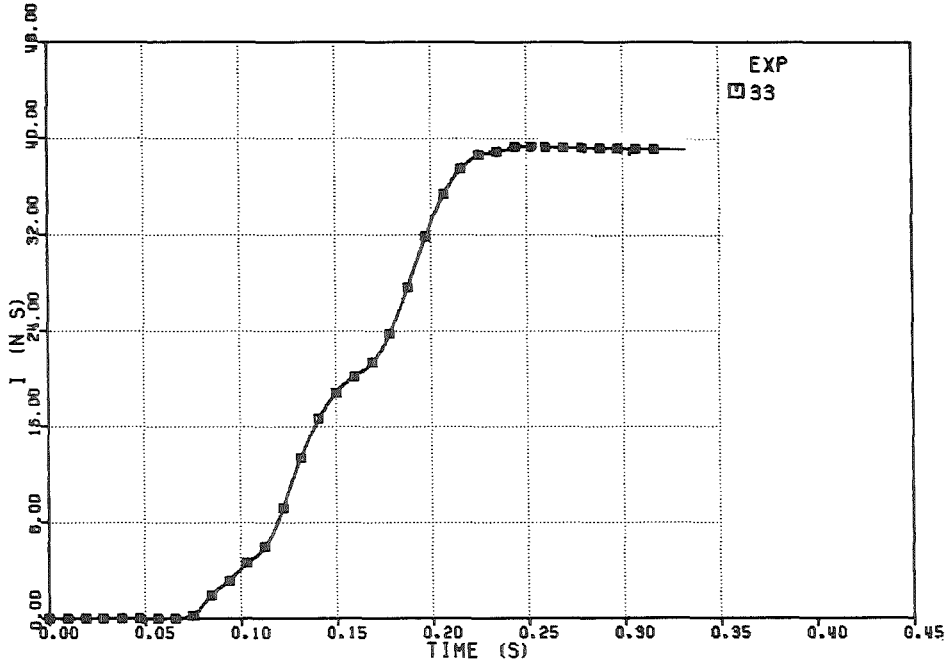

FIG. 6.423 IMPULSE ON THE UPPER PLATE

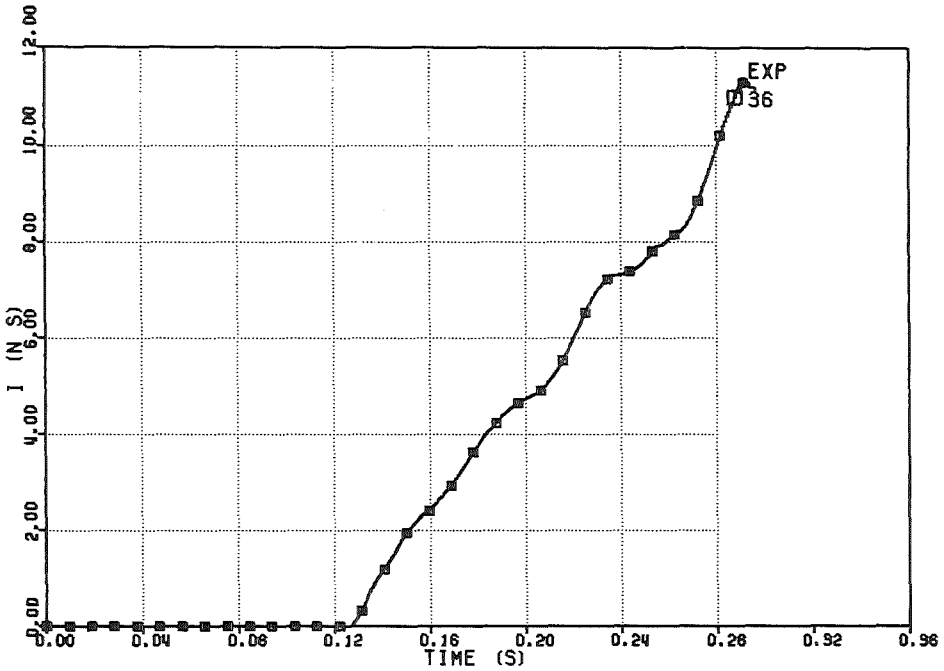

FIG. 6.426 IMPULSE ON THE UPPER PLATE

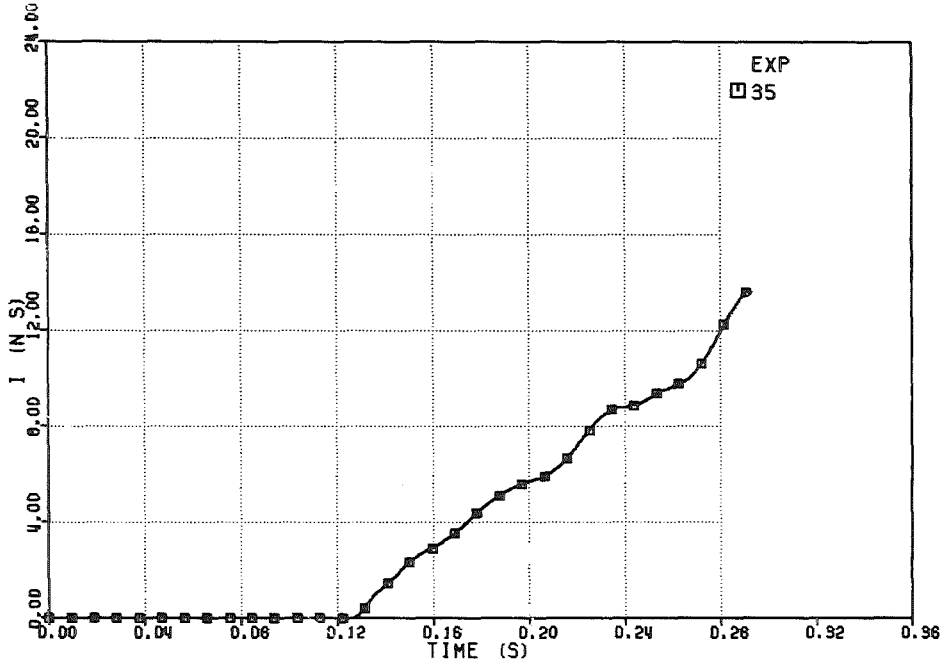

FIG. 6.425 IMPULSE ON THE UPPER PLATE

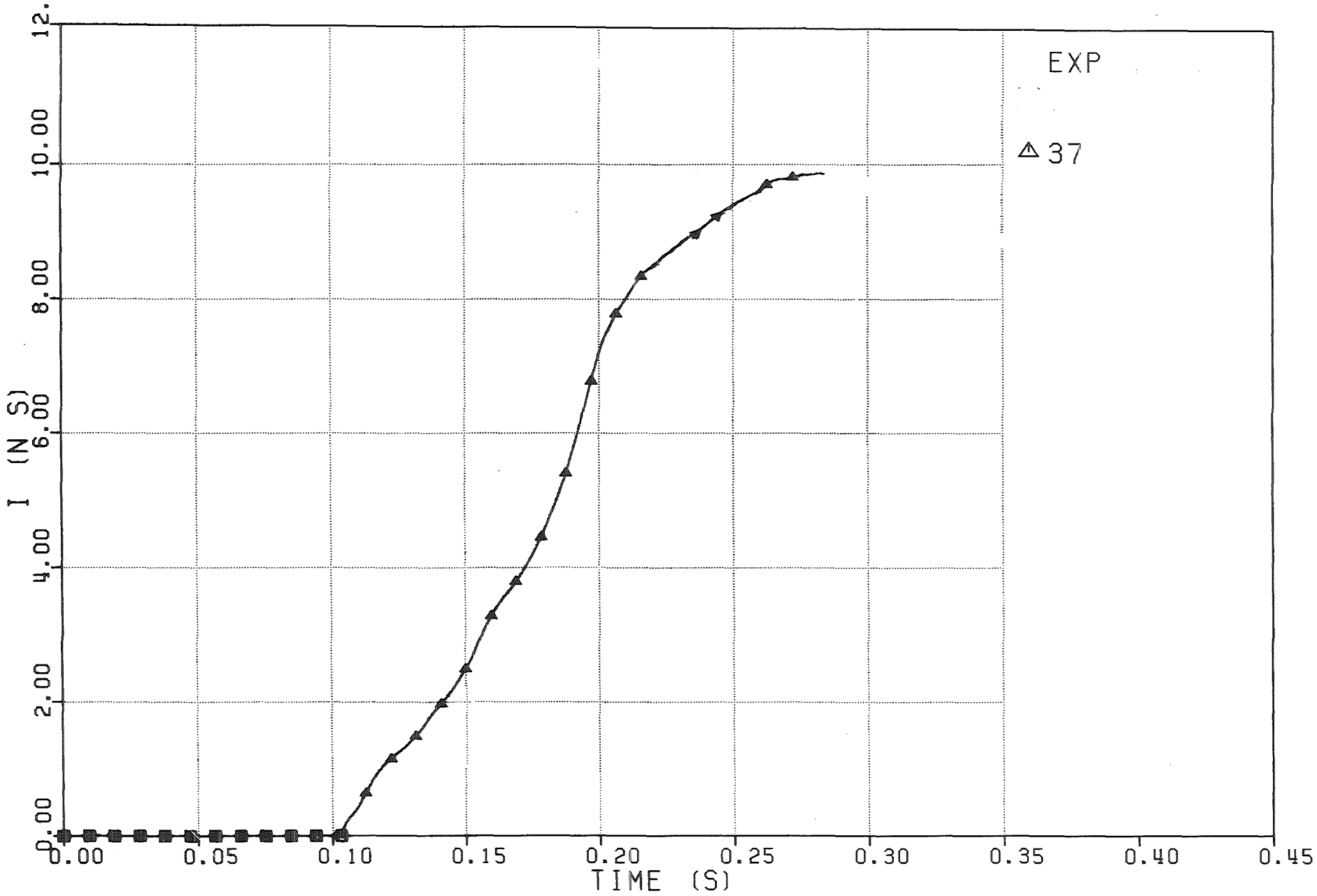

Fig. 6.427 - Impulse on the upper plate

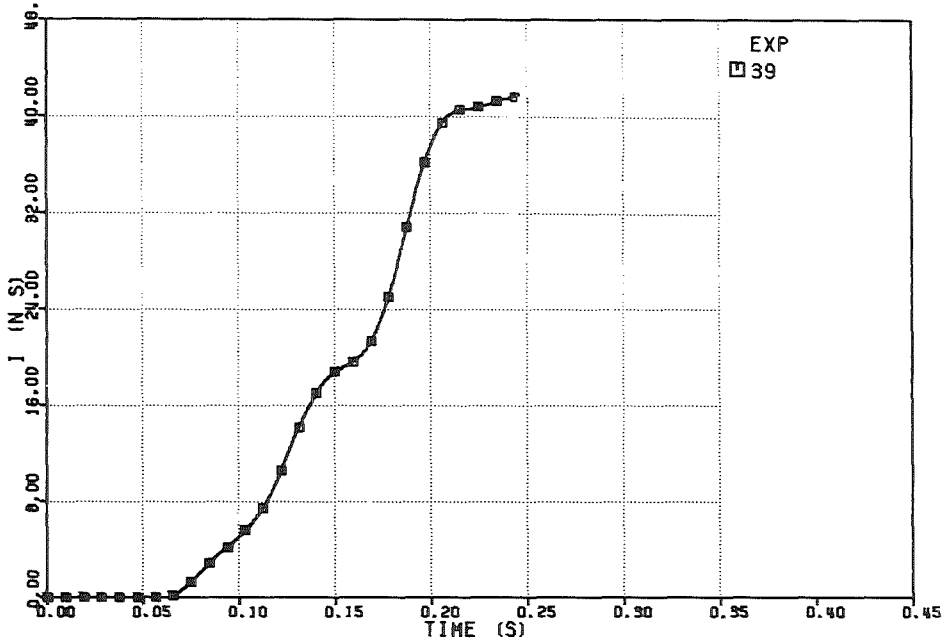

FIG. 6.429 IMPULSE ON THE UPPER PLATE

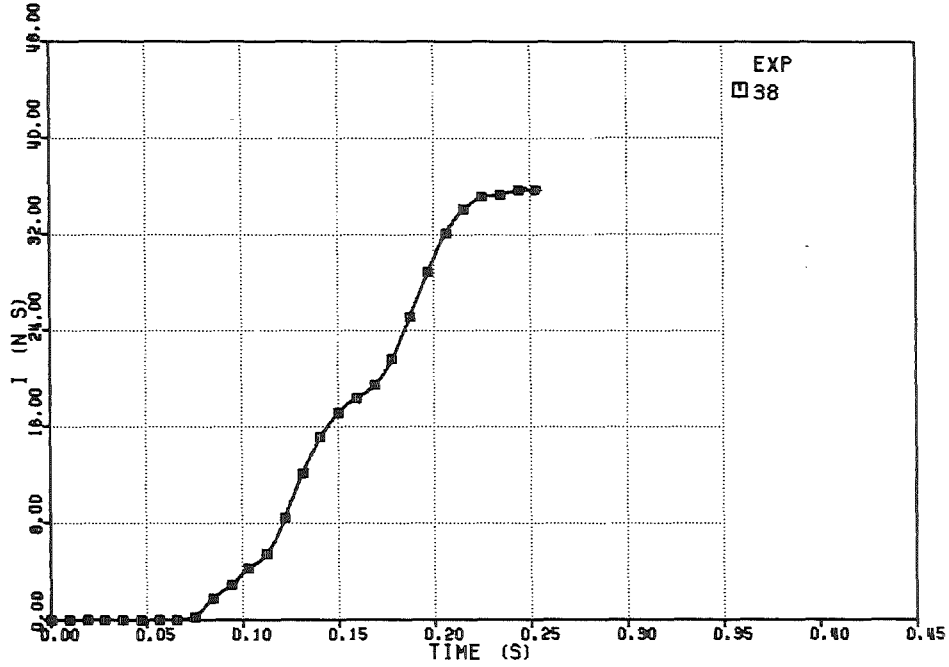

FIG. 6.428 IMPULSE ON THE UPPER PLATE

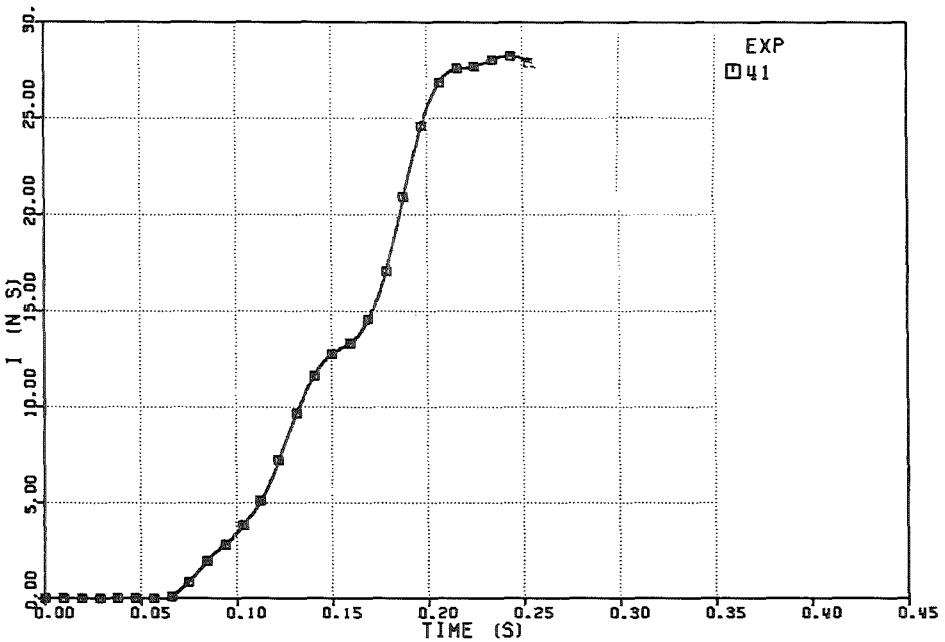

FIG. 6.431 IMPULSE ON THE UPPER PLATE

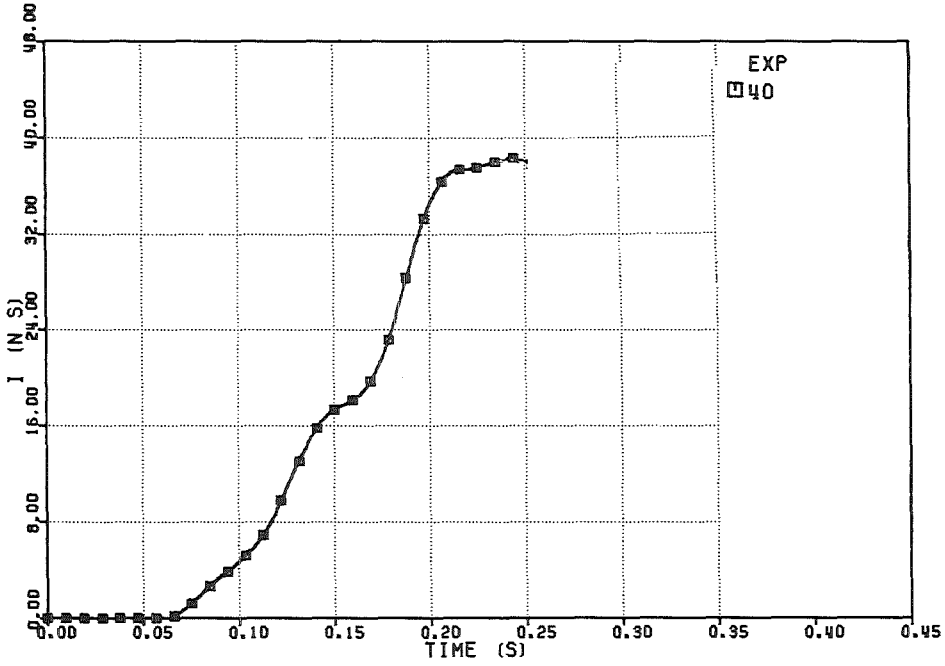

FIG. 6.430 IMPULSE ON THE UPPER PLATE

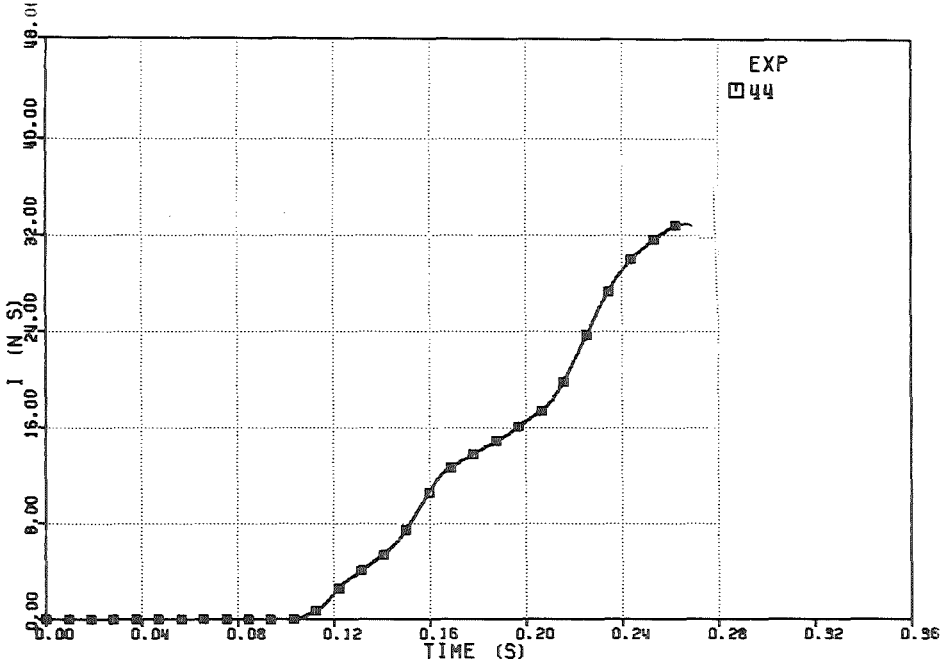

FIG. 6.433 -IMPULSE ON THE UPPER PLATE

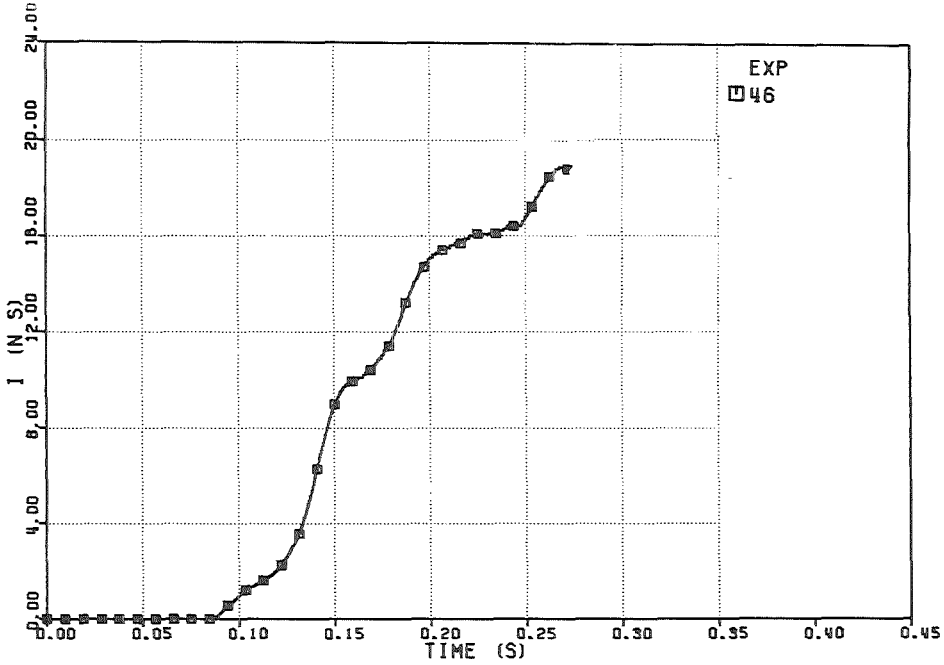

FIG. 6.435 -IMPULSE ON THE UPPER PLATE

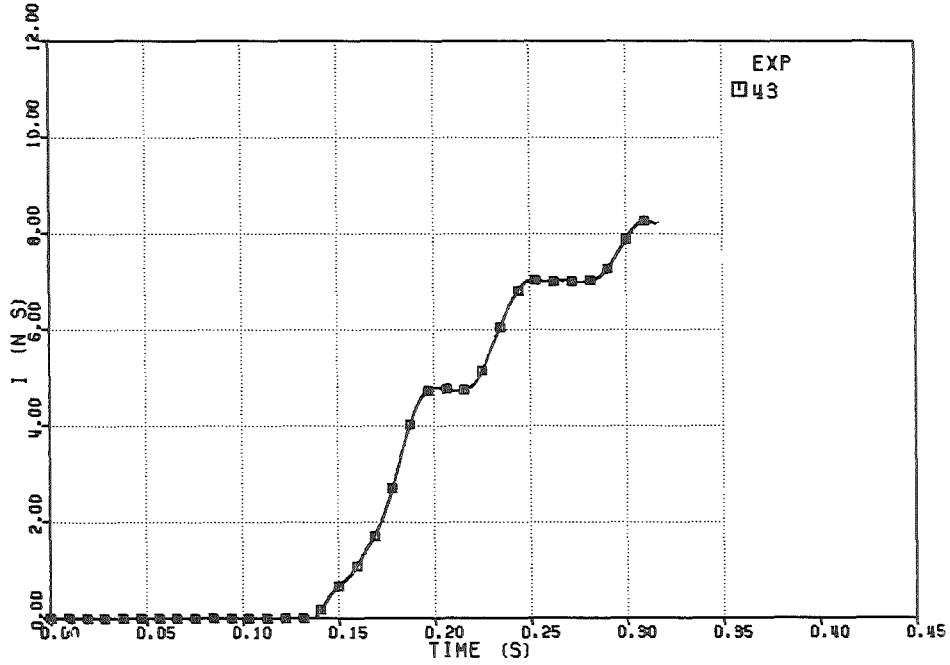

FIG. 6.432 -IMPULSE ON THE UPPER PLATE

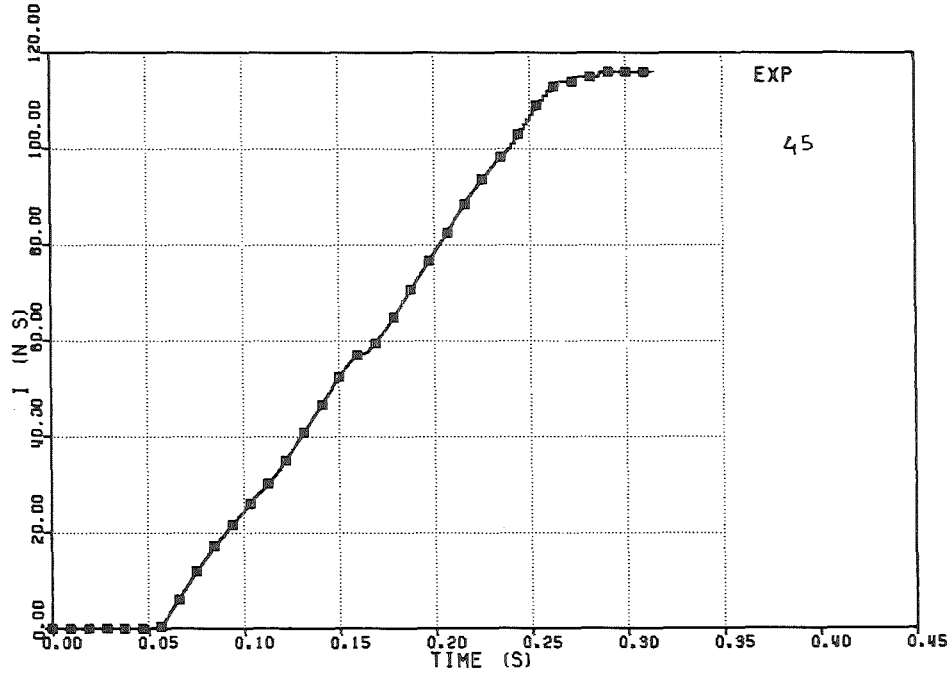

FIG. 6.434 -IMPULSE ON THE UPPER PLATE

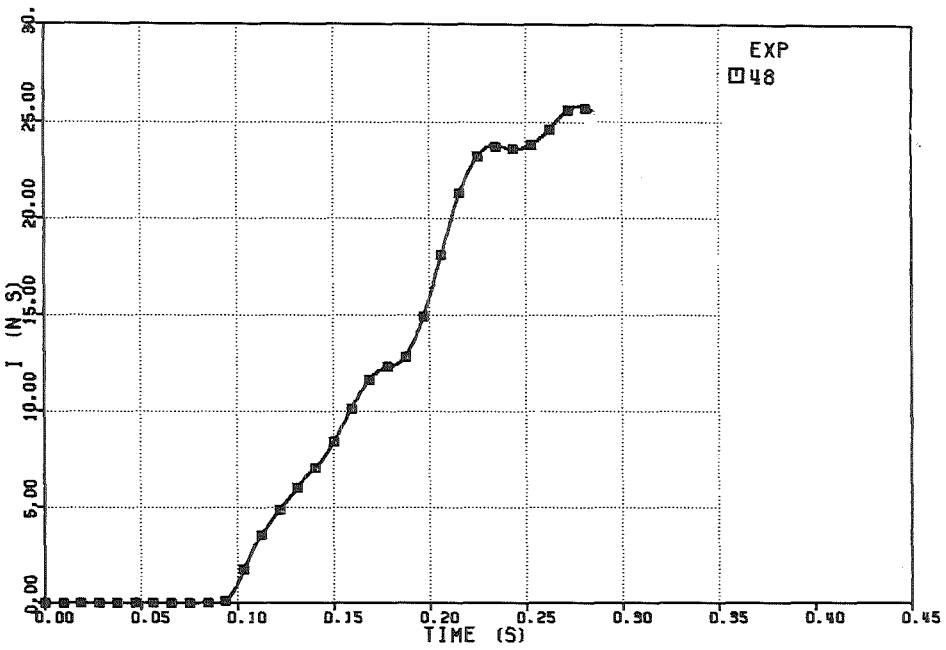

FIG. 6.437 IMPULSE ON THE UPPER PLATE

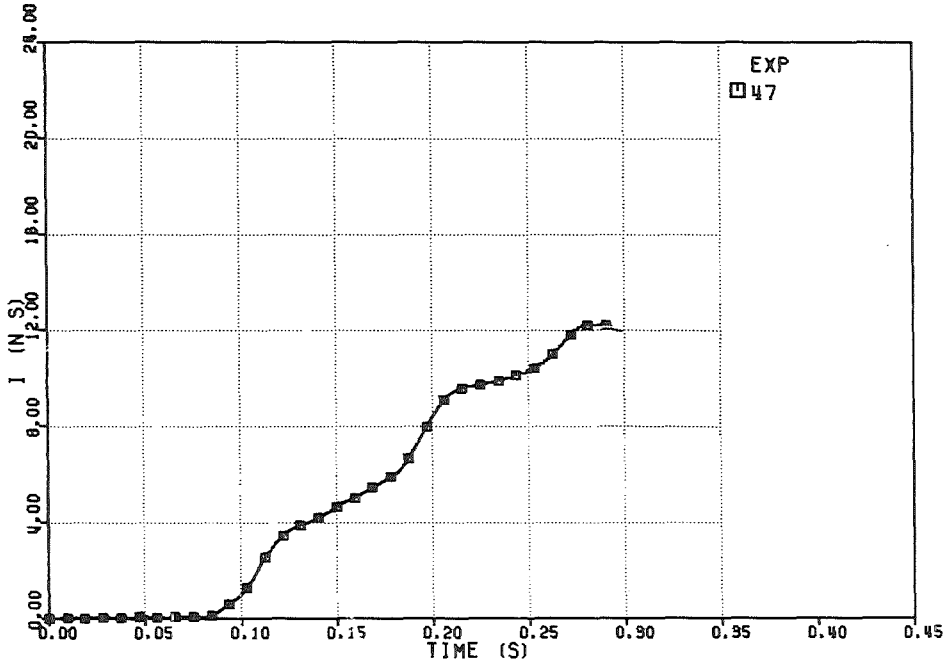

FIG. 6.436 IMPULSE ON THE UPPER PLATE

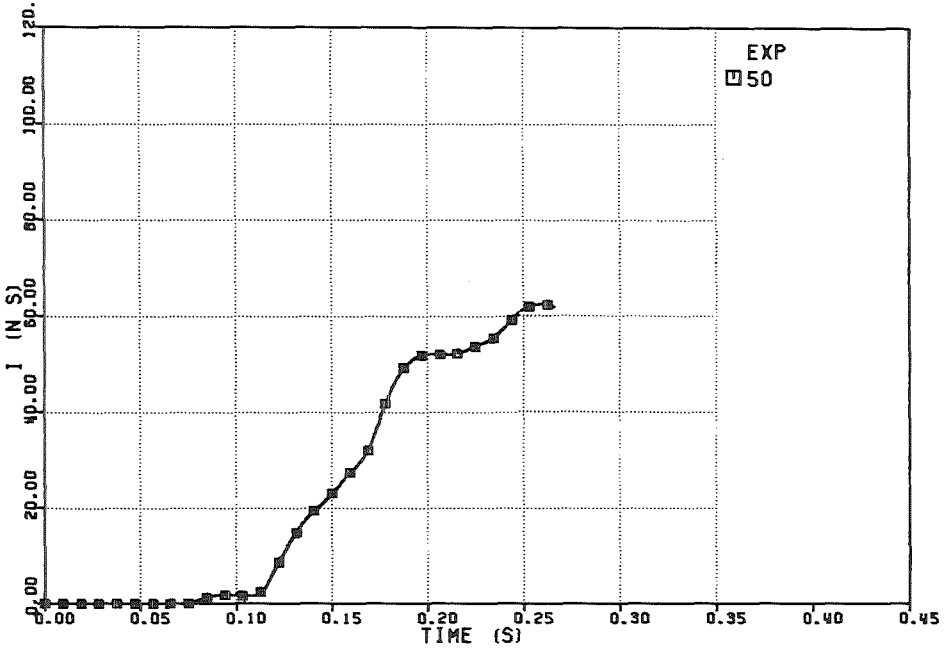

FIG. 6.439 IMPULSE ON THE UPPER PLATE

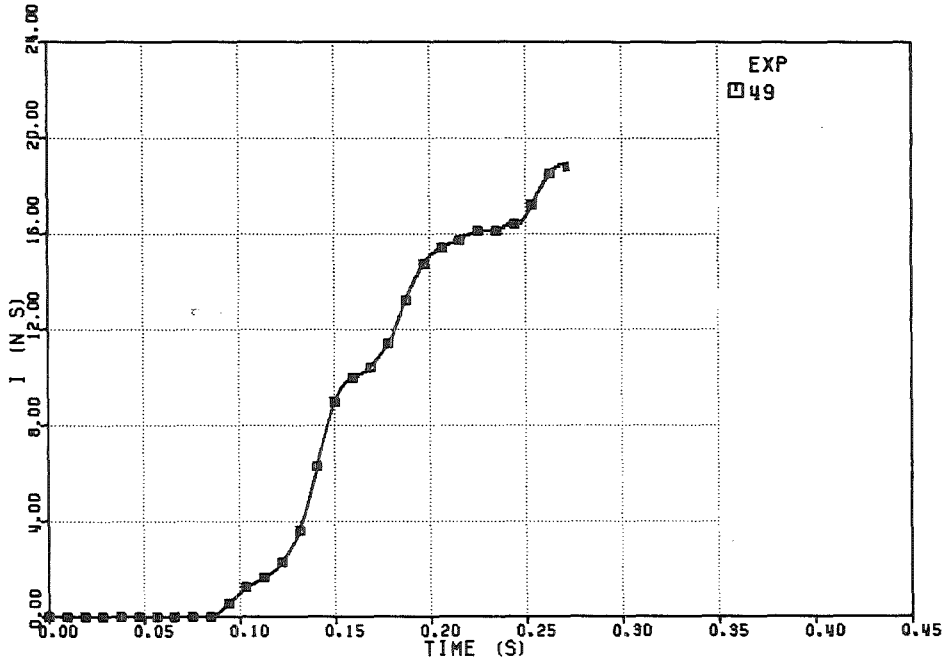

FIG. 6.438 IMPULSE ON THE UPPER PLATE

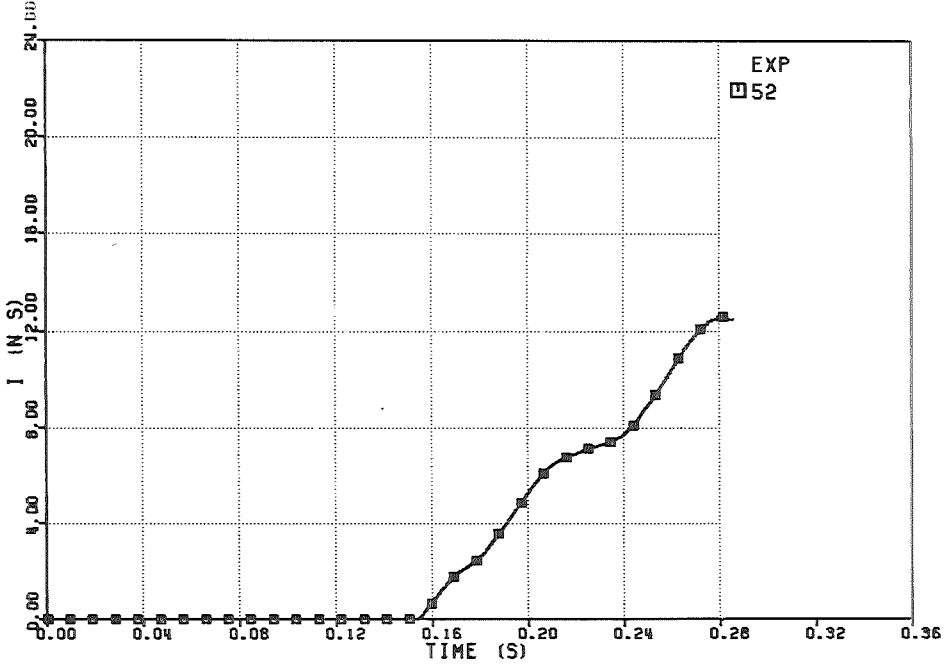

FIG. 6.441 IMPULSE ON THE UPPER PLATE

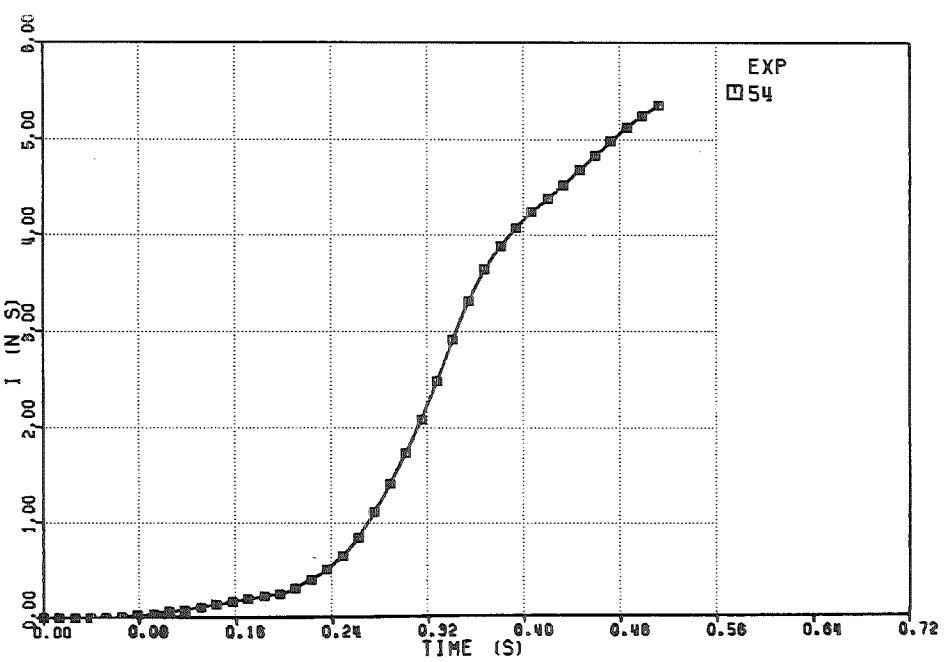

FIG. 6.443 IMPULSE ON THE UPPER PLATE

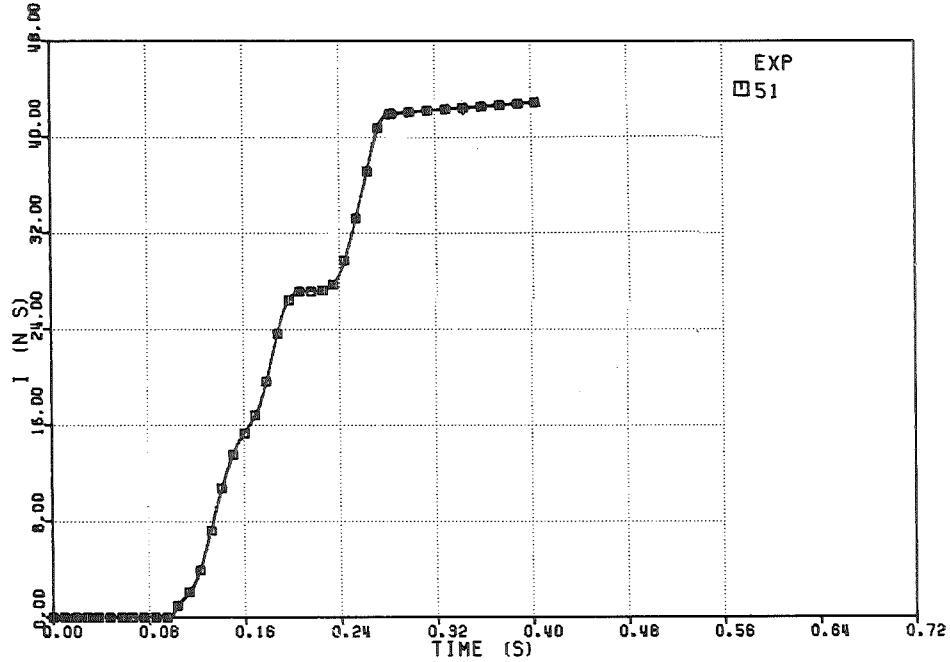

FIG. 6.440 IMPULSE ON THE UPPER PLATE

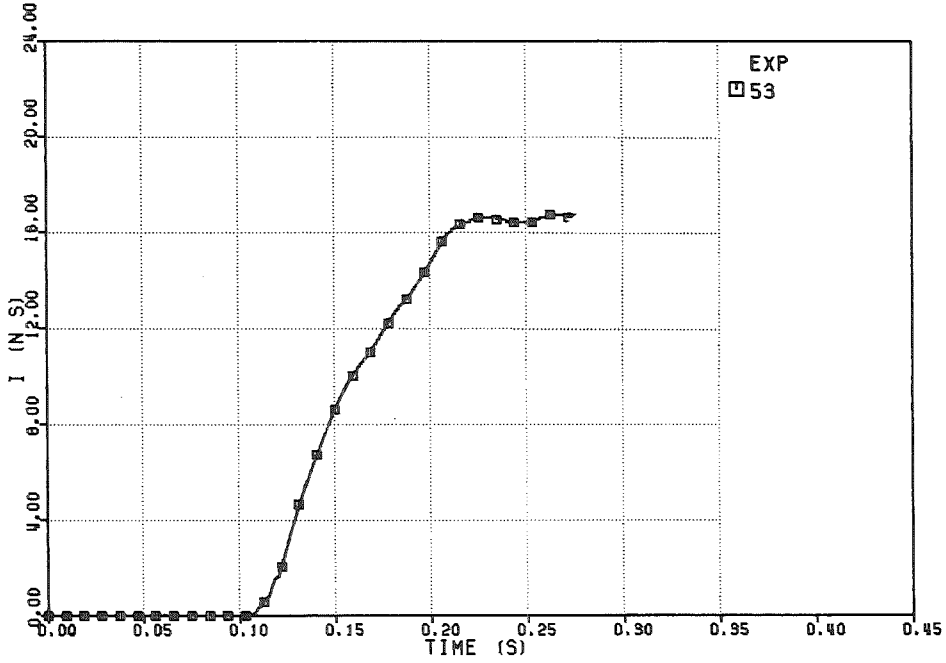

FIG. 6.442 IMPULSE ON THE UPPER PLATE

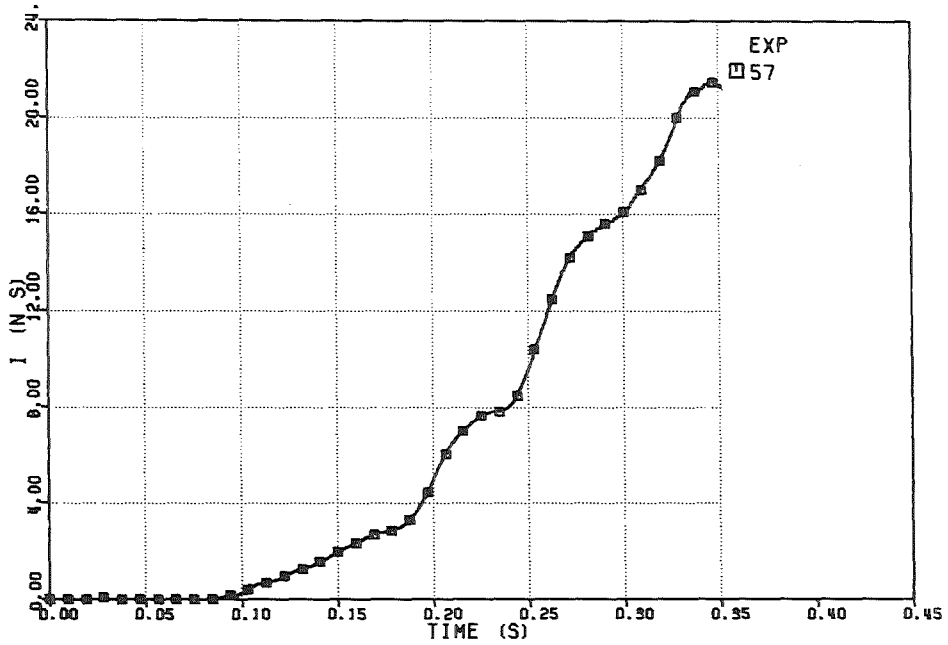

FIG. 6.445-IMPULSE ON THE UPPER PLATE

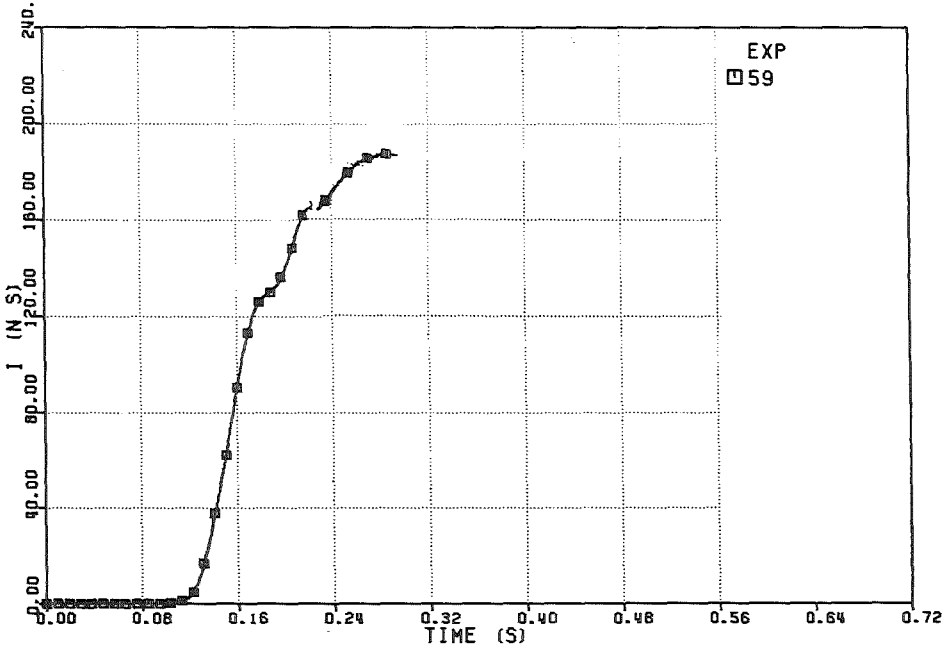

FIG. 6.447-IMPULSE ON THE UPPER PLATE

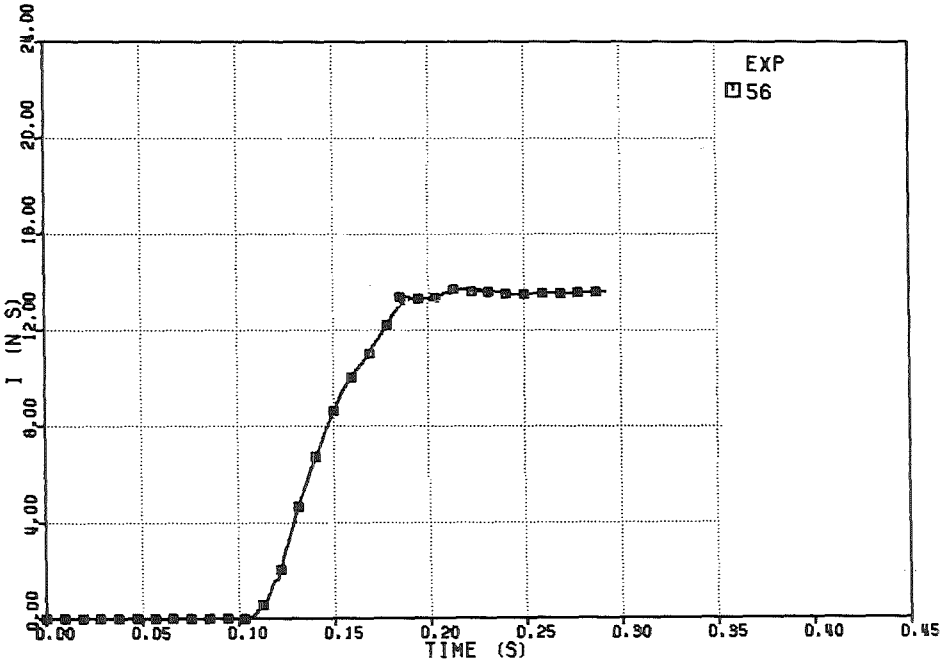

FIG. 6.446-IMPULSE ON THE UPPER PLATE

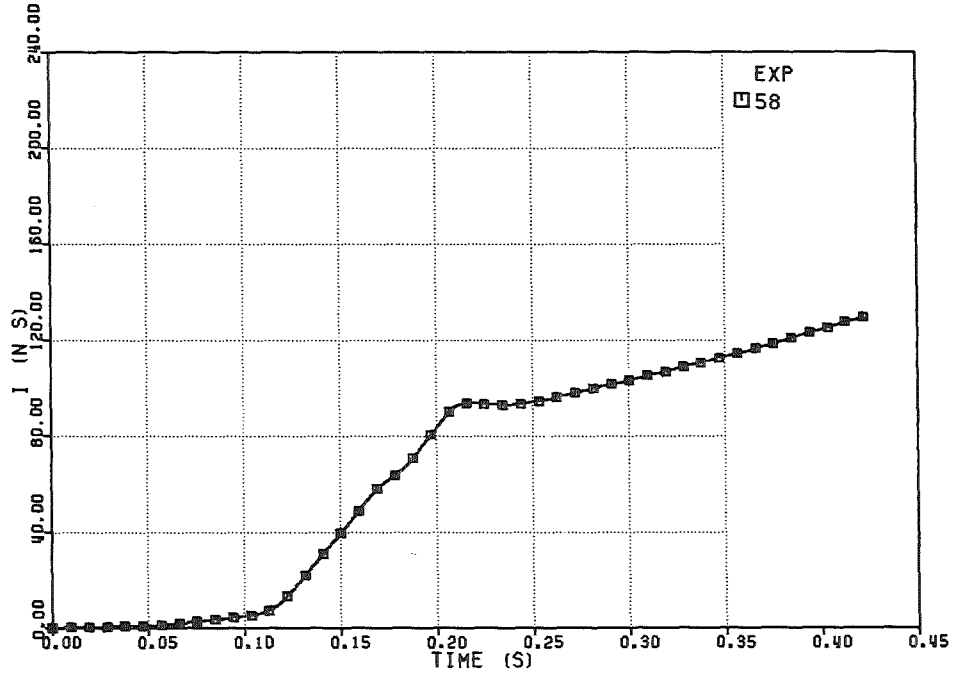

FIG. 6.446-IMPULSE ON THE UPPER PLATE

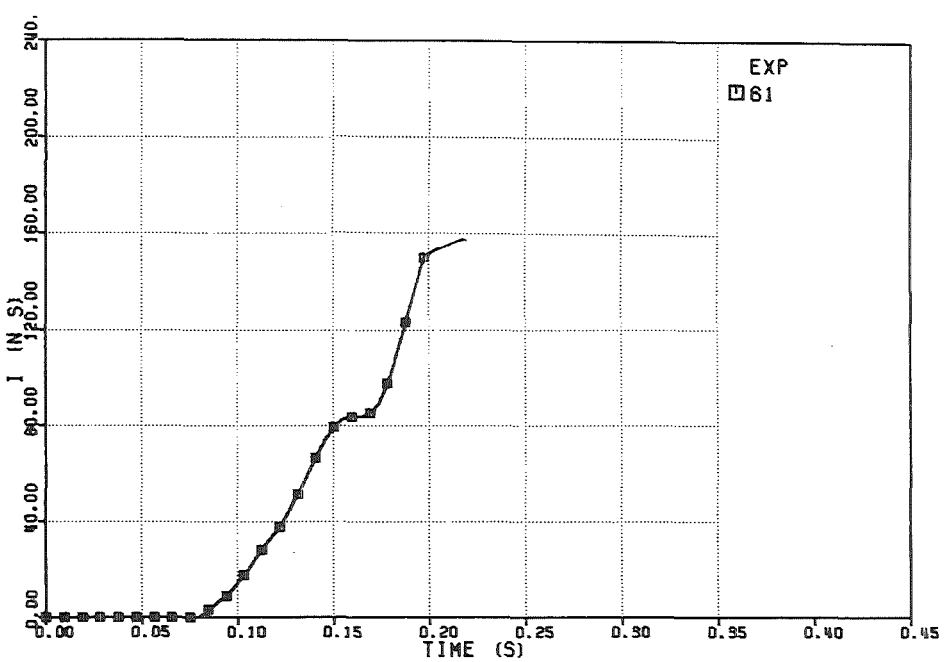

FIG. 6.449 -IMPULSE ON THE UPPER PLATE

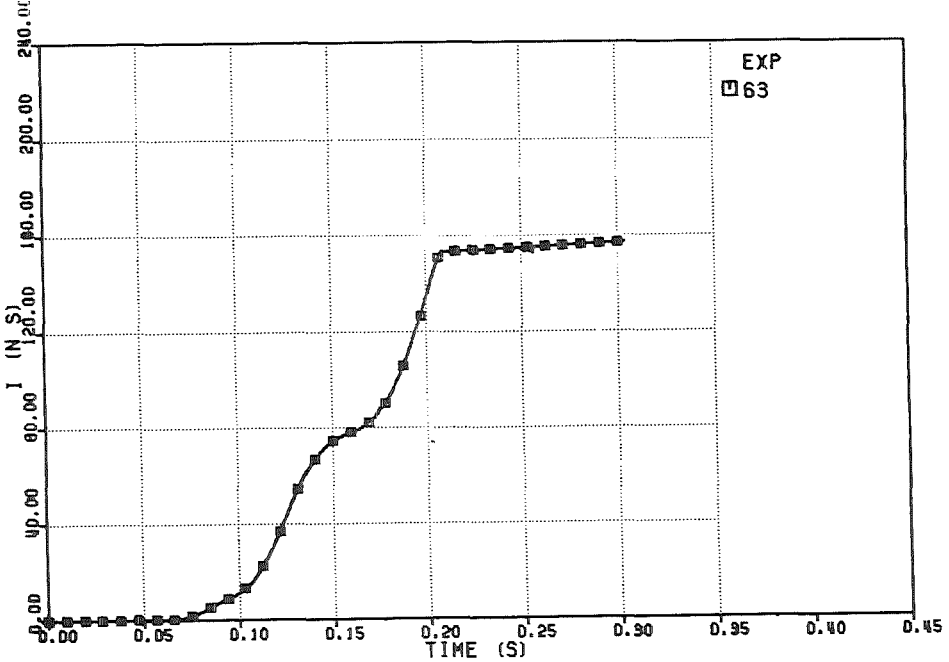

FIG. 6.451 -IMPULSE ON THE UPPER PLATE

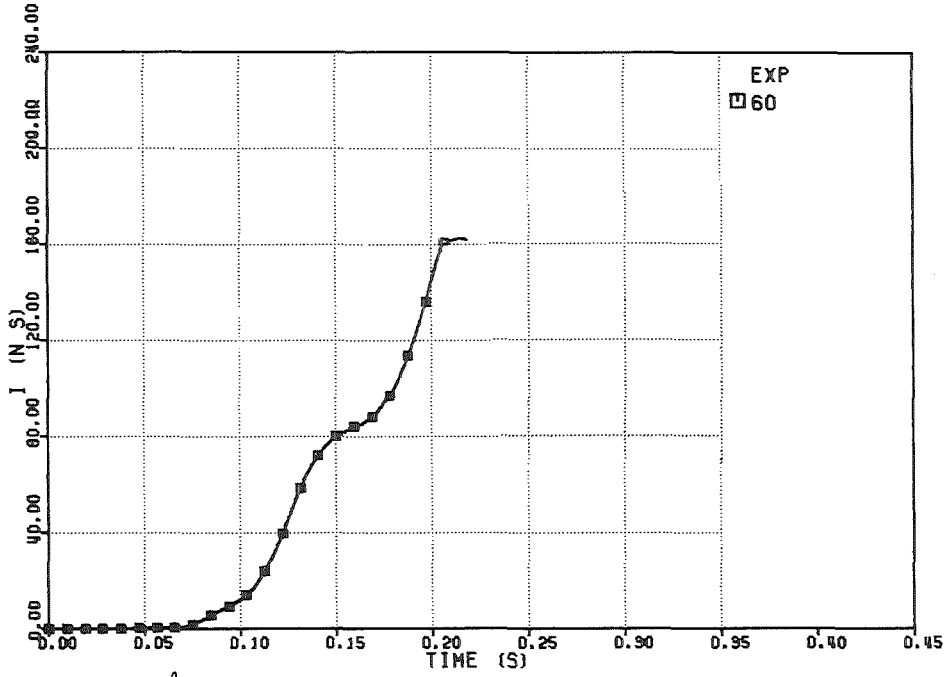

FIG. 6.448 -IMPULSE ON THE UPPER PLATE

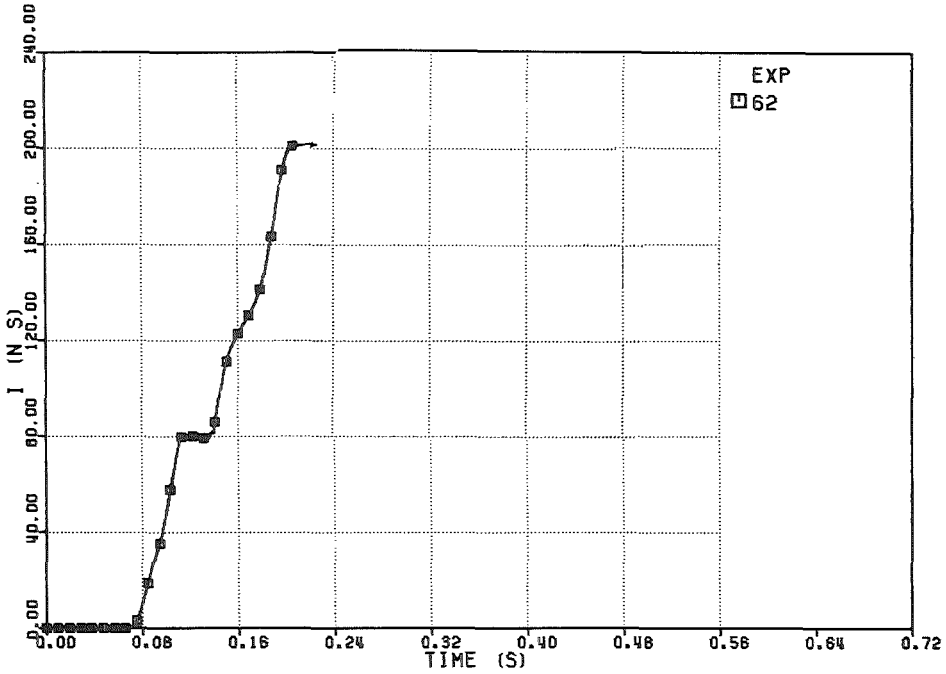

FIG. 6.450 -IMPULSE ON THE UPPER PLATE

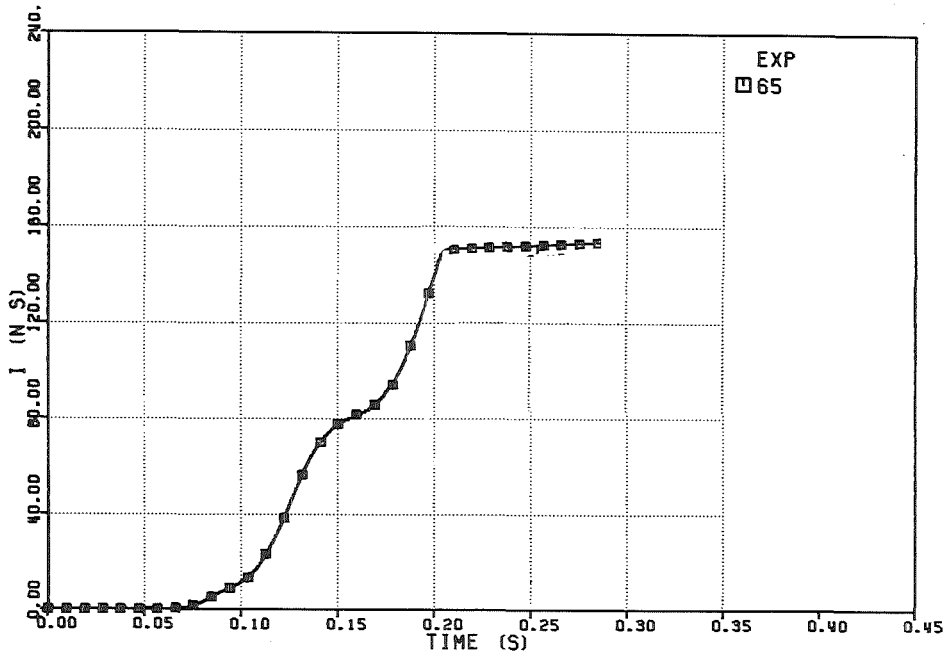

FIG. 6.453 IMPULSE ON THE UPPER PLATE

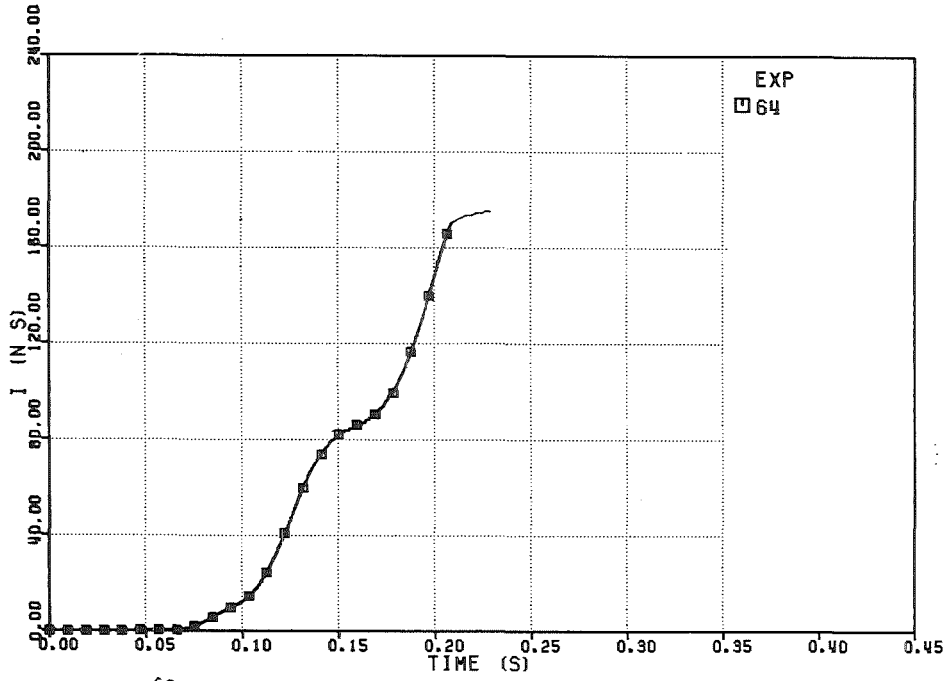

FIG. 6452 IMPULSE ON THE UPPER PLATE

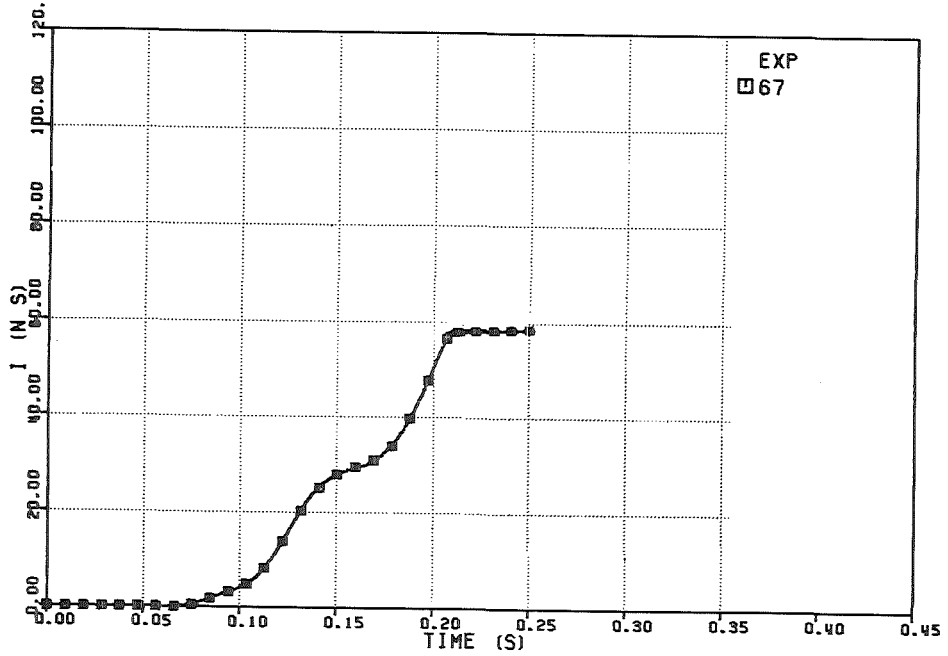

FIG. 6.455 IMPULSE ON THE UPPER PLATE

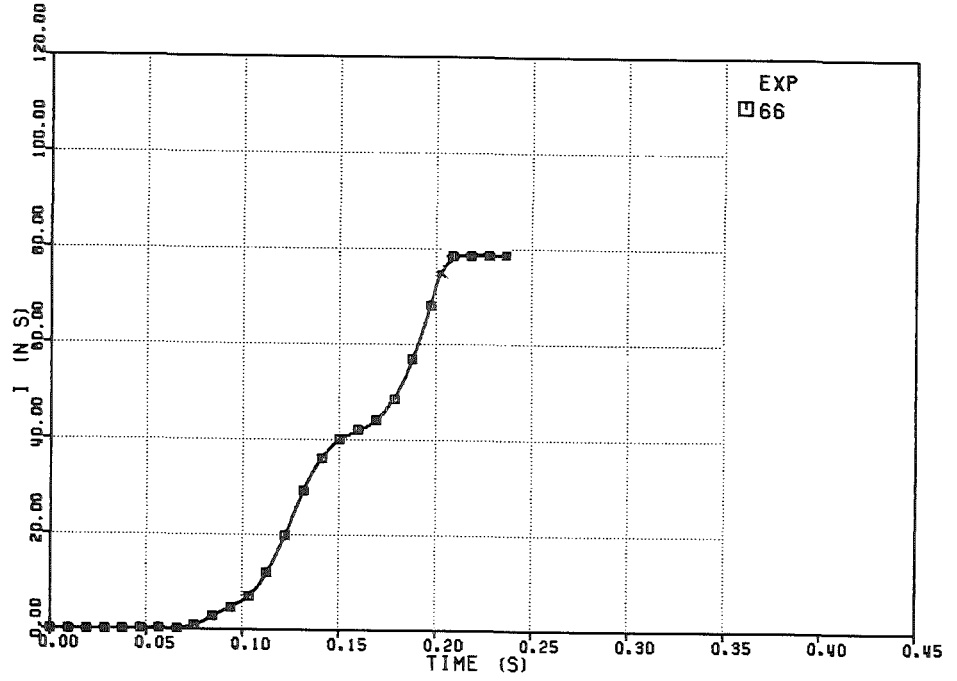

FIG. 6454 IMPULSE ON THE UPPER PLATE

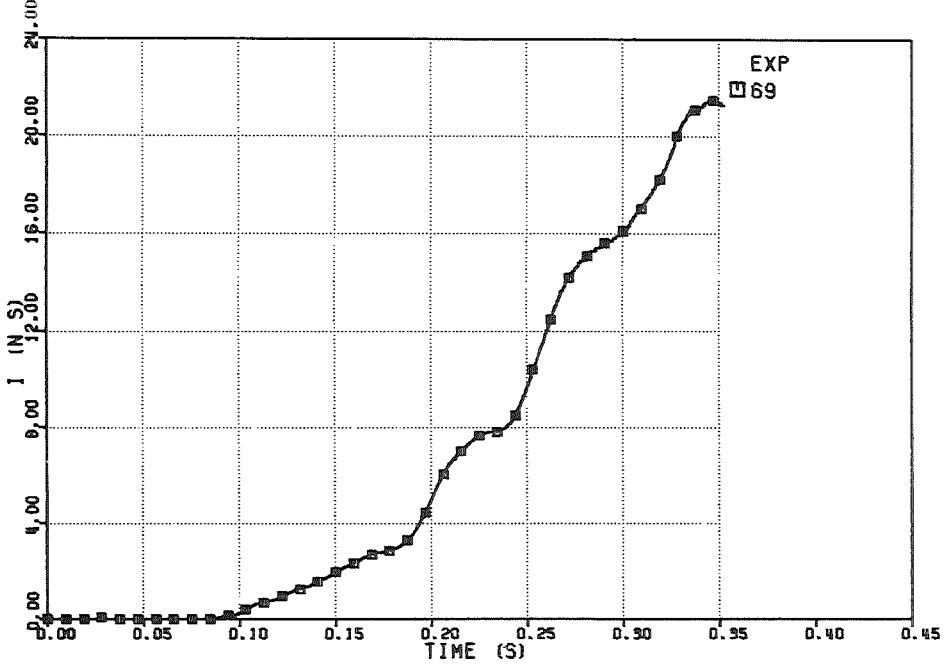

FIG. 6.457 IMPULSE ON THE UPPER PLATE

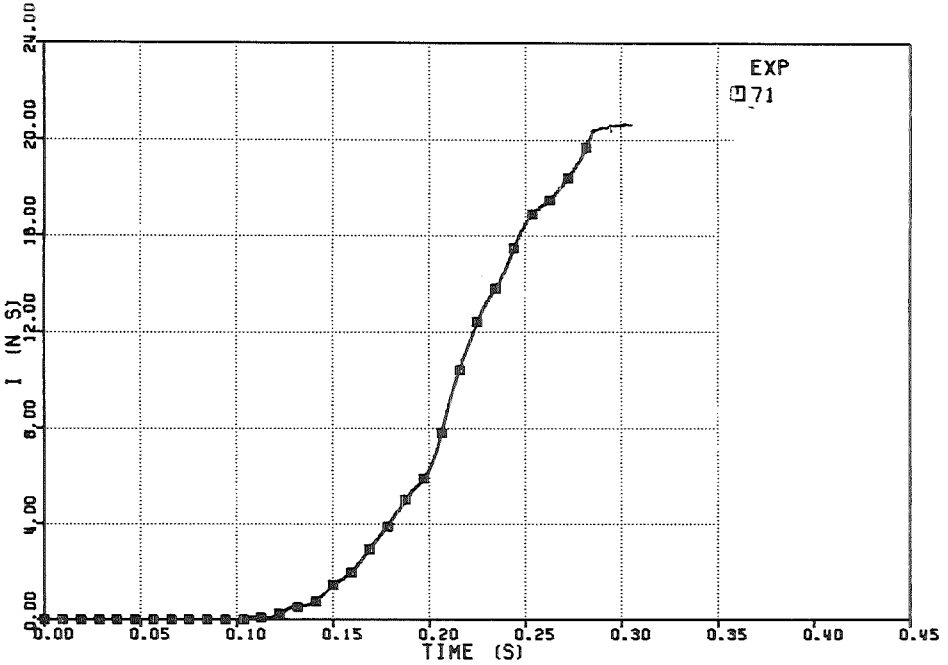

FIG. 6.458 IMPULSE ON THE UPPER PLATE

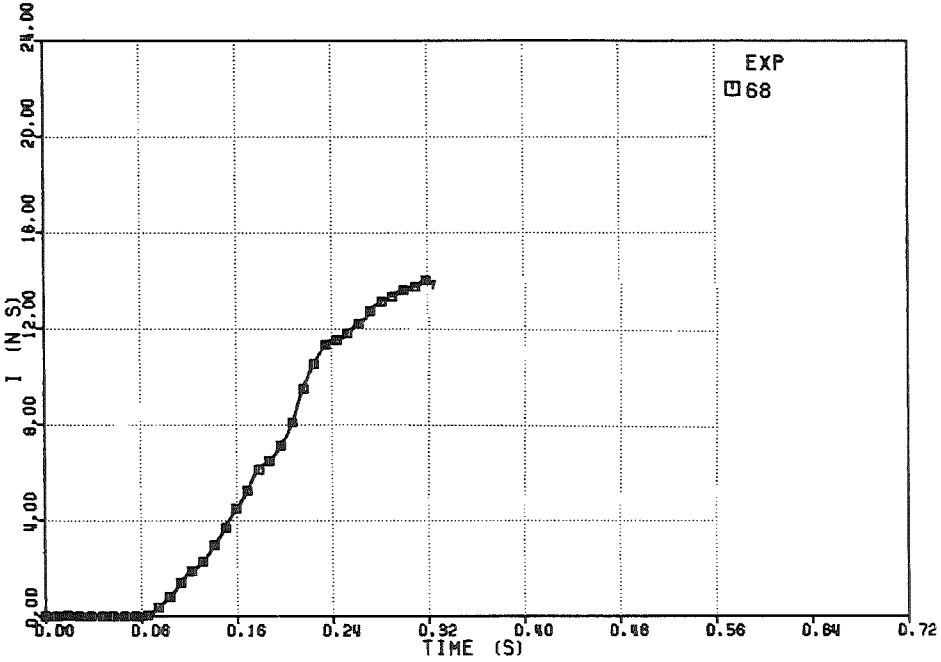

FIG. 6.456 IMPULSE ON THE UPPER PLATE

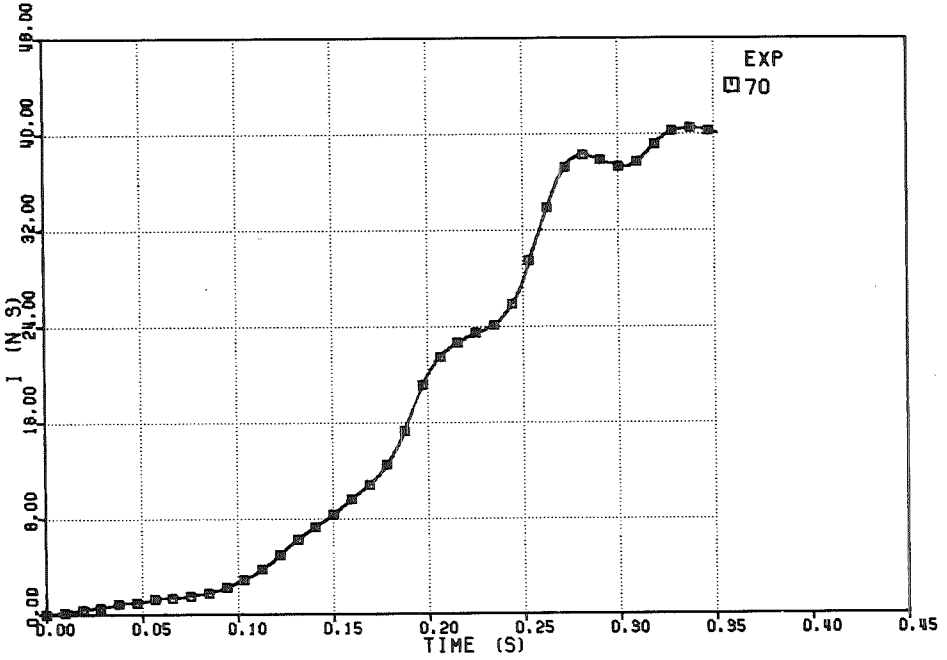

FIG. 6.457b IMPULSE ON THE UPPER PLATE

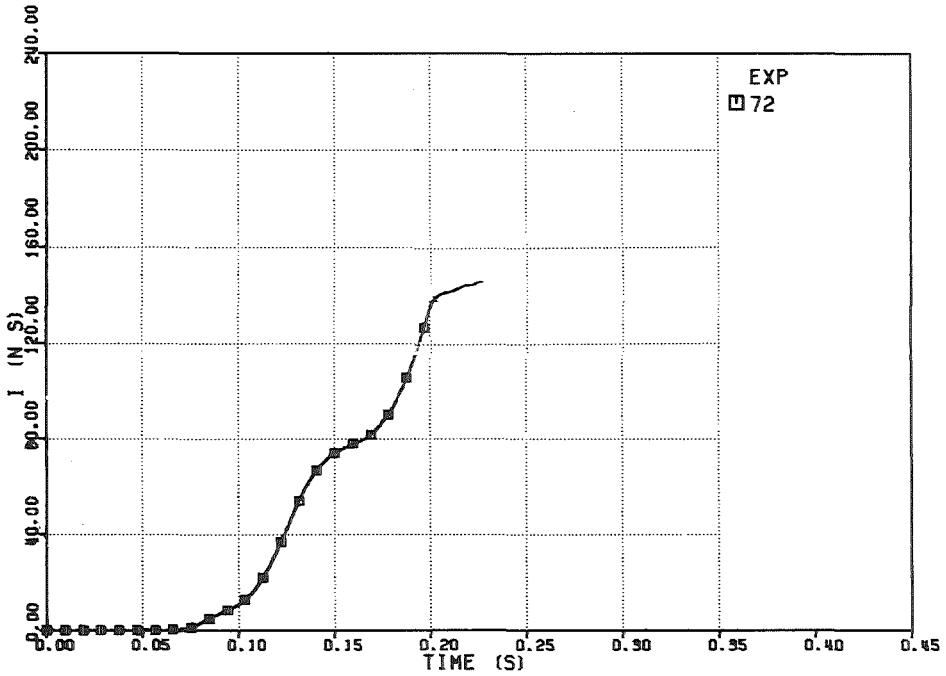

FIG. 6.460 IMPULSE ON THE UPPER PLATE

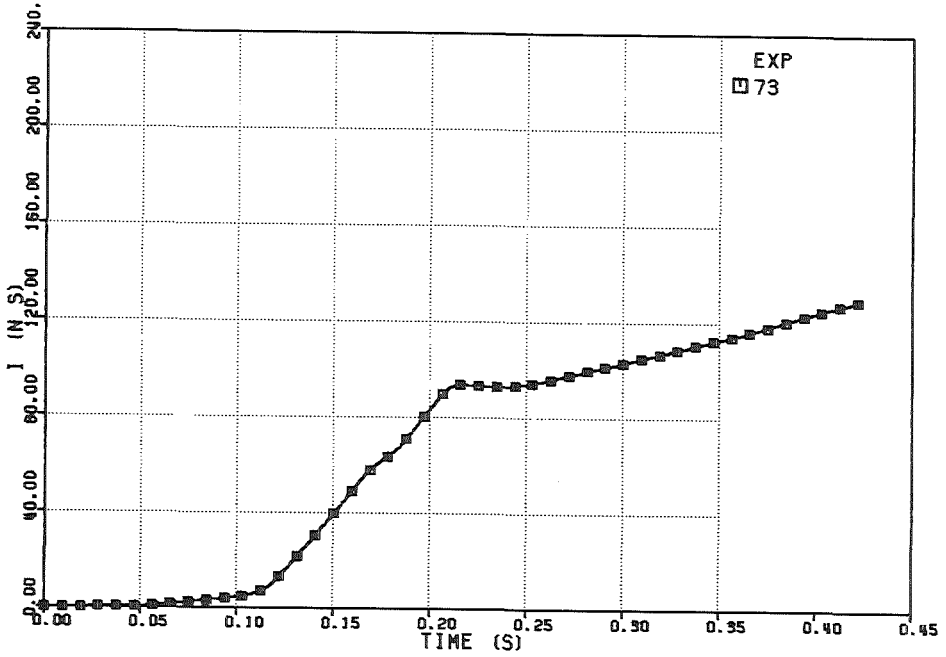

FIG. 6.459 IMPULSE ON THE UPPER PLATE

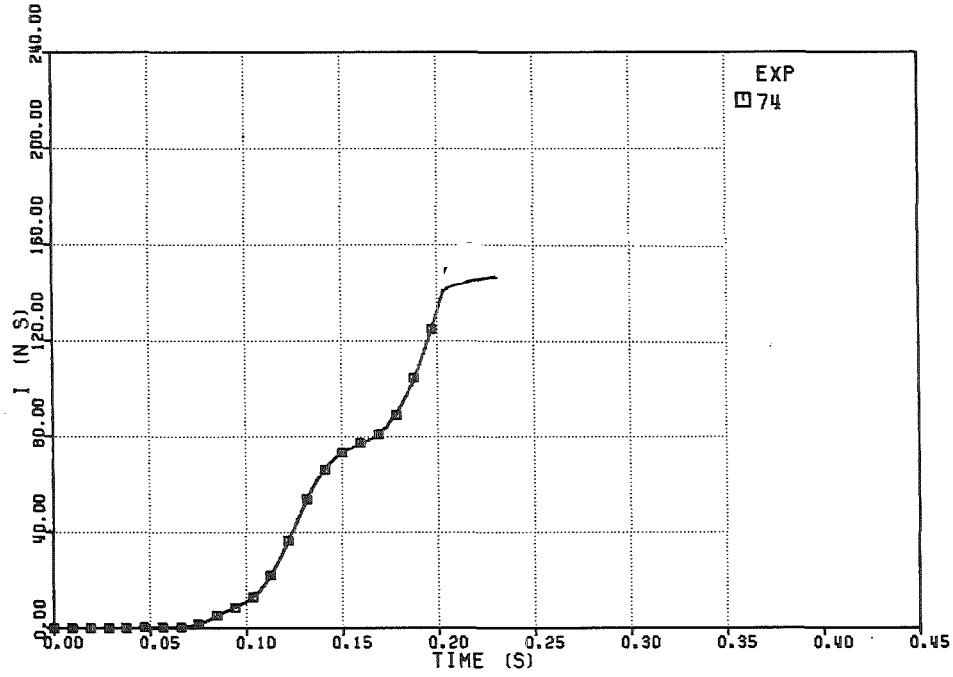

FIG. 6.461 IMPULSE ON THE UPPER PLATE

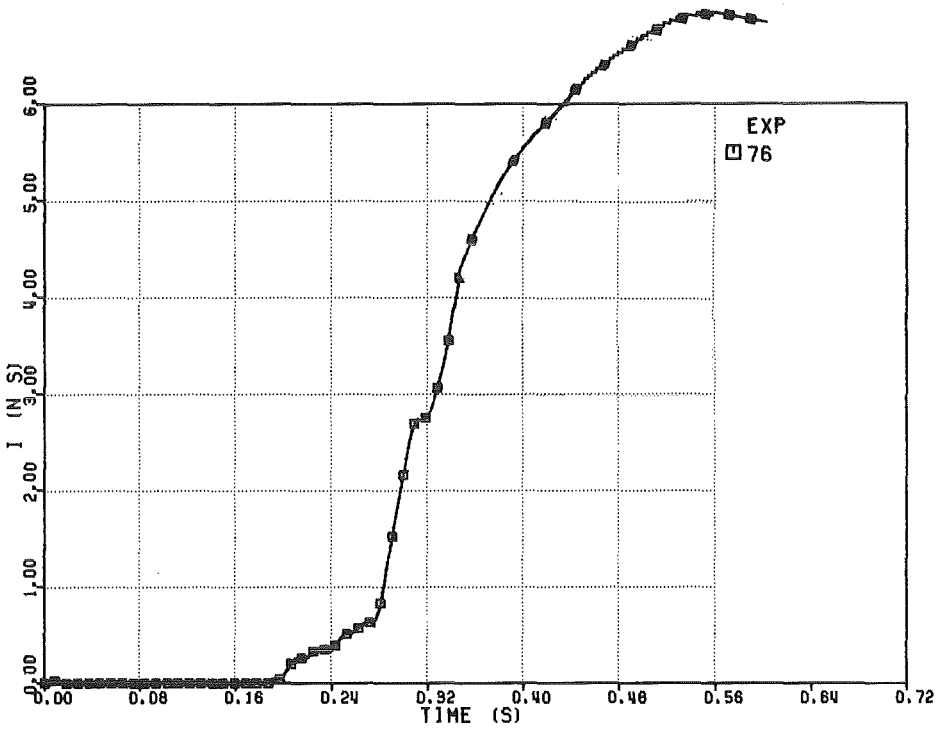

FIG. 6.463 IMPULSE ON THE UPPER PLATE

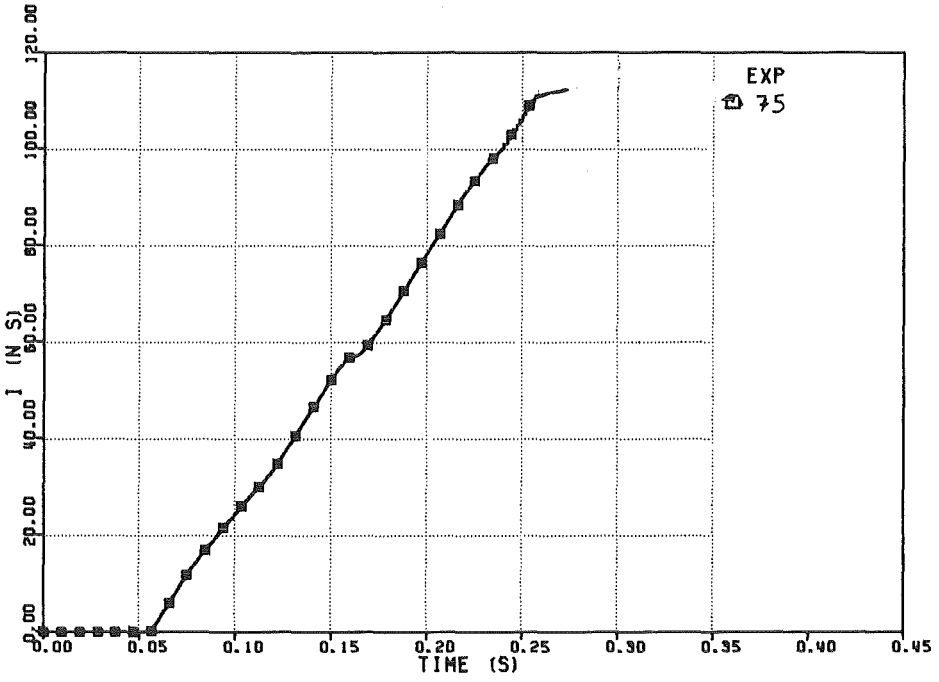

FIG. 6.462 IMPULSE ON THE UPPER PLATE

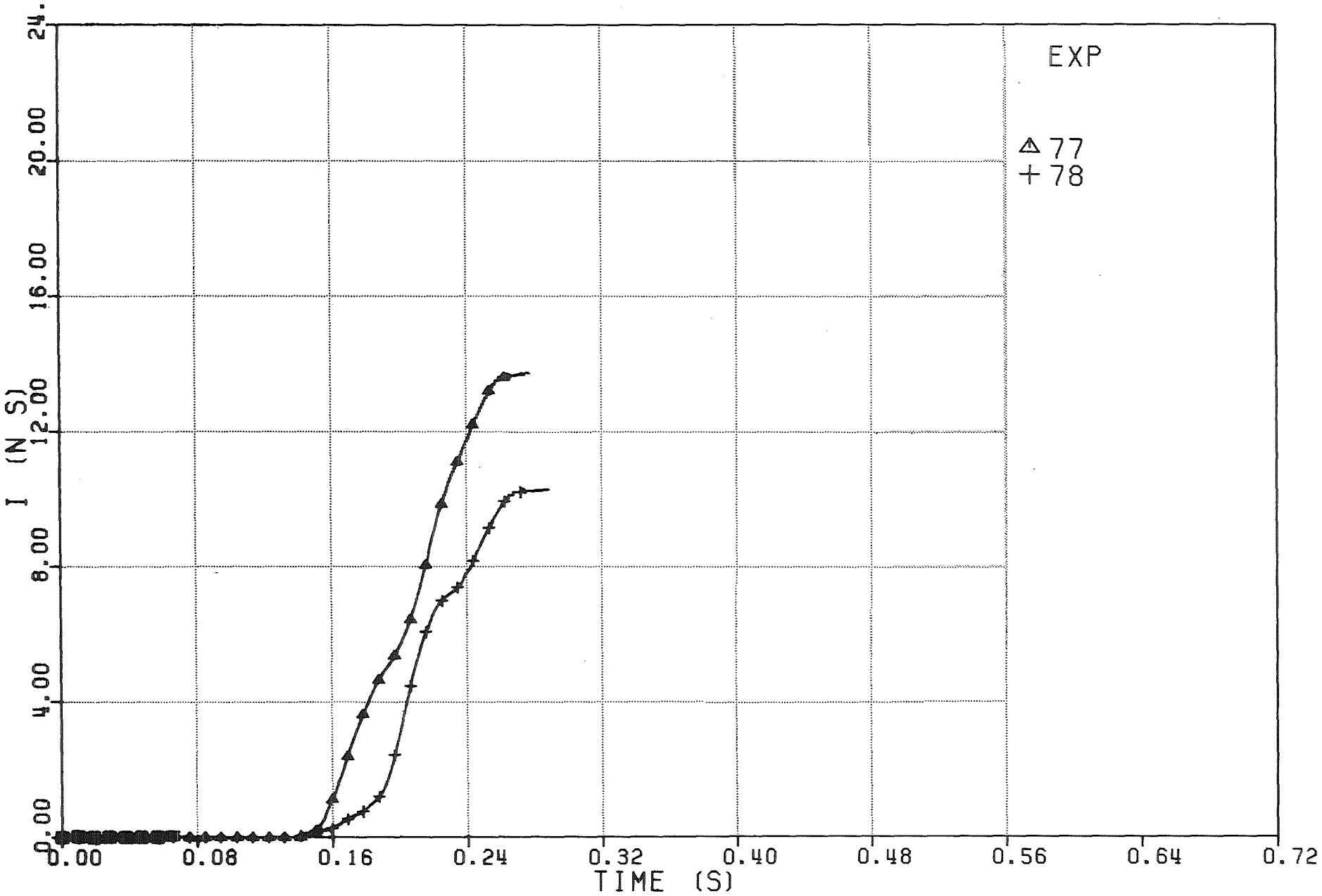

Fig. 6.464 - Impulse on the upper plate

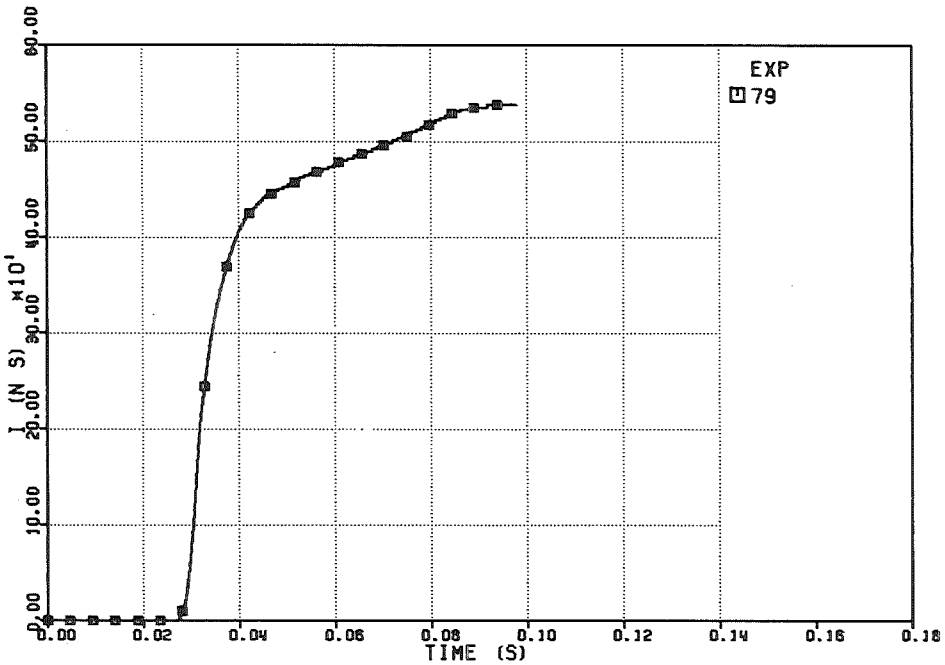

FIG. 6.465 IMPULSE ON THE UPPER PLATE

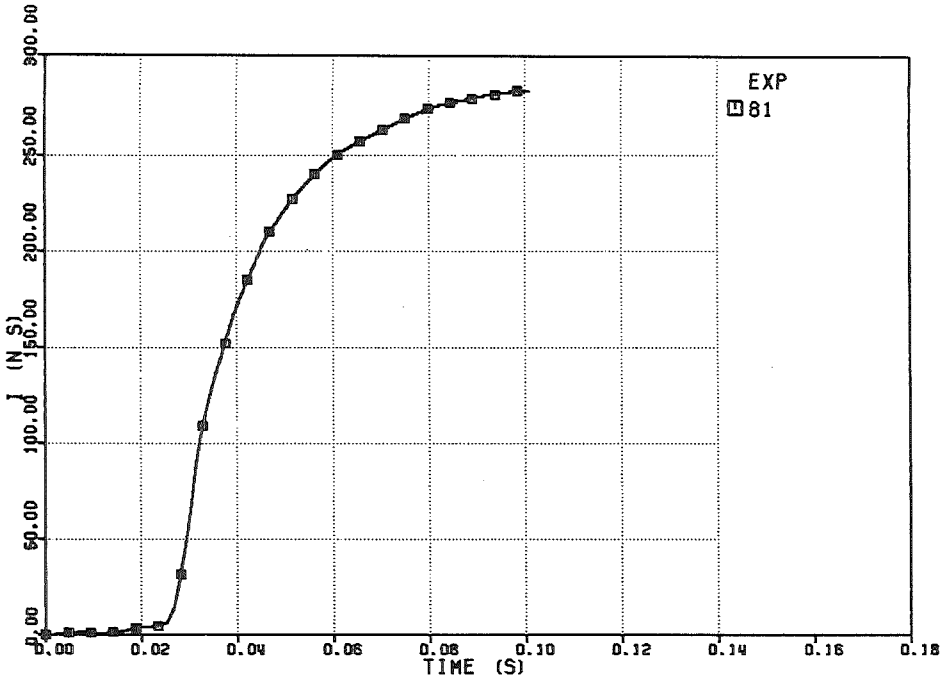

FIG. 6.467 IMPULSE ON THE UPPER PLATE

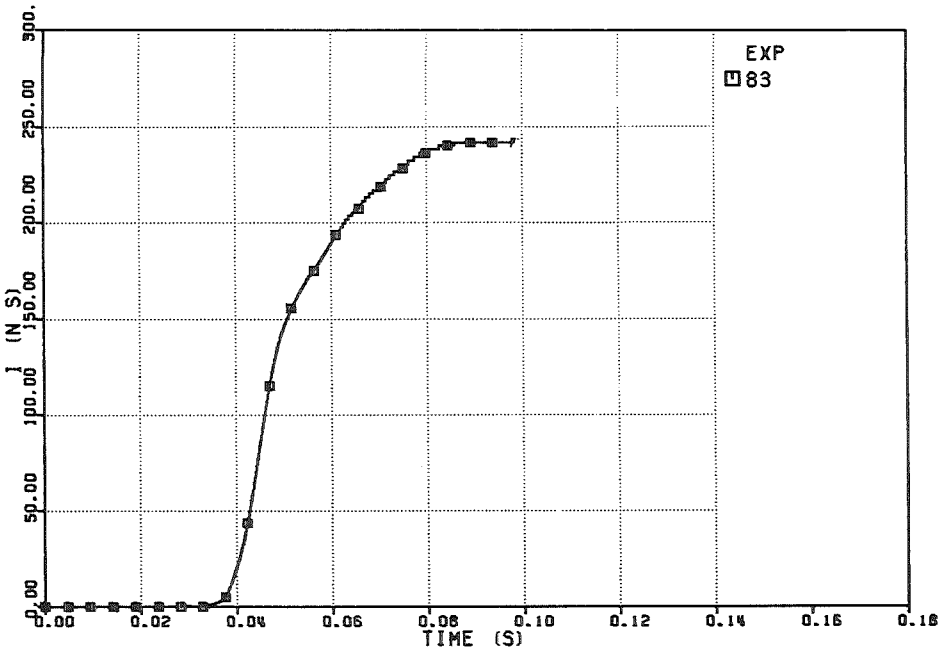

FIG. 6.469 IMPULSE ON THE UPPER PLATE

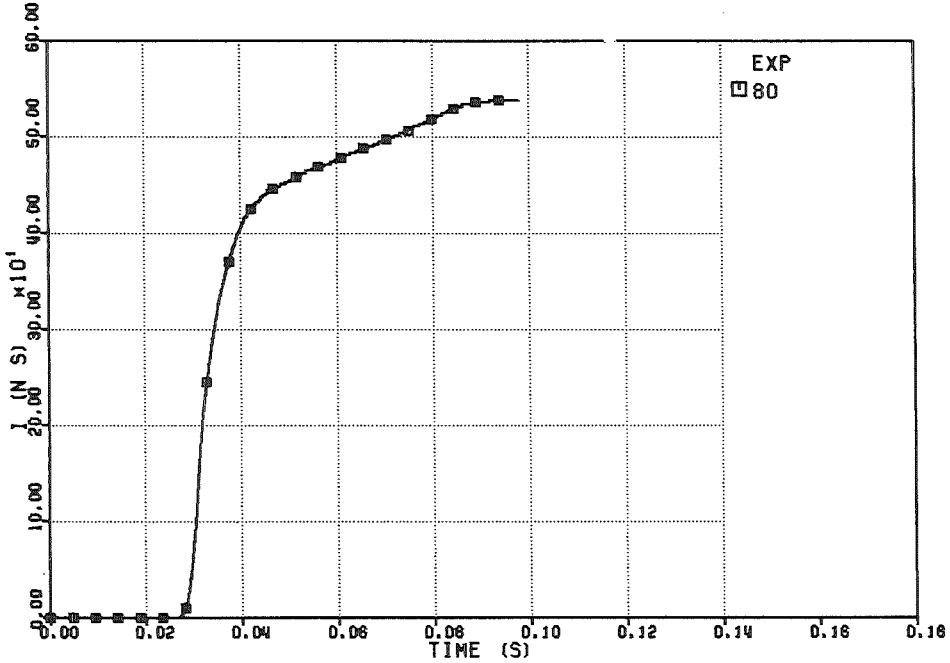

FIG. 6.466 IMPULSE ON THE UPPER PLATE

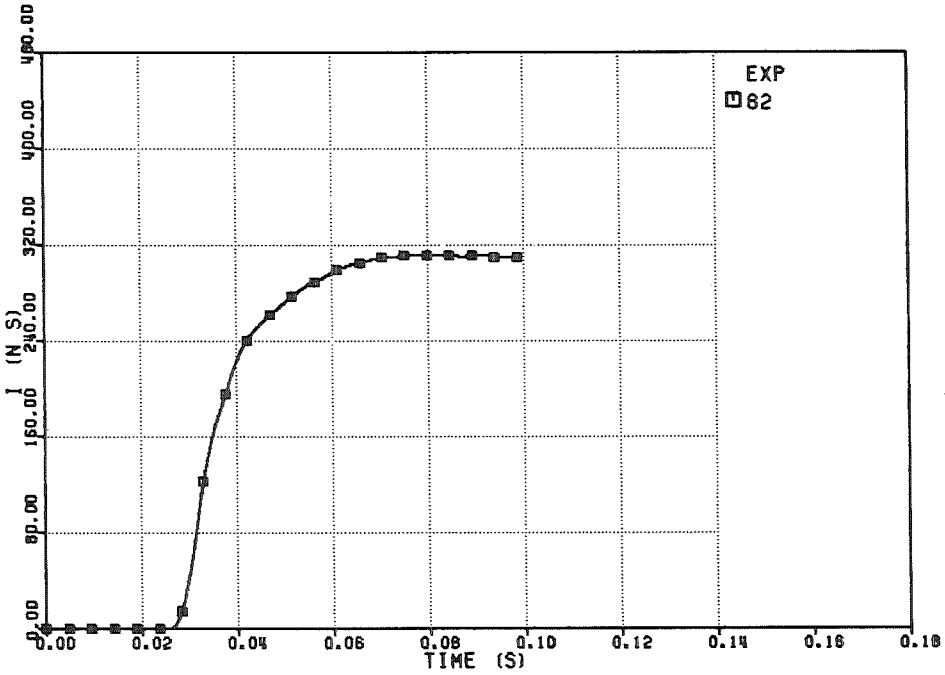

FIG. 6.468 IMPULSE ON THE UPPER PLATE

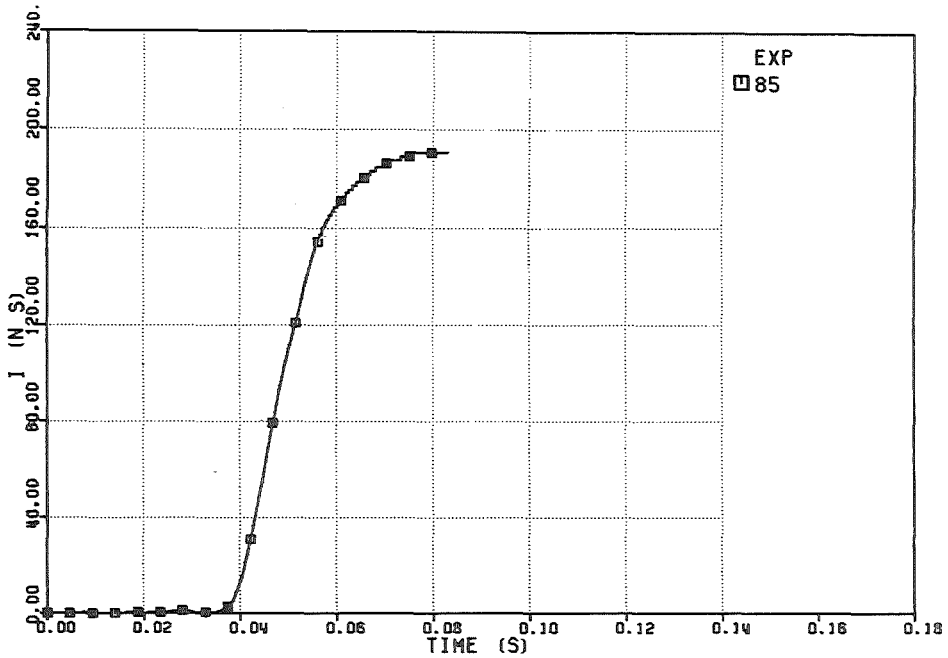

FIG. 6.471 IMPULSE ON THE UPPER PLATE

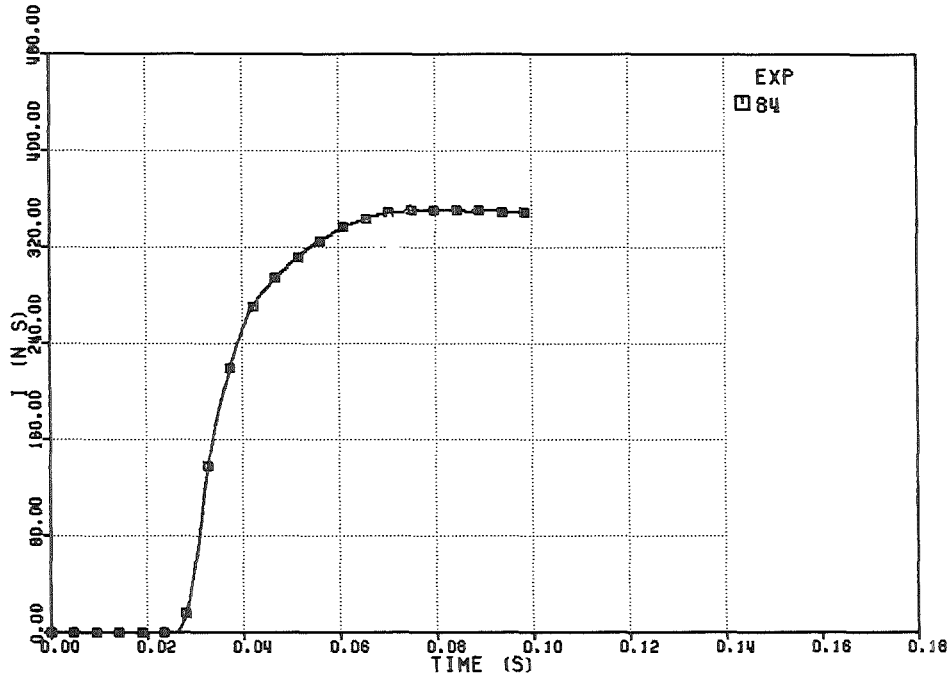

FIG. 6.470 IMPULSE ON THE UPPER PLATE

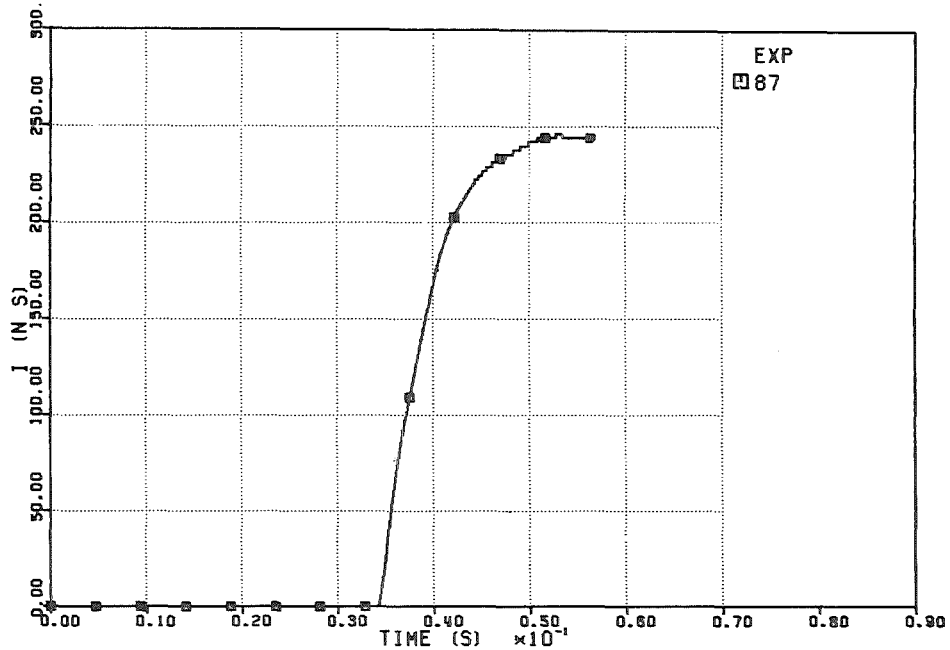

FIG. 6.473 IMPULSE ON THE UPPER PLATE

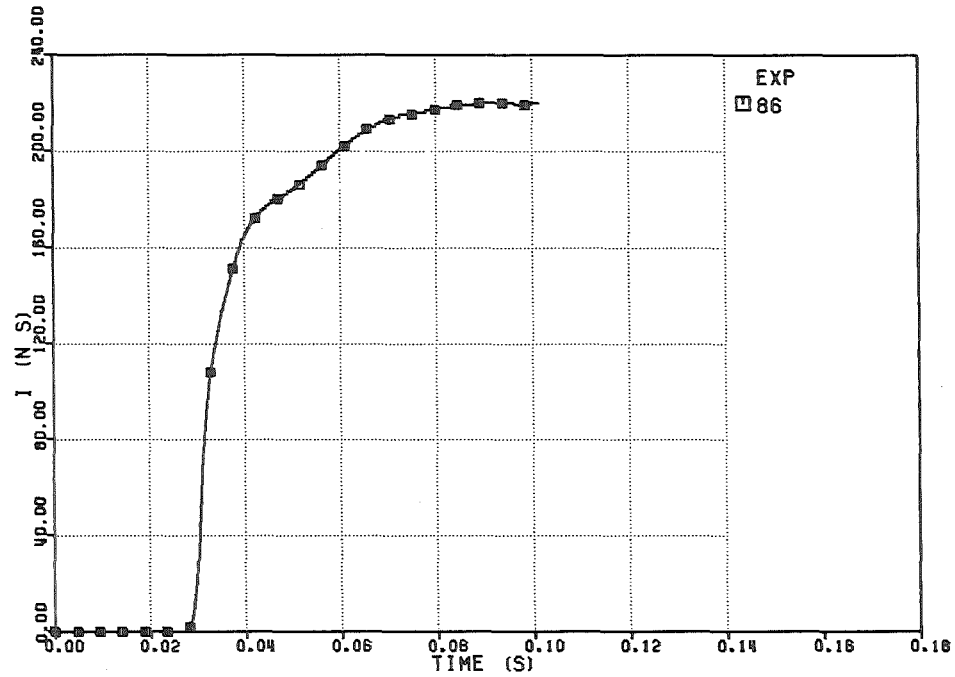

FIG. 6.472 IMPULSE ON THE UPPER PLATE

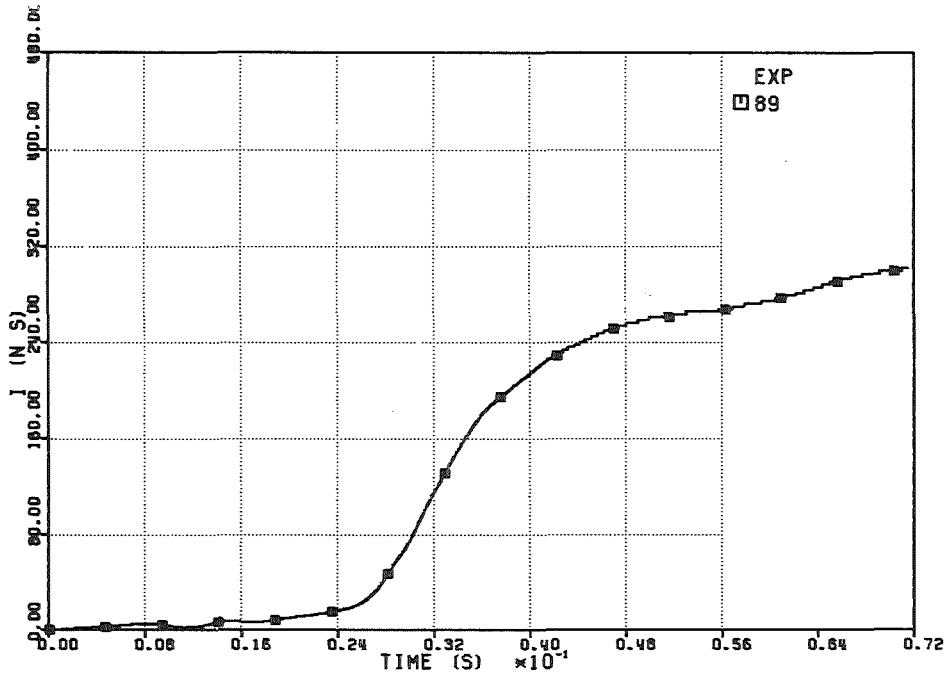

FIG. 6.475 IMPULSE ON THE UPPER PLATE

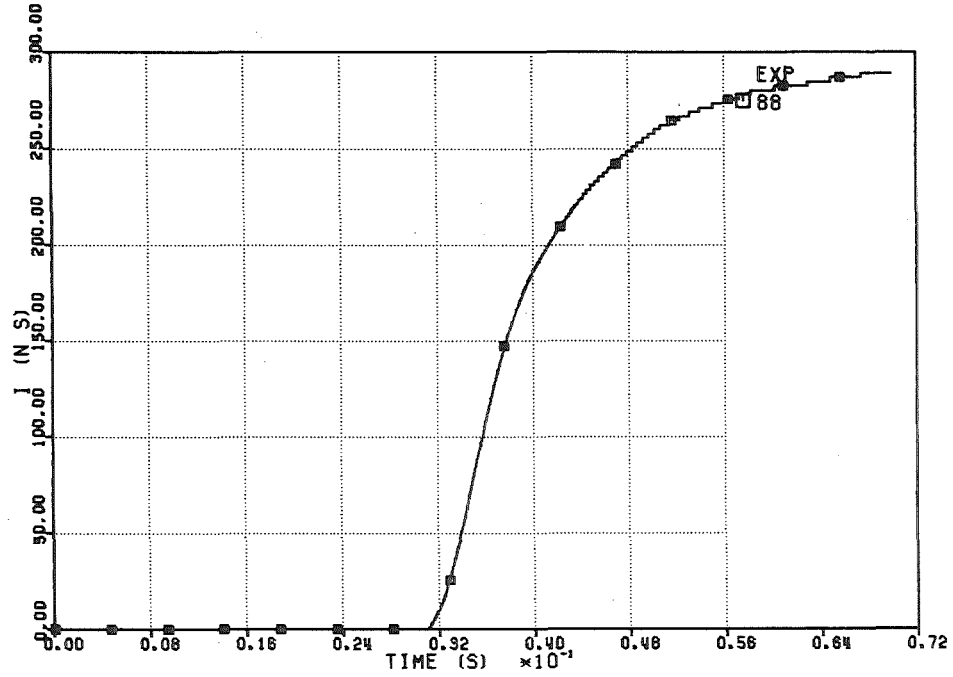

FIG. 6.474 IMPULSE ON THE UPPER PLATE

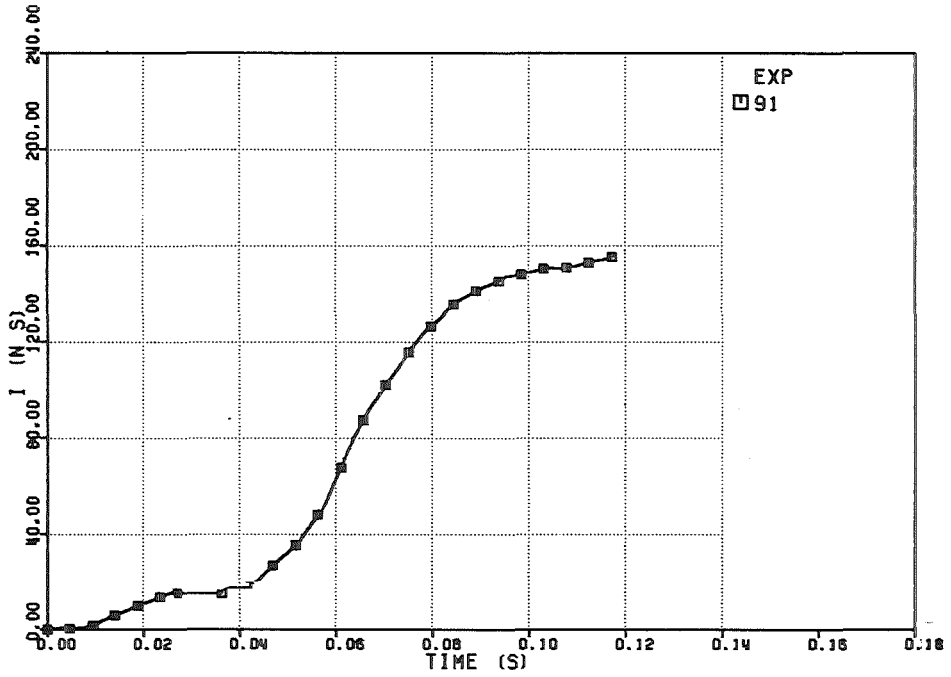

FIG. 6.477 IMPULSE ON THE UPPER PLATE

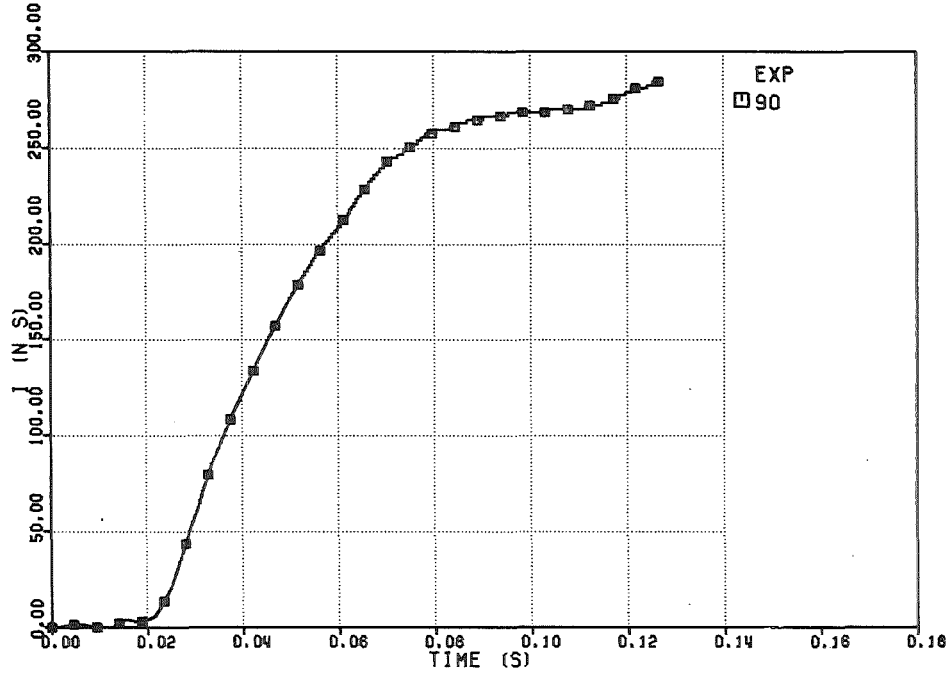

FIG. 6.476 IMPULSE ON THE UPPER PLATE

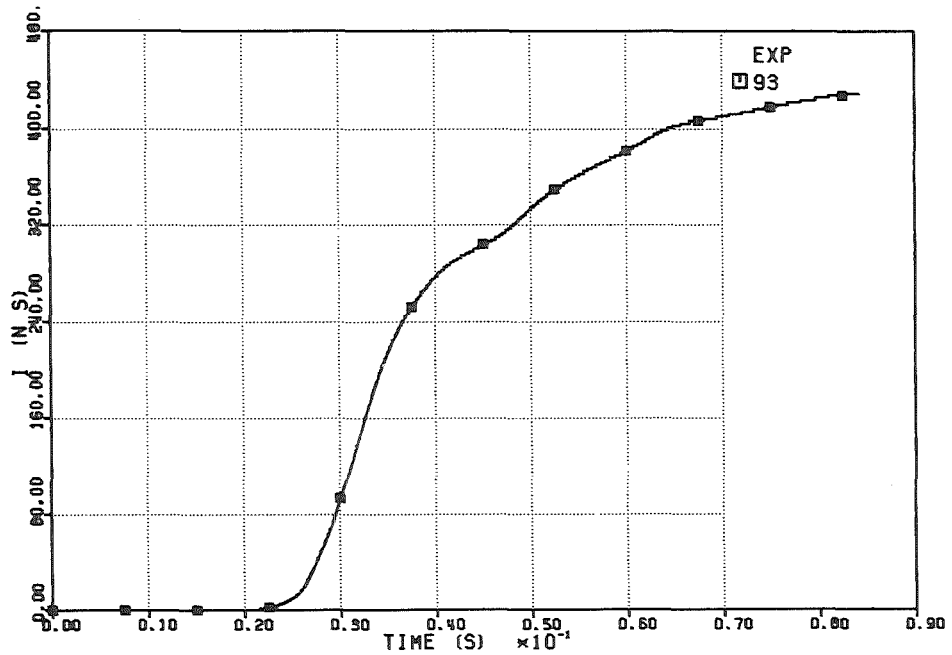

FIG. 6.479 IMPULSE ON THE UPPER PLATE

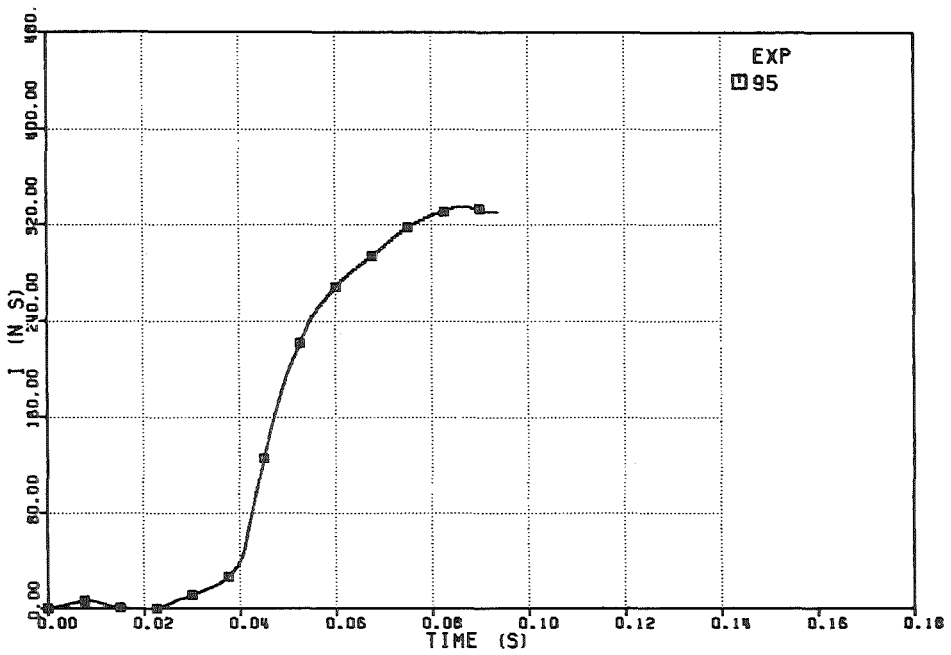

FIG. 6.481 IMPULSE ON THE UPPER PLATE

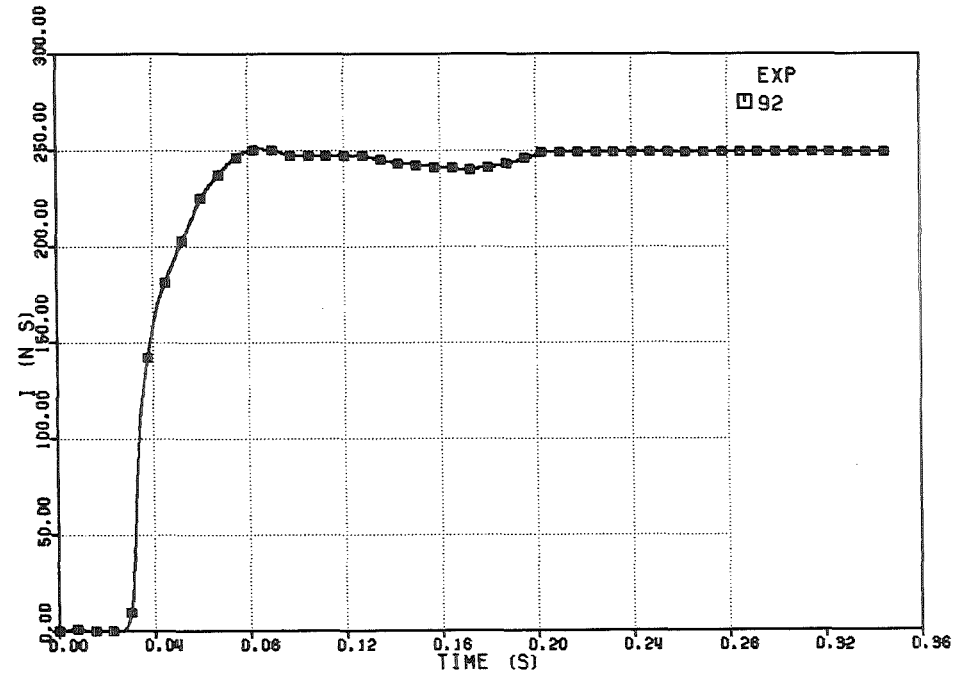

FIG. 6.478 IMPULSE ON THE UPPER PLATE

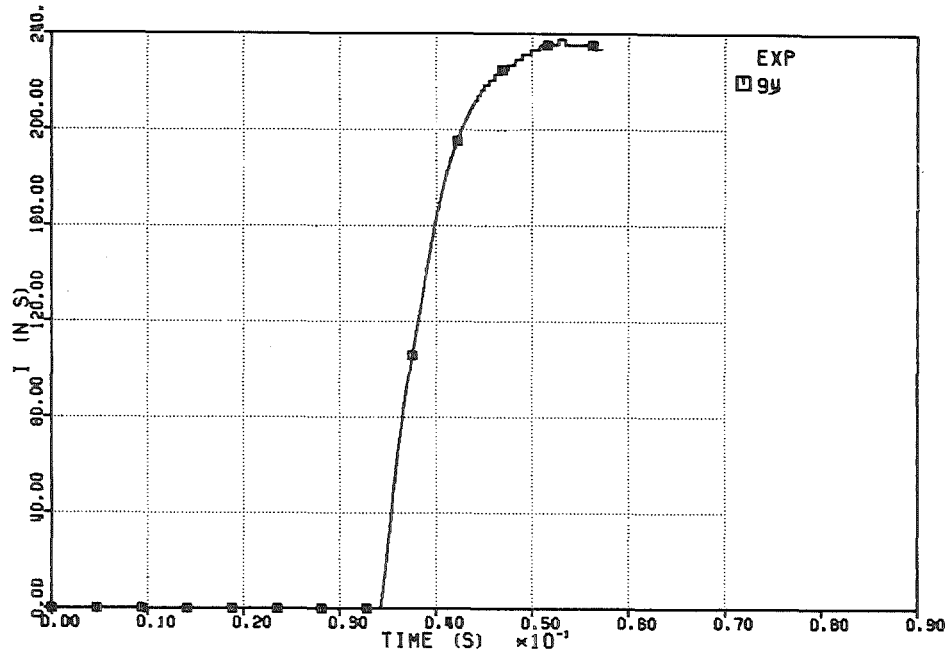

FIG. 6.480 IMPULSE ON THE UPPER PLATE

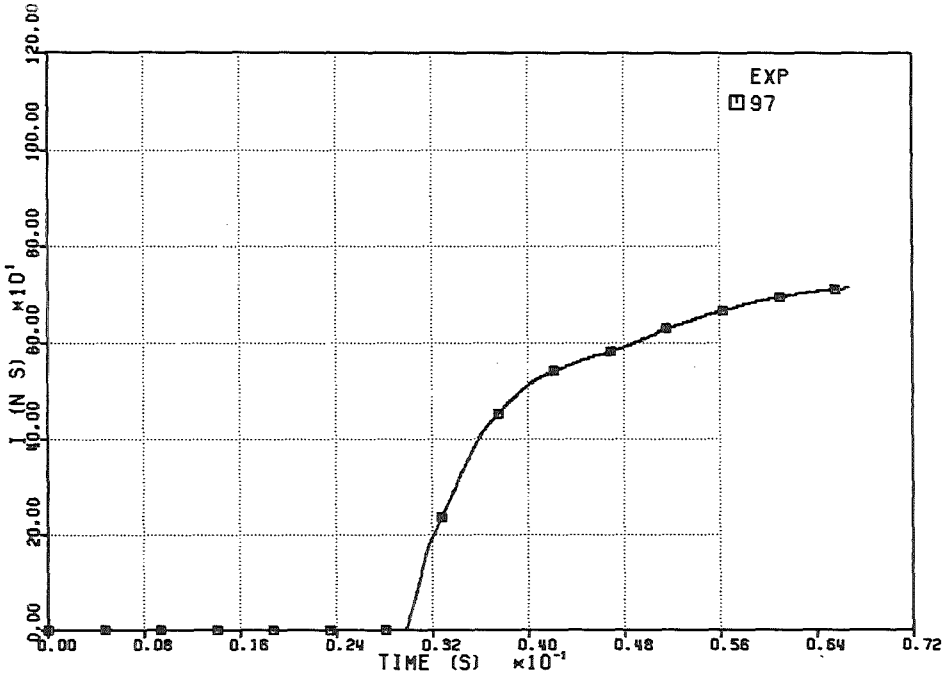

FIG. 6.483 IMPULSE ON THE UPPER PLATE

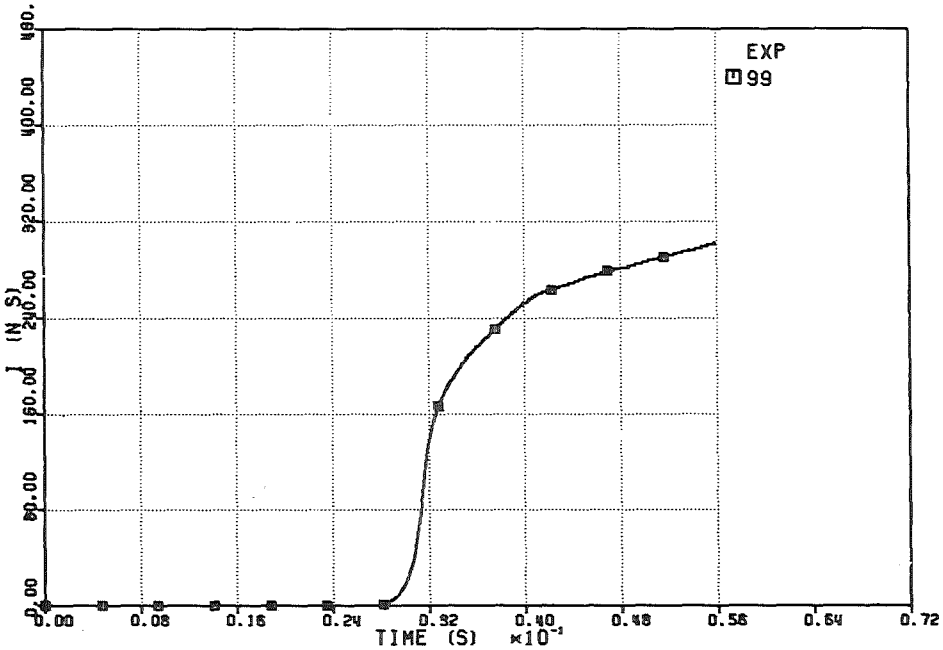

FIG. 6.485 IMPULSE ON THE UPPER PLATE

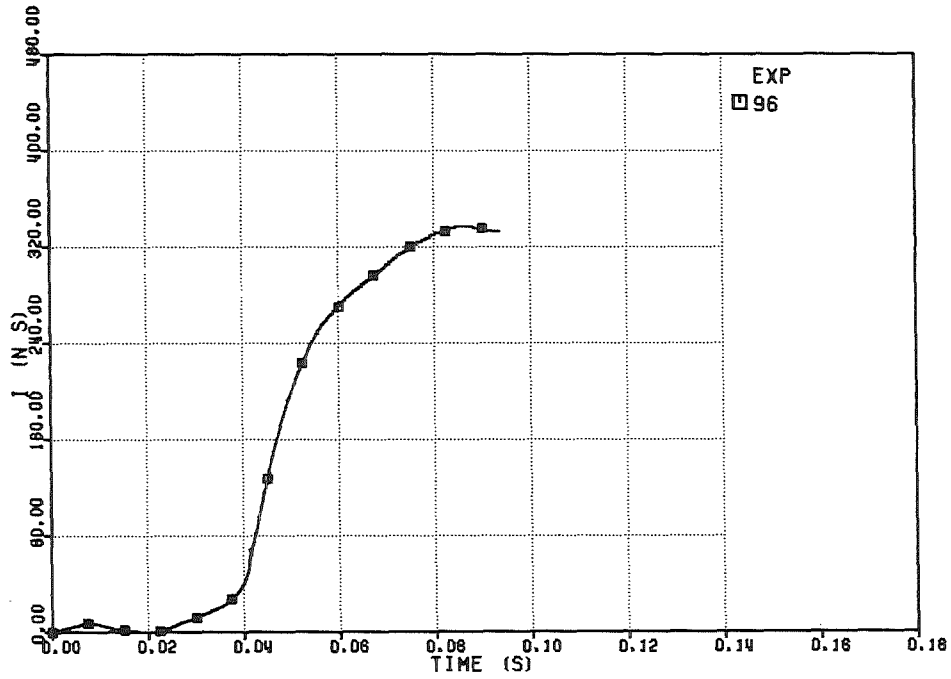

FIG. 6.482 IMPULSE ON THE UPPER PLATE

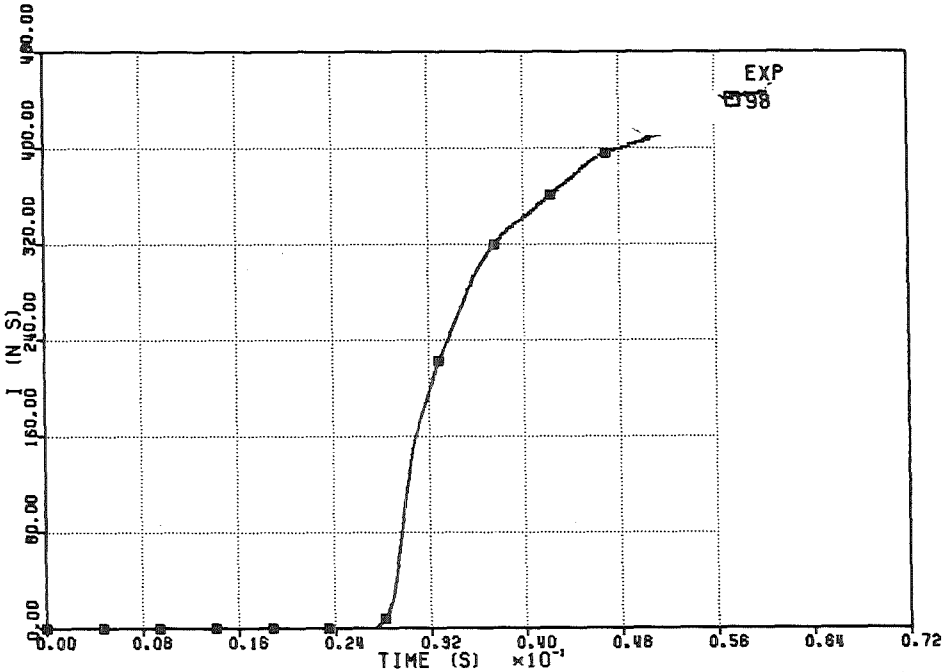

FIG. 6.484 IMPULSE ON THE UPPER PLATE

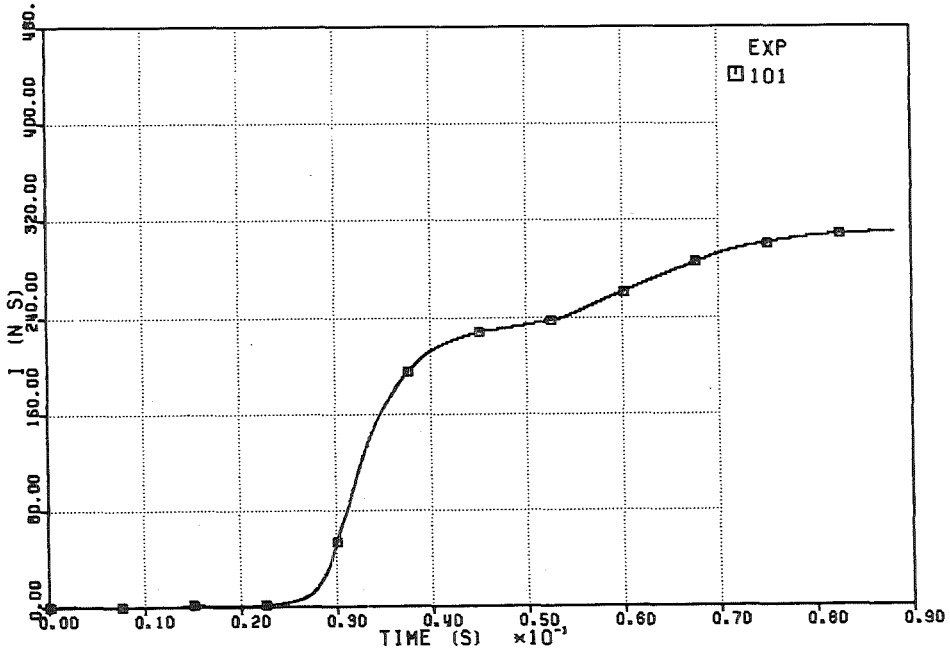

FIG. 6.487 IMPULSE ON THE UPPER PLATE

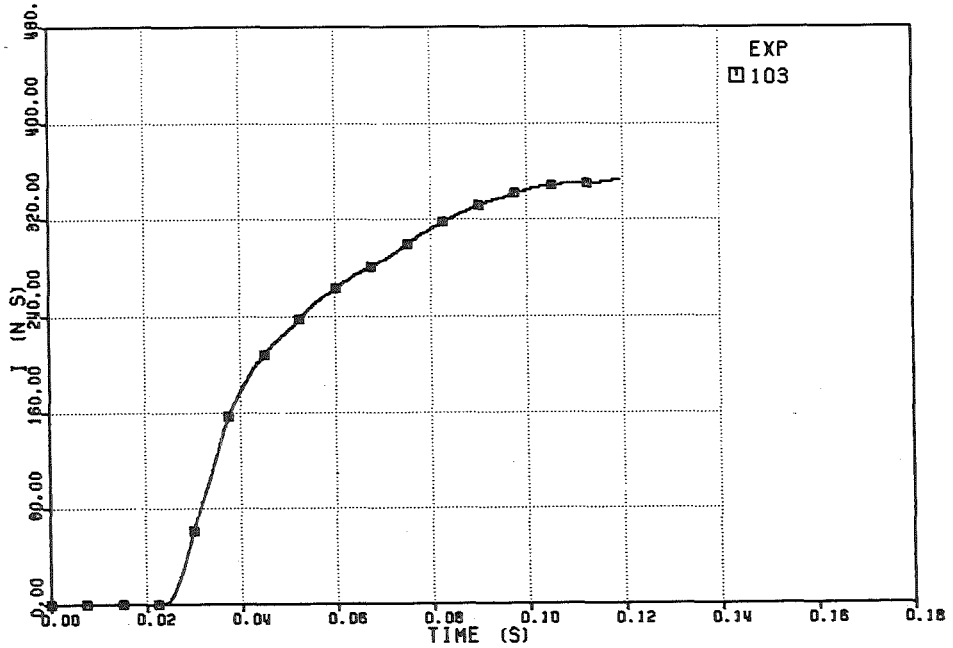

FIG. 6.489 IMPULSE ON THE UPPER PLATE

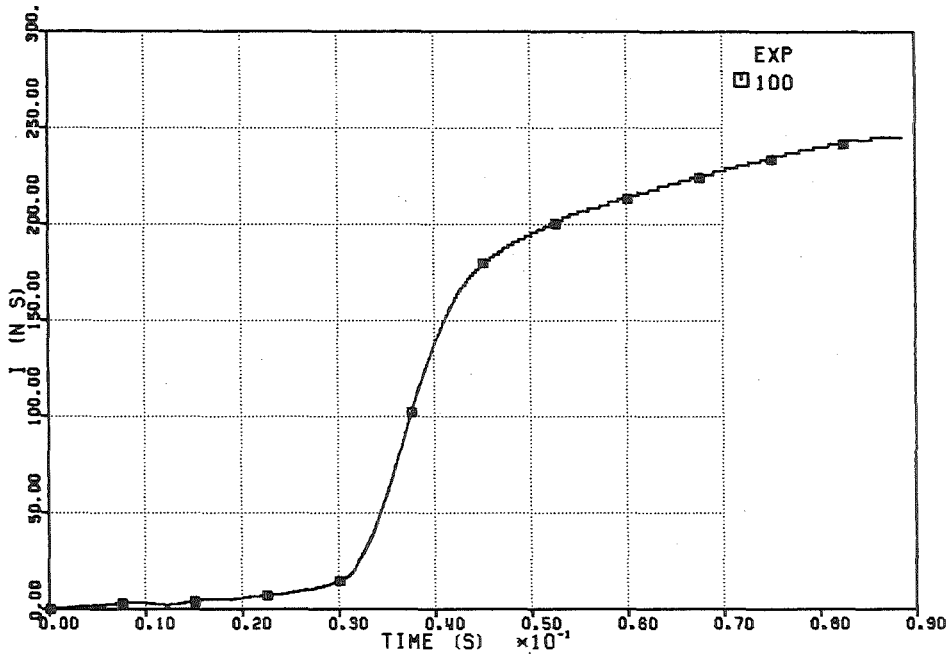

FIG. 6.486 IMPULSE ON THE UPPER PLATE

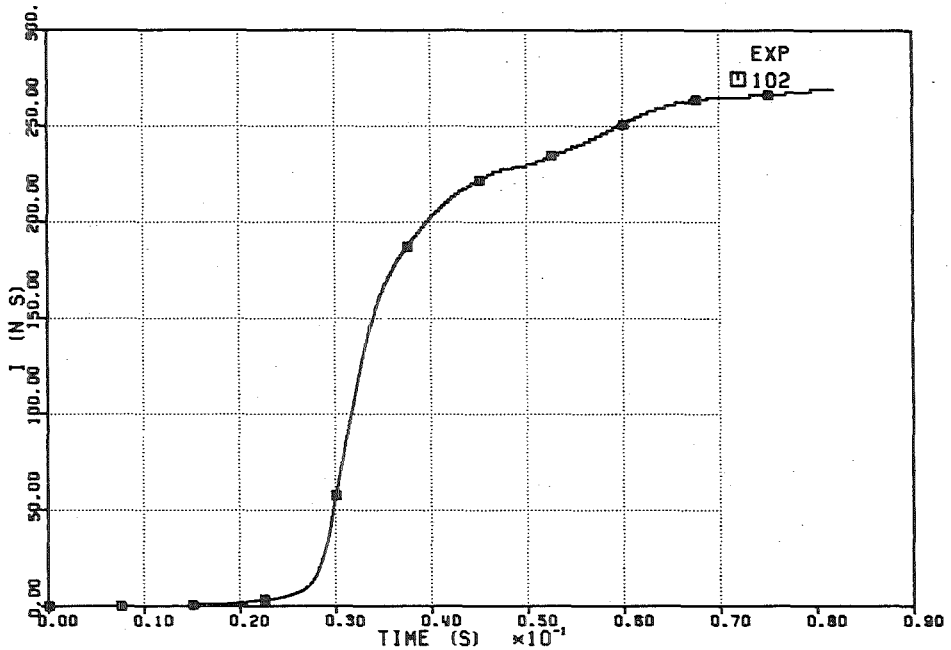

FIG. 6.488 IMPULSE ON THE UPPER PLATE

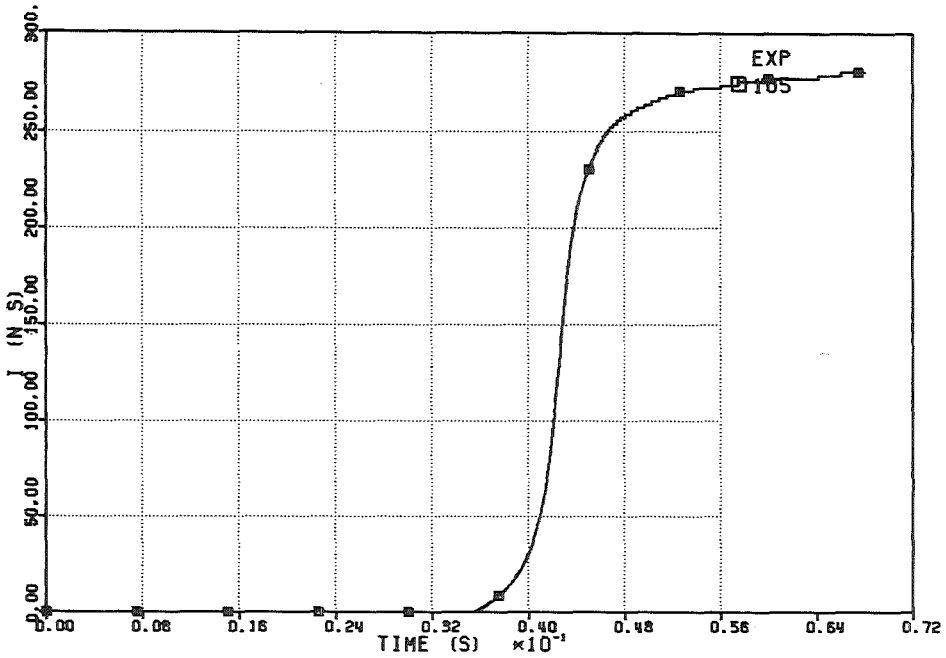

FIG. 6.491 IMPULSE ON THE UPPER PLATE

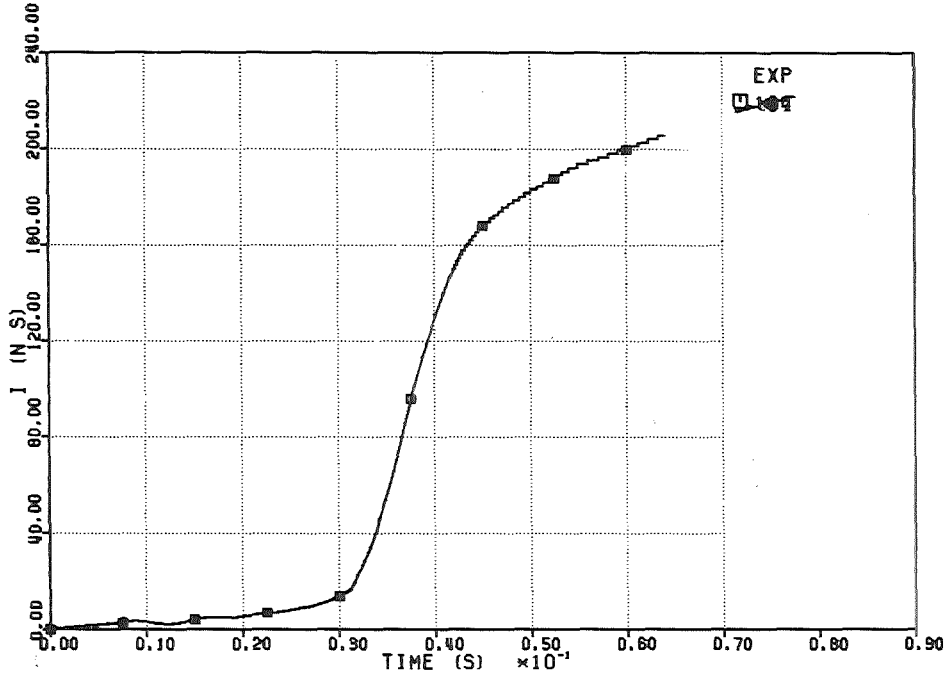

FIG. 6.490 IMPULSE ON THE UPPER PLATE

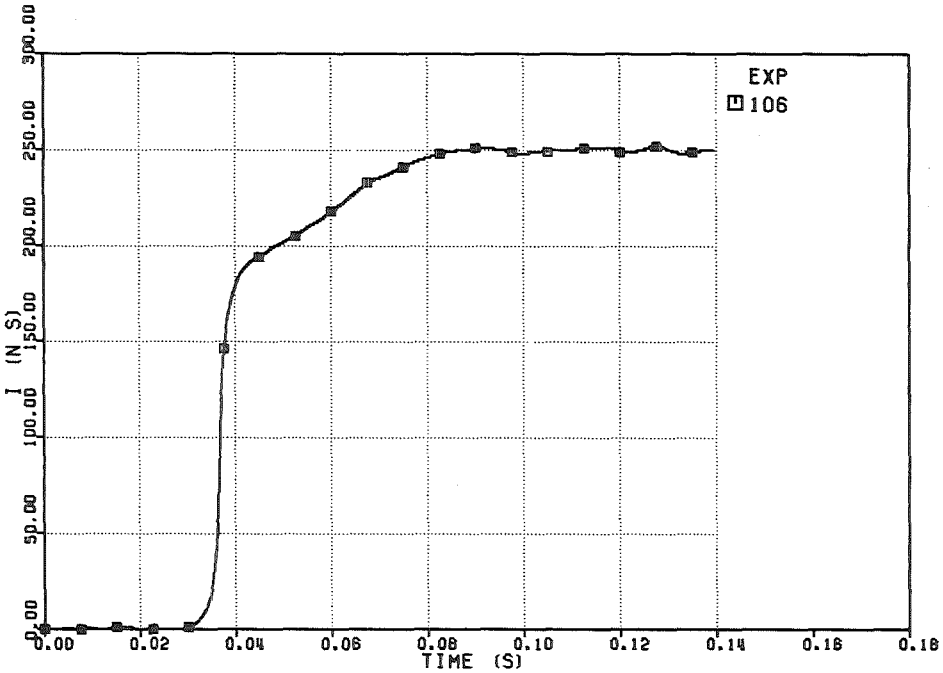

FIG. 6.492 IMPULSE ON THE UPPER PLATE

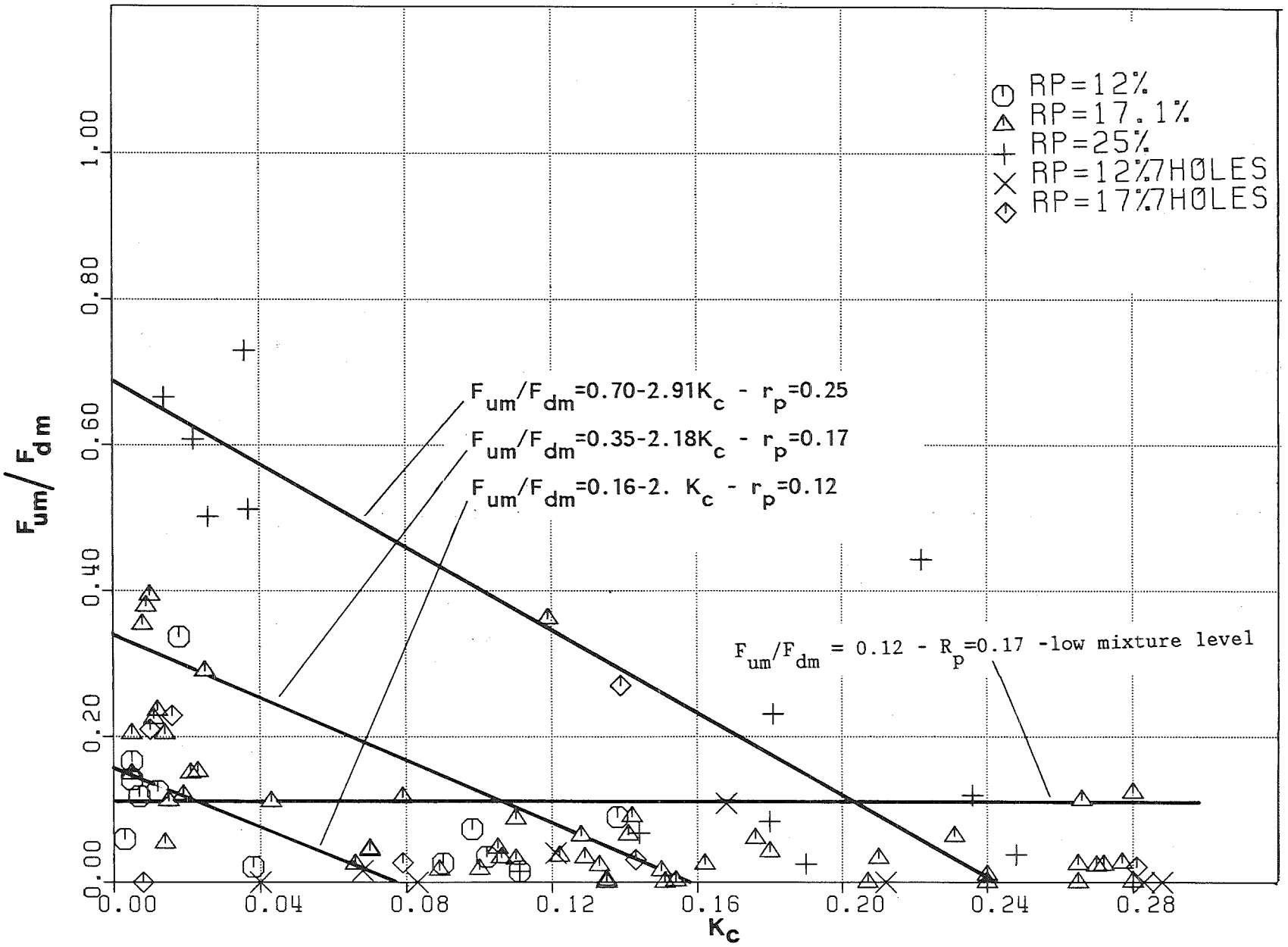

Fig.64 93- Ratio betweeen the maximum values of the forces acting on the upper plate and on the dip-plate as a function of the cavitation number.

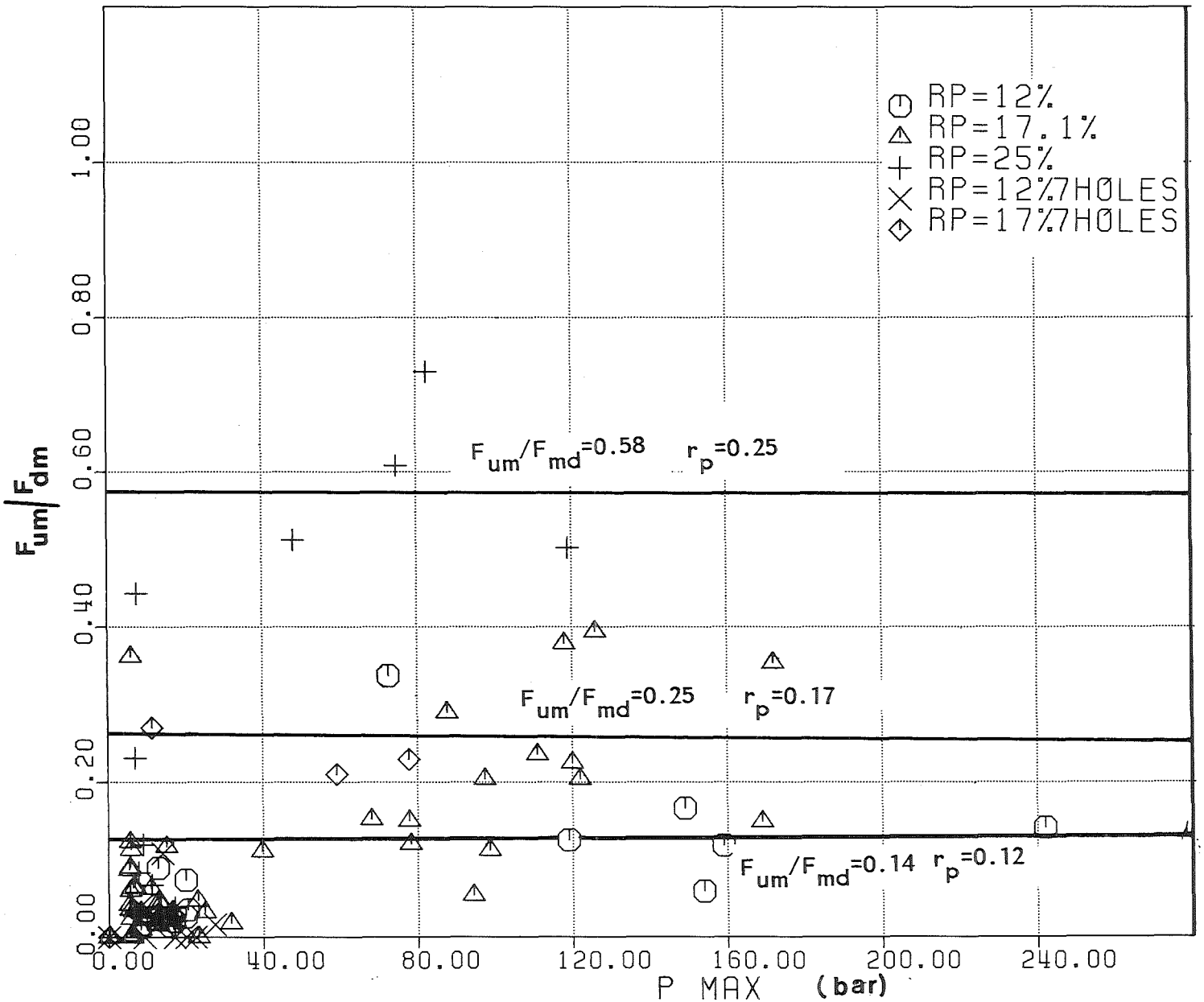

Fig. 6.494- Ratio betweeen the maximum values of the forces acting on the upper plate and on the dip-plate as a function of the maximum value of the pressure below the dip-plate.

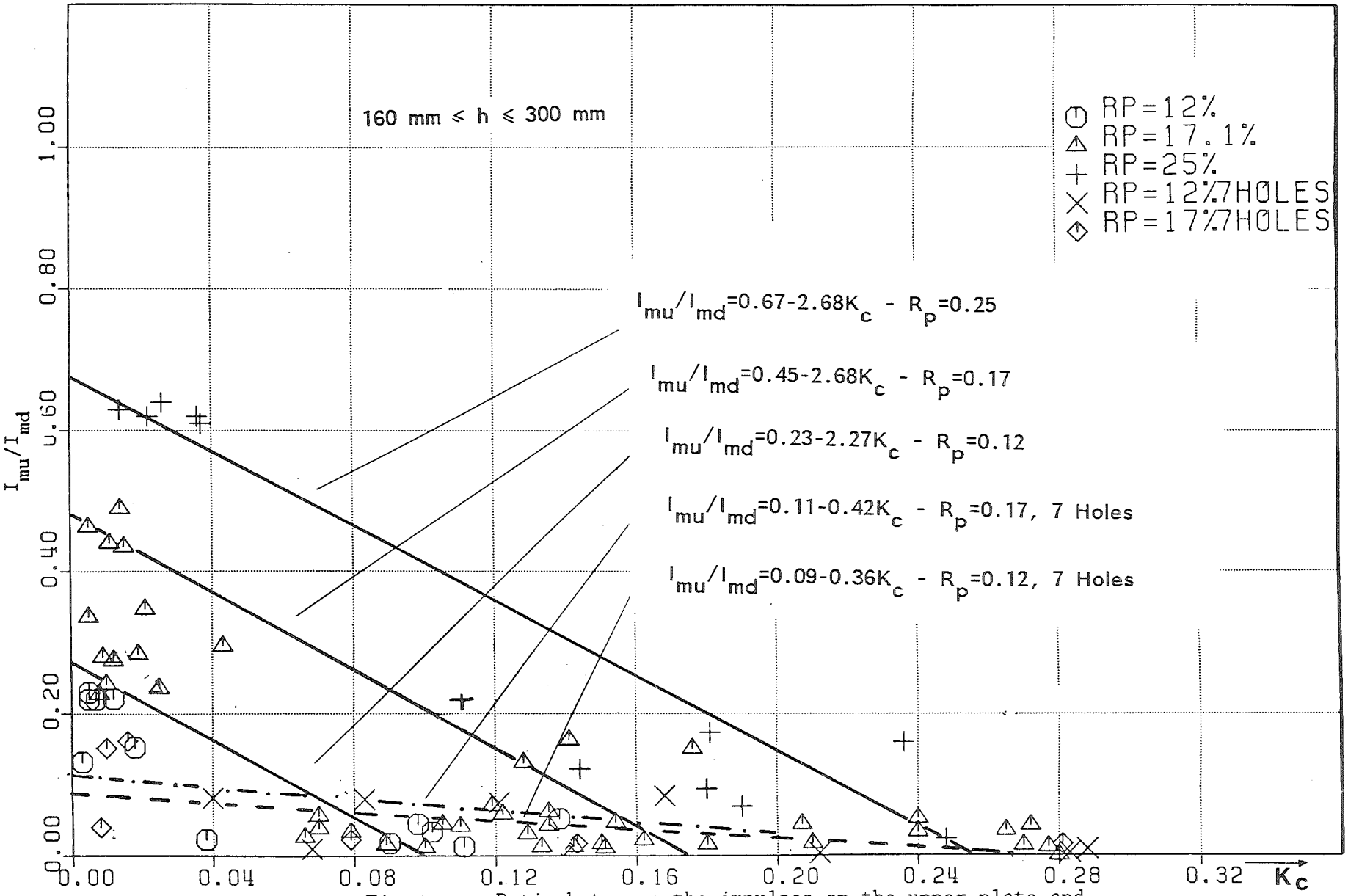

Fig.6.495 - Ratio betweeen the impulses on the upper plate and on the dip-plate versus the cavitation number. (high mixture level)

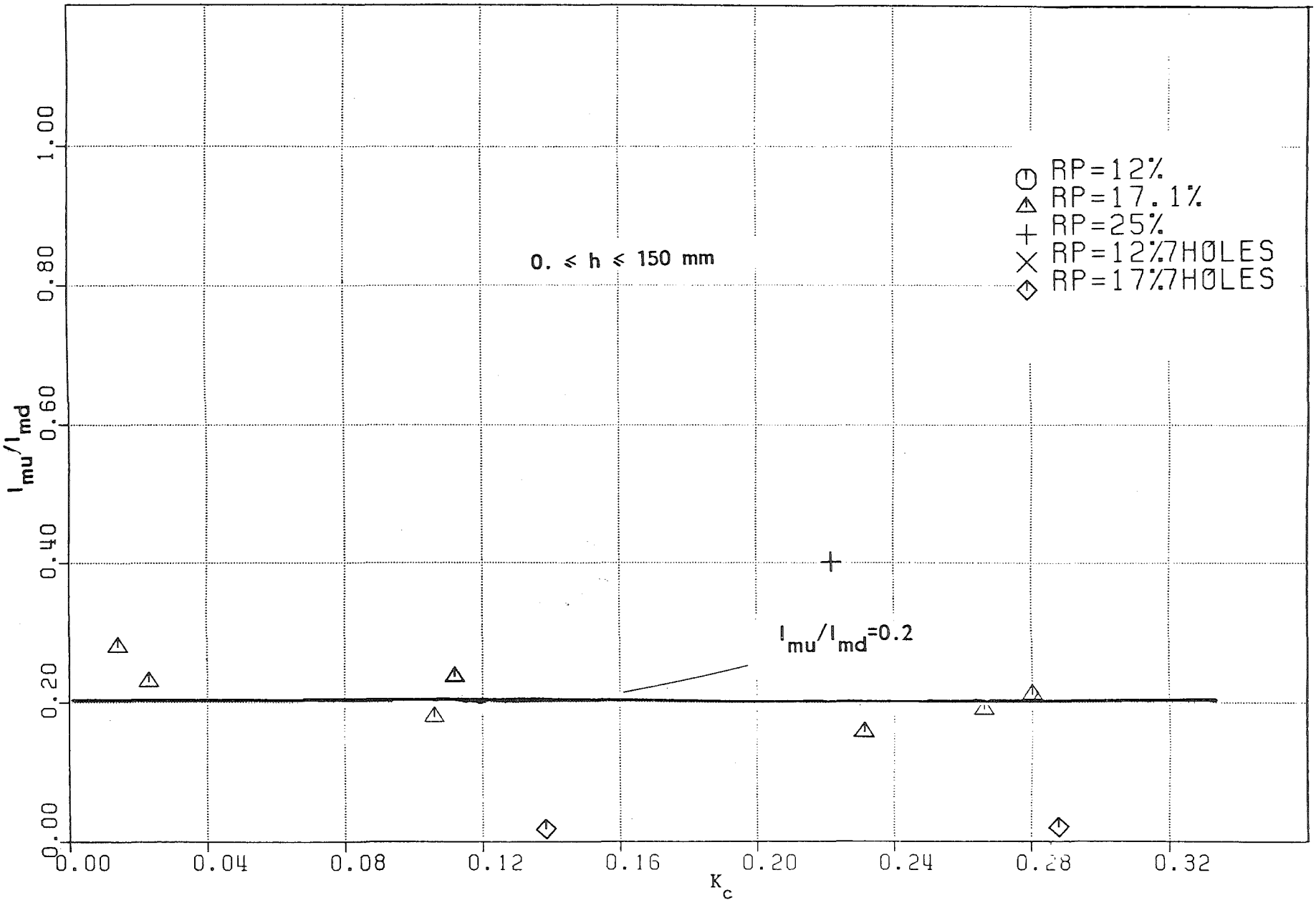

Fig. 6.496 - Ratio betweeen the impulses on the upper plate and on the dip-plate versus the cavitation number.
(low mixture level)

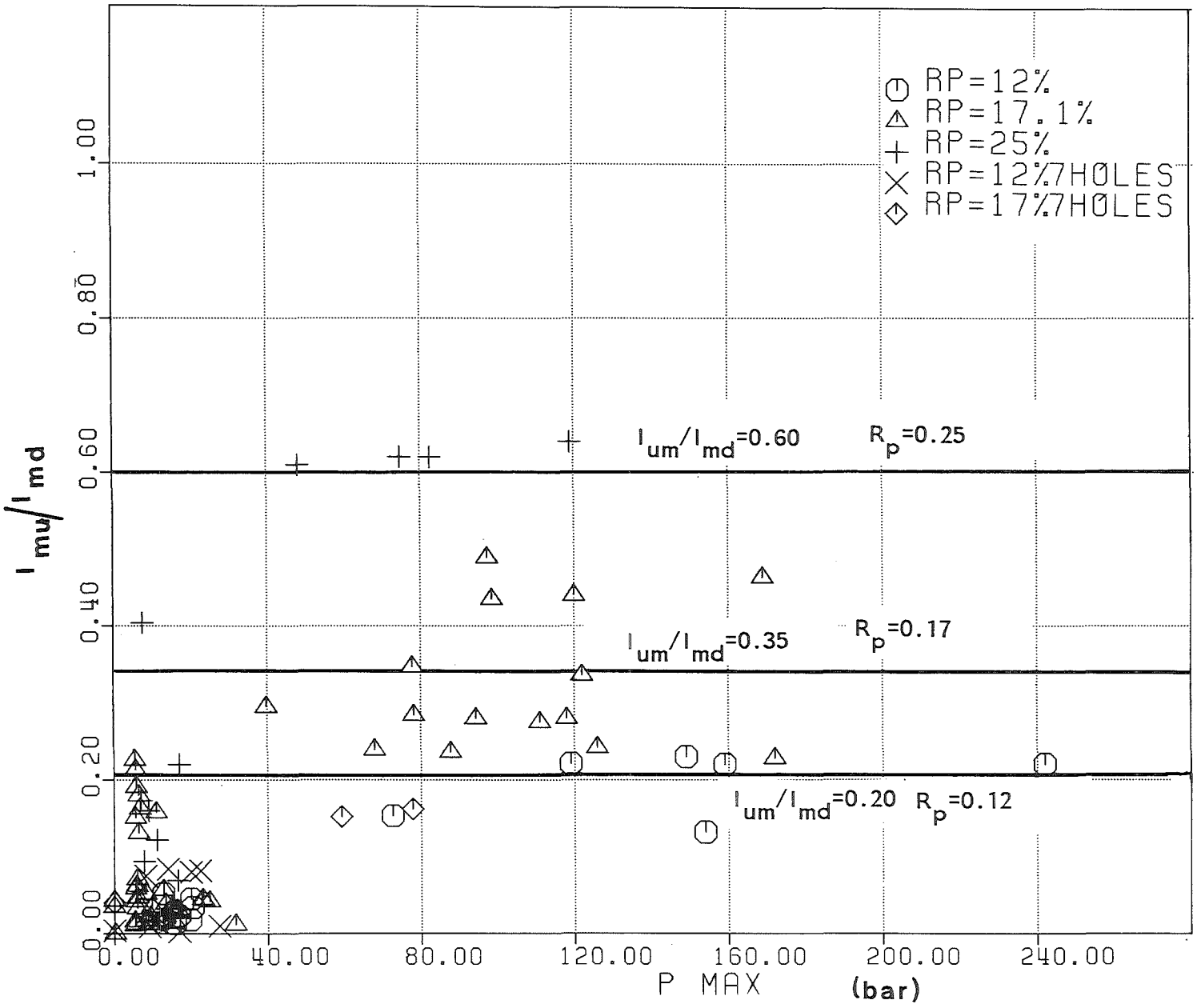

Fig.6.497- Ratio betweeen the impulses on the upper plate and on the dip-plate versus the maximum value of the pressure below the dip-plate.